



FOURTH EDITION

An Introduction to the
**Physiology
of Hearing**

James O. Pickles



AN INTRODUCTION TO THE PHYSIOLOGY OF HEARING

FOURTH EDITION



AN INTRODUCTION TO THE PHYSIOLOGY OF HEARING

FOURTH EDITION

by

JAMES O. PICKLES

School of Biomedical Sciences
University of Queensland



United Kingdom – North America – Japan – India – Malaysia – China

Emerald Group Publishing Limited
Howard House, Wagon Lane, Bingley BD16 1WA, UK

Fourth edition 2012. Previous editions 1982, 1988, 2008

Copyright © 2012 Emerald Group Publishing Limited

Reprints and permission service
Contact: booksandseries@emeraldinsight.com

No part of this book may be reproduced, stored in a retrieval system, transmitted in any form or by any means electronic, mechanical, photocopying, recording or otherwise without either the prior written permission of the publisher or a licence permitting restricted copying issued in the UK by The Copyright Licensing Agency and in the USA by The Copyright Clearance Center. No responsibility is accepted for the accuracy of information contained in the text, illustrations or advertisements. The opinions expressed in these chapters are not necessarily those of the Editor or the publisher.

British Library Cataloguing in Publication Data

A catalogue record for this book is available from the British Library

ISBN: 978-1-78052-166-4



Certificate Number 1985
ISO 9001
ISO 14001

ISOQAR certified
Management Systems,
awarded to Emerald for
adherence to Quality
and Environmental
standards ISO 9001:2008
and 14001:2004,
respectively



INVESTOR IN PEOPLE

To Wendy

CONTENTS

<i>Preface to the fourth edition</i>	<i>xiii</i>
<i>From the Preface to the first edition</i>	<i>xv</i>
<i>Abbreviations</i>	<i>xvii</i>
<i>Reading plan</i>	<i>xxiii</i>
1 The physics and analysis of sound	1
1.1 The nature of sound	1
1.2 The decibel scale	3
1.3 Impedance	4
1.4 The analysis of sound	5
1.5 Linearity	9
1.6 Summary	9
2 The outer and middle ears	11
2.1 The outer ear	11
2.1.1 The pressure gain of the outer ear	11
2.1.2 The outer ear as an aid to sound localization	14
2.2 The middle ear	15
2.2.1 Introduction	15
2.2.2 The middle ear as an impedance transformer	16
2.2.3 The middle ear muscles	22
2.3 Summary	24
2.4 Further reading	24
3 The cochlea	25
3.1 Anatomy	25
3.1.1 General anatomy	25
3.1.2 The organ of Corti	28
3.1.3 The innervation of the organ of Corti	33
3.2 The mechanics of the cochlea	35
3.2.1 The travelling wave	35
3.2.2 Current measurements of the travelling wave	38
3.2.3 Theories of cochlear mechanics	46

3.3	The fluid spaces of the cochlea	52
3.3.1	The endolymphatic and perilymphatic spaces	52
3.3.2	The endolymph	53
3.3.3	The perilymph	56
3.4	Hair cell responses	57
3.4.1	Hair cell responses in vitro	57
3.4.2	Inner hair cell responses in vivo	60
3.4.3	Outer hair cell responses in vivo	64
3.5	The gross evoked potentials	66
3.5.1	The cochlear microphonic	66
3.5.2	The summatting potential	68
3.5.3	The gross neural potentials	68
3.6	Summary	69
3.7	Further reading	71
4	The auditory nerve	73
4.1	Anatomy	73
4.2	Physiology	74
4.2.1	Response to tones	75
4.2.2	Response to clicks	83
4.2.3	Frequency resolution as a function of intensity and type of stimulation	85
4.2.4	Response to complex stimuli	89
4.3	Summary	98
4.4	Further reading	100
5	Mechanisms of transduction and excitation in the cochlea	101
5.1	Introduction	101
5.2	The structure of the transducer region	102
5.2.1	Stereocilia and cuticular plate	102
5.2.2	The cross-linking of stereocilia	104
5.2.3	The mechanotransducer channels	109
5.3	The electrophysiological analysis of mechanotransduction	110
5.3.1	Cell membrane potentials	110
5.3.2	Mechanotransduction	111
5.4	The origin of sharp tuning in the cochlea	123
5.4.1	Is an active process necessary theoretically?	124
5.4.2	Models incorporating an active mechanical process	125
5.4.3	Outer hair cells: needed for low thresholds and sharp tuning	128
5.4.4	Active mechanical processes in the cochlea: cochlear emissions	128

5.4.5	Motility in outer hair cells	131
5.4.6	Cochlear micromechanics	135
5.4.7	Conclusions on cochlear mechanical amplification	137
5.5	Hair cells and neural excitation	137
5.5.1	Stimulus coupling to inner and outer hair cells	137
5.5.2	Activation of auditory nerve fibres	139
5.5.3	Neurotransmitter release	141
5.6	Cochlear non-linearity	142
5.6.1	The non-linear growth of cochlear responses	143
5.6.2	Two-tone suppression	145
5.6.3	Combination tones	147
5.7	Summary	150
5.8	Further reading	153
6	The subcortical nuclei	155
6.1	Considerations in studying the auditory central nervous system	155
6.2	The cochlear nuclei	157
6.2.1	Output pathways	157
6.2.2	Input pathways	158
6.2.3	The ventral binaural sound localization stream: the bushy cells of the anteroventral and posteroventral cochlear nucleus	159
6.2.4	Cells of the posteroventral cochlear nucleus: contributions to both binaural localization and to identification	162
6.2.5	The dorsal cochlear nucleus: sound identification and localization in the vertical plane	164
6.2.6	Excitation and inhibition in the cochlear nucleus	167
6.2.7	Functions of the cochlear nucleus	170
6.3	The superior olivary complex	173
6.3.1	Innervation and overall anatomy	173
6.3.2	The ventral sound localization stream: comparing the intensities of the stimuli at the two ears	175
6.3.3	The ventral sound localization stream: comparing the timing of the stimuli at the two ears	181
6.3.4	Summary of role of superior olivary complex in sound localization	184
6.4	Ascending pathways of the brainstem and the nuclei of the lateral lemniscus	185
6.4.1	The ventral nucleus of the lateral lemniscus	185
6.4.2	The dorsal nucleus of the lateral lemniscus	186
6.5	The inferior colliculus	186
6.5.1	General anatomy	187
6.5.2	The central nucleus	187
6.5.3	The external nucleus and dorsal cortex	195

6.6	The medial geniculate body	197
6.6.1	Overall anatomy and inputs	197
6.6.2	The ventral nucleus	199
6.6.3	The medial and dorsal nuclei	202
6.7	Brainstem reflexes	203
6.7.1	Middle ear muscle reflex	203
6.7.2	Acoustic startle	204
6.7.3	Orientation	204
6.7.4	Audiogenic seizures	205
6.8	Summary	205
6.9	Further reading	208
7	The auditory cortex	211
7.1	Organization	211
7.1.1	Anatomy and projections	211
7.1.2	Tonotopic organization	219
7.1.3	Organization along the frequency-band strips	219
7.2	The responses of single neurones	221
7.2.1	Responses in the core	221
7.2.2	Responses in the belt	225
7.3	Cortical processing of sound location	226
7.3.1	Behavioural experiments	226
7.3.2	Electrophysiological responses	228
7.4	Cortical processing and stimulus complexity	235
7.4.1	Behavioural experiments	235
7.4.2	Physiological responses	236
7.5	Overview of functions of the auditory cortex	238
7.6	Summary	239
7.7	Further reading	241
8	The centrifugal pathways	243
8.1	Introduction	243
8.2	The olivocochlear bundle	244
8.2.1	Anatomy	244
8.2.2	Neurotransmitters	245
8.2.3	Physiology and function	247
8.3	Centrifugal pathways to the cochlear nuclei	257
8.3.1	Anatomy	257
8.3.2	Neurotransmitters	259
8.3.3	Physiology and function	259
8.4	Centrifugal pathways in higher centres	260

8.4.1	Anatomy	261
8.4.2	Physiology and function	262
8.5	Summary	264
8.6	Further reading	265
9	Physiological correlates of auditory psychophysics and performance	267
9.1	Introduction	267
9.2	The absolute threshold	268
9.3	Frequency resolution	268
9.3.1	A review of the psychophysics of frequency resolution	268
9.3.2	Quantitative relations between psychophysics and physiology in frequency resolution	273
9.3.3	Frequency resolution in the auditory central nervous system	276
9.3.4	Co-modulation masking release: analysis across filters	277
9.4	Frequency discrimination	278
9.4.1	Place and time coding	278
9.4.2	A psychophysical model for pitch perception and its relation to physiology	281
9.5	Intensity and loudness	283
9.5.1	Stimulus coding as a function of intensity	283
9.5.2	Loudness	290
9.6	Sound localization and spatial hearing	293
9.6.1	Introduction	293
9.6.2	Mechanisms of sound localization	294
9.6.3	Spatial release from masking and the binaural masking level difference	299
9.7	Speech	301
9.7.1	What is special about speech?	301
9.7.2	Auditory nerve and brainstem responses	303
9.7.3	Cortical responses to vocalizations in non-human species	306
9.7.4	Responses to speech in the human cortex	308
9.8	Summary	314
9.9	Further reading	316
10	Sensorineural hearing loss	319
10.1	Types of hearing loss	319
10.2	Sensorineural hearing loss of cochlear origin: mechanisms of pathology	320

10.2.1	Ototoxicity	320
10.2.2	Acoustic trauma	324
10.2.3	Genetic causes	326
10.2.4	Ageing	328
10.3	Sensorineural hearing loss of cochlear origin: functional changes	329
10.3.1	Physiological changes	329
10.3.2	Psychophysical correlates	332
10.4	Physiological aspects of the cochlear prosthesis	337
10.4.1	Introduction	337
10.4.2	Physiological background	338
10.4.3	Results	342
10.5	Cellular replacement, protection and gene therapy in the inner ear	344
10.5.1	Introduction	344
10.5.2	Production of new hair cells by transdifferentiation of supporting cells	346
10.5.3	Production of new hair cells by mitosis in the mammalian cochlea	347
10.5.4	Gene therapy	348
10.5.5	Stem cell therapy	348
10.5.6	Cell protection	350
10.6	Summary	351
10.7	Further reading	353
References		355
Index		405

PREFACE TO THE FOURTH EDITION

This book is centred around the way that the auditory system processes acoustic signals. In the five years since the last edition, substantial progress has been made in many areas of the subject, and in particular in our understanding of the auditory central nervous system, and in clinical aspects. The chapters dealing with the latter have been expanded; in addition, all parts of the book have been brought thoroughly up to date. Given the rapid expansion in the amount of material available, severe selection has had to be applied, both in the topics presented and in the references that could be quoted, in order to ensure adequate treatment of the main theme of the book in a reasonable length.

The underlying aim is to show the principles that may apply to the human auditory system. Given that the overriding intention is to show the underlying mechanisms as clearly and precisely as possible, much of the information in the book has necessarily been drawn from experimental animals. For this reason, relatively little attention is given to non-mammals, except where they illustrate principles relevant to mammals and where information can be obtained more clearly and precisely than in mammals. Similarly, mammals with specializations remote from those used by human beings are not included, except where they can be used to illustrate mechanisms more clearly than less specialized mammals. Nevertheless, and particularly as a result of genetic and functional imaging studies, an increasing amount of high-quality fundamental information is now available in human beings.

Although substantial advances have been made in the developmental and molecular aspects of the subject, as before I have maintained the focus on the processing of auditory signals, lest the book become too diverse. A small exception has been made in Chapter 10. This chapter deals with sensorineural hearing loss, including current physiological aspects of cochlear pathology, and ways that are being used to reverse the pathology. Here, some molecular and developmental information has been included.

As with previous editions, the intention is to bring those readers with only a little background in neuroscience to a level where they are able to appreciate current research issues and current research frontiers. The subject is still small enough for this to be possible within a volume of reasonable size; however, the chapters dealing with the central nervous system have, in particular, become significantly more dense than in the previous editions. Therefore, it is suggested that non-specialist readers will find the summaries of those chapters particularly useful. It is also suggested that for non-specialist readers, Chapters 5–8 will now

function more as a resource for reference than as chapters to be read in their entirety. A reading scheme is provided (p. xxiii) to guide readers to the sections of the book most appropriate for their interests.

I am very grateful to many colleagues who have commented and very helpfully responded to the many queries that I have raised with them during the course of this revision. I am also very grateful to colleagues who have provided original figures, either unpublished figures of original data, new plots of previously published data or full-resolution versions of previously published figures. My thanks for this go to David Corey, Bertrand Delgutte, Anders Fridberger, Rudolf Glueckert, James Hudspeth, Matthew Kelley, Cornelia Kopp-Scheinpflug, Dave Langers, Gareth Leng, Christopher Petkov, Cathy Price and Ian Russell.

During the writing of this edition I received support from the Garnett Passe and Rodney Williams Memorial Foundation, and without their backing it would not have been possible to produce this revision. I give my thanks to the Foundation and their Trustees for the substantial support that they have given me during the writing of this book and for many years previously.

Jim Pickles
Brisbane

FROM THE PREFACE TO THE FIRST EDITION

The last 15 years have seen a revolution in auditory physiology, but the new ideas have been slow to gain currency outside specialist circles. Undoubtedly, one of the main reasons for this has been the lack of a general source for non-specialists, and it is hoped that this book will bring current thinking to a much wider audience.

While the book is primarily intended as a student text, it is hoped that it will be equally useful to teachers of auditory physiology. It should be particularly useful to those teaching physiology to medical students. The increasing concern about the extent of hearing loss in the community should increase the attention paid to auditory physiology in the medical curriculum.

The book is written at a level suitable for a degree course on the special senses or as a basis for a range of postgraduate courses. It is organized so as to be accessible to those approaching the subject at a number of levels and with a variety of backgrounds (see 'Reading plan', p. xxiii). Only the most elementary knowledge of physiology is assumed, and even such basic concepts as ionic equilibrium potentials are explained where appropriate. The treatment is non-mathematical, and only a few elementary algebraic equations appear.

ABBREVIATIONS

16S	(small) component of ribosomal RNA
a.c.	alternating coupled
AAF	anterior auditory field (of cortex)
AES	anterior ectosylvian sulcal field (of cortex)
AI	primary auditory area (of cortex)
AII	secondary auditory area (of cortex)
AL	anterolateral area (of cortex)
AM	amplitude modulation
AMPA	amino-3-hydroxy-5-methylisoxazole-4-propionic acid (receptor type)
AN	auditory nerve
Atoh 1	atausal homologue 1
ATP	adenosine tri-phosphate
ATPase	enzyme that catalyses the decomposition of ATP
AVCN	anteroventral cochlear nucleus
BAPTA	1,2-bis(2-aminophenoxy)ethane-n,n,n',n'-tetraacetaic acid (Ca ²⁺ chelator)
Bcl-2	B-cell lymphoma 2
BIC	brachium of the inferior colliculus
BMLD	binaural masking level difference
C	capacitance
Ca ²⁺	calcium ion
CAP	compound action potentials
CDH23	cadherin-23 gene
CF	characteristic frequency
CF	constant frequency (in bat echolocation)
CGRP	calcitonin gene-related peptide
Cl ⁻	chloride ion
CL	caudolateral field (of cortex)
CM	caudomedian field (of cortex)
CM	cochlear microphonic
CN	cochlear nucleus
COCB	crossed olivocochlear bundle

CT	computerized (x-ray) tomography
CX26, 30	connexin 25 and 30 genes
<i>d</i>	displacement
dB	decibels
d.c.	direct coupled
DCN	dorsal cochlear nucleus
DFN	X chromosome-linked deafness
DFNA	not linked to X or Y chromosomes (i.e. autosomal) and dominant deafness
DFNB	not linked to X or Y chromosomes (i.e. autosomal) and recessive deafness
DLPO	dorsolateral peri-olivary nucleus
DMPO	dorsomedial peri-olivary nucleus
DNA	deoxyribonucleic acid
DNLL	dorsal nucleus of the lateral lemniscus
DP	dorsal posterior area (of cortex)
DPO	dorsal peri-olivary nucleus
DZ	dorsal zone (of cortex)
D-stellate	project <i>dorsalwards</i> within the cochlear nucleus
EC	equalization and cancellation
EE	excited by stimuli in either ear
EI	excited by contralateral stimuli and inhibited by ipsilateral stimuli
Ep	posterior ectosylvian (gyrus of cortex)
EPSP	excitatory post-synaptic potential
EPTC	electrophysiological ‘psychophysical tuning curve’
ERB	equivalent rectangular bandwidth
<i>f</i>	frequency
<i>F</i>	formant
fMRI	functional magnetic resonance imaging
FM	frequency modulation
FTC	frequency-threshold curve
G	energy
GABA	γ -amino butyric acid (inhibitory neurotransmitter)
HSP	heat shock protein
Hz	hertz (i.e. cycles per second)
I	insula
<i>I</i>	intensity
IC	inferior colliculus
ICC	central nucleus of inferior colliculus
ICDC	dorsal cortex of inferior colliculus
ICX	external nucleus of inferior colliculus
IE	inhibited by contralateral stimuli and excited by ipsilateral stimuli
IHC	inner hair cell(s)
I-T	insulo-temporal (area of cortex)
<i>k</i>	Boltzmann's constant
κ	kappa (spring factor: force/distance)

K ⁺	potassium ion
KAlt	lateral auditory koniocortex
KAm	medial auditory koniocortex
KCNJ10	ATP-sensitive inward rectifier potassium channel 10
kHz	kilohertz
LD	lateral division of inferior colliculus
LGB	lateral geniculate body
LNTB	lateral nucleus of the trapezoid body
LOC	lateral olivocochlear bundle or system
LSO	lateral superior olivary nucleus
LV	pars lateralis of the ventral MGB
m	metres
MAPK/JNK	mitogen-activated protein kinase/c-Jun N-terminal kinase
Math-1	mammalian atonal homologue 1
MELAS	mitochondrial encephalomyopathy, lactic acidosis and stroke-like episodes
MGB	medial geniculate body
MKS	metre kilogram second (system of measurement)
ML	middle lateral area (of cortex)
mM	millimolar (concentration)
µm	microns (micrometres)
MNTB	medial nucleus of the trapezoid body
MOC	medial olivocochlear bundle or system
MRI	magnetic resonance imaging
msec	milliseconds
MSO	medial superior olivary nucleus
MYO7A	myosin 7A gene
mV	millivolts
N	newtons (unit of force)
N ₁ and N ₂	neural potentials
Na ⁺	sodium ion
n	nano (10^{-9})
nm	nanometres
NKCC1	Na ⁺ /K ⁺ /Cl ⁻ cotransporter 1
NMDA	N-methyl-d-aspartate (receptor type)
OHC	outer hair cell(s)
OSB	outer spiral bundle
OV	pars ovoidea of ventral nucleus of MGB
p	pressure
p	probability
p	pico (10^{-12})
p27kip1	protein 27 cyclin-dependent kinase inhibitor 1
Pa	pascals
PaAe	external parakoniocortex
PaAc/d	caudo-dorsal parakoniocortex
PAF	posterior auditory field (of cortex)

PET	positron emission tomography
PKD	polycystic kidney disease
PLZF	promyelocytic leukemia zinc finger protein
PSTH	post- (or peri-) stimulus time histogram
PTC	psychophysical tuning curve
PVCN	posteroventral cochlear nucleus
Q_{10} or $Q_{10\text{ dB}}$	centre frequency divided by the bandwidth at 10 dB above the best threshold
R	rostral field (of cortex)
<i>Rb</i>	retinoblastoma gene
RB	restiform body
RMS	root of the mean of the squared value
RNA	ribonucleic acid
ROS	reactive oxygen species
RT	rostromtemporal area (of cortex)
sec	seconds
S	Siemens: inverse of ohms
S1	fragment of myosin
SC	superior colliculus
SG	spiral ganglion
SK2	small conductance Ca^{2+} -activated K^+ channel type 2
SOC	superior olivary complex
SOD1	copper/zinc superoxide dismutase
SP	summating potential
SPL	sound pressure level
SPN	superior para-olivary nucleus
SSA	stimulus-specific adaptation
<i>T</i>	absolute temperature
T	temporal (area of cortex)
TB	trapezoid body
TMA	tetramethylammonium
Tpt	temperoparietal area
TriEA	triethylammonium
TRP	transient receptor potential
TRPA1	TRP type A1
TRPP	transient receptor potential polycystic
TRPV	transient receptor potential vanilloid
T-stellate	project via <i>trapezoid</i> body
UCOCB	uncrossed olivocochlear bundle
<i>USH1C</i>	Usher syndrome 1C gene
v	velocity
V	voltage
VL	ventrolateral division of the ventral MGB
VMPO	ventromedial peri-olivary nucleus
VNLL	ventral nucleus of the lateral lemniscus

VNTB	ventral nucleus of the trapezoid body
VP	ventral posterior field (of cortex)
W	watts
\approx	impedance

READING PLAN

Chapter 1, on the physics and analysis of sound, contains elementary information which should be read by everyone. Readers who need only a brief introduction to auditory physiology may then read only Chapter 3 on the cochlea, and summaries of the later chapters. Those whose interests lie in the psychophysical correlates may read Chapters 1–4, and then turn to Chapter 9 (with some specific references back to Chapters 6, 7 and 8). Readers who are interested in audiological and clinical aspects may read Chapters 1–3, part of Chapter 4 (up to and including Section 4.2.1), and then Chapter 10 (with some specific references back to Chapters 6 and 7). Chapter 5, which explores the more specialized aspects of cochlear physiology, is written at a more advanced level than earlier chapters, and if desired may be omitted without affecting the understanding of the other chapters. Chapters 6, 7 and 8 on the brainstem, cortex and centrifugal pathways should appeal primarily to specialist physiology students. However, many parts of Chapter 7 on the cortex, some parts of Chapter 8 on centrifugal pathways and Chapter 9 on psychophysical correlates contain information that should be of interest for cognitive neuroscience.

THE PHYSICS AND ANALYSIS OF SOUND

Some of the basic concepts of the physics and analysis of sound, which are necessary for understanding the later chapters, are presented here. The relations between the pressure, displacement and velocity of a medium produced by a sound wave are first described, followed by the decibel scale of sound level and the notion of impedance. Fourier analysis and the idea of linearity are then described.

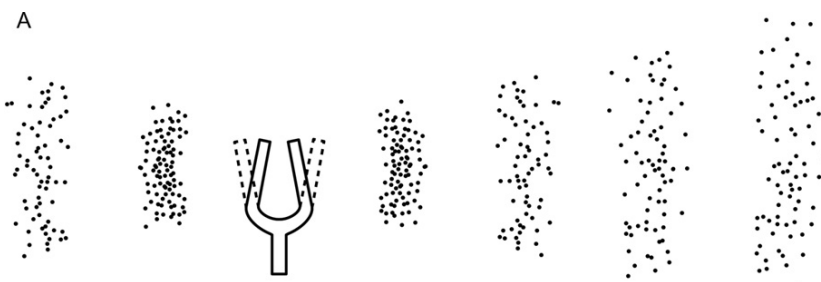
1.1 THE NATURE OF SOUND

In order to understand the physiology of hearing, a few facts about the physics of sound, and its analysis, are necessary. As an example, Fig. 1.1 shows a tuning fork sending out a sound wave and shows the distribution of the sound wave at one point in time, plotted over space, and at one point in space, plotted over time. The tuning fork sends out a travelling pressure wave, which is accompanied by a wave of displacement of the air molecules making them vibrate around their mean positions. There are two important variables in such a sound wave. One is its frequency, which is the number of waves to pass any one point in a second, measured in cycles per second or hertz (Hz). This has the subjective correlate of pitch, sounds of high frequency having high pitch. The other important attribute of the wave is its amplitude or intensity, which is related to the magnitude of the movements produced. This has the subjective correlate of loudness.

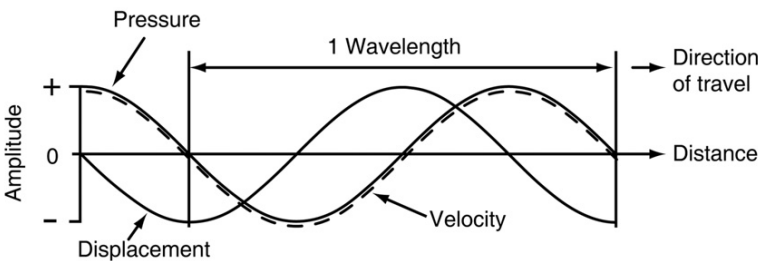
If the sound wave is in a free medium, the pressure and the velocity of the air vary exactly together and are said to be in phase. The displacement, however, lags by a quarter of a cycle. It is important to understand that the pressure variations are around the mean atmospheric pressure. The variations are in fact a very small proportion of the total atmospheric pressure – even a level as high as 140 dB sound pressure level (SPL) (defined in Section 1.2), as intense as anything likely to be encountered in everyday life, makes the pressure vary by only 0.6%. The displacement is also about the mean position, and the sound wave does not cause a net flow of molecules. The different parameters of the sound wave can easily be related to each other. The peak pressure (p) above atmospheric pressure and the peak velocity of the sinusoid (v) are related by the following equation:

$$p = zv \quad (1)$$

A



B



C

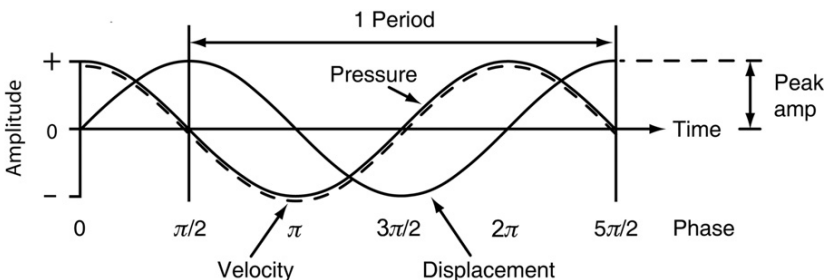


Fig. 1.1 (A) A tuning fork sending out a sound wave. (B) The variations of the pressure, velocity and displacement of the air molecules in a sinusoidal sound wave are seen at one moment in time. The variations are plotted as a function of distance. The pressure and the velocity vary together, and the displacement lags by a quarter of a cycle. (C) The same variations are plotted as a function of time, as measured at one point. Because times further in the past are plotted to the right of the figure, the curve of displacement is here plotted to the right not to the left of the pressure curve, as in part B. The phase increases by 2π (or 360°) in one cycle. The sound wave is defined by its peak amplitude and by its frequency.

where z is the constant of proportionality, called the impedance. It is a function of the medium in which the sound is travelling and will be dealt with later.

The intensity of the sound wave is the amount of power transmitted through a unit area of space. It is a function of the square of the peak pressure and, by

Eq. (1), also of the square of the peak velocity. In addition, it depends on the impedance; for a sine wave,

$$\text{Intensity } I = \frac{p^2}{2z} = \frac{zv^2}{2} \quad (2)$$

In other words, if the intensity of a sound wave is constant, the peak pressure and the peak velocity are constant. They are also independent of the frequency of the sound wave. It is for these reasons that the pressure and velocity will be of most use later.

Unlike the above parameters, the peak displacement of the air molecules does vary with frequency, even when the intensity is constant. For constant sound intensity, the peak displacement is inversely proportional to the frequency:

$$d = \left(\frac{1}{2\pi f} \right) \sqrt{\left(\frac{2I}{z} \right)} \quad (3)$$

where d is the peak displacement and f is the frequency. So for sounds of constant intensity, the displacement of the air particles gets smaller as the frequency increases. We can see correlates of this when we see a loudspeaker cone moving. At low frequencies the movement can be seen easily, but at high frequencies the movement is imperceptible, even though the intensities may be comparable.



1.2 THE DECIBEL SCALE

We can measure the intensity of a sound wave by specifying the peak excess pressure in normal physical quantities, for example newtons/metre², sometimes called pascals. In fact it is often more useful to record the RMS pressure, meaning the square Root of the Mean of the Squared pressure, because such a quantity is related to the energy (actually to the square root of the energy) in the sound wave over all shapes of waveform. For a sinusoidal waveform, the RMS pressure is $1/\sqrt{2}$ of the peak pressure. While it is perfectly possible to use a scale of RMS pressure in terms of newtons per square metre, for the purposes of physiology and psychophysics, it turns out to be much more convenient to use an intensity scale in which equal increments roughly correspond to equal increments in sensation, and in which the very large range of intensity used is represented by a rather narrower range of numbers. Such a scale is made by taking the ratio of the sound intensity to a certain reference intensity and then taking the logarithm of the ratio. If logarithms to the base 10 are taken, the units in the resulting scale, called bels, are rather large, so the scale is expressed in units 1/10th the size, called decibels, or dB.

$$\text{Number of dB} = 10 \log_{10} (\text{sound intensity}/\text{reference intensity})$$

Because the intensity varies with the square of the pressure, the scale in decibels is 10 times the logarithm of the square of the pressure ratio, or 20 times the logarithm of the pressure ratio:

$$\text{Number of dB} = 20 \log_{10} (\text{sound pressure}/\text{reference pressure})$$

It only now remains to choose a suitable reference pressure. In physiological experiments, the investigator commonly takes any reference found convenient, such as that, for instance, given by the maximum signal in the sound-stimulating system. However, one scale in general use has a reference close to the lowest sound pressure that can be commonly detected by human beings, namely $2 \times 10^{-5} \text{ N/m}^2$ RMS or $20 \mu\text{Pa}$ RMS. In air under standard conditions, this corresponds to a power of $10^{-12} \text{ Watts/m}^2$. Intensity levels referred to this are known as dB SPL.

$$\text{Intensity level in dB SPL} = 20 \log_{10} (\text{RMS sound pressure}/2 \times 10^{-5} \text{ N/m}^2)$$

We are then left with a scale with generally positive values, in which equal intervals have approximately equal physiological significance in all parts of the scale, and in which we rarely have to consider step sizes less than one unit. While we often have to use only positive values, negative values are perfectly possible. They represent sound pressures less than $2 \times 10^{-5} \text{ N/m}^2$, for which the pressure ratio is less than 1.

1.3 IMPEDANCE

Materials differ in their response to sound; in a tenuous, compressible medium such as air, a certain sound pressure will produce greater velocities of movement than in a dense, incompressible medium such as water. The relation between the sound pressure and the particle velocity is a property of the medium and is given in Eq. (1) by impedance $z = p/v$. For plane waves in an effectively infinite medium, the impedance is a characteristic of the medium alone. It is then called the specific impedance. In the SI system, z is measured in $(\text{N/m}^2)/(\text{m/sec})$, or Nsec/m^3 . If z is large, as for a dense, incompressible medium such as water, relatively high pressures are needed to achieve a certain velocity of the molecules. The pressure will be higher than is needed for a medium of low specific impedance, such as air.

The impedance will concern us when we consider the transmission of sounds from the air to the cochlea. Air has a much lower impedance than the cochlear fluids. Let us take, as an example, the transmission of sound from air into a large body of water, such as a lake. The specific impedance of air is about 400 Nsec/m^3 and that of water $1.5 \times 10^6 \text{ Nsec/m}^3$, which is 3750 times greater. In other words, when a sound wave meets a water surface at normal incidence, the pressure variation in the wave is large enough to displace the water at the boundary by only $1/3750$ of the displacement of the air near the boundary. However, continuity requires that the displacements of the molecules immediately on both sides of the

boundary must be equal. What happens is that much of the incident sound wave is reflected; the pressure at the boundary stays high, but because the reflected wave is travelling in the opposite direction to the incident wave it produces movement of the molecules in the opposite direction. The movements due to the incident and reflected waves therefore substantially cancel, and the net velocity of the air molecules will be small. This leaves a net ratio of pressure to velocity in the air near the boundary which is the same as that of water.

One result of the impedance jump is that much of the incident power is reflected. Where z_1 and z_2 are the specific impedances of the two media, the proportion of the incident power transmitted is $4z_1z_2/(z_1 + z_2)^2$. At the air–water interface this means that only about 0.1% of the incident power is transmitted, corresponding to an attenuation of 30 dB. In a later section we shall see how the middle ear converts a similar attenuation in the ear to the near-perfect transmission estimated as occurring at some frequencies.

While the most dramatic example of an impedance jump is seen with the transmission of sounds from the air to the cochlear fluids, there are in fact changes in impedance at all stages as the sound travels from the air to the cochlea, for example in the external ear canal, at the tympanic membrane and in the middle ear. All these stages have some degree of impedance mismatch with the adjacent stages and are therefore capable of reducing the efficiency of transmission and giving rise to reflections.

Finally, in analysing complex acoustic circuits, it is convenient to use analogies with electrical circuits, for which the analysis is well described. Impedance in an electrical circuit relates the voltage to the rate of movement of charge, and if we are to make an analogy, we need a measure of impedance that relates to the amount of medium moved per second. We can therefore define a different acoustic impedance, known as acoustic ohms, which is the pressure to move a unit volume of the medium per second. Acoustic ohms will not be used in this book and, where necessary, values will be converted from the literature, which is done by multiplying the number of acoustic ohms by the cross sectional area of the structure in question.



1.4 THE ANALYSIS OF SOUND

Figure 1.2A shows a small portion of the pressure waveform of a complex acoustic signal. There is a regularly repeating pattern with two peaks per cycle. The pattern can be approximated by adding together the two sinusoids shown, one at 150 Hz and the other at 300 Hz. The reverse of this process, the analysis of a complex signal into component sinusoids, is known as Fourier analysis and forms one of the conceptual cornerstones of auditory physiology. The result of a Fourier analysis (or transformation) is to produce the *spectrum* of the sound wave (Fig. 1.2C). The spectrum shows here that, in addition to the main components, there are also smaller components, at 1/15th of the amplitude or less, at 450 and 600 Hz. Such a spectrum tells us the amplitude of each frequency component, and so the energy in each frequency region.

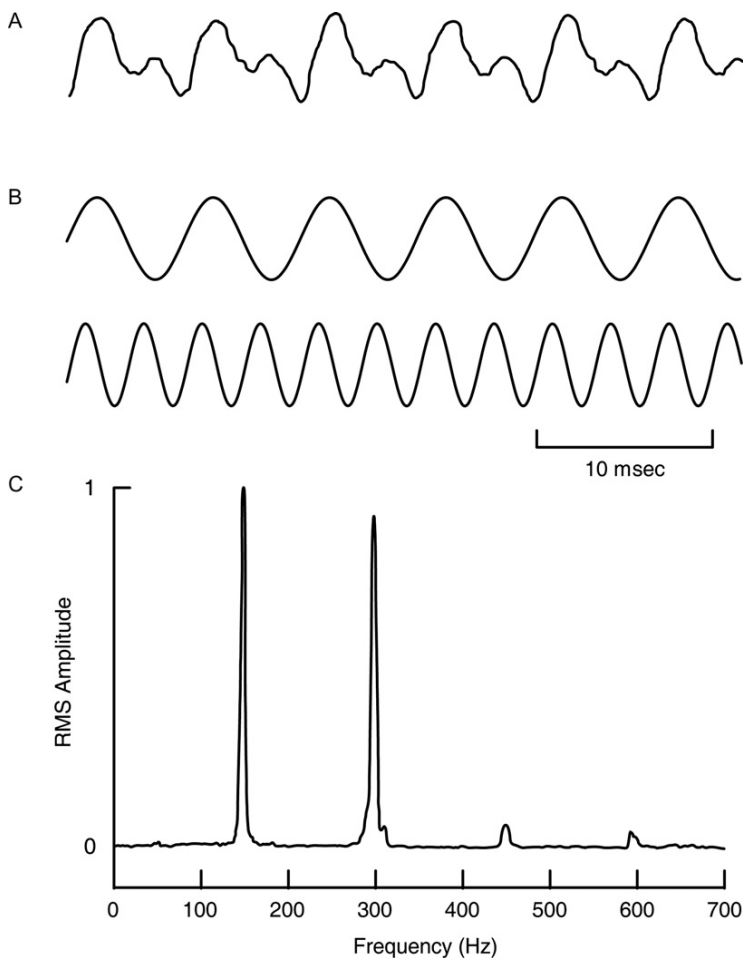


Fig. 1.2 (A) A portion of a complex acoustic waveform. (B) The waveform can be closely approximated by adding together two sine waves. (C) A Fourier analysis of the waveform in A shows that in addition to the main components, there are other smaller ones at higher frequencies. Components at still higher frequencies, responsible for the small high-frequency ripple on the waveform in A, lie outside the frequency range of the analysis and are not shown.

The principles of Fourier analysis can be illustrated most easily by the reverse process of Fourier synthesis, that is by taking many sinusoids and adding them together to make a complex wave. Figure 1.3 shows how it is possible to make a good approximation of a square wave by adding many sinusoids together. If this process were continued indefinitely, it would be possible to make a waveform indistinguishable from a square wave. Fourier analysis is simply the reverse of

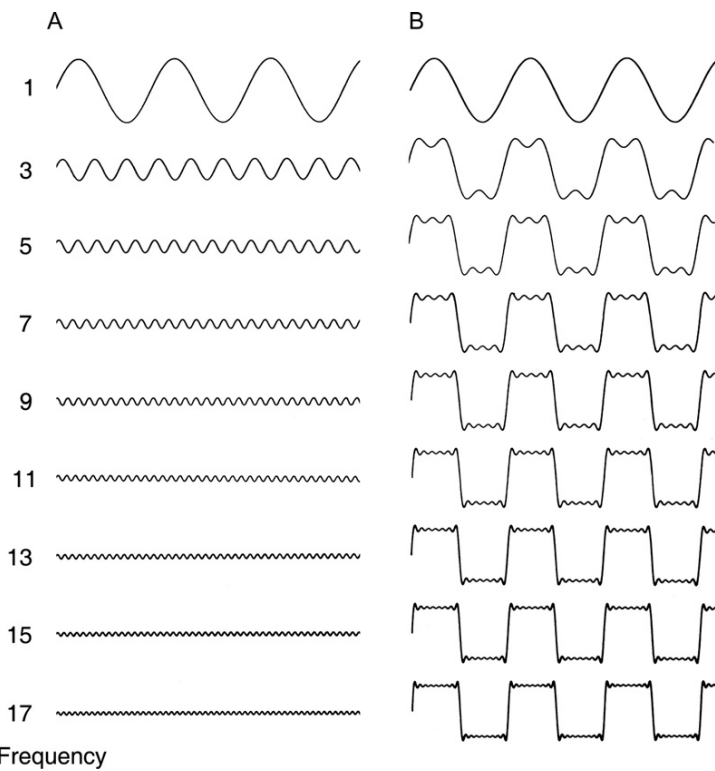


Fig. 1.3 A square wave can be approximated by adding together sinusoids of relative frequencies 1, 3, 5, 7, etc. The column in B shows the effect of successively adding the sinusoids in A.

this – finding the elementary sinusoids, which when added together, will give the required waveform.

Why do we analyse sound waves into sinusoids rather than into other elementary waveforms? One reason is that it is mathematically convenient to do so. Another reason is that sinusoids represent the oscillations of a very broad class of physical systems, so that examples are likely to be found in nature. However, the most compelling reason from our point of view is that the auditory system itself seems to perform a Fourier transform, like that of Fig. 1.2C, although with a more limited resolution. Therefore, sinusoids are simple not only physically, but also physiologically. This has a correlate in our own sensations, and a sinusoidal sound wave has a particularly pure timbre. In understanding the physiology of the lower stages of the auditory system, one of our concerns will be with the way in which the system analyses sound into sine waves, and how it handles the frequency and intensity information in them.

Figure 1.4 shows some common Fourier transforms. In the most elementary case, a simple sinusoid that lasts for an infinite time has a Fourier transform represented by a single line, corresponding to the frequency of the sinusoid (Fig. 1.4A). A wave such as a square wave, similarly lasting for an infinite time, has a spectrum consisting of a series of lines (Fig. 1.4B). But physical signals do not of course last for an infinite time, and the result of shortening the duration of the signal is to broaden each spectral line into a band (Fig. 1.4C). The width of each band turns out to be inversely proportional to the duration of the waveform, and the exact shape of each band is a function of the way the wave is turned on and off.

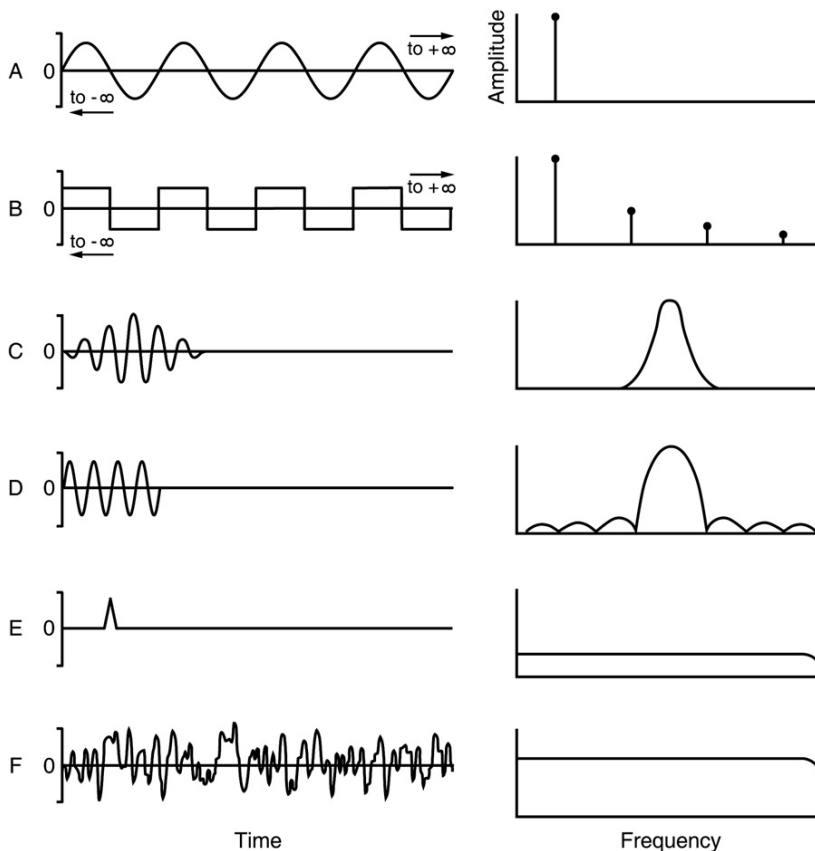


Fig. 1.4 Some waveforms (left) and their Fourier analyses (right). (A) Sine wave. (B) Square wave (in these cases the stimuli last for an infinite time and have line spectra, the components of which are harmonically related). (C) Ramped sine wave. (D) Gated sine wave. (E) Click. (F) White noise.

If, for instance, the waveform is turned on and off abruptly, sidelobes appear around each spectral band (Fig. 1.4D).

In the most extreme case, the wave can be turned on for an infinitesimal time, in which case we have a click. The spread of the spectrum will be in inverse proportion to the duration, and so, in the limit, will be infinite. The spectrum of a click therefore covers all frequencies equally. In practice, a click will of course last for a finite time, and this is associated with an upper frequency limit to the spectrum (Fig. 1.4E). Another quite different signal, namely white noise, also contains all frequencies equally (Fig. 1.4F). Although the spectrum determined over short periods shows considerable random variability, the spectrum determined over a long period is flat. It differs from a click in the relative phases of the frequency components, which for white noise are random.



1.5 LINEARITY

One concept that we shall meet many times is that of a linear system. In such a system, if the input is changed by a certain factor k , the output is also changed by the same factor k , but is otherwise unaltered. In addition, linear systems satisfy a second criterion, which is that the output to two or more inputs applied at the same time is the sum of the outputs that would have been obtained if the inputs had both been applied separately.

We can therefore identify a linear system as one in which the amplitude of the output varies in proportion to the amplitude of the input. A linear system also has other properties. For instance, the only Fourier frequency components in the output signal are those contained in the input signal. A linear system never generates new frequency components. Thus it is distinguished from a non-linear system. In a non-linear system, new frequency components are introduced. If a single sinusoid is presented, the new components will be harmonics of the input signal. If two sinusoids are presented, there will, in addition to the harmonics, be intermodulation products produced, that is Fourier components whose frequency depends on both of the input frequencies. In the auditory system, we shall be concerned with whether certain of the stages act as linear or non-linear systems. The tests used will be based on the properties described above.



1.6 SUMMARY

1. A sound wave produces compression and rarefaction of the air, the molecules of which vibrate around their mean positions. The extent of the pressure variation has a subjective correlate in loudness. The frequency, or number of waves passing a point in a second, has a subjective correlate in pitch. Frequency is measured in cycles per second, known as hertz (Hz).

2. The particle velocities produced by a pressure variation depend on the impedance of the medium. If the impedance is high, high pressures are needed to produce a certain velocity.
3. When a sound pressure wave meets a boundary between two media of different impedance, some of the sound energy is reflected.
4. Complex sounds can be analysed by Fourier analysis, that is by splitting the waveforms into component sine waves of different frequencies. The cochlea seems to do this too, to a certain extent.
5. In a linear system, the output to two inputs together is the sum of the outputs that would have been obtained if the two inputs had been presented separately. Moreover, in a linear system, the only Fourier frequency components that are present in the output are those that were present in the input. Neither is true for a non-linear system.

THE OUTER AND MIDDLE EARS

The outer ear modifies the sound wave in transferring the acoustic vibrations to the eardrum. Firstly, the resonances of the external ear increase the sound pressure at the eardrum, particularly in the range of frequencies (in human beings) of 2–7 kHz. They therefore increase the efficiency of sound transmission at these frequencies. Secondly, the change in pressure depends on the direction of the sound. This is an important cue for sound localization, enabling us to distinguish above from below and in front from behind. The middle ear apparatus then transfers the sound vibrations from the eardrum to the cochlea. It acts as an impedance transformer, coupling sound energy from the low-impedance air to the higher impedance cochlear fluids, substantially reducing the transmission loss that would otherwise be expected. The factors allowing this will be described, and the extent to which the middle ear apparatus acts as an ideal impedance transformer will be discussed. Transmission through the middle ear can be modified by the middle ear muscles; their action, and hypotheses for their possible role in hearing, will be described.



2.1 THE OUTER EAR

The outer ear consists of a partially cartilaginous flange called the pinna, which includes a resonant cavity called the concha, together with the ear canal or the external auditory meatus leading to the eardrum or the tympanic membrane (Fig. 2.1). The effect of the outer ear on the incoming sound has been analysed from two approaches. One is the influence of the resonances of the outer ear on the sound pressure at the tympanic membrane, the other is the extent to which the outer ear provides directionality cues for help in sound localization.

2.1.1 The pressure gain of the outer ear

The external ear collects sound waves over the large area of the pinna and concha and funnels them into the narrower canal of the meatus. Together with the resonances in the external ear, this increases the pressure at the tympanic membrane, which in turn increases the energy transfer to the middle ear (Fig. 2.2A). In human beings, the increase in pressure is a maximum of 15–20 dB in a broad

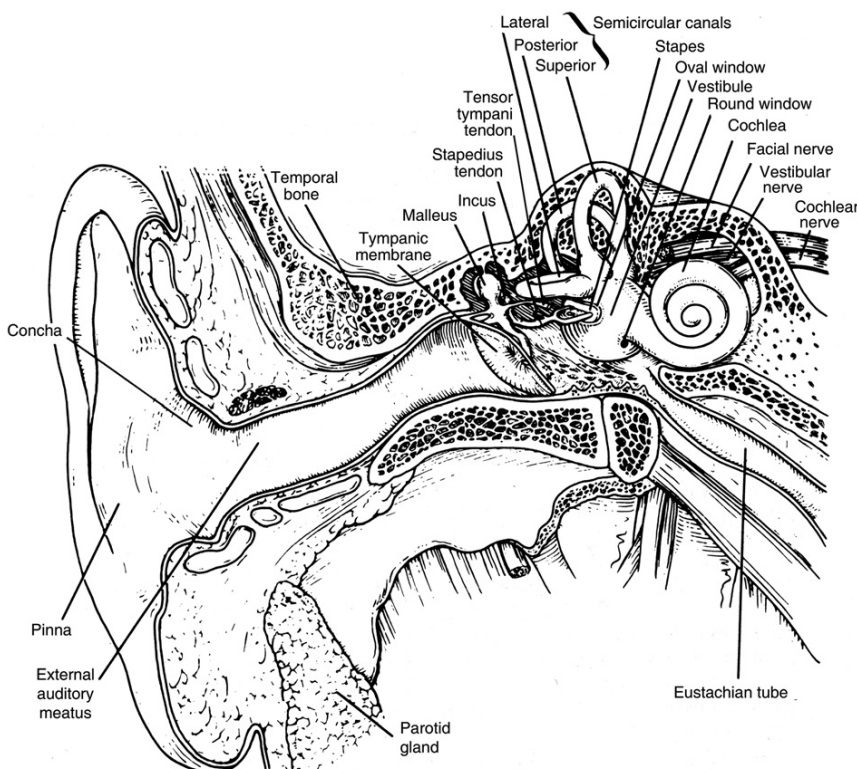


Fig. 2.1 The external, middle and inner ears in human beings. From Kessel and Kardon (1979).

peak around 2.5 kHz (Wiener and Ross, 1946). The contributions of the different elements of the external ear can be studied by adding the different components in a model. The results of such an analysis show that the 2.5-kHz peak is provided by a resonance of the combination of the meatus and concha. The 5.5-kHz peak is due to a resonance in the concha alone. Because the external ear forms a complex acoustic cavity, it can be expected that the changes in sound pressure will be highly frequency-dependent. However, it appears that the main resonances have complementary effects on the pressure gain, so that the increase is relatively uniform over the range from 2 to 7 kHz.

Transmission through the external ear is heavily affected by the major resonance of the ear canal and concha, which in human beings is found at 2.5 kHz. This occurs at a frequency when the canal plus concha is a quarter of a wavelength long. This is the dominant resonance of a tube that is open (i.e. low impedance) at one end and closed (i.e. high impedance) at the other, because then the excursions of the molecules can be high at the open end and low at the

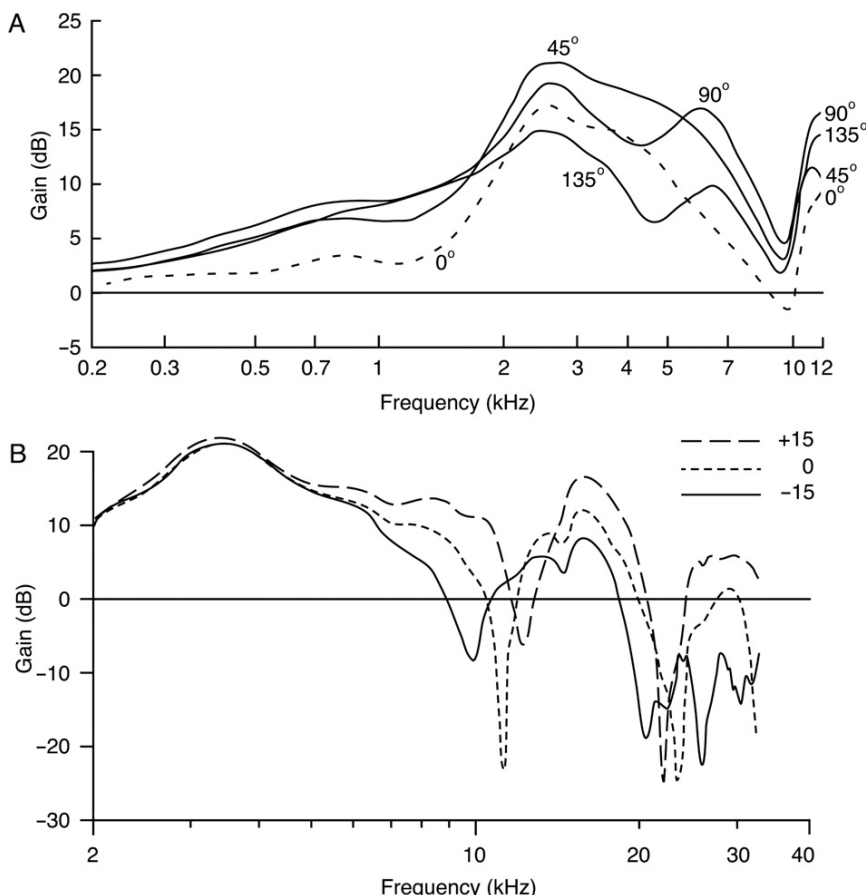


Fig. 2.2 (A) The average pressure gain of the human external ear. The gain in pressure at the eardrum over that in the free field is plotted as a function of frequency, for different orientations of the sound source in the horizontal plane ipsilateral to the ahead. Zero degrees is straight ahead. From Shaw (1974), Fig. 5, with kind permission of Springer Science and Business Media. (B) The change in gain of the outer ear as the elevation of a sound source is altered from -15° to $+15^\circ$ in the cat. Zero degrees is horizontal. The dips around 10 and 20 kHz change in frequency with elevation. From Rice *et al.* (1992), Fig. 5A.

closed end. The pressure also varies, being higher at the closed end. Around the resonant frequency, the increase in pressure at the tympanic membrane substantially enhances the efficiency of power transfer to the middle ear, up to nearly 100% in some species. However, the peak efficiency is rather lower in human beings, and in all species the efficiency is much lower at low frequencies (Fig. 2.3; Rosowski, 1991).

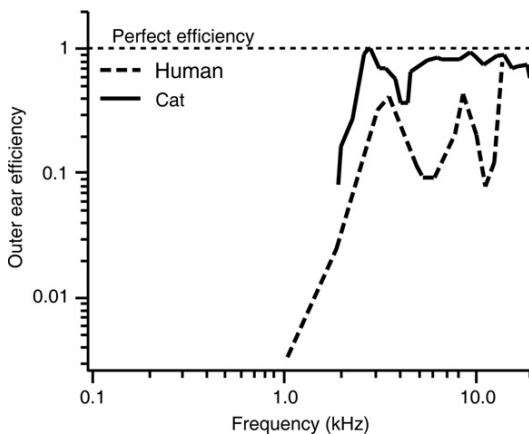


Fig. 2.3 The efficiency of power transfer from the external sound field to the middle ear in two species, according to Rosowski (1991). The efficiency was calculated from the relative impedances of the air in the ear canal and of the tympanic membrane with middle and inner ears attached, using the formula: fraction of power transmitted = $4z_1z_2/(z_1 + z_2)^2$. Reprinted from Rosowski (1991), Fig. 6, Copyright (1991), with permission from American Institute of Physics.

2.1.2 The outer ear as an aid to sound localization

The most important cues for sound localization in human beings are the intensity and timing differences in the sound waves at the two ears. The sound wave from a source on the right will strike the right ear before the left and will be more intense in the right ear. However, this does not account for our ability to distinguish in front from behind, or above from below. The information for such localization comes from the pinna and concha, with the raised ridges of the pinna and concha reflecting sound waves into the ear canal, in a way that depends on the direction and elevation of the sound source.

The human pinna has a raised rim around its rear edge, with the concha giving another rim within that. Waves reflected from the rim and concha will travel further than those entering the meatus directly. If the direct and reflected waves arrive out of phase (i.e. the peak of pressure in one wave arrives at the same time as the trough of pressure in the other wave), there will be partial cancellation or interference, reducing the intensity of the stimulus to the ear. This produces the drop in gain seen around 10 kHz in Fig. 2.2A. Moreover, because the external ear is smaller below the meatus and larger above, sounds reflected from the lower rims (arriving from sound sources above the horizontal) will tend to arrive at the ear canal with smaller delays than those reflected from the upper rims. Therefore as a sound source is raised in space, the trough in the response (e.g. as shown for the cat around 10 kHz in Fig. 2.2B) will tend to move towards higher frequencies. There are further effects; when a sound is moved behind the ear, waves are scattered off the edge of the pinna, interfering with the direct wave and reducing the response

in the 3–6 kHz region (Shaw, 1974). It is in this region that there are the greatest intensity changes as a sound source is moved in the horizontal plane (see Fig. 2.2A). Because of the complex shape of the pinna, multiple reflections contribute to the final colouration of the sound, with the colouration being affected by both the azimuth (direction in the horizontal plane) and the elevation of the source (Rice *et al.*, 1992; Pralong and Carlile, 1994).

When the wavelength is short compared with the dimensions of the pinna, the pinna can show a high degree of directional selectivity in the reception of sound. We expect the pinna to be useful in this way only in the high kilohertz range of frequencies. In the cat, the pinna can produce a gain of up to 21 dB in sound pressure at high frequencies, for sound sources directly in line with the axis of the pinna (Musican *et al.*, 1990). In human beings, there is a broad directional selectivity of the pinna at high frequencies. Above 6 kHz, areas of maximum sensitivity have been measured with a gain of 10–15 dB above the straight-ahead positions, in a frequency-dependent way and over a broad angle some 70° wide (Middlebrooks *et al.*, 1989).

The external ear therefore produces a directionally varying spectral modulation of the incoming sound. In using such a colouration to make directional judgements, we are obviously required to make subtle judgements about the modulation of the spectra of perhaps unknown sound sources (see Middlebrooks and Green, 1991; Moore, 2002, for reviews).



2.2 THE MIDDLE EAR

2.2.1 Introduction

The middle ear couples sound energy from the external auditory meatus to the cochlea, and by its transformer action helps to match the impedance of the auditory meatus to the much higher impedance of the cochlear fluids. In the absence of a transformer mechanism, much of the sound would be reflected. The sound is transmitted from the tympanic membrane to the cochlea by three small bones, known as the ossicles. They are called the malleus, the incus and the stapes (Figs. 2.1 and 2.4). The first two bones are joined comparatively rigidly so that when the tip of the malleus is pushed by the tympanic membrane, the bones rotate together and transfer the force to the stapes. The stapes is attached to a flexible window in the wall of the cochlea, known as the oval window (see Fig. 2.4). The relatively massive heads of the malleus and incus ensure that the centre of inertia of the ossicles is near their centre of rotation, so reducing transfer of bone vibration from the skull.

A second function of the ossicles is to apply force to one window only of the cochlea. If the ossicles were missing, and the pressure of the incoming sound wave was applied equally to both windows, there would be a reduced flow of cochlear fluids. Nevertheless, in many species the other window of the cochlea, the round window, is shielded from the incoming sound wave by a bony ridge. In these cases, if the ossicles are missing, the sound pressure is still primarily applied to one

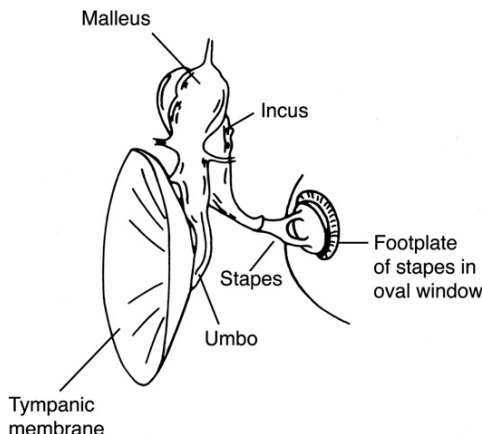


Fig. 2.4 The three ossicles, called the malleus, the incus and the stapes, transmit the sound vibrations from the tympanic membrane (eardrum) to the oval window of the cochlea. The extension of the malleus over the tympanic membrane is called the umbo.

window of the cochlea, and some hearing, although without the benefit of the impedance matching, is still possible.

2.2.2 The middle ear as an impedance transformer

2.2.2.1 The nature of the problem

The middle ear transfers the incoming vibration from the comparatively large, low-impedance tympanic membrane to the much smaller, higher-impedance oval window. As was explained in Chapter 1 (Section 1.3), when a sound wave meets a higher-impedance medium, normally much of the sound energy is reflected. The middle ear apparatus, by acting as an acoustic impedance transformer, reduces this attenuation substantially.

Following the tentative suggestion made by [Wever and Lawrence \(1954\)](#), many authors have said that the cochlear fluids would have an impedance approximately equal to that of sea water, namely $1.5 \times 10^6 \text{ Nsec/m}^3$, and this led to the calculation, detailed in Section 1.3, that if the sound met the oval window directly, only 0.1% of the incident energy would be transmitted. As pointed out by others, and indeed by Wever and Lawrence themselves, while the numerical result may be approximately correct, the physical reasoning behind it is not. Specific impedances are defined for progressive acoustic waves in an effectively infinite medium. In the range of audible frequencies, the cochlea is far smaller than a wavelength of sound in water, and so cannot develop such waves. The actual cochlear impedance is determined entirely by the fact that cochlear fluid flows from one flexible window, the oval window, to another, the round window, with the value of the impedance depending on the way the fluids flow, and on their interaction with the distensible cochlear membranes.

The input impedance of the cochlea has been determined either theoretically (e.g. Zwislocki, 1965; Puria and Allen, 1991) or experimentally (e.g. Lynch *et al.*, 1982 in cats; Aibara *et al.*, 2001 and Nakajima *et al.*, 2009 in human beings). The measurements of Nakajima *et al.* (2009) in human temporal bones suggest a cochlear impedance of about 9×10^4 N sec/m³ at 1 kHz,¹ much lower than that expected from Wever and Lawrence's approximation.

2.2.2.2 The mechanism of the impedance transformer

In matching the impedance of the tympanic membrane to the much higher impedance of the cochlea, the middle ear uses two principles.

1. The area of the tympanic membrane is larger than that of the stapes footplate in the cochlea. The forces collected over the tympanic membrane are therefore concentrated on a smaller area, so increasing the pressure at the oval window. The pressure is increased by the ratio of the two areas (Fig. 2.5A). This is the most important factor in achieving the impedance transformation.
2. The second principle is the lever action of the middle ear bones. The arm of the incus is shorter than that of the malleus, and this produces a lever action that increases the force and decreases the velocity at the stapes (Fig. 2.5B). This is a comparatively small factor in the impedance match.

2.2.2.3 Calculation of the transformer ratio

It might be thought that determining the transformer ratio would be a matter of comparatively simple anatomy and would have been settled in an uncontroversial

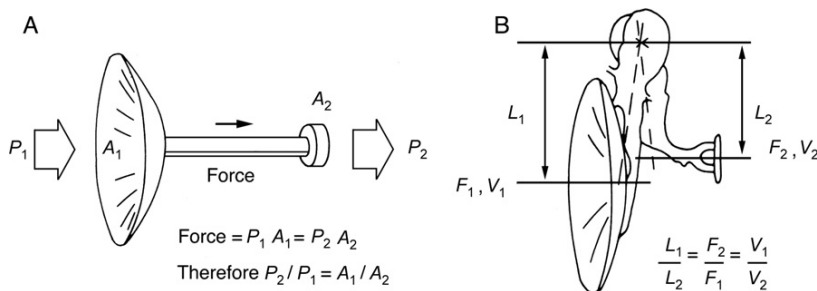


Fig. 2.5 The two mechanisms of the middle ear acoustic impedance transformer. (A) The main factor is the ratio of the areas of the tympanic membrane and the oval window. The middle ear bones are here represented by a piston. (B) The lever action increases the force and decreases the velocity. *A*, area; *F*, force; *L*, length; *P*, pressure; *V*, velocity.

¹This is derived from Nakajima *et al.* (2009)'s measurement of 2.86×10^{10} MKS acoustic ohms, and multiplying by the human stapes footplate area of 3.2 mm^2 (i.e. $3.2 \times 10^{-6} \text{ m}^2$) to get a specific impedance.

way a long time ago. This is not so; the actual transformer ratio depends on the exact way the structures vibrate in response to sound. As the movements are microscopic or submicroscopic, and probably depend on the physiological state of the organism, the determination of the transformer ratio is a rather complex measurement. The values that will be used here are those applicable for human beings and are as given by Kringlebotn (1988) and Gyo *et al.* (1987) (see also Rosowski, 1994).

The most important factor is the ratio of the areas of the tympanic membrane and the oval window. In human beings, the tympanic membrane has an area of 60 mm^2 , and the stapes footplate about 3.2 mm^2 . The pressure on the stapes footplate is therefore increased by $60/3.2 = 18.75$ times.

The geometrical length of the malleus is about 2.1 times that of the incus (Gyo *et al.*, 1987), and so the lever action multiplies the force 2.1 times. However, the velocity is decreased 2.1 times. The lever action therefore increases the impedance ratio (being the pressure/velocity ratio) $2.1^2 = 4.4$ times.

The final transformer ratio, calculated here as a ratio of specific impedances, can be obtained by multiplying these two factors together. The transformer ratio determined in this way is assessed as $18.75 \times 4.4 = 82.5$.²

Does this theoretical transformation ratio give the ideal transformation required to match the cochlea to the air? In order to answer this we need to know the input impedance of the cochlea, a measurement that has been subject to some variability. In human cadavers, Nakajima *et al.* (2009) sealed a tube around the tympanic membrane to apply sound waves to the middle ear and sealed a transducer into the scala vestibuli of the cochlea to measure intracochlear pressures. The velocity of movement of the stapes was measured with a laser. The ratio of intracochlear pressure to velocity of the stapes was used to obtain the cochlear input impedance.

Nakajima *et al.* (2009) found the impedance of the cochlea at 1 kHz to be $9 \times 10^4 \text{ N sec/m}^3$ (here expressed as a specific impedance). The impedance transformer of the middle ear will make this appear to be $9 \times 10^4 / 82.5 = 1090 \text{ N sec/m}^3$ at the tympanic membrane. This is significantly higher than the specific impedance of air, which is 430 N sec/m^3 . The middle ear transformer ratio is not therefore quite adequate for perfect transmission.

The theoretical value of 1090 N sec/m^3 , calculated from the input impedance of the cochlea and the transformer ratio, can be compared to direct measurements of the input impedance of the middle ear as seen at the tympanic membrane. Rabinowitz (1981) sealed a microphone and a small sound source into the human ear canal and measured the sound pressures in the canal resulting from known stimuli. He obtained an impedance for the tympanic membrane of 2500 N sec/m^3 (recalculated here as a specific impedance) at 1 kHz. This is considerably higher than the theoretical value calculated above. The difference can be accounted for by frictional and other losses in the middle ear.

²The reader may be puzzled to see very different numbers in the literature. This may be for two reasons. Firstly, the impedances will probably be defined in acoustic ohms (see Section 1.3). Secondly, the transformer ratio is often quoted as the square root of the impedance ratio in acoustic ohms. Such a ratio is also equal to the pressure transformation ratio. The latter is calculated in Section 2.2.2.4.

Derivations of the middle ear transformer ratio have been a matter of disagreement over the years. For instance, Békésy (1960) showed that the eardrum in man was hinged on one side, so that it flapped like a door rather than moving in and out like a piston. Obviously, a point near the hinge will contribute less to the total force transmitted than a point near the free edge, and this has led to the use of an ‘effective area’ for the tympanic membrane that is less than the real area. Similarly, the way the tympanic membrane moves will affect the effective lever ratio of the middle ear bones. In addition, the lever ratio will depend on the actual position of the centre of rotation of the middle ear bones, which varies with stimulus conditions and has been investigated both experimentally and theoretically (e.g. Homma *et al.*, 2009).

The transformer ratio was calculated only for human beings and applied in one frequency range, around 1 kHz. It seems that at other frequencies, additional factors affect the movement. For instance, above 2 kHz the motion of the tympanic membrane breaks up into separate zones, and as the frequency is raised further, the effective area of the tympanic membrane becomes progressively reduced, until it becomes equal to the area of the arm of the malleus. This will reduce transmission (Khanna and Tonndorf, 1972; Koike *et al.*, 2002). Gyo *et al.* (1987) showed that the effective lever ratio of the middle ear bones changes with frequency, becoming largest around 2 kHz, and modelling suggested that this was due to a change in the centre and direction of rotation of the bones at higher frequencies (Koike *et al.*, 2002; Homma *et al.*, 2009). Transmission through the middle ear is also affected by factors such as elasticity and friction in the bones and their ligaments, particularly at low frequencies. The inertia of the middle ear bones and their imperfect coupling, in addition to acoustic resonances in the middle ear cavity, will also affect transmission. If we wish to determine the way in which the middle ear affects the transmission of sound over a range of frequencies, it is therefore necessary to measure the transmission experimentally. This can be done by measuring the transfer function, that is the ratio of the output to the input, as a function of frequency.

2.2.2.4 The transfer function of the middle ear

The middle ear transforms the sound pressure variations of the ear canal into a sound pressure variation in the scala vestibuli of the cochlea. The transfer function can be shown by plotting the ratio of the two pressures at different stimulus frequencies.

Nedzelnitsky (1980) measured the pressure in the cochlear duct of the cat, just behind the oval window, for constant sound pressures at the tympanic membrane. Similar results have since been obtained for the cat by Voss and Shera (2004). Nakajima *et al.* (2009) performed corresponding measurements in human cadaver temporal bones (see also Aibara *et al.*, 2001 and O’Connor and Puria, 2006). Figure 2.6 shows the pressure gains for both cats and human beings as a function of frequency. The curves have a bandpass characteristic, greatest transmission being seen around 1 kHz. There, the sound pressures are 29 and 20 dB greater than those at the tympanic membrane in the two species. The responses show notches around 4–7 kHz, but otherwise decline gradually towards low and high frequencies.

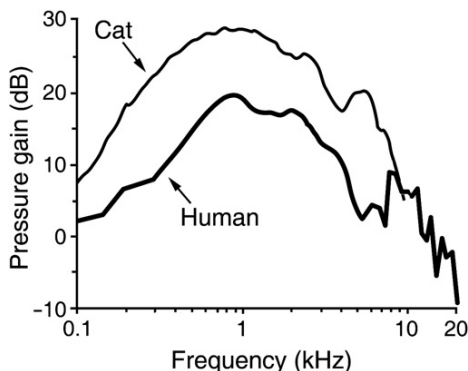


Fig. 2.6 The transfer function of the middle ear. Results from Nakajima *et al.* (2009) are shown for the human being and from Nedzelnitsky (1980) for the cat. The gain of pressure in the cochlea (the scala vestibuli, basal turn) over that at the tympanic membrane is shown as a function of frequency. Reprinted from Nakajima *et al.* (2009), Fig. 4A and from Nedzelnitsky (1980), Fig. 7, Copyright (1980), with permission from American Institute of Physics.

We can attempt to identify some of the factors governing this bandpass characteristic. One factor that attenuates the response at low frequencies is an elastic stiffness. This has been ascribed to an elasticity in the tympanic membrane and in the ligaments of the middle ear bones and to a compression and expansion of the air in the middle ear cavity. For instance, as the tympanic membrane moves in and out, air in the middle ear cavity is compressed and expanded, reducing the movement of the tympanic membrane. The importance of this factor can be shown experimentally, because when the middle ear cavity is vented to the atmosphere, transmission is increased at low frequencies but not at high frequencies (Guinan and Peake, 1967). But why should elastic stiffness be particularly important at low frequencies? This follows simply from the mathematical relation between the pressure of the sound wave and the displacement of the air, and so of the tympanic membrane. Recall from Eq. (3) (Section 1.1) that for a constant sound pressure level, the displacement of the air varies inversely with the frequency. At low frequencies, a constant sound pressure will produce a comparatively large displacement of the tympanic membrane and middle ear structures. The forces to overcome an elasticity depend on displacement, and so the forces will increase as the frequency drops. This explains why transmission is reduced at low frequencies.

The drop at high frequencies is affected by many factors, and their relative importance is not known. For instance, Khanna and Tonndorf (1972) and Koike *et al.* (2002) showed that at high frequencies the vibration pattern of the tympanic membrane broke up into separate zones, reducing the effectiveness of the transmission. We would also expect the mass of the middle ear bones to have a significant effect at high frequencies for the following reason: a constant sound pressure level corresponds to a constant velocity. Therefore, accelerations, and so the forces on the structures involved, increase in proportion to frequency. Further,

the ossicular chain begins to flex at high frequencies, also reducing the transmission, while the motion of the stapes changes from piston-like to include more complex modes of movement (see, e.g. Slama *et al.*, 2010).

The position is in addition complicated by acoustic resonances in the middle ear cavity, in the case of the cat responsible for the peak and dip in the transfer function near 4 kHz. The middle ear cavities of many small animals are enlarged by a bony bulge, called the bulla, extending below the skull (incidentally, this probably serves to increase the low-frequency response of the middle ear, because it will reduce the low-frequency stiffness of the system). In many animals the bulla is divided into two by a bony wall called the septum. The septum has a small hole, and the two cavities with a small intercommunicating hole form coupled acoustic resonators.

In the mid-frequency range, around 1 kHz, many of the factors affecting transmission at lower and higher frequencies will be small. Møller (1965) showed that in this frequency region it was the input impedance of the cochlea itself that was the main factor governing transmission. He disconnected the cochlea by disarticulating the joint between the incus and the stapes, and showed that the input impedance at the tympanic membrane fell substantially. It is in this frequency region that the theoretical calculation of the transformer ratio, described above, will be most nearly accurate; the transfer here will be least affected by factors other than the input impedance of the cochlea. Therefore, we can see here whether the actual pressure gain observed by Nakajima *et al.* (2009) agrees with the value expected from the transformer ratio, as calculated from the displacements of the middle ear structures. The measurements described above would lead us to expect the area ratio to increase the pressure by 18.75 times, and the lever ratio to increase it by 2.1 times. The product is 39.3 times, or 31.9 dB. This is significantly greater than the 20 dB increase in pressure observed by Nakajima *et al.* (2009). The difference is likely to be a result of transmission losses, in particular due to friction in the middle ear.

Power can be calculated from the relations between pressure, velocity and impedance described in Section 1.1. Therefore the efficiency of the middle ear, namely the ratio of (power delivered to cochlea)/(power received by tympanic membrane) can be calculated from the impedance of the cochlea, the velocity of the movement of the stapes and the pressures and velocities of the movements of the tympanic membrane. The middle ear efficiencies for cats and human beings are shown in Fig. 2.7. The efficiency peaks at around 1 kHz, where the factors described above are likely to be smallest. However, even here, the maximum efficiency is only 35%. The plot in Fig. 2.7 was made using older and probably less reliable data for human beings; the more recent data shown in Fig. 2.6 suggest that transmission in human beings is likely to be more efficient at high frequencies than previously thought. However, even so, the middle ear of cats may be more efficient than that of human beings at high frequencies. Therefore it appears that in the cat, the peripheral auditory system is more closely matched to the input impedance of the cochlea in this frequency range.

Consideration of transmission through the middle ear is not complete without a description of the linearity of the response (see Section 1.5). Guinan and

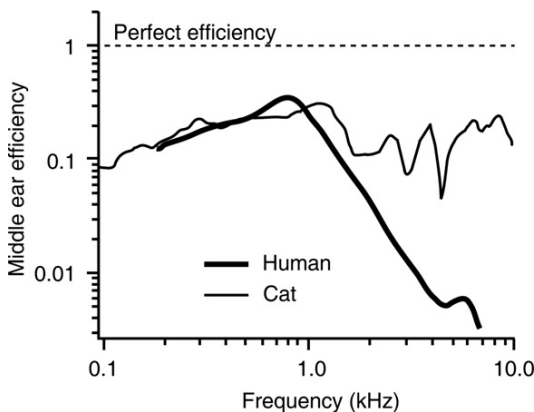


Fig. 2.7 The efficiency of the middle ear, calculated from the ratio of (power delivered to the cochlea)/(power received by the tympanic membrane), in cats and human beings. The data used for this plot are likely to give an underestimate of the efficiency of high-frequency transfer in human beings. Reprinted from Rosowski (1991), Fig. 7, Copyright (1991), with permission from American Institute of Physics.

Peake (1967) found in the cat that the stapes movement increased in proportion to the input up to 130 dB SPL for stimulus frequencies below 2 kHz, and up to 140–150 dB SPL for frequencies above. This suggests that the movements are substantially linear up to these intensities. Aerts and Dirckx (2010) used a more sensitive technique in the gerbil, looking for the distortion products generated when the ear was stimulated with multiple tones simultaneously. They showed that distortion products were approximately 60 dB below the stimulus tones, when the tones were presented at 96 dB SPL, and 40 dB below the stimulus tones, when the tones were presented at 120 dB SPL. In view of these measurements, it appears that the middle ear is substantially linear with acoustic stimuli in the usual range of physiological and psychophysical measurements. In spite of the linear response to acoustic stimuli, static pressures applied to the ear may be enough to affect transmission, possibly by stiffening the joint between the malleus and the incus, and by stretching the annular ligament that holds the stapes in the oval window.

2.2.3 The middle ear muscles

Transmission through the middle ear can be controlled by means of the middle ear muscles. They are two small striated muscles attached to the ossicles. The tensor tympani is attached to the malleus near the tympanic membrane and is innervated by the trigeminal (fifth) cranial nerve. The other muscle, the stapedius muscle, is attached to the stapes and is innervated by the facial (seventh) cranial nerve. The function and anatomy have been reviewed by Mukerji *et al.* (2010).

Contraction of the muscles increases the stiffness of the ossicular chain. As was explained in Section 2.2.2.4, below 1–2 kHz, transmission through the middle ear is stiffness-controlled. The stiffness arises from the elasticity of the tympanic membrane and the ligaments of the ossicles, as well as from the compression and expansion of air in the middle ear cavity. The stiffness reduces the transmission of sounds of low frequency. When it is augmented by a stiffening of the ossicular chain, the low-frequency response is attenuated still further. On the other hand, at high frequencies, above 1–2 kHz, where transmission is not stiffness-controlled, the response is much less affected by the middle ear muscles. Although this seems to be the main mechanism of middle ear muscle action, the real position is more complicated, because there are still some effects in the high-frequency range. In addition, in the cat, the position of the notch in the transfer function around 4 kHz, arising from resonances in the bulla, is changed as well.

Contraction of the middle ear muscles occurs as a reflex in response to loud sound (more than 75 dB above the absolute threshold), and can be elicited by vocalization, tactile stimulation of the head, swallowing or by general bodily movement (Carmel and Starr, 1963; Stach *et al.*, 1984). In some subjects, the middle ear muscles can be contracted voluntarily without any other discernible movement.

Several functions have been suggested for the middle ear muscles that are as follows:

1. The contraction to loud sound suggests that the reflex might be of use in protecting the inner ear from noise damage. While the reflex is too slow to protect the ear against impulsive noises, if the damaging stimulus is preceded by one that is less intense, but still intense enough to activate the reflex, the reflex is able to give some protection (Counter and Borg, 1993).
2. Middle ear muscles may be able to keep intense low-frequency stimuli near a lower part of the intensity range. Wever and Vernon (1955) showed that the reflex kept the intensity of the input to the cochlea relatively constant when the intensity of the stimulus was varied. This near-perfect automatic gain control functioned for a range of 20 dB above the reflex threshold, and applied only to low-frequency stimuli.
3. The middle ear muscles may also have a beneficial effect on the frequency response of the middle ear. As mentioned above, the transmission characteristic shows a sharp dip near 4 kHz, due to resonances in the bulla. Simmons (1964) showed that the middle ear muscles could shift the frequency of the dip slightly. In cats that were awake and had intact middle ear muscles, the dip was not apparent, suggesting that the continually fluctuating tone in the muscles had averaged it out.
4. At high intensities, low-frequency stimuli can mask higher-frequency stimuli over a wide range of frequencies. Pang and Guinan (1997a), by electrically activating the stapedius muscle in anaesthetized cats, showed that the stapedius could reduce the masking of a high-frequency tone by low-frequency noise band by more than 40 dB. Selective attenuation of low frequencies by the

middle ear muscles can therefore be expected to affect the perception of complex stimuli with low-frequency components, such as speech, at high stimulus intensities.



2.3 SUMMARY

1. The outer ear has two roles in transmitting sound to the tympanic membrane or the eardrum. It aids sound localization by altering the spectrum of the sound, in a way that depends on the direction of the source. It also, by resonances, increases the sound pressure at the tympanic membrane.
2. The middle ear apparatus couples sound energy from the tympanic membrane to the oval window of the cochlea. The sound is transmitted by three small bones, the ossicles, called the malleus, the incus and the stapes. The middle ear acts as an acoustic impedance transformer, coupling energy from low-impedance air to the higher-impedance cochlear fluids, thus reducing the reflection of sound energy that would otherwise occur.
3. The middle ear transformer uses two principles. The area of the oval window is smaller than that of the tympanic membrane, increasing the pressure. The lever action of the ossicles increases the force and decreases the velocity.
4. Transmission through the middle ear depends on the frequency of the stimulus. Greatest transmission is produced in the range around 1–2 kHz. Below this frequency, transmission is reduced by the stiffness of the middle ear structures and by compression and expansion of air in the middle ear cavity. Above this frequency, many factors, including the mass of the ossicles and less efficient modes of vibration of the structures, reduce transmission. There are also dips in the response arising from acoustic resonances in the middle ear cavity.
5. Transmission through the middle ear is affected by the middle ear muscles that reduce the transmission of low-frequency sounds. They may serve to protect the ear to some extent from noise damage, reduce the masking effects of low-frequency stimuli on higher-frequency stimuli, act as an automatic gain control for low-frequency stimuli over a narrow range of intensities, and reduce the perturbing effects of middle ear resonances.



2.4 FURTHER READING

The outer and middle ears have been extensively and clearly discussed by Rosowski (1994), who also includes a great deal of comparative information on mammals. Some physiological data on clinical aspects of middle ear physiology are given by Pickles (2007a). Blauert (1997) has an extensive discussion of the sound transformations produced by the outer ear, from a psychophysical perspective. The middle ear muscle reflex has been reviewed by Mukerji *et al.* (2010).

THE COCHLEA

The chapter on the cochlea is a key one and forms the foundation for much of the rest of this book. The anatomy of the cochlea will be described first. This is followed by a description of cochlear mechanics, starting with Békésy's pioneering observations, followed by the more recent measurements. A non-mathematical description of some of the theories of cochlear mechanics is given. The electrophysiology of the cochlea will then be discussed, starting with the standing potentials and hair cell transduction, followed by hair cell responses, their relation to grossly recordable potentials, and nerve excitation. Many of the ideas discussed in this chapter, such as the basis for sharp mechanical tuning in the cochlea, are still a matter of investigation and will be discussed in more depth in Chapter 5.



3.1 ANATOMY

3.1.1 General anatomy

Figure 2.1 (Section 2.1) shows the position of the human cochlea in relation to the other structures of the ear. It is embedded deep in the temporal bone. Overall, the cochlea stands about 1 cm wide and 5 mm from base to apex in human beings, and contains a coiled basilar membrane about 35 mm long. Figure 3.1A shows the turns of the cochlea in more detail, and in particular the longitudinal division into three scalae. The scalae spiral together along the length of the cochlea, keeping their corresponding spatial relations throughout the turns. The osseous spiral lamina divides the scala vestibuli from the scala tympani on the side near the modiolus (see Fig. 3.1B). The scala media is separated from the scala vestibuli above by Reissner's membrane, and from the scala tympani below by the basilar membrane. The two outer scalae, the scala vestibuli and the scala tympani, are joined at the apex of the cochlea by an opening known as the helicotrema (see Fig. 3.1A and C). The scala vestibuli and scala tympani contain perilymph, a fluid which is similar to extracellular fluid in its ionic composition. The scala media forms an inner compartment, which does not communicate directly with the other two. It contains endolymph, which is similar to intracellular fluid in that it has a high K^+ concentration and a low Na^+ concentration. Endolymph is at a high positive potential (e.g. + 80 mV), whereas the other scalae are at or near the potential of the surrounding bone.

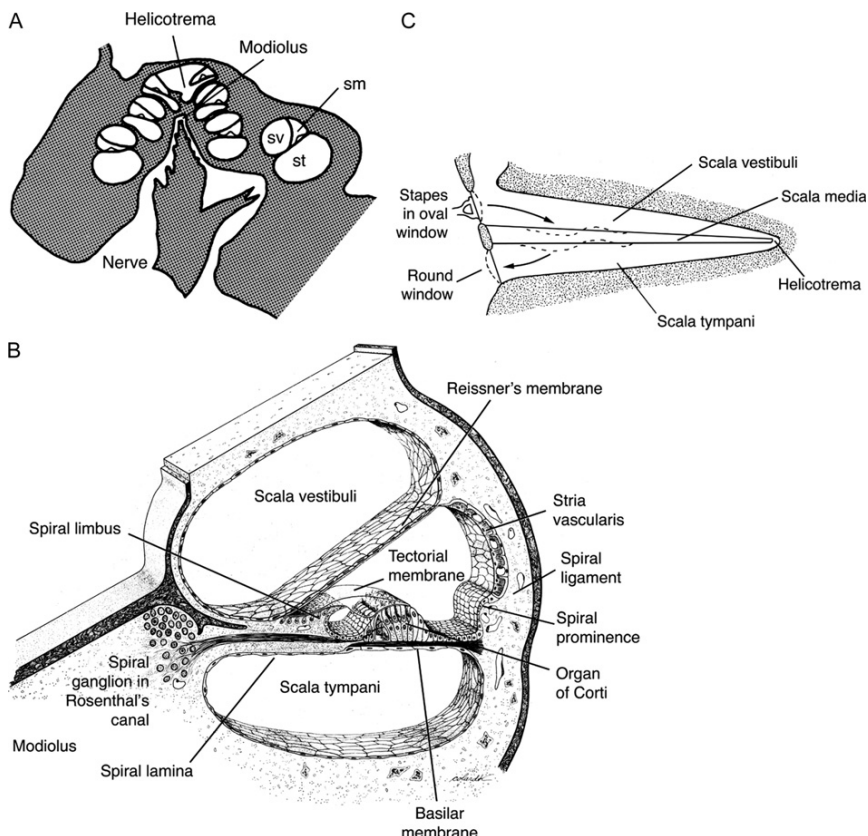


Fig. 3.1 (A) In a transverse section of the whole cochlea, the cochlear duct is cut across several times as it coils round and round. Abbreviations: sv, scala vestibuli; sm, scala media; st, scala tympani. (B) The three scalae and associated structures are shown in a magnified view of a cross section of the cochlear duct. Reproduced from Fawcett (1986), Fig. 35.11. (C) The path of vibrations in the cochlea is shown in a schematic diagram in which the cochlear duct is depicted as unrolled. (D) Cross section of the organ of Corti, as it appears in the basal turn. Deiters' cells send extensions (phalanges) up to the reticular lamina, running in the spaces around the outer hair cells, although they are not shown on this particular cross section. The modiolus is to the left of the figure. From Pickles (2007b). (E) Scanning electron micrograph of a fractured cross section of the human organ of Corti from the mid-turn of the cochlea (the 500 Hz place), oriented as in D. In this specimen, the inner pillar cell (arrowhead) has partly collapsed, and the tectorial membrane has shrunk away from the reticular lamina. There are four rows of outer hair cells (OHCs). BM, basilar membrane; CC, Claudius cell; HP, habenula perforata; HS, Hensen's stripe; IHC, inner hair cell; MP, marginal pillars (of tectorial membrane); OP, outer pillar cell; OSL, osseous spiral lamina; TM, tectorial membrane. From Glueckert *et al.* (2005), Fig. 1.

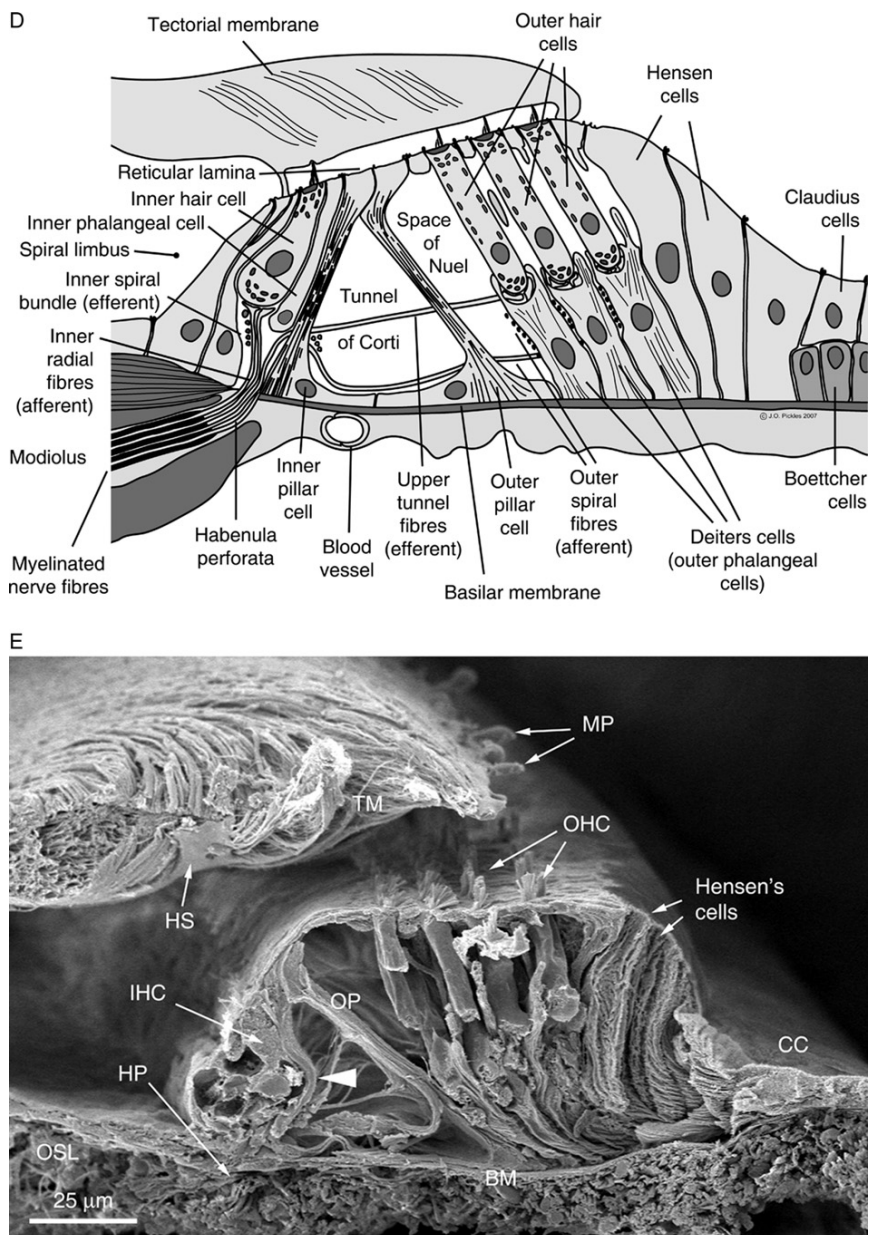


Fig. 3.1 Continued.

The vibrations of the stapes are transmitted to the oval window, a membranous window opening onto the scala vestibuli. The fluid in the cochlea is displaced to a second window, the round window, opening onto the scala tympani. The flow causes a wave-like displacement of the basilar membrane and the structures attached to it (see Fig. 3.1C). It is this that is responsible for the stimulation of the hair cells, and the first stage of the analysis of the incoming sound is performed by the spatial distribution of the resulting displacements.

The basilar membrane undergoes an important gradation in dimensions up the cochlea; although the cochlear duct is broad near the base and narrow towards the apex, the basilar membrane tapers in the opposite direction, the difference being filled by the spiral lamina.

The organ of Corti on the basilar membrane constitutes the auditory transducer and the nerve supply ends here (see Fig. 3.1B, D and E). The nerve supply and the blood vessels of the cochlea enter the organ of Corti by way of the central cavity of the cochlea, the modiolus, the spiral structure of the cochlea imparting a corresponding twist to the nerve and blood vessels during development.

3.1.2 The organ of Corti

The organ of Corti has a highly specialized structure. It contains the hair cells, which are the receptor cells, together with their nerve endings and supporting cells (see Fig. 3.1B and D). The hair cells consist of one row of inner hair cells (IHCs) on the modiolar side of the arch of Corti and between three and, towards the apex, five rows of outer hair cells (OHCs). There are about 15 000 hair cells in each ear in human beings (Ulehlova *et al.*, 1987) and 12 500 in cats (Schuknecht, 1960).

The organ of Corti itself sits on the basilar membrane, a fibrous structure dividing the scala media from the scala tympani. Sometimes, though misleadingly, the whole complex is referred to as ‘the basilar membrane’. The organ of Corti is given rigidity by an arch of rods or pillar cells along its length, the upper ends of the rods ending in the reticular lamina, which forms the true chemical division between the ions in the fluids of the scala media and those of the scala tympani (see Fig. 3.1D). The arch is surrounded by phalangeal cells, that is by cells with processes that end in a plate in the reticular lamina. The inner phalangeal cells completely surround the inner hair cells. The outer phalangeal cells, which are also known as Deiters’ cells, form cups holding the basal ends of the outer hair cells. The outer phalangeal cells extend fine processes, or phalanges, to the reticular lamina, with the phalanges running in spaces between the side walls of the outer hair cells. The upper ends of the outer phalangeal cells become part of the reticular lamina. External to the outer hair cells there is a row of supporting cells known as Hensen’s cells, and on the modiolar side of the organ of Corti there is a further row of supporting cells. The distribution of the supporting cells changes in the different turns of the cochlea (Fig. 3.2).

The organ of Corti is covered by a gelatinous and fibrous flap, the tectorial membrane, composed of collagens and molecules unique to the inner ear, known as tectorins (see Richardson *et al.*, 2011, for review). The tectorial membrane is

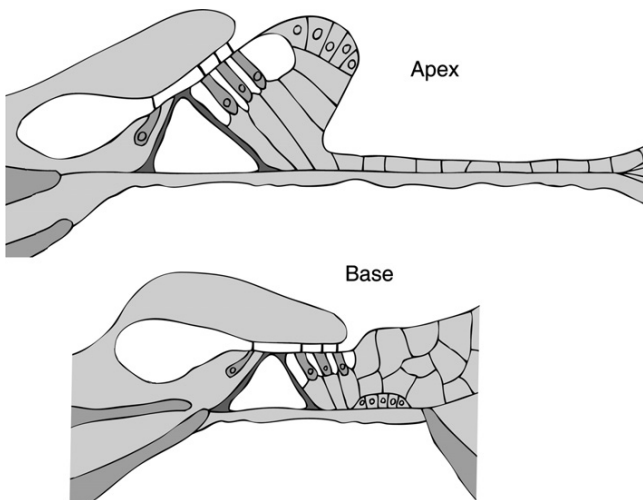


Fig. 3.2 The organ of Corti shows morphological differences along the length of the cochlea. Moreover, near the apex the basilar membrane is wide and near the base it is narrow. The modiolus is to the left of the figure. From Pickles (2007b).

fixed only on its inner edge, where it is attached to the limbus, although it is joined to the reticular lamina by small processes (trabeculae or marginal pillars). Some investigators believe that the tectorial membrane joins and seals onto the reticular lamina along its outer edge. However, this has been difficult to determine definitively because when the cochlea is preserved for histological examination the tectorial membrane tends to shrink away from the reticular lamina, as in Fig. 3.1E. The longer of the hairs on the outer hair cells are shallowly but firmly embedded in the undersurface of the tectorial membrane. The hairs of the inner hair cells are probably not embedded and fit loosely into a raised groove known as Hensen's stripe on the undersurface of the tectorial membrane.

The tectorial membrane is attached only on one side and is raised above the basilar membrane. Therefore, when the basilar membrane moves up and down, a shear or relative movement will occur between the tectorial membrane and the organ of Corti, with the result that the hairs will be deflected (Fig. 3.3). The arch of the pillar cells (the arch of Corti) would seem well suited to maintaining the rigidity of the organ of Corti during such a movement. Although this appears to be true in outline, more recent measurements have also shown that the organ of Corti may well undergo a complex distortion during each cycle of vibration, as will be discussed in Chapter 5 (see, e.g. Nam and Fettiplace, 2010).

Figure 3.4A shows a view of the upper surface of the organ of Corti of a guinea pig once the tectorial membrane has been removed. The hairs or stereocilia of the hair cells are seen projecting through the reticular lamina, with V-shaped rows on the outer hair cells, and nearly straight rows on the inner hair cells. The geometric patterns on the reticular lamina between the hair cells reveal the pattern

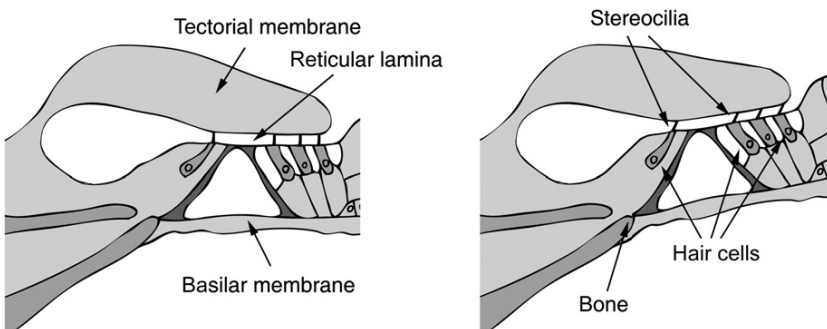


Fig. 3.3 The lever action of the cochlea, showing how the stereocilia on the hair cells are deflected as a result of vertical displacements of the basilar membrane. When the basilar membrane is deflected upwards, the stereocilia are deflected away from the modiolus (the modiolus is to the left of the figure). From Pickles (2007b).

of the supporting cells making up the lamina. The pattern is formed by small microvilli, which cover the apical surfaces of the supporting cells, bunching more thickly around their edges. Figure 3.4B shows the relations between the outer hair cells and the Deiters' cells, as seen from the outer edge of the organ of Corti once the supporting cells have been removed, and shows the spaces around the bodies of the outer hair cells. On each inner hair cell of the guinea pig the hairs are arranged in three to five closely spaced rows (see Fig. 3.4C), whereas on the outer hair cells there are three closely spaced rows (see Fig. 3.4D). In human beings, there are three to five rows of outer hair cells, and each outer hair cell has three to five rows of stereocilia (Glueckert *et al.*, 2005).

Figure 3.5A shows a schematic cross section of the apical portion of a hair cell. This is the portion bearing the stereocilia and is the region involved in the initial sensory transduction. The diagram shows the structures common to acoustico-lateral hair cells, including those of the vestibular system. Three rows of stereocilia are shown in the cross section. The stereocilia themselves are composed of packed actin filaments, which means that stereocilia are more closely related to microvilli, also composed of actin filaments, than to true cilia. The actin filaments give the stereocilia considerable stiffness so that they behave as rigid levers in response to mechanical deflection (Flock *et al.*, 1977). The stereocilia are bonded together by sideways-running links so that all the stereocilia in a bundle tend to move together. There are also fine links emerging from the tips of the shorter stereocilia, called tip links, which couple the stimulus-induced movements to the actual mechano-transducer channels in the membrane (Pickles *et al.*, 1984). When the bundle is deflected in the direction of the tallest stereocilia, the tip links are placed under tension, pulling open the mechanotransducer channels. In the guinea pig, stereocilia are 2–4 µm long and 300 nm in diameter in the row of tallest stereocilia on the hair cell, tapering to some 500 nm long and 100 nm wide for the shortest stereocilia.

Some of the actin filaments of the stereocilia continue, closely packed, into a rootlet which anchors the stereocilium into the cuticular plate. The cuticular plate

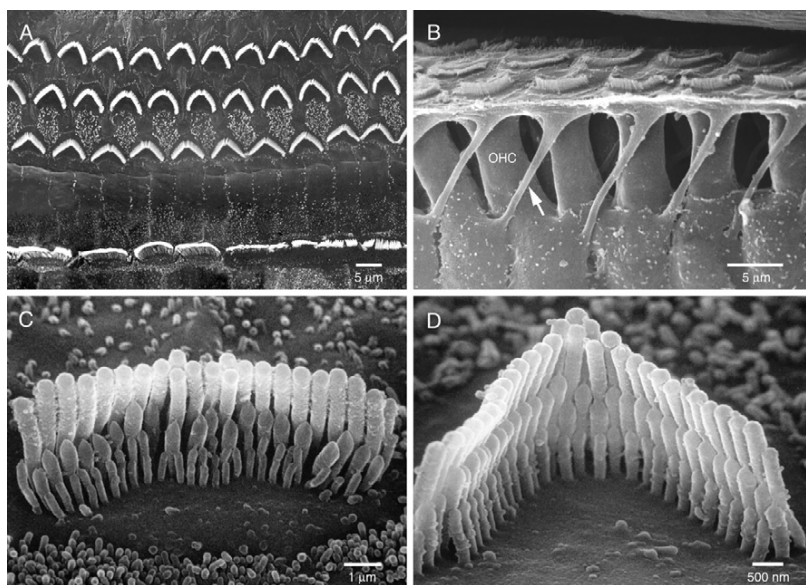


Fig. 3.4 (A) A scanning electron micrograph of the upper surface of the organ of Corti, when the tectorial membrane has been removed, shows three rows of outer hair cells (top) and one row of inner hair cells (bottom). Scale bar, 5 μm . (B) The phalanges of the Deiters' cells (e.g. arrow) run at an angle to the cylindrical bodies of the outer hair cells (OHCs). For this micrograph, the supporting cells on the outer edge of the organ of Corti were removed, and the organ of Corti was viewed looking in towards the modiolus (i.e. looking downwards in Fig. 3.4A). The cochlear apex is to the right of the figure. Scale bar, 5 μm . (C) On inner hair cells, the stereocilia form nearly straight rows. Three to five rows of stereocilia are visible. The stereocilia are viewed from the side nearest to the modiolus (i.e. looking upwards in Fig. 3.4A). Scale bar, 1 μm . (D) On outer hair cells, the stereocilia form V- or W-shaped rows. In the guinea pig, there are three rows of stereocilia, evenly graded in height. The stereocilia are viewed from the side nearest to the modiolus. Scale bar, 500 nm. Guinea pig.

is also composed of actin filaments, this time forming a dense matrix (Flock *et al.*, 1982). Adjacent to the middle of the row of tallest stereocilia, there is a gap in the cuticular plate, with a basal body situated in the gap. The basal body is a centriole-like structure and may be important in development. In vestibular hair cells and in embryonic cochlear hair cells, but rarely in mature ones, a cilium of different appearance known as the kinocilium emerges from the basal body. Unlike the stereocilia, the kinocilium is a true cilium, in that it consists of tubulin-containing microtubules, nine pairs of microtubules being arranged in a ring around the outside of the cilium, with one pair in the centre. In the cell body itself we have the usual intracellular organelles and synaptic junctions at the extreme basal end.

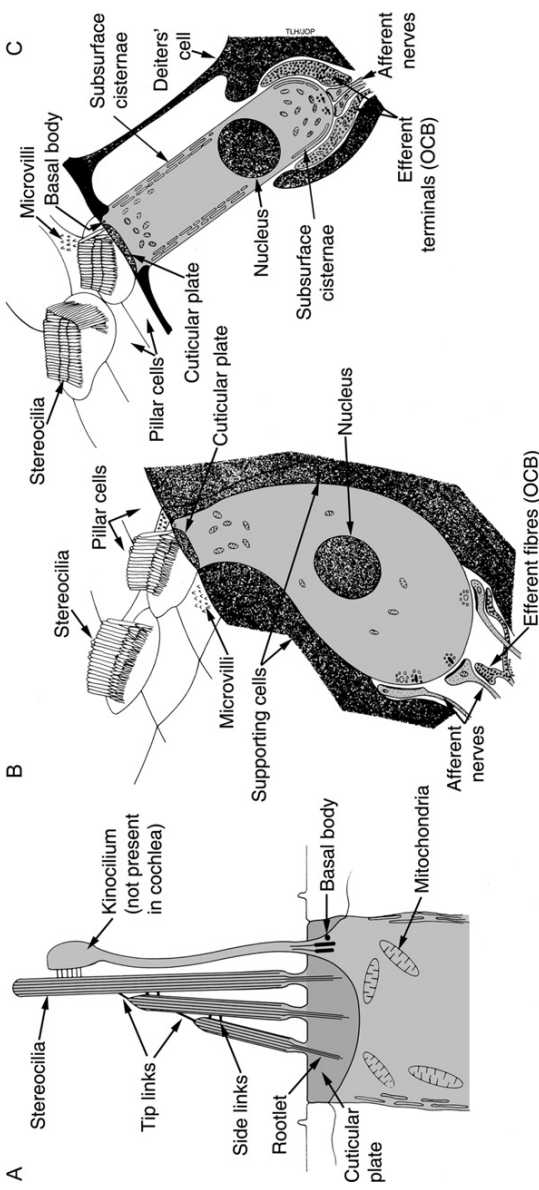


Fig. 3-5 (A) The common structures on the apical portion of acousticolateral hair cells include rows of stereocilia that are graded in height and joined by cross-links. A pull on the tip links opens the transducer channels. The kinocilium is not present in the mature cochlea, although it is present in vestibular cells. (B and C) Inner hair cells are shaped like a flask (B), and outer cells are shaped like a cylinder (C). OCB, olivocochlear bundle. From Pickles (2007b).

An inner hair cell is shown in Fig. 3.5B. Depending on species, it is about 35 µm in length and about 10 µm in diameter at the widest point. The shape is commonly likened to that of a flask. The nucleus is central, the mitochondria are scattered, though denser above the nucleus, and the cellular organelles are most prevalent at the apex, near the cuticular plate. The nerve endings are situated near the base of the cell. These terminals are associated with the afferent fibres of the auditory nerve, conveying information from the cochlea to the brainstem. On the presynaptic membrane, the synapse is often marked by small dense synaptic ribbons at right angles to the cell wall, surrounded by synaptic vesicles (Liberman *et al.*, 1990). The synaptic ribbon marshals the vesicles to release neurotransmitter at the hair cell synapse, so that the coordinated release of neurotransmitter from multiple vesicles is able to reliably activate the synapse (Grant *et al.*, 2010). The neurotransmitter is glutamate, acting on glutamate AMPA receptors in the afferent auditory nerve fibres (Ruel *et al.*, 1999).

Outer hair cells are approximately 25 µm long in the basal turn and 45 µm long in the apical turn, and 6–7 µm in diameter, again depending on species. They have a cylindrical shape. The nucleus is located basally (see Fig. 3.5C). The mitochondria are situated in groups around the lateral wall, at the apex just under the cuticular plate and at the base below the nucleus. The afferent terminals are faced with occasional small synaptic bodies and synaptic vesicles (Liberman *et al.*, 1990).

In both types of hair cells, the tallest stereocilia are situated on the side of the hair cell furthest away from the modiolus, and the shortest stereocilia are situated nearest to the modiolus.

3.1.3 The innervation of the organ of Corti

Each cochlea is innervated by about 50 000 sensory neurones in cats, and about 30 000 in human beings (Schuknecht, 1960; Harrison and Howe, 1974a). There are also about 1400 ‘efferent’ or centrifugal neurones, by means of which the central nervous system is able to influence the cochlea (counted for the cat; see Warr, 1992).

The afferent fibres, which convey auditory information from the cochlea to the central nervous system, have their cell bodies in the spiral ganglion within Rosenthal’s canal in the modiolus on the inner wall of the spiral lamina (see Fig. 3.1B; reviewed by Nayagam *et al.*, 2011). The cells have one process projecting to the hair cells and the other to the cells of the cochlear nucleus in the brainstem. The axons project into the cochlear duct through openings in the bony shelf of the spiral lamina, known as the habenula perforata. About 90–95% (90% in the guinea pig; Brown, 1987; 95% in the cat: Spoendlin, 1972) of the afferent fibres connect directly with the inner hair cells, are thick and myelinated and are called Type I or radial fibres (Fig. 3.6). Each inner hair cell receives 20–30 Type I fibres (Liberman *et al.*, 1990). The remaining 5–10% of fibres are thin and unmyelinated, have monopolar cell bodies, go to the much more numerous outer hair cells, and are called Type II fibres (also called outer spiral fibres). Whereas the axons to the inner hair cells contact the cell directly opposite their habenular opening, those to the outer hair cells take a much more oblique course. They turn basally for five hair

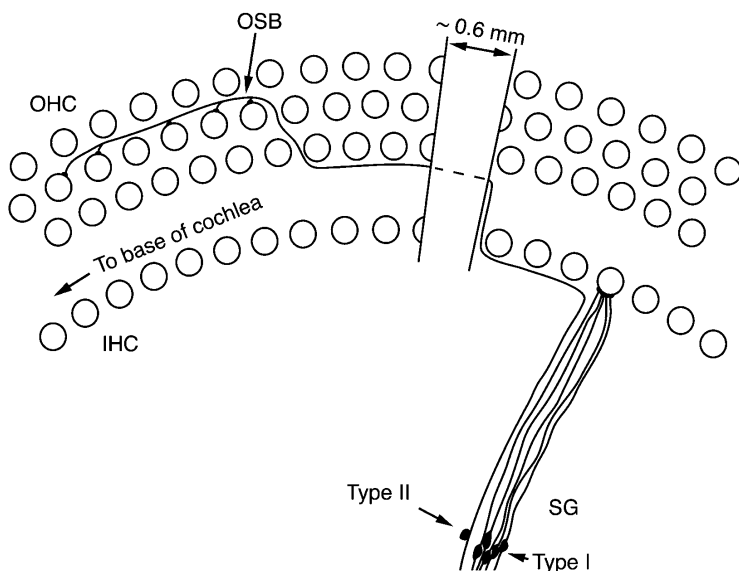


Fig. 3.6 The great majority of afferent auditory nerve fibres (Type I fibres) connect with inner hair cells. A few fibres (Type II) form the outer spiral bundle, and pass to outer hair cells, after running basally for about 0.6 mm. Type I fibres have bipolar cell bodies (i.e. with axon and dendrite contacting the cell body in separate branches), while Type II fibres have monopolar cell bodies (i.e. with axon and dendrite contacting the cell body through a single branch). All rows of outer hair cells receive Type II afferents, although only one afferent to one row is shown here. IHC, inner hair cells; OHC, outer hair cells; SG, spiral ganglion; OSB, outer spiral bundle. From Pickles (2007b).

cells or so and cross the tunnel of Corti on the basilar membrane, where they are known as basilar or lower tunnel fibres. They then run towards the base of the cochlea for some 0.6 mm, first running along the outer edge of the tunnel of Corti, where they are known as the fibres of the outer spiral bundle or outer spiral fibres. They spiral outwards among the rows of the outer hair cells, synapsing with up to about 50 hair cells, generally all of the same row (Simmons and Liberman, 1988; see Fig. 3.6). However, each outer hair cell also has synapses from several other afferent fibres. The innervation of the two types of hair cell is therefore completely different, the neural connections of inner hair cells showing a great deal of divergence and those of outer hair cells showing both convergence and divergence.

The efferent or centrifugal axons arise in the superior olive complex of the brainstem and will be discussed in detail later (Chapter 8). The olivocochlear system has two divisions, known as the medial olivocochlear bundle (MOC) and the lateral olivocochlear bundle (LOC) (see Guinan, 2006, 2010, for reviews). Fibres of the medial olivocochlear bundle arise relatively medially in the brainstem, on the medial surface of the superior olive complex, and give rise to axons

running to the outer hair cells, mainly on the contralateral side (Guinan *et al.*, 1983). Fibres of the lateral olivocochlear system arise more laterally in the superior olfactory complex and innervate the region of the inner hair cells, mainly on the ipsilateral side. In the cat, there are about 500 centrifugal fibres to the outer hair cells and about 900 to the region of the inner hair cells (Warr, 1992). The fibres to the region of the inner hair cells do not generally contact the inner hair cells directly, but rather terminate on the dendrites of the afferent fibres under the inner hair cells. The fibres to the outer hair cells cross the tunnel halfway up the tunnel of Corti, where they are known as the upper tunnel fibres, and then ramify outwards among the outer hair cells, showing considerable branching. Near the base of the cochlea, each hair cell receives four to eight efferent terminals and near the apex, rather fewer (Liberman *et al.*, 1990). The efferent terminals on the outer hair cells are large and vesiculated and tend to surround the base of the cell and its afferent terminals.

The cochlea also receives an adrenergic, sympathetic innervation (Vicente-Torres and Gil-Loyzaga, 2002; Maison *et al.*, 2010). Most of the fibres appear to end on blood vessels in the spiral lamina. There are also adrenergic receptors in the stria vascularis, on the hair and supporting cells of the organ of Corti and on the cell bodies of the cochlear nerve fibres, that is the spiral ganglion cells, which would be capable of responding to circulating adrenaline (Fauser *et al.*, 2004; Khan *et al.*, 2007).



3.2 THE MECHANICS OF THE COCHLEA

3.2.1 The travelling wave

When a sound impinges on the eardrum, the vibrations are transmitted to the oval window by the middle ear bones. The vibrations then cause a movement of the cochlear fluids and the cochlear partitions, displacing the fluid to the round window (see Fig. 3.1C). This initiates a wave of displacement on the basilar membrane, which then travels apically in the cochlea. The wave is a very important stage in the analysis of sound by the auditory system, because the pattern and position of the wave depends on the frequency of the stimulus. For a sine wave of a single frequency, the vibration has a sharp peak which is confined to a narrow region of the basilar membrane. Moreover, the position of the peak depends on the frequency of the stimulus. The mechanical analysis of frequency by the cochlea underlies the frequency selectivity shown by the later stages of the auditory system and the selectivity that can be shown psychophysically. The frequency selectivity depends on the physical mechanics of the basilar membrane and the cochlear fluids, and their interaction with physiological hair cell responses. The most recent results are a development of the approach pioneered by G. von Békésy, and a discussion of his results still provides the best way of introducing current work.

Békésy in a long series of experiments, described in a collected form by Békésy (1960), examined the movement of the cochlear partition in human and animal

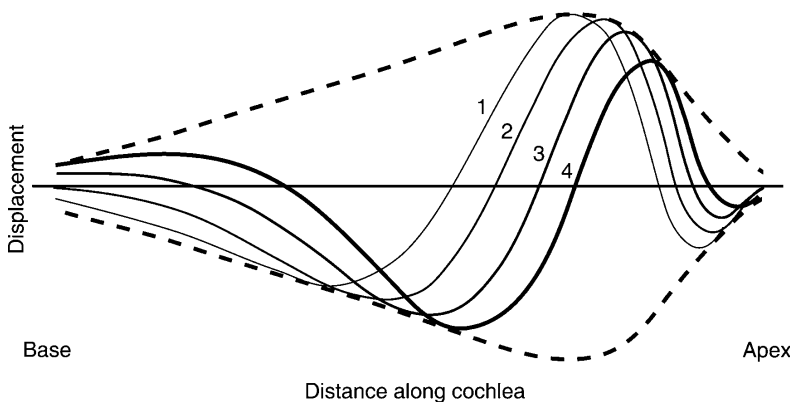


Fig. 3.7 Travelling waves in the cochlea were first shown by Békésy. The full lines show the pattern of the deflection of the cochlear partition at successive instants, as numbered. The waves are contained within an envelope that is static (dotted lines). Stimulus frequency, 200 Hz. Reprinted from Békésy (1953), Fig. 22, Copyright (1953), with permission from American Institute of Physics.

cadavers. Temporal bones were rapidly dissected soon after death and were immersed in saline solution. Rubber windows were substituted for the round and oval windows, and a mechanical vibrator was attached to one of them. The cochlear wall was opened under water for observation of the partitions within. By microscopic and stroboscopic observation of silver particles scattered on Reissner's membrane, Békésy was able to plot out the now-classic travelling wave pattern shown in Fig. 3.7. He presumed that this was similar to the movement of the membrane carrying the transducers themselves, namely the basilar membrane. For a stimulus of fixed frequency, the cochlear partition vibrated with a wave that gradually grew in amplitude as it moved up the cochlea from the stapes, reached a maximum, and then rapidly declined. The wave of displacement moved more and more slowly as it passed up the cochlea, so the phase changed with distance at an accelerating rate and the apparent wavelength of the vibration decreased. However, the frequency of vibration at any point was, of course, the same as that of the input.

Békésy's plots were made in two ways. By opening a length of cochlea, it was possible to see the pattern of movement distributed along the membrane, and so plot the waveforms and their envelopes for sounds of different frequencies. The vibration envelopes found by Békésy are shown in Fig. 3.8. They show the important point that as the frequency of the stimulus was increased, the position of the vibration maximum moved towards the base of the cochlea. Thus high-frequency tones produced a vibration pattern peaking at the base of the cochlea. Low-frequency tones, in contrast, produced most vibration in the apex of the cochlea, although, because of the long tail of the vibration envelope, there was some response near the base as well.

A second way in which Békésy measured the vibration pattern is indicated in Fig. 3.9. He opened the cochlea at certain points and measured the vibration at

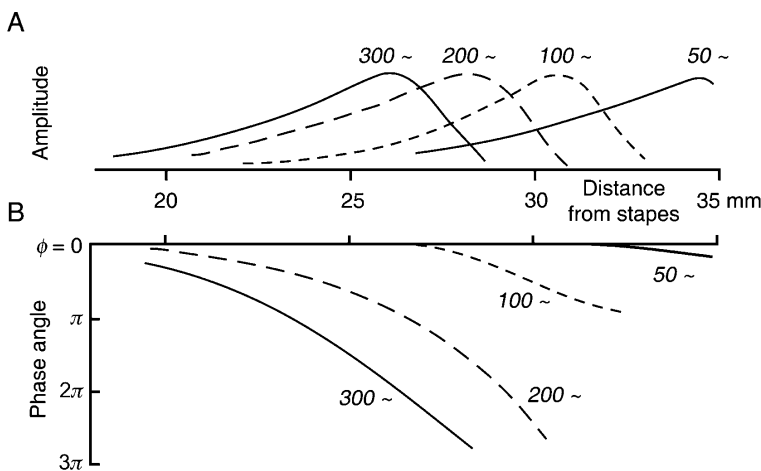


Fig. 3.8 (A) Displacement envelopes on the cochlear partition are shown for tones of different frequencies. (B) The relative phase angle of the displacement. Reprinted from Békésy (1947), Fig. 5, Copyright (1947), with permission from American Institute of Physics.

those points as the frequency was varied. Figure 3.9 shows his results for six points on the membrane, the peak-to-peak stapes displacement being kept constant as he varied the frequency at each point. Note that, as before, it is the most basal point that responds best to the highest frequencies. Note the shallow slope on the low-frequency side and the much steeper slope on the high-frequency side. In going from the space axis of Fig. 3.8 to the frequency axis of Fig. 3.9, the direction of variation of the parameters marked on the curves and the abscissa has to be reversed, although the positions of the steep and shallow slopes are the same.

Békésy's results can be summarized as follows: vibration of the stapes gives rise to a travelling wave of displacement on the basilar membrane. For a vibration of a particular frequency, the vibration on the basilar membrane grows in amplitude as the wave travels towards the apex, and then beyond a certain point dies out rapidly. The wave travels more and more slowly as it travels up the cochlea. Low-frequency sounds peak a long way along the membrane, near the apex, and high-frequency sounds peak only a short way along, near the base. His results showed that the frequency selectivity at single points on the basilar membrane was very poor, with a very shallow slope on the low-frequency side, though a steeper slope on the high-frequency side. On the basis of his results, therefore, the basilar membrane appeared to act substantially as a low-pass filter.¹

¹ In Fig. 3.9, the peak-to-peak stapes displacement was kept constant as the stimulus frequency was varied. However, as described in Chapter 1, constant sound pressure level at different frequencies corresponds to constant peak velocities. If the data are recalculated for constant peak velocity, the low-frequency slopes in Fig. 3.9 become flat, that is, the cochlea appears to act purely as a low-pass filter.

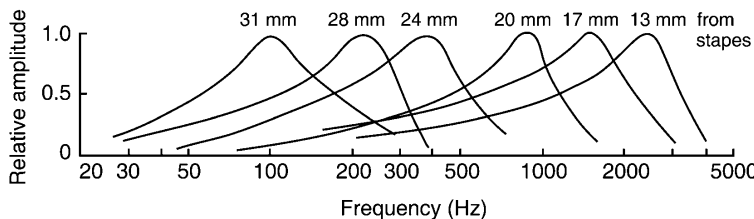


Fig. 3.9 Frequency responses are shown for six different points on the cochlear partition. The amplitude of the travelling wave envelope was measured as the stimulus frequency was varied with constant peak stapes displacements. The position of the point of observation is marked on each curve. Reprinted from Békésy (1949), Fig. 7, Copyright (1949), with permission from American Institute of Physics.

3.2.2 Current measurements of the travelling wave

3.2.2.1 Historical introduction

Békésy's observations had been questioned on two grounds. Firstly, visual observations meant that the vibration amplitude had to be at least of the order of the wavelength of light, and the high intensities (130 dB SPL) that are necessary make extrapolation to a more physiological range unjustified. Secondly, his measurements were performed on cadavers. It is now known that the cochlea vibrates non-linearly so that responses measured at high stimulus intensities are not a valid measure of the responses at lower stimulus intensities (first shown by Rhode, 1971). Moreover, it is now known that not only does the experimental animal have to be alive, but also the cochlea has to be in extremely good physiological condition to show a satisfactory mechanical response (first shown by Sellick *et al.*, 1982). The history of the measurements of basilar membrane vibration over the years is the story of the progress that has gradually been made in meeting the latter requirements. The impetus came from studies on the auditory nerve, which showed that single auditory nerve fibres, innervating single points on the basilar membrane, could show sharply tuned bandpass characteristics, at variance with Békésy's observations.

Since Békésy, only a few researchers have managed to open the cochlea and successfully measure the responses as a pattern distributed over space. Because the degree of opening needed is highly traumatic for the cochlea, the more general approach has been to make only a small hole and confine the observations to a single place. The responses at that point are then measured as the frequency of stimulation is altered. However, the measurements made by the two methods agree. Current measurements use laser interferometry to determine the vibration of the cochlear partition. The basilar membrane is illuminated with laser light, and the reflected light is allowed to combine (interfere) with a sample of the illuminating light, producing either partial cancellation or summation of the light waves. The resulting light intensity is detected by a sensor, and high degrees of

amplification are used so that very small changes in intensity, resulting from movements of the sample by much less than a wavelength of light, can be detected. The light may be either reflected from reflective beads applied to the basilar membrane (e.g. Nuttal *et al.*, 1991; Ruggero and Rich, 1991a; Rhode and Recio, 2000; Ren *et al.*, 2011) or reflected directly from the basilar membrane itself (e.g. Nilsen and Russell, 2000; Ren, 2002; Choudhury *et al.*, 2006). These techniques have superseded earlier techniques based on radioactive detection (i.e. the Mössbauer technique; see Robles and Ruggero, 2001, for review).

Because the response of the basilar membrane underlies the performance of the whole of the auditory system, the results of measurements of basilar membrane vibrations will be presented in several different ways.

3.2.2.2 Current measurements of basilar membrane vibration: pattern over space

Recent measurements of the response of the basilar membrane will be introduced here by showing the spatial pattern of vibration along the basilar membrane, in response to a single tone. This is analogous to the measurements made by Békésy, as shown in Figs. 3.7 and 3.8. In contrast to the experiments of Békésy, the more recent measurements are all shown for cochleae with a normal physiological degree of sensitivity, and with stimuli in the physiological range of intensities.

Figure 3.10A shows the response of the basilar membrane, at one instant in time during stimulation by a 16-kHz tone. This is analogous to one of the curves in Fig. 3.7 (e.g. the curve labelled 4) and gives a snapshot view of the travelling wave as it moves from base to apex along the basilar membrane.

Figure 3.10B shows the peak amplitude of the wave on the basilar membrane, as a function of distance, in response to a tone of 15 kHz. The amplitude of the envelope of the wave (analogous to the upper dotted line in Fig. 3.7) is plotted for five different intensities of tone stimulation. At 20 dB SPL, there is a small narrow peak, situated 3.55 mm from the base of the cochlea. As the intensity is raised to 40 and then 60 dB SPL, the peak grows in size and the tip of the peak becomes slightly broader. At higher intensities, the peak becomes much broader and moves towards the base of the cochlea, while the slope towards the base becomes much shallower.

Two points can be noted. Firstly, the basilar membrane is very responsive, because the lowest-intensity stimulus produces a relatively large (1.5 nm – but still very small!) response at the most sensitive point. Secondly, with low-intensity tones, the basilar membrane shows a high degree of spatial selectivity to frequency. For a tone of one frequency, the amplitude of vibration drops away rapidly on either side of the most sensitive point, and only a limited length of the basilar membrane is activated. At higher intensities of stimulation, however, the sharp spatial selectivity is reduced. A tone of one frequency can now activate a broad patch of the basilar membrane.

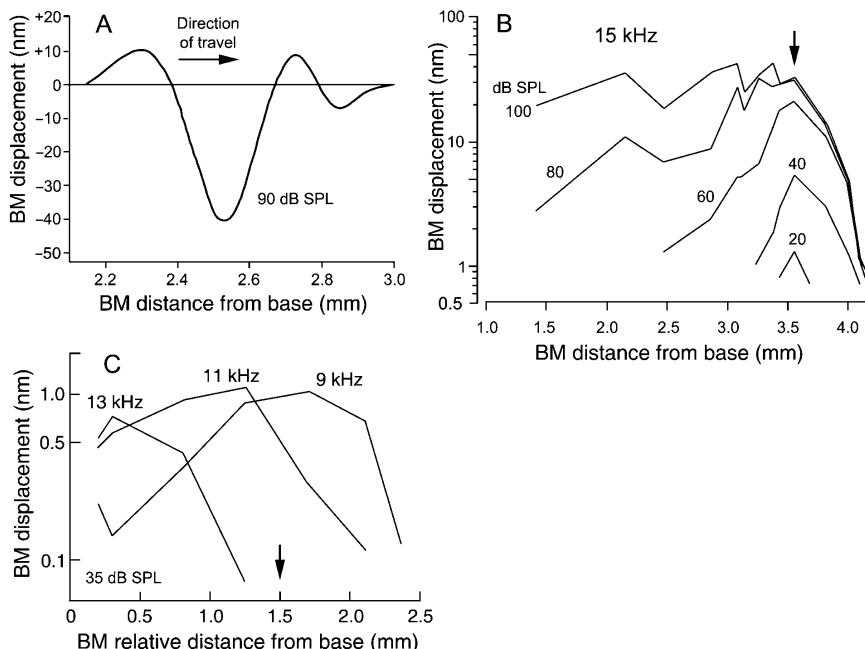


Fig. 3.10 Current measurements of the travelling wave as a function of position along the cochlear duct. (A) Instantaneous waveform of the vibration of the basilar membrane in response to a 90 dB SPL 16-kHz tone, for one moment in time, and plotted as a function of distance from the base of the cochlea. Gerbil. Displacements were calculated from velocity data kindly supplied by T. Ren (see Ren, 2002). (B) Amplitude of vibration of the basilar membrane in response to a 15-kHz tone, presented at several different intensities, and measured as a function of position along the cochlear duct. At the lowest intensities (20 and 40 dB SPL), the vibration is sharply localized to one area. At higher intensities (80 and 100 dB SPL), the pattern of vibration becomes broader, particularly towards the base of the cochlea. Guinea pig. From Russell and Nilsen (1997), Fig. 1D, Copyright (1997), National Academy of Sciences, USA. (C) Amplitude of vibration of the basilar membrane in response to tones of frequencies 9, 11 and 13 kHz, measured as a function of position along the cochlear duct. The 13-kHz tone peaks towards the base, and the 9-kHz tone peaks towards the apex. Arrow: see text. Chinchilla. Note distances are relative to a certain zero point and are not absolute distances from the base of the cochlea. Reprinted from Rhode and Recio (2000), Fig. 7. Copyright (2000), with permission from American Institute of Physics.

Figure 3.10C shows the amplitude of the envelope of vibration as a function of distance along the cochlea, for three different frequencies of stimulation. As anticipated from the results of Békésy (Fig. 3.8), stimuli of higher frequency produce their greatest response near the base of the cochlea, while stimuli of lower frequency produce their greatest response near the apex.

3.2.2.3 Current measurements of basilar membrane vibration: response of single points as a function of frequency

If a measurement is made at a single point (e.g. at the point marked by the arrow in Fig. 3.10C) and if the tone frequency increased from low frequency to high, the peak of the travelling wave will sweep across the measurement point. The amplitude of the response at that place will therefore go from low, to high, to low. Plots made in this way are called frequency responses. By opening the cochlea at only one place, it is easier (though still very difficult) to measure physiologically valid responses compared with opening the cochlea over a wider region.

Figure 3.11A shows the amplitude of vibration of a point on the chinchilla basilar membrane, at a site 3.5 mm from the base of the cochlea. The lowest curves are for stimuli of 10 and 20 dB SPL and show that as the stimulus frequency is varied, a sharp peak of vibration is produced around one frequency. For tones of this

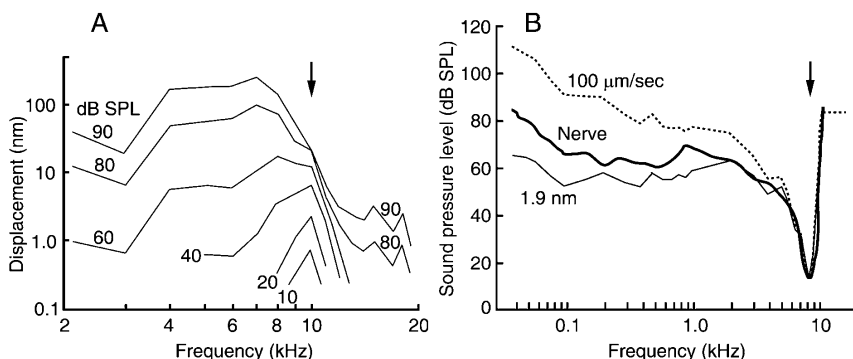


Fig. 3.11 Current measurements of the travelling wave measured at a single point on the basilar membrane, as a function of frequency. (A) Peak displacements of the chinchilla basilar membrane show a bandpass characteristic for low intensities of stimulation and develop more of a low-pass characteristic for high intensities of stimulation. The stimulus intensity is marked on each curve. Arrow: the characteristic frequency, that is the frequency of greatest sensitivity. The response has been recalculated as peak displacement, rather than as peak velocity, as in the original figure. Measured by laser light at a point 3.5 mm from the base of the cochlea. Data recalculated from Ruggero *et al.* (1997). (B) Tuning curves of chinchilla basilar membrane vibration. Thresholds are shown for two different criteria: for peak velocities of $100 \mu\text{m/sec}$ (dashed line) and for a peak displacement of 1.9 nm (thin solid line). The thick solid line shows the average tuning curve of a large number of low-threshold, sharply tuned auditory nerve fibres innervating the same frequency region. The average fibre tuning curve lies in between the iso-velocity line and the iso-amplitude line. The threshold criteria have been chosen so that the curves overlap in the region of the tip. Arrow: characteristic frequency. See Ruggero *et al.* (2000) for further related data. Reprinted from Ruggero *et al.* (1990), Fig. 22. Copyright (1990), with permission from American Institute of Physics.

intensity, the cochlea is sharply tuned, because changing the stimulus frequency by only a little produces a large change in the amplitude of vibration. The basilar membrane therefore shows a bandpass filter function, with a high degree of frequency selectivity.

At higher intensities of stimulation, the sharp tuning disappears (e.g. at 90 dB SPL). The response now shows only a broad peak. Not only does the pattern spread preferentially in the low-frequency direction, but also the frequency giving the maximum response moves towards lower frequencies. This occurs because as the stimulus intensity is raised, the response grows only slowly in the region of the peak, and faster for lower frequencies of stimulation.

Figure 3.11B shows the same data plotted as tuning curves, or frequency-threshold curves (FTCs), determined for two different criteria of vibration. The dotted line shows the sound intensities necessary to produce a vibration velocity of 100 $\mu\text{m/sec}$ as a function of stimulus frequency. The dotted line, like the lowest curve in Fig. 3.11A, shows that the system is very sensitive at one frequency, and is very sharply tuned. This frequency is known as the characteristic frequency (CF) of the place or nerve fibre being measured (in this case, 8.3 kHz). The basilar membrane is sensitive because at this frequency the criterion response is produced by a stimulus intensity of only 13 dB SPL. It is sharply tuned because if the stimulus frequency is moved away from this frequency, the stimulus intensity has to be increased markedly to produce the same criterion response. An advantage of presenting the data in this way is that it is possible to compare directly the tuning from different stages of the auditory system. For instance, if we go through a similar procedure and construct a tuning curve for an auditory nerve fibre innervating the same region of the cochlea, using as our criterion a certain number of evoked action potentials per second, we obtain a tuning curve that is similar in general shape to the mechanical iso-velocity one (thick solid line, Fig. 3.11B). This shows that the tuning of the auditory nerve fibres matches, approximately at least, the tuning of the basilar membrane. The systematic differences between the curves will be discussed in Chapter 5.

The plots in Fig. 3.10, with distance on the horizontal axis, and those in Fig. 3.11, with frequency on the horizontal axis, are equivalent representations of the same data. They can be calculated from each other as long as we know how the position of the peak of the travelling wave depends on the frequency of the stimulus and how the shape of the travelling wave changes for different frequencies of stimulation. Figure 3.12 shows how the plots are interrelated. It is a useful exercise for the reader to become practiced in understanding the relation between the two representations so that he or she can immediately understand the implications in the spatial domain of data presented in the frequency domain, and vice versa.

3.2.2.4 Non-linearity of the response

Figures 3.10B and 3.11A show that as the stimulus intensity is raised, the amplitude of the response can grow non-linearly, that is it can grow less than in proportion to

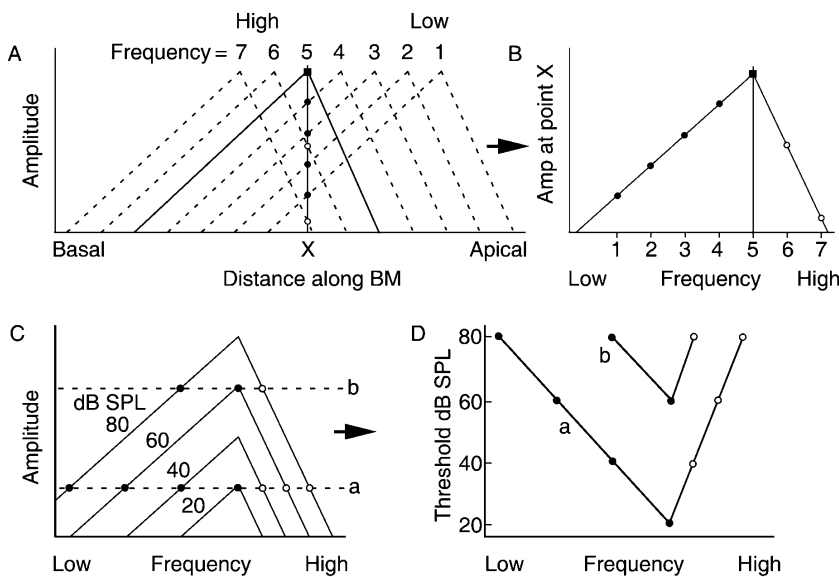


Fig. 3.12 (A and B) Relation between amplitude plots made as a function of distance (A) and amplitude plots made as a function of frequency (B). Full and dotted lines in A show responses for different frequencies of stimulation. Frequency 7 is high and frequency 1 is low. The plot in B can be derived from the data in A, by looking at the amplitude of the response at one point (\times) on the basilar membrane. Closed circles show data derived from frequencies of stimulation below that giving the maximum response at point \times and open circles from frequencies above. It is also possible to construct the plots in A from the plot in B, if the place–frequency map is known, that is if the relation between the position of the peak of the travelling wave and the frequency of stimulation is known, and if the change in shape of the travelling wave with change in frequency is known. It is generally a reasonable assumption that for small changes in frequency, the travelling wave maintains the same overall shape as it changes in position. (C and D) Construction of tuning curves from amplitude–frequency plots. (C) Amplitudes of response as a function of frequency, for different intensities of stimulation (dB SPL marked on curves). Tuning curves in D are shown for two amplitude criteria (a and b).

the increase in stimulus intensity. This compressive non-linearity is particularly visible near the peak of the travelling wave (arrow, Fig. 3.10B), or in frequency plots at the characteristic frequency (arrow, Fig. 3.11A).

The non-linearity is shown more explicitly in the amplitude plots of Fig. 3.13. In Fig. 3.13A, the amplitude of the basilar membrane vibration is shown for different amplitudes and frequencies of stimulation. At the characteristic frequency, 10 kHz, the response increases approximately linearly with intensity until about 20 dB SPL and then increases with a slope of about 0.3 (on log–log axes). Higher frequencies of stimulation (e.g. 11 kHz) show a similar non-linearity. However, at frequencies well below the characteristic frequency, the non-linearity is reduced or

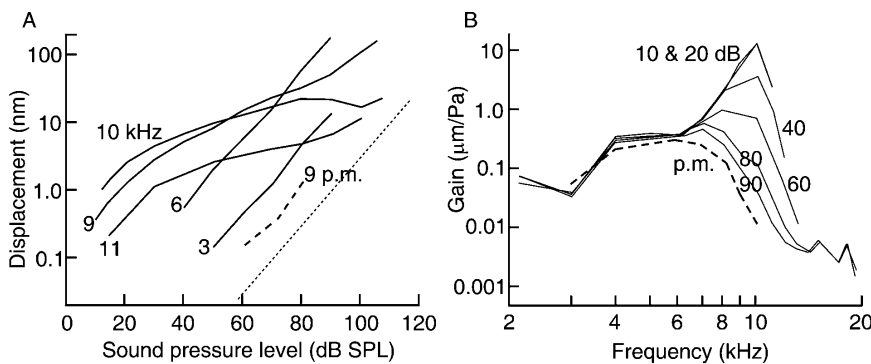


Fig. 3.13 The non-linearity of basilar membrane vibration. (A) Magnitude of basilar membrane vibration is shown as a function of stimulus intensity (horizontal scale) and for different frequencies of stimulation (as marked on curves, in kHz). The heavy dotted line marked p.m. was measured after death (at stimulus frequency 9 kHz). The graph has log–log axes, because the decibel scale uses a logarithmic transformation of stimulus intensity. The fine dotted line has a slope of 1, that is as for linear growth. Near and above the characteristic frequency (near and above 10 kHz), and for stimulus intensities above 20–30 dB SPL, the slope of the intensity functions is less than 1, that is the responses show a compressive non-linearity. At lower frequencies, the slope is 1 or near 1. After death, the cochlea loses sensitivity and the response becomes linear. Data recalculated from Ruggero *et al.* (1997). (B) The data of Fig. 3.11A, replotted as a gain (i.e. amplitude of displacement divided by stimulus intensity) and shown as a frequency response. The intensity of stimulation (in dB SPL) is marked on the curves. The dotted line marked p.m. was measured after death. Data recalculated from Ruggero *et al.* (1997) and from Recio *et al.* (1998) (post-mortem).

absent. After death (p.m., at 9 kHz) the cochlea becomes much less sensitive and the response becomes linear.

In Fig. 3.13B, the response is plotted as a gain, that is as response amplitude divided by stimulus amplitude, as a function of frequency. If the responses were entirely linear, all curves would lie on top of each other. Figure 3.13B shows how the gain of the basilar membrane response is greatest around the characteristic frequency, and at the lowest intensities of stimulation (e.g. 10 and 20 dB SPL). At the highest intensity of stimulation (90 dB SPL), the gain is much lower, and after death the gain is a little lower still (p.m., dotted line). The pattern of vibration is now similar to the insensitive, broadly tuned and substantially low-pass filter response, originally found by Békésy.

This gives a hint as to the mechanism behind sharp tuning and suggests that when the cochlea is in good physiological condition, a sensitive and sharply tuned component of the response is added to an insensitive and broadly tuned component. The sensitive component disappears when the cochlea is in a poor condition.

The most widely accepted hypothesis for the production of the sharply tuned tip in the tuning curve is a rather surprising and revolutionary one. The hypothesis says that the cochlea contains an active mechanical amplifier. The amplifier is

triggered by the acoustic stimulus and feeds mechanical energy back into the travelling wave, thus increasing the amplitude of the mechanical vibration. It also produces the sharply tuned response. The mechanism of this mechanical amplification is still controversial, and some of the thinking behind the hypotheses will be described in Section 3.2.3 when theories of cochlear mechanics are discussed. However, a more detailed consideration of the evidence will be delayed until Chapter 5. Here, we note that the presence of a mechanically active factor in cochlear mechanics could explain the extreme physiological vulnerability of the low-threshold, sharply tuned component of the travelling wave.

The non-linearity also has a very important functional consequence, because it allows the discrimination of auditory stimuli over a very wide (120 dB) range of stimulus intensities.

3.2.2.5 Phase of the response

Because the travelling wave moves from base to apex, its phase increases with distance along the cochlear duct. This was shown by Békésy (see Fig. 3.8B) and has been confirmed by more recent measurements. Figure 3.14A shows the phase

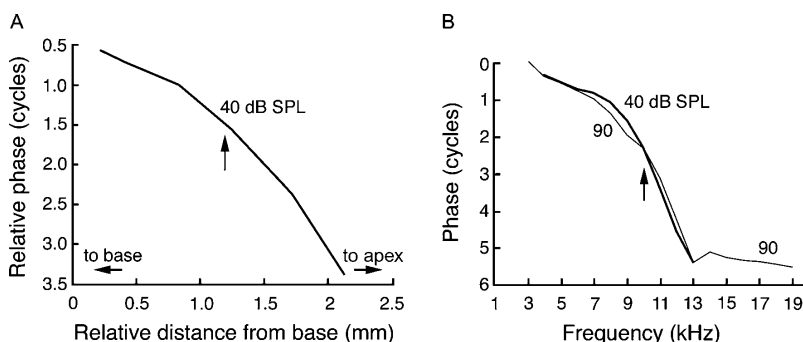


Fig. 3.14 Phase of basilar membrane response (dB SPL marked on curves). Increasing phase lags at the point of measurement are plotted downwards. (A) Phase of basilar membrane response to a 10-kHz tone, as a function of relative (not absolute) distance along the basilar membrane, in the chinchilla cochlea. The vertical arrow shows the position of the peak of the travelling wave. The wave shows increasing phase lag as it moves towards the apex of the cochlea. Reprinted from Rhode and Recio (2000), Fig. 5D, Copyright (2000), with permission from American Institute of Physics. (B) Phase of response, at a single point 3.5 mm from the base of the chinchilla cochlea, as a function of frequency of stimulation. The vertical arrow shows the characteristic frequency of the point being measured (10 kHz). Note difference in vertical scale from part A. Measurements were made at two different stimulus intensities (40 and 90 dB SPL). Phase = 0 means that displacement to scala tympani is in phase with low pressure at the eardrum. Reprinted from Ruggero *et al.* (1997), Fig. 13, Copyright (1997), with permission from American Institute of Physics.

response to a tone of fixed frequency, as a function of distance, and demonstrates a similar increase in phase with distance from the cochlear base. With this technique, the spatial restrictions of the window into the cochlea did not permit the observation of the whole length of the travelling wave and therefore the total phase change accumulated by the travelling wave along its whole length could not be measured. An alternative method is shown in Fig. 3.14B. Here, the observation is made at a single point, and the frequency of stimulation is varied. This sweeps the whole travelling wave across the point of observation, permitting the total phase shift of a wave to be measured.

The phase data show that there are three regions in the travelling wave. The phase curve has a shallow slope towards the left of Fig. 3.14A. This means that here the phase of the wave increases only a little with distance along the duct, which means that the wave travels relatively rapidly over the first part of the cochlear duct. Near the peak of the travelling wave (arrow in Fig. 3.14A), the phase changes more rapidly with distance, meaning that the wave moves more slowly as it travels through this region. We note that at the peak of the travelling wave, the total phase shift is approximately two to three cycles (shown in the frequency plot, in Fig. 3.14B), though this varies with species, frequency region and investigator. Well beyond the peak of the travelling wave, when the wave has become very small, the phase response becomes essentially flat (Fig. 3.14B). This means that the whole apical region of the cochlea beyond the region where the travelling wave is developed, known as the ‘plateau region’, vibrates in phase, though admittedly at a very small amplitude.

3.2.3 Theories of cochlear mechanics

The vibration of the cochlear partition has been investigated theoretically, initially by means of mechanical models, and more recently mathematically, through analytic approaches or with computer models. There seems to be a satisfactory explanation of the broadly tuned wave that is seen in cochleae in poor physiological condition. This will be described first. The basis of the sensitive and sharply tuned component of the wave, seen in cochleae in good physiological condition, is more controversial, and some ideas will be discussed later. The issues discussed here will be dealt with in greater detail in Chapter 5.

3.2.3.1 The broadly tuned component of the travelling wave: passive cochlear mechanics

A consensus seems to be emerging about the physical basis of the broadly tuned component of the travelling wave (see, e.g. de Boer, 1996; Patuzzi, 1996; Robles and Ruggero, 2001). In the most general terms, the wave is analogous to a wave on the surface of water. In such a water wave, once the energy is introduced, it is carried passively along the wave by the inertia of fluid motion in the horizontal direction. Gravity provides the restoring forces in the vertical direction. The passive

cochlear wave is similar, except that the restoring forces come from the stiffness of the cochlear partition (i.e. from the stiffness of the basilar membrane and all its associated structures, such as the organ of Corti and the tectorial membrane). The inertial forces include a component from the mass of the cochlear partition, as well as from the mass of the fluid. Theories are expressed in terms of either shallow-water waves (also known as long waves) in which the wavelength is long compared to the depth of the cochlear duct, or deep-water waves (also known as short waves) in which the wavelength is short compared to the depth of the cochlear duct. While the rather simpler long-wave analysis is possible well basal to the peak of the travelling wave, the wavelength becomes short near the peak, and here a short-wave analysis is necessary.

The passive cochlear travelling wave differs from a water surface wave in two respects. Firstly, it always travels from base to apex of the cochlea, whereas a water wave radiates away from the source in all directions. Secondly, the cochlear travelling wave has a particular dependence on the distance of travel along the cochlea, since unlike a water wave it grows in amplitude as it passes down the cochlea, comes to a maximum, and then declines sharply, with the position of the peak depending on the stimulus frequency. The different behaviour in these two respects is a result of the variation in the stiffness of the cochlear partition from base to apex.

It was originally shown by Békésy, and more recently confirmed by Emadi *et al.* (2004), that the cochlear partition is relatively stiff near the base and relatively compliant near the apex (see also de La RocheFoucauld and Olson, 2007). This affects the way that the partition vibrates in response to sound. Near the base, where the stiffness is high, stiffness is the most important factor governing the vibration of the partition. Vibrations here are known as stiffness-limited. Towards the apex, where the stiffness is lower, the masses and inertias of the system instead limit the vibration, and the vibration is known as mass-limited. In response to an applied force, a stiffness-limited system will always start to move before a mass-limited one. This means that when a pressure difference is applied across any one small segment of the cochlear partition, the more stiffness-limited part towards the base will move first followed by the more mass-limited part towards the apex. A wave of deflection therefore travels up the cochlea, from base to apex, the direction depending only on the gradation of compliance and not how the pressure difference is introduced.

The relative delay in the movement of the more apical portion induces longitudinal flow of the fluid, and the inertia of this flow carries the energy towards the apex. The travelling wave therefore primarily depends on the interaction between the stiffness of the partition in response to deflection and the inertia of fluid moving along the duct.

Why does the travelling wave grow in amplitude as it passes up the duct, and why is there a peak in the vibration? In order to answer this, we need to know more about how the mechanical properties of the cochlear partition vary along the duct.

Firstly, the partition becomes less stiff towards the apex so that a certain pressure difference across the partition will induce greater amplitudes of movement towards the apex. This is shown in the plot of the admittance of the membrane in Fig. 3.15A, where on the left of the diagram, for the stiffness-limited region

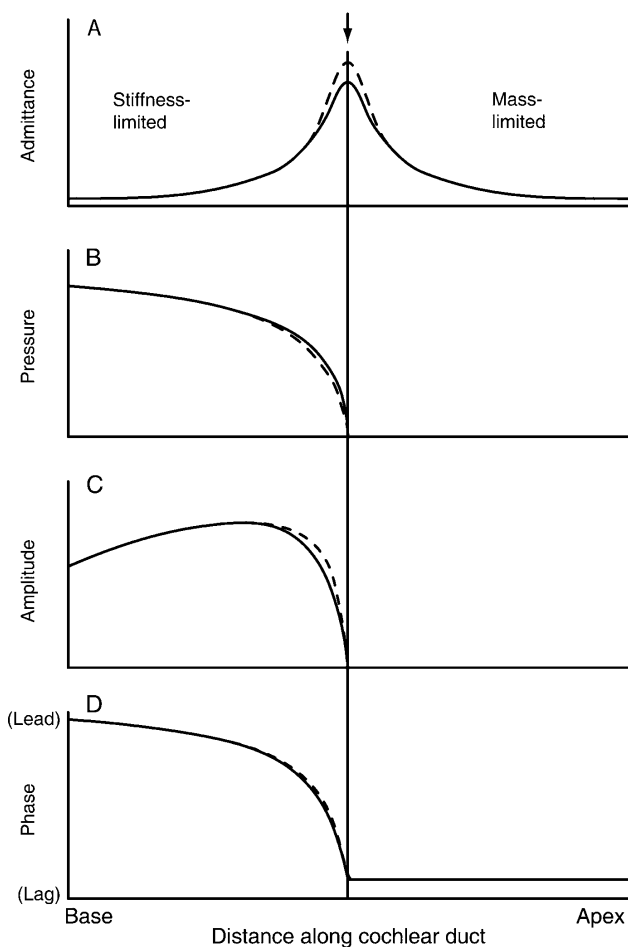


Fig. 3.15 The mechanisms giving rise to the different aspects of the broadly tuned, passive mechanical component of the travelling wave. (A) The admittance of the cochlear partition for a stimulus of one frequency is plotted as a function of distance along the cochlea. The admittance is the membrane velocity (proportional to displacement) divided by the driving pressure ratio. The admittance is highest at the resonant point (vertical line: arrow), where the effects of stiffness limitation and mass limitation cancel because they are equal in magnitude but opposite in phase. Dotted line: curve for decreased damping. (B) The pressure across the cochlear partition drops as the point of maximum admittance is reached. (C) The displacement of the cochlear partition, derived from the product of curves A and B for each point along the cochlea, shows a peak basal to the point of maximum partition admittance and a sharp drop as the point of maximum admittance is reached. (D) Phase changes along the cochlear partition.

between the base and the centre of the diagram, the admittance of the membrane increases towards the centre of the diagram, that is towards the apex.

Near the apical end of the cochlea, however, the admittance becomes low again because here the mass of the basilar membrane and cochlear fluids are large enough to limit the movement (see Fig. 3.15A, mass-limited right half). In between the stiffness-limited and the mass-limited portions, at the point of resonance, the effects of mass and stiffness become equal in magnitude while being exactly opposite in phase. Due to the phase opposition, their effects cancel, and the admittance becomes high. At this point, the partition therefore shows a relatively large amplitude of movement in response to a certain applied pressure difference across the partition.

For a wave that travels up the cochlear duct, we can trace the following sequence of events:

1. As the wave travels towards the apex, the admittance of the partition at first increases. The amplitude of vibration of the partition is derived from the product of the admittance and the pressure difference between the scalae, and so the wave grows in amplitude.
2. As the wave approaches the point of maximum admittance, the admittance of the partition increases still further and the amplitude of vibration increases further. However, towards the point of maximum admittance, the wave travels more and more slowly, and the effects of damping make the amplitude decline. Moreover, because of the high admittance of the membrane, the pressure difference is short-circuited across the membrane. For these reasons, the driving pressure across the membrane drops sharply as the point of maximum membrane admittance (i.e. the natural resonant point) is reached (see Fig. 3.15B). The amplitude of vibration, given by the product of pressure and admittance, therefore has a maximum that occurs basal to the point of maximum admittance (see Fig. 3.15C).
3. Beyond the point of maximum admittance, the movement of the partition becomes mass-limited rather than stiffness-limited. But to produce a travelling wave, we need interaction between a stiffness (in the partition) and a mass (in the fluids). Since stiffness is no longer dominant in the partition, wave motion becomes impossible. The wave therefore dies away at the point of maximum admittance, and the whole apical region of the partition moves in the same phase. The phase curve therefore becomes flat (see Fig. 3.15D).
4. Resonance occurs when stiffness and mass limitation are equal in magnitude (though opposite in phase), and this point occurs at different places along the duct, depending on the stimulus frequency. Since inertial forces are relatively greater for high-frequency stimuli, they will match the forces due to the stiffness near the relatively stiff base for high-frequency stimulation and near the apex for low-frequency stimulation. High-frequency waves therefore peak near the base of the cochlea, while low-frequency waves peak towards the apex.
5. Near the point of maximum admittance, the amplitude of the response is limited by damping, or friction, in the cochlear partition. If the damping is decreased, the peak in the admittance function becomes larger, but the travelling wave becomes

only very slightly larger and only very slightly more sharply tuned (dotted lines, Fig. 3.15).

3.2.3.2 Sharp tuning in the travelling wave: active cochlear mechanics

The principles described above have been formulated in many different mathematical and computational models of varying degrees of complexity and realism. It has been possible to adjust the model parameters so as to match Békésy's data showing a broad, low-amplitude peak in the travelling wave (e.g. Viergever and Diependaal, 1986). However, a consensus has been reached in that it does not seem possible to produce travelling waves that match the functions shown in Figs. 3.10 and 3.11. In some models, although low degrees of damping can produce large and sharply tuned peaks in the calculated travelling wave pattern, so far it has not been possible to match both the size of the peak and its relative width with the same set of parameters. If the parameters are adjusted so that the amplitude of the peak of the response is the same as measured physiologically, the width near the tip is far too narrow. The discrepancy reveals a fundamental inadequacy of the types of model that have been described so far, since very narrow peaks are intrinsic to the models if the peak size is made large.

It has been possible to produce functions similar to those in Figs. 3.10 and 3.11 only if the computations assume that there is an active source of mechanical energy in the cochlear partition that amplifies the travelling wave as it passes through. The idea that an apparently passive mechanoreceptor might contain an active mechanical process has proved fascinating to those in the field. While this model is now generally supported, the mechanisms of the motility are still controversial. Some indications of the possible basis of the active mechanical process will be evaluated in detail in Chapter 5.

The models that have succeeded in matching the experimental frequency functions have incorporated the active source of mechanical energy in a limited region on the basal slope of the travelling wave (Fig. 3.16). It is suggested that as the wave passes through this region, the hair cells are stimulated and, by an active motile process, in turn feed mechanical energy of biological origin into the travelling wave (e.g. Neely and Kim, 1986; Ashmore, 2008). The feedback makes the wave grow as it passes through the active region, which produces still more stimulation of the hair cells, and a still greater input of mechanical energy. The travelling wave grows more and more steeply. Soon, however, the wave passes beyond the region where travelling waves are possible for this particular frequency, and now the amplitude drops sharply. Models incorporating these assumptions have been able to produce tuning curves similar to those seen in basilar membrane responses and in auditory nerve fibres. It leads to the idea that the observed travelling wave has two components, a relatively small amplitude and broadly tuned wave that depends only on passive mechanical processes, as described above, and a large amplitude and sharply tuned active component superimposed on that, which is seen only in cochleae in good physiological condition.

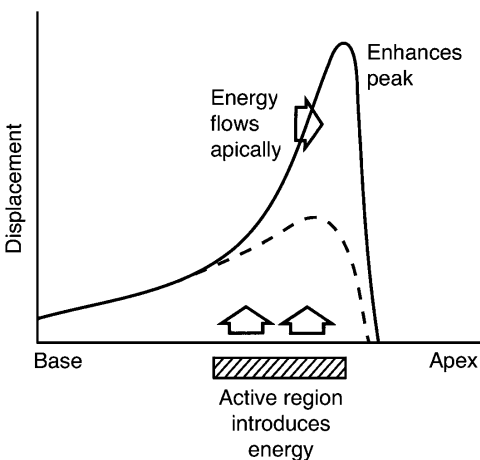


Fig. 3.16 Possible production of a sharply tuned travelling wave by a mechanically active process on the basal slope of the wave. Dotted line: passive component of the wave. The exact extent of the active region is still controversial.

Under conditions producing sharp tuning, that is with stimuli of middle and low intensity and with cochleae in good physiological condition, both the active and passive mechanical processes contribute. With cochleae in poor condition, or with stimuli of high intensity, the active mechanical component makes relatively less of a contribution, and the passive mechanical process dominates. The cochlea becomes less sensitive and less sharply tuned. As the stimulus intensity is raised, therefore, there is a gradual transition from the very sharp tuning seen at low intensities to the broader tuning of passive mechanics. This accounts for the broadening of the travelling wave, seen in Figs 3.10B and 3.11A, as the stimulus intensity is raised. The change with stimulus intensity occurs, because the passive process grows entirely linearly with stimulus intensity. The active process, however, makes a limited contribution at higher intensities because of the limited dynamic range of the mechanotransducer channels on the outer hair cells (see below).

The model explains many details of the data satisfactorily, such as why the peak of the wave is so dependent on the good physiological state of the cochlea and why manipulations of the cochlea have such a large effect on its sensitivity and sharp tuning.

It is not definitive as to what is responsible for the active mechanical process. It is clear that the movements are produced, directly or indirectly, by the outer hair cells. This is based on the finding that if outer hair cells are damaged, the sensitive and sharply tuned component of the travelling wave is lost, leaving the insensitive and broadly tuned component. Active movements of two sorts have been demonstrated in outer hair cells:

1. In response to intracellular depolarization and hyperpolarization, there is a lengthwise contraction and expansion of the outer hair cell body, mediated by

- the protein prestin, which is expressed in the cell wall (Brownell *et al.*, 1985; Zheng *et al.*, 2000a; Dallos *et al.*, 2008). While this is the favoured mechanism for the active mechanical process, it is not yet certain whether it is the only one, and it is not yet certain that the changes are of the correct type to feed back and amplify the travelling wave.
2. Ca^{2+} ions that enter through the open mechanotransducer channels may change the conformation of the mechanotransducer apparatus, leading to an output of mechanical energy that can feed back into the mechanical system (Kennedy *et al.*, 2006).

While there is evidence that both of these processes occur in the cochlea, at the moment a complete theoretical framework is lacking and the position is therefore uncertain. The arguments concerning active mechanical amplification are of necessity complex and indirect, and a more detailed evaluation will be delayed until Chapter 5 (for review, see e.g. Ashmore, 2008; see also discussion by Dallos *et al.*, 2008). Under all theories, however, the mechanical amplification that has been demonstrated uses the chemical and electrical energy that is stored in the fluid spaces of the cochlea.

3.3 THE FLUID SPACES OF THE COCHLEA

The electrochemical environment of the organ of Corti is important for the normal generation of the sharply tuned travelling wave, and for the normal operation of the transduction process. The environment is maintained by the division of the cochlear scalae into endolymphatic and perilymphatic spaces. The high positive standing potential and high K^+ concentration of the endolymph appear to play an essential role in cochlear function. They form a battery that drives both mechanotransduction and the active mechanical amplification of the travelling wave.

3.3.1 The endolymphatic and perilymphatic spaces

The labyrinthine cavity is composed of two separate compartments. The larger, outer compartment, which is formed by the scala vestibuli and the scala tympani, runs the length of the system and is filled with perilymph. There is a smaller, inner compartment also extending the entire length of the system, which is formed by the scala media, and is filled with endolymph. In the cochlea itself, the inner, endolymphatic space is bounded above by Reissner's membrane, laterally by the stria vascularis, and below by the reticular lamina on the upper surface of the organ of Corti (see also Fig. 3.1B). Figure 3.17 shows the generally accepted borders of the endolymphatic space. The ionic composition of the endolymph is very different from that of the perilymph, being high in K^+ and low in Na^+ . In accordance with this, the endolymphatic space is bounded on all sides by occluding

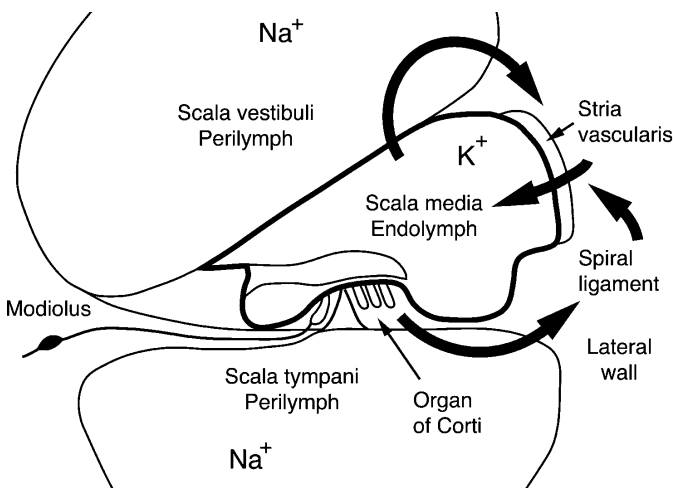


Fig. 3.17 The boundaries of the scala media, formed by occluding tight junctions, are shown by thick solid lines. The large arrows show the paths of K^+ flow (K^+ recycling). From Pickles (2007b).

tight junctions, known to inhibit the movement of ions. The positive potential and high K^+ concentration of the endolymph gives rise to a flow of K^+ out of the endolymphatic space. This may occur through the mechanotransducer channels in the hair cells, possibly through ion transporters in other cell membranes, and, deeper in the cochlear walls, through gap junctions between the cells (large arrows, Fig. 3.17). The K^+ is thereby recycled to the stria vascularis. Genetic defects in the gap junction proteins, particularly in connexin-26, are responsible for a high proportion of all inherited hearing losses (see Chapter 10).

3.3.2 The endolymph

3.3.2.1 The composition and electric potential of the endolymph

The composition of the endolymph can be measured by ion-selective electrodes. It contains a high level (150 mM) of K^+ and a low level (1.3 mM) of Na^+ . The endolymph therefore has an ionic composition approximately similar to that found intracellularly and is unique among extracellular fluids of the body for this reason (for reviews of the endolymph and the generation of the electrocochlear potential, see Wangemann, 2006 and Hibino *et al.*, 2010).

The potential within the scala media, the endocochlear potential, has been measured to be +97 to +100 mV in the basal turn, declining to +87 to +93 mV in higher turns (measured in cat, rat and mouse; Sterkers *et al.*, 1984; Wangemann *et al.*, 2004). Again, it is unique in the body for an extracellular fluid

to have such a high positive potential. Both the chemical and electrical properties of the endolymph therefore point to its having a special role in the cochlea, and many investigations of its functions have been undertaken. The evidence has supported its role in mechanotransduction and in mechanical amplification of the travelling wave.

3.3.2.2 The origin of the endolymph and the endocochlear potential

The endolymph and the endolymphatic potential are both produced by the stria vascularis. Under the light microscope, the cells of the stria vascularis can be divided into superficially located darkly staining cells, called the marginal cells, and more lightly staining basal and intermediate cells (e.g. [Spicer and Schulte, 2005](#)). Under the electron microscope, it can be seen that the marginal cells have long infoldings on the side furthest away from the endolymph and contain many mitochondria. The stria is also richly supplied with blood capillaries. The marginal and intermediate cells appear to be critical both for secreting endolymph and for maintaining its ionic and electrical state.

Although the endolymph has a high K^+ concentration and a low Na^+ concentration similar to that found inside cells, its electric potential, unlike that found intracellularly, is strongly positive. This immediately suggests that the endocochlear potential is not a simple K^+ diffusion potential as found within cells, as this would lead to a potential of the opposite sign. That is it is not due to K^+ diffusing passively down its concentration gradient out of the endocochlear space, taking positive charge with it and leaving a net negative charge behind. Nor does it seem to be a Na^+ diffusion potential, although the Na^+ concentration difference is in the right direction. [Johnstone and Sellick \(1972\)](#) increased the Na^+ concentration in scala media by perfusing with 20 mM Na^+ Ringer's solution. They found that the endocochlear potential actually increased: if it was a Na^+ diffusion potential it should have decreased, because the Na^+ concentrations in the endolymph and the perilymph had become more equal.

The positive endocochlear potential is, in contrast, closely tied to the energy-consuming, ion-pumping processes in the stria vascularis, although a diffusion potential internal to the stria vascularis itself is included in the mechanism. Anoxia, which of course inhibits the energy-consuming processes rapidly, causes the endocochlear potential to decay to zero within 1–2 min, confirming its dependence on active transport ([Johnstone and Sellick, 1972](#)). Evidence that the stria vascularis is the source of the endocochlear potential comes from several sources (for review, see [Hibino *et al.*, 2010](#)):

1. [Tasaki and Spyropoulos \(1959\)](#) destroyed Reissner's membrane so that the endolymph and the perilymph could mix. The stria vascularis was the only site from which positive potentials could then be recorded. That any potentials at all could be recorded is evidence that the endocochlear potential is not a diffusion

potential between endolymph and perilymph, because the ionic gradient would have been destroyed.

2. The stria vascularis is a site of high metabolic activity. Kuijpers and Bonting (1969) analysed Na^+/K^+ -ATPase in several structures of the cochlea and found that its activity was some 12 times higher in the stria vascularis than in any other cochlear structure. The ATPase was inhibited by ouabain, a specific inhibitor of Na^+/K^+ -ATPase, and showed a concentration function for its effect on the ATPase similar to that for its effect on the endocochlear potential (Kuijpers and Bonting, 1970).
3. Ototoxic agents such as ethacrynic acid that have a preferential effect on the stria vascularis reduce the endocochlear potential.
4. Isolated stria vascularis can generate a potential of the same sign as the endocochlear potential and will transport K^+ (Wangemann *et al.*, 1995). Microelectrode penetrations in the stria vascularis show that the marginal cells and the intrastrial fluid, in the spaces between the cells of the stria vascularis, have a high positive potential, more positive even than the endolymph (Melichar and Syka, 1987; Offner *et al.*, 1987; Salt *et al.*, 1987). These are the only positions in the cochlea from which such high positive potentials have been recorded.
5. Mice with genetic modifications that interfere with the normal expression of proteins in the stria vascularis have reduced or no endocochlear potentials (e.g. Marcus *et al.*, 2002; Gow *et al.*, 2004).

The generation of the endocochlear potential has been successfully explained by a model, known as the two-cell model, in which the endolymphatic potential is generated as a diffusion potential across the intermediate and basal cell layers (Marcus *et al.*, 2002; Fig. 3.18). The potential is generated because the K^+ concentration is maintained at very low levels (1–2 mM) within the intrastrial fluid. Therefore, K^+ has a high tendency to enter this space from the intermediate and basal cells, taking positive charge with it and driving the intrastrial fluid positive (+ 90 mV). The existence of just such a compartment within the stria vascularis, with a very high positive potential and with a very low K^+ concentration, was found by Salt *et al.* (1987) using ion-selective electrodes.

K^+ is maintained at low levels in the intrastrial space by an active transporter in the inner (intrastrial) surfaces of the marginal cells. This takes up K^+ by pumping it into the marginal cells. The transporter also produces a Na^+ gradient across the junction between the marginal cells and the intrastrial fluid, which activates a $\text{Na}^+/\text{2Cl}^-/\text{K}^+$ cotransporter, further lowering the K^+ concentration in the intrastrial fluid.

K^+ passively diffusing from the marginal cells raises the K^+ concentration of the endolymph and also communicates the high positive potential of the intrastrial fluid and marginal cells to the endolymph. Further evidence for this model has come from demonstrations of the existence of the required channels and transporters in the required locations and from mutant mice in which different channels and transporters have been knocked out (Marcus *et al.*, 2002; Wangemann, 2006).

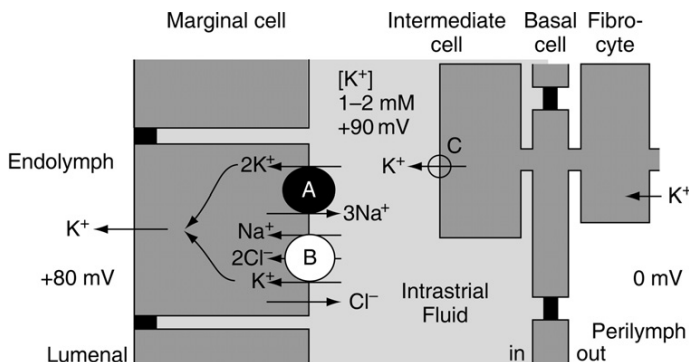


Fig. 3.18 The generation of the endocochlear potential according to Marcus *et al.* (2002) and Wangemann (2006), in a mechanism often referred to as the two-cell mechanism. The stria vascularis consists of marginal cells, intermediate cells and basal cells, the latter connected by gap junctions to the fibrocytes of the spiral ligament. The endolymphatic potential is generated as a diffusion potential across the intermediate and basal cell layer. This occurs because the K⁺ concentration is maintained at very low levels (1–2 mM) in the intrastrial fluid. Therefore K⁺ has a high tendency to enter this space from the intermediate and basal cells, taking positive charge with it and driving the intrastrial fluid positive (+ 90 mV). K⁺ is maintained at low levels in the intrastrial fluid by the ATP-consuming active transporter (A: Na⁺/K⁺-ATPase) in the inner surfaces of the marginal cells. This transporter also produces a gradient of Na⁺ concentration between the marginal cells and the intrastrial fluid. The Na⁺ gradient activates a Na⁺/2Cl⁻/K⁺-cotransporter (B: called NKCC1; also called Slc12a2), which further lowers the K⁺ concentration in the intrastrial fluid. K⁺ diffusing across the luminal surfaces of the marginal cells raises the K⁺ concentration of the endolymph and also communicates the high positive potential of the intrastrial fluid and marginal cells to the endolymph. The K⁺ channel marked C on the intermediate cell is called Kir 4.1 (also called KCNJ10). There is also a contribution from ion pumps (not shown) in the fibrocytes (Hibino *et al.*, 2010). Modified from Wangemann (2006), Fig. 2.

Once produced, the endolymph flows out of the cochlea by way of the ductus reunions, through the endolymphatic duct, and is absorbed in the endolymphatic sac. Malabsorption or obstruction of the flow causes an increase in the pressure of the endolymph, known as endolymphatic hydrops, such as is found in Ménière's disease (for review, see Salt and Plontke, 2010).

3.3.3 The perilymph

The ionic composition of the perilymph, situated in the outer fluid compartments of the cochlea, is similar to that of extracellular fluid or cerebrospinal fluid. Its electric potential is close to that of the surrounding plasma, being reported to be +7 mV in the scala tympani and +5 mV in the scala vestibuli (Johnstone and Sellick, 1972). Perilymph appears to be at least partially produced by transcellular

transport of solutes from blood plasma, likely to be via the capillaries in the walls of the perilymphatic space. In contrast to the endolymph, the perilymph has a K^+ concentration of 4–6 mM and a Na^+ concentration of 140–150 mM and is therefore similar to most other extracellular fluids (for review, see Wangemann and Schacht, 1996).

X-ray microanalysis of frozen tissue shows that the spaces within the organ of Corti have the same ionic content as perilymph (Anniko and Wroblewski, 1986). The fluid within the extracellular spaces of the organ of Corti has a potential of approximately 0 mV (Dallos *et al.*, 1982).



3.4 HAIR CELL RESPONSES

The measurement of hair cell responses was one of the important landmarks in the progress of cochlear physiology, permitting the link to be made between the mechanical responses of the basilar membrane and the electrophysiological responses of the auditory nerve. Inner hair cells of the mammalian cochlea were first recorded from by Russell and Sellick (1978). Since the very great majority of afferent auditory nerve fibres make their synaptic contacts with inner hair cells, it must be presumed that it is the job of inner hair cells to signal the movements of the cochlear partition to the central nervous system. Outer hair cells are much more difficult to record from, and we have fewer reports. The role of the outer hair cells is to amplify the mechanical travelling wave, although the exact details of the mechanisms by which they do this are still controversial.

Hair cell responses will be dealt with in terms of the resistance-modulation and battery theory of Davis (1958), as it appears in the light of more recent evidence and summarized in Fig. 3.19. The endocochlear potential and the negative hair cell intracellular resting potential combine to form a potential gradient across the apical membrane of the hair cell. Movement of the cochlear partition produces deflection of the stereocilia, as shown in Fig. 3.3. Deflection in the excitatory direction (the bundle moving towards the tallest stereocilia) opens mechanosensitive ion channels in the stereocilia, by a direct mechanical action (Fig. 3.19B). Ions are driven into the cell by the potential gradient, causing intracellular depolarization. The depolarization causes the release of transmitter, likely to be glutamate, activating the auditory nerve fibres (see Fig. 3.19A). These stages, and the evidence for them, will be dealt with in more detail in Chapter 5. Hair cell responses from non-mammalian cochleae and the vestibular system, which give basic information on the transduction process, are also dealt with in Chapter 5.

3.4.1 Hair cell responses *in vitro*

It is possible to isolate the cochlear sensory epithelium, namely the organ of Corti together with its surrounding structures, and mechanically stimulate the bundles of

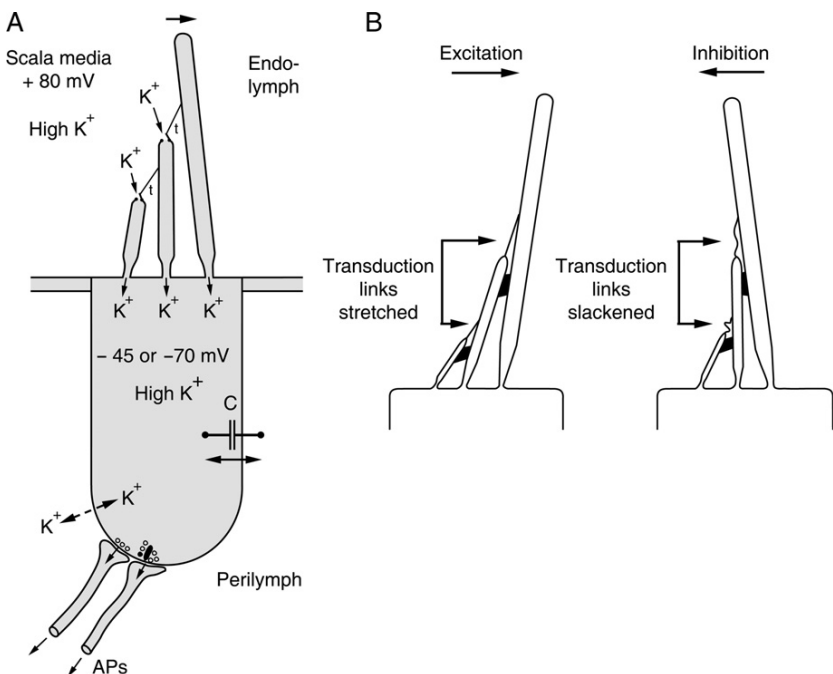


Fig. 3.19 (A) The operation of hair cells: mechanotransducer channels at the apex of the hair cells act as variable resistances. Ions flow into the cell, driven by the battery of the endolymphatic potential and the intracellular potential. Intracellular depolarization causes the release of transmitter and auditory nerve fibre activation. Increased current flow through the hair cells also makes the scala media less positive and the scala tympani more positive. The mechanotransducer channels (drawn here diagrammatically as little doors) are opened by tension on the tip links running between the tips of the stereocilia. The molecular identity of the mechanotransducer channels is not known. The large arrow shows the direction for excitatory (depolarizing) movement of the stereocilia, which is always towards the tallest stereocilia in the bundle. t, tip links. The resting potentials marked (-45 and -70 mV) are for inner and outer hair cells, respectively. (B) The tip link model for mechanotransduction, according to Pickles *et al.* (1984). Deflection of the bundle in the direction of the tallest stereocilia, which is always the excitatory direction, applies tension to the links and pulls open the mechanotransducer channels. Deflection in the reverse direction takes tension off the links and allows the channels to close. For the purposes of illustration, the deflection of the stereocilia has been massively magnified from that expected *in vivo*. From Pickles *et al.* (1984), Fig. 9.

stereocilia with either a fluid jet or an applied probe. Figure 3.20 shows responses from an outer hair cell recorded in such a manner. Similar responses have also been obtained from inner hair cells recorded *in vitro* (e.g. Russell *et al.*, 1986a,b; Jia *et al.*, 2007).

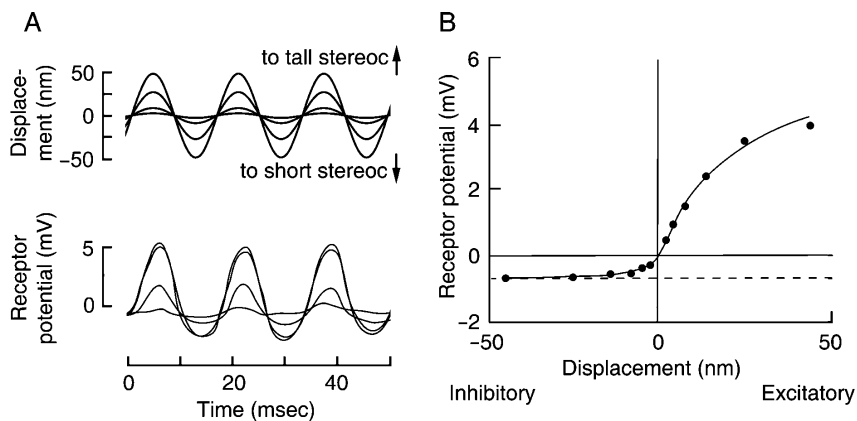


Fig. 3.20 Responses of an outer hair cell recorded *in vitro*, in cultures from neonatal mice. In these cultures, the tectorial membrane does not develop, so hair bundles can be moved directly. (A) Intracellular voltage responses to sinusoidal stimulation at 50 Hz. The top trace shows the displacement of the hair bundle at different amplitudes of stimulation. The lower trace shows the voltage response in the hair cell. The displacement of the stereocilia modulates the intracellular voltage, with an asymmetric response to the sinusoidal stimulus. Displacements in the excitatory direction (stereocilia moving towards the tallest in the bundle) produce much larger changes in intracellular voltage than displacements in the opposite direction (stereocilia moving towards the shortest in the bundle). (B) Responses of the same cell shown as an input–output function. The voltage changes (vertical axis), measured from the peaks of plots as in Part A, are plotted as a function of bundle displacement (horizontal axis). The resulting function shows the degree of channel opening as a function of displacement of the hair bundle. The dotted line shows that with a large negative displacement of the hair bundle, the intracellular voltage changes by about -0.6 mV , so the channels are only 10% open at rest. From Russell *et al.* (1986b), Fig. 5.

Movements of the hair bundle open and close the mechanotransducer channels, modulating the current through the cell. While the change in current approximately follows the waveform of the stimulus, the changes in the excitatory direction (upwards in lower part of Fig. 3.20A) are much larger than the changes in the inhibitory direction (downwards). The input–output function, which describes the moment-by-moment relation of current flow (and hence channel opening) to displacement of the hair bundle, is an asymmetric sigmoid (see Fig. 3.20B). In these particular experiments, at the resting point of the bundle (i.e. in the absence of mechanical stimulation), the channels were only slightly open, and movements in the inhibitory direction closed them completely. We can also note from Fig. 3.20B that the responses are nearly linear in the middle of the function. However, the responses also have a limited dynamic range and start to saturate for movements more than about 20 nm from the centre point of the function.

3.4.2 Inner hair cell responses *in vivo*

3.4.2.1 Intracellular potentials

The responses of inner hair cells can be measured in the intact cochlea, by impaling the cells with microelectrodes. The cells can then be stimulated by sounds delivered to the ear. Russell and Sellick (1978) found resting potentials of some -45 mV . This is rather more depolarized than most nerve cells, which commonly have intracellular potentials of some -70 mV .

In response to a tone of low frequency, in which the individual cycles of the waveform can be distinguished, the hair cells give potential changes which followed a distorted version of the input stimulus (upper traces, Fig. 3.21). These responses are generally similar to those shown in Fig. 3.20, although in this case with less distortion. As with responses recorded *in vitro*, the excursions in the positive direction are greater than the excursions in the negative direction. It is

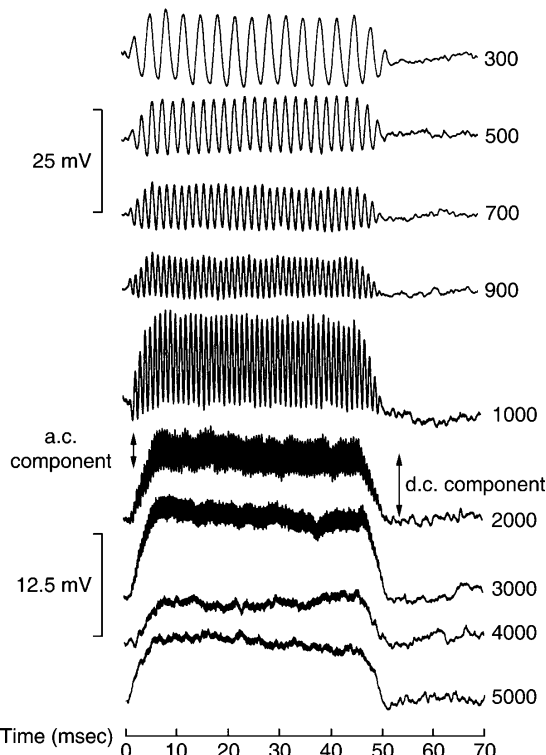


Fig. 3.21 Intracellular voltage changes in an inner hair cell for different frequencies of stimulation show that the relative size of the a.c. component declines at higher stimulus frequencies (numbers on the right of curves). Note change of scale for the lower four traces. Reprinted from Palmer and Russell (1986), Fig. 9.

therefore possible to describe the potential changes as an a.c. response at the stimulus frequency, superimposed on a sustained d.c. depolarization.

As the stimulus frequency is raised, the a.c. component of the voltage response declines relative to the d.c. component so that at frequencies of a few kilohertz and above, the a.c. component is much smaller than the d.c. component (lower traces, Fig. 3.21). Russell and Sellick (1983) ascribed this to the capacitance of the hair cell membranes. Hair cell membranes, like all cell membranes, have a capacitance, and capacitances offer a low impedance to a.c. currents at high frequencies. At high frequencies, therefore, the a.c. current was short-circuited by the low impedance of the hair cell membranes, reducing the a.c. voltage response in the cell. Because depolarization leads to the release of transmitter at the base of the hair cells, we expect the release of transmitter, to a first approximation at least, to follow the waveforms of Fig. 3.21.

3.4.2.2 Relation to basilar membrane responses

The close correspondence between hair cell responses and basilar membrane responses can be shown in several ways. Firstly, the tuning curves for inner and outer hair cells are shown in Fig. 3.22. The curves have a low-threshold, sharply

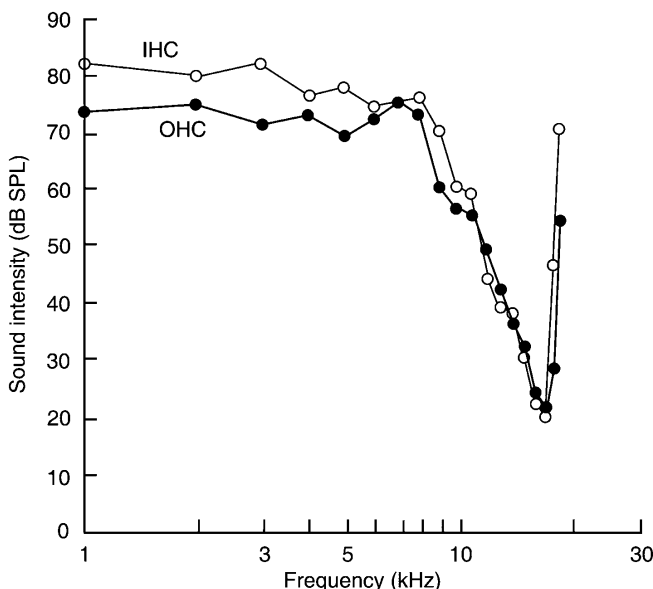


Fig. 3.22 Inner (○) and outer (●) hair cells have very similar tuning curves. The curves are also very similar to those for the mechanical response of the basilar membrane (compare to Fig. 3.11B). The IHC threshold criterion was 0.8 mV d.c. depolarization; the OHC criterion was 0.3 mV a.c. response. From Cody and Russell (1987), Fig. 7.

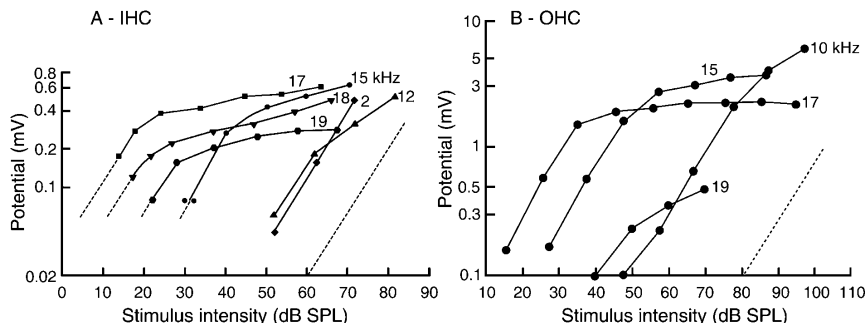


Fig. 3.23 (A) The a.c. intensity functions for an inner hair cell show an approximately linear increase in potential at the lowest intensities at each frequency, followed by a saturation. The numbers marked on the curves show the frequency of stimulation in kilohertz; this cell was most sensitive at 17 kHz. Dotted lines: slope for linear growth. From Russell and Sellick (1978), Fig. 3, modified. (B) Intensity functions for an outer hair cell are similar to those of inner hair cells. The a.c. response is plotted. In part B, but not part A, the voltages have been compensated for the attenuating effects of the current flowing through the capacitance of the hair cell walls. From Cody and Russell (1987), Fig. 6.

tuned tip, at the best or characteristic frequency (CF). There is also a high-threshold and broadly tuned tail, stretching to low frequencies. The shape is similar to that of the tuning curve for the mechanical response of a single point on the basilar membrane when the stimulus frequency is varied, as shown in Fig. 3.11B. The tuning of hair cells therefore appears to be derived from the tuning of the basilar membrane, although it is possible that there are some differences in the low-frequency tail.

Correspondingly, intensity functions for inner hair cells are similar to those of the basilar membrane mechanical response (Fig. 3.23A; compare with Fig. 3.13A). Around the characteristic frequency (17 kHz for this particular hair cell), the response grew linearly at first, at the rate of a 10-fold voltage change for a 20 dB increase in stimulus intensity, parallel to the dotted line. When the intensity was raised further, the response at and near the characteristic frequency grew non-linearly, that is with a more shallow slope (remember these are log-log scales). At frequencies above the characteristic frequency, the response saturated at a low maximum output voltage, while in contrast well below the characteristic frequency (e.g. 2 kHz), the response grew much more linearly. Again, both of these indicate that inner hair cell responses closely follow basilar membrane mechanical responses.

3.4.2.3 Input–output functions

As with hair cells recorded from *in vitro*, it is possible to make input–output functions, relating the instantaneous magnitude of the input signal to the

instantaneous magnitude of the voltage response. Figure 3.24 shows input–output functions for inner and outer hair cells measured in the third turn of the guinea pig cochlea (800 Hz place). In order to construct these curves, the amplitude of the stimulating sinusoid was varied, and the peak voltage excursions in the positive and negative directions were plotted as a function of the peak positive and negative pressure excursions in the stimulating waveform. Both the inner and outer hair cells show an asymmetric saturating sigmoidal function. As in Fig. 3.20B, the changes in the depolarizing direction are much greater than in the hyperpolarizing direction. Also as in Fig. 3.20B, the maximum depolarization is reached much more gradually and at much greater sound pressure excursions than the maximum hyperpolarization. The asymmetric functions in Fig. 3.24 show the basis for the production of the d.c. component superimposed on the a.c. component of the response. However, and in comparison with the hair cell measured *in vitro*, the zero point of the function shows that in inner hair cells the mechanotransducer channels are about 30% open at rest, compared with 10% in the hair cell of Fig. 3.20B (mechanisms determining the zero point will be described in Chapter 5).

Intensity functions (see Fig. 3.23) and input–output functions (see Fig. 3.24) for hair cells measured *in vivo* tend to saturate more sharply than either the intensity functions for the basilar membrane vibration (see Fig. 3.13A) or the

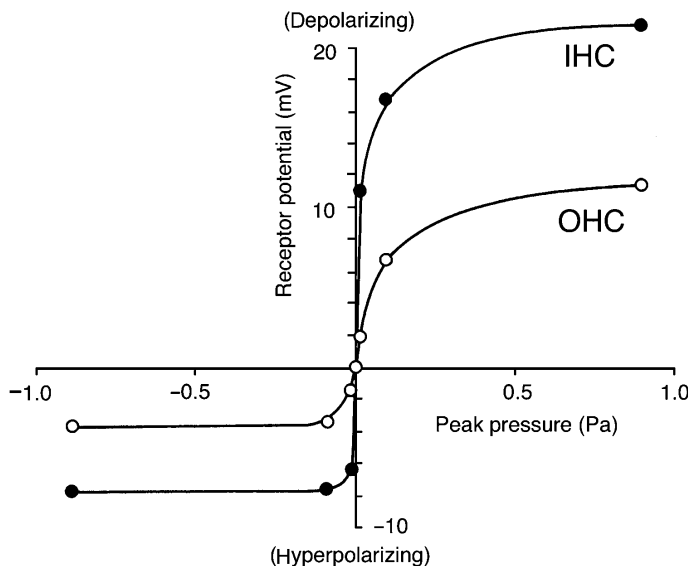


Fig. 3.24 Input–output functions for hair cells recorded *in vivo* were constructed by plotting peak voltage responses (in depolarizing and hyperpolarizing directions) as a function of the peak positive and negative pressures in the stimulus waveform. The results give asymmetric sigmoids, as in Fig. 3.20. Hair cells in the 800 Hz region (third turn) of the guinea pig cochlea were stimulated at 800 Hz. Reprinted from Dallos (1986), Fig. 8.

input–output function of hair cells stimulated directly *in vitro* (see Fig. 3.20). This is because when a hair cell is measured *in vivo* using acoustic stimulation, it is driven by two saturating processes in series (i.e. basilar membrane saturation and transducer channel saturation), rather than either alone.

3.4.3 Outer hair cell responses *in vivo*

3.4.3.1 Intracellular potentials

Outer hair cells have proved to be particularly difficult to record from. One reason may be that outer hair cells are suspended by their apical and basal ends within the organ of Corti so that an advancing electrode tends to push them aside rather than penetrate. In contrast, inner hair cells are closely surrounded on all sides by supporting cells. The position of outer hair cells halfway across the cochlear duct, rather than near the edge, may also mean that they can move more easily away from the electrode. It is also likely that stimulus-induced vibrations are greater at the outer hair cell position so that the electrode is thrown out more easily when acoustic stimulation is applied. We have only a few reports of outer hair cell recordings *in vivo*. [Dallos et al. \(1982\)](#), [Dallos \(1986\)](#), [Cody and Russell \(1987\)](#) and [Russell and Kössl \(1991\)](#) have recorded from outer hair cells in the guinea pig cochlea. They reported resting potentials to be considerably more negative than inner hair cells (-70 mV as against -45 mV). Like inner hair cells, outer hair cells can show both a.c. and d.c. voltage responses. However, the voltage responses in outer hair cells are only one-half to one-third the size of those of inner hair cells, possibly reflecting the difficulty of making the recordings.

3.4.3.2 Relation to basilar membrane responses

Like inner hair cells, outer hair cells have responses which closely follow the mechanical response of the basilar membrane. [Figure 3.22](#) shows the tuning curve for an outer hair cell a.c. response, recorded from the base of the cochlea. The frequency selectivity is very similar to that of the inner hair cell that was recorded immediately adjacent to it ([Cody and Russell, 1987](#)). [Figure 3.23B](#) shows intensity functions for the response of an outer hair cell. Again, they are generally similar to the functions of an inner hair cell (see [Fig. 3.23A](#)) and the basilar membrane (see [Fig. 3.13A](#)), although they may saturate rather more abruptly than the basilar membrane responses.

3.4.3.3 a.c. and d.c. components and input–output functions

While there is agreement about the sharpness of tuning and the general shape of the intensity functions found by the different groups of workers, there are differences in the shapes of the input–output functions and in the relative sizes of the a.c. and d.c. components of the response.

Dallos and his colleagues recorded in the apical (low-frequency) end of the guinea pig cochlea (Dallos *et al.*, 1982; Dallos, 1986). With stimulation at moderate intensities at the characteristic frequency, they showed that there was a depolarizing d.c. response superimposed on the a.c. component, in accordance with the asymmetric sigmoidal input–output function of Fig. 3.24. Unlike the position in inner hair cells, however, the function changed form as the stimulus frequency was varied, with the result that the d.c. component could become hyperpolarizing at frequencies just below characteristic frequency. If the stimulus intensity was raised, the frequency range over which depolarization could be obtained spread so that the response became consistently depolarizing.

Cody and Russell (1987), recording in the basal (high-frequency) turn of the guinea pig cochlea, found that with low-frequency stimulation, well below the characteristic frequency, the input–output function had the opposite symmetry to that shown in Fig. 3.24 – that is the changes in the hyperpolarizing direction were greater than those in the depolarizing direction. As the stimulus frequency was raised to 2 kHz and above, the input–output functions became symmetrical so that no d.c. components were generated in the response. However, at high stimulus intensities, the response became depolarizing at all frequencies, although this happened at some 90 dB SPL, a higher intensity than in the experiments of Dallos (1986).

The differences in the input–output functions of inner and outer hair cells may be partly explained by the different ways their stereocilia are coupled to the mechanical stimulus. The stereocilia of inner hair cells are not embedded in the tectorial membrane; rather they fit loosely into the groove of Hensen's stripe and are moved by fluid flow in the subtectorial space, being driven by the velocity of the movement. Hence they are unresponsive to any static offsets or biases in the position of the basilar or tectorial membranes. In contrast, the stereocilia of outer hair cells are embedded in the tectorial membrane and will be affected by such biases. The different responses that have been measured from outer hair cells suggest that such biases or offsets in the mechanical travelling wave are a complex function of cochlear region, stimulus frequency and stimulus intensity. In particular, the lack of a d.c. response in basal hair cells to high-frequency stimulation as found by Cody and Russell (1987) suggests that under these conditions, the tectorial membrane normally biases the stereocilia to the midpoint of the input–output function of Fig. 3.20.

Russell and colleagues' high-intensity depolarizing component was rather different from the d.c. components described hitherto. Unlike the other d.c. components that appeared and disappeared instantaneously with the a.c. response, the high-intensity d.c. component in basal turn outer hair cells took several cycles to develop and several cycles to disappear after the end of the stimulus. This suggests that it cannot simply be thought of as a distortion component of the a.c. response and that a description in terms of an input–output function (see Fig. 3.20) is not appropriate. They suggested that this component of the d.c. response was due to the accumulation of K^+ ions around the basal ends of the hair cells, as a result of the acoustic stimulation.

3.5 THE GROSS EVOKED POTENTIALS

When electrodes are placed in or near the cochlea, it is possible to record gross stimulus-evoked potentials that are derived from the massed activity of large numbers of the individual receptor and nerve cells. The gross evoked potentials can be divided into three groups. Firstly, the cochlear microphonic (CM) is an a.c. response that approximately follows the acoustic stimulating waveform (Fig. 3.25). The cochlear microphonic is derived mainly from the currents flowing through the outer hair cells. Secondly, there is a d.c. shift in the record, known as the summatting potential (SP), which depends on the d.c. components generated by the hair cells. Thirdly, there are a series of deflections at the beginning, and sometimes also at the end, of the stimulus, called the N_1 and N_2 neural potentials (or compound action potentials, CAP). The neural potentials are produced by the summed activity of auditory nerve fibres, producing synchronized action potentials at the onset and sometimes at the end of the stimulus.

3.5.1 The cochlear microphonic

Wever and Bray (1930) placed a wire electrode in the auditory nerve, connected to an amplifier in a room 16 m away, and from there to a loudspeaker. As they reported, ‘the action currents, after amplification, were audible in the receiver as sounds which, so far as the observer could determine, were identical with the original stimulus. Speech was transmitted with great fidelity. Simple sounds, commands and the like were easily received. Indeed, under good conditions the system was employed as a means of communication between operating and sound-proof rooms’.

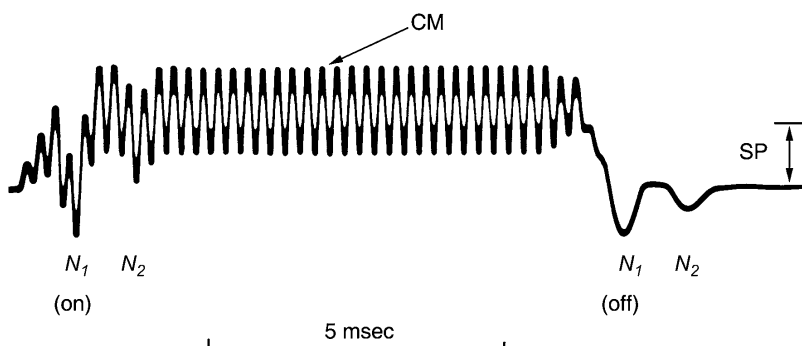


Fig. 3.25 Diagram of the response to a tone burst, recorded with gross electrodes, shows the cochlear microphonic (CM), N_1 and N_2 phases of the compound action potential (CAP) to both the beginning and the end of the stimulus and, in the d.c. shift of the microphonic from the baseline, the summatting potential (SP).

3.5.1.1 Generation

Tasaki *et al.* (1954) presented clear evidence as to the site of production of the cochlear microphonic. They advanced a microelectrode from the scala tympani, through the basilar membrane and the organ of Corti, into the endolymphatic space and the scala media. They recorded the cochlear microphonic as they advanced the electrode and showed that the microphonic reversed polarity at the same time as the endocochlear potential appeared. This fixes the site of generation of the cochlear microphonic as the border of the endolymphatic space, namely the reticular lamina. The reticular lamina is the surface carrying the transducing structures of the hair cells, the stereocilia. It is now clear that the cochlear microphonic is generated by the hair cells. When the transducer channels open so that current flows into the hair cells, making them more positive, current is drained from the scala media, making it less positive (see Fig. 3.19). When the channels shut, the current flow is reduced, and the scala media moves more positive. Potential changes are therefore produced, which in the scala media are in the opposite phase to the changes in the hair cells and the scala tympani.

3.5.1.2 Spatial localization

As might be expected from the mechanism of its production, the cochlear microphonic is spatially localized in the same way as the mechanical travelling wave.

Low frequencies give the greatest response near the apex and high frequencies near the base. The position of the peak of the response at low intensity compares well with the position of the peak of the travelling wave envelope (Eldredge, 1974). In addition, when the intensity is raised, the peak of the response moves towards the base of the cochlea. Part of the shift is due to the basalward shift in the travelling wave envelope at high stimulus intensities (see Fig. 3.10B).

Within the organ of Corti itself, extracellular microelectrodes situated near the basolateral walls of the outer hair cells will record the cochlear microphonic, in a form that is heavily dominated by the adjacent outer hair cells. This ‘organ of Corti potential’ can be used as an indicator of local outer hair cell activity and therefore can be used to draw conclusions about outer hair cell activity without the necessity of making the extremely difficult intracellular penetrations of outer hair cells (e.g. Cheatham and Dallos, 2000).

3.5.1.3 Intensity functions

With increases in intensity, responses grow similarly to those measured for the basilar membrane and outer hair cells, as shown in Figs 3.13A and 3.23B. As with the basilar membrane responses, the cochlear microphonic measured near the peak of the travelling wave grows nearly linearly only for the lowest intensities and then starts to saturate. Responses measured in the basal region of the travelling wave

grow linearly with stimulus intensity to much higher intensities (e.g. to 100 dB SPL for a 1-kHz stimulus; [Tasaki et al., 1952](#)).

The cochlear microphonic can be easily recorded using an electrode placed outside the cochlea and adjacent to it. One favourite site giving good potentials is the round window, the membrane-covered opening between the scala tympani and the middle ear cavity. For low- and mid-frequency stimuli, microphonics recorded from an electrode in this position, right at the base of the cochlea, will be dominated by the basal parts of the travelling wave. The round-window microphonics will therefore show the activity of the basal parts of the travelling wave, with their high degree of amplitude linearity, and may not show the activity produced near the peak.

3.5.2 The summatting potential

The d.c. change produced in the cochlea in response to a sound is known as the summatting potential (SP) and is visible as a baseline shift in the recorded signal of [Fig. 3.25](#). Depending on the circumstances, it is recorded as a sustained positive or negative deviation in the scala media during acoustic stimulation. The summatting potential has correlates in the d.c. stimulus-evoked potentials in hair cells and is probably derived directly from them. When the input-output functions of hair cells are such as to produce intracellular d.c. depolarization of the hair cells, the d.c. component of the current into the cells is greater than normal. The scala media will tend to move more negative, because of the K⁺ ions moving out of the scala media, and the scala tympani will tend to move more positive. Because the intracellular d.c. depolarizations or hyperpolarizations of outer hair cells change with the stimulus parameters in a complex way (see [Section 3.4.3](#)), and differently from those of the inner hair cells, the summatting potential can be affected in a similarly complex way. In addition, other changes in potential, such as those ascribed to the accumulation of K⁺ ions within the organ of Corti after acoustic stimulation ([Cody and Russell, 1987](#)) and those resulting from possible metabolic changes from structures such as the stria vascularis, will also contribute.

3.5.3 The gross neural potentials

Electrodes that are too large to record from single neural elements can nevertheless record summed neural activity produced by the simultaneous activation of many neurones. An electrode in or near the cochlea will record a gross neural response, or compound action potential, of the cochlea to a click or to a tone onset, as in [Fig. 3.25](#).

The two dominant waves of the gross neural response are known as N₁ and N₂, the first coming about 1 msec after the start of the microphonic and the second about 1 msec after that. As the intensity is raised from low levels, N₁ is the first to appear, followed at higher intensities by N₂. At still higher intensities, the response becomes more complex, with the appearance of other components of different latency. The gross potential is interpreted as the summed effect of massed action

potentials travelling in a volley down the auditory nerve. Detailed experiments have supported this conclusion. An analysis of the mechanisms behind this potential is useful because it is the gross potential, rather than the activity of single fibres of the auditory nerve, that can be recorded clinically.

Özdamar and Dallos (1978) sampled the activity of auditory nerve fibres in response to tone bursts. The N_1 potential occurred at the same time as the first action potentials triggered in the auditory nerve fibres, and the N_2 potential occurred at the same time as the action potentials immediately following, though a contribution from the cochlear nucleus could not be ruled out. With high-frequency tone pips (4 kHz and above), the greatest contribution to the N_1 and N_2 potentials was made by fibres tuned to the stimulus frequency, and this was true for both high- and low-intensity stimuli. On the other hand, with low-frequency tone pips, fibres tuned to the frequency of the tone pip made the greatest contributions only for low-intensity stimuli. At higher intensities, fibres innervating more basal regions dominated the response. This occurred because as the stimulus intensity was raised, auditory nerve fibres of a wider range of characteristic frequencies became activated (due to the basalward spread of the travelling wave at high intensities, shown in Fig. 3.10B). A gross summed potential can be produced only by neural action potentials that are substantially in synchrony. The travelling wave travels most rapidly over the basal part of the cochlea, and more and more slowly thereafter (Figs. 3.8 and 3.14). Therefore, with a low-frequency stimulus of high intensity that activates fibres of a wide range of characteristic frequencies, it is only the fibres from the high-frequency, basal, region that will be activated in synchrony. We therefore expect fibres from the basal region to dominate the grossly recorded N_1 and N_2 potentials under these stimulus conditions, since the gross potentials summate responses over many fibres.



3.6 SUMMARY

1. The cochlea is a coiled tube, divided lengthways into three scalae. The three divisions are known as the scala vestibuli, the scala media and the scala tympani. The two outer scalae, the scala vestibuli and the scala tympani, contain perilymph, which is like normal extracellular fluid in composition, and is at or near ground potential. The scala media contains endolymph, which is more like intracellular fluid, and has a positive potential. The positive potential is generated as a diffusion potential across the intermediate and basal cell layers of the stria vascularis, driven by concentration gradients arising from Na^+/K^+ -ATPase and $\text{Na}^+/2\text{Cl}^-/\text{K}^+$ -ATPase ion pumps in the stria vascularis.
2. The organ of Corti contains the auditory transducers. The organ sits on the basilar membrane dividing the scala media from the scala tympani. The transducing cells are called hair cells. Hair cells are of two types, known as inner and outer hair cells. They have many hairs, or stereocilia, projecting from

their apical surface. Deflection of the hairs initiates transduction, via a pull on the tip links between the stereocilia, which opens the mechanotransducer channels near the tips of the stereocilia by a direct mechanical action. The molecular identity of the mechanotransducer channels is not known.

3. Deflection of the hairs is produced by deflection of the basilar membrane. The latter occurs as a result of a sound-induced displacement of the cochlear fluids, which interacts with the stiffness of the basilar membrane, to produce a progressive travelling wave on the membrane. The wave passes up the cochlea from base to apex.
4. Travelling waves produced by sounds of high frequency come to a peak near the base of the cochlea. High-frequency sounds are therefore transduced near the base of the cochlea. The travelling wave produced by low-frequency sounds comes to a peak further up the cochlea, and low-frequency sounds are transduced near the apex.
5. The travelling wave has a sharply tuned peak. The sharp peak underlies the sensitivity and frequency selectivity shown by the rest of the auditory system, and indeed the sensitivity and frequency selectivity shown by the whole organism. The sharply tuned peak arises because the outer hair cells, when stimulated by the movement, make an active mechanical response which amplifies the vibration of the basilar membrane as the travelling wave passes through. The travelling wave therefore increases in amplitude as it passes along the cochlear duct, until it dies away abruptly when it reaches a point where the cochlear partition can no longer sustain vibrations of that particular frequency. This point is nearer to the base for high-frequency stimuli and nearer to the apex for low-frequency stimuli.
6. The active amplification has its largest effect at low stimulus intensities. At higher intensities, it makes a smaller contribution. The result is that the basilar membrane moves with a compressive non-linearity, that is the response does not grow as fast as the input. This has an important functional consequence, because it allows the auditory system to discriminate stimuli over a very wide range of stimulus intensities.
7. Deflection of the stereocilia by the travelling wave, by opening and closing ion channels in the stereocilia, modulates the current being driven into the hair cells by the combined effects of the positive endocochlear potential and the negative intracellular potential. The current produces potential changes that can be measured in the hair cells with fine microelectrodes, and grossly in the cochlea with larger electrodes.
8. Inner hair cells have resting potentials of about -45 mV . They produce both an a.c. voltage and a steady d.c. depolarization in response to sound. The potentials have sharp tuning curves and amplitude functions similar to those shown by the basilar membrane vibrations. Outer hair cells have resting potentials of about -70 mV . They show a.c. potential changes in response to sound and, depending on the circumstances, either no, or a depolarizing, or a hyperpolarizing, d.c. response. Like inner hair cells, they show sharp tuning curves and amplitude functions similar to those shown by basilar membrane vibrations.

9. The potential changes in inner hair cells serve to govern the release of the neurotransmitter glutamate, to produce action potentials in the auditory nerve fibres. Outer hair cells amplify the mechanical travelling wave, producing a mechanical motile response in the hair cells. The motile response may arise from one or both of the following: (1) a lengthwise contraction and expansion of the outer hair cell body in response to intracellular depolarization and hyperpolarization or (2) Ca^{2+} ions entering through the open mechano-transducer channels, which may change the conformation of the mechano-transducer apparatus, leading to an output of mechanical energy that can feed back into the mechanical system.
10. The cochlear microphonic is the extracellular correlate of the a.c. current flowing through hair cells. It is generated predominantly by outer hair cells. The summing potential is primarily the extracellular correlate of the d.c. component of the current flowing through hair cells. Depending on circumstances, it can be recorded as either a positive or a negative shift in the scala media and probably receives contributions from both inner and outer hair cells, and possibly from other sources.
11. The massed synchronized activity of auditory nerve fibres, called the compound action potential (CAP) or the N_1 and N_2 potentials, can be recorded with gross electrodes in response to stimulus onsets.



3.7 FURTHER READING

Cochlear anatomy has been reviewed by Santi and Mancini (2005) and hair cell biology by Schwander *et al.* (2010). Differences in cochlear anatomy between animals and human beings have been reviewed by Felix (2002). The anatomy of the auditory nerve (with an emphasis on its central connections) has been reviewed by Nayagam *et al.* (2011). Molecular information on the mechanotransducer channel has been reviewed by Fettiplace (2009). Cochlear mechanics have been reviewed by Robles and Ruggero (2001), and by Ashmore (2008). Mechanically active processes in the cochlea have been reviewed in several chapters of Vol. 30 of the Springer Handbook of Auditory Research ‘Active Processes and Otoacoustic Emissions in Hearing’ (2008), eds G.A. Manley, R.R. Fay and A.N. Popper. The electrochemical environment of the cochlea has been reviewed by Wangemann and Schacht (1996), Wangemann (2006) and Hibino *et al.* (2010). Hair cell responses have been reviewed by Kros (1996). The genetics of deafness and their relation to basic cochlear anatomy and physiology have been reviewed by Richardson *et al.* (2011) and Schwander *et al.* (2010). Mechanisms of transduction and of cochlear pathology are further dealt with in Chapters 5 and 10 of the present work.

THE AUDITORY NERVE

We now have a comprehensive description of the responses of auditory nerve fibres to a variety of stimuli in normal, albeit anaesthetized, animals. We also understand some of the changes that occur in auditory nerve activity during cochlear pathology. The responses of auditory nerve fibres underlie the responses of the later stages of the auditory system and closely relate to the psychophysical capabilities of the intact organism. For these reasons, knowledge of the material presented in this chapter is essential for the understanding of the later chapters on the central auditory system (Chapters 6–8), psychophysical correlates of auditory physiology (Chapter 9) and sensorineural hearing loss (Chapter 10). Those whose interest is primarily in Chapter 10 need here only read up to and including Section 4.2.2.



4.1 ANATOMY

Auditory nerve fibres, with their cell bodies in the spiral ganglion, provide a direct synaptic connection between the hair cells of the cochlea and the cochlear nucleus. Each ear has about 50 000 fibres in cats and 30 000 in human beings (Harrison and Howe, 1974a; Felix, 2002). The very great majority (90–95%, depending on species) of auditory nerve fibres make their synaptic contacts directly and exclusively with the inner hair cells (Spoendlin, 1972; Liberman *et al.*, 1990). A diagram summarizing Spoendlin's scheme is shown in Fig. 3.6. The reader is reminded that the fibres innervating the inner hair cells innervate the hair cells nearest to their point of entry into the cochlea, whereas those innervating the outer hair cells run basally for about 0.6 mm before terminating. About 20 afferent fibres innervate each inner hair cell, whereas about 6 fibres innervate each outer hair cell. Each fibre to the inner hair cells connects with one and only one hair cell, whereas those to the outer hair cells branch and innervate about 10 hair cells (Simmons and Liberman, 1988). Differentiation in the targets is associated with a morphological differentiation in the cell bodies and axons. A total of 95% of cells (in cats) connect with the inner hair cells, have bipolar cell bodies in the spiral ganglion, and have myelinated cell bodies and axons (Spoendlin, 1978). They are called Type I cells. Type II cells connect with outer hair cells, are monopolar and are not myelinated. Retrograde transport of horseradish peroxidase from the cochlear

nucleus to the cochlea confirms that both types send axons to the cochlear nucleus (Ruggero *et al.*, 1982).

It is generally thought that the very great majority of auditory nerve responses have been measured from Type I cells. Type I cells are typically driven strongly by tones and can show high levels of spontaneous activity. We have only one confirmed instance, by tracing a horseradish peroxidase injection, of a record from a Type II cell (Robertson, 1984; see also Robertson *et al.*, 1999). Here, the cell was silent in response to acoustic stimulation. We do not therefore know the function of the Type II system in audition, although some ideas will be discussed in Chapter 5.

4.2 PHYSIOLOGY

We must assume, provisionally at least, that all, or substantially all, the auditory nerve fibres or cells that have been recorded from innervate the inner hair cells. Although our knowledge of the responses of inner hair cells is still relatively sketchy, we do have a fairly complete knowledge of the responses of the auditory nerve. Our knowledge has accumulated over the past 50 years or so and has depended on a careful control of stimulus and physiological parameters, together with the surveying of large populations of fibres, sometimes as many as 418 fibres in one animal (Kim *et al.*, 1980). This has been achieved in spite of the inaccessibility of the nerve deep in the bone, and the lack of mechanical stability of the adjacent brainstem, which means that nerve fibres can easily be lost in recording. In fact, it was not until 1954 that the first responses of auditory nerve fibres were published (Tasaki, 1954), and it is now recognized that the records indicate that the cochlea must have been in poor physiological condition. Tasaki's approach was to drill through the temporal bone until the auditory nerve was encountered in the internal auditory meatus. The approach commonly used nowadays is to open the occipital bone at the back of the skull and, by inserting a retractor around the edge of the cerebellum, to retract the cerebellum and the brainstem medially away from the wall of the skull until the stub of the nerve running between the internal auditory meatus and the cochlear nucleus becomes visible. Microelectrodes can then be inserted under direct vision. Alternative approaches are to record from cells of the spiral ganglion directly through holes in the cochlear wall or to record from within the internal auditory meatus by means of microelectrodes inserted stereotactically through the brainstem. When appropriate measures are taken to stabilize the preparation, fibres or cells can now be recorded for many tens of minutes, compared with the 10 sec or so managed by Tasaki.

With microelectrodes with a tip size 0.3 µm or less, single fibres can be recorded from and give waveforms corresponding to those in Fig. 4.1. Many fibres show random spontaneous activity. There is a highly asymmetric distribution of spontaneous discharge rates. About a quarter of the fibres discharge at below 20/sec, and most of these discharge at 0.5/sec or less. The other fibres have a mean

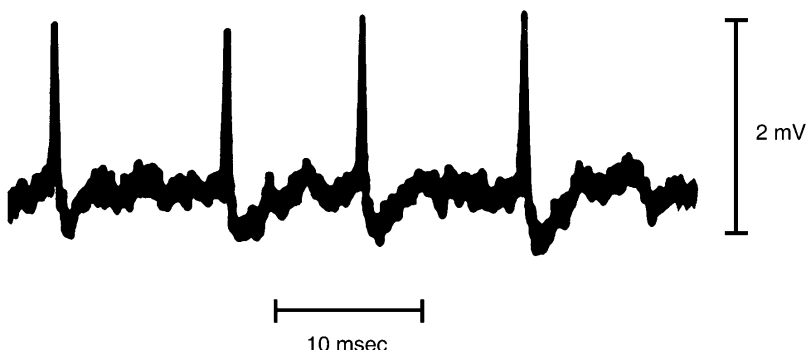


Fig. 4.1 Action potentials recorded extracellularly from a single auditory nerve fibre. The waves are initially positive and nearly monophasic. By courtesy of G. Leng.

rate of 80–100 discharges/sec, with a maximum of 160/sec (Liberman and Kiang, 1978; Temchin *et al.*, 2008b).

4.2.1 Response to tones

4.2.1.1 Threshold responses and frequency selectivity

Fibres are responsive to single tones, and in the absence of other stimuli the tones are always excitatory and never inhibitory. The responses can be demonstrated by means of a post- (or peri-) stimulus-time histogram (PSTH). In making such a histogram, a stimulus is presented many times, and the occurrence of each action potential is plotted on the histogram by incrementing the count in the column, or bin, corresponding to the time after the beginning of the stimulus. Tone bursts produce a sharp onset response, which drops rapidly over the first 10–20 msec (Fig. 4.2), and then more and more slowly over the next several minutes. The fibres can be characterized by their threshold as a function of frequency of the tone. The intensity of a tone burst is adjusted until an increment in firing is just detectable. This increment is commonly between 5 and 30 spikes/sec, depending on the spontaneous firing rate of the fibre and the method used to detect the increment. The procedure is repeated for different frequencies of stimulation. Examples of the resulting tuning curves relating threshold to frequency are shown in Fig. 4.3. Each fibre has a low threshold at one frequency, the ‘characteristic’ or ‘best’ frequency, and the threshold rises rapidly as the stimulating frequency is changed.

Figure 4.3 shows the typical change in shape of tuning curves across frequencies, if the frequency scale is logarithmic. At low frequencies, below 1 kHz, tuning curves are nearly symmetric. At higher frequencies, the curves become increasingly asymmetric, with steep high-frequency slopes and less steep low-frequency slopes. A distinction between two parts of the tuning curve also becomes obvious in high-frequency units. There is a very sensitive, frequency-selective ‘tip’

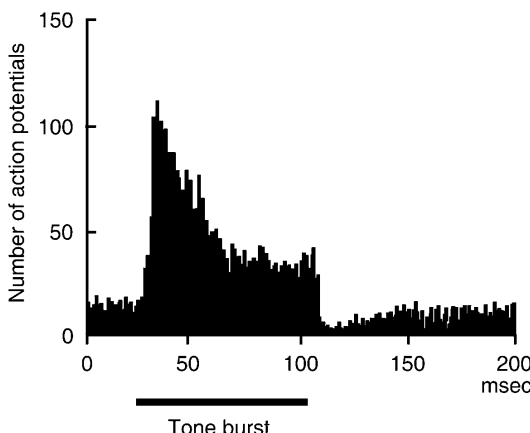


Fig. 4.2 Single fibres of the auditory nerve show an initial burst of activity at the beginning of a tone burst, a gradual decline and a transient off-suppression of the spontaneous activity at the end of the stimulus. Here, a post-stimulus-time histogram was made by presenting tone bursts many times and incrementing the count at the corresponding point on the histogram whenever an action potential occurred. Author's data.

of the tuning curve and a long, broadly tuned 'tail', stretching to low frequencies. The tail has a broad dip around 1 kHz. This is probably derived from the boost given to the input by the middle ear characteristics, since it disappears if the stimulus intensity is plotted with respect to constant stapes velocity (Kiang *et al.*, 1967). Single auditory nerve fibres therefore appear to behave as bandpass filters, with an asymmetric filter shape. The frequency selectivity is generally similar to that of the basilar membrane and the hair cells, from which the frequency selectivity is derived (see Figs. 3.11B and 3.22; Ruggero *et al.*, 1997). All mammals investigated show tuning curves broadly similar to those of Fig. 4.3, although details such as the degree of frequency selectivity and the depth of the tip may vary from species to species.

Liberman (1978) showed that there is a 60–80 dB spread of fibre thresholds at any one characteristic frequency. Ninety per cent of fibres have high spontaneous firing rates and have thresholds within the bottom 10 dB of the range. The remainder, which have medium and low spontaneous rates, are spread over the rest of the range (Fig. 4.4).

Intracellular labelling of nerve fibres after electrophysiological recording shows that fibres with different thresholds and spontaneous rates can innervate the same inner hair cell. The differences must therefore be due to differences in the fibres or synapses, rather than to differences in the hair cells themselves (Tsuiji and Liberman, 1997). In addition, there are anatomical variations in the fibres with different physiological properties. Fibres with high levels of spontaneous activity are thicker than the others and innervate the pillar (i.e. the non-modiolar or outer hair cell)

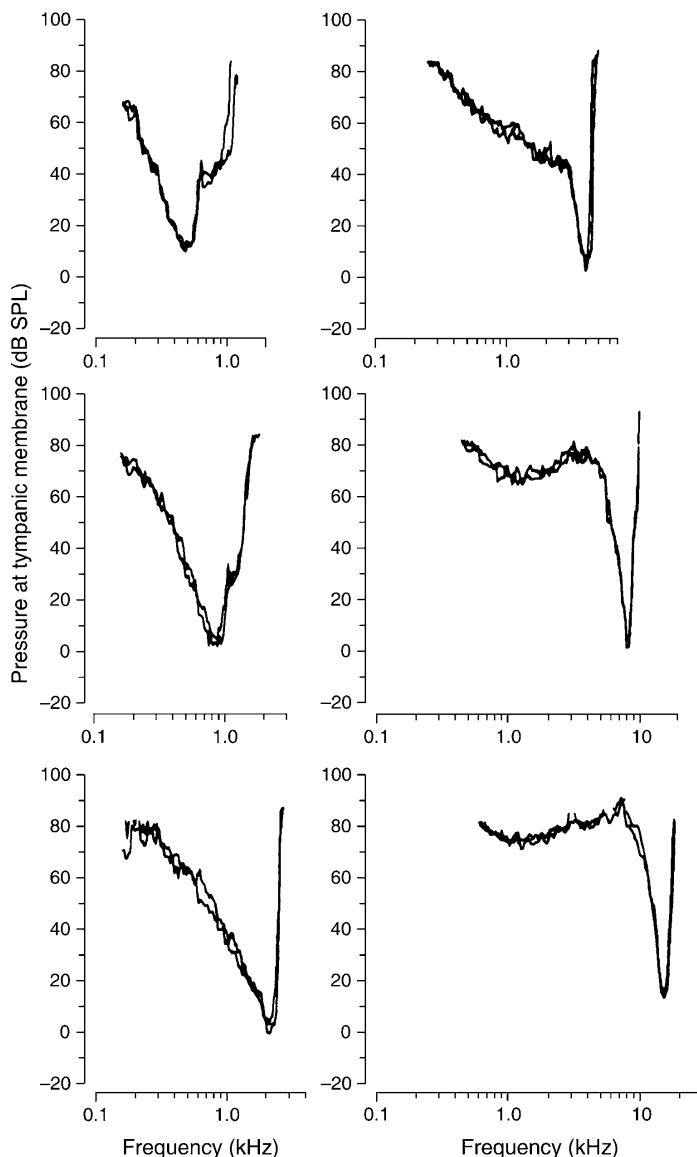


Fig. 4.3 Representative tuning curves (FTC) of cat auditory nerve fibres are shown for six different frequency regions. In each panel, two fibres from the same animal of similar characteristic frequency and threshold are shown, indicating the constancy of tuning under such circumstances. From Liberman and Kiang (1978), Fig. 1.

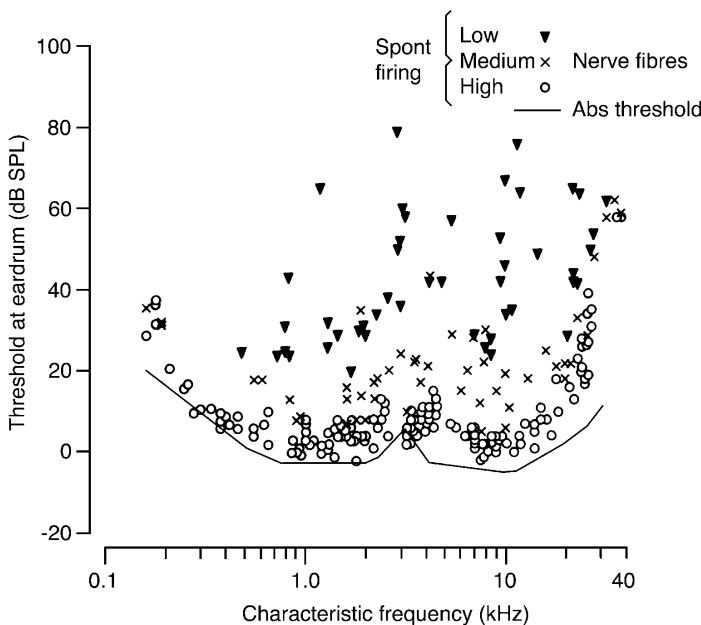


Fig. 4.4 Distribution of best thresholds of auditory nerve fibres in a cat. Fibres with high spontaneous firing rates (\circ , $>18/\text{sec}$) have low thresholds, and those with low spontaneous firing rates (\blacktriangledown , $<0.5/\text{sec}$) have high thresholds. Fibres with intermediate spontaneous firing rates (\times) have thresholds in between. The behavioural absolute threshold of the cat, expressed in terms of the intensity at the eardrum, lies just below the lowest thresholds of the auditory nerve fibres. Neural data from Liberman and Kiang (1978), Fig. 2. Behavioural data from Elliott *et al.* (1960).

and more apical (i.e. nearer the cuticular plate) pole of the inner hair cells, while fibres with low and medium rates of spontaneous activity are finer and innervate the modiolar and more basal pole (Liberman, 1982; Tsuji and Liberman, 1997; Liberman *et al.*, 2011). One suggestion is that neurons with lower thresholds have larger postsynaptic receptor patches facing the hair cells (Liberman *et al.*, 2011; see Chapter 5).

The degree of frequency selectivity has been expressed in two ways. One is by the slopes of the tuning curve above and below the characteristic frequency. The slopes are a function of the characteristic frequency of the fibres concerned, with, in many species, the fibres in the 10-kHz region having the steepest slopes. Here the high-frequency slopes measured between 5 and 25 dB above the best threshold range from 100 to 600 dB/octave, and the low-frequency slopes from 80 to 250 dB/octave (Evans, 1975). Further up the slope of the tuning curves, the low-frequency slopes become shallower as the ‘tail’ is approached, but the high-frequency slopes become even steeper, sometimes increasing to as much as 1000 dB/octave (Evans, 1972).

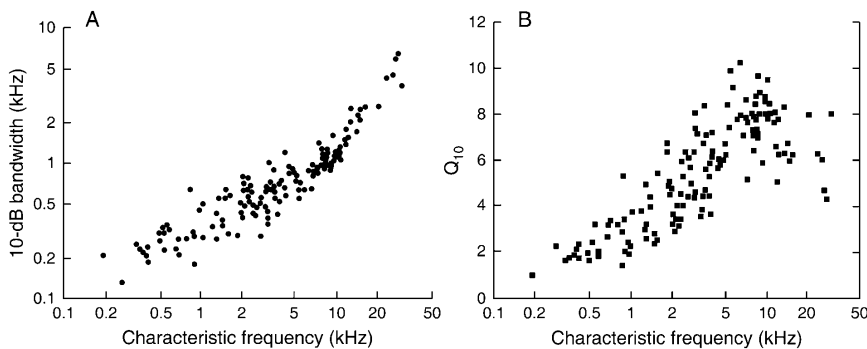


Fig. 4.5 (A) The bandwidths of tuning curves of cat auditory nerve fibres are plotted as a function of the fibres' characteristic frequency. Here, the bandwidths were measured 10 dB above the best threshold. Data calculated from Q_{10} s of Evans (1975). (B) Q_{10} s of auditory nerve fibres are shown as a function of characteristic frequency. ($Q_{10} = \text{CF}/\text{bandwidth measured 10 dB above best threshold}$.) From Evans (1975), Fig. 10, with kind permission of Springer Science and Business Media.

A second way that resolution can be expressed is by measuring the bandwidth of the tuning curve at some fixed intensity above the best threshold. By analogy with the practice in the measurement of the bandwidths of electrical filters, it might be thought appropriate to measure the half-power bandwidth, that is the bandwidth 3 dB above the best threshold. However, because it is difficult to measure thresholds sufficiently accurately, bandwidths 10 dB above the best threshold have been used instead. The 10-dB bandwidths plotted as a function of characteristic frequency show a restricted spread (Fig. 4.5A). A related way in which the resolution can be expressed is by analogy with the electrical 'quality' or 'Q' factor of a filter, defined as the centre frequency divided by the bandwidth, the bandwidth here being defined at 10 dB above the best threshold. The quality factor so defined is called Q_{10} or $Q_{10\text{dB}}$, and a high-quality factor, or high Q_{10} , corresponds to a narrow bandwidth. Figure 4.5B shows that for cats the minimum relative bandwidth occurs around 10 kHz, where it averages about one-eighth of the characteristic frequency. Comparable values have been measured for basilar membrane and hair cell responses (Russell and Sellick, 1978; Sellick *et al.*, 1982; Ruggiero *et al.*, 1997; see also Robles and Ruggiero, 2001 for review, and Temchin *et al.*, 2008a for a cross-species review of the data).

4.2.1.2 Response to tones as a function of stimulus intensity

The tuning curves of Fig. 4.3 show the intensity necessary to raise the firing rate above the spontaneous rate by a certain criterion amount, plotted as a function of stimulus frequency. We can also measure the firing rate as a function of intensity for different frequencies, giving rate-intensity functions (Fig. 4.6A). The functions show a sigmoidal shape, and for stimuli of the characteristic frequency they

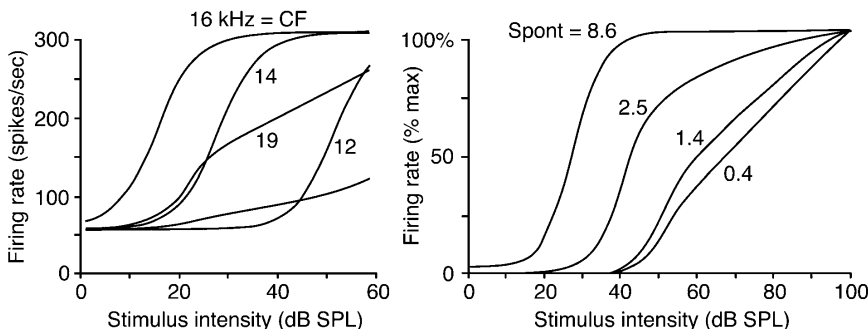


Fig. 4.6 (A) Rate-intensity functions are shown for one auditory nerve fibre for different frequencies of stimulation (marked on curves in kHz). At the characteristic frequency (16 kHz), the fibre goes from threshold to saturation (= dynamic range) in about 30 dB. At frequencies below the characteristic frequency (CF), the rate-intensity function in this fibre is as steep as at characteristic frequency. Above the characteristic frequency, however, the slope of the function is shallower. This behaviour is similar to that of the basilar membrane. (B) Rate-intensity functions measured at the characteristic frequency, for four fibres of different thresholds and different spontaneous firing rates (numbers on curves). The low-threshold fibre with the high spontaneous firing rate (8.6/sec) has a steep rate-intensity function, with a dynamic range of about 30 dB. Fibres of higher threshold, and with lower spontaneous firing rates, have functions with shallower slopes and wider dynamic ranges. All fibres illustrated had CFs in the range 19–20 kHz. From Yates *et al.* (1990), Figs. 1 and 2A, Copyright (1990).

saturate at an intensity some 20–50 dB above the threshold at that frequency. For stimuli below the characteristic frequency, the functions are as steep as at the characteristic frequency, or steeper. Above the characteristic frequency, however, the slope is shallower and the dynamic range is greater (see Fig. 4.6A). The intensity behaviour of the auditory nerve mirrors that of the basilar membrane, which shows a generally similar dependence on frequency in relation to the characteristic frequency, although it does not saturate quite so sharply (see Fig. 3.13A). The sharper saturation of auditory nerve firing can be ascribed to the other stages of the system, such as limitations in the maximum sustained firing rate that is possible.

Fibres of different spontaneous firing rate and threshold also have different slopes in their rate-intensity functions. Low-threshold fibres have steep rate-intensity functions and narrow dynamic ranges. In contrast, high-threshold fibres have much shallower rate-intensity functions ('sloping saturation' or 'straight' functions; Fig. 4.6B). These high-threshold fibres also tend to have much wider dynamic ranges (e.g. 60 dB), and at the characteristic frequency some are able to signal changes in stimulus intensity up to the highest stimulus intensities tested. The shallower slopes and sloping saturations of high-threshold fibres reflect the shallow slopes of the basilar membrane intensity functions to characteristic frequency tones at high stimulus intensities (see Fig. 3.13A, Yates *et al.*, 1990).

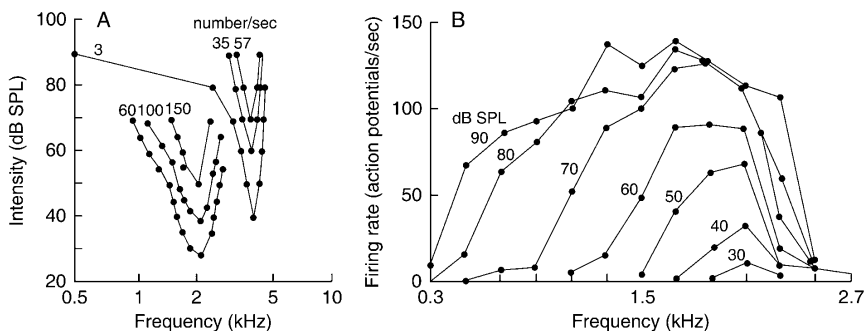


Fig. 4.7 (A) Tuning curves constructed at different firing rate criteria (rate shown by numbers on curves) show that frequency resolution can be maintained at higher rate criteria as long as the fibre is not driven into saturation. From Evans (1975), Fig. 13, with kind permission of Springer Science and Business Media. (B) Iso-intensity functions of auditory nerve fibres show that at the lowest intensity the greatest response is produced by tones near the CF, but that at higher intensities the most effective frequency moves to lower frequencies (for CFs above 1 kHz). Numbers on curves: intensity in dB SPL. Used with permission from Rose *et al.* (1971), Fig. 2B.

The suprathreshold response can be plotted in three ways. We can, as in Fig. 4.6, plot the firing rate at a constant frequency for different intensities of stimulation (rate-intensity functions). We can also continue the analogue of the frequency threshold curve to higher firing rates by plotting the combinations of intensities and frequencies necessary to evoke a constant increment in firing rate, giving iso-response or iso-rate contours (Fig. 4.7A). Or the firing rate can be plotted as the frequency is varied, the curves then being called iso-intensity plots (see Fig. 4.7B). Each of the ways is best for showing a different property. The iso-rate, iso-response or tuning curves are best at showing the degree of frequency selectivity, at least for intensities below saturation. These curves show that the frequency selectivity can stay the same or indeed become sharper as a higher rate criterion is used (see Fig. 4.7A), although resolution may deteriorate at still higher stimulus intensities. The iso-intensity functions show that the frequency evoking the highest firing rate can shift as the intensity is raised, moving upwards for fibres with characteristic frequencies below 1 kHz and downwards for fibres with characteristic frequencies above 1 kHz (see Fig. 4.7B). The curves in Fig. 4.7A are similar to the tuning curves for the basilar membrane shown in Fig. 3.11B. Correspondingly, the curves in Fig. 4.7B are similar to the iso-intensity curves for the membrane in Fig. 3.11A.

4.2.1.3 Temporal relations

In response to sinusoids of high frequency, auditory nerve fibres fire with equal probability in every part of the cycle of the stimulus. At lower frequencies,

however, it is apparent that the spike discharges are locked to one phase of the stimulating waveform. That is not to say that each fibre fires once every cycle: the fibres fire randomly, perhaps as little as once every 100 cycles on average. But when they do fire, they do so in only one phase of the stimulus. The phase locking can be most easily demonstrated by means of a period histogram. In making a period histogram, the occurrence of each spike is plotted in time, but the time axis is reset in every cycle at a constant point on the stimulus waveform, perhaps at the positive zero crossings (Fig. 4.8). The period histogram appears to follow a half-wave rectified version of the stimulating waveform. It is reasonable to suppose that this corresponds to deflection of the cochlear partition in the effective direction.

The rarefaction phase of the stimulus will move the oval window outwards, and so move the basilar membrane upwards, towards the scala vestibuli. Because of the velocity coupling between the cochlear fluids and the inner hair cell stereocilia (see Chapter 3), we expect the most effective phase of excitation to correspond to the maximum velocity of the movement of the partition in the direction of the scala vestibuli, a direction that presumably deflects the stereocilia in the direction of the tallest in the bundle and corresponds to inner hair cell depolarization. When

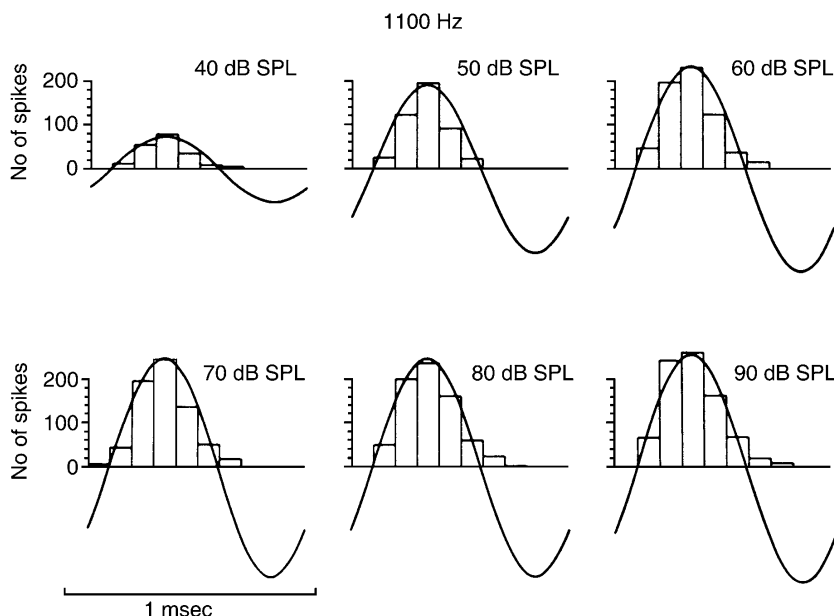


Fig. 4.8 Period histograms of a fibre activated by a low-frequency tone indicate that spikes are evoked in only one-half of the cycle. The histograms have been fitted with a sinusoid of the best-fitting amplitude but fixed phase. Note that although the number of spikes increases little above 70 dB SPL, meaning that the firing is saturated, the histogram still follows the sinusoid without any tendency to square. Used with permission from Rose *et al.* (1971), Fig. 10.

the basilar membrane is driven in the opposite direction, we expect the hair cells to hyperpolarize, reducing the spontaneous activity of the fibre. For apical regions of the cochlea and low stimulus intensities, this indeed seems to be the case. However, this does not hold towards the base, where the position becomes complicated (see [Ruggero *et al.*, 2000](#) for review, and Chapter 5 for a fuller discussion).

One explanation for the loss of phase locking at high frequencies is that there is some jitter at the time of initiation of action potentials. While that may be true to some extent, it was also suggested by [Russell and Sellick \(1978\)](#), on the basis of their hair cell records, that the phase locking disappears when the cell's a.c. response becomes small in comparison with the d.c. response, owing to the attenuation of the intracellular a.c. component by the capacitance of the cell walls. In this case all the spikes would become initiated by the continuous d.c. depolarization of the cell, rather than by the depolarizing half cycles of the a.c. response. Indeed, phase locking in auditory nerve fibres declines directly in proportion to the decline in inner hair cells' a.c./d.c. ratio ([Palmer and Russell, 1986](#)). Phase locking and mean firing rates therefore can be thought of as being related to different aspects of inner hair cell function, the phase locking being related to the a.c. component and the mean firing rate to the square-law non-linearity in the a.c. component, or in other words, to the d.c. response. Phase locking diminishes for frequencies above 2 kHz, and although 5 kHz is often quoted as an upper frequency limit, with appropriate averaging techniques some phase-locked responses are detectable up to 12 kHz ([Recio-Spinoso *et al.*, 2005](#)).

Phase locking is a sensitive indicator of the activation of a fibre by a low-frequency tone. At low stimulus intensities, a tone can produce significant phase locking even though the mean firing rate is not increased. Tuning curves based on a criterion of a certain degree of phase locking are similar to those based on an increase in firing rate, although for the above reason they may be more sensitive by 20 dB or so ([Evans, 1975](#)). As the intensity is raised, phase locking is preserved (see [Fig. 4.8](#)). Note that, although the total number of spikes evoked does not increase above 70 dB SPL, meaning that the firing rate is saturated, the period histogram still follows the waveform of the stimulus and does not show any sign of squaring. This occurs because the hair cells' a.c. responses are still approximately sinusoidal at high stimulus intensities ([Dallos, 1985](#)).

4.2.2 Response to clicks

A click, which lasts a short time but which spreads spectral energy over a wide frequency range, can be thought of as the spectral complement of a tone, which lasts a long time but which has only a narrow frequency spread. [Figure 4.9](#) shows the post-stimulus-time histograms of the auditory nerve fibres to clicks. The histograms of low-frequency fibres show several decaying peaks. It looks as though they would be produced by a decaying oscillation, that is as though the basilar membrane rings in response to the stimulus. The frequency of the ringing is equal to the characteristic frequency of the cell ([Kiang *et al.*, 1965](#)). This ringing at the characteristic frequency

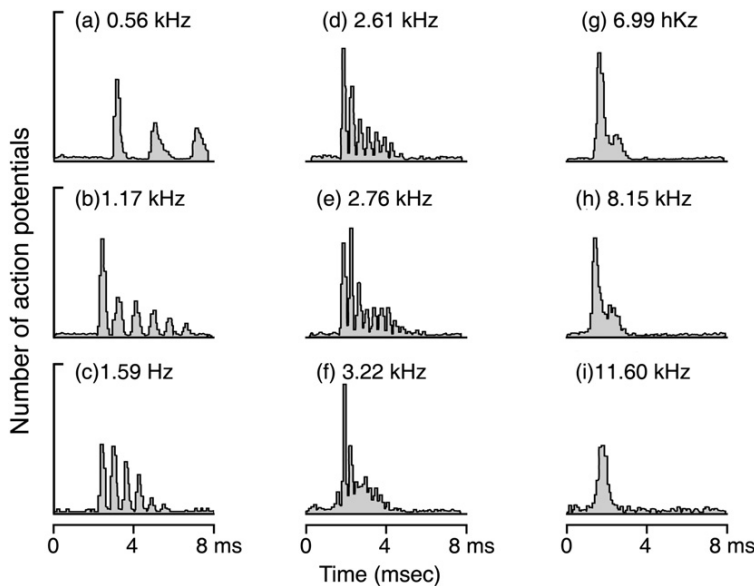


Fig. 4.9 The form of the post-stimulus-time histograms to clicks depends on the characteristic frequency of the fibre. Low-frequency fibres show ringing (a–e) at the characteristic frequency, whereas high-frequency fibres do not (f–i). High-frequency fibres also show a later phase of activation (g), corresponding to a response to the broad dip seen in the tail of the tuning curve of high-frequency fibres (Fig. 4.3). Data from Kiang *et al.* (1965).

is exactly what would be expected if the tuning of the auditory nerve fibres was produced by an approximately linear filter. We would also expect the rate of decay of the ringing to be inversely proportional to the bandwidth of the tuning curve, so that a sharply tuned fibre would ring for a long time.

As with the response to tones, it appears as though only one phase of the basilar membrane movement is effective. The histogram corresponds to half cycles of the decaying oscillation produced on the basilar membrane (Fig. 4.10A). As with tones, for low-frequency fibres it appears as though the velocity of movement of the membrane towards the scala vestibuli is responsible for excitation, since for these fibres at high stimulus intensities, a rarefaction click produces the earliest activation (see Fig. 4.10B). An approximate picture of the excitatory oscillation can be produced by inverting the histogram of the response to a condensation click under that to a rarefaction click, to produce what has been called a compound histogram (see Fig. 4.10C). Histograms to clicks can also show that the suppression of activity during the less effective half cycle of the stimulating waveform is not due to refractoriness from previous activity, because the first sign of influence on a fibre can sometimes be a suppression of spontaneous activity produced by the less effective half cycle.

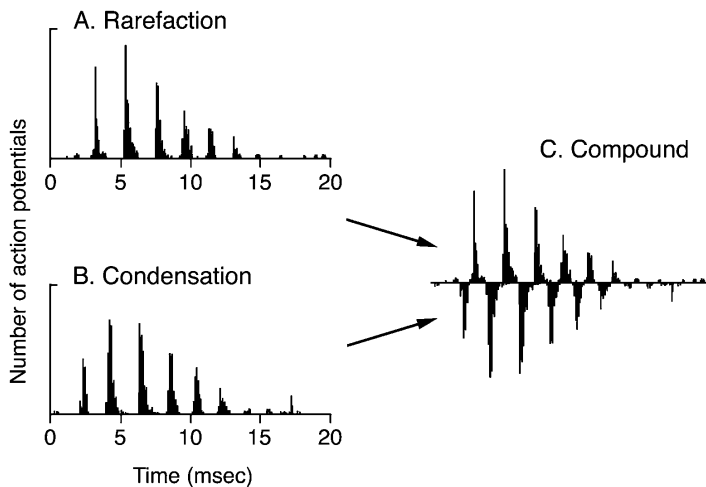


Fig. 4.10 (A) Post-stimulus-time histograms to (A) rarefaction and (B) condensation clicks show that the peaks and troughs occur in complementary places for the two stimuli. (C) A compound histogram is formed by inverting the histogram of condensation clicks under that of rarefaction clicks. Reprinted from Goblick and Pfeiffer (1969), Fig. 1, Copyright (1969), with permission from American Institute of Physics.

As the intensity is raised, earlier, previously subthreshold cycles of activation become effective, and so the histograms shift to shorter latencies. Other complexities are also visible that cannot be fitted into the above scheme. Some fibres that are of too high a frequency to show phase locking can show an earlier phase of activation at high intensities. This must be of a different origin, since these units do not show phase locking to the effective half cycles of the stimulus, and the early phase is more than $1/CF$ before the normal one. Some fibres also show a late phase in the post-stimulus-time histogram, which may be related to the broad dip in the low-frequency tail of high-frequency fibres (see, e.g. Fig. 4.3).

4.2.3 Frequency resolution as a function of intensity and type of stimulation

The tuning curves of Fig. 4.3 clearly show the degree of frequency-resolving power of auditory nerve fibres, that is they show the extent to which the fibres will respond to one tone rather than another on the basis of frequency. This reflects the mechanical tuning of the basilar membrane. It is reasonable to suppose that this neural resolution underlies the frequency resolution of the whole auditory nervous system. It is therefore important to consider the ways in which the fibres' frequency-resolving power varies for different intensities and different types of stimulation.

4.2.3.1 Frequency resolution with broadband stimuli

The tuning curves are produced in response to individual tones; yet we know that a considerable frequency selectivity must be shown in the response to clicks, which have broadband spectra, because of the ringing shown by fibres. In principle, we can calculate the tuning curve of the filter behind the ringing response by taking a Fourier transform of the compound histogram of Fig. 4.10C. If this is done, the frequency selectivity of the tuning curve is found to be approximately comparable to that determined with pure tones (Goblick and Pfeiffer, 1969). This shows that the frequency selectivity of the auditory nerve is, roughly at least, the same to a broadband stimulus as to a narrowband stimulus. This is what would be expected if the tuning was produced by a quasi-linear filter such as the cochlear travelling wave and rules out theories that the sharp tuning is due to lateral inhibition. Lateral inhibition is widespread in sensory systems and increases the contrast of the peaks and troughs of intensity in a sensory pattern; but a narrow click, which has a broad spectrum, has no spectral peaks and troughs, at least in the frequency range of interest.

There are further ways of showing the tuning of the auditory nerve to broadband stimuli, which also depend on using the timing information in the auditory nerve responses. One way of showing sharp tuning with broadband stimuli is to use a stimulus that consists of many tones, presented simultaneously. For frequencies in the range giving phase locking, and under certain conditions, the strength of phase locking to each tone in the complex is proportional to the extent to which each tone activates the fibre. By analysing the strength of phase locking to each of the frequency components in the stimulus, it is possible to measure the relative activation of the fibre by the different components, and so construct a tuning curve. Curves constructed in this way are similar to the tuning curves determined conventionally, that is by plotting the threshold to tones of different frequencies presented one after the other (Horst *et al.*, 1990). This again shows, to a first approximation at least, that frequency resolution is independent of the type of stimulation.

The above method in effect involves cross-correlating the firing pattern of the fibre with the waveforms of each of the component tones in the stimulus. It is possible to use an exactly analogous method but with broadband noise stimulation, where the pattern of action potential is cross-correlated with the waveform of the noise stimulus itself. This is known as the reverse correlation technique. Broadband noise will of course stimulate the fibre, which will fire with an irregular pattern of discharge. We can imagine the noise as being made of a random collection of sinusoidal waves of different durations, phases and frequencies. If there is a particular wavelet of just the right frequency to stimulate the nerve fibre in question, and if it is of sufficient amplitude, the fibre will be activated and an action potential will be recorded. The action potential will be phase locked to the stimulating wavelet if the fibre's characteristic frequency is below 4–5 kHz. Of course, because the noise is random, other frequency components will be present, all of which will be in random phase and amplitude relations to the action potential. Therefore, if we add together all the samples of the original broadband

noise occurring just before the recorded action potentials, all the component wavelets will cancel, except those that were in the right frequency and phase relations to fire the fibre. The resulting average, the reverse correlation function, is the average best waveform that triggers the fibre. Mathematically, the waveform turns out to be the same as the impulse response (i.e. the response to a click) of the nerve fibre, but reversed in time (de Boer and de Jongh, 1978). Once we have obtained the impulse response, we can perform a Fourier transformation on the impulse response to obtain the frequency response, or tuning curve. Figure 4.11A shows the tuning curve of a fibre measured by the reverse correlation technique and compares it with the tuning curve (frequency-threshold curve) measured directly (solid line). The result for the lowest noise intensities shows that the tuning to a low-intensity broadband stimulus is approximately the same as that to a narrowband stimulus.

A further extension of this technique is known as Wiener kernel analysis. In Wiener kernel analysis, the responsiveness is described in terms of a series of coefficients, of zero order, first order, second order and higher orders, although it is not usually possible to go beyond the second order with the amount of data obtainable from auditory nerve fibres. The zero-order kernel is related to the overall mean rate of firing, the first-order kernel in a linear system is related to the reverse correlation function described in the last paragraph and the second-order kernel in an otherwise linear system is related to the square-law distortion (see, e.g. van Dijk *et al.*, 1994). Figure 4.11C shows the iso-intensity function of a fibre, as a function of frequency, determined from the first-order Wiener kernel. This produces a set of filtering functions which are analogous to those shown, as frequency-threshold curves, in Fig. 4.11A. Under some circumstances, the technique can also be adapted to permit the analysis of fibres of much higher frequency, that is out of the range for phase locking (for details, see Recio-Spinoso *et al.*, 2005).

4.2.3.2 Frequency resolution as a function of intensity

We are now in a position to assess how the frequency resolution of auditory nerve fibres changes with intensity. A priori we might expect the tuning of auditory nerve fibres to follow that of the basilar membrane. We would expect it to show a transition from a sensitive, sharply tuned response as seen at low intensities and associated with the cochlear active mechanical process to a poorly sensitive and broadly tuned response as seen at high intensities and associated with passive cochlear mechanics. This expectation is in fact borne out by the data.

The width of the tuning curve is smallest at medium and low intensities, and this has sometimes been taken to mean, erroneously, that the fibres' frequency-resolving power is necessarily greatest near threshold and deteriorates as the intensity is raised and the tuning curve becomes wider. This is not necessarily so: if the fibre is not driven into saturation, the relative importance of stimuli near and away from the characteristic frequency may be unchanged. Tuning curves constructed at higher firing rate criteria (iso-rate or iso-response curves) show

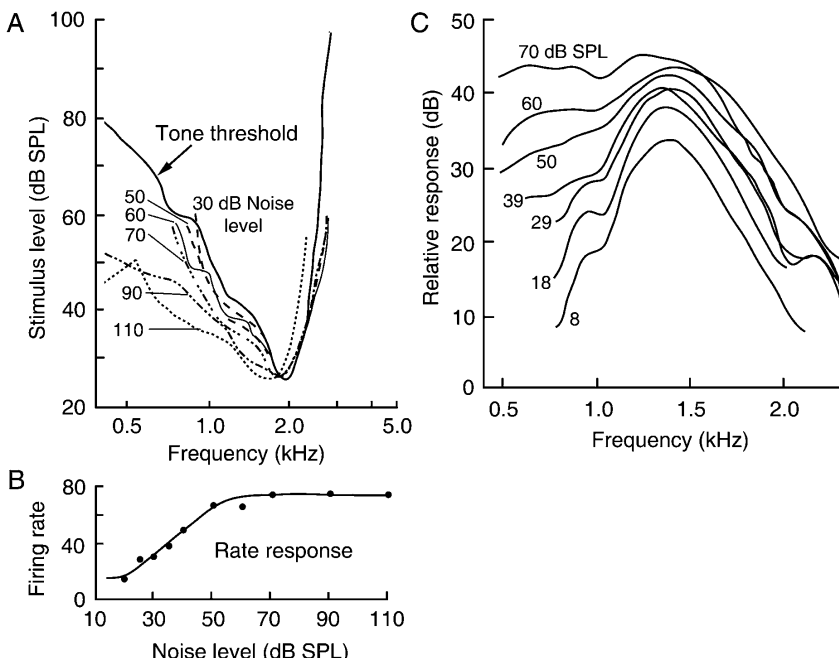


Fig. 4.11 (A and B) Frequency resolution as a function of intensity, as determined by the reverse correlation technique and plotted as tuning curves. For this figure, the curves have been shifted in vertical position, to align at the tip of the tuning curve. For noise levels of 30–70 dB SPL, the calculated tuning curves (broken lines) show good agreement with the tuning curve obtained with tones at threshold (solid line), at least over the bottom 10 dB of the tuning curve. This occurs even though with the 70 dB noise level, the mean firing rate is 20 dB into saturation (rate response in B). With higher intensities of stimulation, the tuning curve broadens to lower frequencies, although some tuning is preserved even with a noise level of 110 dB, when the fibre is 60 dB into saturation. Evans (1977), Fig. 5. (C) Iso-intensity functions (frequency–amplitude responses) of an auditory nerve fibre, for different intensities of stimulation, as determined from the first-order Wiener kernel (see text). For low intensities of stimulation, the function is similar to the iso-intensity function of the fibre determined with tones. At higher intensities, the frequency resolution deteriorates, and the function widens on the low-frequency side, as with the fibre in part A. This behaviour is also similar to that of the iso-intensity functions for the basilar membrane (Fig. 3.11A). Numbers on curves: intensity of noise stimulus in dB SPL in a bandwidth equal to the effective bandwidth of the fibre at threshold. Calculated from data in Recio-Spinoso *et al.* (2005), Fig. 13B. Used with permission from Recio-Spinoso *et al.* (2005).

similar, or sometimes slightly sharper, degrees of frequency selectivity as the intensity is raised, at least for small increases in criterion (see Fig. 4.7A). However, the frequency resolution as shown by the mean firing rate deteriorates when the fibre is driven into saturation. The fibre is now firing as fast as it can, and the firing

rate does not change over a wide frequency range. This is shown by the flat tops of the iso-intensity plot of Fig. 4.7B.

Does this mean, however, that the mechanism behind the fibre's filter function has become inoperative? It is possible, using the reverse correlation technique or the first-order Wiener kernel, to calculate the fibre's frequency-resolving power in spite of a saturation of the firing rate. Such a calculation is possible because the techniques depend only on the accuracy of the timing of the action potentials and not on the mean rate. As was shown in the period histograms of Fig. 4.8, the temporal relations of the firings are preserved at high intensities in spite of the saturation of the mean firing rate. The results of the reverse correlation technique in Fig. 4.11A show that although the firing rate is saturated at noise intensities of 50 dB SPL (see Fig. 4.11B), substantial tuning is still visible for up to 60 dB above that. The downwards shift in best frequency in high-frequency fibres and the broadening of tuning are similar to those seen in the basilar membrane responses of Figs. 3.10B and 3.11A.

These studies show that some degree of frequency resolution of the auditory nerve is preserved at high stimulus intensities, even in low-threshold fibres. We also expect that the high-threshold fibres of Fig. 4.6B, which have an extended dynamic range into the high intensities, would also be able to show some degree of frequency tuning in their responses at high intensities and that this could be revealed in their mean rate responses. We expect the tuning at these intensities to match the broader tuning of the basilar membrane seen at higher stimulus intensities.

4.2.4 Response to complex stimuli

4.2.4.1 Two-tone suppression

It was stated above that single tones produce excitation in auditory nerve fibres, and never sustained inhibition. However, the presence of one stimulus can affect the responsiveness of nerve fibres to other stimuli, and if the relative frequencies and intensities of two tones are arranged correctly, the second tone can inhibit, or suppress, the response to the first. This can occur even though the second tone produces no inhibition of spontaneous activity when presented alone. Figure 4.12 shows the post-stimulus-time histogram produced by a suppressing tone superimposed on a continuous excitatory tone. The pattern of response to the suppressing tone looks like the inverse of the pattern to an excitatory one. The suppressing tone produces an initial maximum of suppression when turned on and produces a prominent rebound of activity when turned off. The dip in activity at the beginning of the suppressing tone looks like the transient suppression seen at the end of an excitatory stimulus, and the activity at the end looks like the onset burst seen at the beginning of an excitatory stimulus (cf. Fig. 4.2). This suggests that the suppressing tone simply turns the effect of the excitatory tone off. The fact that only stimulus-evoked, and not spontaneous, activity can be suppressed makes the same point.

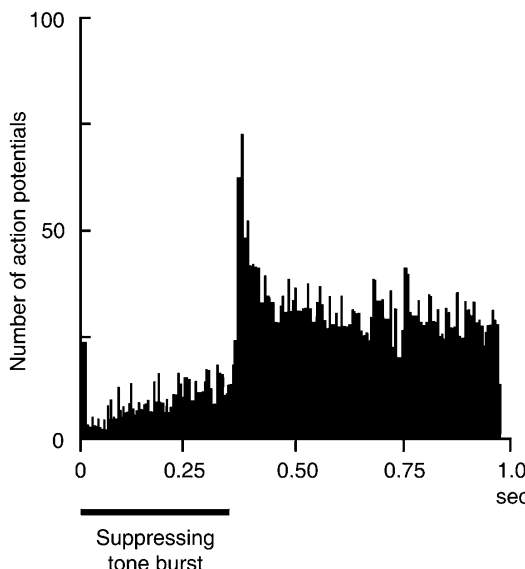


Fig. 4.12 The post-stimulus-time histogram of a suppressing tone burst superimposed on a continuous excitatory tone. Reprinted from [Sachs and Kiang \(1968\)](#), Fig. 1, Copyright (1968), with permission from American Institute of Physics.

[Arthur et al. \(1971\)](#) made detailed measurements of the relative latencies of excitation and suppression to tone onsets and found that on average excitation and suppression differed in latency only by 0.1 msec. The latency of suppression has more recently been measured by measuring the temporal fluctuations in the response to one tone, when a low-frequency suppressing tone is superimposed (e.g. [van der Heijden and Joris, 2005](#)). These results suggested that, when travel times along the cochlear duct were taken into account, suppression occurs on a time-scale of about two cycles. The very short time constants of suppression suggest very strongly that suppression is not the result of inhibitory synapses in the cochlea, even if possible synapses had been demonstrated anatomically, because there is no time for synaptic delay (about 1 msec). The latency argument also means that the suppression cannot be a result of the activity of the olivocochlear bundle, the ‘feedback’ pathway from the brainstem nuclei to the hair cells (see Chapter 8), as has also been confirmed by direct experiment ([Kiang et al., 1965](#)). Because it is believed that two-tone suppression is not the result of inhibitory synapses, the more neutral term ‘suppression’ rather than ‘inhibition’ is often used. Of course, ‘inhibition’ is still used for the process mediated by inhibitory synapses, which is seen in the later stages of the auditory system, in, for instance, the cochlear nucleus. ‘Suppression’ is used only for the process occurring in the cochlea.

It is now clear that suppression occurs at the mechanical stage. Two-tone suppression can be seen in the vibration of the basilar membrane, and in the responses of cochlear hair cells ([Sellick and Russell, 1979; Rhode, 2007](#)). The

basilar membrane and the hair cells have the advantage over the auditory nerve in that it is easier to assess the effects of the exciting and suppressing tones separately. In the case of the inner hair cell shown in Fig. 4.13, the excitatory tuning curve was first measured from the d.c. response to an excitatory tone. The cell was then stimulated with a continuous tone (the probe), having the intensity and frequency indicated by the triangle in Fig. 4.13. A suppressive tone was then swept across the response area, and the contours for 20% suppression of the a.c. response at the probe's frequency determined (Sellick and Russell, 1979). The results show that the suppressing tone can reduce the response to the exciting tone when presented over a wide range of frequencies. The suppressive area is more broadly tuned than the excitatory response area and overlaps it at the tip. In other words, a stimulus can suppress even though it does not excite and can still suppress the response to another stimulus, even though it excites when presented alone.

The overlap of excitatory and suppressive areas that has been demonstrated in inner hair cells can also be shown in auditory nerve fibres, for tones of low frequencies, by taking advantage of the fact that the firing will follow the waveform of an exciting stimulus. If two tones are presented, the firing will follow the waveform of the sum of the two in an appropriate combination of amplitude and phase. By looking at the degree of phase locking of the firing to any one tone

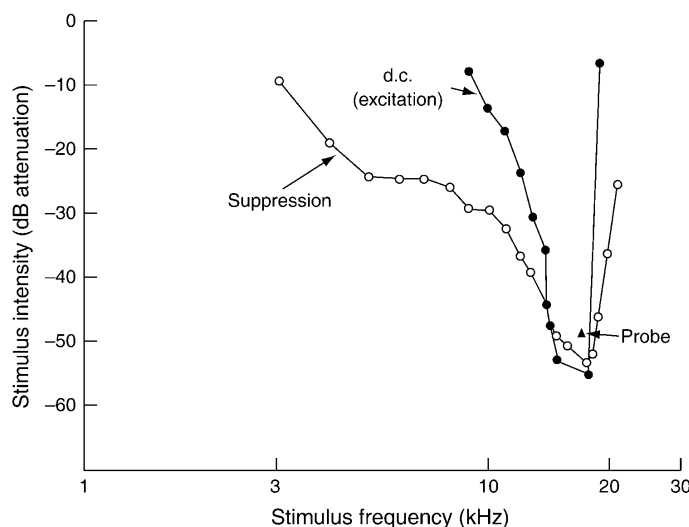


Fig. 4.13 Excitatory and suppressive tuning contours for an inner hair cell. The d.c. contour is the d.c. depolarization to a single tone and shows the excitatory tuning curve. The triangle shows the frequency and intensity of the probe tone, and the open circles show the contour for 20% suppression of the a.c. response to the probe. All stimuli within the excitatory contour excite, and all within the suppressive contour suppress. Stimuli within both contours both suppress and excite. From Sellick and Russell (1979), Fig. 3.

in a complex, it is possible to calculate the degree to which the fibre is activated by that frequency component and to measure the extent to which the response to that component is suppressed by the other stimulus. In this way, Javel *et al.* (1983) showed that the narrow excitatory response area was overlaid by a broader suppressive area.

If, of course, the second tone is in the suppressive area but outside the excitatory area, it will be easy to measure the suppression by measuring the total firing rate to the stimulus complex. The second tone produces only suppression and does not contribute any excitation of its own. The overall mean firing rate will then be a measure of the activation produced by the excitatory tone and the extent to which it is suppressed by the suppressor. Plots of the combinations of intensity and frequency necessary to reduce the mean firing rate in response to a constant excitatory tone by a certain criterion amount (20% has been commonly taken) show the suppressive areas where they flank the excitatory area (Sachs and Kiang, 1968; Arthur *et al.*, 1971; Fig. 4.14A). When the suppressing tone reaches the boundary of the excitatory area, it will begin to activate the fibre on its own account, and so the total number of action potentials will increase. Suppression areas plotted in this way therefore stop at, or near, the boundary of the excitatory area.

It is most likely that two-tone suppression derives from the non-linear responses of outer hair cells as shown in the saturating input–output function of Fig. 3.20B. When hair cells are stimulated with one stimulus, a superimposed stimulus will drive the stereocilia to greater displacements, that is further into the flatter part of the input–output curve. Because of the non-linearity of the outer hair cells' responses, the response in the outer cells to the two stimuli together will be less than the sum of the responses to the two stimuli considered separately. Therefore, each stimulus will reduce the active amplification of the travelling wave to the other one. (In addition, of course, the non-linearity means that each stimulus could be said to reduce the active amplification of its own travelling wave, resulting in the saturating non-linearity of basilar membrane intensity functions.)

This explains two-tone suppression where both tones are in the excitatory part of the tuning curve, such that their travelling waves overlap. Similarly, we can see how a higher-frequency tone might be able to suppress, even though it does not excite (e.g. in the upper shaded two-tone suppression area of Fig. 4.14A). As shown in Fig. 4.14B, a higher-frequency suppressor produces a travelling wave on the basilar membrane, with a peak basal to that produced by the exciter, or probe, tone. This will overlap the region where the active amplification of the suppressed tone f_1 is occurring, and so reduce the amplification of f_1 . Further up the cochlea, the travelling wave to the high-frequency suppressor f_2 will be filtered out by the mechanics, leaving the wave to the lower-frequency tone f_1 , but at a reduced amplitude (Fig. 4.14B).

Note, however, that this explanation of how a stimulus can suppress without causing excitation does not apply to the low-frequency suppression area. The mechanism of low-frequency two-tone suppression will be discussed further in Chapter 5.

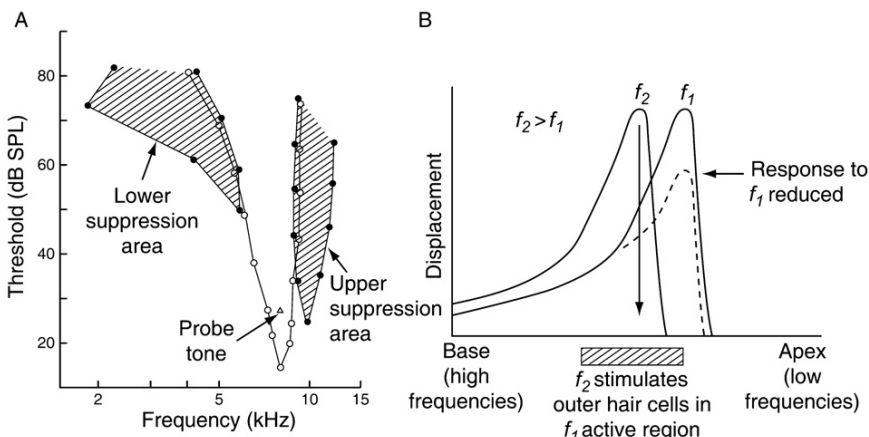


Fig. 4.14 (A) The upper and lower suppression areas of an auditory nerve fibre (shaded) flank the excitatory tuning curve (open circles). A stimulus in the shaded suppression areas was able to reduce the mean firing rate to the probe by 20% or more. From Arthur *et al.* (1971), Fig. 2. (B) Two-tone suppression explained where the suppressor (f_2) is of higher frequency than the suppressed tone (f_1). The travelling wave to the higher-frequency tone overlaps the region on the basilar membrane where the travelling wave to the lower-frequency tone f_1 is being actively amplified. Because of the saturating non-linearity in the responses of outer hair cells, this reduces the active amplification produced by the f_1 tone, and so reduces the magnitude of the f_1 vibration on the basilar membrane. This explanation holds where the excitatory areas of the suppressor and suppressed tones overlap, and in the upper suppression area of part (A).

Suppression has a number of effects on the discriminability of auditory stimuli, depending on circumstances. Figure 4.14A indicates that a stimulus is able to reduce the driven response of fibres tuned to neighbouring frequencies. Two-tone suppression is therefore potentially able to increase the contrast in a complex sensory pattern, so that, for instance, the peaks of activation produced by dominating frequencies will tend to stand out in stronger contrast against the background. However, because suppression reduces the active mechanical amplification in the cochlea, it makes the cochlea more linear, less sensitive and more broadly tuned, which will tend to reduce resolution. The possible effects of two-tone suppression on the discrimination of complex stimuli will be discussed in Chapter 9.

4.2.4.2 Masking

Masking denotes the general phenomenon in which one stimulus obscures or reduces the response to another. We can identify three mechanisms of masking:

1. The ‘line busy’ effect. If one stimulus has pre-empted the firing of a fibre, superimposed stimuli will not be able to provoke an increment in firing. In one

statement of the hypothesis, if the firing is saturated to one stimulus, superimposed stimuli will not be able to increase the rate further (Smith, 1979). This mechanism will also be operative to some extent below saturation. If one signal has a greater effective intensity than the other, the less intense one will add negligible activity of its own. Such an effect will be greater than might appear at first sight, because the summation of effective intensities will occur on a linear scale rather than on the logarithmic scale of decibels. For instance, a signal added 10 dB below another will produce an increase in net stimulus intensity of only 0.4 dB.

2. Two-tone suppression, by the mechanism discussed above, reduces responses and broadens tuning to the suppressed stimulus (Pang and Guinan, 1997b).
3. Adaptation forms a further mechanism of masking: in response to prolonged background stimulation, the extra firing that can be evoked by a superimposed stimulus is reduced, presumably due to depletion of neurotransmitter at the hair cell synapse.

Figure 4.15 shows an example of masking by all three mechanisms. The figure shows rate-intensity functions for a tone both with and without wideband masking noise. The tone alone could produce a maximum firing rate just over

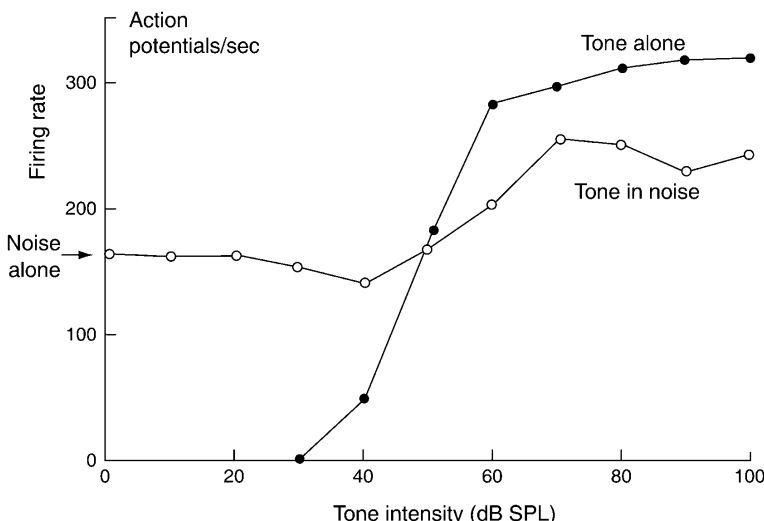


Fig. 4.15 Rate-intensity functions to a tone with and without masking noise. The tone was presented at 2.9 kHz, the CF. The noise band was centred around the CF and covered 2.5–4 kHz. At low tone intensities, the noise activates the fibre on its own ('line busy' effect). At higher tone intensities, it is possible to see how the noise reduces the response to the tone. Suppression by the noise also shifts the tone's rate-intensity function to the right. Used with permission from Rhode *et al.* (1978), Fig. 3E.

300/sec. The continuous noise was then presented at an intensity that gave a firing rate of 160/sec. Tones were superimposed on the noise; tones less intense than 50 dB SPL did not produce a greater firing rate than the noise, and so did not increase the response. In this intensity range, the tone was masked by the line busy effect. Once the tone is intense enough to activate the fibre in the presence of the noise, its rate-intensity function in noise is seen to be shifted 10 dB to the right compared with that without noise, showing the effects of suppression. In addition, for the most intense tones, the maximum firing rate to the tone plus noise is lower than to the tone alone. This shows the effect of both adaptation and suppression.

We are now in a position to understand some of the complex interactions between the components of multicomponent stimuli. If two stimuli of comparable levels are presented, both well inside the excitatory area, each will suppress the other strongly, but both will excite the fibre even more strongly. Below saturation, the firing rate in response to both will be greater than that to either one alone, and they will therefore appear to summate in their effects. For low-frequency units, the firing will follow a waveform that can be composed of the waveforms of the component stimuli added together with suitable amplitudes and phases (Rose *et al.*, 1971). The relative amplitudes and phases giving the best fit are not necessarily those presented in the acoustic stimulus. The frequency selectivity of the fibre, as well as the mutual suppression of the components, will alter their relative amplitudes. In the case of the phases, the effects of suppression are complex and not entirely understood (see Chapter 5).

In a more trivial case where one stimulus has much less influence over the fibre than the other, the most effective stimulus will dominate both the firing rate and the temporal pattern of the action potentials. When the effects of suppression are strong, the temporal pattern can follow the waveform of the suppressing as well as of the exciting stimulus (Rose *et al.*, 1971).

The different effects of suppression and summation can also be seen in the mean firing rates to bands of noise of different widths. As a narrow band of noise of constant spectral density is widened around the characteristic frequency of a fibre, the first effect is for the firing rate to increase, because the greater number of noise components in the excitatory area summate and drive the fibre more intensely (Gilbert and Pickles, 1980). As the bandwidth becomes still broader, the extra noise components added come to fall on the parts of the suppressive area outside the excitatory area, and now not only fail to contribute excitation, but contribute a net suppression. The firing rate therefore comes to a maximum, and then declines. Ruggero (1992) reviews some of the complexities in the interactions of the components of complex stimuli.

4.2.4.3 Combination tones

If the ear is stimulated with two tones at the same time, combination tones may be heard that are not physically present in the stimulus. The presence of combination tones was first demonstrated psychophysically rather than physiologically. It is now

known that they occur as a result of a non-linearity in the basilar membrane mechanics, as a result of hair cell non-linearity.

One set of combination tones has certain fascinating properties and can be heard even at low sound levels. The best known representative of this group is the tone known as the cubic distortion tone or $2f_1-f_2$, from the frequency at which it is heard, where f_2 is above f_1 in frequency. Figure 4.16 shows the frequency and level of the cubic distortion tone in relation to the primaries. In this experiment, the level of each distortion tone was measured psychophysically by introducing a third, cancellation, tone into the stimulus, and altering its level and phase until it just cancelled the sensation of the distortion tone.

The frequency at which $2f_1-f_2$ appears might be explained by supposing that the auditory system undergoes a distortion such that the output contains a component that is the cube of the input. If two tones of frequency f_1 and f_2 are presented (waveform $\cos 2\pi f_1 + \cos 2\pi f_2$), the output distortion component = $(\cos 2\pi f_1 + \cos 2\pi f_2)^3$.³ This can be decomposed into a series of cosines containing frequencies such as f_1 , $3f_1$, f_2 , $3f_2$, $2f_1+f_2$, $2f_2+f_1$, $2f_1-f_2$ and $2f_2-f_1$. Of these, only $2f_1-f_2$ is at a frequency below the primaries and we can provisionally suppose that the others are masked or filtered out by a high reject filter later in the auditory system. At the moment we can note that the name ‘cubic distortion tone’ arises because the tone can hypothetically be produced by a cubic distortion. However, it can also be produced by non-linearities such as that shown for the outer hair cell input–output function in Fig. 3.24, which is a saturating non-linearity, such that the response starts to saturate for excursions of

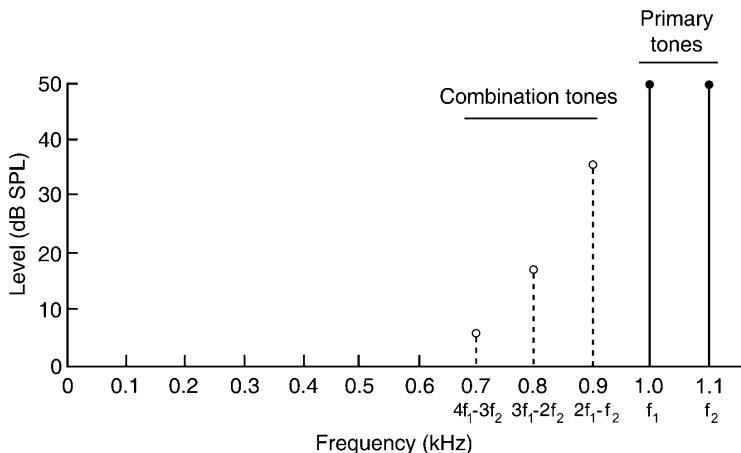


Fig. 4.16 The subjective cubic and related combination tones form a series below the primaries, of frequency spacing equal to the separation of the primaries. The levels indicated were found psychophysically, by the cancellation method (see text) according to Goldstein (1967).

the stereocilia in both the positive and negative directions. If the non-linear input–output function is expressed as a power series:

$$\text{output} = a_1.\text{input} + a_2.\text{input}^2 + a_3.\text{input}^3 + a_4.\text{input}^4 + a_5.\text{input}^5 + \dots$$

where a_i are constants, the cubic term will give rise to the combination tones described above. The other odd-exponent terms will in addition give rise to terms such as $3f_1 - 2f_2$ and $4f_1 - 3f_2$, for the distortion components below f_1 and f_2 in frequency. Such additional distortion components are detectable psychophysically, although at a lower amplitude than $2f_1 - f_2$ (see Fig. 4.16).

Models behind the generation of $2f_1 - f_2$ will be discussed further in Chapter 5. At the moment we can note that similar non-linearities are present in the responses of the basilar membrane, and that the basilar membrane vibrates as though real tones at the distortion frequencies are present in the mechanical travelling wave (see Robles and Ruggero, 2001, for review). The distortion tones are generated because the active mechanical amplification produced by outer hair cells is non-linear, as a result of the non-linear and saturating input–output functions of the outer hair cells (see Figs. 3.20 and 3.24). This generates a non-linear vibration of the basilar membrane. The non-linear vibration can be decomposed into the primaries, at frequencies f_1 and f_2 , as well as components at all the other frequencies described above. Components of each of these frequencies are therefore generated by the active mechanical amplifier on the basilar membrane at the sites where the travelling waves of the primaries overlap. However, only those components that have frequencies lower than the primaries are capable of setting up travelling waves that move apically on the basilar membrane. This is because any distortion components that are higher in frequency than the primaries will be generated apical to the point on the basilar membrane at which they can propagate as travelling waves. They will therefore be filtered out by the mechanics, leaving only the distortion components that are lower in frequency than the primaries (described in more detail in Section 5.6.3).

The intensity of the cubic distortion tone, both as measured in the vibration of the basilar membrane and in the responses of the auditory nerve fibres, depends strongly on the frequency separation of the primaries (Cooper and Rhode, 1997). This is to be expected if combination tones are produced only in the region where the travelling wave to one primary overlaps the mechanically active region in the travelling wave to the other primary.

Correlates of the cubic distortion tone in the responses of fibres of the auditory nerve were first reported by Goldstein and Kiang (1968). Goldstein and Kiang presented two tones f_1 and f_2 such that both lay outside the response area of the fibre, neither provoking a response when they were presented singly. If, however, the calculated frequency $2f_1 - f_2$ lay at the characteristic frequency of the fibre, it is possible for the fibre to be excited by both stimuli together. In other words, the fibre could be excited by the combination tone, in the absence of a response to the primaries. The same point was made by studies of the phase locking to the stimuli for low-frequency fibres; it was possible to show significant phase locking to $2f_1 - f_2$ without any phase locking to f_1 or f_2 . Moreover,

Kim *et al.* (1980) showed that the fibres' frequency selectivity to $2f_1-f_2$ was the same as that to introduced real tones of the same frequency. This shows that as far as the auditory nerve was concerned, it was as though a real tone at the frequency $2f_1-f_2$ was present in the stimulus.

The cubic distortion tone can be seen in the responses of auditory nerve fibres and detected psychophysically, even near threshold, presumably because the input–output functions of the outer hair cells start showing some degree of saturating non-linearity, even for small excursions of their stereocilia around their resting point.

A further combination tone is the difference tone, which is at a frequency f_2-f_1 , where f_2 and f_1 are the frequencies of the primaries. At high signal levels, the level of the difference tone is almost completely independent of the frequency separation of the primaries. It was once thought that it originated as an overloading type of distortion in the middle ear (e.g. Helmholtz, 1863). However, direct measurements have shown that the middle ear has insufficient non-linearity (e.g. Aerts and Dirckx, 2010), and an intracochlear origin is now suspected. Intracochlearly, a difference tone can be measured even with low-level stimuli. It can be measured in the vibration of the basilar membrane, in the responses of hair cells and in the responses of auditory nerve fibres. In these cases the level of the tone is highly dependent on the separation of the primaries, as with the cubic distortion tone (Kim *et al.*, 1980; Cheatham and Dallos, 1997; Cooper and Rhode, 1997). It is likely that it has an origin similar to that of the cubic distortion tone, although the parameters necessary to evoke it make it much more difficult to analyse.

It is interesting that the production of combination tones, which has important implications for the perception of complex stimuli, can be traced to the input–output functions of the outer hair cells, and hence to the basic thermodynamic properties of the mechanotransducer channels themselves (see Chapter 5).

4.3 SUMMARY

1. The very great majority of the fibres present in the auditory nerve innervate inner hair cells.
2. Single fibres of the auditory nerve are always excited by auditory stimuli and never show sustained inhibition to single stimuli.
3. The fibres have lower thresholds to tones of some frequencies than of others. The relation between threshold and stimulus frequency is known as the 'tuning curve'. Tuning curves show one threshold minimum, at what is known as the characteristic frequency. The threshold rises sharply for frequencies above and below the characteristic frequency. The tuning curve therefore shows a sharp dip in this frequency region. Tuning curves of auditory nerve fibres are similar to the tuning curves of hair cells and of the mechanical response of the basilar membrane.

4. The great majority (90%) of auditory nerve fibres have minimum thresholds in a 10-dB range near the animal's absolute threshold. The others have thresholds spread over a 60-dB range above that. The low-threshold fibres have particularly high rates of spontaneous activity in the absence of sound.
5. Fibres show a sigmoidal relation between firing rate and stimulus intensity. Low-threshold fibres also have steeper rate-intensity functions, often going from threshold to maximum rate in 20–30 dB (the dynamic range) at any one frequency. Fibres of higher threshold have shallower rate-intensity functions and wider dynamic ranges, up to 60 dB or more.
6. The frequency-resolving power of auditory nerve fibres has been measured by a 'quality' factor, by analogy with a quality factor for filters. The quality factor is the characteristic frequency divided by the bandwidth of the fibre to tones at an intensity 10 dB above the best threshold. This is called ' Q_{10} ' or ' $Q_{10\text{ dB}}$ '. Therefore, fibres with a high Q_{10} have good frequency selectivity. At any one frequency, different fibres have $Q_{10\text{s}}$ in a restricted range. In any one animal, the range of $Q_{10\text{s}}$ at one frequency is twofold or less. In cats, the greatest $Q_{10\text{s}}$ are reached at around 10 kHz, where they have an average value of eight. The $Q_{10\text{s}}$ match, to a first approximation at least, the Q_{10} of the basilar membrane vibration.
7. During tonal stimulation, auditory nerve fibres fire preferentially during one part of the cycle of the stimulating waveform if the frequency of the stimulus is below 4–5 kHz. The fibres are excited by deflection of the basilar membrane in only one direction.
8. For fibres with characteristic frequencies below 4–5 kHz, clicks preferentially evoke responses at certain intervals after the stimulus. A histogram of action potentials made with respect to time after the stimulus suggests that the fibres are activated by the half cycles of a decaying oscillation of the mechanical resonance on the basilar membrane. The frequency of the oscillation is equal to the characteristic frequency of the fibre.
9. One tone can reduce, or suppress, the response to another, even though single tones are only excitatory. This is called two-tone suppression. The suppression arises from the non-linear properties of the basilar membrane mechanics. Two-tone suppression can also be seen in the basilar membrane mechanics and the responses of inner hair cells. Stimuli other than tones cause suppression too.
10. One stimulus can mask the response to another. Masking mainly occurs because the masking stimulus produces a greater firing rate than the masked stimulus. The other mechanisms of masking are the suppression of the response to one stimulus by another, and adaptation in the fibre produced by an ongoing stimulus.
11. When two-tone stimuli are used, auditory nerve fibres can respond to distortion products as a result of non-linear interactions in the cochlea. One distortion tone, known as the cubic distortion tone, is at a frequency $2f_1-f_2$, where f_1 is the lower of the tones presented and f_2 the higher.



4.4 FURTHER READING

The developmental biology of the peripheral connections of the auditory nerve has been reviewed by [Defourney *et al.* \(2011\)](#), while the anatomy of the nerve (with an emphasis on its central connections) has been reviewed by [Nayagam *et al.* \(2011\)](#). The physiology of the auditory nerve has been reviewed by [Ruggero \(1992\)](#). Some information is also included in a review of cochlear mechanics by [Robles and Ruggero \(2001\)](#). Mechanisms of activation of the nerve fibres, and further details on the role of cochlear nonlinearity, are discussed in Chapter 5.

MECHANISMS OF TRANSDUCTION AND EXCITATION IN THE COCHLEA

The study of cochlear processing has shown rapid advances in recent years. We now have detailed information on the mechanotransducer apparatus, with information on the molecular identity of many of the proteins associated with mechanotransduction, although the molecular identity of the mechanotransducer channels still eludes us. We also have detailed information on the biophysics of the transducer process. In addition, it is now clear that the outer hair cells must mechanically amplify the travelling wave in the cochlea. The motility arises, in part at least, from the motility of a protein called prestin, which is expressed in the basal membranes of the outer hair cells. The overall pattern of mechanical vibration of the cochlea is not in doubt, at least in the basal turn. However, the micro-mechanical pattern of movement (i.e. the pattern of vibration within the organ of Corti), how the hair cell motility is translated into movement of the basilar membrane, and the details of how the vibration excites the inner hair cells and then the synapse, are not clear. This chapter is written at a more advanced level than the rest of the book and may be omitted without affecting the comprehensibility of the other chapters.



5.1 INTRODUCTION

Electrophysiological experiments show that deflections of the stereocilia open ion channels near the tips of the stereocilia. The channels are opened by fine links running between the stereocilia, called tip links, and the tip links pull the channels open by a direct mechanical action. The molecular nature of the mechano-transducer channel is at present unknown. Once the channels are opened, ions are driven into the hair cells by the combined effects of the positive endocochlear potential and the negative intracellular potential. Intracellular depolarization causes the release of transmitter at the synapse, evoking action potentials in the afferent auditory nerve fibres.

The cytoskeletal structures in the apical portions of the hair cells are important in determining the electrophysiological responses of the hair cells to mechanical stimulation: the way in which the stereocilia deflect in response to mechanical stimulation and the way in which the movement is transferred to the

mechanotransducer channels are dependent on the mechanical properties of the stereocilia and the way in which the stereocilia are coupled together. In response to deflection of the stereocilia, a shear is developed between the different rows of stereocilia on the hair cell, which is then coupled to fine tip links, of macromolecular dimensions, which transmit the movement to the transducer channels themselves.

In addition, outer hair cells are known to be motile and actively generate movements when stimulated. The motility depends on a specialized motor protein, called prestin, expressed in the basal membranes of the cells. The motility may also depend on a reverse motion generated by the mechanotransducer channels in the apical portions of the hair cells. The motility is responsible for amplifying the mechanical travelling wave on the basilar membrane and for generating the sharply tuned, low-threshold component of the mechanical response.

5.2 THE STRUCTURE OF THE TRANSDUCER REGION

5.2.1 Stereocilia and cuticular plate

Micromanipulation experiments show that stereocilia act as stiff, rigid, levers, bending only at the point of insertion into the cuticular plate and fracturing as though brittle when pushed too far (Flock *et al.*, 1977). Stereocilia gain their considerable rigidity from a core of tightly packed actin filaments. The actin filaments are tightly bonded together in what is known as a paracrystalline array, the high degree of bonding contributing to the rigidity to the stereocilia (Tilney *et al.*, 1980). After acoustic overstimulation, the paracrystal is seen to be disordered, with an irregular spacing of the filaments in longitudinal view and loss of the striations due to bonding (Tilney *et al.*, 1982). The regions of disorder are associated with a bending or kinking of the stereocilia. This suggests that the mechanical rigidity of the stereocilia is indeed associated with the integrity of the paracrystal.

Within the paracrystal, all the actin filaments have the same polarity so that when decorated with the heavy (S1) fragments of myosin, the S1 fragments make a pattern of arrowheads pointing down into the cell body (Tilney *et al.*, 1980; Fig. 5.1). This also has the implication that actin–myosin interactions as in other living cells will tend to carry the myosin molecules up towards the tips of the stereocilia. In addition, from the orientation of the filaments, we expect that any new actin monomers added to the stereocilia will tend to be added at the tips (the ‘plus’ ends) of the filaments, while actin monomers will tend to be removed at the basal ends (the ‘minus’ ends). This ‘treadmilling’ can occur, though very different estimates of the turnover time of the stereociliary proteins has been obtained in the different experiments, ranging from 2 to 3 days to weeks or many months (Pickles *et al.*, 1996a; Rzadzinska *et al.*, 2004; Zhang *et al.*, 2012).

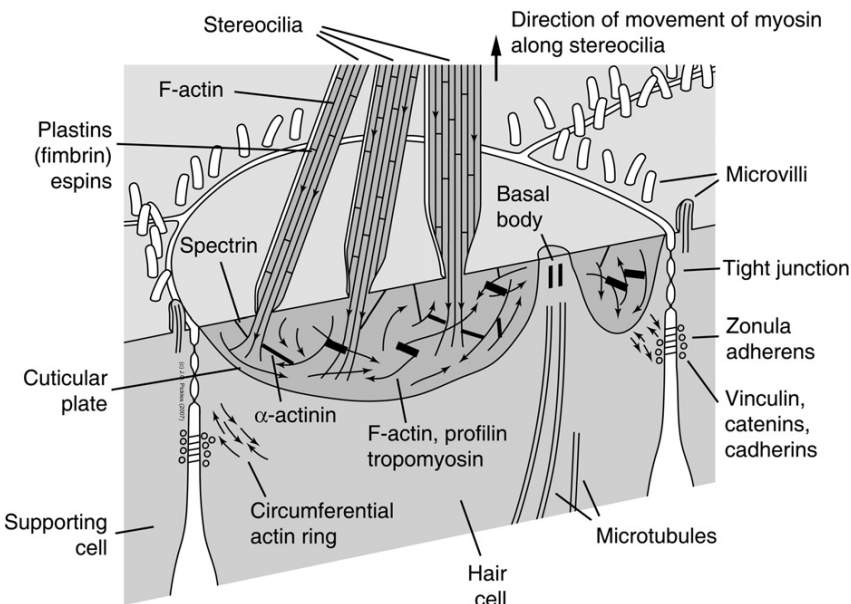


Fig. 5.1 The arrangement of actin and other cytoskeletal proteins in the apical regions of hair cells. The molecular organization of the upper ends of the stereocilia is shown separately in Fig. 5.6. Arrows show the direction of the arrowhead complexes formed after decoration with myosin heads (Sl-myosin), and show the similarity of stereocilia to microvilli. A few of the links between the actin filaments are also shown. From Pickles (2007b).

The actin filaments are cross-linked by means of the actin-linking proteins I-plastin (i.e. fimbrin), T-plastin and the espins, shown by means of immunological techniques (Daudet and Lebart, 2002; reviewed by Schwander *et al.*, 2010). A mutation in the espin gene in the strain of mice known as jerker mice leads to stereociliary degeneration, deafness and vestibular dysfunction, and similar changes have been detected in human beings (Donaudy *et al.*, 2006). The tip region of each stereocilium is capped, and stereociliary growth regulated, by a number of proteins, including the myosins 3, 7a and 15a, which may be involved via direct interactions, as well as by transporting other proteins involved in the capping (whirlin, twinfilin and espin-1) (reviewed by Schwander *et al.*, 2010). Genetic defects associated with these proteins, and the roles of further stereociliar proteins, are reviewed by Richardson *et al.* (2011).

The stereocilium is able to flex at its lower end, just before it enters the cuticular plate, because it tapers at this point before continuing into the cuticular plate as a dense rootlet. About 10 (counted in the lizard basilar papilla) of the actin filaments in the stereocilium enter the rootlet in this way, the rest ending in association with the membrane of the stereocilium where it tapers (Tilney *et al.*, 1980). The taper is controlled by another myosin, myosin 6, which unlike other

myosins tends to move to the minus ends of actin filaments. There is evidence that myosin 6 in this region links to a membrane-associated protein, known as protein tyrosine phosphatase receptor Q, thus tying the stereociliar membrane to the actin core (Sakaguchi *et al.*, 2008; for further review of the rootlet see Richardson *et al.*, 2011).

The cuticular plate itself is also composed of actin filaments, here in a dense mesh-work. The cuticular plate also contains tropomyosin, α -actinin (a component of the muscle Z-line), myosins, fimbrin, profilin, tropomyosin and the Ca^{2+} -binding proteins calbindin and calmodulin (for review, see Slepecky, 1996). It has been suggested that spectrin, originally known as a component of the erythrocyte membrane, bonds the matrix of the cuticular plate to the overlying membrane (Drenckhahn *et al.*, 1985). The dense matrix of interlinked actin filaments in the cuticular plate would be expected to give the plate considerable rigidity.

In contrast to the apparently haphazard matrix of filaments in the cuticular plate, organized actin filaments can be found running in a ring-like arrangement just inside the zonula adherens at the apical end of the hair cell. The rings contain actin filaments oriented in opposite polarities. The suggested arrangements of actin filaments and associated cytoskeletal structures in the apical region of hair cells are shown in Fig. 5.1.

5.2.2 The cross-linking of stereocilia

The stereocilia in a hair bundle are heavily cross-linked in a variety of ways. Firstly, the stereocilia are bonded together sideways by links that run predominantly parallel to the cuticular plate. The side links run between the stereocilia of the different rows on the hair cell as well as between the stereocilia of the same row (Pickles *et al.*, 1984). These side links serve to couple the stereocilia mechanically, with the result that in micromanipulation experiments all stereocilia in a bundle tend to move together when some are pushed. Fig. 5.2 shows an example of the side links running between stereocilia of the same row on an inner hair cell, and Fig. 5.3 shows side links joining stereocilia of different rows. Most of the side links (arrowheads, Fig. 5.3) are concentrated in a broad band just below the tips of the shorter stereocilia and hold the tips of the shorter stereocilia in towards the adjacent taller stereocilia. The rows of stereocilia therefore make triangles when seen in sideways view.

The links of a second set are rather different and have generated interest because they couple the stimulus-induced movements to the transducer areas of the stereocilia (Pickles *et al.*, 1984). A single vertically pointing link emerges from the tip of each shorter stereocilium on a hair cell and runs up to join the adjacent taller stereocilium of the next row. The links are 150–180 nm long. Figure 5.3 shows these tip links by transmission electron microscopy and Fig. 5.4A by scanning electron microscopy. Each tip link consists of a fine 8–11-nm strand, surrounded by a variable coat (Osborne *et al.*, 1988; Gillespie *et al.*, 2005). Figure 5.4B and C shows the central strand in more detail. It bifurcates at the top end and at high resolution has a spiral structure (Kachar *et al.*, 2000; Tsuprun *et al.*, 2004).

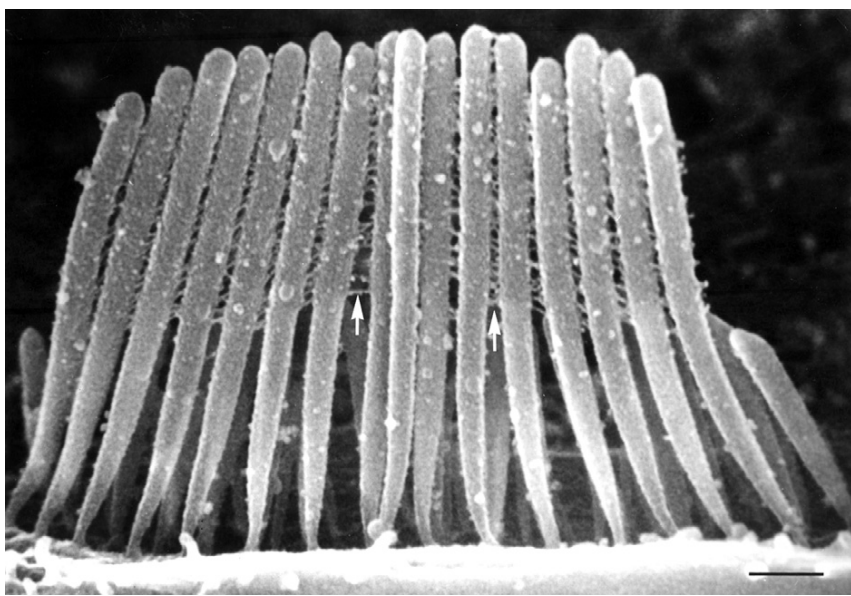


Fig. 5.2 Inner hair cell of the guinea pig cochlea, showing side links (arrows) running between the stereocilia of the tallest row on the hair cell. Note also that the surface membranes of the stereocilia appear rough, particularly at the level of the links. Scale bar, 500 nm.

The link inserts into specialized densities in the stereocilia, while the surrounding coat is probably a continuation of the glycoconjugate material that surrounds the surfaces of the stereocilia (Santi and Anderson, 1987). As suggested by Pickles *et al.* (1984), if the tallest stereocilium in Fig. 5.3 was deflected away from the shorter stereocilia, the tip links would tend to be stretched. This could pull open mechanotransducer channels situated at the links' points of insertion into the stereocilia, by a direct mechanical action (see Fig. 3.19B).

In addition to electrophysiological evidence to be described in the next section, supporting anatomical evidence for the role of tip links in mechano-transduction is the following:

1. Their position on the stereocilia, being ideal to detect movements of the bundle in the excitatory direction (see Fig. 3.19B).
2. They are the only structures known that are oppositely stressed by excitatory and inhibitory deflections of the stereocilia, through the different types of manipulations (e.g. pushing or pulling the bundle) that have been used experimentally.
3. The geometrical arrangement of the bundle is such that maximum energy from the stimulus is coupled to the tip links, in contrast to the other types of links on the hair cell (Pickles, 1993).

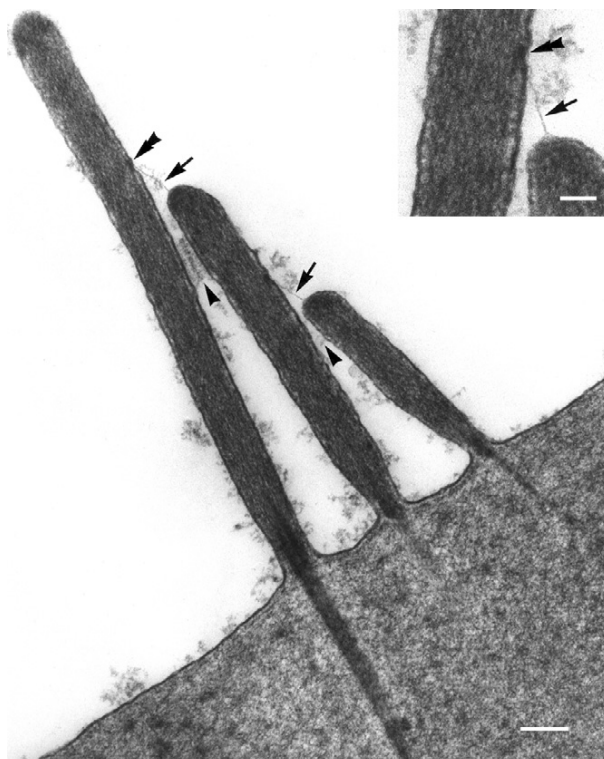


Fig. 5.3 The three rows of stereocilia on an outer hair cell are shown in cross section. The stereocilia of the different rows are joined by horizontal (between-row) side links just below their tips (arrowheads). The inset shows a higher magnification of the lower tip link. Tip links (arrows) have a fine central core, surrounded by amorphous material (see also inset). Double arrowhead: upper density. Guinea pig. Scale bar on main figure: 200 nm, on inset 100 nm. From Osborne *et al.* (1988), Figs. 3 and 4.

4. In hair cells of many different configurations, the tip links always run parallel to, or nearly parallel to, the excitatory–inhibitory axis of the cell (Pickles *et al.*, 1989).

The outer hair cell shown in Fig. 5.4A was viewed almost exactly parallel to the axis of bilateral symmetry, that is along the anticipated excitatory–inhibitory axis, and so looking radially across the cochlear duct. The tip links run parallel to the line of view, rather than across it (see also Fig. 3.4D). Figure 5.5A shows the direction of the links plotted from another outer hair cell, seen in top view.

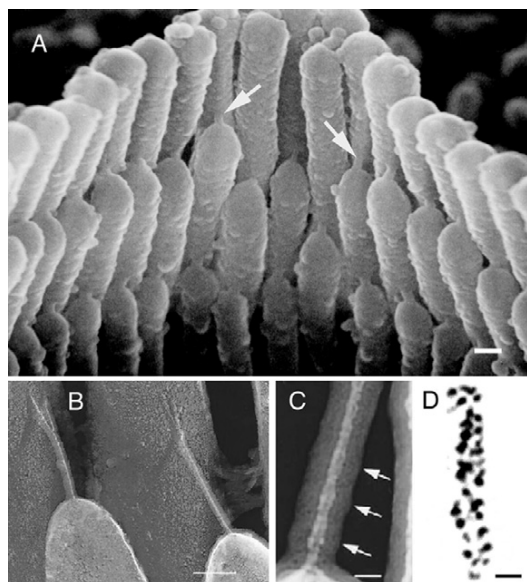


Fig. 5.4 (A) Tip links (arrows) shown by scanning electron microscopy, in the apex of the 'V' of stereocilia on a guinea pig outer hair cell. The stereocilia were viewed nearly parallel to the axis of bilateral symmetry, showing that the tip links run parallel to that axis, that is parallel to the excitatory–inhibitory axis, and approximately radially across the cochlear duct. In this micrograph, the central cores of the tip links are covered by glycocalyx. Scale bar, 200 nm. (B) The central cores of two tip links shown at higher resolution, by freeze-etch transmission electron microscopy, and showing how the links can bifurcate at their upper ends. The preparations were frozen and fractured, the surface was given texture by permitting evaporation, and then was coated with platinum and carbon to give a layer that could be visualized with a transmission electron microscope. Scale bar, 100 nm. (C) A tip link at higher magnification, prepared with the same technique, showing the spiral structure. Arrows point to repeats of the spiral. Scale bar, 15 nm. (D) The fine structure of a part of a tip link, obtained from a noise-filtered electron micrograph image at high magnification. Globular elements are visible aligned in two spiral strands. Scale bar, 10 nm. B and C from Kachar *et al.* (2000), Figs. 3A and 2C, Copyright (2000), National Academy of Sciences, USA. D From Tsuprun *et al.* (2004), Fig. 1E.

A similar result holds true over hair cells of many different geometrical configurations. For instance, stereocilia on hair cells of lizard and bird basilar papillae are packed tightly in a hexagonal array. Here again, the tip links are oriented parallel to the cell's axis of bilateral symmetry, that is parallel to the excitatory–inhibitory axis, and therefore in a position to be maximally stretched by excitatory deflections of the bundle (see Fig. 5.5B; Pickles *et al.*, 1989).

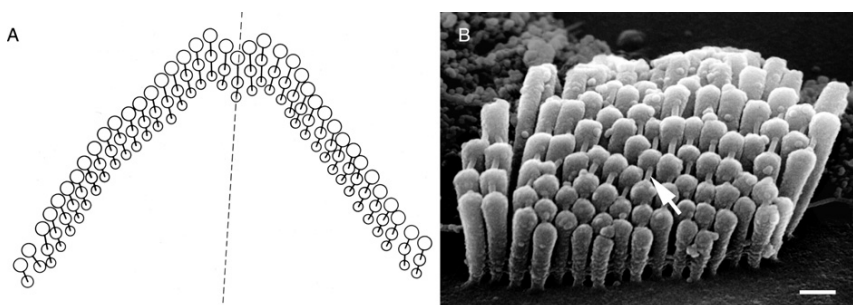


Fig. 5.5 (A) Direction of tip links in a guinea pig outer hair cell plotted from top view. The dotted line shows the axis of bilateral symmetry, that is the excitatory-inhibitory axis. (B) Stereocilia of a hair cell from the chick cochlea, viewed nearly along the excitatory-inhibitory axis, parallel to the gradation in heights of the stereocilia. The tip links (e.g. arrow) run parallel to the axis. Scale bar, 500 nm. A from Comis *et al.* (1985), Fig. 7. B from Pickles (1992), Fig. 1.

5.2.2.1 The molecular nature of the tip links and their attachments

The physical nature of the tip link is important because the link has to be able to transmit very small (subnanometre) displacements to the transducer channel, while being able to accommodate the very large – micron – extensions that occur when the bundle undergoes large deflections. The upper two-thirds of the tip link is composed of two twisted strands of the cell adhesion molecule cadherin-23, which has a long filamentous extracellular domain. The evidence was derived from immunolabelling and from the effects of genetic mutation (Siemens *et al.*, 2004; Söllner *et al.*, 2004). Similar evidence shows that the lower third of the tip link is composed of two twisted strands of protocadherin-15. The genes coding for cadherin-23 and for protocadherin-15 are among those mutated in the Usher syndrome Type 1 in human beings, which leads to blindness and deafness (Kazmierczak *et al.*, 2007; Richardson *et al.*, 2011). It has been suggested that the repeats of the extracellular domain of cadherin-23 are normally folded, bonded by Ca^{2+} ions, and that in response to excessive tension, the molecule progressively unfolds, thus allowing it to extend, while maintaining its ability to transmit small forces to the mechano-transducer channels (Sotomayor *et al.*, 2005; see also Sotomayor *et al.*, 2010).

The intracellular insertion of the upper end of the tip link is thought to attach to a protein complex which includes harmonin, sans and either myosin 7a or myosin 1c (Grati and Kachar, 2011; see also Richardson *et al.*, 2011). The myosin itself attaches to the actin filaments in the core of the stereocilia, so not only can forces from the core of the stereocilium be transmitted to the tip link, but the tension on the tip link can be controlled by movement of the myosin on the actin core (see Section 5.3.2.7). We have less information on the lower insertion of the tip link. The protocadherin-15 is likely to attach directly or indirectly onto the mechanotransducer channel, thought to be situated at this point

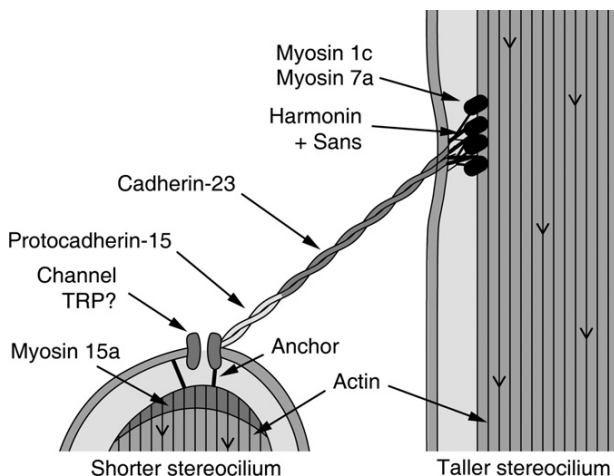


Fig. 5.6 Conjectured arrangement of mechanotransducer channels, tip link and associated proteins are shown for a tip link between a taller and a shorter stereocilium (e.g. as in inset to Fig. 5.3). The mechanotransducer channel is shown situated in the cell membrane at the lower end of the tip link. The tip link, composed of cadherin-23 and protocadherin-15, is here drawn as attaching directly onto the channel, although it may connect via intermediary proteins. The channel is provisionally shown as being tethered to the underlying cytoskeleton via an anchor: the tips of the shorter stereocilia are known to have a number of strands running between the cell membrane around the tip link insertion site and the underlying density on the actin core. At the upper end of the tip link, the tip link may attach via harmonin (in conjunction with another scaffolding protein, sans) to myosin 7a, which provides the adaptation motor. Myosin 1c may also be involved in the adaptation. Myosin heads tend to crawl up the actin filaments, tensioning the tip link as part of the slow adaptation mechanism. Myosin 15a forms parts of the cap over the actin filaments at the tips of shorter stereocilia. Arrows on actin filaments show the direction of arrowheads formed by decoration of actin by myosin heads (opposite to the direction of myosin movement). Data from Pickles *et al.* (1984, 1991), Dumont *et al.* (2002), Sidi *et al.* (2003), Corey (2006), Rzadzinska *et al.* (2004, 2005), Siemens *et al.* (2004), Schneider *et al.* (2006), Vollrath *et al.* (2007), Kazmierczak *et al.* (2007) and Grati and Kachar (2011).

(see Section 5.3). The channel is then likely to be attached directly or indirectly via anchors to the density covering the upper ends of the actin filaments of the shorter stereocilium (Fig. 5.6).

5.2.3 The mechanotransducer channels

The channels are likely to be situated on the tips of the shorter stereocilia on the hair bundle, attached to the lower end of the tip link (see Section 5.3). However, molecular nature of the channel is not known. This search has been difficult for

two reasons: (i) there are only a few active channels per stereocilium, and only relatively few hair cells per animal, which means that only a few molecules are likely to be available for analysis and (ii) the channels are not operated by chemical ligands which restricts the molecular tools that can be used to label or extract them.

Initial research deriving from random mutation experiments in flies, followed by targeted interference in zebrafish and mice, suggested that members of the TRP channel family could be candidates (Sidi *et al.*, 2003; Corey *et al.*, 2004) (TRP: transient receptor potential; named after the first member of the family to be found, which coded for a membrane channel expressed in the *Drosophila* visual system). However, knockout of the candidate in mice, TRPA1, left hair cell mechanotransduction intact, casting doubt on the interpretation of the earlier results in zebrafish (Kwan *et al.*, 2006). Nevertheless, based on channel properties, the channel may still be a member of the TRP family (Corey, 2006). One recent suggestion based on channel properties, but without definitive molecular information, is that the channel is composed of different members of the TRPP family (also known as PKD or polycystin channels) (Fettiplace, 2009).

A functional channel is likely to exist as a multimer of subunits linked together. Therefore it is quite possible that the expressed mechanotransducer channel is a heteromer of different subunits, the composition possibly varying with hair cell type and with cochlear location.

Figure 5.6 shows the current model of how the stereocilia, tip link and mechanotransducer channels fit together to detect movements. In addition to the evidence described in this section, the evidence is also derived from electrophysiological experiments, which will be described in Section 5.3.

5.3 THE ELECTROPHYSIOLOGICAL ANALYSIS OF MECHANOTRANSDUCTION

It is difficult to record intracellularly from single cochlear hair cells while manipulating the stereocilia, and so the best information on transduction has been obtained from hair cells of the vestibular system. However, where data from cochlear hair cells are available, they have supported the data from vestibular cells.

Before considering the process of transduction, it is useful to review a few of the basic facts about cell membrane potentials.

5.3.1 Cell membrane potentials

Nerve cell membranes are more permeable to some ions than to others – for instance, in the resting state they are many more times permeable to K^+ than to Na^+ ions. Because there is a high K^+ concentration inside the cell and because the cell membrane is permeable to K^+ , K^+ ions tend to diffuse out passively down their concentration gradient, taking positive charge with them and leaving the inside of the cell with a net negative potential. This potential is known as a diffusion potential. Diffusion continues until the negative potential inside the cell is sufficient to stop the further movement of ions, at which point in an ideal

system K^+ would be held in equilibrium. The value of potential at which this occurs is known as the equilibrium potential. It is possible to think of various schemes for the modulation of ion flows in hair cells. If, for instance, the apical surface of the hair cell faced an endolymph that, as well as having a low electrical potential, had a low K^+ concentration, increasing the permeability to K^+ alone would generate a negative diffusion potential across the apical membrane of the hair cell. K^+ would tend to diffuse out of the hair cell, tending to take the membrane towards the K^+ equilibrium potential. The inside of the cell would then become hyperpolarized, that is more negative. Increasing membrane permeability alone does not therefore necessarily produce a reduction in the membrane potential; the important point is that the membrane potential tends to move in a direction towards the equilibrium potential of the diffusible ion, or to a weighted mean of the various equilibrium potentials if more than one ion is involved.

In mammals the K^+ concentration in endolymph is approximately the same as that inside the cell, and the Na^+ concentration is very low. Therefore no substantial diffusion potential will be produced by the flow of these ions across the apical membrane of the hair cell, and decreasing the resistance will simply pull the negative intracellular potential towards the endolymphatic potential, producing a depolarization. As a bonus, in mammals the endolymphatic potential is 80 mV or so positive. This increases the driving force across the apical membrane from 45 mV or so to 125 mV in the case of the inner hair cells.

It is presumably advantageous for the current to be carried by K^+ rather than by Na^+ . Because K^+ is in equilibrium across the basal membrane of the hair cell, any K^+ entering the cell will diffuse out automatically through K^+ channels in the basal membrane, and K^+ will not accumulate inside the cell. In this case, the energy driving the current flow is ultimately derived from ion pumps in the stria vascularis. It has the advantage of allowing the main blood supply to be removed well away from the organ of Corti, with a consequent reduction in possible vascular noise.

Although there are considerable advantages in the transducer current being carried by K^+ , we must not forget that other schemes are possible. For instance, if the apical surface faced a normal extracellular fluid that was high in Na^+ and low in K^+ and if the channels are non-specific for Na^+ and K^+ (which is the case – see below), then lowering the membrane resistance would tend to bring the potential to a weighted mean of the Na^+ and K^+ equilibrium potentials, that is to around 0 mV if there is no endocochlear potential. The cell would again tend to depolarize. This is in fact the position in many investigations of hair cell transduction undertaken *in vitro*. In addition, other ions, such as Ca^{2+} , also carry some of the transducer current.

5.3.2 Mechanotransduction

5.3.2.1 Mechanotransduction depends on deflection of the stereocilia

The most straightforward information on transduction comes from direct manipulation of the stereocilia on single hair cells during intracellular recording.

This was undertaken, for instance, in the hair cells of the bullfrog sacculus. [Hudspeth and Corey \(1977\)](#) excised the saccular macula and removed the covering otoliths and membranes. They directly manipulated the stereocilia with a glass rod while recording intracellularly with fine microelectrodes. They showed that deflection of the stereocilia in the direction of the kinocilium, that is in the direction of the tallest stereocilia, caused intracellular depolarization, and so was associated with neural excitation, while deflection in the opposite direction caused hyperpolarization ([Fig. 5.7](#)). They therefore confirmed the conclusion that had

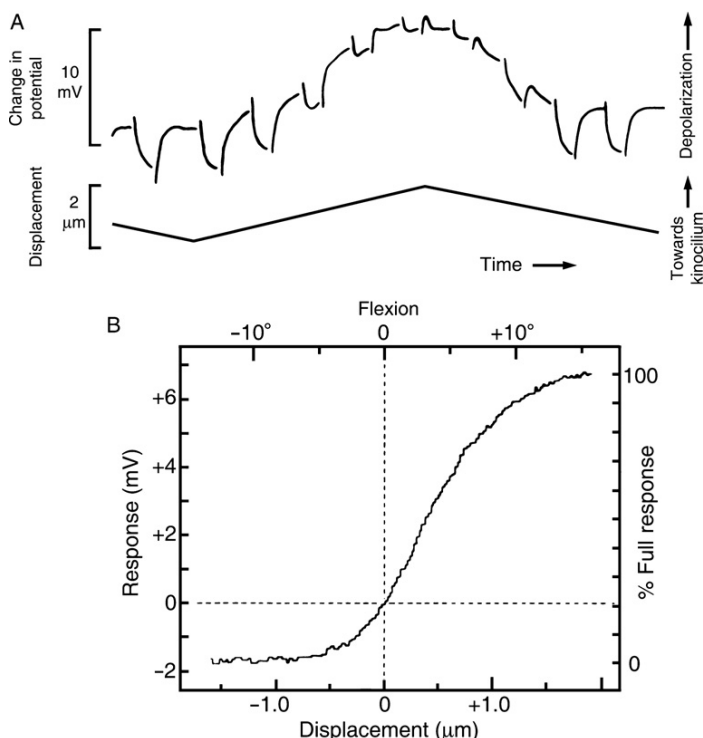


Fig. 5.7 (A) Deflection of the stereocilia towards the kinocilium produced depolarization, and deflection away from the kinocilium produced hyperpolarization, in a hair cell of the bullfrog sacculus. The kinocilium, a specialized cilium found in vestibular but not mammalian cochlear hair cells, is adjacent to the centre of the row of tallest stereocilia. The small pulses on the upper trace show the voltage response to current pulses in the recording electrode. Large voltage changes show that the membrane resistance was high, and small changes show that it was low. The membrane resistance was smaller when the cell was depolarized. (B) The relation between hair deflection and voltage change. The function is saturating, and symmetric around its mid point. However, because the channels are substantially closed at zero deflection, the function is asymmetric around its resting point (see Fig. 3.20 for corresponding data from mammalian cochlear hair cells). From [Hudspeth and Corey \(1977\)](#), Fig. 3.

been made less directly many years earlier from vestibular nerve responses in whole animals, that deflection of the stereocilia in the direction of the kinocilium is excitatory, while deflection in the opposite direction is inhibitory (Löwenstein and Wersäll, 1959). This has since been confirmed in mammalian cochlear hair cells by direct manipulation of the stereocilia (e.g. Geleoc *et al.*, 1997; see Fig. 3.20).

In cells that have a kinocilium as well as stereocilia, it can be shown that transduction depends only on the movement of the stereocilia. If the kinocilium is teased away from the bundle of stereocilia, transducer currents are evoked only by manipulation of the stereocilia, and not the kinocilium alone (Hudspeth and Jacobs, 1979). In cochlear hair cells, of course, there was never any question that transduction might depend on the kinocilium, since cochlear hair cells do not have a kinocilium when mature.

5.3.2.2 Mechanotransduction opens channels at the tips of the stereocilia

Depolarization of the cell is associated with a decrease in membrane resistance, while hyperpolarization is associated with an increase. Hudspeth and Corey (1977) introduced current pulses down their recording electrode and found that the resulting intracellular voltage changes were small when the stereocilia were deflected towards the kinocilium, that is when the cell was depolarized, and large when the stereocilia were deflected in the other direction, that is when the cell was hyperpolarized (see Fig. 5.7A). A small voltage response to the introduced current suggests that the introduced current had been able to leak out of the cell relatively easily. This shows that the resistance was low when the cells were depolarized and suggests that the depolarization had been produced by ion channels opening in the cell membrane.

A number of different experiments have shown that the transduction channels are situated at or near the tips of the stereocilia (Hudspeth, 1982). The clearest demonstration has come from imaging the entry of Ca^{2+} ions. Cells can be pre-loaded with dyes that fluoresce in the presence of Ca^{2+} . Because the resting level of Ca^{2+} in the cells is very low, and because Ca^{2+} enters through the mechanotransducer channels, the fluorescent signal is a sensitive indicator of the sites of ion entry into the cell. Figure 5.8A–C shows how the fluorescent signal starts at the tip of a stereocilium and then spreads down the stereocilium with time. This shows that the mechanotransducer channels are indeed situated at the upper ends of the stereocilia.

If, as seems possible from these experiments, the mechanotransducer channels are situated at or near the insertions of the tip links, the question arises whether channels are associated with the top end, the bottom end or with both ends, of the tip link. Beurg *et al.* (2009) measured the fluorescence in rat inner hair cell stereocilia, in response to deflection of the bundle. They found a fast fluorescent signal, showing Ca^{2+} entry, in stereocilia of the two shorter rows on the bundle, but not in the stereocilia of tallest row (Fig. 5.8D and E). This suggests that in the mammalian cochlea, the mechanotransducer channels are situated only at the lower end of the tip links. This result is in contrast to an earlier result obtained by

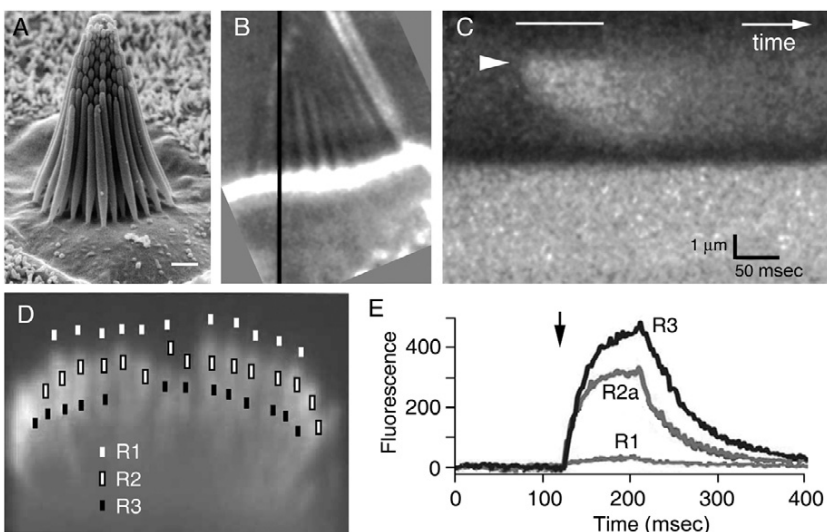


Fig. 5.8 (A) Scanning electron micrograph of a hair cell of the bullfrog saccus. Scale bar, 1 μm . (B) Light micrograph of a hair cell of the bullfrog saccus, seen from the side. The solid vertical line shows the line along which fluorescence in the single stereocilium in part C was measured. (C) Distribution of fluorescent signal in stereocilium marked in B, as a function of height in the bundle (vertical) and time (horizontal). A mechanical stimulus was applied during the white bar. The fluorescent signal appeared first at the top of the stereocilium (arrowhead) and then spread down the stereocilium. (D) Fluorescence due to mechanotransduction-induced Ca^{2+} ion entry in an inner hair cell of the rat cochlea. The microscope was aligned so that the tips of the stereocilia on all three rows were in focus. Symbols show analysis points at the tips of the stereocilia. No fluorescence is visible in the tallest stereocilia (R1: row 1), but is visible in most shorter stereocilia (R2 and R3: rows 2 and 3). However, two stereocilia in the centre of R2 do not show a signal. (E) Time-course of fluorescence change in part D. Signals were averaged over all stereocilia of the different rows, except that for row 2, only active stereocilia (R2a) are shown. There is negligible response in the tallest stereocilia (R1). The signal in R3 is probably overestimated because of show-through from signals in R2. The arrow shows the time at which an induced change in membrane potential allowed movement-induced mechanotransducer currents to enter the cell without introducing movement-induced artefacts (see original paper for details). A from Holt and Corey (2000), Fig. 1A, Copyright (2000), National Academy of Sciences, USA. B and C from Lumpkin and Hudspeth (1995), Fig. 2A and C, Copyright (1995), National Academy of Sciences, USA. D and E from Beurg *et al.* (2009), Fig. 2 (modified).

Denk *et al.* (1995) in the bullfrog saccus, who showed that tall as well as shorter stereocilia were able to carry some of the mechanotransducer current. The reason for the difference is not known; it may be related to the presence of the kinocilium in the vestibular hair cells, which could possibly activate channels in the adjacent tall stereocilia.

5.3.2.3 Mechanotransduction depends on the tip links

Strong evidence that tip links are involved in mechanotransduction came from experiments in which the tip links were broken by the calcium chelator BAPTA (Assad *et al.*, 1991). If all Ca^{2+} is removed from around the hair bundle, the tip links break (as shown anatomically), and mechanotransduction disappears irreversibly (Fig. 5.9). Mechanotransduction does not reappear even after the BAPTA has been removed and the level of Ca^{2+} has returned to normal. This manipulation is now commonly used in investigations of mechanotransduction to confirm that the currents investigated are indeed mechanotransducer currents.

5.3.2.4 Single-channel recording: only one or two channels per stereocilium

In many analyses of channels in other types of cell, it is possible to record from single channels, because it is possible to apply a patch-clamp (i.e. gigaohm seal) electrode to the cell membrane and find instances when only a single channel is included in the patch under the electrode. It is not possible to use a similar technique to record from single mechanotransducer channels in hair cells, because patch electrodes cannot be applied to the stereocilia while keeping mechanotransduction intact. Instead, briefly lowering the extracellular Ca^{2+} concentration can reduce the number of active channels on the cell, presumably by breaking most of the tip links (Crawford *et al.*, 1991; Ricci *et al.*, 2003). In occasional cases, this has allowed single mechanotransducer channels to be measured with an electrode attached to the cell body. Patch-clamp electrodes are used, which have wide (about 1 μm) tips, giving low access resistances and allowing the recording of fast electrical events inside the cell.

When single channels are found, they spontaneously flicker between their open and closed states. Channel openings and closings are shown by the discrete transitions between the two states (Fig. 5.10A). Applied mechanical stimuli cause a

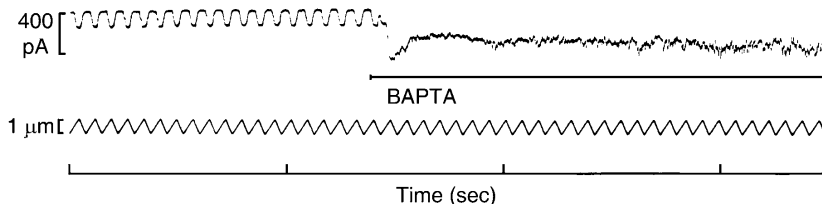


Fig. 5.9 Mechanotransducer currents (top trace) were measured in a single hair cell of the bullfrog sacculus, in response to cyclic displacement of the stereocilia (lower trace). The Ca^{2+} -chelator BAPTA was applied to the bundle at time marked by the horizontal bar. Mechanotransducer currents disappeared and did not recover. From Assad *et al.* (1991), Fig. 1A.

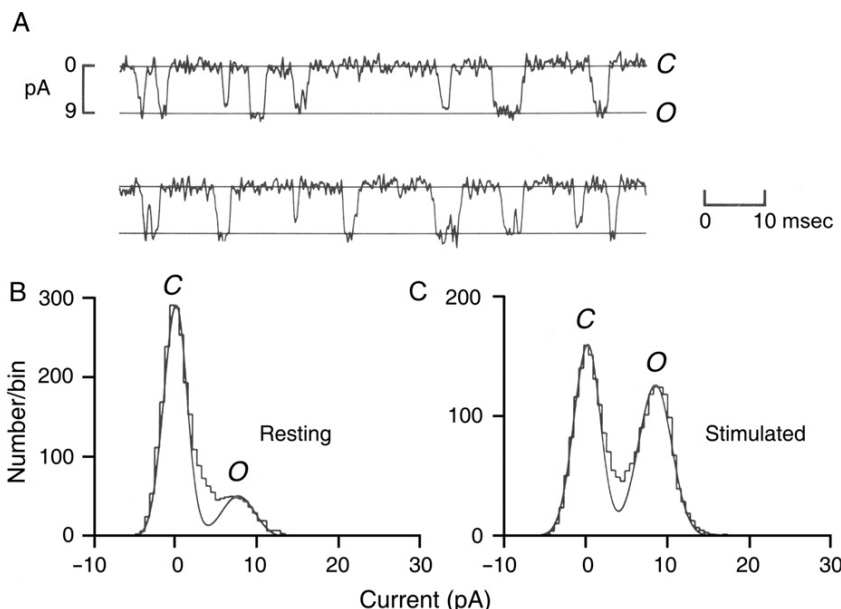


Fig. 5.10 (A) Single mechanotransducer channel recorded in the turtle cochlea. C, closed state; O, open state. pA: current through the cell in picoamperes. (B) and (C) Distribution of membrane currents over time, recorded in another channel. When the bundle is unstimulated (B), the channel spends most of its time in the closed state. When stimulated (C), the channel spends more time in the open state. From Crawford *et al.* (1991), Figs. 11 and 13.

redistribution in the states, an excitatory stimulus causing the channel to spend more time in the open state (see Fig. 5.10B and C). The analysis of current flows shows that single channels in rat cochlear hair cells have a conductance of 145–260 pS,¹ with higher conductances being found at the high frequency end of the cochlea (Beurg *et al.*, 2006). These are much larger than the earlier, less direct, estimates. Comparing these values with the total conductance change seen in intact hair cells, and taking into account the number of stereocilia per hair cells, suggests that there are between 1.2 and 1.7 active channels per tip link (Beurg *et al.*, 2006). This is consistent with the model shown in Fig. 5.6, particularly if two channels are present at the lower point of attachment of the tip link, possibly one associated with each of the two strands of protocadherin-15 in the tip link. The single-channel conductances that have been found are comparable with those that have been found for some TRP channels in other systems (e.g. 172 and 310 pS for TRPV3 and TRPV4).

¹ Conductance is measured in siemens (S), which is the inverse of ohms; the conductance in siemens = current divided by driving voltage.

5.3.2.5 The ionic selectivity of the channel

Corey and Hudspeth (1979a) varied the ionic content of the solution bathing the apical surfaces of their hair cells and showed that a range of ions could carry the transducer current. The alkali cations, including Na^+ and K^+ , could carry the transducer current to an approximately equal extent. Ca^{2+} can also carry the transducer current, though it appears to partially block the channel as well. The channel therefore appears to be relatively non-specific and to belong to the class of non-specific cation channels. Tetramethylammonium (TMA), triethylammonium (TriEA) and other amines can also carry the current, although with a lower permeance, suggesting that the pore diameter is approximately 1.2 nm (Farris *et al.*, 2004; Fettiplace, 2009).

By far the most abundant cation in the endolymph is K^+ , and since K^+ has a high permeance through the transducer channel, it is reasonable to suppose that K^+ carries a high proportion of transducer current in the mammalian cochlea. This is supported by experimental evidence since K^+ accumulates in the space around the base of the outer hair cells during acoustic stimulation (Johnstone *et al.*, 1989). Moreover, the reversal potential of the transducer current in inner hair cells of the guinea pig cochlea is approximately equal to the endocochlear potential (Russell, 1983). This would be expected if the stereocilia were faced by an endolymph with the high positive potential and if current were carried by an ion with the same concentration in the endolymph as intracellularly. However, and very importantly, a substantial proportion of the mechanotransducer current is also carried by Ca^{2+} . Ca^{2+} is driven into the cell both by a concentration gradient and by its electrochemical gradient. Once inside the cell, Ca^{2+} is able to have further effects, for example it is able to alter the conformation of the molecules associated with mechanotransduction (see below).

5.3.2.6 Kinetic evidence on the nature of mechanotransduction and gating spring theory

The transducer channels open and close with a very short delay. Corey and Hudspeth (1979b) showed that the transducer current, in response to pulse stimuli, changed with a delay of only 40 μsec at 22°C. The short latency agrees with the latencies that would be required to subserve hearing at the upper frequency limits of mammalian perception, for instance, 120 kHz for dolphins and 150 kHz for seals (Brown and Pye, 1975). The latency has a temperature dependence, decreasing by a factor of 2.5 for every 10°C increase between 1 and 38°C.

These results suggest that the transduction process has a fairly simple mechanism, with its short latency and its low temperature dependence arguing against any great complexity (Corey and Hudspeth, 1983). By contrast, one could imagine rather more complex models in which, for instance, a protein kinase was activated or a second messenger released, opening the channels by a biochemical reaction. A further continuously active enzyme would then return the channels to their non-conducting state. The likelihood of these models is

limited by the short latency of channel opening and the speed at which the channels can close at the end of a stimulus, which mean that the biochemical reactions would have to proceed at unrealistically high rates (Corey and Hudspeth, 1983).

More plausible are models in which the displacement opens the channel by a direct mechanical action, such as shown in Figs. 3.19B and 5.6 where the channel is opened by a direct mechanical pull from the tip link. Put in terms of a kinetic analysis, the pull alters the energy difference between the open and closed states of the channel plus associated structures. Thermal energy would continuously move the channel between its opened and closed states so that the proportion of the time spent in one state would depend on the energy difference and so on the displacement (Fig. 5.11). Since it is supposed that the channel fluctuates between its open and closed states under the influence of thermal energy, the relative probabilities of the two states can be calculated from the Boltzmann distribution (Corey and Hudspeth, 1983).

In its simplest form, such a model can be described in the following way, which also forms the basic analysis to which gating in all other types of mechanosensitive channels is referred (Hamill and Martinac, 2001; Sukharev and Corey, 2004).

In the analysis of Corey and Hudspeth (1983), the channel is assumed to be pulled open by an elastic link, called the gating spring (see also Howard *et al.*, 1988; Markin and Hudspeth, 1995; Sukharev and Corey, 2004). The gating spring is directly attached to the gate of the channel, which is provisionally viewed as a door that opens and closes. The gating spring is elastic so that as the door opens, the gating spring is slackened, and as it closes, the gating spring is stretched (see Fig. 5.11A). The energy level of the mechanotransducing element (channel plus gating spring) can be represented in an energy diagram (see Fig. 5.11B).

If a spring is stretched, the force at the end of the movement is equal to the spring constant (stiffness of the spring) multiplied by the distance of the stretch. The work required to produce this movement can be calculated by integrating the force over the distance, and is equal to the spring constant κ multiplied by the square of the distance of the stretch, all divided by 2.

Consider the case where there is no resting tension on the gating spring when the channel is open. If the channel closes (e.g. spontaneously as under the influence of thermal energy), the gating spring is stretched by a distance y . The work performed on the spring is $\int \kappa y \, dy = \kappa y^2/2$.

If the other end of the gating spring had been stretched by a distance x before the gate closes, the work done by the gate on closing increases because of the increased force on the spring; the work is now larger: it is $\int \kappa(y+x) \, dy = \kappa(y^2/2 + xy)$. The difference between the two terms is κxy , which is a linear function of the externally applied stretch x of the gating spring.

In the absence of any initial tension on the gating spring, the closed and open states of the channel plus spring have an intrinsic energy difference C . With an externally applied stretch of the gating spring, the energy difference ΔG between the closed and open states becomes $\kappa xy + C$.

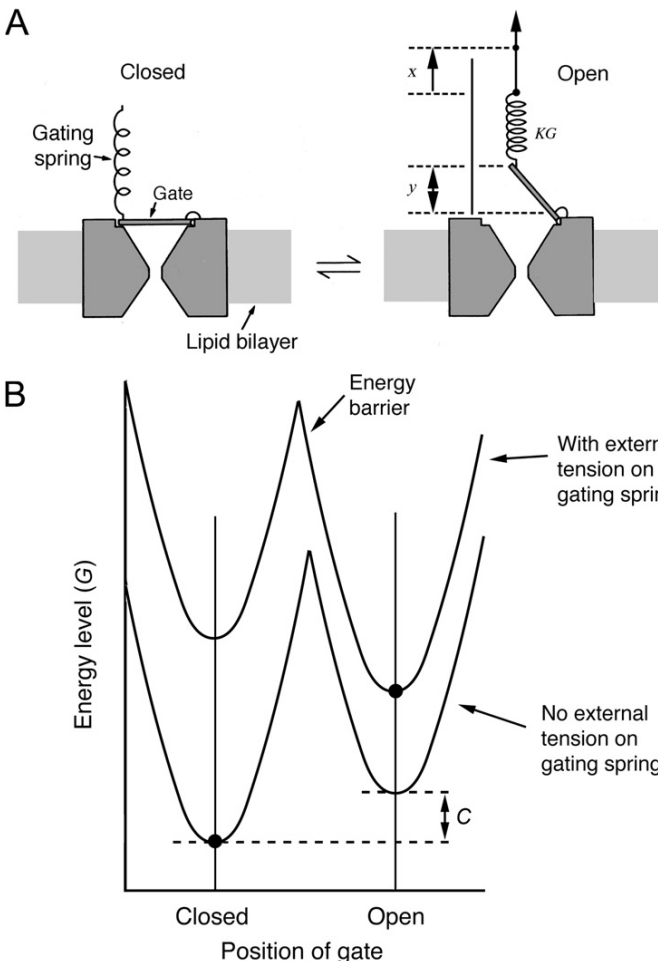


Fig. 5.11 (A) Kinetic description of the mechanotransducer channel and gating spring in a two-state model. The channel opens and closes under the influence of thermal energy. When it closes, it stretches the gating spring by an amount y . The external stimulus separately stretches the other end of the gating spring by a distance x . From Howard and Hudspeth (1988), Fig. 1. (B) Energy level of the channel plus gating spring, as a function of position of the gate. On the horizontal axis, the displacement of the gate is marked on a hypothetical scale of distance. The lower curved line is the hypothetical relation between internal energy and displacement of the gate, in the absence of external displacement of the other end of the gating spring. The function shows two minima, one in the open position and one in the closed position. (C) The energy of the closed state minus the energy of the open state, when there is no tension on the gating spring. The position of the lowest energy (the closed position in this case) is the favoured state in which the channel spends most of its time. External stretch of the gating spring changes the shape of the function, increasing the energy level more when the gate is closed than when it is open (see calculations in text) so that now the open state is favoured. The two most favoured states, with and without external extension of the gating spring, are marked by the black dots.

From Boltzmann's law, the probability p_1 that a system at equilibrium is in state 1 rather than the probability p_2 that it is in state 2 is related to the energy difference ΔG between the states, according to the following formula:

$$\frac{p_1}{p_2} = e^{-\Delta G/kT}$$

where k is Boltzmann's constant and T the absolute temperature.

Here

$$\frac{p_c}{p_o} = e^{-\Delta G/kT}$$

where $p_o = p(\text{open})$ and $p_c = p(\text{closed})$. Because at equilibrium $p_o + p_c = 1$,

$$p_o = \frac{p_o}{p_o + p_c} = \frac{1}{1 + (p_c/p_o)} = \frac{1}{1 + e^{-\Delta G/kT}} = \frac{1}{1 + e^{-(\kappa xy + C)/kT}}$$

This is the basic formula that relates the open probability of the channel at equilibrium to the extension of the gating spring x produced by an external stimulus, in the two-state kinetic model. Because the stretch of the gating spring can be related to the deflection of the stereociliary bundle by simple geometry, the open probability can now be related to the deflection of the bundle. The function is a symmetrical sigmoid, going from zero open probability at large negative deflections to open probability of one at large positive deflections. This function corresponds to the relation between open probability and magnitude of the input stimulus for some (e.g. Fig. 5.12), but not all (see, e.g. Fig. 3.20B) experimental results. Apart from the position of the curve along the horizontal axis, the only free parameter that needs to be adjusted in fitting the theoretical function is the product $\kappa\gamma$, which is equal to the effective stiffness of the gating spring multiplied by the swing of the channel's gate; in the case of Fig. 5.12, this had a value of 4.3×10^{-14} N per channel.

Where experimental functions deviate from the symmetric sigmoid, the function commonly saturates relatively sharply for low open probabilities and saturates relatively slowly for high open probabilities (as in Fig. 3.20B). This can be accounted for with a model with three or more states, by supposing that, as with many other channels, there are at least two closed states C_1 and C_2 and one open state (see, e.g. Corey and Hudspeth, 1983; Markin and Hudspeth, 1995).

The model explains some otherwise curious results, such as the way in which the time constants of channel opening decrease for large stimulus steps (Corey and Hudspeth, 1983). This occurs because the energy of the closed state (upper curve, Fig. 5.11B) becomes relatively larger with larger deflections of the stereocilia so that the energy barrier for opening defined in Fig. 5.11B becomes smaller relative to the closed state, with the result that the transitions become

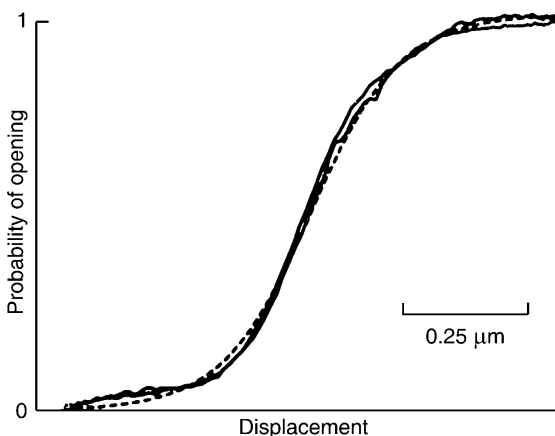


Fig. 5.12 Symmetrical change in transducer current, as recorded with a patch-clamp electrode in a single cell of the bullfrog sacculus. The curves for the measured transducer current (solid lines) have been fitted with a curve calculated from the two-state kinetic model described in the text (dotted line). From Holton and Hudspeth (1986), Fig. 12.

faster. In addition, it suggests that the channel does not have any absolute threshold for opening, since the opening is probabilistic, under the influence of thermal energy. Such processes are required to account for the very low threshold of auditory sensitivity.

The energy diagram of Fig. 5.11B has another implication. As an external force moves the channel from its closed state to the open state, the channel has to move over the energy barrier between the states. Once just over the top of the barrier, the channel will tend to jump spontaneously to the next energy minimum, the open state. From the top of the barrier, therefore, the gate will move spontaneously in the direction of the applied force, or in other words, show a negative stiffness. This can be detected as a drop in the stiffness of the bundle as a whole (Howard and Hudspeth, 1988; Markin and Hudspeth, 1995). The fact that channel opening and closing can affect the stiffness of the whole bundle is a strong confirmation of the idea that the channels are opened by a direct mechanical action.

The anatomical structure that corresponds to the gating spring is at the moment uncertain. Initially it was suggested that the tip link might be elastic and that the link, as well as coupling the mechanical stimulus to the mechanotransducer channel, could act as the gating spring. However, the micrographs of Kachar *et al.* (2000) suggested that the link might be stiff, not elastic, and it is difficult to see how cadherin-23 or protocadherin-15 could have sufficient elasticity. Instead, it has been suggested that the gating spring might be provided by the proteins that attach the tip link to the channel, or by the proteins that anchor the mechanotransducer channel to the underlying actin core (Fig. 5.6). However, the basic kinetic analysis of the gating spring model would remain unchanged.

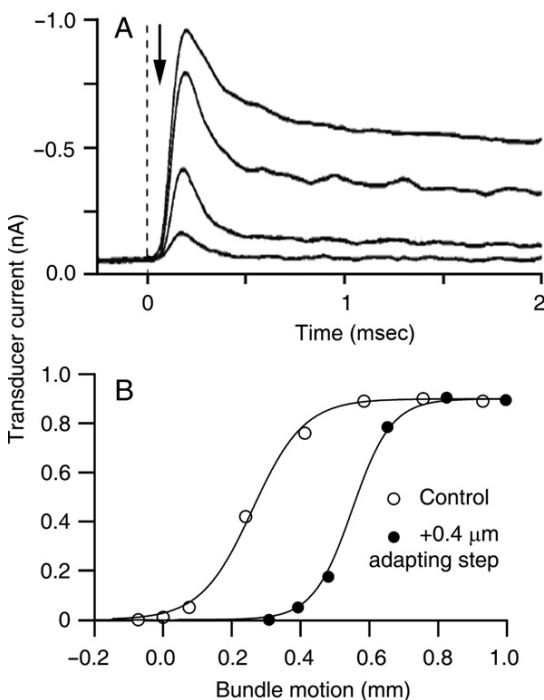


Fig. 5.13 Fast adaptation in an outer hair cell isolated from the rat cochlea. (A) The responses to steady displacement steps applied to the stereocilia decline with time. For the second smallest step in (A), the time constant was 0.16 msec. The arrow shows the moment at which the deflection of the bundle started. From Kennedy *et al.* (2003), Fig. 1. (B) Response of an outer hair cell of the rat cochlea as a function of displacement of the stereocilia, before (control) and nearly immediately (5 msec) after an adapting step. From Fettiplace (2006), Fig. 1B.

5.3.2.7 Adaptation

When hair cells are stimulated with a sustained deflection of the stereocilia, their responses decline over time (Fig. 5.13A). In cochlear hair cells, the adaptation occurs with a time constant of 0.15–4 msec. This adaptation, known as fast adaptation, has been seen in hair cells of the turtle cochlea as well as the mammalian cochlea (Kros *et al.*, 1992; Ricci *et al.*, 2000; Kennedy *et al.*, 2003; see also reviews by Fettiplace, 2006 and Peng *et al.*, 2011). Fast adaptation can be affected by manipulations that alter the Ca^{2+} levels within the stereocilia, such as varying the external Ca^{2+} concentration (since Ca^{2+} enters through the mechanotransducer channels), depolarizing the hair cells to prevent Ca^{2+} from entering, or by experimentally varying the intracellular concentration of Ca^{2+} buffers such as BAPTA (Ricci *et al.*, 1998). The rapid action of Ca^{2+} that enters through the

mechanotransducer suggests that it acts within 15–35 nm of the channel. On one current model, the Ca^{2+} binds within the mechanotransducer channel, making it more likely to close. This shifts the channel's operating point so that the channel requires a larger stimulus force to open, lowering the open probability (Fig. 5.13B; Wu *et al.*, 1999; Cheung and Corey, 2006). The shift in the operating point actively adjusts the point on the input–output function at which the cells remain when there is no applied displacement to the stereocilia (see, e.g. Fig. 3.20B). When adapted, the cells do not lose overall responsiveness, because the slope of the activation curve remains steep. The time constant of fast adaptation varies with cochlear location, being faster in hair cells tuned to high frequencies (Ricci *et al.*, 2005).

Vestibular hair cells and turtle cochlear hair cells also show another type of adaptation, called slow adaptation, which occurs over a longer timescale of 20 msec or more. Slow adaptation, like fast adaptation, causes a shift in the operating point of the hair cell along the displacement axis. However, unlike fast adaptation, which probably depends on a change in the gating properties of the mechanotransducer channel, slow adaptation depends on a geometrical change within the stereociliary bundle. The polarity of the actin filaments of the stereocilia, as shown by the arrowheads formed when the filaments are decorated with heavy actin heads (S1 myosin), suggests that the myosin 7a and possibly also myosin 1c situated at the upper end of the tip link would tend to crawl up the actin filaments within the stereocilia, towards the tips of the stereocilia, thereby tensioning the tip link and pulling the mechanotransducer channels open (see Fig. 5.6). The entry of Ca^{2+} through open mechanotransducer channels tends to make the myosin motor slip so that the adaptation mechanism comes to equilibrium when the entry of Ca^{2+} through the partially open channels is just sufficient to hold the motor back against the tension of the tip link and the channels, thus setting the zero point of the bundle. Slow adaptation, unlike fast adaptation, can be affected by intracellular myosin ATPase inhibitors (see Gillespie, 2004, for review). It is possible that slow adaptation does not exist in mammalian cochlear hair cells, because it has not been seen in electrophysiological records. However, the candidate myosins, myosins 7a and 1c, are expressed at the requisite sites on the hair cell stereocilia (Dumont *et al.*, 2002; Grati and Kachar, 2011; see also a general discussion of adaptation in the review by Peng *et al.*, 2011).

5.4 THE ORIGIN OF SHARP TUNING IN THE COCHLEA

As described in Chapter 3, passive mechanical models of the cochlea have difficulty in reproducing the low-threshold, sharply tuned component of the travelling wave. The only theories to be successful in matching mechanical, hair cell, and auditory nerve tuning suppose that the cochlea contains an active mechanical amplifier. The amplifier, involving outer hair cells, detects the movement of the basilar membrane and feeds mechanical energy back into the travelling wave. The issue will now be examined in more detail. The discussion

will be based initially on models of the type discussed in Chapter 3, that is with a cochlear partition having a gradation of stiffness, mass and damping, and that separates two fluid-filled compartments with a pressure difference between them.

5.4.1 Is an active process necessary theoretically?

The argument turns on whether tuning curves of the type observed experimentally can be produced in models containing purely passive mechanics. As described in Chapter 3, some passive models can produce large and sharply tuned peaks, but of the wrong shape. In addition, if the peaks are made large, the phase changes become too abrupt. But how reliable is this as evidence that purely passive processes are inadequate?

de Boer and Nuttall (1999) addressed this further by starting with observed basilar membrane tuning curves and calculating back to the expected power fluxes within the cochlea. If the power flux stayed constant or declined from base to apex, passive models could apply, but if the power flux increased along the cochlear duct, then clearly extra energy must have been introduced. Their results show that broad tuning, such as is seen post-mortem, is associated with a constant or a declining power flux (Fig. 5.14A). In addition, the real membrane impedance in Fig. 5.14A is always positive. Real impedance is a measure of the impedance that is in phase with the velocity of the vibration, and positive real impedance is equivalent to damping, that is loss of energy. However, where animals show sharp tuning, the power flux increases near the peak of the travelling wave (see Fig. 5.14B). Moreover, the real part of the cochlear impedance now becomes negative on the basal slope of the travelling wave, just basal to the peak. Negative real impedance indicates the introduction of energy. Correspondingly, the power flux in the cochlea increases in this region of negative damping. This is strong and robust evidence that sharp tuning is associated with the introduction of energy into the travelling wave, that is there is active amplification of the experimentally observed mechanical travelling wave.

Further points can be raised to show that purely passive models are unrealistic.

1. If large resonant peaks are to be produced in purely passive systems, then the amount of damping has to be very low indeed. This is unrealistic in view of the levels of viscous damping to be expected in the cochlea.
2. As described above, if the amplitude of the travelling wave is matched with the physiological data, the tuning becomes far too sharp and the phase changes too abrupt.
3. Other attempts have been made to mimic the observed basilar membrane responses by varying the parameters of the cochlear model, and in particular to broaden the tip of the tuning curve while keeping the resonance peak large. This might, for instance, be done by supposing that there is appreciable longitudinal coupling along the cochlear partition. However, calculations show that the effect is to make the apical slope of the travelling wave too shallow, while still keeping an unrealistic sharply tuned tip on the travelling wave (Viergever and Diependaal, 1986).

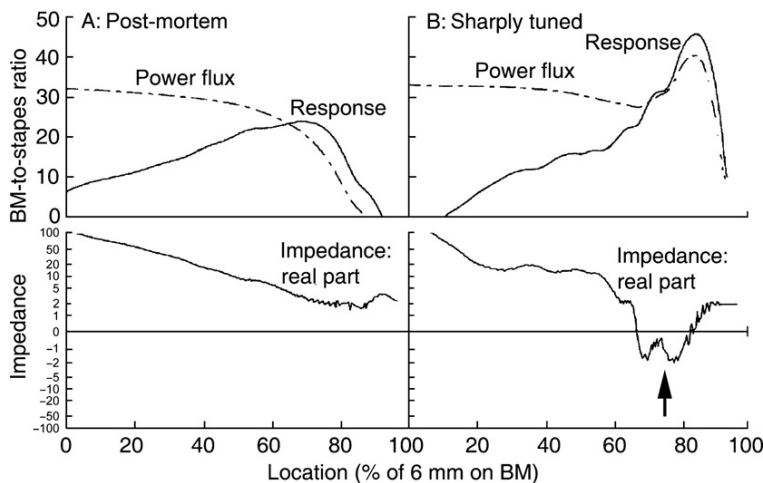


Fig. 5.14 Calculated power fluxes through the guinea pig basilar membrane and the real part of the basilar membrane impedance. (A) Results for a broadly tuned basilar membrane response, as measured post-mortem. (B) Results for a sharply tuned response measured in the living animal. In A the power flux declines smoothly towards the apex of the cochlea, and the real part of the impedance is always positive, meaning that the cochlea always absorbs energy. In B the power flux increases around the peak of the travelling wave, and the real part of the impedance becomes negative (arrow), meaning that in this region energy is being introduced into the travelling wave (as also shown in the diagrammatic representation of Fig. 3.16). The impedance scale is non-linear: values from +1 to -1 are spaced linearly, more extreme values are spaced logarithmically. Value $1 = 2 \times 10^3 \text{ kg/m}^2/\text{sec}$. Reprinted from de Boer and Nuttall (1999), Figs. 1 and 3, Copyright (1999), with permission from American Institute of Physics.

5.4.2 Models incorporating an active mechanical process

Models that simulate sharp tuning by means of an active process suppose that the outer hair cells, when stimulated, feed energy into the travelling wave. By appropriate choice of frequency and spatial dependence of the active process, it is possible to produce tuning curves of realistic shape. Moreover, the models are in agreement with the considerable body of data suggesting that normal functioning of outer hair cells is necessary for the development of sharp tuning in the wave. The evidence on this point will be discussed in Section 5.4.3.

One group of successful models suppose that the tectorial membrane, as well as simply hingeing as in the Davis model (see Fig. 3.3), can undergo compression and expansion vibrations in a direction radial across the cochlear duct (Fig. 5.15). The mass of the tectorial membrane as it undergoes radial oscillations, together with the stiffness of the stereocilia, form a second resonant system sitting on the cochlear partition (Zwislocki, 1980; Neely and Kim, 1986). The second system would be set into resonance by the motion of the basilar membrane and would then increase the stimulus

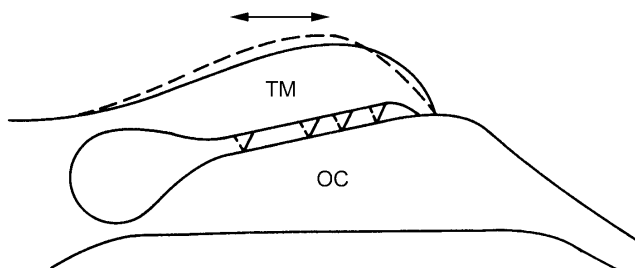


Fig. 5.15 A model of cochlear micromechanics, as originally suggested by Zwischenberger (1980), and as modelled by Neely and Kim (1986). The vertical vibration of the cochlear partition, in conjunction with the lever action of the organ of Corti (Fig. 3.3), sets the tectorial membrane into compression and expansion vibrations in a direction radial across the cochlear duct. TM, tectorial membrane; OC, organ of Corti.

to the outer hair cells. The outer hair cells would, by means of their motile properties, contribute to the pressure difference across the cochlear partition, thus amplifying the travelling wave. In this model, the resonance of the second system serves to confine the feedback to one region of the travelling wave, set to be just basal to the peak of the travelling wave. The active process in this region would amplify the travelling wave, the wave continuing along the cochlear duct to peak at its own characteristic place. Such models can produce responses that match the observed neural and basilar membrane tuning curves with a high degree of precision (Fig. 5.16), as well as matching most of the observed non-linearities and phase responses of the cochlea.

Models that successfully imitate observed cochlear tuning commonly use some mechanism to limit the active region to one part of the travelling wave. These include a second resonant system within the organ of Corti and the tectorial membrane, as described above, or factors such as a longitudinal variation in mechanical or geometrical parameters with distance along the cochlear duct, or frequency-specific delays, to effectively limit the active region to one part of the travelling wave (e.g. Lim and Steele, 2002; see also models reviewed by de Boer, 1996; Robles and Ruggero, 2001). However, not all successful models need to incorporate such an element (e.g. de Boer and Nuttall, 2002).

Successful models must also account for the correct phase relations. The effect of damping, which is akin to friction, depends on velocity. If the active process is to counter the effect of damping, it has to be delivered in phase with the velocity of movement of the basilar membrane. In other words, if the basilar membrane is moving upwards, then the peak of the active drive upwards has to be delivered when the basilar membrane is moving with maximum velocity upwards, which is $\frac{1}{4}$ of a cycle ahead of its displacement.

Active amplification has substantial advantages in performance, because the final thermal noise limit would be set by the noise in the amplification pathway, rather than by the noise in the mechanotransducer channels. Since the former is a

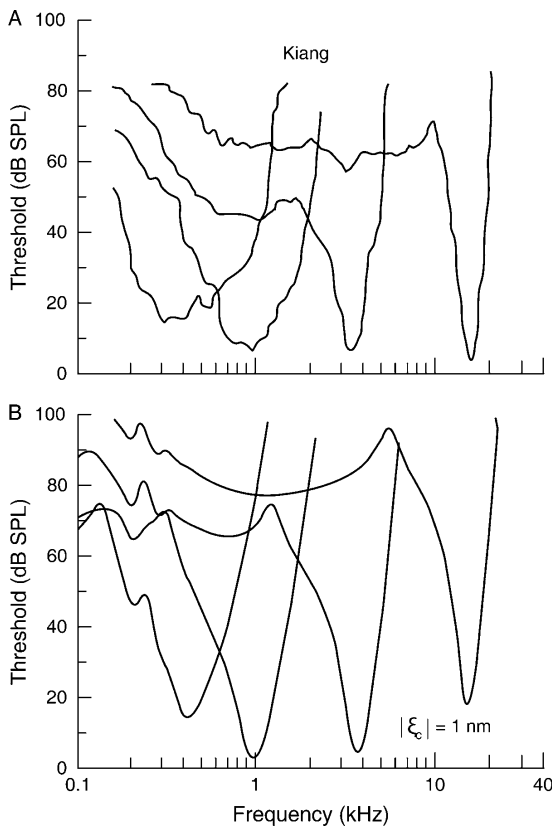


Fig. 5.16 (A) Sample cat auditory nerve fibre tuning curves, compared with predictions (B) from the active mechanical model of Neely and Kim (1986). Reprinted from Kiang (1980), Fig. 3, Copyright (1980), with permission from American Institute of Physics, and from Neely and Kim (1986), Fig. 12, Copyright (1986), with permission from American Institute of Physics.

narrowband-tuned element, but the channels are not, the noise limit can be lowered substantially.

The movements that occur within the organ of Corti and the tectorial membrane is an area known as cochlear micromechanics, and are further discussed in Section 5.4.6.

There are three main issues to be discussed in analysing the general validity of these models. Firstly, what is the evidence that outer hair cells are necessary for the development of low thresholds and sharp tuning? Secondly, is there evidence that outer hair cells can act as active mechanical amplifiers? And thirdly, can we measure the way in which hair cells might move so as to amplify the movements of the organ of Corti?

5.4.3 Outer hair cells: needed for low thresholds and sharp tuning

The most direct evidence that outer hair cells affect the tuning of the basilar membrane comes from experiments in which the medial olivocochlear bundle (MOC) is stimulated. The MOC is an efferent neural pathway that arises in the brainstem and ends specifically on the outer hair cells (discussed further in Chapter 8). It can be stimulated electrically where it crosses in the floor of the fourth ventricle in the brainstem. Stimulation reduces the amplitude of the mechanical vibration of the basilar membrane, increasing the thresholds particularly near the sharply tuned tip of the tuning curve (Fig. 5.17A; Murugasu and Russell, 1996; Dolan *et al.*, 1997; see also Fig. 8.4). These effects are closely paralleled by the effects on the inner hair cells, which are driven by basilar membrane vibrations but do not receive a medial olivocochlear innervation directly (Fig. 5.17B). Similar effects are seen in the auditory nerve fibres which are driven by the inner hair cells (see Chapter 8). The fact that activation of a neural pathway that ends exclusively on the outer hair cells affects the mechanical response of the basilar membrane shows that the outer hair cells influence the response of the basilar membrane.

Manipulations that affect the motility outer hair cells also influence cochlear thresholds and tuning. For instance, transgenic mice have been engineered to express a non-motile form of the protein prestin, the protein that is expressed in outer hair cells that normally confers the motile function (Dallos *et al.*, 2008). These mice have basilar membrane responses with high thresholds and broad tuning (Fig. 5.18C; Weddell *et al.*, 2011).

Further manipulations that affect outer hair cells also affect cochlear tuning. The ototoxic drug furosemide, which reduces the endocochlear potential and hence the electrical driving force through the outer hair cells, raises the thresholds and broadens the tuning of the mechanical response of the basilar membrane (Ruggero and Rich, 1991b), while the ototoxic drug salicylate, which primarily affects the outer hair cells, has the same effect (Murugasu and Russell, 1995). Kanamycin, an ototoxic drug that destroys outer hair cells while having less effect on other cells, raises the thresholds and broadens the tuning curves of auditory nerve fibres (see Fig. 5.17D). When the outer hair cells are inactivated, the insensitive, broadened tuning now comes to resemble that seen in the dead animal (see Fig. 3.13B).

5.4.4 Active mechanical processes in the cochlea: cochlear emissions

There is considerable evidence that the cochlea can generate movements, whether spontaneously or when stimulated by sound, and that the outer hair cells are responsible for the motion.

Kemp (1978) sealed both a microphone and a speaker into the ear canal of human subjects. An acoustic click presented through the speaker produced a brief wave of pressure in the ear canal. However, a second much smaller sound wave, delayed by 5–15 msec, could also be recorded. The results of a replication of his

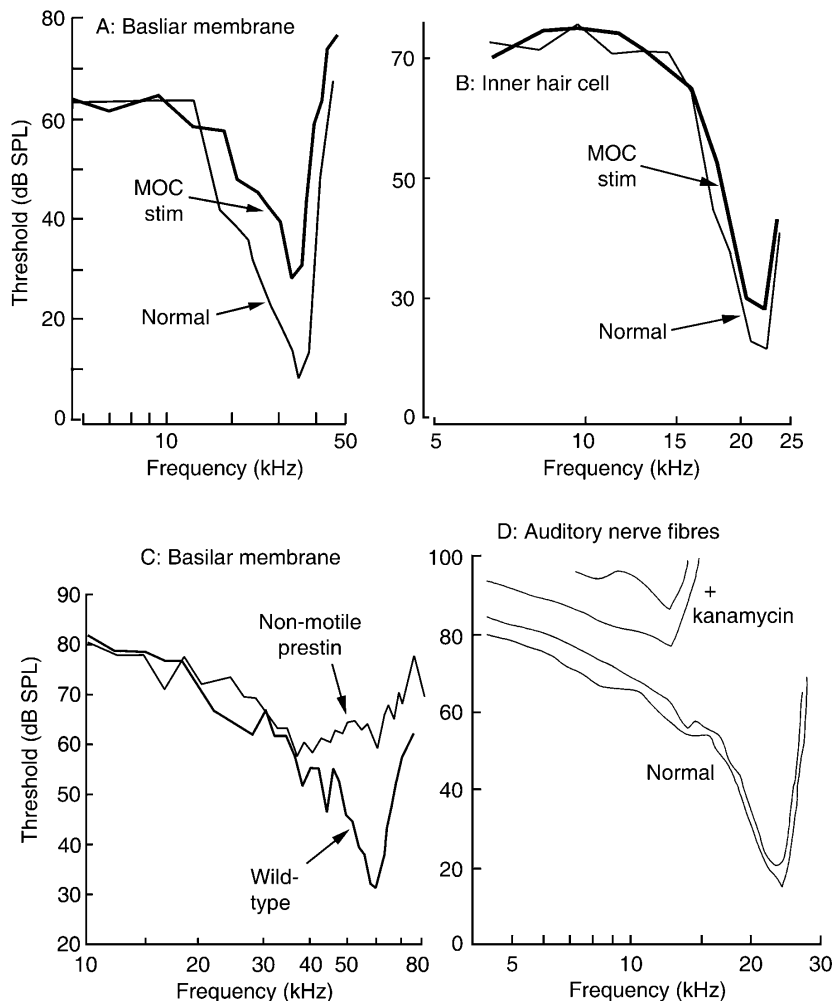


Fig. 5.17 Four manipulations that show the influence of the outer hair cells on cochlear thresholds and tuning. (A) Electrical stimulation of the medial olivocochlear bundle (MOC) which ends on the outer hair cells, raises the threshold of tuning curves for the mechanical vibration of the basilar membrane. Data from Murugasu and Russell (1996). (B) Effect of stimulation of the medial olivocochlear bundle on the tuning curve of an inner hair cell. From Brown and Nuttall (1984), Fig. 9. (C) Basilar membrane tuning curves in a normal mouse (wild-type) and in a mouse engineered to express a non-motile form of prestin in the outer hair cells. Data from Weddell *et al.* (2011), Fig. 1E. (D) Effect of damaging the outer hair cells with kanamycin, on the tuning curves of auditory nerve fibres. Reprinted from Robertson and Johnstone (1979), Fig. 1, Copyright (1979), with permission from American Institute of Physics.

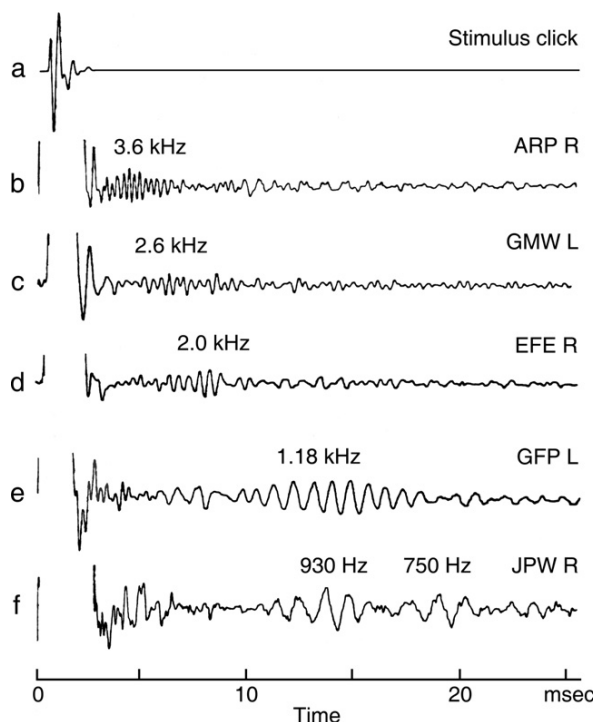


Fig. 5.18 When the ear is stimulated with a click, the cochlea returns an acoustic echo to the external auditory meatus. The form of the echo is different for each subject. The original stimulus in the meatus is shown in trace a. In traces b–f, shown with a much magnified vertical scale, the stimulus has clipped but the waveform of the echo is visible. Lower-frequency echoes tend to occur later, consistent with the longer travel times to the more apical low-frequency regions of the cochlea. Each trace is the average of many responses. From Wilson (1980), Fig. 2.

experiment by Wilson (1980) are shown in Fig. 5.18. The ‘echo’ was strongest relative to the input for low-intensity clicks. The suggestion was made that the mechanical impulse travelling up the basilar membrane at some point met a discontinuity in the impedance of the membrane. This caused a certain proportion of the energy to be reflected, setting up a pressure wave that travelled back to the base of the cochlea. The fact that the delayed response could be affected by ototoxic agents and was absent in sensorineurally deaf subjects indicated a cochlear origin for the effect. With suitable signal retrieval techniques it could be measured for stimuli well below the sensory threshold. Moreover, it preserved many details of the stimulus waveform and inverted its waveform when the stimulus was inverted. These suggest that it was generated by a stage before the synapse and it was not the result of the middle ear muscle reflex.

Analogous echoes can be seen with other types of stimuli. If, for instance, the ear is stimulated with a single continuous tone, the cochlea reflects the tone back into the ear canal. With two-tone stimulation, acoustic distortion products produced by intermodulation between the stimulus tones can also be detected in the ear canal. The amplitude of the reflected intermodulation tones can be affected by stimulation of the olivocochlear bundle, showing that the outer hair cells are involved in its generation (Mountain, 1980; Siegel and Kim, 1982). Moreover, ototoxic agents that target outer hair cells are able to reduce the echo (e.g. Hotz *et al.*, 1994). Further experiments suggest that the reflections occur from a sharply tuned late stage of the transduction process. For instance, it is possible to use a continuous tone to mask the echo to a click. The frequency and intensity relations of the tone necessary to mask any particular frequency component of the echo show that the generators behind the echo must be very sharply tuned (e.g. Kummer *et al.*, 1995).

These observations do not in themselves prove that the echo results from a mechanically active process and is of a type that uses metabolic energy. However, observations with more radical implications are shown in Figure 5.19. Figure 5.19A illustrates the sound pressure fluctuations in the ear canal of a human subject who heard a continuous tonal tinnitus, while Fig. 5.19B shows recordings of basilar membrane vibrations in a guinea pig that produced a spontaneous oscillation of its basilar membrane at 15 kHz. Incredibly, this oscillation was also directly audible to one of the investigators who put his ear near the opened ear. Clearly, where the cochlea shows oscillations in the absence of an acoustic stimulus, or where the oscillations far outlast a triggering stimulus, the cochlea must be able to produce mechanical energy. This is a very strong evidence that not only are intracochlear events able to affect the sound pressure in the ear canal, but that an amplifying and mechanically active physiological process must be involved. The necessity for an amplifying stage was also shown by Kemp (1978), who calculated that even when a click did not evoke tinnitus, more energy could be produced by the cochlea than was originally introduced. The obvious but revolutionary hypothesis that was put forward was that when the hair cells are stimulated, the cochlear partition is actively moved in return.

5.4.5 Motility in outer hair cells

Motility of a variety of forms has been demonstrated in outer hair cells. Two types that may be involved in the active amplification of sounds are (1) cell-body motility, in which outer hair cells change length and (2) active movements of the stereocilia, as a result of stimulus-induced motility of the mechanotransducer apparatus. It is likely that both forms of motility are simultaneously functional in the mammalian cochlea (Kennedy *et al.*, 2006). However, it is not certain whether only one or both forms of motility contribute to the active amplification of the travelling wave.

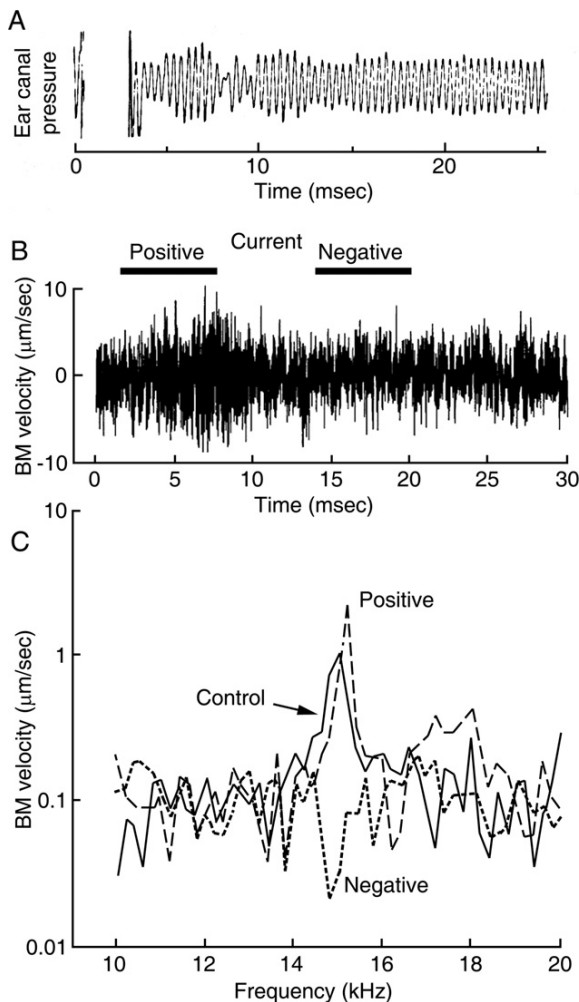


Fig. 5.19 (A) Spontaneous mechanical oscillations recorded from the cochlea. The acoustic waveform, recorded in the human external auditory meatus, of spontaneous cochlear oscillations. The click at the beginning of the trace (heavily clipped) synchronized the continuous ongoing oscillations, so that they became visible in the averaged waveform. The displayed waveform is the average of multiple repeats. From Wilson (1980), Fig. 5. (B) Mechanical vibration of the basilar membrane in a guinea pig that showed spontaneous oscillations of the basilar membrane at 15 kHz (spectrum in C). Short periods of positive and negative current were able to lock the oscillations into sufficient synchrony for a response to be shown in an average waveform. (C) The spectrum of the waveforms in B shows that positive current enhanced the oscillation and shifted its peak to higher frequencies. B and C reproduced from Nuttall *et al.* (2004), Fig. 3, with permission of the Association for Research in Otolaryngology.

5.4.5.1 Motility of the outer hair cell body

Brownell *et al.* (1985) showed that outer hair cells isolated from the guinea pig cochlea were able to change length in response to voltage changes produced via an electrode. The cells shortened when the cells were depolarized and elongated when the cells were hyperpolarized. The changes are fast and are able to follow applied transmembrane voltage changes up to at least 80 kHz, sufficient for motility at the upper reaches of hearing in many mammals (Grosh *et al.*, 2004). The motility depends on the presence of a protein called prestin, which is heavily expressed in the basolateral membranes of outer hair cells (Zheng *et al.*, 2000a). Transgenic mice that either under-express prestin or express abnormal prestin have outer hair cells that do not show the motile response and show abnormal mechanical tuning (Liberman *et al.*, 2002; Dallos *et al.*, 2008; Weddell *et al.*, 2011; Fig. 5.17C). Prestin in the membrane undergoes a conformational change in response to changes in transmembrane voltage, so that it alters its packing in the membrane and alters the area of the basolateral membrane (Matsumoto and Kalinec, 2005). When there is a change in area, cytoskeletal attachments under the membrane confine the extent to which the outer hair cell body can expand sideways so that any change in area is translated into a change in length of the cell (Holley *et al.*, 1992). These movements could be driven by the electrical gradient across the hair cell membranes, and therefore could use energy of metabolic origin stored in the endolymphatic potential as modulated by resistance changes in the mechano-transducer channels (for further review, see Dallos *et al.*, 2006).

There are two views of how the cell motility could amplify the movements of the basilar membrane. Firstly, we expect the outer hair cells to depolarize when the stereocilia are deflected in the excitatory direction. The resulting depolarization induces the motile response, shortens the outer hair cell bodies and alters the geometry of the organ of Corti (e.g. Nilsen and Russell, 2000). A different view of the contribution of somatic motility comes from Jia and He (2005), who examined the movements of outer hair cell stereocilia, when the hair cells were still within the isolated organ of Corti. Jia and He demonstrated that electrical stimulation could evoke movements of the bundle itself. Because the movements were absent in prestin-knockout mice, they presumably depend on the prestin expressed in the cell's soma. They were therefore most likely transmitted from the soma, possibly by tilting of the cuticular plate or by deformation of the reticular lamina. Such motility could amplify the vibration of the basilar membrane by the stereocilia actively pushing against the tectorial membrane.

At high (i.e. audio) frequencies, intracellular voltages will follow the transducer current with $\frac{1}{4}$ cycle delay. Therefore in the most straightforward model the voltages are not in the correct phase to amplify the movement, which would require the voltages to be in phase with the velocity, that is $\frac{1}{4}$ cycle in advance of, instead of $\frac{1}{4}$ cycle behind, the current and displacement (see Section 5.4.2).

Motility based on this mechanism faces a further, and possibly major, problem. The motility is driven by the transmembrane voltage. Although the motile mechanism itself is very fast, above about 1 kHz an increasing proportion of the transmembrane current passes through the capacitance of the cell wall, substantially

decreasing the fluctuations of the transmembrane voltage at high frequencies such that they may be too small to drive the motility. One solution was proposed by Dallos and Evans (1995a,b). They suggested that at high frequencies, where currents were substantially passing through the capacitances of the cell walls, all the capacitances of the organ of Corti would act as simple voltage dividers. The resulting division of voltage would be substantially independent of frequency (Fig. 5.20A). That is, as long as there were significant extracellular voltages produced by the outer hair cells, there would also be significant transmembrane voltages (coupled via the capacitances). A further factor was demonstrated by Johnson *et al.* (2011). They pointed out that in OHCs *in vivo*, not only are approximately 50% of the mechanotransducer channels open at rest, but voltage-gated conductances in the basal cell wall are substantially activated. These serve to lower the cells' resistance and so shorten the membrane time constant (which is given by the product of resistance and capacitance). Moreover, in OHCs from high-frequency regions of the cochlea, the cellular geometry and the conductances of the membrane channels change, shortening the membrane time constant

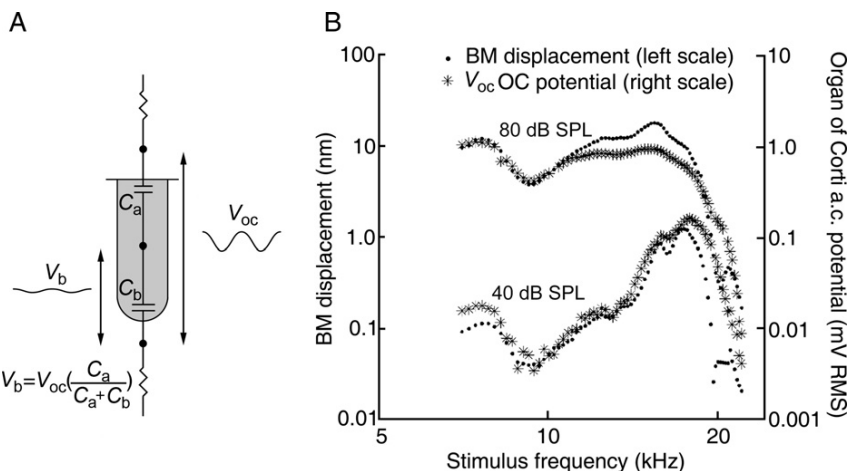


Fig. 5.20 (A) According to the suggestion of Dallos and Evans (1995a,b), at high frequencies, when most of the transcellular currents pass through the capacitances of the outer hair cell membranes, the apical and basal capacitances of an outer hair cell (shown in A) will act as a simple voltage divider. Mechanotransducer currents produce an oscillating voltage across the organ of Corti (V_{oc}). Since the impedance of a capacitor C is proportional to $1/C$, the voltage across the basal membrane of adjacent hair cells $V_b = V_{oc} \cdot C_a / (C_a + C_b)$. The estimated values of C_a and C_b suggest that V_b should be about 20% of V_{oc} , with the ratio being substantially independent of frequency above about 2 kHz. C_a and C_b are the capacitances of the apical and basal membranes of the hair cell. (B) High-frequency extracellular voltages within the organ of Corti are detectable and nearly proportional to basilar membrane displacement as a function of frequency. Figure supplied by Dr. A. Fridberger (based on original data from Fridberger *et al.*, 2004).

further. The result is that in high-frequency cells the membrane time constant is some 25 μ sec, as against the 1 msec otherwise expected.

Fridberger *et al.* (2004) showed that, as expected with the formulation of Dallos and Evans (1995a,b), there were indeed extracellular potentials within the organ of Corti at high frequencies, that they had the same frequency distribution as the mechanical response, and that they were potentially large enough to drive to motile response (see Fig. 5.20B).

5.4.5.2 Motility of hair cell stereocilia

Motility of different types has been seen in stereociliar bundles of hair cells of different types and from different species. Stereociliar-based motility is moreover the only option in non-mammalian species and mammalian vestibular hair cells that do not have the basal membrane specializations of mammalian outer hair cells. For instance, Martin *et al.* (2003) showed that hair cells of the bullfrog sacculus could sometimes spontaneously oscillate at frequencies between 5 and 50 Hz. The oscillation was affected by manipulations that would affect the myosin slow adaptation motor (Section 5.3.2.7) and was therefore thought to depend on the activity of the myosin molecules found at the upper ends of the tip links (see Fig. 5.6). Any myosin-based motility would, however, be too slow to serve motility in cochlear hair cells in the auditory range of frequencies. Any such motility is instead thought to depend on rapid Ca^{2+} -induced conformation changes within the mechanotransducer apparatus (Cheung and Corey, 2006). Different forms of fast stereocilia-based motility have been observed; in rat cochlear outer hair cells, Kennedy *et al.* (2005, 2006) found that the stereociliar bundles could produce an active movement to a stimulus that was in the same direction as the applied force. This could potentially magnify the movement to the stimulus. In contrast, in the turtle cochlea, stimulation generated a delayed movement opposite in direction to the applied force (Ricci *et al.*, 2000). While it appears that both types of motility may be related to fast adaptation, different mechanisms must be involved in the two cases, because opposite effects were produced on bundle movement. Either type of motility could generate a power stroke, if Ca^{2+} altered the conformation of a protein in a concentration-dependent manner, since Ca^{2+} ions are driven into the hair cell by the electrochemical gradient across its apical surface. Presumably, by pushing against the tectorial membrane, the stereocilia could transmit a movement to the organ of Corti and basilar membrane as a whole. Hair bundle motility, and its possible relation to channel adaptation, have been reviewed by Fettiplace (2006).

5.4.6 Cochlear micromechanics

Understanding the secret of how outer hair cells amplify the cochlear vibrations, and present a high-amplitude and sharply tuned stimulation to the inner hair cells, is likely to depend on knowing the detailed vibrations and displacements that occur within the organ of Corti itself, and within the tectorial membrane. This is

the area known as cochlear micromechanics. If measuring the vibration of the basilar membrane was a technical challenge that took many decades to surmount, measuring cochlear micromechanics presents a further order of difficulty. Therefore it is not surprising that results at the moment have to be viewed as only provisional.

Firstly, how could length changes in the outer hair cells affect the vibration of the basilar membrane? If the outer hair cells change length as a result of the motile process, we would expect the reticular lamina and basilar membrane to move with different amplitudes of vibration. [Chen et al. \(2011\)](#) imaged the reticular lamina through the basilar membrane using a technique known as optical coherence tomography, in which phase changes in laser light waves are detected when a reflecting surface is displaced. They showed that the reticular lamina vibrated with an amplitude that was about three times greater than that of the basilar membrane, and with similar sharpness of tuning, though tuned to a slightly higher frequency. Figure 3.4B shows how the geometry of the organ of Corti could accommodate such a movement. The phalanges of the Deiters' cells run up at an angle within the organ of Corti, to surround the next-but-one outer hair cell towards the apex. If the outer hair cells, which run directly across the organ, actively changed length, this difference in angle would allow the whole organ to change thickness. It is suggested that when outer hair cells shorten as they depolarize, they further pull the basilar membrane towards the scala vestibuli, that is upwards as depicted in most diagrams, so enhancing the cochlear travelling wave (e.g. [Nilsen and Russell, 2000](#)).

Secondly, is there any evidence supporting the model described in Fig. 5.15, which suggested that the tectorial membrane undergoes a radial vibration, as well as the vertical vibration shown in Fig. 3.3? [Gummer et al. \(1996\)](#) used laser interferometry of the top surface of the tectorial membrane in isolated preparations taken from the apex of the guinea pig cochlea. They showed that just such a radial component was indeed present. The radial vibration was tuned differently from the basilar membrane, having a natural resonant frequency half an octave below the characteristic frequency of the basilar membrane at the same point.

The difference in resonant frequency has important implications for the drive to the outer hair cells. A resonator driven well above its natural resonant frequency is mass-limited (see right half of Fig. 3.15A) and its displacement will lag the driving force by half a cycle. The flow of current into the OHCs is in phase with the deflection of the stereocilia. At high (audio) frequencies the resulting intracellular voltage changes will be delayed with respect to the current by a further $\frac{1}{4}$ cycle. Therefore at high stimulus frequencies, we expect the voltage change within the OHCs, which drives the motile process, to lag the vibration of the basilar membrane by $\frac{3}{4}$ of a cycle, or in other words, to lead it by $\frac{1}{4}$ of a cycle. As described in [Section 5.4.2](#), such a change is in the correct phase to amplify the movement ([Gummer et al., 1996](#); see also [Lukashkin et al., 2010](#)).

This mechanism naturally limits the active process to a region basal to the peak of the travelling wave, to the region between where the tectorial membrane has its natural resonant frequency at the frequency of stimulation (where the phase relations first become correct to drive the vibration), and the peak of the travelling

wave. In the guinea pig, this region extends approximately 1 mm basalwards from the peak of the travelling wave.²

5.4.7 Conclusions on cochlear mechanical amplification

Active mechanical amplification is definitely required to produce the tuning and sensitivity that has been observed in the cochlea. Outer hair cell somatic motility definitely exists; the transmembrane voltages go to sufficiently high frequencies to drive the motility in many mammalian species, although this is still uncertain particularly for very high-frequency mammals such as bats. It is likely that the length changes in OHC alter the thickness of the organ of Corti, serving to enhance the vibration of the basilar membrane by producing an upwards force on the basilar membrane in phase with the membrane's velocity of movement upwards. Stereocilia-based motility, probably dependent on a conformational change in the mechanotransducer apparatus, has been demonstrated in non-mammalian hair cells and in isolated mammalian cochlear hair cells. It is still not certain whether it amplifies vibrations in the intact cochlea. It is possible that both types of motility contribute together to the amplification of the travelling wave. The amplification is likely to involve additional mechanisms, such as a resonance within the tectorial membrane. Because the cochlea is a complex feedback system, it is difficult to measure the effect of any manipulation in isolation; and an accurate view will only be formed once a complete picture has been put together, and matched with the behaviour of mathematical models.

A collection of views of many of those working in the area is to be found in the review by [Ashmore *et al.* \(2010\)](#).



5.5 HAIR CELLS AND NEURAL EXCITATION

5.5.1 Stimulus coupling to inner and outer hair cells

The tips of the tallest stereocilia of outer hair cells are embedded in the tectorial membrane, while the stereocilia of inner hair cells fit loosely into a groove called Hensen's stripe without any evidence that the tips are embedded. This has suggested that, while the stereocilia of outer hair cells are moved directly by displacements of the tectorial membrane, the stereocilia of inner hair cells are moved by viscous drag of the fluid in the subtectorial space. Since viscous drag is dependent on the velocity of the flow, we would expect that for low frequencies

² The peak tectorial membrane resonance occurs basal to the peak of resonance of the basilar membrane for the following reason. The tectorial membrane has a natural resonance at a frequency half an octave below that of the basilar membrane. Therefore with a 10 kHz driving stimulus the point in the cochlea where the tectorial membrane is set into its 10 kHz natural resonance is at the 14 kHz characteristic place for basilar membrane vibration. The 14 kHz basilar membrane characteristic place is basal to the 10 kHz basilar membrane characteristic place.

of stimulation, inner hair cells would respond to the velocity of basilar membrane movement, while outer hair cells would respond directly to the displacement.

It has been possible to address this issue in the special case of low-frequency stimulation, where the timing of the responses can be readily determined from the recordings. Dallos *et al.* (1972) and later Sellick and Russell (1980) stimulated the cochlea with a low-frequency triangular acoustic wave, which is calculated to give a trapezoidal pattern of displacement on the basilar membrane. They showed that the conjecture of the previous paragraph was indeed the case, with inner hair cells giving a large response in phase with the velocity of the movement, and with the cochlear microphonic, generated by the outer hair cells, following the displacement (Fig. 5.21). In accordance with the functional polarization of hair cells, depolarization in inner hair cells was produced by velocity towards the scala vestibuli, which can be expected to displace the stereocilia in the excitatory direction, that is in the direction of the tallest stereocilia (see Figs. 3.3 and 3.19). The velocity coupling of the inner hair cells suggests that they would not be directly sensitive to any d.c. bias in the position of the basilar membrane, but would only pick up the a.c. component in the vibration. On the other hand, outer hair cells would be directly affected by d.c. biases in the position of the membrane, and this may be important in affecting the way they produce the hypothesized active mechanical feedback. The two types of coupling can therefore be associated with the different roles of the two types of hair cells in cochlear function, with inner

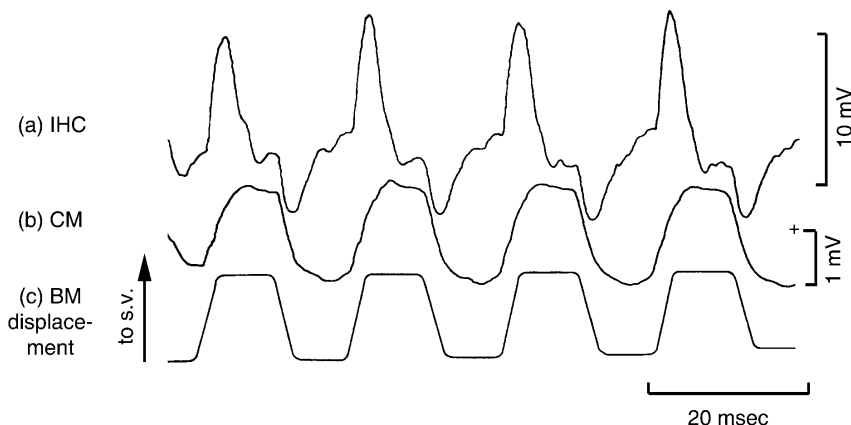


Fig. 5.21 The cochlear microphonic (trace b), dominated by outer hair cells, follows the displacement of the basilar membrane (trace c), whereas the inner hair cell responses (trace a) follow the velocity. In both cases, movement towards the scala vestibuli caused positivity below the reticular lamina, indicating a similar functional polarization for inner hair cell and outer hair cells. In this figure, recordings were made from the base of the guinea pig cochlea. The velocity response has also been confirmed for inner hair cells from the apex of the cochlea (Cheatham and Dallos, 1999). The displacement of the basilar membrane was calculated from the rate of change of sound pressure applied to the ear. From Sellick and Russell (1980), Fig. 1.

hair cells detecting the movement of the membrane and the outer hair cells helping to generate it.

This result is in accordance with the original view of cochlear micromechanics shown in the lever action of Fig. 3.3, modified by a velocity coupling to the IHC stereocilia. However, it is subject to a number of caveats. At higher frequencies, at or beyond 200 Hz, the response changes to one that follows the displacement of the basilar membrane (Sellick and Russell, 1980). It is expected that at these frequencies, the viscous drag on the stereocilia becomes strong enough to change the response to a displacement response. Secondly, the timings will be affected by any additional vibrations within the tectorial membrane or organ of Corti, such as described in Fig. 5.15 and Section 5.4.6. At higher frequencies, these effects change the response in complex ways that are not completely understood.

5.5.2 Activation of auditory nerve fibres

The phase of activation of the auditory nerve afferents by the inner hair cells is a complex issue and one that has not been fully resolved. On the basis of the above analysis, we would expect auditory nerve fibres to be activated in phase with the velocity of the basilar membrane movement towards the scala vestibuli, since this is the phase giving inner hair cell depolarization. This is indeed the case for fibres innervating the apical regions of the cochlea, in response to intense clicks or to tones with frequencies well below the characteristic frequency of the region investigated (Ruggero and Rich, 1987; Cheatham and Dallos, 1999).

The position is different, however, at the base of the cochlea or with higher-frequency tones. At the base of the cochlea and with low-frequency tones, peak inner hair cell responses occur, as expected, in phase with the maximum velocity of the basilar membrane movement towards the scala vestibuli. However with low-intensity stimuli, auditory nerve fibres in this region have a response phase that is nearly 180° different from the expected value, corresponding instead most closely to the maximum velocity towards the scala tympani (Fig. 5.22A). This of course could be determined only at low frequencies, in the frequency range for phase locking of the auditory nerve fibres. Figure 5.22A also shows that as the intensity is raised, at about 85 dB SPL, there is an abrupt jump in the phase of activation of the auditory nerve fibres so that at that intensity and above, the peak phase of activation now most closely corresponds to the peak velocity to the scala vestibuli, in agreement with the direction initially expected. Similar jumps in the phase of activation of auditory nerve fibres have been known for many years (e.g. Kiang and Moxon, 1972). Figure 5.22B shows how the rate-intensity function can also suddenly dip at this point. In the region of the dip, the period histogram becomes more complex, with multiple phases of activation, while the phase reverses on either side of the dip (see Fig. 5.22C). A reasonable hypothesis to explain the results is that there are two modes of activation of the auditory nerve fibres, one associated with high intensities of stimulation, and the other with low, and that they are in phase opposition. At some intensity in between, the two modes can cancel, giving rise to a dip in the response and the abrupt phase shift. At this point, small

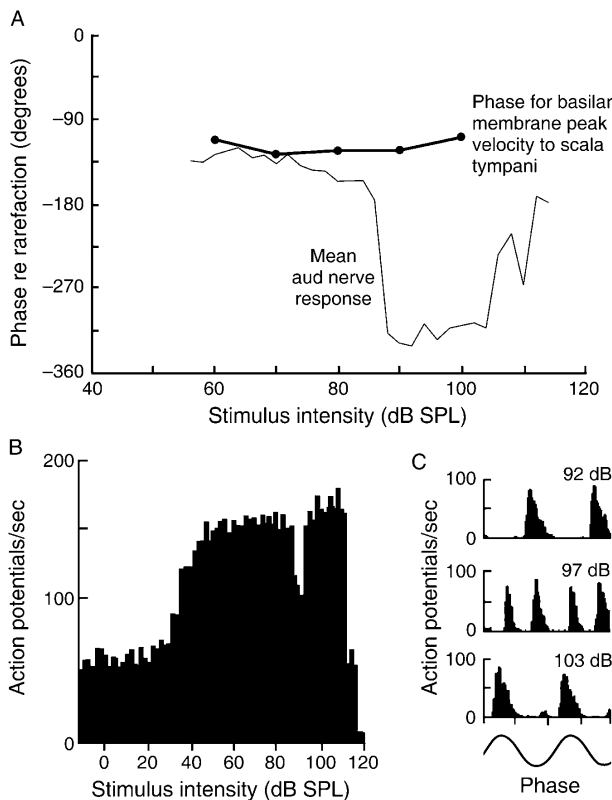


Fig. 5.22 (A) Phase of basilar membrane vibration and mean phase of auditory nerve activation, as a function of stimulus intensity, for neurons innervating the middle/basal region of the cochlea. Below about 85 dB SPL, the mean activation of the nerve fibres is nearly in phase with the velocity of the basilar membrane towards scala tympani. Above 85 dB SPL, nerve activation suddenly jumps 180° to being more in phase with the basilar membrane velocity to scala vestibuli. Responses were measured to 600 Hz tones and the auditory nerve fibres had CFs of 8–12 kHz, similar to that of the basilar membrane at the point of measurement. From Ruggiero *et al.* (2000), Fig. 6A, Copyright (2000), National Academy of Sciences, USA. (B) Firing rate of an auditory nerve fibre as a function of stimulus intensity. The rate shows a sharp dip around 90 dB SPL. From Kiang (1990), Fig. 8. (C) Period histograms of a different auditory nerve fibre firing to a continuous tone presented at different intensities (dB SPL marked on curves). The response reverses phase over this small range of intensity. At the middle intensity, multiple phases of activation are visible. From Kiang (1990), Fig. 7.

differences between the waveforms of the two driving stimuli become apparent in the period histogram.

Because of the phase of the auditory nerve responses at high stimulus intensities, depolarization of the inner hair cells is likely to form the high-intensity

mode of activation. The second process must therefore drive the activation at low intensities. One candidate for the low-level excitation is the a.c. extracellular current flowing through the outer hair cells, which can be sufficient to reverse the expected a.c. voltage change across the inner hair cell synapses (Cheatham and Dallos, 1999). The result is that displacement of the basilar membrane towards the scala tympani, which causes hyperpolarization of the outer hair cells and of the spaces of the organ of Corti, can drive the release of neurotransmitter at the base of the inner hair cells. Distortion of the extracellular waveforms with high-intensity stimulation would be expected to cause further phase shifts (for full discussion, see Cheatham and Dallos, 1999).

Note that this excitation of the inner hair cell synapse by the outer hair cell currents is likely to apply only to the special case of low-frequency stimulation of fibres innervating the high-frequency region of the cochlea. With high-frequency stimulation, the individual phases of depolarization and hyperpolarization are too fast to affect the release of neurotransmitter. However, the inner hair cells develop substantial distortion components, giving a d.c. component (i.e. sustained depolarization) in their response that instead triggers the release of neurotransmitter in response to high-frequency stimuli.

Further complications arise when the frequency of stimulation is within half an octave of the characteristic frequency of the region. As described in Fig. 5.15 and Section 5.4.6, the tectorial membrane may be set into transverse vibrations. We expect this vibration to be up to half a cycle out of phase with the movement of the basilar membrane, if the results of Gummer *et al.* (1996) hold up in other cochlear regions. This will add another factor to the complexity of the responses. Some of these complexities have been analysed by Temchin and Ruggero (2010), for apical auditory nerve fibres stimulated at and around their characteristic frequency.

The mixed velocity and displacement drives to the auditory nerve fibre synapse, associated with the inner and outer hair cells, mean that in the low-frequency tails of tuning curves of high-frequency auditory nerve fibres, the tuning curves have a slope intermediate between those of the velocity and displacement tuning curves of the basilar membrane (see Fig. 3.11B).

5.5.3 Neurotransmitter release

Each afferent Type I auditory nerve fibre makes only a single synaptic contact with a single inner hair cell. The synapses are of a type known as ribbon synapses. The ribbon synapses allow the inner hair cells to activate each afferent fibre (i) reliably, needed because there is only a single synapse for each nerve fibre, (ii) rapidly, which preserves the precise timing needed for time-based sound localization and for the time-coding of frequency and (iii) sustainably, which permits the ongoing generation of action potentials, not only so that they can continue firing during long acoustic stimuli but also to permit the high spontaneous firing rate of auditory nerve fibres (reviewed by Meyer and Moser, 2010 and Defourne *et al.*, 2011).

The ribbon of the synapse appears to tether the vesicles and biochemically prepare them for exocytosis, allowing their initial rapid release at the active zones.

The release of the neurotransmitter, glutamate, is triggered by Ca^{2+} influx through L-type voltage-gated Ca^{2+} channels, triggered by reduction in the transmembrane potential of the inner hair cells. Synaptic vesicles fuse in two phases after the elevation of intracellular Ca^{2+} , as detected by changes in the capacitance of the cell membrane when the vesicles fuse. There is an initial fast phase, corresponding to the release of five to eight vesicles per active zone, which presumably triggers the initial fast burst of firing in the nerve at the start of a stimulus (see Fig. 4.2). These vesicles are likely to be those situated on the ribbon and close to the sites of Ca^{2+} entry, supported by the anatomical correspondence between the ribbon synapses and sites of Ca^{2+} entry and by the fact that intracellular Ca^{2+} chelators have little effect on this initial phase of the release (see Prescott and Zenisek, 2005, for review). There is a second, slower and more sustained phase of release that can be affected by intracellular Ca^{2+} chelators, which therefore probably depends on changes in Ca^{2+} levels further away from sites of Ca^{2+} entry, and which is likely to involve the release of vesicles that are stored further away in the cell. This phase is likely to permit continued firing during long acoustic stimuli and to support the spontaneous activity of the nerve fibre.

Auditory nerve fibres differ in spontaneous activity and threshold, fibres with high levels of spontaneous activity having lower thresholds (see Fig. 4.4). All nerve fibres innervate the same population of inner hair cells, and it is easy to see how threshold and spontaneous activity could be dependent on the same mechanism, with low-threshold fibres having lower thresholds for release of neurotransmitter. Liberman *et al.* (2011) showed that there were multiple gradients of synaptic ribbon and postsynaptic receptor properties along the cochlea and across each inner hair cell. Synapses on the basal and modiolar pole of each inner hair cell, where we expect the innervating auditory nerve fibres to have high thresholds and low levels of spontaneous activity, have relatively small postsynaptic receptor patches, and large presynaptic ribbons. In contrast, in synapses on the non-modiolar and more apical pole of each inner hair cell, where we expect the auditory nerve fibres to have low thresholds and higher levels of spontaneous activity, the postsynaptic patches are larger and the presynaptic ribbons smaller. Liberman *et al.* suggested that the large postsynaptic receptor patches contribute to the low thresholds of these fibres, while the smaller presynaptic ribbons could facilitate fast and coordinated release of vesicles.

5.6 COCHLEAR NON-LINEARITY

One of the most intriguing aspects of cochlear function is its non-linearity. The non-linearity of the basilar membrane vibration is produced by the process generating sharp tuning. That process, namely the active amplification of the travelling wave by the outer hair cells, derives most or all of its non-linearity from the intrinsic non-linearity of hair cell transduction. Cochlear non-linearity is revealed in three main ways: (1) by the non-linear growth of cochlear responses

with stimulus intensity, (2) by the reduction in the response to one stimulus by a second stimulus ('two-tone suppression') and (3) by the generation of combination tones, or in other words intermodulation distortion products.

5.6.1 The non-linear growth of cochlear responses

Figure 3.13A shows that basilar membrane responses grow non-linearly with intensity, for stimulus frequencies around the characteristic frequency. The figure shows that for stimulus frequencies between 9 and 11 kHz and for stimulus amplitudes greater than 30 dB SPL, the amplitude function has a slope of approximately 0.3 on log-log scales, indicating that basilar membrane vibration grows in proportion to the stimulus amplitude raised to the power of 0.3.

The non-linearity arises from the active mechanical amplification of the travelling wave which starts to saturate or reach its maximum output, by about 30–40 dB SPL. Such saturation of the active component is shown by the solid line in Fig. 5.23. The overall amplitude function of the basilar membrane response can therefore be separated into two parts:

1. A nearly linear growth up to about 30 dB SPL, which is dependent on an approximately linear growth of the outer hair cell input–output functions and hence of the active mechanical process.

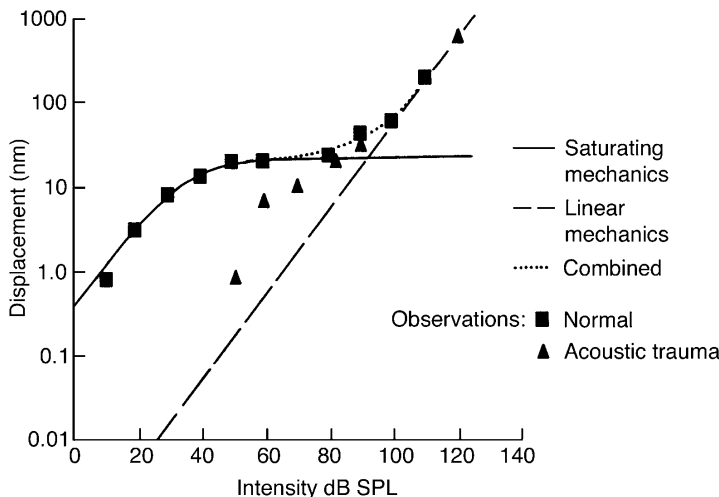


Fig. 5.23 Amplitude functions of the basilar membrane, showing theoretical contributions from the active process (solid line) and the passive process (long dashes), making a net function shown by the dotted line. ■, Measured basilar membrane response when cochlea in good condition. ▲, Measured response after acoustic trauma. Not all investigators have shown the second high-intensity linear phase plotted here. From Johnstone *et al.* (1986), Fig. 5.

2. A saturating function up to 80–100 dB SPL, which is dependent on the saturation of the outer hair cell response.

Some investigators have also shown a further phase of linear growth at the highest stimulus intensities, in cases where the linear passive component has become larger than the active component (see Fig. 5.23). However it is possible that this linearity is a result of the cochlear damage that occurs at high stimulus intensities. The saturating function is seen only around and above the characteristic frequency, because it is only here that the active process is dominant.

Noise trauma might be expected to impair a physiologically active process, and amplitude functions made before and after the induction of noise trauma show a change from the initial three-part function to one that more closely approximates a simple linear growth (see Fig. 5.23, triangles). Analogous results are seen with the many manipulations that can be expected to affect the active mechanical amplification, and that linearize the intensity functions as well as making cochlea less sensitive (see, e.g. Fig. 3.13, dashed lines).

Why does the active contribution start to saturate at such a low stimulus intensity? The saturation could occur at two possible stages: (1) saturation of the transducer current as a function of stereociliary displacement and (2) saturation of the motile mechanism as a function of transducer current.

The evidence suggests that saturation of mechanotransduction is likely to be the dominant factor. As described above, manipulation of the stereocilia on all types of hair cells, including outer hair cells, shows that transducer current is limited at larger deflections (see Fig. 3.20). We also expect the responses to rise nearly linearly at very low stimulus intensities, because the hair cell input–output functions have a short approximately linear region around their midpoints.

The motile process from outer hair cells is therefore expected to be initially nearly linear and then saturate. Basilar membrane responses will then show a similar pattern of non-linearity, because outer hair cell transduction saturates (Russell *et al.*, 1986a,b). The form of the saturation can therefore be directly related to the kinetics of mechanotransducer gating, and hence to the Boltzmann function, since this underlies the input–output function of hair cells (see Fig. 5.12).

While the cell body-based motile process is also non-linear, the degree of non-linearity is probably not enough to contribute to the overall non-linearity of the response (Santos-Sacchi, 1993). Stereociliar-based motility is likely to share the non-linear properties of the mechanotransduction with which it is so closely related.

Because the outer hair cells in the basal turn do not show d.c. responses with low intensities of stimulation, it can be concluded that *in vivo* the outer hair cells are biased towards the central part of the input–output functions, that is to the point around which the function is most symmetric. Because their stereocilia are embedded in the tectorial membrane, the hair cells' zero point is influenced by the zero position of the cochlear partition as a whole. This suggests that the zero point is set to within a few tens of nanometres, extraordinary for a structure that is 100 or more micrometres wide. This further suggests that the point must be set actively, that is the outer hair cells detect a shift from the central position and, by

mechanisms that are not certain, act to correct it. This is an issue that has been subject to speculation without resolution for many years. Some possible mechanisms are adaptation, which in outer hair cells can shift the input–output function by at least 50 nm (see Fig. 5.13B), the fast somatic motile mechanism, which can generate movements of up to 1 µm in basal turn outer hair cells, or slow somatic motility (Zenner *et al.*, 1985). It was earlier speculated that a reflex arc via the Type II afferents from the outer hair cells (which could be driven by a static depolarization of the outer hair cells), to the brainstem, and back to the outer hair cells via the medial olivocochlear bundle could affect the static position of the basilar membrane; however, Murugasu and Russell (1996) found that stimulation of the olivocochlear bundle affected only the oscillatory, and not the static, position of the basilar membrane.

5.6.2 Two-tone suppression

It was described in Chapter 4 how the presence of one stimulus can reduce the response of the cochlea to other stimuli. Figure 4.14A shows the tuning curve for the suppressive effect when the suppressed tone ('probe') is set to the nerve fibre's characteristic frequency and the suppressing tone is moved in frequency. The explanation given in Chapter 4 for two-tone suppression was the following: because of the saturating input–output functions of the outer hair cells, each stimulus will push the response to the other into the flatter part of the input–output function. This means that each stimulus will reduce the active amplification of the other's mechanical travelling wave (as well as of course reducing the active amplification of its own travelling wave, revealed in the saturation of basilar membrane mechanics).

Further evidence on the possible mechanism of two-tone suppression has been produced by measuring the mechanical response of the basilar membrane to a high-frequency stimulus at the characteristic frequency of the region, while presenting an intense tone of very low frequency. The excursions of the low-frequency tone displace the outer hair cells to the ends of their operating ranges, suppressing the mechanical response to the characteristic frequency tone twice per cycle (e.g. Geisler and Nuttall, 1997). The major phase of suppression was seen when the basilar membrane was displaced towards the scala tympani, with a second smaller phase of suppression during displacements towards the scala vestibuli.

Similar effects have been seen in the tuning curves of inner hair cells, made during different phases of the intense low-frequency tone. The tuning curves moved upwards and increased in width during the suppressive phases, with the greatest effect being seen during deflections to the scala tympani (Fig. 5.24; Patuzzi and Sellick, 1984). The effect was not simply due to the low-frequency tone moving the basilar membrane to the mechanical limits of its response in either direction, because the effect was greatest for characteristic frequency test tones, and completely absent for test tones of much lower frequency. The results are consistent with the explanation given above that the suppressing tone had biased the outer hair cells towards the more saturating parts of their input–output

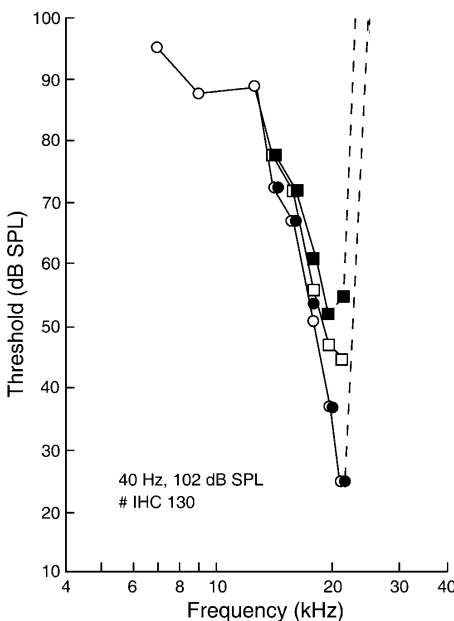


Fig. 5.24 Inner hair cell tuning curves, measured during the different phases of a simultaneously presented low-frequency stimulus. The tuning curve is sharpest at the moments at which the low-frequency stimulus is going through its zero crossings (○ ●) and broader and of higher threshold during the extremes of movement towards the scala tympani (■) and the scala vestibuli (□). The tuning curves were made for d.c. receptor potentials of 0.9 mV. From Patuzzi and Sellick (1984), Fig. 3.

functions so that the superimposed test stimulus would be unable to produce as much active mechanical feedback.

Because outer hair cells normally operate around the steepest part of their input–output function, any shift in the operating point can be expected to reduce the amount of active mechanical feedback, and reduce the response around the characteristic frequency. We can explain the greater suppression with biases towards the scala tympani, because hair cell functions are commonly more sharply saturating in the inhibitory, that is scala tympani, direction.

The above theory suggests that in order to produce suppression, the travelling wave to the suppressing stimulus must overlap the active region of the travelling wave to the suppressed stimulus. This explanation easily shows how tones can mutually suppress when they are very close in frequency so that their travelling waves substantially overlap. As described in Chapter 4, it also shows how a higher-frequency suppressor can reduce nerve fibres' response to a lower-frequency tone without itself producing excitation. A higher-frequency tone produces its peak of activity basal to the peak of activity produced by a lower-frequency tone. Therefore, as shown in Fig. 4.14B, a higher-frequency suppressor can easily overlap the active

region of a lower-frequency tone, and so can reduce the active amplification of the lower-frequency tone, while being filtered out by the mechanics before it reaches the suppressed tone characteristic place. However, this filtering out does not occur with a low-frequency suppressor. Because a lower-frequency suppressed tone peaks more apically in the cochlea, its travelling wave will always overlap the whole travelling wave of a higher-frequency suppressed tone.

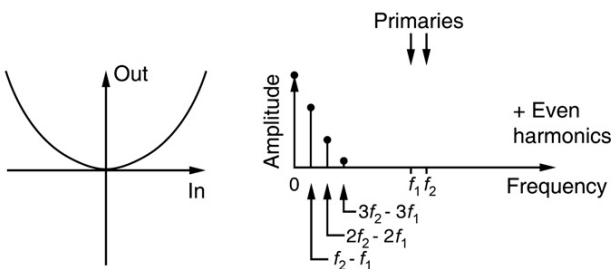
Therefore, how does a lower-frequency suppressor suppress without itself causing excitation? In other words, how can we explain the shaded lower suppression area of Fig. 4.14A? Surely, if the travelling wave to a lower-frequency tone produces enough displacement to drive the outer hair cells into their non-linear range, it also produces enough displacement to activate the inner hair cells in the same region?

An explanation proposed by Temchin *et al.* (1997) relates to the different driving stimuli to the outer hair cells and auditory nerve fibres. Outer hair cells respond to the displacement of the cochlear partition. However, for some frequency ranges, auditory nerve fibres are driven by the velocity of the basilar membrane, or by a combination of velocity and displacement (Section 5.5.2). This means that below characteristic frequency, the tuning curves of basilar membrane displacement (and hence of outer hair cell activation) will have a shallower slope and a lower threshold than those of the auditory nerve fibres (e.g. in Fig. 3.11B compare the line for 1.9 nm displacement of the basilar membrane and the tuning curve for the auditory nerve fibres). Stimuli in the intensity range in between the two curves will suppress, because they activate the outer hair cells, but will not excite, because they do not activate the auditory nerve fibres.

5.6.3 Combination tones

Combination tones provide powerful evidence for cochlear non-linearity. If a system is entirely linear, its output waveform will contain only the same frequency components as the input. If a system is non-linear, single tones will also produce harmonics. A pair of input tones will, in addition, produce combination tones, that is tones whose frequencies depend on the frequencies of both of the input tones. The pattern of such harmonics and combination tones immediately tells us a great deal about the non-linearity. If the input–output function through the non-linearity is symmetric around the line at $\text{input} = 0$ (otherwise called even-order), we shall have even harmonics ($2f_1$, $4f_1$, etc.) and sum and difference tones of the form $f_2 \pm f_1$, $2f_2 \pm 2f_1$, etc. (Fig. 5.25). If the input–output function through the non-linearity is antisymmetric, or odd-order, we shall, in addition to the original frequencies, have odd harmonics and combination tones of the form $2f_1 \pm f_2$, $3f_1 \pm 2f_2$, etc. Combination tones of the form $2f_1 - f_2$ (the cubic distortion tone) and of the form $f_2 - f_1$ (the difference tone) can be demonstrated in the responses of the basilar membrane and in the electrophysiological responses of the cochlea (Kim *et al.*, 1980; Cooper and Rhode, 1997; Robles *et al.*, 1997). This suggests that the input–output function through the non-linear stage is a sum of both symmetric and antisymmetric components.

A. Symmetric



B. Antisymmetric

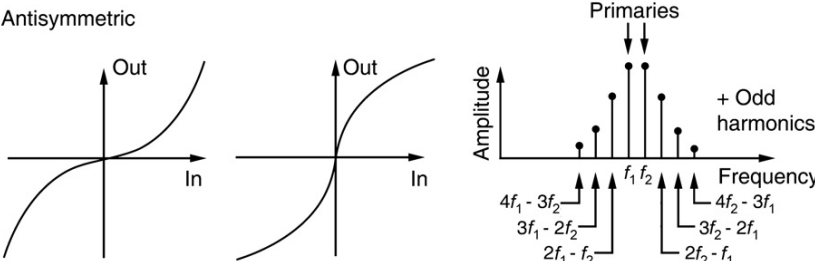


Fig. 5.25 Combination tones generated by different non-linearities. (A) A non-linearity with an input–output function symmetrical around the line: $\text{input} = 0$ (even-order function) generates an output with terms of the form $n(f_1 \pm f_2)$, and even harmonics. (B) Examples of antisymmetric input–output functions (odd-order functions). Such functions generate the primaries, combination tones of the form $nf_1 \pm mf_2$ ($n \neq m$) and odd harmonics. All realizable input–output functions can be made by combinations of even-order and odd-order functions.

Responses to combination tones can be seen in the vibration of the basilar membrane, in the responses of inner hair cells and in the firing of auditory nerve fibres. Figure 5.26 shows the spectrum of the mechanical vibrations of the basilar membrane, in response to two-tone stimulation. The frequencies were chosen such that the calculated frequency $2f_1 - f_2$ was equal to the characteristic frequency of the point being measured. In Fig. 5.26A, the frequency ratio is 1.05, and a large number of different combination tones could be detected at the point being measured, in addition to the two tones, or primaries, presented. In Fig. 5.26B, however, the frequency ratio of the two tones being presented was much larger at 1.25, and only the $2f_1 - f_2$ combination tone could be detected at the point being measured. The responses to the primaries had been filtered out by the mechanics of the cochlea, showing that the combination tone had set up a travelling wave on the basilar membrane that was separate from those of the primaries. The mechanics of the cochlea had carried this wave apically in the cochlea, where it peaked at its own characteristic place.

Similar results have been found by other methods, such as by measuring the responses of auditory nerve fibres. For instance, Kim *et al.* (1980) measured the responses of large numbers of fibres in one animal and built up a picture of the

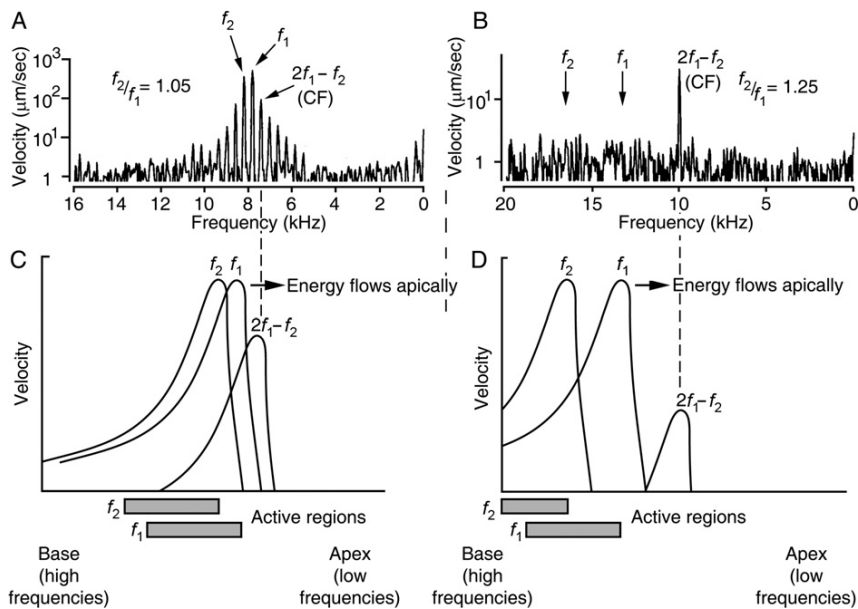


Fig. 5.26 (A) Spectrum of response of the basilar membrane to two-tone stimulation. The tones (frequencies f_1 and f_2) were chosen such that $2f_1 - f_2$ lay at the characteristic frequency (CF) of the point being measured. The frequencies were in the ratio $f_2/f_1 = 1.05$. Because of this small ratio, a large number of combination tones were generated and detectable at this point on the basilar membrane. (B) The frequency ratio f_2/f_1 was 1.25, again chosen so that $2f_1 - f_2$ lay at the CF of the point being measured. Because of the larger ratio, the travelling waves to f_1 and f_2 had been filtered out by the basilar membrane mechanics before reaching the $2f_1 - f_2$ place, producing a negligible measurable response at this point in the cochlea. The response to the $2f_1 - f_2$ tone confirms that the $2f_1 - f_2$ tone had set up its own travelling wave on the basilar membrane. Because of the larger ratio, the combination tone is seen at a lower level than in A (note difference in vertical scales). Also note reversed frequency scales in both parts A and B. Stimulus intensity in A and B: 70 dB SPL. (C) and (D) Diagram of travelling waves and energy flows in the cochlea for the stimuli in A and B. The combination tones are generated where the active regions of f_1 and f_2 overlap. Energy from this region sets up travelling waves that carry energy apically in the cochlea, to peak at their own characteristic places. For clarity, $2f_1 - f_2$ is the only combination tone shown. A and B used with permission from Robles *et al.* (1997), Fig. 2.

activation of different regions of the basilar membrane in response to single- and two-tone stimulation (Kim *et al.*, 1980). In each fibre, the response to each of the component tones was measured from the phase locking at that frequency. The results again showed that the combination tone produced its own travelling wave in the cochlea, which peaked at its own characteristic place.

The presence of odd-order combination tones in the cochlear responses suggests that an odd-order, or antisymmetric, non-linearity, is present in the generator, that is, in the active mechanical process and so in the input–output functions of outer hair cells, anticipated to be the major stage of non-linearity. These findings are entirely consistent with the shapes of the input–output functions of outer hair cells (see Figs. 3.20B, 3.24, 5.7 and 5.12), which become less sensitive and saturate for both excitatory and inhibitory displacements. Even-order distortion is also present, since difference tones (f_2-f_1) and second ($2f$) harmonics have been measured in basilar membrane responses, the former at levels comparable to the odd-order intermodulation products (Cooper and Rhode, 1997; Cooper, 1998). This is consistent with the even-order asymmetry that is present in the outer hair cell input–output functions, since they saturate more sharply for movements in the inhibitory direction (see Figs. 3.20 and 3.24). The fact that the cubic distortion tone can be detected even near threshold suggests that the hair cells' input–output functions have some degree of antisymmetric (odd-order) non-linearity even for very small displacements around the resting position.

Just as an externally introduced tone can produce a cochlear emission, so can an internally produced combination tone. Some of the energy produced by the active mechanical process is transmitted, presumably by a compression wave in the cochlear fluids, to the middle and outer ears, where it can be detected with a microphone (see, e.g. Shera *et al.*, 2002; He *et al.*, 2007 for different views on reverse transmission in the cochlea). Because the combination tone at $2f_1-f_2$ is at a frequency that is not present in the external stimulus, it is technically relatively easy to detect the emitted tone at very low levels. The combination tone can therefore be used as a sensitive non-invasive indicator of the state of the active mechanical amplifier, and hence of the outer hair cells, in for instance human beings.

Because the stimulus frequencies can be chosen at will, it is possible to monitor the state of the cochlea over a range of frequencies. The involvement of the outer hair cells in the emission has been confirmed in experiments in which the medial olivocochlear bundle was stimulated in chinchillas. The medial olivocochlear bundle ends only on the outer hair cells, and stimulation of the bundle can modulate the amplitude of the emitted tone (Siegel and Kim, 1982; Guinan, 2006).



5.7 SUMMARY

1. The stereocilia on hair cells are composed of tightly packed actin filaments, bonded by a number of proteins (I-plastin or fimbrin, T-plastin and the espins), which give them considerable rigidity. Their rootlets insert into the cuticular plate, also composed of actin filaments though with a less regular organization. The stereocilia in a bundle are cross-linked so that the whole bundle tends to move together when the stereocilia are deflected.
2. Links of one class, the tip links, emerge from the tips of the shorter stereocilia in the bundle to join to the side of the adjacent taller stereocilium. Tip links

are composed of cadherin-23 and protocadherin-15. Deflection of the stereocilia in the excitatory direction (towards the tallest stereocilia) pulls on the tip links and pulls open the mechanotransducer channels by a direct mechanical action.

3. The molecular identity of the mechanotransducer channel is not known. It is possible that the channels are a member of the TRP (transient receptor potential) family.
4. Ca^{2+} imaging shows that the mechanotransducer channels are situated at or near the tips of the shorter stereocilia on the bundle, likely to be in association with the lower ends of the tip link. Mechanotransduction also depends on the integrity of the tip links, since it disappears if the links are broken by the removal of Ca^{2+} from around the bundle with chelators.
5. The single-channel conductance is 145–260 pS. The channel is a non-specific cation channel, with a pore diameter of around 1.2 nm. We therefore expect mechanotransducer currents to be carried by K^+ and to a lesser extent by Ca^{2+} .
6. Electrophysiological analysis shows that the channels open with a very short delay (20 μsec) and with a low temperature dependence, consistent with the channels being opened by a direct mechanical action. Theoretical analysis of channel activation is undertaken in the framework of ‘gating spring’ theory, in which the channel opens and closes under the influence of thermal energy, pulled open by an elastic spring. Depending on the number of channel states that are chosen and their relative energies, realistic input–output functions for channel opening as a function of stereociliar deflection can be obtained. The functions are derived from the Boltzmann distribution. The gating spring may be formed by an elastic protein associated with the tip link or with the proteins that anchor the mechanotransducer channel to the underlying cytoskeleton.
7. Hair cells adapt, that is shift their operating range, in response to sustained stimuli. Fast adaptation (time constant 0.15–4 msec) depends on the molecular reorganization within the mechanotransducer channels following the entry of Ca^{2+} , while slow adaptation (time constant 10–500 msec) depends on the myosin-based motility of the upper insertion point of the tip link.
8. Sharp tuning in the cochlea depends on the active mechanical amplification of the travelling wave by the outer hair cells. The theoretical necessity for the amplification can be shown by mathematical analysis, which shows that experimentally obtained response patterns can be obtained only if there is an input of energy into the travelling wave, in a restricted region on the rising part of the travelling wave.
9. Outer hair cells put energy into the travelling wave. The involvement of outer hair cells is shown by manipulations that affect the outer hair cells, which also affect the magnitude and sharp tuning of the mechanical travelling wave.
10. The production of energy by the hair cells has been shown by the existence of cochlear emissions, when the cochlea, either spontaneously or in response to acoustic stimulation, emits sound. The emissions depend on the integrity of the outer hair cells. Isolated outer hair cells generate two forms of motility, one depending on length changes in the cell body driven by the protein

- prestin in the cell body, and the other depending on motility in the mechanotransducer apparatus, perhaps linked to the adaptation mechanism.
- 11. It is possible that the feedback of energy into the travelling wave is governed by the tectorial membrane acting as a second resonator within the cochlea, tuned to a frequency approximately half an octave below the basilar membrane at the same point in the cochlea.
 - 12. Outer hair cells, whose stereocilia are embedded in the tectorial membrane, are driven by the displacement of the cochlear partition. However, the stereocilia of inner hair cells are not embedded and are moved by viscous drag of the surrounding fluid. They, therefore, respond to the velocity of basilar membrane, though this becomes a displacement response at higher stimulus frequencies.
 - 13. Inner hair cells drive the Type I auditory nerve fibres. However, unlike the inner hair cells, auditory nerve fibres can show mixed velocity and displacement responses, depending on the stimulus conditions. For high-frequency fibres driven by low-intensity, low-frequency stimuli, there is evidence that the inner hair cell synapses may be activated by extracellular currents from the outer hair cells, rather than only by the mechanotransducer currents from the inner hair cells themselves. There may also be an influence from superimposed resonances of the tectorial membrane. These phenomena may explain the phase of activation of the auditory nerve fibres, and the sudden odd phase jumps seen in the activation.
 - 14. Inner hair cells release the neurotransmitter glutamate to activate the auditory nerve fibres. The synapse (a ribbon synapse) shows specializations that permit the rapid and reliable activation of the nerve fibres. Low-threshold auditory nerve fibres with high spontaneous firing rates may receive their properties from their larger postsynaptic receptor areas.
 - 15. Cochlear vibrations show an amplitude non-linearity, because the active amplification of the travelling wave in the cochlea is strongest with low-intensity stimuli. The non-linearity, therefore, probably derives from the non-linearity of the outer hair cells' input–output functions. The amplitude non-linearity permits auditory discrimination over a very wide range of stimulus intensities.
 - 16. Cochlear non-linearity gives rise to two-tone suppression, where one stimulus reduces the response to a second stimulus. This occurs because the travelling wave of the suppressing stimulus overlaps the mechanically active (amplifying) region of the travelling wave of the suppressed stimulus. Because outer hair cells' input–output functions are non-linear and saturating, the degree of amplification of the second stimulus is reduced, and hence the response to the second stimulus is reduced.
 - 17. Cochlear non-linearity also gives rise to combination tones or intermodulation distortion products when multiple tones are presented simultaneously. One prominent intermodulation product is the cubic distortion tone at a frequency $2f_1-f_2$, where f_1 and f_2 are the frequencies of the two primary tones presented and $f_2 > f_1$. The combination tone is produced when the travelling wave of one primary overlaps the active region of the travelling wave of the other

primary. The non-linearity means that the active process generates a travelling wave at the frequency of the distortion product which then travels apically and peaks at its own characteristic place in the cochlea. It can also generate a cochlear emission. A second prominent intermodulation product is the difference tone ($f_2 - f_1$), which also produces a travelling wave on the cochlear partition. The cubic distortion tone would be generated by an antisymmetric (e.g. cubic) distortion, while a difference tone would be generated by a symmetric (e.g. square-law) distortion. The presence of both types of distortion product suggests that the cochlear non-linearity has both symmetric and antisymmetric components, consistent with the observed non-linearity of the outer hair cell input–output functions.



5.8 FURTHER READING

Molecular information on mechanotransduction and its associated structures has been reviewed by Schwander *et al.* (2010), Richardson *et al.* (2011) and Peng *et al.* (2011). Hair cell mechanotransducer channels have been reviewed by Fettiplace (2009) and Peng *et al.* (2011), and the kinetic analysis of mechanotransduction by Sukharev and Corey (2004), and Markin and Hudspeth (1995). Experimental results on cochlear mechanics have been reviewed by Robles and Ruggero (2001), and its theoretical basis by Patuzzi (1996), de Boer (1996) and Hubbard and Mountain (1996). Hair cell adaptation has been reviewed by Fettiplace (2006) and Fettiplace and Ricci (2003). Hair cell motility has been reviewed by Ashmore (2008) and Dallos (2008) and a number of different views of the area are given by Ashmore *et al.* (2010). Hair cell motility, with an emphasis on hair bundle motility, has been reviewed by Hudspeth (2008). Ideas on the role of the tectorial membrane are described by Lukashkin *et al.* (2010). Cochlear emissions have been reviewed by Kemp (2002). Transmission at the inner hair cell synapse has been reviewed by Defourne *et al.* (2011) and Meyer and Moser (2010). Many chapters in the Springer Handbook of Auditory Research, Vol. 8 'The Cochlea' (1996), eds P. Dallos, A.N. Popper and R.R. Fay, Vol. 27 'Vertebrate Hair Cells' (2006), eds R. A. Eatock, R.R. Fay and A.N. Popper, and Vol. 30 'Active Processes and Otoacoustic Emissions in Hearing' (2008), eds G. Manley, R.R. Fay and A.N. Popper, are relevant for the material discussed in this chapter.

THE SUBCORTICAL NUCLEI

Fundamental auditory features such as frequency spectrum, temporal variations and sound location are extracted by progressive analyses in the auditory nuclei. At the cochlear nucleus, the auditory pathway divides into two separate streams, one mainly for binaural sound localization and one mainly for sound identification. The ventral stream, predominantly subserving sound localization, projects to the superior olfactory complex, where the direction of the sound source is extracted by comparing the intensities and timing of the stimuli at the two ears. The pathway then projects to the inferior colliculus. In the dorsal stream, mainly subserving sound identification, temporal variation and spectral information are extracted in the cochlear nucleus, and then mapped onto the inferior colliculus. The inferior colliculus therefore combines the information from the two streams, to begin to form the representation of an ‘auditory object’. This information is then mapped to the specific thalamic relay for the auditory system, the medial geniculate body and then to the auditory cortex.



6.1 CONSIDERATIONS IN STUDYING THE AUDITORY CENTRAL NERVOUS SYSTEM

Auditory nerve fibres have qualitatively uniform properties, although the fibres may vary quantitatively in factors such as bandwidth, spontaneous firing rate and threshold. It is therefore relatively easy to describe the properties of the whole population from a small number of experiments. In the cochlear nucleus, however, there are many different cell types and regions. These multiple cell types permit the simultaneous extraction of multiple features of the stimulus. Already at this stage of the system, therefore, giving a complete description is very difficult, and it is much easier to undertake experiments and analyse the results, if we have some theories as to the function of the system.

Three themes can be discerned in the analysis of sensory systems. One concerns ‘feature detection’. In such an analysis, we suppose that certain features of the sensory input are selectively extracted. In the visual system, the scheme following from the work of Hubel and Wiesel (1962) has been extremely successful. In the primary visual cortex, cells respond selectively to orientation, colour and eye of stimulation. In the auditory system, some of the critical features appear to be frequency spectrum, temporal fluctuations and sound location.

However, in the auditory system, these features do not appear to be as clearly and as separately extracted and encoded in readily definable stages, as are the basic features in the visual system.

A second theme is the localization of functions to the activity of individual cells. In the context of feature detection, it involves finding cells that respond to specific features, so that the detection of a feature can be defined by the activity of single cells studied in isolation. At the other end of a continuum, detection might only be defined by the pattern of activity over many cells. In a common analogy, the first case might be compared to a photograph, in which each point on the photograph represents one point in space, whereas the opposite end of the continuum might be compared to a hologram, in which each point on the hologram represents many points in space, and in which individual points in space can be reconstructed only by the integration of information from many points on the hologram. It is likely many of the more complex features will only be represented in the second form, and at any level of the auditory system, we might expect to find many coexisting stages in between the two extremes.

A third theme is that of hierarchical processing, in which successively more complex analyses are performed at ascending levels of the nervous system, and in which analysis of more complex features is based on an earlier analysis of more simple features.

Schemes for sensory analysis based on the logical extremes of each of the three themes – that is on the extraction of specific features, on the representation of the features in the activity of single cells and on hierarchical analysis of features – naturally spring to mind. But it seems that the auditory system operates far from these logical extremes at least on the first two points. For instance, a feature may be represented only in a pattern of activity across many cells, with different patterns of activity within the same population of cells representing different features. Such a mode of operation has contributed greatly to the difficulty of the electrophysiological analysis of the central auditory nervous system.

The likely reason is that many of the critical features of the acoustic stimulus are intermingled in the stimulus, and the neural extraction of some of the features degrades the neural representation of other features. As an example, sound localization that is based on interaural timing requires the preservation of precise time information. However, neuronal circuits that extract the features of complex spectra degrade time information. These two aspects of the stimulus cannot therefore be simultaneously extracted in the same neural circuit: the nervous system extracts them in separate circuits and combines the information at a later stage. This means that extraction of a number of features has to occur in separate parallel systems, with the results being integrated at one or more later stages. When the recombination occurs, the different features are resynthesized to form a neural representation of the auditory properties of the object that gave rise to them, that is they begin to define what has been called an ‘auditory object’.

The result is that, as we move through the auditory system, we see a progressive enhancement of the different features over many stages, with the gradual emphasis of, for instance, spectral contrast, temporal fluctuations and sound location, being built up over multiple stages of the system, and being represented in

separate functional channels. At the later stages where the resynthesis occurs (particularly in the inferior colliculus and beyond), the neurones become driven by multiple and selected aspects of the features that were strongly represented in the earlier channels.

Analysis of feature extraction in the central auditory pathway suggests a general division into different functional streams at an early stage. At the cochlear nucleus, two streams are already visible, one of which is involved in binaural sound localization, and the other of which is predominantly involved in sound identification, although with some involvement in sound localization. The information from these streams is then progressively recombined in the higher nuclei, namely in the nuclei of the lateral lemniscus, the inferior colliculus and the medial geniculate body.

A different type of functional division is also visible in the auditory pathway. Both the streams mentioned above are parts of the specific, core or lemniscal auditory system. This can be distinguished from a non-specific, diffuse, extra-lemniscal or belt system, which is concerned with auditory reflexes and multimodal integration. The nuclei of this system are the nuclei surrounding the central nucleus of the inferior colliculus, the dorsal and medial divisions of the medial geniculate body, and the secondary and association auditory cortices. This system receives a heavy input from the dorsal cochlear nucleus which, as well as being part of the specific auditory system, could for this reason also be said to be the first stage of the non-specific auditory system.



6.2 THE COCHLEAR NUCLEI

6.2.1 Output pathways

In view of the diversity of the properties of cochlear nucleus neurones, anatomical studies are vital in aiding physiologists in analysing the functions of the nuclei. Classification of the different cells, firstly by linking physiological responses with anatomical cell type, and then by analysing the cells in terms of their output connections, has permitted a straightforward link to be made between anatomy and function.

Cells of the cochlear nucleus project to higher nuclei through two main streams (Fig. 6.11). Cells that project via a ventral stream, running in the trapezoid body on the ventral surface of the brainstem, primarily project to the superior olive nuclei of the two sides. Here, the timings and intensities of the stimuli at the two ears are compared, and the information is used for sound localization. This pathway forms the binaural sound localization stream. Cells that project via a more dorsal stream, in the dorsal and intermediate acoustic striae, project mainly to the contralateral nuclei of the lateral lemniscus and inferior colliculus. They are mainly involved in the complex analysis of auditory stimuli, forming a stream mainly subserving sound identification.

6.2.2 Input pathways

Each fibre of the auditory nerve branches on entering the nucleus, sending one branch rostrally and the other caudally. The rostral or anterior branch carries information for the ventral binaural sound localization stream and innervates the division known as the anteroventral cochlear nucleus (AVCN) (Fig. 6.1A). The caudal or posterior branch carries information for both sound identification and sound localization and innervates the posteroventral cochlear nucleus (PVCN) as well as the dorsal cochlear nucleus (DCN). The orderly arrangement of the incoming fibres, arriving from different regions of the cochlear duct and tuned to different frequencies, gives rise to an orderly arrangement of characteristic frequencies of the neurones they innervate, leading to ‘tonotopic’ frequency maps. Such maps are indeed found, one corresponding to each of the above-named divisions of the nucleus. Within each nucleus, low frequencies tend to be represented anteriorly and ventrally and high frequencies posteriorly and dorsally (for review, see Nayagam *et al.*, 2011).

The auditory nerve uses glutamate as a neurotransmitter. The postsynaptic glutamate receptors are of both the AMPA type, associated with fast kinetics, and the NMDA type, associated with slower kinetics (Cao and Oertel, 2010).

Different cell types are found within the different regions of the cochlear nucleus (Fig. 6.2). This has allowed physiologists to refine our knowledge of the relation between the different cell types, their location in the nucleus and their function.

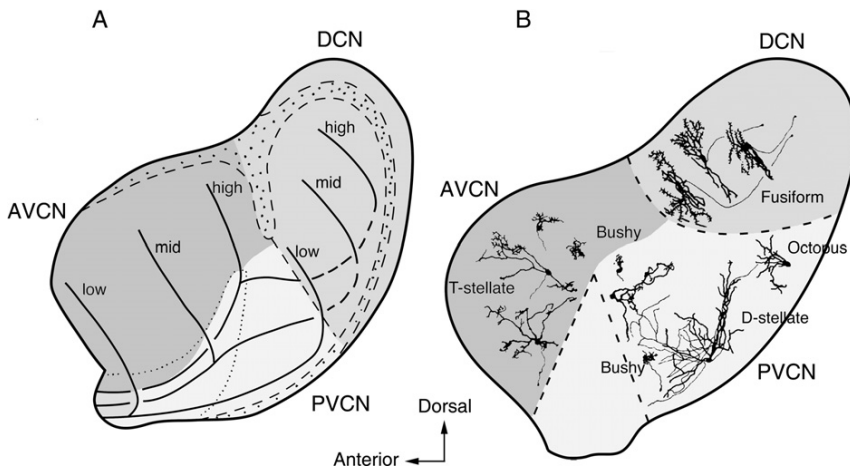


Fig. 6.1 (A) A sagittal section of the cat cochlear nucleus shows the three divisions of the nucleus. The paths of branching auditory nerve fibres, of high, mid and low frequency, are illustrated. (B) Diagram of the principal cell types in each division of the nucleus. AVCN, anteroventral cochlear nucleus; DCN, dorsal cochlear nucleus; PVCN, posteroventral cochlear nucleus. From Osen (1969), Fig. 2 and Oertel (1991), Fig. 1.

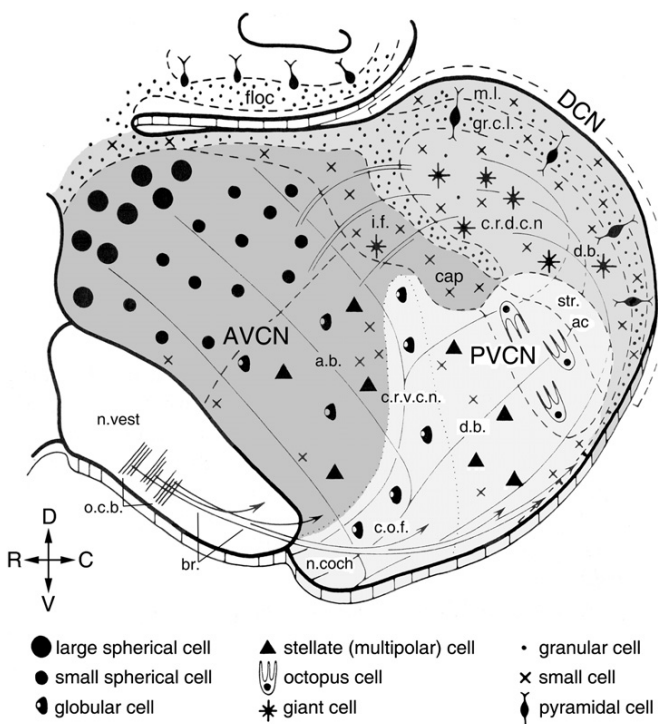


Fig. 6.2 Cytoarchitectonic map of the cochlear nucleus as shown in a sagittal section. The predominant cell types in each region are represented. AVCN, anteroventral cochlear nucleus; cap, peripheral cap of small cells; c.r.d.c.n., central region of the DCN; c.r.v.c.n., central region of the ventral nucleus; DCN, dorsal cochlear nucleus; floc, flocculus (cerebellum); gr.c.l., granular cell layer; if, intrinsic fibres; m.l., molecular layer; PVCN, posteroventral cochlear nucleus; strac, dorsal and intermediate acoustic striae. From Osen and Roth (1969), Fig. 1.

6.2.3 The ventral binaural sound localization stream: the bushy cells of the anteroventral and posteroventral cochlear nucleus

The anteroventral cochlear nucleus (AVCN) contains bushy cells, named for the bushy pattern of their dendrites. Bushy cells can be divided into spherical and globular types (Fig. 6.3). The posteroventral cochlear nucleus (PVCN) contains several types of cells, also including globular bushy cells.

Spherical bushy cells receive inputs from one to four auditory nerve fibres per cell, via giant synaptic terminals called end bulbs of Held, which wrap around the cell bodies. Each terminal contains many synaptic contacts (Fig. 6.3C and D; Kuenzel *et al.*, 2011).

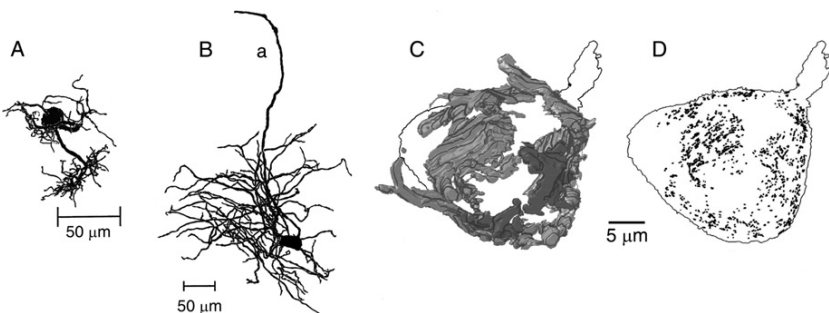


Fig. 6.3 (A) Spherical and (B) globular bushy cells in the anteroventral cochlear nucleus. a, axon. (C) Four end bulbs of Held (shown by different shades of grey) surrounding the soma of a spherical bushy cell. (D) The individual synaptic contacts underlying the end bulbs, in the same cell. From Ostapoff *et al.* (1994), Fig. 10B; Smith and Rhode (1987), Fig. 5; Nicol and Walmsley (2002), Fig. 4A and B.

These large synapses transmit the activity of the auditory nerve fibres to the cells of the AVCN with an overall high degree of reliability (but see Section 6.2.6.3) and with very low synaptic delays and low variability in timing, important if the timing and intensity information critical for binaural sound localization is to be transmitted effectively.

The direct, relatively secure, activation of the spherical bushy cells by the afferent auditory nerve fibres means that the bushy cells have response properties that are similar to those of the auditory nerve fibres. Each action potential in an innervating fibre has a high probability of giving an action potential in the spherical bushy cell. This can be revealed by recordings showing that each action potential in a bushy cell is preceded by a pre-potential, which is thought to be the presynaptic potential in the end bulbs of Held (Fig. 6.4A; Pfeiffer, 1966; Kopp-Scheinplug *et al.*, 2002). The close relation between the afferent action potentials and the firing of the spherical bushy cells means that the post-stimulus time histograms resemble those of primary auditory nerve fibres, giving the name primary-like for these responses (Fig. 6.4B; cf. Fig. 4.3).

The spherical bushy cells project directly to the medial superior olfactory nuclei on both sides, where the times of arrival at the two ears are compared. They also project to the ipsilateral lateral superior olive, where the intensities of the stimuli at the two ears are compared (Smith *et al.*, 1993).

The globular bushy cells are contacted by smaller modified end bulbs of Held, arising from between 4 and 40 auditory nerve fibres which end mainly on the soma and initial segment of the axon. The larger number of inputs to each globular bushy cell means that the cell will fire with a very high probability at the onset of a stimulus, giving the response pattern known as ‘primary-like with notch’ (Smith and Rhode, 1987). The convergence of inputs will moreover increase the temporal accuracy of the cells’ action potentials because of the opportunity for averaging (Cao and Oertel, 2010). Note in Fig. 6.4D how the

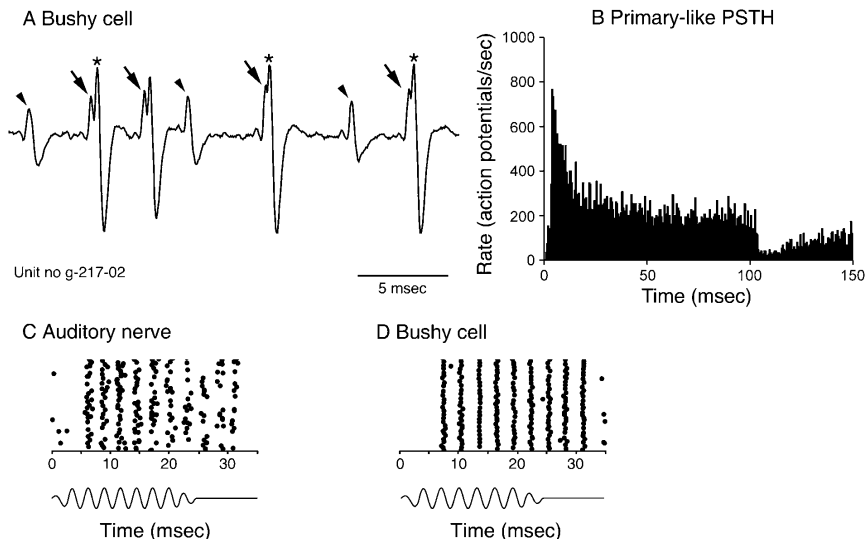


Fig. 6.4 (A) Extracellularly recorded response from an anteroventral cochlear nucleus unit (AVCN), likely to be a spherical bushy cell. Each action potential (star) is preceded by a pre-potential (arrow) representing a presynaptic potential. Pre-potentials marked by arrowheads are not followed by action potentials. Failure of transmission may occur when the cell is refractory from a previous action potential, or when the cell is also receiving an inhibitory input. (B) Post-stimulus time histogram of primary-like cells in the AVCN. The histogram shown here is the averaged response from 25 cells. Bar: stimulus. A and B kindly provided by Dr. C. Kopp-Scheinpflug (see also [Kopp-Scheinpflug et al., 2002](#)). (C) Raster diagram of firing of auditory nerve fibre to tone burst. The stimulus is repeated many times, and each action potential is marked by a dot, with successive stimulus presentations shown one below the other. (D) Raster diagram of bushy cell (type not described) to tone burst as in C, output axon recorded in the trapezoid body. Note greater precision of firing in D than in C. Redrawn using data from [Joris et al. \(1998\)](#).

temporal precision of firing to a tone burst is much higher in the bushy cell than in the comparable auditory nerve fibre shown in Fig. 6.4C. Both types of bushy cells also receive inhibitory inputs from interneurones within the nucleus and from other auditory nuclei, with the inhibitory inputs ending on the dendrites. Because these inhibitory inputs can be driven by sound, most of the cells can be inhibited by tones of the appropriate intensity and frequency ([Kopp-Scheinpflug et al., 2002](#)).

The globular bushy cells project primarily to the contralateral medial nucleus of the trapezoid body, a stage in the pathway to the contralateral lateral superior olive, where the intensities of the stimuli at the two ears are compared ([Smith et al., 1991](#)).

6.2.4 Cells of the posteroventral cochlear nucleus: contributions to both binaural localization and to identification

The posteroventral cochlear nucleus (PVCN) is more complex than the anteroventral nucleus, since it contains four major types of cells. In addition to globular bushy cells, its major cells are octopus cells and two types of stellate cells. Cells in this group contribute both to the ventral binaural localization stream and to the dorsal, mainly sound-identification, stream.

Octopus cells, found in only one area of the PVCN, are large cells of complex shape (Fig. 6.5A). They receive a very large number (>60) of auditory nerve afferents, and are driven only when a large number of the relatively small excitatory postsynaptic potentials arrive together within a short time period and summate (McGinley and Oertel, 2006). They therefore fire particularly strongly at the onset of a stimulus, giving what is called the ‘onset’ response (Fig. 6.5B). Octopus cells

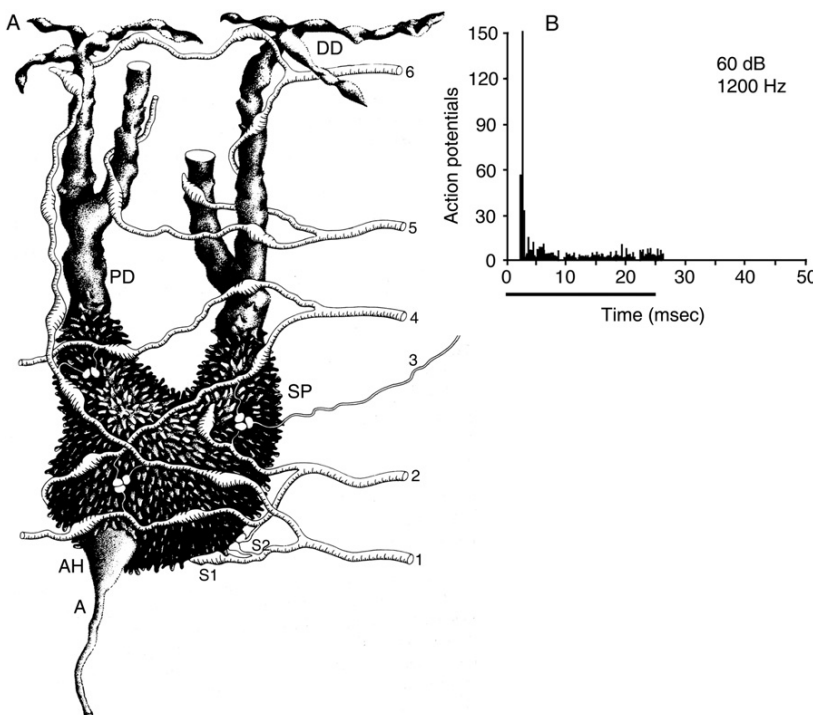


Fig. 6.5 (A) An octopus cell of the posteroventral cochlear nucleus. The cell is covered with stubby appendages (SP). A, axon; AH, axon hillock; DD, distal dendrites; PD, proximal dendrites. From Morest *et al.* (1973), Fig. 2. (B) An onset response: the post-stimulus time histogram of a cell identified as an octopus cell. Bar: stimulus. From Rhode *et al.* (1983a), Fig. 1B.

also respond readily to the transients in an ongoing stimulus, which they can follow at a high rate (greater than 500 repetitions/sec). They also respond to tones over a very wide range of stimulus frequencies (Smith *et al.*, 2005). They are therefore specialized for extracting the temporal fluctuations in complex broadband stimuli such as speech sounds (Cao and Oertel, 2010).

Octopus cells project, via the dorsal pathway (in their case, in the intermediate acoustic stria), primarily to the ventral nucleus of the lateral lemniscus of the opposite side.

Stellate cells are of two types (Doucet and Ryugo, 1997). Approximately 95% of stellate cells are T-stellate cells. T-stellate cells project bilaterally to the inferior colliculus and contralaterally to the ventral nucleus of the lateral lemniscus, as well as sending collaterals widely within the ipsilateral cochlear nuclei and to the superior olfactory complex (Cant and Benson, 2003; reviewed by Oertel *et al.*, 2011). Each one has on average 6.5 functional excitatory inputs from the auditory nerve, as determined from the incremental response to shocks of increasing intensity to the auditory nerve (Cao and Oertel, 2010). The cells tend to fire repetitively during a sustained tone burst at a rate that is unrelated to the period of the stimulus waveform, giving what is known as a ‘sustained chopper’ response (Fig. 6.6A). The post-stimulus time histogram therefore shows a series of peaks, which, because the timing of the spikes becomes rather ragged during the latter part of the tone burst, flatten towards the end. The cells are called stellate cells because they have three to four dendrites that project around the cell in a ‘stellate’ pattern, that is in many directions (Smith and Rhode, 1989). T-stellate cells tend to have narrow excitatory bandwidths, sometimes surrounded by wider inhibitory bands, and therefore could encode complex sounds, or narrowband stimuli in a noisy background. They are particularly suited to conveying the spectral shape of broadband stimuli. Because of their sustained firing, unrelated to the period of the driving stimulus, they are also suited to conveying the fluctuations in the envelopes of ongoing stimuli. T-stellate cells are also called T-multipolar, Type I multipolar or planar multipolar cells.

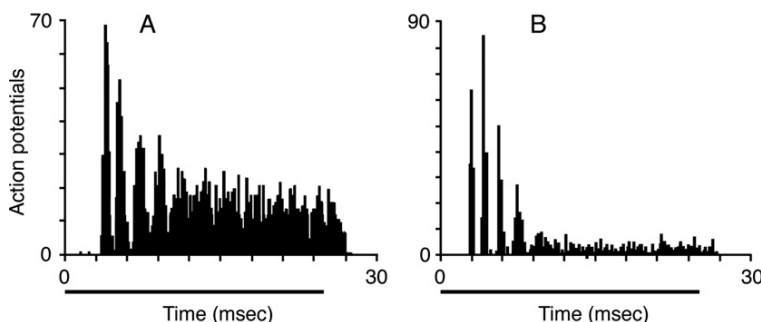


Fig. 6.6 (A) Post-stimulus time histogram showing sustained chopper response, recorded in the ventral cochlear nucleus. (B) Onset-chopper response. 25-msec tone bursts (bars). From Smith and Rhode (1989), Figs. 1C and 2C.

A small proportion of stellate cells are called D-stellate cells. D-stellate cells fire with what is called an onset-chopper response, with the first few spikes at regular intervals, but with a response that is not sustained throughout the stimulus (Fig. 6.6B). The decline in response is due to delayed inhibition of the cell probably via interneurones (Paolini and Clark, 1999). D-stellate cells receive auditory nerve inputs from a wide range of frequencies. They send inhibitory glycinergic projections to the cochlear nuclei of the opposite side as well as inhibitory collaterals widely within the ipsilateral cochlear nuclei, particularly to the dorsal cochlear nucleus, where they contribute wideband inhibition (Paolini and Clark, 1999; Smith *et al.*, 2005). D-stellate cells are also called D-multipolar, Type II multipolar or radiate multipolar cells. The AVCN also contains stellate cells, probably with similar properties and projections (Arnott *et al.*, 2004a).¹

6.2.5 The dorsal cochlear nucleus: sound identification and localization in the vertical plane

The dorsal cochlear nucleus has a more complex structure than the ventral nucleus. It also processes acoustic signals in a complex way and, as well as being part of the specific auditory system, has a major input to the diffuse, ‘belt’, non-specific or extra-lemniscal auditory system. The dorsal nucleus has a number of layers. The most superficial layer consists of small interneurones, granule cells and the axons of granule cells, which give rise to a system of parallel fibres running just under the surface of the nucleus (Oertel and Young, 2004). The second layer, the pyramidal cell layer, contains the fusiform (or pyramidal) cells, which form the major cell type of the dorsal nucleus. It also contains cartwheel cells. The deepest layer contains giant cells and vertical cells.

Fusiform (pyramidal) cells have extensive branches of dendrites which are oriented towards and away from the surface of the nucleus (Fig. 6.7A). The extensive dendritic arbor towards the surface of the nucleus receives inputs from the granule cell interneurones via the parallel fibres. The more basal dendrites receive inputs directly from auditory nerve fibres as well as indirectly via other interneurones. The fusiform cells project to the inferior colliculus, primarily on the contralateral side, as well as sending collaterals to other fusiform cells. Their responses to auditory stimuli are complex, reflecting the interplay of multiple excitatory and inhibitory inputs to the cells. The inhibitory inputs are particularly vulnerable to anaesthesia, so a classification of responses based on recordings obtained in anaesthetized animals may not reflect the actual position *in vivo*.

Fusiform cells commonly show what are called pauser responses, where the initial burst of activity is followed by an inhibitory pause (Fig. 6.7B). Others show a build-up response, where the response increases gradually during presentation of the stimulus (Fig. 6.7C). Both response types reflect a transient potassium

¹ T-stellate cells were so named because they project via the trapezoid body and D-stellate cells because they project dorswards within the cochlear nucleus (Oertel *et al.*, 1990).

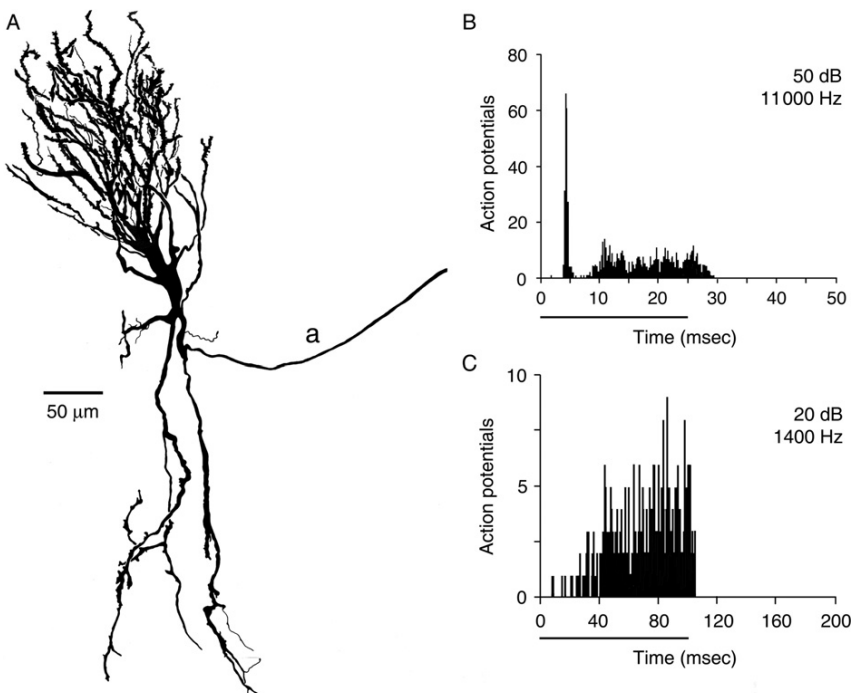


Fig. 6.7 (A) Fusiform (pyramidal) cell in dorsal cochlear nucleus. a, axon. The surface of the nucleus would be upwards in this diagram. (B) Post-stimulus time histogram showing pauser response recorded from a fusiform cell. (C) Post-stimulus time histogram showing a build-up response recorded from another fusiform cell. Bars: acoustic stimulus. From Rhode *et al.* (1983b), Figs. 13, 4B and 8A.

conductance that makes the cell less likely to fire, which is turned on by the initial acoustically driven depolarization of the cell. In human beings, fusiform cells are scattered and do not have a clear organization, although the dorsal cochlear nucleus itself is large in human beings (Moore, 1980).

The other cell types in the dorsal nucleus will not be described here in detail and information can be found in reviews and papers by Oertel and Young (2004), Sedlacek *et al.* (2011) and Ma and Brenowitz (2012). The cartwheel cells are large cells that, like the fusiform cells, have dendrites that arborize within the parallel fibre layer. However, unlike fusiform cells, they do not have a second group of dendrites ramifying deeper within the nucleus. They have complex temporal responses, and show complex patterns of tone-evoked excitation and inhibition (Portfors and Roberts, 2007). Their outputs inhibit other cartwheel cells and the fusiform cells (Mancilla and Manis, 2009). The giant cells project out of the cochlear nucleus to the inferior colliculus and to other brainstem nuclei, as well as within the nucleus. Vertical cells (also called tuberculo-ventral cells) have narrowly

tuned auditory responses and send glycinergic narrowband inhibition widely within the cochlear nuclei (Rhode, 1999; Spirou *et al.*, 1999). Many of these cells act as excitatory or inhibitory interneurones, sending axons to the ventral as well as dorsal divisions of the nucleus and themselves receiving excitatory and inhibitory inputs from interneurones within the nucleus.

Figure 6.8 summarizes the main cell types of the cochlear nuclei and their connections.

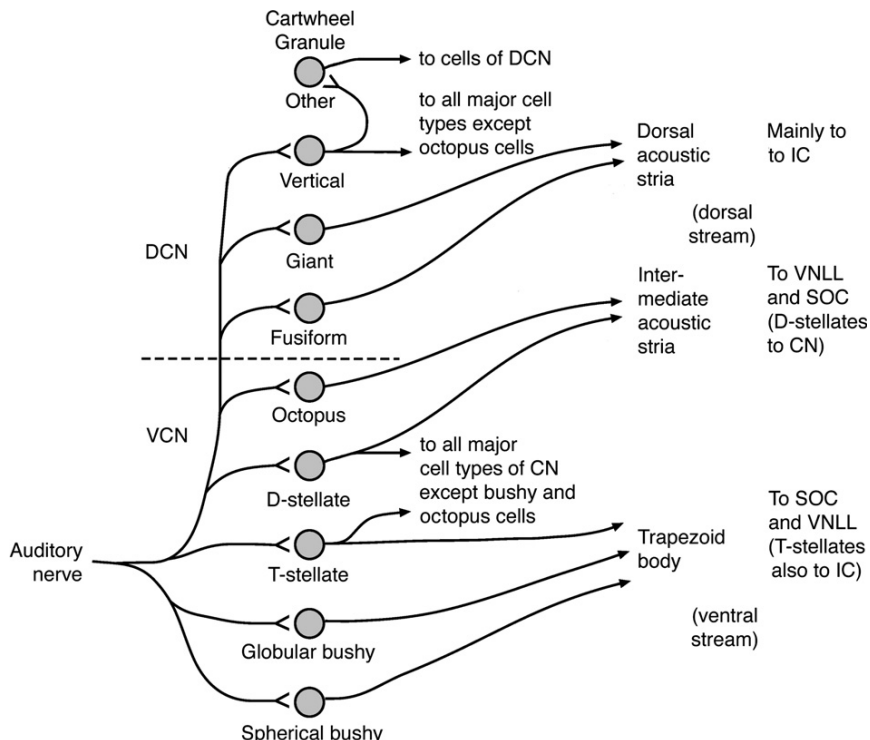


Fig. 6.8 Overall neuronal circuitry and output pathways of the cochlear nuclei. Fusiform cells are also called pyramidal cells, stellate cells are also called multipolar cells and vertical cells are also called tuberculo-ventral cells. For clarity, the interneuronal pathways are not drawn in detail. The ‘Other’ cells of the dorsal cochlear nucleus (DCN) include cells in the most superficial, that is molecular or granular, layer, namely cartwheel cells, granule cells, cells of stellate morphology plus further cell types (see also Fig. 6.2). Many minor projections and minor targets are not shown. The dorsal nucleus of the lateral lemniscus also receives an input from the cochlear nucleus (CN), but the cell types of origin in the CN have not been described. DCN, dorsal cochlear nucleus; IC, inferior colliculus; SOC, superior olive complex; VNLL, ventral nucleus of the lateral lemniscus; VCN, ventral cochlear nucleus. Data from Cant and Benson (2003) and Young and Oertel (2004).

6.2.6 Excitation and inhibition in the cochlear nucleus

The analysis of excitatory and inhibitory tuning curves enables the experimenter to show how the cochlear nucleus transforms the acoustic stimulus in the frequency domain.

6.2.6.1 Patterns of excitation and inhibition

No neural inhibitory responses are seen in single fibres of the auditory nerve. All suppressive phenomena arise from the non-linearity of the excitatory transduction process or from rebounds following a period of excitation. However, cells of the cochlear nucleus show strong inhibition generated by inhibitory synapses. In contrast to the auditory nerve, spontaneous as well as stimulus-evoked activity can be reduced. In general, least inhibition is found in the anteroventral division of the cochlear nucleus, where the cells seem closest to the auditory nerve fibres in their response characteristics, and increasing degrees of inhibition are found as the posteroverentral, and then the dorsal, cochlear nuclei are approached.

Descriptions in terms of excitatory and inhibitory response areas were carried out by [Evans and Nelson \(1973\)](#) and extended by [Shofner and Young \(1985\)](#). In the terminology of Shofner and Young, Type I cells have purely excitatory response areas, similar to those of auditory nerve fibres (Fig. 6.9).

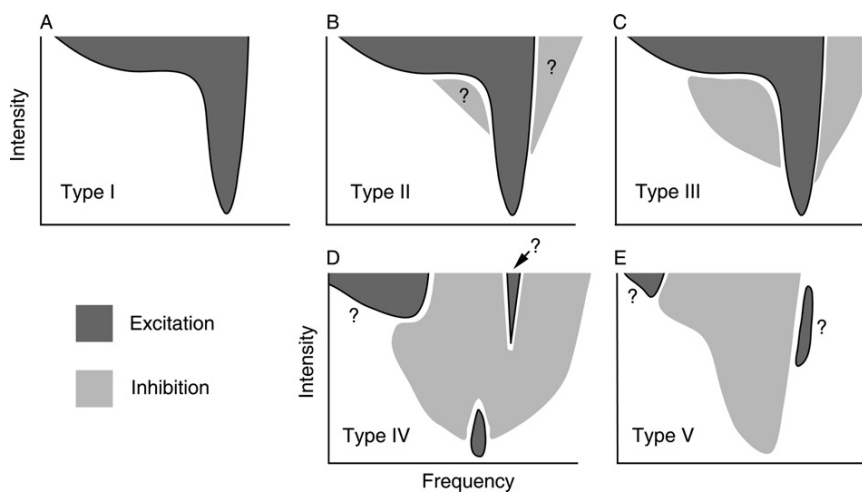


Fig. 6.9 Tuning curves of excitation and inhibition in the cat cochlear nucleus are shown in order of increasing amounts of inhibition (A–E). Purely excitatory responses are predominant in the anteroventral cochlear nucleus. Greater amounts of inhibition are found towards the dorsal cochlear nucleus (especially in the cat; D and E). Question marks show variable features.

They have no inhibitory responses. They are widely seen in the anteroventral cochlear nucleus and to a lesser extent in the posteroventral nucleus. Type III cells have a central excitatory response area, surrounded by inhibitory sidebands. They are found in both divisions of the ventral nucleus and in the deep layers of the dorsal nucleus. Type II units, which are also found in the deep layer of the dorsal nucleus, also give excitatory responses to tones, but give little or no response to wideband noise. They are therefore likely to receive strong wideband inhibition, although this cannot be tested directly with single stimuli because the cells do not show spontaneous activity. Type IV cells, found in all layers of the dorsal nucleus, have strong inhibitory areas, though giving excitatory responses to characteristic frequency tones near threshold (see the little "island" of excitation at tip of response area in Fig. 6.9D). Type V cells, also found in the dorsal nucleus, are similar to Type IV cells, but without the excitatory area at the characteristic frequency. Type IV and V cells are found more commonly in the cat than in the other species investigated such as rodents. The high degrees of inhibition are blocked by barbiturate anaesthesia, and these predominantly inhibitory responses are only seen in chloralose-anaesthetized or decerebrate animals. In general, the cells showing inhibition have non-monotonic rate-intensity functions, as the balance between excitation and inhibition moves further towards inhibition at the higher stimulus intensities (Fig. 6.10).

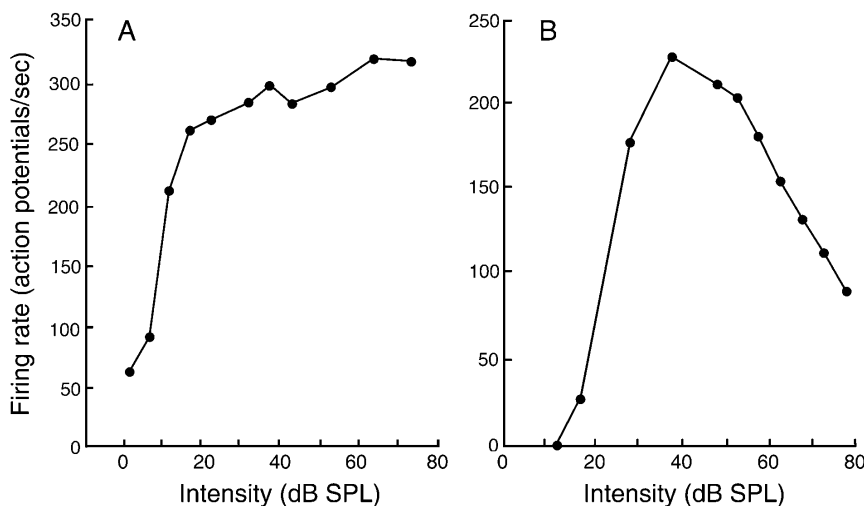


Fig. 6.10 Monotonic (A) and non-monotonic (B) rate-intensity functions in the cochlear nucleus. A is typical of neurones showing only weak inhibitory sidebands, and B of those with strong ones. Reprinted from Greenwood and Goldberg (1970), Figs. 1 and 4, Copyright (1970), with permission from American Institute of Physics.

6.2.6.2 Excitation and inhibition in relation to cell type

While it may seem reasonable to try to identify the inhibitory response types with the anatomical cell types described above, in practice this has been fraught with difficulty. For instance, for many years it appeared reasonable that most Type I cells would be identified with spherical bushy cells, since they have a simple direct input from the auditory nerve, and are heavily represented in the areas giving a high proportion of Type I responses. However, spherical bushy cells have some synaptic terminals which on anatomical grounds appear to be inhibitory, and the responses of spherical cells can be affected by blockers of the inhibitory neurotransmitters GABA and glycine. When care is taken in the analysis, a very high proportion of spherical bushy cells can be shown to have inhibitory responses, giving inhibitory sidebands (Kopp-Scheinplug *et al.*, 2002). One reason for not finding inhibition when it is in fact present is that the cells may show no spontaneous activity, so the inhibition cannot be shown with single-tone stimulation. A second reason for not finding inhibition is that in some cells the inhibitory tuning curve may closely match the excitatory tuning curve, so that it is not possible to separate their effects with one- or two-tone stimulation. The effects of inhibition that is otherwise hidden can sometimes be revealed by blocking the inhibition pharmacologically (Caspary *et al.*, 1994). The likely conclusion is that where Type I responses have been found, the cells in fact had inhibitory responses that were not picked up by the analysis and that the cells should have been classified as Type II or Type III. In other words, cells of the Type I classification may not in fact exist in the cochlear nucleus.

With similar provisos, one can attempt to draw broad associations between cell types and patterns of excitation and inhibition. T-stellate cells, which give sustained chopper responses, have narrow tuning curves that are excitatory with inhibitory sidebands (i.e. Type III; Smith and Rhode, 1989; Caspary *et al.*, 1994). Onset-chopper cells, identified with D-stellate morphology, have similar types of responses, though the excitatory part of the area is much broader (i.e. also Type III; Smith and Rhode, 1989; Paolini and Clark, 1999). Octopus cells have broad excitatory tuning curves, but inhibition has not been reported (i.e. provisionally Type I; Rhode *et al.*, 1983a; Smith *et al.*, 2005). Fusiform cells are likely to have Type III or Type IV responses, depending on species. These responses predominate in the fusiform layer of the dorsal nucleus and also in the dorsal acoustic stria which carries the projection axons of the fusiform cells (Rhode *et al.*, 1983b; Nelken and Young, 1997; Joris, 1998). Type II responses are also recordable deep in the dorsal nucleus, but not from the output pathway of the dorsal nucleus, the dorsal stria. Type II responses in the dorsal nucleus are therefore likely to represent interneurones, including the vertical cells which act as glycinergic inhibitory interneurones within the nucleus (Nelken and Young, 1994). Voigt and Young (1980), by simultaneously recording and cross-correlating the activity of Type II and Type IV neurones, showed that at least some of the inhibitory inputs onto the Type IV neurones arose from Type II neurones within the nucleus.

6.2.6.3 Roles of inhibition in the cochlear nucleus

A general consequence of inhibition is that auditory performance can be maintained relatively constant over a wide range of stimulus intensities. The inhibitory sidebands of Type II and Type III cells can stop the cell's frequency response area from widening at higher intensities, so that frequency resolution can be maintained. Lateral inhibition also reduces the influence of wideband background noise on auditory performance. Inhibition also raises the threshold of firing at higher stimulus intensities, so that the dynamic range is adjusted and details of the stimulus, such as small fluctuations in its intensity or its exact timing, can be transmitted with equal, and in some cases increased, accuracy. The latter can be demonstrated in bushy cells, where inhibition adjusts the threshold for initiation of action potentials. With higher intensity stimuli, where a greater number of synaptic terminals are activated, inhibition reduces the sensitivity of the cell. Individual terminals no longer activate the cell, and advantage can then be taken of the opportunity for greater averaging of the time-locked input which can increase the temporal accuracy of the cell's firing (see Fig. 6.4C and D; Kopp-Scheinflug *et al.*, 2002; Dehmel *et al.*, 2010; Kuenzel *et al.*, 2011).

In more complex cases, where cells with inhibitory sidebands such as Type II cells themselves inhibit further cells within the nucleus, further types of interaction are possible. These will be described in Section 6.2.7.4.

6.2.7 Functions of the cochlear nucleus

In this section, some transformations of the representation of the acoustic stimulus in the cochlear nucleus will be discussed. As the auditory signal is transmitted through the auditory system, critical aspects of the stimulus are emphasized. In this way, the representation is gradually transformed to give a clear-cut representation of the features that will be used by the decision-making mechanisms later in the brain. The transformations that have been most obvious to experimenters will be described in this section; however, it should be emphasized that these are likely to be only some of the key transformations of the representation of the acoustic stimulus in the auditory system.

6.2.7.1 The sound localization stream: binaural comparisons and localization in the horizontal plane

Sound localization in the horizontal plane involves comparing the timing and intensities of the stimuli at the two ears: a stimulus on the left side of space will hit the left ear first and will also be more intense in the left ear. For this comparison to be made, information about timing and intensity has to be transmitted to the superior olive, where the comparisons are made, as accurately as possible.

The threshold for sound localization in the horizontal plane shows that we can judge a time difference of 10 µsec between the ears, and therefore we know that timing is preserved to this level of accuracy in the population response. Bushy cells

have a low membrane resistance, and this means that large synaptic currents are needed to provide the depolarization to fire the cells. Also, the low resistance means that the time constants of the cells are short, so that temporal summation of inputs will occur over a short time period (Oertel, 1983). Moreover, the placement of the synapses on the soma itself means that the postsynaptic changes are transmitted as quickly as possible to the site of initiation of action potentials. These factors, together with temporal averaging arising from the convergence of the inputs, mean that bushy cells fire with a high degree of temporal precision. Indeed, bushy cells can produce action potentials with a greater degree of synchrony with the stimulus, and a more accurate representation of timing, than do single fibres of the auditory nerve (Cao and Oertel, 2010; van der Heijden *et al.*, 2011; see Fig. 6.4C and D).

6.2.7.2 Spectral contrast is enhanced and dynamic range adjusted in the cochlear nuclei

Many cells (Type II and III cells) have inhibitory sidebands, and in these cells, lateral inhibition serves to enhance the spectral contrasts, maintaining and enhancing the response to the predominant stimulus in spite of background masking noise. Some further consequences of inhibition were described in Section 6.2.6.3: lateral inhibition means that tuning curves do not widen with stimulus intensity as fast as in the auditory nerve, and neuronal responses therefore become relatively independent of the overall intensity of the stimulus. This does not necessarily require lateral inhibition (i.e. inhibition from cells tuned to adjacent frequencies); it also occurs where the inhibitory inputs substantially or completely overlap the excitatory inputs, as described for bushy cells in Section 6.2.6.3.

6.2.7.3 Temporal fluctuations are emphasized in the cochlear nuclei

In the frequency region for phase locking, the pattern of action potentials in the auditory nerve follows the waveform of the individual cycles of the stimulus (Fig. 4.9). Fluctuations in the amplitude of the stimulus will be similarly represented by fluctuations in the numbers of action potentials. When the stimulus frequency is too high for phase locking to the individual cycles of the stimulus, the numbers of action potentials can still be modulated by variations in the overall envelope of the stimulus. As the rate of modulation of the envelope is increased, the degree of modulation of the firing stays constant, until an upper cut-off frequency for modulation is reached, when the fibre no longer follows fluctuations in the stimulus amplitude (Rhode and Greenberg, 1994).

Many cells of the cochlear nucleus show degrees of modulation of their firing rate, in response to amplitude-modulated stimuli, that are greater than those seen in fibres of the auditory nerve. Onset-chopper cell and ‘primary-like with notch’ cells (Section 6.2.3) show the highest degrees of modulation. The suggested

mechanism is that these neurones are subject to a high degree of averaging of the input: because of the high degree of convergence of auditory nerve fibres onto the neurones, only those portions of the waveform which evoke the greatest probability of activation would be able to trigger firing, which therefore occurs at those times with a high degree of temporal precision (Fig. 6.4D; Rhode and Greenberg, 1994).

6.2.7.4 Complex stimulus analysis in the dorsal cochlear nucleus and sound localization in the vertical plane

The principal cells of the dorsal nucleus, the fusiform cells, receive direct inputs from the auditory nerve and also indirect inputs from Type II inhibitory interneurones, the vertical cells. These interactions lead to the complex Type IV or Type V response areas, with small islands of excitation among large inhibitory areas (Fig. 6.9D and E).

When a tone is presented in wideband noise, we might expect inhibitory sidebands to suppress the weaker parts of the stimulus pattern, so emphasizing the stronger parts. This is the case for cells with simpler inhibitory sidebands such as Type II or III cells. In these cases, we expect that the firing would depend on the net contrast in the stimulus pattern rather than on the overall intensity. We would also expect that stimuli with uniform wideband spectra would be poor at driving the cells.

More detailed investigation shows that, although this picture may be true for Type II and III cells, it may not be so for cells with more complicated response areas, such as Type IV cells. Young and Brownell (1976) in unanaesthetized cats showed that broadband noise was able to drive such cells more strongly than any tone. In some cases, both tones and noise were excitatory near threshold, but at higher intensities, tones became inhibitory and noise was excitatory. Such a finding may seem rather paradoxical, since we would expect the interplay of excitation and inhibition in a complex response area to reduce the response to broadband stimuli in comparison with that to tones. However, the responses can be understood simply in terms of the circuitry worked out by Young and colleagues, described in Section 6.2.6.2. They showed that the Type IV cells were themselves inhibited by cells with the simpler organization of an excitatory centre and an inhibitory surround, that is by Type II cells, now known to be vertical cells. Because vertical cells respond strongly to tones, but are themselves inhibited by wideband stimuli, the dominant inhibition from the vertical cells is turned off by wideband stimuli, to reveal excitation. Therefore, wideband stimuli can activate Type IV or V cells more strongly than can single tones, in spite of the apparently wideband inhibition implied by Fig. 6.9D and E (Young and Davis, 2002).

The complex interactions in the inputs driving fusiform cells can enhance the responses to spectrally complex wideband stimuli. Notch noise can strongly drive fusiform cells, if the rising edge of the notch is at or near the best frequency of the cell (Reiss and Young, 2005). In this case, the stimulus energy just above the upper edge of the notch falls in the excitatory response area of the cell. Such notches in

the spectra of broadband stimuli are produced by the transformation of sound field by the pinna (Fig. 2.2B). We would therefore expect the fusiform cells to be responsive to the elevation of broadband sound sources, which are judged on the basis of pinna-derived spectral cues. This agrees with behavioural data, because after lesions of the dorsal acoustic stria, the output pathway of the fusiform cells, cats are less able to make reflex orientations to sound sources as a function of elevation (Sutherland *et al.*, 1998a; May, 2000).

The deficit described by Sutherland *et al.* (1998a) was one to reflexive orientation, in which the cats made an automatic unlearned movement of the head upwards towards a sound source at different elevations. This response was upset by lesions that included the dorsal and intermediate acoustic striae. In contrast, after similar lesions, cats could still learn to discriminate between sound sources at different elevations, using a behavioural conditioning task (Sutherland *et al.*, 1998b). In other words, it is the automatic reflexive nature of the response that was critical for the deficit found by Sutherland *et al.* (1998a). This suggests that the dorsal nucleus might be part of an automatic reflex circuit. The ventral pathway, which of course also contains information on the spectrum of the sound, might in contrast be used for behaviour that is learned. It has been in fact speculated that the dorsal cochlear nucleus has much in common with the cerebellum, also involved in automatic motor activity (Oertel and Young, 2004).

The dorsal cochlear nucleus is likely to have a role in many other complex functions as well. For instance, it is affected by somatosensory inputs, and this has suggested that it may help suppress sounds produced by self-generated vocalizations and by movements (Kanold *et al.*, 2011; Koehler *et al.*, 2011). Changes in the responses of cells in the dorsal cochlear nucleus are also seen in experimentally produced tinnitus in animals, suggesting that the nucleus may have a role in generating tinnitus (see Chapter 10; Kaltenbach, 2011; Middleton *et al.*, 2011).

6.3 THE SUPERIOR OLIVARY COMPLEX

6.3.1 Innervation and overall anatomy

The outflows from the cochlear nucleus can be divided into two main streams. A ventral stream, in the ventral acoustic stria, is concerned with binaural sound localization. A dorsal stream, which is mainly concerned with sound identification, runs near the dorsal surface of the brainstem in the dorsal and intermediate striae (Fig. 6.11).

The binaural sound localization stream runs ventrally to the superior olivary nuclei of both sides (Fig. 6.12). The stream has two divisions. In the first division, the intensities of the stimuli at the two ears are compared in the lateral superior olive (LSO). The fibres to the ipsilateral LSO run directly to the nucleus, while those to the contralateral LSO project via a synapse in the contralateral medial nucleus of the trapezoid body (MNTB). The second division compares the timings

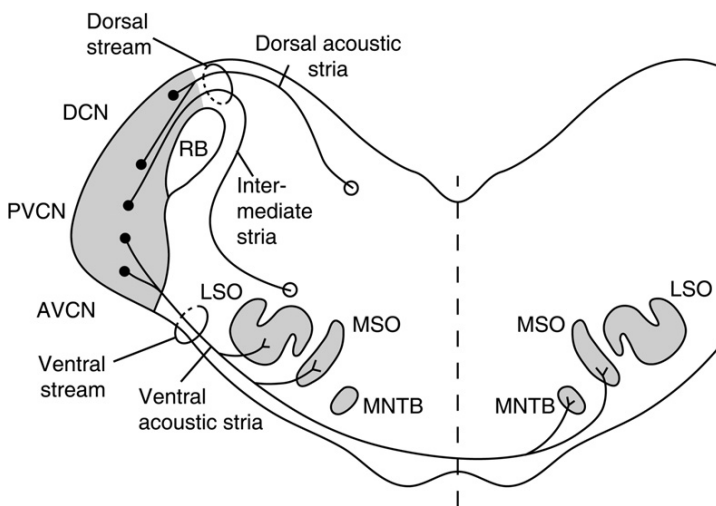


Fig. 6.11 The major outflows from the cochlear nucleus are shown on a transverse section of the cat brainstem. The ventral stream (binaural sound localization stream) arises in the anteroventral cochlear nucleus (AVCN) and posteroventral cochlear nucleus (PVCN) and runs in the ventral acoustic stria to the superior olfactory nuclei of both sides (see Fig. 6.8 for further details). The dorsal stream (mainly sound identification stream) runs in the dorsal and intermediate acoustic striae and passes dorsally over the restiform body (RB), or inferior cerebellar peduncle. It arises in the dorsal cochlear nucleus (DCN) and PVCN. Most fibres of the dorsal stream leave the plane of the section (shown by small circles) to run to higher levels of the brainstem, while others (not shown) run to the cells surrounding the lateral superior olive (LSO). MSO, medial superior olive nucleus; MNTB, medial nucleus of the trapezoid body. Other fibres (not shown) run between the cochlear nuclei of both sides. The fibres are represented diagrammatically and do not necessarily branch or join as indicated. For this diagram, anterior sections containing the AVCN and more posterior sections containing the PVCN and DCN have been superimposed.

of the stimuli at the two ears. This comparison is undertaken in the medial superior olive (MSO). The fibres from the AVCN project directly to the MSOs of both sides without an intervening synapse.

The dorsal stream, mainly involved in sound identification, runs primarily to the inferior colliculus of the opposite side, with some fibres synapsing in the nuclei of the lateral lemniscus on the way. Many of the fibres in the intermediate acoustic stria, which is also part of the dorsal stream, arise from the octopus cells of the PVCN and project to the contralateral VNLL, with some also projecting to the nuclei surrounding the LSO and MSO, or the peri-olivary nuclei.

Within the superior olfactory complex itself, several subnuclei can be distinguished (Fig. 6.13), all receiving different distributions of fibres from the different regions of the cochlear nuclei. The main nuclei associated with the ascending auditory pathways are the lateral and medial nuclei of the superior

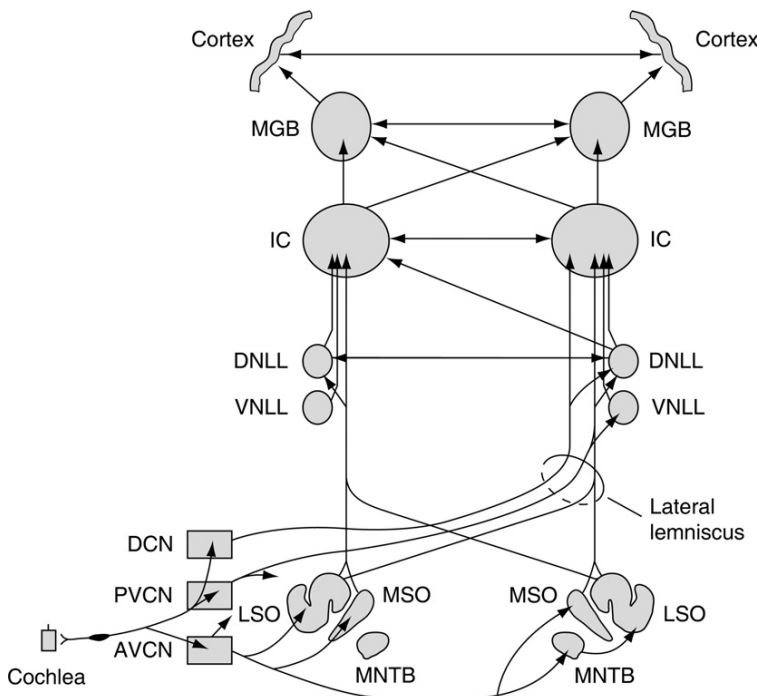


Fig. 6.12 The main ascending pathways of the brainstem. Many minor pathways, including many inhibitory pathways, are not shown. DNLL, dorsal nucleus of the lateral lemniscus; IC, inferior colliculus; MGB, medial geniculate body; VNLL, ventral nucleus of the lateral lemniscus. For other abbreviations, see caption to Fig. 6.11. The branching and joining of arrows does not necessarily mean that fibres branch or join.

olive (LSO and MSO), and the medial nucleus of the trapezoid body (MNTB). These nuclei are surrounded by other nuclei, known as the pre-olivary and periolivary nuclei, which send connections to the other olivary nuclei, as well as being associated with the centrifugal auditory system. They will be discussed in Chapter 8.

6.3.2 The ventral sound localization stream: comparing the intensities of the stimuli at the two ears

6.3.2.1 The lateral superior olivary nucleus

The lateral superior olivary nucleus (LSO) compares the intensities of the stimuli at the two ears and is excited by sounds on the ipsilateral side. The LSO has the form of a folded sheet of cells, which in cross sections in the cat has an S-shaped

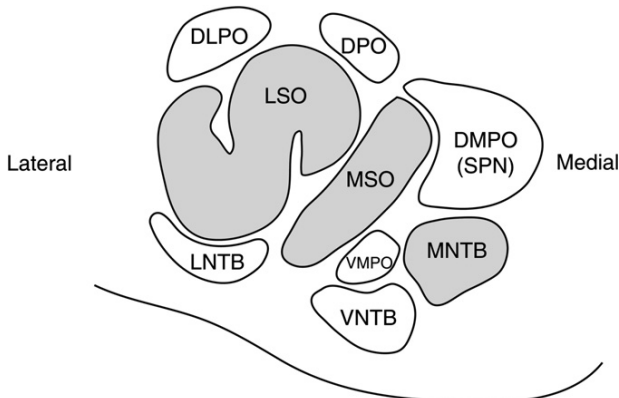


Fig. 6.13 The nuclei of the superior olfactory complex are shown in a transverse section in the cat. The main nuclei associated with the ascending system are shaded. DLPO, dorsolateral peri-olivary nucleus; DMPO, dorsomedial peri-olivary nucleus (corresponding to the superior para-olivary nucleus SPN in rodents); DPO, dorsal peri-olivary nucleus; LSO, lateral superior olfactory nucleus; LNTB, lateral nucleus of the trapezoid body; MSO, medial superior olfactory nucleus; MNTB, medial nucleus of the trapezoid body; VMPO, ventromedial peri-olivary nucleus; VNTB, ventral nucleus of the trapezoid body (medial pre-olivary nucleus). From [Harrison and Howe \(1974b\)](#), Fig. 8, with kind permission of Springer Science and Business Media.

appearance, though this varies with species. The major cell type is known as the principal cell (see, e.g. [Schwartz, 1992](#), for review). The dendrites spread extensively in the rostro-caudal direction, but with a distribution that is flattened so that the cells appear spindle shaped (i.e. fusiform) in transverse sections (Fig. 6.14A).

The LSO receives two major inputs. It receives a direct, glutamatergic, excitatory input from the ipsilateral AVCN, predominantly from the spherical bushy cells (Fig. 6.15A). The second major input is glycinergic and inhibitory, arriving via a synapse in the adjacent MNTB, from globular bushy cells of the contralateral AVCN ([Wu and Kelly, 1992](#); [Srinivasan et al., 2004](#)). Fibres from the ipsilateral and contralateral sides enter the folded sheet of the LSO by similar routes, with inhibitory inputs tending to terminate closer to the cell body and on the proximal dendrites and excitatory inputs terminating on the more distal dendrites.

The great majority of cells in the LSO are excited by ipsilateral stimuli and inhibited by contralateral ones (e.g. [Boudreau and Tsutsumi, 1968](#); [Tollin et al., 2008](#)). These cells are described as being of the 'IE' type.² In the experiment shown in Fig. 6.16, the rate-intensity function was first determined for tones in the

² In the terminology that is most widely used, the response to the contralateral ear is put first, and the response to the ipsilateral one second (see [Goldberg and Brown, 1969](#)). For example EE cells are excited by stimuli in both ears, EI cells are excited by contralateral stimuli and inhibited by ipsilateral ones and EO cells are excited by contralateral stimuli but not affected by ipsilateral ones.

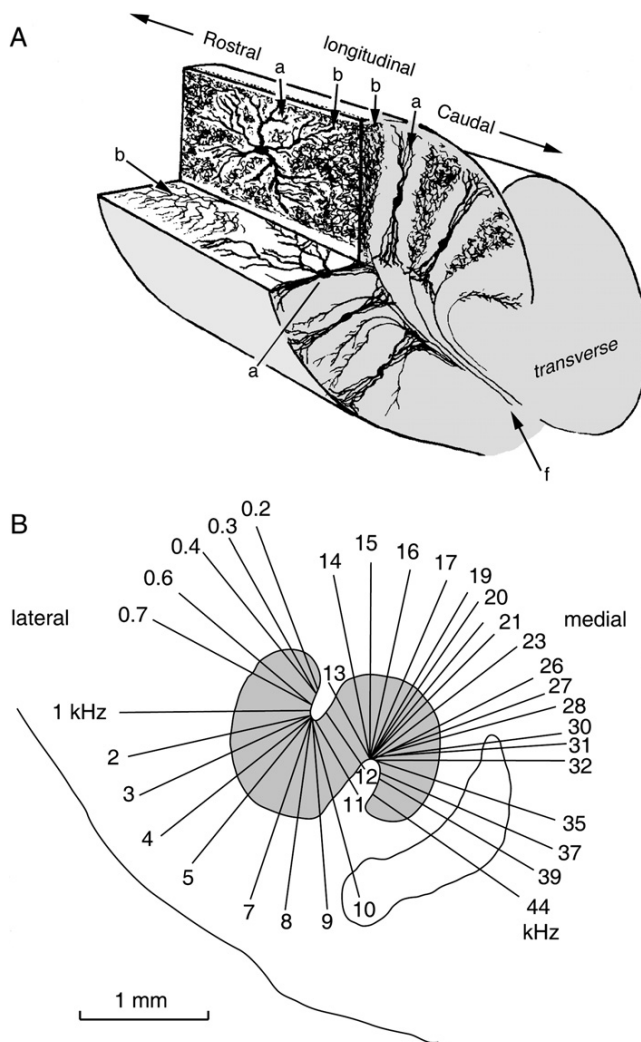


Fig. 6.14 (A) Neural organization of the lateral superior olive (LSO), showing how the dendrites of the principal cells (a) have a flattened arborization in the rostro-caudal direction. The terminal plexuses (b) of the afferent fibres ramify in the same planes as the dendrites of the principal cells. f, afferent fibres. From Scheibel and Scheibel (1974), Fig. 4A. (B) The tonotopic organization of the LSO. A large proportion of the nucleus is devoted to high frequencies. The numbers denote the characteristic frequencies of the sectors. Used with permission from Tsuchitani and Boudreau (1966), Fig. 6.

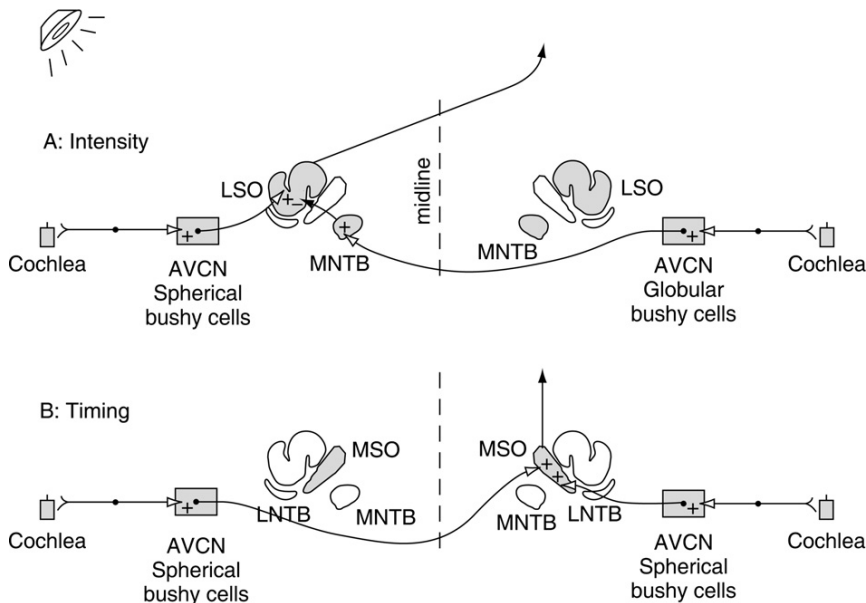


Fig. 6.15 The pathways (A) for comparing interaural intensity differences and (B) for comparing interaural timing differences, shown diagrammatically for the cat. Both sections show the pathways dominant when the stimulus is on the left. + –, excitatory and inhibitory inputs. The MSO receives further inhibitory inputs, not shown here, from the MNTB and LNTB.

ipsilateral (excitatory) ear alone (Fig. 6.16A). The tone in the ipsilateral ear was then presented at 20 dB SPL, and a further tone was simultaneously presented to the contralateral (inhibitory) ear. With the contralateral stimuli at very low levels (e.g. -10 dB SPL), the firing rate was the same as when no contralateral tone was present (dotted line). But as the intensity of the contralateral tone was increased, the cell's firing rate was reduced (Fig. 6.16B). When the intensity in the contralateral ear was the same as in the ipsilateral one (20 dB SPL), the firing rate of the cell was decreased near to zero, with 50% reduction being found with an interaural level difference of 10 dB.

The thresholds and tunings for the ipsilateral and contralateral effects are approximately comparable, so that cells of the LSO are able to extract interaural intensity differences in a frequency-specific manner (Caird and Klinke, 1983; Tollin and Yin, 2002). However, the inhibitory tuning curves of cells of the LSO are slightly wider than the excitatory tuning curves measured in the MNTB. This suggests that there is a convergence of inputs from MNTB cells onto cells of the LSO (Tsuchitani, 1997). The convergence increases the range of thresholds and dynamic ranges of LSO neurones and, by averaging, increases the temporal precision of the inhibitory inputs to the LSO.

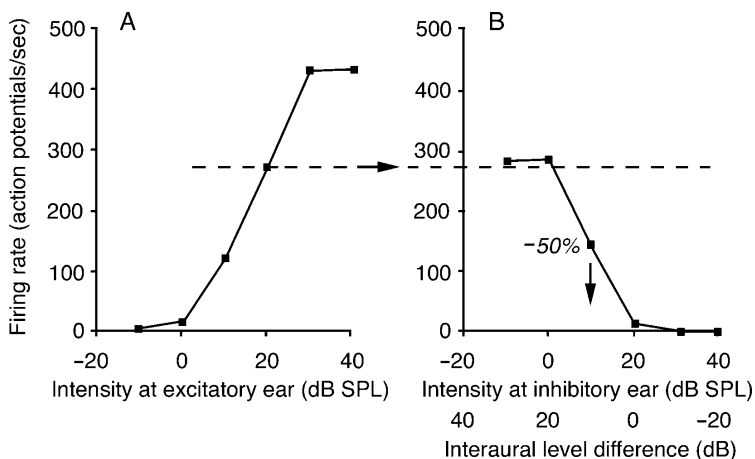


Fig. 6.16 (A) Rate-intensity function of an IE cell in the lateral superior olive, in response to an ipsilateral (excitatory) stimulus presented alone. (B) The cell was stimulated with the tone in the ipsilateral ear at 20 dB SPL (the dotted line showing the firing rate to the ipsilateral stimulus alone), and the response plotted as the function of the intensity of a superimposed tone presented to the contralateral (inhibitory) ear. Fifty per cent reduction in firing rate was produced with a contralateral stimulus intensity of 10 dB SPL (shown by vertical arrow: corresponding to interaural level difference of 10 dB). Used with permission from Park *et al.* (2004), Figs. 1A and 2A.

The intensity differences related to sound source location will be largest at high frequencies, where the degree of diffraction or bending of the sound waves around the head will be small. In accordance with this, most of the LSO is devoted to high frequencies (Fig. 6.14B).

The excitatory and inhibitory effects arrive at the LSO only after synaptic and neural transmission delays. If the two ears are stimulated simultaneously, the delays mean that the inhibitory effect from the contralateral ear arrives on average 200 µsec after the excitatory effect from the ipsilateral ear (Joris and Yin, 1998).

Therefore, for maximum inhibition of the excitatory response, the contralateral stimulus has to be applied 200 µsec before the ipsilateral one. This will occur when the sound source is on the contralateral side of the head. This is also the direction in which the intensity of the contralateral stimulus is greater and therefore has the maximum inhibitory effect based on relative intensities. The two effects, interaural intensity differences and the relative timing of the two stimuli, therefore summate to maximally suppress the LSO responses when the stimulus is on the contralateral side of the head, although the intensity effect is much more potent. While the temporal effects can be seen on a cycle-by-cycle basis with low-frequency stimuli, because the LSO is mainly a high-frequency nucleus, the temporal effect will be seen mainly in the onset responses and in the envelope fluctuations of high-frequency stimuli, as neurones do not phase-lock to the

individual cycles of high-frequency stimuli (Caird and Klinke, 1983, Tollin and Yin, 2005).

The LSO projects bilaterally to the central nucleus of the inferior colliculus (ICC), with the contralateral projection being substantially excitatory and the ipsilateral projection primarily inhibitory but with an excitatory component as well (Glendenning *et al.*, 1992). Because cells of the LSO are excited by stimuli on the ipsilateral side, this pattern of projection is in accordance with the generally crossed representation of stimuli in the central nervous system.

6.3.2.2 The medial nucleus of the trapezoid body

The medial nucleus of the trapezoid body (MNTB) acts primarily as a relay, conveying the excitation from the globular bushy cells of the contralateral AVCN to the LSO, as described in Section 6.3.2.1, as well as to the MSO. The axons from the contralateral AVCN are thick and end in large single calyces of Held on the principal cells of the MNTB, with the calyx of Held covering about half of the surface of the soma (Nakamura and Cramer, 2011). The single excitatory calyx on each principal cell means that this structure has become a favoured model for investigating synaptic physiology, particularly because the inputs can be activated precisely and specifically in tissue slices *in vitro*.

The single, large synapse arising from a thick axon can be expected to generate an activation that is secure, of high fidelity and short latency. Cells of the MNTB commonly have primary-like discharge patterns and tuning curves like those of the globular bushy cells of the AVCN (e.g. Tolnai *et al.*, 2008). In addition to the excitatory input, however, there are also inhibitory terminals on the principal cells of the MNTB, with GABAergic and glycinergic boutons having been shown immunocytochemically. These represent an input from surrounding nuclei such as the ventral nucleus of the trapezoid body (VNTB) and the superior para-olivary nucleus (SPN: also known as DMPO; see Fig. 6.13). Extracellular recordings from cells of the MNTB, like those from bushy cells of the AVCN (Fig. 6.4), show pre-potentials arising from depolarization of the calyx of Held, as well as postsynaptic action potentials from the cells themselves. As in the AVCN, some of the pre-potentials are not followed by action potentials, showing a failure in transmission a certain proportion of the time, suggestive of a superimposed inhibitory input (Kopp-Scheinpflug *et al.*, 2003). Tones set in the inhibitory part of a cell's response area can have a greater effect on the postsynaptic response than on the presynaptic pre-potentials, confirming the existence of the additional inhibitory input to the postsynaptic membrane. Comparison of the pre-potentials and principal cells' action potentials shows that the MNTB does not act simply as a relay and that the fineness of tuning, degree of phase locking and sharpness of onset responses are enhanced in the MNTB.

The principal cells of the MNTB project primarily to the principal cells of the adjacent ipsilateral LSO via inhibitory, glycinergic, synapses. In addition, cells of the MNTB send axons to the MSO and to the peri-olivary and pre-olivary cell

groups surrounding the superior olivary complex (Fig. 6.13) as well as to other nuclei of the brainstem (Schwartz, 1992).

6.3.3 The ventral sound localization stream: comparing the timing of the stimuli at the two ears

The medial superior olivary nucleus (MSO or accessory olive) receives a direct innervation from the spherical bushy cells of the AVCN of both sides. Because the spherical bushy cells have a secure, short latency activation arising from only a few very large end bulbs of Held, the cells of the MSO receive temporally accurate signals from the two ears. The nucleus performs sound localization by comparing the times of arrival of the activity from the two ears (Fig. 6.15B).

The MSO has a thin, sheet-like structure, with a single layer of principal (or fusiform) cells which have two groups of dendrites projecting towards the two sides of the sheet (Fig. 6.17). The axons from the AVCNs of the two sides innervate opposite sides of the sheet, with those from the ipsilateral AVCN contacting the lateral dendrites and those from the contralateral AVCN contacting the medial dendrites, that is those nearer the midline of the brainstem. Both types of inputs are excitatory and use glutamate as a transmitter. In addition to the principal cells, there are other cells, such as stellate and marginal cells (the latter situated around the edge of the nucleus; see Schwartz, 1992). As well as the excitatory input, cells of the MSO receive glycinergic inhibitory inputs via the LNTB and MNTB (Brand *et al.*, 2002). The MSO sends a presumed excitatory projection to the ipsilateral dorsal

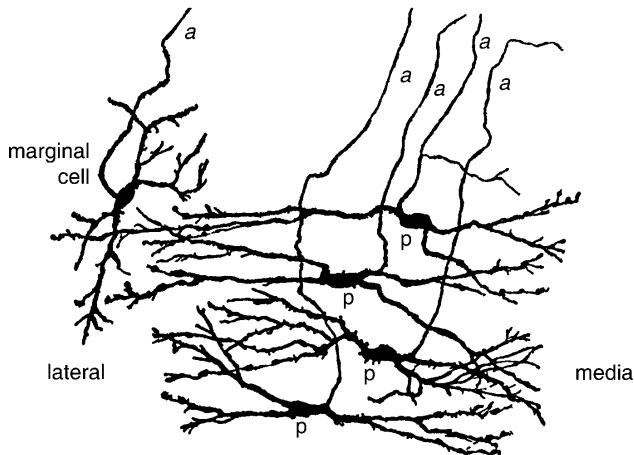


Fig. 6.17 Four principal cells (p) and one marginal cell in a small part of the medial superior olive (MSO). Axons from the ipsilateral and contralateral AVCNs contact dendrites on opposite sides of the sheet of cells. a, output axons. Mouse foetus. From Cajal (1909), Fig. 346, modified.

nucleus of the lateral lemniscus (DNLL) and to the ipsilateral inferior colliculus (Helfert *et al.*, 1989).

Studies of single unit activity in the MSO face severe difficulties, because the sheet of cells is thin and because gross potentials from neighbouring cell groups tend to swamp the single unit action potentials. In the dog, where the MSO is particularly large, Goldberg and Brown (1969) found that almost all the cells were binaural. Three-quarters of the cells were excited by both ears (EE cells), while the remainder were excited by one and inhibited by the other (EI or IE cells). The majority of cells in the MSO are low-frequency cells, and this allowed Goldberg and Brown to measure the timing of the responses by looking at the phase locking of the responses (the low best frequencies meant that they could not use click stimuli to measure the timing). They showed that the preferred phase of the response could differ at the two ears, which could be explained by a difference in the time of transmission of the neural signals to the nucleus from the two ears. The two delays calculated for the ipsilateral and contralateral stimuli could be used to predict the optimal interaural phase disparity. In this way, when the relative phases of the two stimuli were adjusted so that their excitatory effects coincided, there was

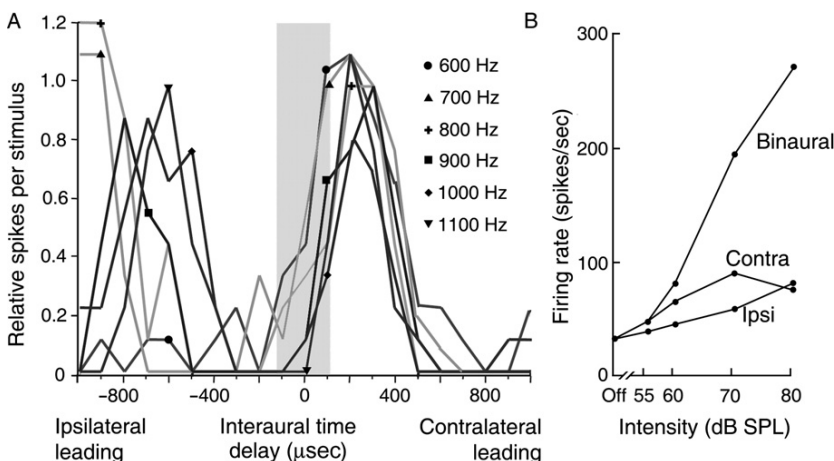


Fig. 6.18 (A) Response of a cell in the medial superior olive (MSO) to binaural stimulation, as a function of time delay between the stimuli to the two ears. The peak response is produced when the contralateral ear leads by 200 μsec . The position of the peak is independent of the actual frequency used for stimulation. Functions such as these are cyclic, because sinusoids as used for the stimulation repeat with the period of the stimulus. The grey area shows the range of interaural time differences expected from a single acoustic source external to the animal ($\pm 120 \mu\text{sec}$). Data for gerbil. From Brand *et al.* (2002), Fig. 1B. (B) Rate-intensity functions are shown for monaural and binaural stimulation in the dog MSO. The binaural stimulus was in the optimal phase relation, and could produce a much greater maximum firing rate than could either monaural stimulus alone. Used with permission from Goldberg and Brown (1969), Fig. 11.

a particularly large binaural response. This was true for neurones where both stimuli had a net excitatory effect (EE neurones), as it was for many IE neurones.

Figure 6.18A shows a more recent replication of Goldberg and Brown's experiment, this time in the gerbil. The interaural time delay giving the maximum response is independent of the frequency of the stimulus, consistent with the idea that the activation reaches the MSO cell after a time delay which depends on the cell rather than on the stimulating conditions. Further confirmation that the delay is primarily a property of the cell rather than of the stimulating conditions has come from experiments in which noise as well as tones are used as stimuli, all of which give similar time delays (Yin and Chan, 1990). The time difference that gives the peak of the function leads to the idea of a characteristic delay, different for each cell. The cell acts as a coincidence detector, so that at the characteristic delay the response to the two stimuli together can be greater than the sum of the responses to the stimuli presented separately. Moreover, when in the optimum relation, binaural stimuli can drive the neurones far harder than even more intense monaural stimuli (Fig. 6.18B). Similarly, at the minimum, the response is less than the response to either separately. This shows that in the excitatory phase relation, the interaction is one of facilitation rather than simple summation.

The findings can provisionally be interpreted in terms of Jeffress's (1948) model of sound localization, in which the direction of a sound source is measured from the difference in time of arrival of the stimuli at the two ears. The physiological results will be described in relation to that model in more detail in Chapter 9. Here, we note that if the characteristic delay for a cell matches, and exactly compensates for, the difference in time of arrival of the stimuli at the two ears, the cell will give a maximal response, and could be said to be specialized for detecting a sound source in that direction in space. In the great majority of cells, the characteristic delays are such that, as in Fig. 6.18A, the maximum response is produced with the contralateral ear leading. This means that overall the MSO represents sound sources on the contralateral side of the head.

Jeffress (1948) suggested that characteristic delays would be produced by axons of different lengths acting as neural delay lines. This indeed appears to be the situation in birds (Overholt *et al.*, 1992). In mammals, branches of axons of different lengths have indeed been found for the innervation from the AVCN, although with considerable variability (Beckius *et al.*, 1999). However, the role of axonal length in generating delays has been disputed. Brand *et al.* (2002) found that if the glycinergic inhibitory inputs to cells were blocked by the application of strychnine, the characteristic delays shifted to zero. The inhibition has to arrive in the correct temporal window, because tonically applied inhibition (via the iontophoretic application of glycine) also shifts the characteristic delays towards zero (Pecka *et al.*, 2008). It was suggested that fast and temporally precise inhibitory inputs via the LNTB and MNTB instead drove the coincidence detection, to generate the functions shown in Fig. 6.18A (see Grothe *et al.*, 2010, for review).

A second issue with the simple model of Jeffress is that in mammals the characteristic delays commonly fall outside the times that would be expected to arise from a sound source external to the head in space. This is illustrated in Fig. 6.18A, where the characteristic delay for the cell (200 µsec) lies outside the

maximum range calculated from the separation of the animal's ears and the speed of sound (120 µsec, grey area in the figure). Cells such as this therefore do not represent the actual direction, but rather whether the source is on one side or the other of the head. It is also a common finding that the steepest part of the curve occurs at zero interaural disparity. This means that the overall population response will change progressively with direction in the horizontal plane, with the greatest sensitivity to changes in direction occurring for sound sources nearest the midline.

6.3.4 Summary of role of superior olivary complex in sound localization

We can summarize the role of the LSO and MSO in sound localization as follows. In the LSO, most cells are IE cells and so respond to intensity differences between the ears. The majority of the cells are high-frequency cells and so have characteristic frequencies in the range where a sound source to one side will produce significant interaural intensity differences. In addition, the cells have a degree of sensitivity to temporal disparities in the time of arrival of the sound waveforms. By contrast, in the MSO most cells are EE cells and so will not respond to interaural intensity differences. Most MSO cells respond to direction on the basis of interaural temporal cues and in general are most responsive to low frequencies where phase information is preserved. Anatomical evidence suggests a picture in agreement with the division of functions. Animals with small heads and good high-frequency hearing, who might be expected to favour intensity cues, have large LSO nuclei and small MSO nuclei, whereas animals with large heads and good low-frequency hearing tend to have the reverse (Masterton and Diamond, 1967).

It should also be remembered that, just as some cells of the LSO respond to differences in interaural timing, some cells in the MSO are IE or EI cells; in other words, they can respond to the difference in intensities at the two ears. Therefore, like most cells of the LSO, they could contribute to sound localization on the basis of interaural intensity differences. Given that cells of each nucleus can in some ways respond on the basis of the cues used by the other, the segregation of functions between the two systems is not complete.

The above discussion applies to the main experimental animals used in auditory physiological research such as the cat and rodents. However, primates are somewhat different, and human beings show a large divergence from the pattern described above. As might be expected from the relatively large size of the human head, the human MSO is large. As also might be expected, the LSO is relatively small (Kulesza, 2007). In contrast to previous reports, it appears that human beings do have an MNTB, previous negative findings resulting from difficulties in identification (for discussion, see Grothe *et al.*, 2010). Sound localization will be further discussed in Chapter 9.

6.4 ASCENDING PATHWAYS OF THE BRAINSTEM AND THE NUCLEI OF THE LATERAL LEMNISCUS

The principal ascending pathways are shown diagrammatically in Fig. 6.12. The fibres running from the superior olfactory complex to the inferior colliculus run in a tract known as the lateral lemniscus. There are two major nuclei within the tract, known as the dorsal and ventral nuclei of the lateral lemniscus (Kelly *et al.*, 2009). A further division, the intermediate nucleus of the lateral lemniscus, has been distinguished although it is often included with the ventral nucleus, and will not be discussed separately here. Some fibres in the lateral lemniscus run directly to the colliculus, while others enter after a synapse in the nuclei of the lateral lemniscus.

6.4.1 The ventral nucleus of the lateral lemniscus

The ventral nucleus of the lateral lemniscus (VNLL) is part of the monaural sound identification stream. It receives its input from all cell types of the contralateral ventral cochlear nucleus (i.e. bushy cells, stellate cells and octopus cells) as well as from the ipsilateral MNTB (Kelly *et al.*, 2009). It does not receive an input from the major binaurally innervated nuclei of the superior olive (the MSO and LSO) and therefore does not appear to be involved in binaural sound localization. In addition, it is very poorly developed in human beings (Moore, 1987). It projects ipsilaterally to the inferior colliculus, with a complex pattern and interdigitating patchiness in the neuronal connections between the VNLL and the colliculus.

Some cells of the VNLL, with response patterns similar to the octopus cells of the ventral cochlear nucleus which project to the VNLL, can show precise temporal responses, appropriate for processing temporal information. Many neurones have complex, multipeaked tuning curves (Nayagam *et al.*, 2005; Zhang and Kelly, 2006). Therefore, the neurones appear to be specialized for extracting the temporal patterns in complex sounds. The laminae within the nucleus have been described as having a helical shape, and Langner has speculated that the VNLL is organized as a pitch helix, able to extract harmonic relations between stimuli (Langner, 2005). Together, these anatomical and physiological observations suggest that the VNLL might contribute a complex pattern of cross-frequency interactions to the central nucleus of the inferior colliculus (Merchan and Berbel, 1996; Malmierca *et al.*, 1998). In the colliculus, this input is likely to be superimposed on the direct input from the lower nuclei that bypasses the VNLL. The projection from the VNLL to the ipsilateral colliculus is substantially inhibitory; two-thirds of the cell bodies in the VNLL co-localize GABA and glycine, while the remaining one-third of cells are presumed to be excitatory (Riquelme *et al.*, 2001).

6.4.2 The dorsal nucleus of the lateral lemniscus

The dorsal nucleus of the lateral lemniscus (DNLL) is part of the binaural sound localization stream. It serves to increase the accuracy, contrast and dynamic range of the localization information, compared with that found in the superior olive (Pecka *et al.*, 2010). It receives its inputs from the ipsilateral MSO, the LSOs of both sides and the contralateral cochlear nucleus. The DNLL sends a substantially inhibitory, GABAergic, projection to the inferior colliculi of both sides as well as to the contralateral DNLL (Adams and Mugnaini, 1984; Ammer *et al.*, 2012). Most neurones of the DNLL are excited by contralateral stimuli and inhibited by ipsilateral ones. Neurones are also sensitive to interaural time differences, such that they represent sounds on the opposite side of the head (Kuwada *et al.*, 2006; Siveke *et al.*, 2006). The crossed inhibitory input from the contralateral DNLL to the inferior colliculus increases the neural contrast between the responses to sound sources localized in different positions in the horizontal plane. The enhancement can be reversed by local lesions: lesions of the DNLL made by local injections of kainic acid, which destroys the cells of the nucleus while not affecting fibres of passage, substantially interfere with the animals' ability to lateralize sound sources behaviourally, that is to tell whether the sound sources are on the left or the right, consistent with the role of the DNLL in lateralization. Similar effects were produced by surgical lesions of the commissure of Probst which carries the crossing fibres, also supporting the hypothesis (Ito *et al.*, 1996; Kelly *et al.*, 1996; reviewed by Kelly, 1997). The inhibition within the DNLL can be particularly long-lasting, suggesting that the cells may also enhance lateralization by suppressing echoes in an echoic environment (Pecka *et al.*, 2007).

The inhibition from the DNLL therefore enhances the lateralization of sound sources which was initially established in the lower stages of the auditory system. The lateralization is first seen at the superior olive, where the LSO predominantly represents sounds on the ipsilateral side of the head and sends its main excitatory projection to the contralateral inferior colliculus, whereas the MSO represents sounds on the contralateral side of the head, and sends its main excitatory projection to the colliculus on the same side as the MSO (Elverland, 1978; Adams, 1979). The result is that, from the inferior colliculus onwards, sound sources are predominantly represented on the contralateral side of the brain.



6.5 THE INFERIOR COLICULUS

The inferior colliculus (IC) is the main receiving station for the ascending pathways from lower stages of the brainstem. It forms the primary site of convergence of the sound identification and sound localization streams. Because the colliculus is tonotopically organized, fibres from different sources but of the same characteristic frequency manage to meet in the same isofrequency plane. The inferior colliculus shows a jump in the complexity of responses: the

integration of the sound identification and the sound localization streams, and the response to temporally complex stimuli, suggest that this is a critical stage in the transformation from responses dominated by the simple acoustic characteristics, to those which integrate acoustic properties in a way that begins to define an auditory object.

Although the inferior colliculus has been described as an obligatory relay for all the auditory input to the medial geniculate body, some neurones projecting to the medial geniculate body bypass the colliculus (Malmierca *et al.*, 2002).

6.5.1 General anatomy

The inferior colliculi form the rear pair of a set of four lobes on the dorsal surface of the midbrain. The anterior pair, the superior colliculi, form an important integrative reflex centre with a large visual input. The inferior colliculi are an auditory processing, relay and reflex centre. There are three main divisions to the inferior colliculus, namely the central nucleus, the external cortex and the dorsal cortex (Morest and Oliver, 1984; see Casseday *et al.*, 2002, for review). These different divisions have different neuronal architectures, different patterns of innervation and different functions. The central nucleus is the specific auditory nucleus and sometimes referred to as the ‘lemniscal’ nucleus, because of its heavy input from fibres running in the lateral lemniscus. The external nucleus and dorsal cortex, sometimes referred to as non-lemniscal or extra-lemniscal nuclei, mark a less specific, ‘diffuse’ and sometimes multisensory auditory pathway, which surrounds the specific auditory pathway. The inferior colliculus in human beings has the same general form as in the cat (Moore, 1987). The terminology used here is the current one which supersedes earlier terminologies.

6.5.2 The central nucleus

6.5.2.1 The spatial organization of the nucleus and its afferents

Oliver and Morest (1984) gave an authoritative account of the structure of the central nucleus (ICC). The central part of the central nucleus has a dramatic laminar structure (Figs. 6.19A and 6.20A). The laminae are strongly tilted with respect to the horizontal plane. The laminae are formed by the layering of the afferent axons and the dendrites of the intrinsic neurones.

A high proportion (about 80%) of neurones in the ICC are classed as disc-shaped neurones. Their dendrites arborize in a flat plane, along the plane of the laminations, so that when seen in transverse sections through the colliculus, the arborization appears flat, but when seen orthogonal to the plane of the lamination, the field of dendrites becomes disc shaped. Disc-shaped cells predominate in all parts of the ICC, even in the lateral division of the central nucleus where the laminations are not obvious. Stellate cells make up nearly all the remainder of the cells; their dendritic fields are in contrast spherical or ovoid, so that their dendrites

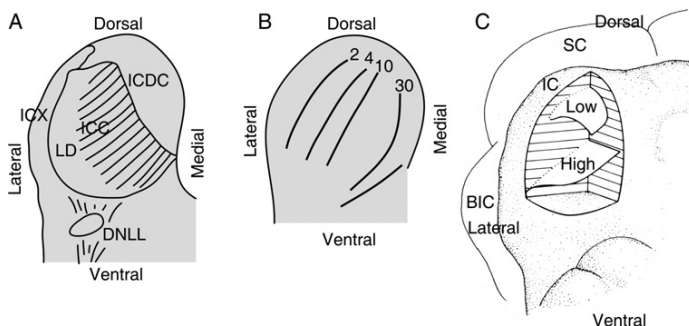


Fig. 6.19 The inferior colliculus in the cat. (A) Transverse section of the inferior colliculus, showing the main divisions, and the direction of the laminae in part of the central nucleus (ICC). The laminae repeat with a period of approximately 150 µm. Data from [Morest and Oliver \(1984\)](#), Fig. 2. (B) Isofrequency sheets shown in a transverse section of the inferior colliculus, as defined by 2-deoxyglucose reaction. The isofrequency sheets extend beyond the laminae shown in part A. Frequency in kHz are marked for the sheets illustrated. From [Brown et al. \(1997\)](#), Fig. 7F. (C) Low-frequency and high-frequency isofrequency sheets in the central nucleus of the inferior colliculus, as seen in caudolateral view (left side of brainstem, looking forward). Used with permission from [Semple and Aitkin \(1979\)](#), Fig. 5. BIC, brachium of the inferior colliculus; DNLL, dorsal nucleus of the lateral lemniscus; IC, inferior colliculus; ICDC, dorsal cortex of inferior colliculus; ICX, external nucleus of inferior colliculus; LD, lateral division of ICC; SC, superior colliculus.

cross over multiple laminations. As well as sending axons to the output nuclei, both types of cells, and particularly the stellate cells, send axon collaterals within the nucleus, so are able to act as interneurons.

The afferent fibres ramify along the laminae and contribute strongly to the laminated appearance. The afferent input from any one fibre therefore tends to be confined to a single layer of the lamination, but to spread very widely within that layer. Given that the dendrites of the disc-shaped cells also ramify within the same plane, this region of the nucleus seems to function as separate sheets of cells, with a relatively restricted interaction between the sheets, the interaction being carried by the stellate cells. The different fibrodendritic laminae appear to correspond to different isofrequency planes, with low frequencies represented dorsally and high frequencies ventrally (Fig. 6.19B and C). Like the laminations shown anatomically, the isofrequency planes are tilted down laterally and caudally. However, and unlike the anatomical laminations, the isofrequency planes extend beyond the area of clear lamination, to enter the lateral division of the ICC and the dorsal cortex. Adjacent laminae may form functionally discrete modules, because electrode penetrations show discrete jumps in best frequency as the electrode moves across the laminae, with a spatial periodicity roughly corresponding to the physical separation of the laminae ([Schreiner and Langner, 1997](#); [Malmierca et al., 2008](#)). Each anatomical lamina may itself cover a small range of frequencies, so that all frequencies are eventually represented in the nucleus. For this reason, the term

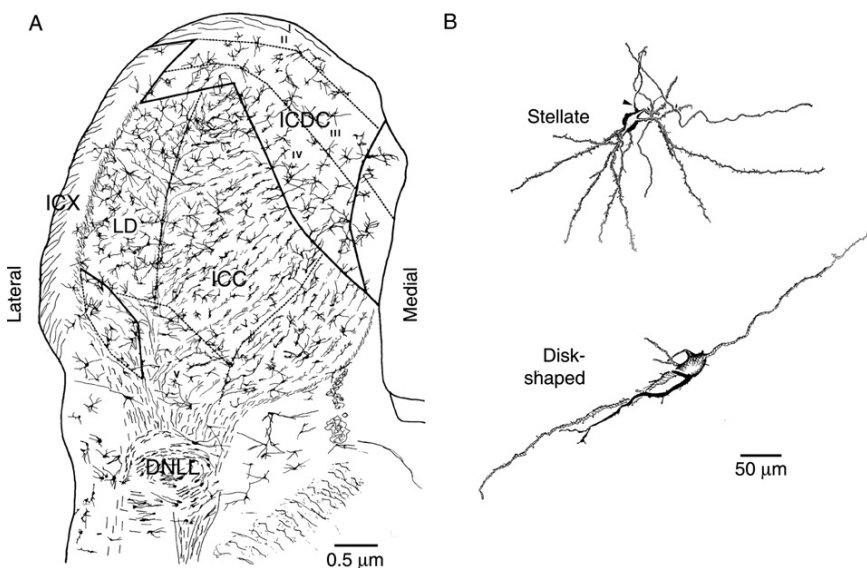


Fig. 6.20 (A) Drawing of the inferior colliculus from Golgi-impregnated material, showing divisions of the nucleus according to [Morest and Oliver \(1984\)](#), and the lamination in part of the central nucleus (ICC). I–IV, layers of dorsal cortex. ICDC, dorsal cortex of inferior colliculus; ICX, external nucleus of inferior colliculus; DNLL, dorsal nucleus of the lateral lemniscus; LD, lateral division of ICC. (B) Large disc-shaped cell of the central nucleus, seen edge-on as in transverse sections, plus a simple stellate cell, seen in same plane of section as the disc-shaped cell. Arrowhead: axon of stellate cell. From [Morest and Oliver \(1984\)](#), Fig. 2 and [Oliver and Morest \(1984\)](#), Figs. 1C and 3C.

'frequency-band lamina' rather than 'isofrequency plane' will sometimes be used here when the correspondence between anatomical and physiological results is being discussed.

Figure 6.21 summarizes the main direct ascending inputs to the central nucleus of the inferior colliculus ([Cant and Benson, 2003](#); [Kelly et al., 2009](#)). The major ascending excitatory inputs arise from the contralateral cochlear nucleus, the contralateral LSO, the ipsilateral MSO and 30% of the cells of the ipsilateral VNLL. Those inputs are glutamatergic, with different groups of nerve terminals having glutamate transporters of different functional types ([Ito and Oliver, 2010](#)). The major ascending inhibitory inputs arise from the DNLL bilaterally (GABAergic), the ipsilateral LSO (glycinergic) and the ipsilateral VNLL (GABAergic and glycinergic). About 30% of the intrinsic neurones of the ICC are GABAergic. They would be able to act as interneurones and provide inhibition within the nucleus via their collateral axons, as well as sending inhibitory projections to the medial geniculate body ([Oliver et al., 1994](#); [Winer et al., 1996](#); [Merchan et al.,](#)

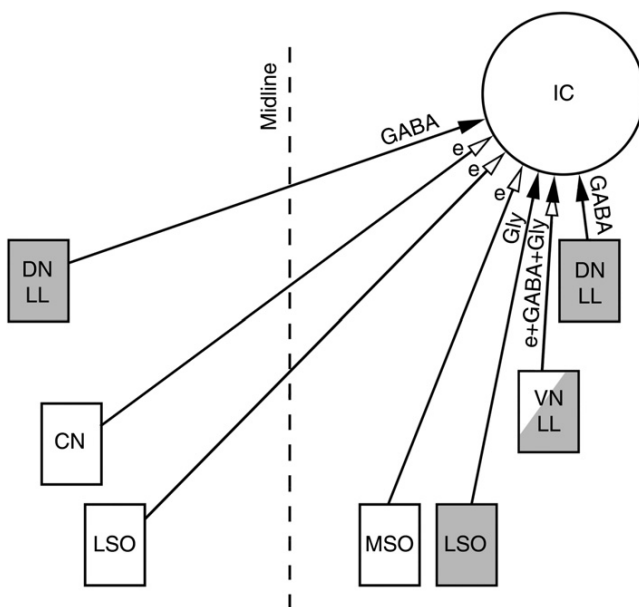


Fig. 6.21 The main ascending excitatory (open arrows) and inhibitory (closed arrows) pathways to the central nucleus of the inferior colliculus. Nuclei sending a predominantly inhibitory input are shown shaded. Some nuclei (e.g. VNLL) send a mixed input. Many minor ascending pathways, and all descending pathways, are not shown. In addition, there is an innervation from the contralateral inferior colliculus (IC). For the inhibitory pathways, the main neurotransmitter is shown. CN, cochlear nucleus; DNLL, dorsal nucleus of the lateral lemniscus; e, excitatory neurotransmitter; gly, glycine; LSO, lateral superior olive; MSO, medial superior olive; VNLL, ventral nucleus of the lateral lemniscus. Data on neurotransmitters and projections from DNLL, Adams and Mugnaini (1984); LSO, Glendenning *et al.* (1992); MSO, Helfert *et al.* (1989); VNLL, Riquelme *et al.* (2001).

2005). In addition, there is an input from the contralateral inferior colliculus (not shown in Fig. 6.21).

6.5.2.2 Patterns of excitation and inhibition

In anaesthetized animals, the majority of neurones in the ICC have sharp tuning curves, while a minority have long, shallow, low-frequency tails to the curves (Fig. 6.22A and B). In unanaesthetized animals, the response areas can be more complex in some neurones, with more than one excitatory area and multiple areas of inhibition (Ramachandran *et al.*, 1999; Fig. 6.22C). In some neurones, flanking inhibitory areas stop the excitatory area widening at higher stimulus intensities, so that sharp tuning is maintained at all intensities. In some cases, this is so extreme

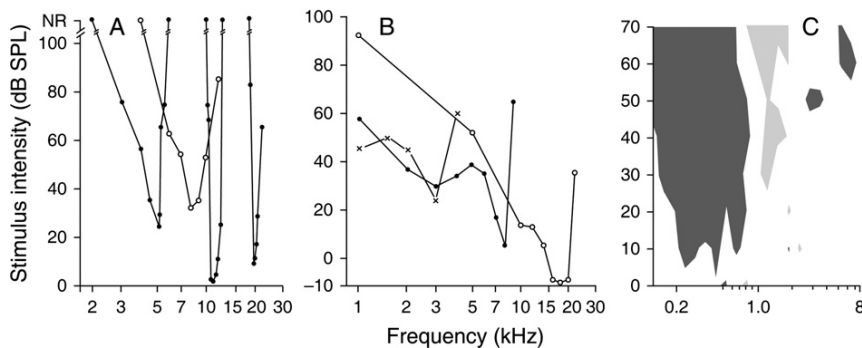


Fig. 6.22 Responses of neurones in the central nucleus of the inferior colliculus. (A) Tuning curves showing sharply tuned responses in the anaesthetized cat. (B) Tuning curves with shallow low-frequency tails in the anaesthetized cat. (C) Complex response areas in a neurone recorded in the unanaesthetized chinchilla. Dark grey: excitation; light grey: inhibition. A and B used with permission from Aitkin *et al.* (1975), Fig. 7; C from Biebel and Langner (2002), Fig. 1.

that the excitatory response area disappears at the highest intensities, giving a so-called closed excitatory response area, while in others there may be an inhibitory island within the excitatory response curve (Alkhateeb *et al.*, 2006).

The inhibition within the ICC may arise from either the inhibitory inputs to the nucleus or the inhibitory collaterals of the intrinsic neurones of the ICC. In neurones with simple V-shaped response areas (Fig. 6.22A), blocking the inhibition increases neuronal firing to a similar extent both in the central excitatory part of the response area and in the inhibitory flanks. Therefore in these cells, the inhibitory synapses on cells of the ICC tend to affect the whole response area equally (LeBeau *et al.*, 2001). The inhibition in these cells is likely to have a role such as maintaining the response to complex signals relatively constant over a wide range of stimulus intensities. In addition, the inhibition, by lowering the transmembrane resistance and so shortening the membrane time constant, may increase the temporal accuracy of the response to stimuli with rapid temporal fluctuations (Wu *et al.*, 2004). On the other hand, in neurones with more complex response areas (Fig. 6.22C), blocking the inhibition reduces the inhibitory sidebands, returning cells to the simple V-shaped response area. In these cases, inhibition can affect the frequency selectivity of the cells (LeBeau *et al.*, 2001).

6.5.2.3 Binaural responses and sound localization

Cells in the ICC show directional selectivity; recordings from cells of the (presumed) central nucleus of the unanaesthetized rabbit show that many cells have a broad directional selectivity towards the contralateral spatial hemifield. The responses are dominated by inputs from the contralateral ear, but refined and enhanced by input from the ipsilateral ear (Kuwada *et al.*, 2011).

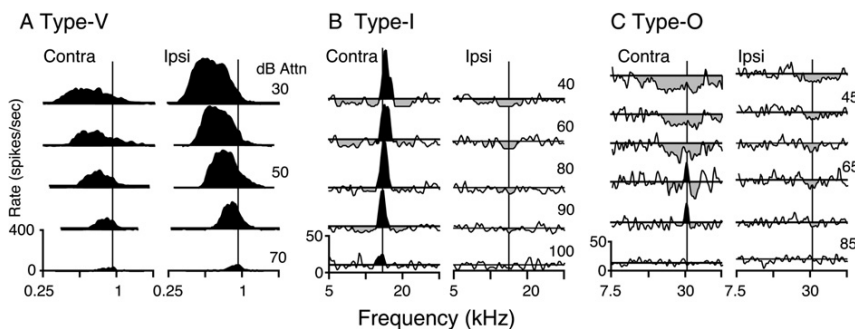


Fig. 6.23 Binaural responses in the inferior colliculus recorded in the decerebrate cat. (A) Type V neurones tend to have V-shaped frequency response areas, no inhibition, low characteristic frequencies and EE responses. (B) Type I neurones have narrow response areas that stay narrow at high intensities, with inhibitory sidebands, and EI responses at their characteristic frequency. (C) Type O neurones have an area of excitation at their characteristic frequency, which becomes inhibitory at higher stimulus intensities. They have wide inhibitory areas, may have small additional excitatory areas and EI responses. Stimulus intensities are marked as dB attenuation below the maximum sound level produced at each particular frequency by the sound system. Contra, contralateral; Ipsi, ipsilateral. Modified and used with permission from Davis *et al.* (1999), Fig. 1.

Evidence of the possible interactions giving rise to the directional selectivity has come from anatomical studies of the detailed innervation patterns. In areas where interaural timing differences dominate, there was found to be an input from the ipsilateral MSO, which processes interaural time differences. However, some of these areas also received an input from the ipsilateral LSO which primarily responds to interaural intensity differences (Loftus *et al.*, 2004). On the other hand, the DCN processes location using monaural information based on high-frequency spectral notches. However, some high-frequency areas where there was a major input from the DCN also received inputs from the contralateral and ipsilateral LSO. These nuclei also process sound location based on high-frequency information, but in their case using interaural level differences (see also Section 6.5.2.5).

Functional separations within the ICC seem also to be related to the type of frequency response area. Some of the relationships are shown in Fig. 6.23. Units with V-shaped symmetrical tuning curves and no inhibitory inputs tend to be low-frequency units, which are binaurally excited (EE) and sensitive to interaural timing differences (Ramachandran and May, 2002). These are the Type V units as shown in Fig. 6.23A. It is likely that their response is dominated by inputs from the MSO which have similar characteristics. These are the types that do not show changes in response area when their inhibitory synapses are blocked. On the other hand, Type I (Fig. 6.23B) cells are EI³ cells sensitive to differences in interaural

³ EI – excitation by the contralateral ear, inhibition by ipsilateral one.

intensity. They are therefore presumed to have a dominant input from the LSO (see also Greene *et al.*, 2010). Cells with complex, wide inhibitory areas and only narrow islands of excitation have response areas to contralateral stimulation reminiscent of DCN neurones (Type O cells, Fig. 6.23C; cf. Fig. 6.9). They have a dominant input from the DCN and have EI responses to binaural stimuli, the ipsilateral inhibition presumably arising from the ipsilateral LSO and possibly from the DNLL. In Type I and O cells, blocking the inhibition pharmacologically at the ICC reduces the inhibitory sidebands, so some of the inhibition in the sidebands must be shaped by inhibition at the ICC (LeBeau *et al.*, 2001).

Low-frequency neurones are sensitive to interaural time delay, giving functions relating firing rate to interaural time delay which are similar to those seen in the MSO (Fig. 6.18). Cells of the ICC would therefore be able to code sound direction in a way similar to cells of the MSO. However, inhibition at the ICC can increase the slopes of the functions relating firing rate to interaural time delay. This has been shown in unanaesthetized animals by blocking the GABAergic inhibition at the ICC (D'Angelo *et al.*, 2005). In this way, inhibition at the inferior colliculus has been shown to enhance the accuracy of judgements of sound location based on timing information. GABAergic inhibition at the ICC can also contribute to sound localization based on differences in interaural intensity. When GABAergic inhibition is blocked in some cells, the sensitivity to differences in interaural intensity can be either shifted to favour one ear or the other or can be markedly reduced overall (reviewed by Pollak *et al.*, 2003).

Some of the inhibition that enhances the sensitivity to differences in interaural intensity and timing arises from the contralateral DNLL. As pointed out above (Section 6.4.2), the DNLL enhances the lateralization of stimuli established elsewhere in the system: blocking excitatory synapses in the contralateral DNLL with kynurenic acid reduces the sensitivity of cells in the ICC both to differences in interaural intensity and to differences in interaural timing, in accordance with this suggestion (Li and Kelly, 1992; Kidd and Kelly, 1996; see Kelly, 1997, for review). In addition, inhibition in the inferior colliculus helps in gain control, maintaining neural responses relatively constant in spite of variation in overall stimulus intensity (Ingham and McAlpine, 2005). This would for instance help maintain the accuracy of localization based on intensity and timing information, over a wide range of stimulus intensities.

The different inputs onto a binaurally sensitive cell in the ICC can arrive at slightly different times, and the different inputs can adapt at different rates, so that in many cells the pattern of excitation and inhibition from the two ears changes over time (Zhang and Kelly, 2010). A further implication of this is that some cells in the ICC might be sensitive to the direction of movement of sound sources. Some cells in the inferior colliculus are sensitive to the dynamic aspects of changes in interaural phase. The enhanced response to moving sound sources appears to come from the timing of the excitatory inputs to collicular neurones, rather than from phasic GABAergic inhibition arriving from the DNLL, as it can be maintained and indeed enhanced after blockage of the GABAergic input onto the cells (McAlpine and Palmer, 2002).

6.5.2.4 Temporal sensitivity

Neurones in the ICC commonly show onset, pauser and sustained response types, with a smaller proportion of cells being choppers. In some neurones, inhibition is the first effect seen although the overall response may be excitatory. Multiple phases of excitation and inhibition are likely to arise from the different times of arrival of the inputs from the different projecting nuclei, as well as from the different temporal properties of the various ion channels on the neurones (e.g. Koch and Grothe, 2003; Wu *et al.*, 2004). We expect these effects to enhance the response to temporal modulations in the stimuli.

Amplitude-modulated stimuli give bandpass rate functions in a high proportion (50%) of cells. In these cells, the mean firing rate shows a peak for certain frequencies of amplitude modulation, with suppression of the mean rate for higher and lower frequencies of modulation (Langner and Schreiner, 1988; Krishna and Semple, 2000). It is possible that these neurones have a role in periodicity detection (for discussion, see Chapter 9, Section 9.4.2). In some neurones, inhibitory inputs help shape the bandpass response, by selectively suppressing the firing rates for stimuli with low rates of amplitude modulation. This can be shown by blocking the inhibitory input with a GABA blocker, which can increase the firing rate for stimuli which have a low rate of amplitude modulation. This changes the plot of firing rate as a function of frequency of amplitude modulation, from a bandpass function to a lowpass function (Caspari *et al.*, 2002).

Cells in the ICC can also show preferential responses to frequency-modulated stimuli. In the study of Poon *et al.* (1992) in the rat, 75% of cells showed an enhanced response to frequency-modulated stimuli, in a way that could not be simply predicted from their ongoing responses to continuous tones (see also Escabi and Schreiner, 2002). Some cells were driven particularly well by fast sweeps and also were selective to the direction of the sweep. Intracellular labelling and later morphological analysis of the latter cells showed that they were stellate cells, that is the cells with large spherical or ovoid dendritic trees which cross the isofrequency laminae and which therefore would be in a position to detect cross-frequency information.

In the bat, cells are also responsive to amplitude modulation and frequency modulation, and some show specializations not found in non-echolocating mammals, such as detecting the duration of auditory stimuli and detecting the delays between auditory stimuli (for review, see Casseday *et al.*, 2002).

6.5.2.5 Maps in the ICC?

The frequency-band laminae define one axis in the ICC, related to stimulus frequency. However, each frequency-band lamina is two-dimensional, and this has led many researchers to suggest that there might be further functional zones or specializations within the two-dimensional laminae, which may have an organization that runs orthogonal to the frequency axis. Some support has come from anatomical studies, which have shown that endings from different structures

are not uniform within a lamina, but are grouped in patches, giving rise to a variety of specializations or differentiations within the frequency-band laminae (Oliver *et al.*, 1997). It can be speculated that this would permit a strong interaction between neurones of similar properties, and so facilitate the extraction of certain stimulus properties. For instance, axons from the LSO end only in the ventromedial part of the ICC; here, the inputs from the ipsilateral and contralateral LSO are concentrated in complementary patches side by side (Shneiderman and Henkel, 1987; Loftus *et al.*, 2004; Henkel *et al.*, 2005).

Areas of primarily monaural input are found in the rostral and caudal ICC. Here, the responses reflect the monaural properties of cells in the cochlear nucleus. The VNLL may provide a monaural inhibitory input to this area, via glycinergic and GABAergic synapses. This area may be specialized for extracting spectral and temporal patterns, and for monaural sound localization using cues from the pinna as extracted by the DCN (Loftus *et al.*, 2010).

In the dorsolateral ICC, there is a low-frequency area where the cells are sensitive to interaural time differences. This area has a major input from the ipsilateral MSO (which responds to interaural time differences). It also receives an input from the lateral, or low-frequency, region of the ipsilateral LSO, which is likely to be a source of glycinergic inhibition (Loftus *et al.*, 2010). This area is likely to be involved in low-frequency sound localization, with the response areas sharpened by the inhibitory inputs from the LSO.

Apart from the above functional zones, it has been difficult to show any convincing maps apart from the tonotopic map. For instance, a map of auditory space has been defined in the external nucleus of the inferior colliculus (see Section 6.5.3), but not in the central nucleus. A further suggested map has been related to periodicity information. Investigating the response to amplitude-modulated sounds, Schreiner and Langner (1988) found that, within a single frequency-band lamina, cells responding with the shortest latency and to the highest frequencies of modulation were situated towards the ventrolateral edge of the lamina (see also Langner *et al.*, 2002). This spatial segregation was used by the authors to suggest that different periodicities were represented along an axis which was orthogonal to the tonotopic axis (Langner, 2004).

6.5.3 The external nucleus and dorsal cortex

The external nucleus receives inputs from the contralateral cochlear nucleus, including the contralateral DCN, and from the ICC. It also receives a somatosensory input from the dorsal columns and the trigeminal nuclei. The dorsal cortex, on the other hand, does not receive a direct ascending auditory projection, but receives inputs from the contralateral inferior colliculus and descending inputs from the auditory cortex (for review, see Irvine, 1986).

Neurones in the external nucleus and dorsal cortex tend to be broadly tuned (Fig. 6.24) and to habituate rapidly (Aitkin *et al.*, 1975). Neurones in the dorsal cortex are driven monaurally, while in the external nucleus a high proportion (70%) of neurones show binaural responses. Aitkin *et al.* (1978) found that 54% of

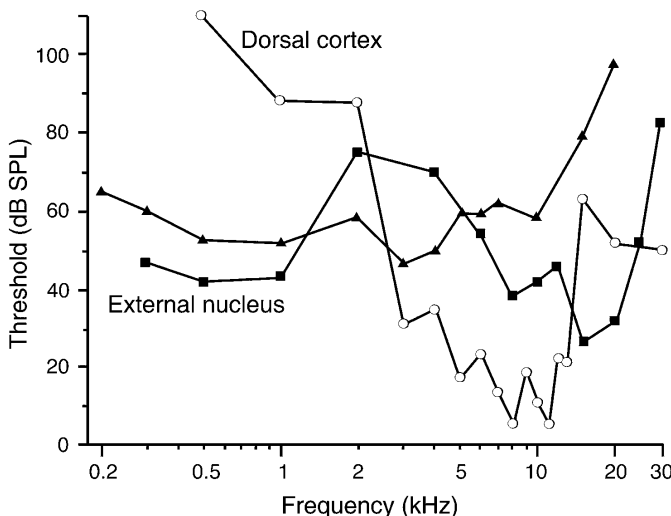


Fig. 6.24 Examples of tuning curves of cells in the dorsal cortex and external nucleus of the inferior colliculus. Open circles: cell in dorsal cortex; triangles and squares: cells in external nucleus. Used with permission from Aitkin *et al.* (1975), Fig. 6.

neurones in the external nucleus were bimodal, most of those being excited by auditory stimuli and inhibited by somatosensory ones. In the dorsal cortex, neurones show strong responses at the onset of stimuli. They also can adapt to ongoing stimuli, but show a strong response to changes, a phenomenon known as stimulus-specific adaptation (SSA). This suggests that the nucleus might be important for detecting novel sounds (Lumani and Zhang, 2010).

While there is little definitive evidence on the functions of the dorsal cortex and the external nucleus, the external nucleus is likely to be an auditory and somatosensory integrative area, governing spatial reflex responses to sound, rather than being a simple auditory relay (e.g. Jain and Shore, 2006). Both nuclei are likely to form part of the separate ‘diffuse’, ‘belt’, non-specific or extra-lemniscal auditory system, often with multisensory interactions, that surrounds the specific, ‘core’ or lemniscal, auditory system. This division into specific and diffuse auditory systems is carried up through the medial geniculate body to the auditory cortex (see Lee and Sherman, 2011, for further analysis of the distinction between the two types of pathways).

In the owl, there is a map of auditory space in the lateral rim of the lateral dorsal mesencephalic nucleus, in an area suggested to be homologous to the mammalian external nucleus (Knudsen and Konishi, 1978; Gutfreund and Knudsen, 2006). Neurones in the lateral rim code the direction of a sound source. Points forward are represented anteriorly, and points to the side are represented posteriorly. Each nucleus represents space on the contralateral side, although in front the field crosses 15° over to the ipsilateral side. In addition,

points high in space are represented high in the nucleus, and points low are represented low. The owl achieves this map with two specializations which do not appear in the mammal. Firstly, auditory neurones in owls phase-lock up to much frequencies than in mammals (10 kHz), with the result that their functions for interaural time delay, as in Fig. 6.18A, can be very steep. Secondly, the two ears are set at different heights on the head, and this, combined with the ruff feathers around the head, means that elevation of the source is coded as an interaural intensity difference.

Searches for similar maps have been made in the mammal. Binns *et al.* (1992) found a space map in the external nucleus of the guinea pig. Neurones preferentially responded to the direction of a broadband noise stimulus, with different neurones responding to sound sources in different directions. Neurones situated rostrally in the nucleus responded preferentially to sound sources in front of the animal, and neurones situated caudally in the nucleus responded best to sound sources behind the animal. The selectivity primarily depended on monaural cues, as the map was maintained if one cochlea was ablated. It is likely that the spatial selectivity was determined, in part at least, from the spectral cues introduced by the pinna and processed by the DCN. In animals in which both ears were functional, the map was essentially the same, but did not broaden at high stimulus intensities in the way that the monaural map did, suggesting that the second ear provided gain control or lateral inhibition at higher intensities. The external nucleus projects to, among other areas, the superior colliculus, and it is likely that the space map in the external nucleus contributes to the joint visual and auditory space map in the superior colliculus which is used for behavioural orientation (e.g. Burnett *et al.*, 2004).



6.6 THE MEDIAL GENICULATE BODY

The medial geniculate body is the specific thalamic relay of the auditory system, receiving afferents from the inferior colliculus, and projecting to the cerebral cortex. It also has heavy reciprocal connections back from the cortex, indicating that the cortex and medial geniculate body are grouped together as a functional unit.

6.6.1 Overall anatomy and inputs

Figure 6.25A shows the divisions of the nucleus recognized in the cat. There is a ventral, principal division, plus the adjacent dorsal and medial divisions. In primates, instead of a dorsal division there is a posterodorsal division with an adjacent anterodorsal division (Jones, 2003).

The ventral division is the specific auditory relay and is classed as part of the lemniscal auditory pathway. Its afferents run mainly ipsilaterally from the central nucleus of the inferior colliculus. The afferent fibres run in the brachium of the

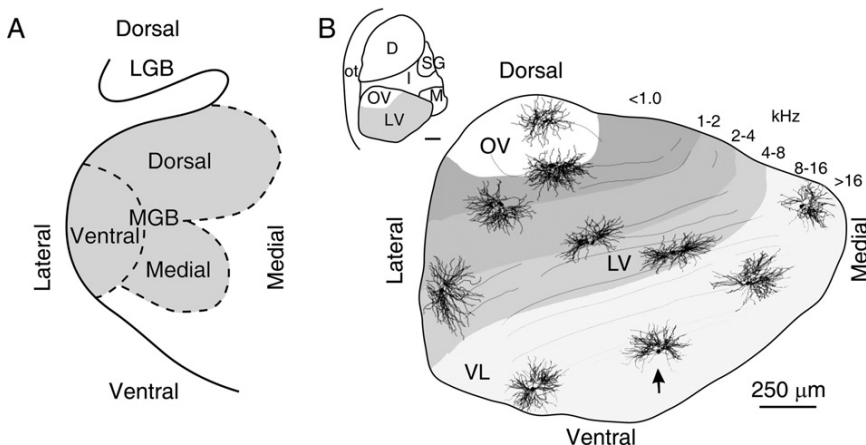


Fig. 6.25 (A) Major divisions of medial geniculate body in the cat in coronal section, showing the dorsal, medial and ventral divisions. MGB, medial geniculate body; LGB, lateral geniculate body. From Harrison and Howe (1974a), Fig. 8, with kind permission of Springer Science and Business Media. (B) Orientation of laminae and tonotopic organization of the ventral division of the medial geniculate body in the rabbit. Numbers and gradient of shading show the frequency gradient in kHz across the nucleus. Also shown are typical dendritic arbours of the tufted neurones. Arrow: cell with asymmetric dendritic arbour. The laminations are most clear in the pars lateralis (LV) region of the ventral division. Other parts of the ventral division are the pars ovoidea (OV) and the ventrolateral part (VL). The inset shows the region of the main figure in relation to the rest of the MGB. In the rabbit, the internal division (I) is more prominent than in the cat. D, dorsal division; M, medial division; ot, optic tract; SG, supra-geniculate nucleus. Scale bars in main figure and inset: 250 μ m. From Cetas *et al.* (2003), Fig. 1.

inferior colliculus, a bulge on the lateral surface of the brainstem between the inferior colliculus and the geniculate bodies (Fig. 6.19C). The ventral division projects principally to the core areas of the auditory cortex, that is to AI, the anterior auditory field (AAF) and the posterior auditory field (PAF) (defined for the cat in Fig. 7.1; see also Read *et al.*, 2011).

In contrast, the medial and dorsal divisions receive a multiplicity of inputs and project to the cerebral cortex in a less specific way. The medial division, as well as receiving inputs from the central nucleus of the inferior colliculus (the ICC), receives inputs from the external nucleus of the inferior colliculus (ICX), from the lateral tegmental system running just medial to the brachium of the inferior colliculus, from the superior colliculus and from the spinal cord. It therefore has somatosensory and visual as well as auditory inputs. It also receives some fibres directly from the contralateral dorsal cochlear nucleus and from parts of the ventral cochlear nucleus (Malmierca *et al.*, 2002). The medial division projects widely to the different auditory cortices, as well as to the core. In addition, it has connections with the lateral nucleus of the amygdala. The dorsal division in the cat receives

afferents primarily from the dorsal cortex of the inferior colliculus and also from the region medial to the brachium and from the somatosensory system. It projects to the cortical areas known as AII, Ep and I-T, which surround the core auditory cortex, and to AAC within the core (defined in Fig. 7.1; Calford and Aitkin, 1983; Winer, 1985). The medial and dorsal divisions, classed as part of the extra-lemniscal auditory pathway, therefore can be viewed as the ‘diffuse’ or non-specific auditory system surrounding the specific auditory system. The different patterns of inputs and the different patterns of projections suggest that the three divisions of the medial geniculate body are parts of three separate and parallel projection pathways to the auditory cortex (Calford and Aitkin, 1983; Smith *et al.*, 2012; reviewed by Winer *et al.*, 2005).

6.6.2 The ventral nucleus

6.6.2.1 Anatomy and frequency organization

The ventral nucleus or division has a laminar structure, formed by the interdigitating layers of afferent axons and intrinsic neurones. There are two types of intrinsic neurones, namely tufted neurones and short-axon interneurones. The tufted neurones have large dendritic fields (approximately 450 µm across) and axons that project out of the nucleus (Fig. 6.25B). The dendritic trees commonly ramify in two diametrically opposed directions. The short-axon interneurones (Golgi Type II cells) may have large or small dendritic trees depending on species and are inhibitory, using GABA as a neurotransmitter (Huang *et al.*, 1999). The tufted cells receive a multiplicity of inputs, including excitatory and inhibitory inputs from the inferior colliculus, excitatory inputs from the auditory cortex, inhibitory inputs from the short-axon interneurones and inhibitory inputs from the reticular thalamic nucleus.

The laminae are particularly clear in the rabbit; in the large central region of the ventral nucleus, the pars lateralis (LV), the laminae are relatively flat and tilted downwards laterally, whereas in the more dorsal part of the ventral nucleus, the pars ovoidea (OV), the laminae form tighter curves (Fig. 6.25B; Cetas *et al.*, 2003). The laminae are almost certainly parallel to the isofrequency planes in the nucleus, with low frequencies represented dorsally in the nucleus and high frequencies ventrally.

An electrode inserted through the ventral nucleus in a dorsal to ventral direction shows that it has a tonotopic organization, with low frequencies represented dorsally and high frequencies represented ventrally (Fig. 6.25B). However, as the electrode passes through the nucleus, the best frequency does not increase steadily, but rather in jumps of around 0.8 octave (Cetas *et al.*, 2001; Fig. 6.26). This has suggested that there is a further level of organization within the nucleus and that patches of neurones are joined into functional groups which represent a range of frequencies. The functional groups have been termed ‘slabs’ (McMullen *et al.*, 2005). Each slab corresponds to a thick, two-dimensional curved sheet, formed from groups of several adjacent anatomical laminae. The large dendritic arbours of the tufted neurones ramify within one slab. Because all

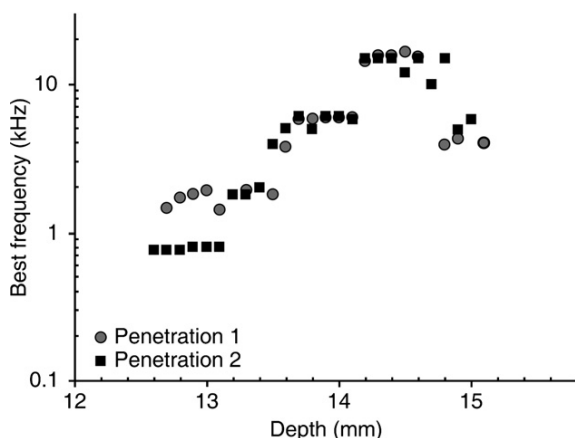


Fig. 6.26 Tonotopicity in the ventral division of the medial geniculate body: as an electrode is advanced from the dorsal side through the nucleus in the ventral direction, the best frequency of the region goes from low to high frequencies. However, the changes are stepwise, suggesting the presence of functional modules. From Cetas *et al.* (2001), Fig. 3.

intermediate frequencies are represented, as well as those shown in a single track as in Fig. 6.26, this model also implies that the intermediate frequencies are represented in other parts of the two-dimensional slab. The finding of frequency jumps is analogous to the finding of frequency jumps in the ICC by Schreiner and Langner (1997), although in the ICC the frequency jumps are smaller (about 0.3 octave) and have an anatomical spacing corresponding to the separation of the individual anatomical laminae.

There is a further organization orthogonal to the isofrequency planes, since the neurones with different classes of binaural response (EE vs. EI) are segregated in different patches within the isofrequency planes. This is correlated with a patchiness in the projections to the auditory cortex and a patchiness in the different cells' binaural response types within the cortex (Velenovsky *et al.*, 2003).

6.6.2.2 Responses to sound

Neurones in the ventral division, the specific auditory nucleus, have relatively sharp tuning curves (Aitkin and Webster, 1972; Bartlett and Wang, 2011). A great variety of temporal response patterns have been found. In anaesthetized animals, onset responses are most common, although onset plus inhibition, offset, on–off or sustained excitatory types also occur (Calford, 1983; Cetas *et al.*, 2002). Sustained excitation or sustained inhibition is more common in unanaesthetized animals (Aitkin and Prain, 1974). In general, neurones with complex temporal properties have non-monotonic rate–intensity functions and complex frequency response

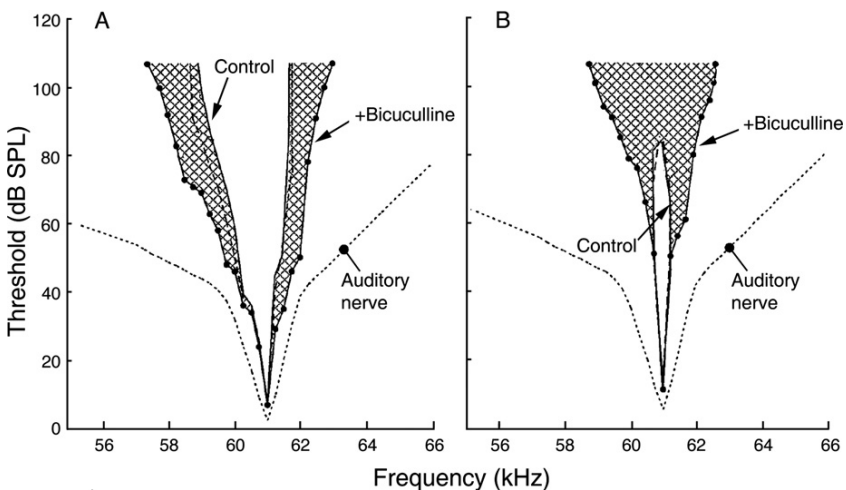


Fig. 6.27 (A) Role of inhibition in sharpening tuning curves in the ventral division of the moustache bat medial geniculate body. Control tuning curves (inner open areas) are sharply tuned, more sharply tuned than auditory nerve fibres tuned to the same frequency region (dotted lines). After GABAergic inhibition was blocked with bicuculline, the tuning curves expanded (shaded areas). Thirty-seven per cent of neurones of this class showed a similar effect; the remainder showed no effect. Part B shows a neurone with a particularly narrow, closed, excitatory tuning curve. Neurones were Doppler-shifted constant-frequency neurones, that is those specialized for picking up echolocation echoes at a precise frequency and hence corresponding to a precise relative velocity of the target (note expanded frequency scale on abscissa). Used with permission from Suga *et al.* (1997), Fig. 2.

areas, as would be expected for neurones with a multiplicity of excitatory and inhibitory inputs.

The role of inhibition in tuning has been shown in the moustached bat, where blocking GABAergic inhibition by the local application of bicuculline widened tuning curves in some of the neurones (Fig. 6.27). The widening was particularly dramatic at the higher stimulus intensities, and it is expected therefore that the normal role of inhibition in the medial geniculate body is to maintain frequency resolution at these intensities. Correspondingly, blocking inhibition changed the rate-intensity functions from the highly non-monotonic functions expected with high degrees of inhibition at high stimulus intensities to more monotonic ones (Suga *et al.*, 1997).

Figure 6.27 shows that in the moustached bat, the tips of the tuning curves are much sharper than those of the auditory nerve fibres. Similarly sharp tuning has been found in a high proportion (76%) of MGB neurones in the awake marmoset (Bartlett *et al.*, 2011). However, many other authors have reported that the tips of tuning curves in the medial geniculate body are equally as sharply tuned as, or only occasionally more sharply tuned than, those of the auditory nerve fibres (Aitkin

and Webster, 1972; Calford *et al.*, 1983). In all species, the tuning curves do not increase in width with stimulus intensity to the same extent as in the auditory nerve, meaning that frequency resolution is independent of stimulus intensity to a much greater extent than in the auditory nerve. There are also further roles for the lateral inhibitory interactions; one is that of enhancing the cues for sound localization in the vertical direction. These cues are dependent on the spectral peaks and troughs introduced by the pinna at certain sound source directions (Fig. 2.2B) and are initially extracted by inhibitory networks in the dorsal cochlear nucleus and enhanced in the medial geniculate body (Samson *et al.*, 2000).

Bats show a number of specialized responses which may be related to echolocation, such as responses to tone combinations, and neurones that are sensitive to the duration of auditory stimuli or to delays between auditory stimuli. Some of these complexities may reflect cortical processing, as there are substantial corticofugal influences on the medial geniculate body which can for instance change the frequency resolution of neurones in the medial geniculate (Zhang and Suga, 2000; see also Chapter 8). While these may be specializations in the bat, it is likely that they are examples of basic neural mechanisms that also occur in other mammalian species. In addition, the close bi-directional interaction between the medial geniculate body and the auditory cortex means that the two must be considered as one unit. This close interaction enhances the difficulty of analysing the specific stimulus transformations that occur in the medial geniculate.

6.6.3 The medial and dorsal nuclei

The medial division is part of the ‘diffuse’ or extra-lemniscal auditory system which projects more generally to the auditory cortex. It has sometimes been grouped with a number of adjacent nuclei which together are known as the paralaminar nuclei and which have similar innervations and functions. A further candidate for inclusion is the posterior thalamic nucleus which is adjacent to the MGB rostrally, although the posterior thalamic nucleus has response properties more reminiscent of the ventral division than of the extra-lemniscal nuclei (Anderson and Linden, 2011).

In the medial division, Aitkin (1973) in the unanaesthetized cat showed many very wide, multipeaked and complex response areas. Three-quarters of the neurones were binaural. In the anaesthetized mouse, many neurones have short first-spike latencies, and highly reliable firing at the onsets of stimuli (Anderson and Linden, 2011). The neurones also show stimulus-specific adaptation (SSA), in which the response to an ongoing stimulus declines with time but returns on presentation of a novel stimulus (Anderson *et al.*, 2009; Antunes *et al.*, 2010; Bäuerle *et al.*, 2011). Both of these findings suggest a particular role in the response to novel stimuli.

The responses in the medial nucleus are affected by associative learning. They change as a result of a conditioned fear response, in which sounds have been associated with a negative stimulus, such as a puff of air to the cornea (McEchron *et al.*, 1996). The amygdala is involved in learning fear in response to negative

stimuli. The medial division of the MGB and the posterior intralaminar nucleus, both of which receive an input from the inferior colliculus, have particularly close anatomical associations with the amygdala (for a review of the role of the auditory nuclei in fear, see [Weinberger, 2011](#)). Reversible inactivation of the medial division of the medial geniculate nucleus together with adjacent nuclei (the posterior intralaminar nucleus and supra-geniculate nucleus) stops the acquisition and retention of eyeblink conditioning in response to an electric shock ([Halverson et al., 2008](#)). In turn, input from the amygdala modifies the responses of neurones in the medial MGB, as shown by pairing the auditory stimulus with a fear-inducing stimulus such as an electric shock to the foot ([Duvel et al., 2001](#)).

The dorsal division projects to the auditory areas surrounding the primary auditory cortex ([Smith et al., 2012](#)). Neurones in the deep division of the dorsal nucleus show short latency and sharply tuned responses to sound in anaesthetized cats; those situated more dorsally and medially respond more weakly and with much habituation ([Calford and Aitkin, 1983](#); see also [Anderson and Linden, 2011](#)). The responses show strong stimulus-specific adaptation ([Antunes et al., 2010](#)) and may also be modulated by training paradigms. In conscious guinea pigs, when a tone was followed by an aversive stimulus (an electric shock to the paws), the responsiveness of neurones in the dorsal division was enhanced to the tone of the frequency used in the training but not to tones of other frequencies ([Edeline and Weinberger, 1991](#)). The medial and dorsal divisions of the medial geniculate body, by showing responses that are modifiable depending on the behavioural environment of the animal and by projecting widely to many areas of the auditory cortex, would be able to prepare the cortex for responding to stimuli which are of particular significance for the organism.



6.7 BRAINSTEM REFLEXES

The brainstem is the main auditory reflex centre of lower vertebrates, and it would be surprising if some of these functions were not retained in human beings and in other mammals.

6.7.1 Middle ear muscle reflex

One of the most elementary auditory reflexes is the middle ear muscle reflex. Both the tensor tympani and stapedius muscles contract reflexively in response to loud sounds, and protect against overstimulation. However, in human beings, while the stapedius muscle is predominantly driven by intense sounds, the tensor tympani is also activated by self-generated actions such as swallowing and vocalizations. An arc of two to four neurones is involved, consisting of a projection from the ventral cochlear nucleus to the motor nuclei of the trigeminal nerve, and other neurones projecting from the cochlear nucleus via the MSO to the motor nuclei of the facial and trigeminal nerves (e.g. [Billig et al., 2007](#)). But in addition to this short latency

pathway, there is also evidence for a slower pathway, perhaps projecting via the red nucleus or the reticular formation, both of which receive an auditory input. The middle ear muscle reflex has been reviewed by [Mukerji *et al.* \(2010\)](#).

6.7.2 Acoustic startle

Acoustic startle is a stereotyped fast contraction of facial and body muscles in response to an auditory stimulus. It has a latency of 5–10 msec and forms a way of rapidly withdrawing the head and tensing the muscles to protect against physical damage. The reflex arc is thought to involve the ventral cochlear nucleus which projects contralaterally to a small cluster of giant neurones in a part of the reticular formation known as the nucleus reticularis pontis caudalis ([Yeomans and Frankland, 1996](#)). The giant neurones are known to project to the spinal cord, and blockade of glutamate receptors on the giant neurones reduces the startle response. Lesion studies suggest that other nuclei such as the ventrolateral tegmental nucleus are also involved, particularly in the reflex response of the head musculature (for review, see [Koch, 1999](#)). Because startle is a simple, reliable response, it is heavily used for behavioural screening. Because it is enhanced by fear and attenuated by presumed pleasurable states, it can also be used as a measure of the subject's central state, for instance, when testing the effects of drugs that either increase or reduce anxiety. It can also be used for analysing sensory processing, since an immediately preceding weaker auditory or visual stimulus can reduce the response (prepulse inhibition or PPI). In the case of an auditory prepulse stimuli, the pathway for inhibition involves the inferior and then the superior colliculi ([Fendt *et al.*, 2001](#)).

6.7.3 Orientation

Orientation to acoustic stimuli is also an automatic stereotyped response which involves the brainstem, and in particular the superior colliculus, where lesions upset orientation responses to auditory stimuli (e.g. [Burnett *et al.*, 2004](#)). The deep layers of the superior colliculus receive an input from the external nucleus of the inferior colliculus (ICX), an area which contains neurones selective for the directions of sounds in space. The ICX receives an input from the dorsal cochlear nucleus, where sound elevation is extracted on the basis of the spectral notches introduced by the pinna and where lesions interfere with automatic reflexive orientation to sounds of different elevations ([Sutherland *et al.*, 1998a](#)). The deep layers of the superior colliculus in addition receive an input from the anterior ectosylvian sulcus (AES) area of the auditory cortex, which is also involved in sound localization (see Chapter 7). In the deep layers of the superior colliculus, a high proportion of the acoustically responsive cells are high-frequency EI cells, which respond to spatial location on the basis of interaural intensity differences, being excited by stimuli on the contralateral side ([Campbell *et al.*, 2006](#)). It appears moreover that these layers of the superior colliculus contain a map of auditory space, which is approximate register with the visual map and which is influenced in development by input from

the ICX (Palmer and King, 1982; Thornton and Withington, 1996; Vachon-Presseau *et al.*, 2009). Nevertheless in the superior colliculus registration of the two maps is not complete, at least in primates (Maier and Groh, 2009). In the owl, plasticity in both the ICX and the optic tectum (superior colliculus) helps to contribute to aligning the maps in the tectum (DeBello and Knudsen, 2004).

6.7.4 Audiogenic seizures

Audiogenic seizures also seem to require structures up to the level of the inferior colliculus, but not beyond. In certain susceptible strains of animals, early deprivation of auditory input ('priming') leads to a hypersensitivity of the central nervous system, so that a later auditory stimulus produces a motor seizure (Saunders *et al.*, 1972). The inferior colliculus seems particularly involved in the initiation of the seizures, because during the onset of a seizure, neuronal activity starts to increase first in the inferior colliculus, and bilateral lesions of the colliculus abolish the seizures. Seizures can also be induced by interfering with GABAergic inhibition in the inferior colliculus (Faingold, 2002). On the other hand, lesions of structures higher in the auditory system, such as the medial geniculate, do not abolish the seizures. The external nucleus and dorsal cortex of the inferior colliculus seem to be the structures responsible, since fos immunoreactivity, a measure of neuronal activation, increases in these structures with the stimuli producing audiogenic seizures, but not in the central nucleus (Kwon and Pierson, 1997). Following activation of the inferior colliculus, activity spreads to the reticular formation, the superior colliculus and basal ganglia (for reviews, see Faingold, 1999; Ross and Coleman, 2000). Audiogenic seizures have become a valuable general model for analysing epilepsy and for studying the effects of anti-convulsant medication and neuronal implants.



6.8 SUMMARY

1. The analysis of auditory stimuli is progressively undertaken over many stages of the auditory system, where the critical features are progressively extracted to a greater and greater extent as the information is passed up the auditory pathway. The likely reason is that many of the critical features of the acoustic stimulus are intermingled in the stimulus, such that the neural extraction of some of the features degrades the neural representation of other features. This means that extraction of a number of features has to occur in separate parallel streams, with the results being integrated at one or more later stages. When the recombination occurs, the responses to the different features are resynthesized to form a neural representation of the auditory properties of the object that gave rise to them, that is they begin to define what has been called an 'auditory object'.

2. The auditory system shows an early division into two streams with broadly different functions, forming a stream involved in binaural sound localization and a stream predominantly involved in sound identification. At the level of the cochlear nucleus, the binaural sound localization stream involves the anteroventral cochlear nucleus and some cells of the posteroventral cochlear nucleus, which project ventrally over the brainstem in the trapezoid body to the superior olivary complex of both sides. Here, the location of sound sources in the horizontal direction is extracted on the basis of interaural timing and intensity cues. The stream predominantly involved in sound identification includes other cells of the posteroventral cochlear nucleus and dorsal cochlear nucleus and projects directly to the contralateral ventral nucleus of the lateral lemniscus and the contralateral inferior colliculus.
3. The cochlear nucleus has three divisions, known as the anteroventral, posteroventral and dorsal cochlear nuclei. Each division of the nucleus is tonotopically organized, so that the best frequencies of the neurones make a spatially ordered map in each division. In the anteroventral division, the neuronal responses are similar to those of auditory nerve fibres, with simple tuning curves, no inhibitory sidebands and monotonic rate-intensity functions. Globular and spherical bushy cells predominate, each receiving synaptic terminals of the auditory nerve fibres in the form of a few large end bulbs of Held, giving fast and secure activation of the neurones. They project to the superior olivary complex via the ventral, binaural sound localization, stream.
4. In the posteroventral cochlear nucleus, as well as globular bushy cells, there are octopus cells, which have broad tuning curves and fast temporal responses. Octopus cells can follow the temporal variations in broadband stimuli up to high rates. The cells project via the dorsal predominantly sound identification pathway, primarily to the contralateral ventral nucleus of the lateral lemniscus. The posteroventral cochlear nucleus also contains stellate cells (also present in the anteroventral nucleus). Stellate cells (also known as multipolar cells) are of two types, the more numerous T-stellate cells and the less numerous D-stellate cells. T-stellate cells project bilaterally to the inferior colliculus and to the ventral nucleus of the lateral lemniscus as well as to the cochlear nucleus and superior olive. D-stellate cells send inhibitory collaterals widely within the cochlear nuclei.
5. The dorsal cochlear nucleus has multiple cell types, the major output cells being the fusiform cells. Cells of the dorsal nucleus tend to have very complex tuning curves, strong bands of inhibition and non-monotonic rate-intensity functions. Cells of the dorsal nucleus, as well as projecting within the nucleus, project via the dorsal stream which is predominantly involved in sound identification to the contralateral inferior colliculus. Some of the cells of the dorsal nucleus respond well to spectral notches and may be involved in judging the elevation of sound sources based on spectral cues introduced by the pinna. Many cells in the cochlear nucleus emphasize spectral contrast and temporal fluctuations in the stimulus.
6. The superior olivary complex receives an input from the anteroventral and posteroventral cochlear nuclei. The superior olivary complex has several

component nuclei. The largest component nucleus, the lateral superior olive (LSO), receives an input from both sides, the ipsilateral input being excitatory and the contralateral input inhibitory, via a synapse in the medial nucleus of the trapezoid body. The nucleus is therefore responsive to differences in interaural sound intensity. It is mainly a high-frequency nucleus and uses the differences in interaural sound intensity and time of arrival of transients in the stimulus to code the direction of mainly high-frequency sound sources, being most strongly driven by sound sources on the ipsilateral side of the head. Another component nucleus, the medial superior olive, is mainly a low-frequency nucleus. It is responsive to differences in interaural timing and uses these to code the direction of low-frequency sound sources in space, being most strongly driven by sound sources on the contralateral side of the head.

7. The projections from the superior olfactory complex, and some of the projections from the cochlear nucleus, travel to the inferior colliculus in the tract known as the lateral lemniscus. Some of the fibres in the tract synapse in the dorsal and ventral nuclei of the lateral lemniscus. The ventral nucleus of the lateral lemniscus (VNLL) is part of the sound identification stream. Its anatomical structure has a complex patchiness which suggests that it contributes complex cross-frequency interactions to the inferior colliculus. The dorsal nucleus of the lateral lemniscus (DNLL) is part of the sound localization stream and enhances the lateralization of stimuli in the auditory system. The fibres within the lateral lemniscus and from the VNLL and DNLL project to the inferior colliculus in such a way that neurones in the colliculus, and in all stages in the auditory system thereafter, predominantly represent sound sources on the contralateral side of the head.
8. The inferior colliculus marks a jump in the complexity of the responses. Here, the results of the different analyses that were undertaken in separate streams at the lower levels of the auditory system are combined to give responses that begin to define an auditory object. The inferior colliculus has three main divisions, namely a central nucleus (the specific, core or lemniscal auditory relay) and two non-specific, diffuse, belt or extra-lemniscal nuclei, called the dorsal cortex and external nucleus. The central nucleus has a pronounced laminar structure, with the lamina corresponding to isofrequency planes, otherwise known as frequency-band laminae. The nucleus receives a multiplicity of excitatory and inhibitory inputs from the lower auditory nuclei. A great variety of response types are seen in the central nucleus, with some very sharp and some very wide tuning curves. Many cells show enhanced responses to temporal fluctuations, and most neurones are responsive to the location of sound sources. There is evidence that some of these properties are distributed differentially and in patches across each frequency-band lamina. Neurones in the less specific dorsal cortex and external nucleus are often broadly tuned and tend to habituate rapidly. Neurones in the dorsal cortex show a particularly strong response to novel stimuli, and so may have a role in processing novel stimuli. Neurones in the external nucleus commonly respond to the directions of sound sources and often have multimodal responses (e.g. to auditory and somatosensory stimuli).

The external nucleus is therefore likely to be an auditory and somatosensory integrative area, governing among other things spatial reflex responses to sound.

9. The medial geniculate body is the specific thalamic relay of the auditory system, receiving afferents from the inferior colliculus and projecting to the auditory cortex. It has three divisions, namely the ventral, dorsal and medial divisions. The ventral division is the specific, core or lemniscal auditory relay and projects to the primary auditory cortex. It has a laminar structure, where individual adjacent laminae are likely to be organized together into functional units called 'slabs'. The ventral division further sharpens frequency resolution and in species with auditory specializations performs further analyses related to those specializations. It also has heavy reciprocal connections with the auditory cortex and must be seen as a functional unit with the cortex. The medial and dorsal divisions of the medial geniculate body form part of the non-specific, diffuse, belt or extra-lemniscal auditory system. They project widely to the areas of cortex surrounding the primary auditory cortex. They have multimodal interactions (i.e. visual and somatosensory as well as auditory responses) and have responses that are modifiable as a result of learning. The dorsal division in particular seems to be involved in the response to novel stimuli. The medial division has a close association with the amygdala, and is likely to be involved in the learning of responses to fear-evoking stimuli.
10. Brainstem auditory reflexes include (i) the middle ear muscle reflex, which involves a reflex arc of two to four neurones, starting at the cochlear nucleus and going to the motor nuclei of the facial and trigeminal nerves, either directly or via the superior olive; (ii) acoustic startle, which is a reflexive contraction of the muscles of the head and neck and which uses a projection from the ventral cochlear nucleus to a nucleus in the reticular formation, the nucleus reticularis pontis caudalis; (iii) reflexive orientation to auditory stimuli, which involves the external nucleus of the inferior colliculus and the superior colliculus; (iv) audiogenic seizures which depend on the inferior colliculus, especially its external nucleus and dorsal cortex. The seizures arise from a hypersensitivity of the auditory system, probably in these nuclei, that develops in certain susceptible strains of animals in response to early auditory deprivation.

6.9 FURTHER READING

Volumes in the Springer Handbook of Auditory Research (Pub. Springer: series editors R.R. Fay and A.N. Popper) deal with the auditory subcortical areas. The older literature was reviewed in Vols. 1 and 2 ('The Mammalian Auditory Pathway: Neuroanatomy', 1992, and 'The Mammalian Auditory Pathway: Neurophysiology', 1991). Further reviews are found in several chapters of Vol. 15 'Integrative Functions of the Mammalian Auditory Pathway' (2002; eds D.

Oertel, R.R. Fay and A.N. Popper) and Vol. 23 ‘Plasticity of the Auditory System’ (2004; eds T.N. Parks, E.W. Rubel, R.R. Fay and A.N. Popper). Volume 41 ‘Synaptic mechanisms in the Auditory System’ (2011; eds L.O. Trussell and A.N. Popper) also has many chapters relevant to this chapter.

The auditory nerve and its inputs to the cochlear nucleus have been more recently reviewed by Nayagam *et al.* (2011). The cell types of the nucleus have been reviewed by Oertel and Young (2004), and the inputs to the different cells of the ventral cochlear nucleus have been usefully reviewed by Cao and Oertel (2010) and Oertel *et al.* (2011). The superior olive was reviewed by Schwartz (1992). The role of the olfactory nuclei in sound localization has been reviewed by Grothe *et al.* (2010) and Grothe and Koch (2011). The DNLL was reviewed by Kelly (1997). ‘The Inferior Colliculus’ (2005; eds J.A. Winer and C.E. Schreiner) has many valuable chapters not only on the inferior colliculus but also on its relation with the rest of the auditory brainstem. The inferior colliculus was also reviewed by Casseday *et al.* (2002), and spectral processing in the colliculus by Davis (2005). The medial geniculate body was reviewed by Winer *et al.* (2005), and its role in fear conditioning by Weinberger (2011). For a general review of the processing of amplitude-modulated stimuli in the auditory brainstem, see Joris *et al.* (2004), and for a general review of the processing of communication calls, see Suta *et al.* (2008).

The middle ear muscle reflex was reviewed by Mukerji *et al.* (2010). Acoustic startle has been reviewed by Koch (1999) and Davis *et al.* (2008), and the prepulse inhibition of startle by Fendt *et al.* (2001). Orientation to auditory stimuli was reviewed by Maier and Groh (2009). The brain mechanisms underlying audiogenic seizures were reviewed by Ross and Coleman (2000).

THE AUDITORY CORTEX

The auditory cortex consists of core areas, surrounded by belt and parabelt areas. Auditory stimuli are analysed first in the core areas and then in the belt and the parabelt areas. The core areas and some of the surrounding areas are tonotopically organized, with further patterns of organization (e.g. ear dominance, latency and degree of sensitivity to frequency-modulated stimuli) superimposed on the tonotopic organization. Cells in the auditory cortex can show a wide variety of tuning curves, with either broad or narrow tuning, and single or multiple peaks of frequency sensitivity. They can show specific responses to amplitude and frequency-modulated stimuli and to the location of sound sources. Neurones show a general progressive increase in complexity of responses from the core to the belt. Behavioural studies suggest that the core auditory cortex is necessary for the response to relatively basic features of the auditory stimulus, such as detecting the direction of frequency change, and for sound localization, while the belt and parabelt areas detect more complex features. It is suggested that the auditory cortex is necessary for the representation of ‘auditory objects’, that is the assembly of information about all auditory features of a stimulus, including its location. It has been speculated that in primates the information is then divided into two general streams, with ‘what’ information being passed anteriorly in the cerebral cortex and with both ‘what’ and ‘where’ information being passed posteriorly and dorsally.



7.1 ORGANIZATION

7.1.1 Anatomy and projections

The auditory areas of the cerebral cortex are divided into core areas, with further surrounding areas. The initial detailed analysis of the auditory cortex was performed in the cat. This was undertaken in accordance with the concepts prevailing at the time, which included a single primary receiving area (AI), plus an adjacent secondary area (AII) and further surrounding ‘association’ areas. However, later analysis in the cat and in particular the extension of the analysis to a wider range of species including primates has led to a reassessment of this approach. The specific receiving area, which receives its input from the specific or ‘lemniscal’ ventral division of the medial geniculate body, is now known to contain many areas and is now called the core, while there are multiple adjacent areas, called the

belt, and further areas surrounding those, called the parabelt. In many mammalian species, there are believed to be three separate areas with the characteristics of core auditory cortex, and up to eight separate auditory areas in the adjacent belt, with further areas in the parabelt. These multiple cortical representations are thought to contribute to parallel processing of the auditory stimulus, with the different areas preferentially processing selected aspects of the auditory input.

7.1.1.1 Core areas

Core areas of the auditory cortex are defined by a number of criteria. Firstly, the areas can be defined by histological criteria. The cytoarchitectonic appearance of the cortex, determined with Nissl staining which marks the cell bodies and proximal dendrites, shows that the core auditory cortex has the same appearance as the primary sensory cortex for other modalities. Cortex with this appearance is known as 'koniocortex' ('dustcortex'), defined as having a large number of small cells with relatively even packing. Layer IV, which receives the afferent axons, is well developed, while there are no large pyramidal cells, normally the large output cells, in the deepest, output layers. Core sensory cortices also are marked by certain common histochemical characteristics such as a dense reaction for the metabolic enzyme cytochrome oxidase, a dense reaction for the enzyme that deactivates the neurotransmitter acetylcholine (acetylcholinesterase) and a dense reaction for the calcium-binding protein parvalbumin (see [Kaas and Hackett, 2000](#)).

Secondly, the core areas have substantial direct inputs from the specific auditory division of the medial geniculate body, that is from the ventral or 'lemniscal' division. In contrast, the belt or adjacent areas have few or no connections with the specific ventral division, but receive their major inputs from the core auditory areas. They also receive inputs from the non-specific medial and dorsal divisions of the medial geniculate ([Winer, 1992](#); [Kaas and Hackett, 2000](#)).

Thirdly, each core area shows a tonotopic organization. A single area is defined as having a single progression of neural characteristic frequencies across the cortical area, from high frequencies to low, or vice versa. Therefore, a progression of characteristic frequencies across an area of cortex that goes from low to high and to low again, in other words, that includes a frequency reversal, can be taken as a good indication that the area in fact contains two cortical areas, one for each frequency progression.

The core areas are heavily interconnected by reciprocal connections, and this forms a further criterion by which they are grouped together.

In terms of its cytoarchitecture, core auditory cortex shares some properties with other primary sensory cortex, with six layers and a high density of pyramidal and granule cells in layers II, III and IV, but with sparse staining in layer V ([Rose, 1949](#); see also review by [Winer, 1992](#)). In layers II–IV, the cortical cells are organized in vertical columns, separated by zones of dendrites and axons and situated around the periphery of small vertical cylinders 50–60 µm in diameter which are oriented orthogonal to the cortical surface. The columnar arrangement is also visible in human beings, where the cell bodies appear in what have been

called a ‘rain-shower’ formation (von Economo and Koskinas, 1925; Moore and Guan, 2001). The main cells receiving the thalamo-cortical inputs are pyramidal cells in layers III and IV (Smith and Populin, 2001). This is in contrast with visual cortex, where the main receiving cells are spiny stellate cells. Overall, 25% of the neurones in primary cortex are GABAergic and therefore inhibitory; this proportion rises to 94% for neurones within layer I (Prieto *et al.*, 1994). Axons and dendrites within AI have substantial patchy lateral ramifications that run across as well as along the frequency-band strips (Matsubara and Phillips, 1988). There is also a particularly rich ramification vertically within each column of cells. Callosal afferents, from the contralateral cortex, similarly ramify vertically within ‘callosal columns’, that is within columns of cells having a particularly rich callosal innervation (Code and Winer, 1986).

There are reciprocal connections between the cortical areas and the medial geniculate body, such that cortical activation enhances activity in the region that projects to that area of the cortex and suppresses activity in adjacent areas of the cortex (Zhang and Suga, 1997). The corticofugal fibres also form a way that activity can be transmitted from core cortical areas to other areas (for review, see Smith and Spirou, 2002).

Figures 7.1 and 7.2 show the auditory cortical areas in the cat and macaque. In the cat, areas currently classed as core by the above criteria are the traditional primary auditory cortex AI, the anterior auditory field AAF and the posterior auditory field PAF (Reale and Imig, 1980). In the macaque, the areas most commonly classed as core are the auditory area 1 (AI), the rostral area (R) and the rostrotemporal area (RT). As well as projecting heavily to each other, the core areas project to the adjacent belt areas, but without connections to the more distant auditory fields. The belt areas therefore form an obligatory stage in the output from the core.

7.1.1.2 The belt and parabelt

The belt areas are adjacent to the core. Belt areas are defined by the following criteria: (i) major connections with the dorsal or medial divisions of the medial geniculate, (ii) no or only minor connections with the ventral division of the medial geniculate and (iii) having recordable auditory responses. Each belt area receives inputs from multiple core areas, though with a heavier input from the nearest core area. Therefore, we expect each belt area to have its own separate representation of the cochlea. This is borne out functionally in the macaque, where four of the belt areas have their own frequency progressions (Fig. 7.2E).

The macaque parabelt consists of two areas, the rostral and caudal parabelt areas, lateral to the belt. While the core and belt are buried in the lateral sulcus, the parabelt is visible on the lateral surface of the superior temporal gyrus (Fig. 7.2B). The parabelt is defined as an area where injections of tracers give heavy labelling of neurones in the belt, but little in the core itself (Hackett *et al.*, 1998). It is divided into rostral and caudal halves on the basis of heavier connections of each part with the more rostral and caudal divisions of the belt. Figure 7.3 shows the suggested

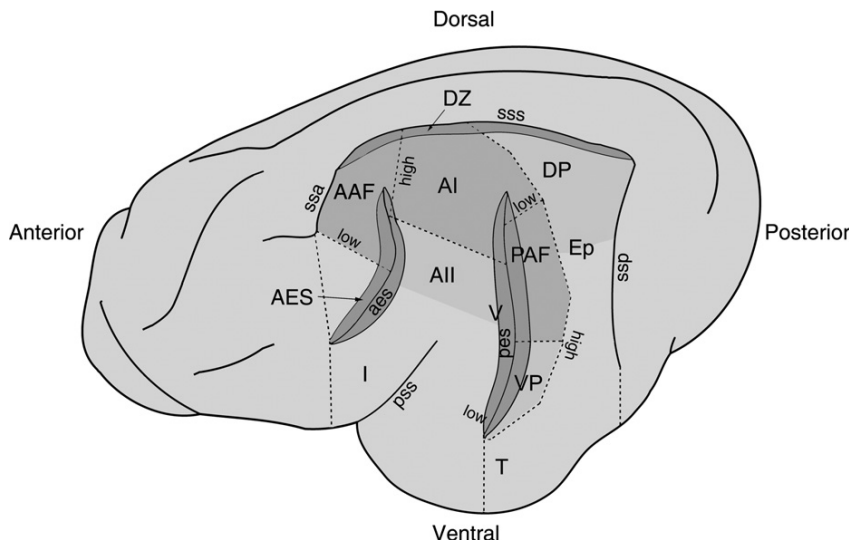


Fig. 7.1 Auditory areas recognized in the cat cortex. Core areas: AI, AAF and PAF. Other areas are belt, surrounded by parabelt. Where the fields are tonotopically organized (AI, AAF, PAF and VP), the representation of highest frequencies (high) and lowest frequencies (low) are marked. Areas shaded darker are hidden in the sulci, which have been opened slightly to show the fields within the sulci. AI, primary auditory cortex; AII, secondary auditory cortex; AAF, anterior auditory field; AES, field of anterior ectosylvian sulcus (buried in sulcus); DP, dorsal posterior area; DZ, dorsal zone, buried on the ventral (lower) surface of the suprasylvian sulcus; Ep, posterior ectosylvian gyrus; I, insula; PAF, posterior auditory field; Sulci, aes and pes, anterior and posterior ectosylvian sulci; pss, pseudosylvian sulcus; ssa and ssp, anterior and posterior suprasylvian sulci; sss, suprasylvian sulcus; T, temporal area; V, ventral field; VP, ventral posterior field. Adapted from Reale and Imig (1980), Fig. 1, including data from Clarey and Irvine (1990).

interconnections of the core, belt and parabelt areas in the macaque. The parabelt also connects to several areas of the frontal lobes, including the frontal eye field, which is involved in directing eye movements.

The callosal afferents connect corresponding areas of core, belt and parabelt cortices on the two sides of the brain. There is relatively little crossover between the different types of cortical area, and this forms an additional criterion by which the areas can be distinguished (Hackett *et al.*, 1999).

7.1.1.3 The human auditory cortex

The position in human beings is less certain, in view of the difficulty of obtaining detailed functional information about sound representation in the human auditory cortex and the substantial variability from one individual to another. Anatomical

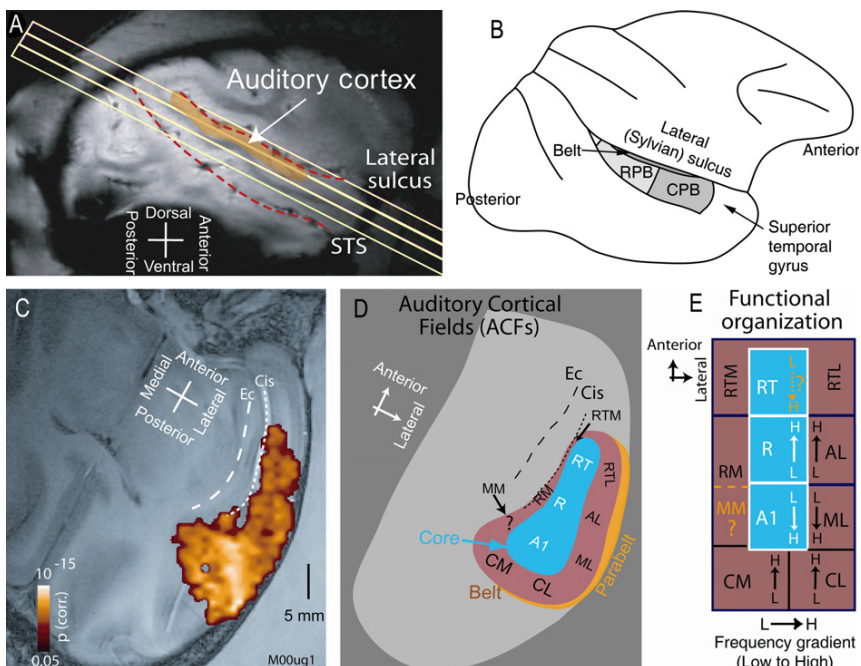


Fig. 7.2 Areas of the monkey (macaque) right auditory cortex as shown by functional magnetic resonance imaging (fMRI). fMRI uses the response to changes in intense magnetic fields to detect activity-related changes in the oxygen depletion of blood. (A) Side view of cortex, showing the planes, through the lower edge of the lateral sulcus, over which images were taken. (B) Diagrammatic representation of the macaque cortex from the same point of view as in part A. The rostral and caudal parabelt areas (RPB, CPB) are shown on the surface of the superior temporal gyrus. (C) Response to broadband noise in one animal. (D) The three core auditory areas (R, RT, A1) are surrounded by eight belt areas. (E) Tonotopicity of the three core areas and four of the belt areas, shown by representation of high (H) and low (L) frequencies. A1, primary auditory area; AL, anterolateral area; Cis, circular sulcus; CL, caudolateral area; CM, caudomedian area; CPB, caudal parabelt; Ec, external capsule; ML, middle lateral area; MM, middle medial area; R, rostral area; RM, rostromedial area; RPB, rostral parabelt; RT, rostrotemporal area; RTL, lateral rostrotemporal area; RTM, medial rostrotemporal area; STS, superior temporal sulcus. Figure 7.2A, C–E from Petkov *et al.* (2006), Fig. 2. See Plate 1.

studies have therefore been essential for the precise delimitation of the different functional areas.

The auditory cortex is situated on the upper surface of the temporal lobe, on an area known as the superior temporal plane, which is buried within the lateral or Sylvian sulcus or fissure (Fig. 7.4). Because of the depth of the sulcus, and the deep infoldings of the area, the extent of the auditory cortex cannot be appreciated from

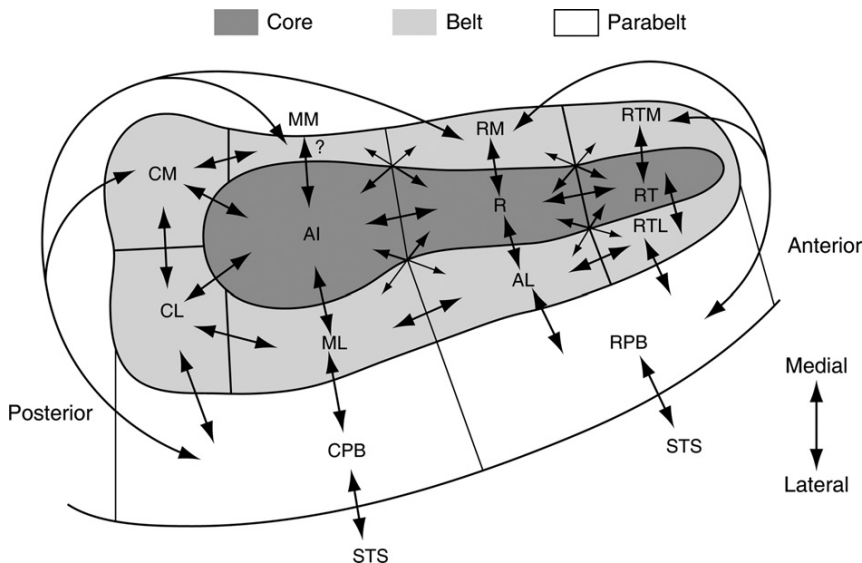


Fig. 7.3 Interconnections of the core, belt and parabelt areas in the macaque, shown on a projection of the upper surface of the superior temporal lobe, according to Hackett *et al.* (1998). AL, anterolateral area; CL, caudolateral area; CM, caudomedian area; ML, middle lateral area; MM, middle medial area; R, rostral area; RM, rostremedial area; RPB, rostral parabelt; RTL, lateral rostrotemporal area; RTM, medial rostrotemporal area. From Hackett *et al.* (1998), Fig. 11.

external views. Figure 7.4B shows a surface view of the superior temporal plane once the overlying cortex has been removed and shows a top view of the deep infoldings of the cortical surface on the plane. The primary auditory cortex or core area is situated in the posterior-medial part of Heschl's gyrus, corresponding to Brodmann's area 41 (Brodmann, 1909). The primary cortex is surrounded by several belt and parabelt areas, most of which are also buried within the sulcus. Figure 7.4C shows a vertical transverse (i.e. coronal) section through the superior temporal plane, and shows the core, belt and parabelt areas of the auditory cortex extending over Heschl's gyrus and then laterally over the superior temporal plane to the superior temporal gyrus (see also Fig. 7.4D and E).

The anatomical criteria for the core are the presence of koniocortex and the pattern of cytochrome oxidase and acetylcholinesterase staining. Using Nissl stain, Galaburda and Sanides (1980) identified two distinct divisions within the koniocortex, which they called KAm (medial auditory koniocortex) and KA_{lt} (lateral auditory koniocortex), both of which are likely to be core (Fig. 7.4E). Dense cytochrome oxidase and acetylcholinesterase staining define a similar core area (Rivier and Clarke, 1997; Wallace *et al.*, 2002a; Sweet *et al.*, 2005). More detailed cytoarchitectural analyses have further divided medial koniocortex KAm into three sub-areas (Fullerton and Pandya, 2007).

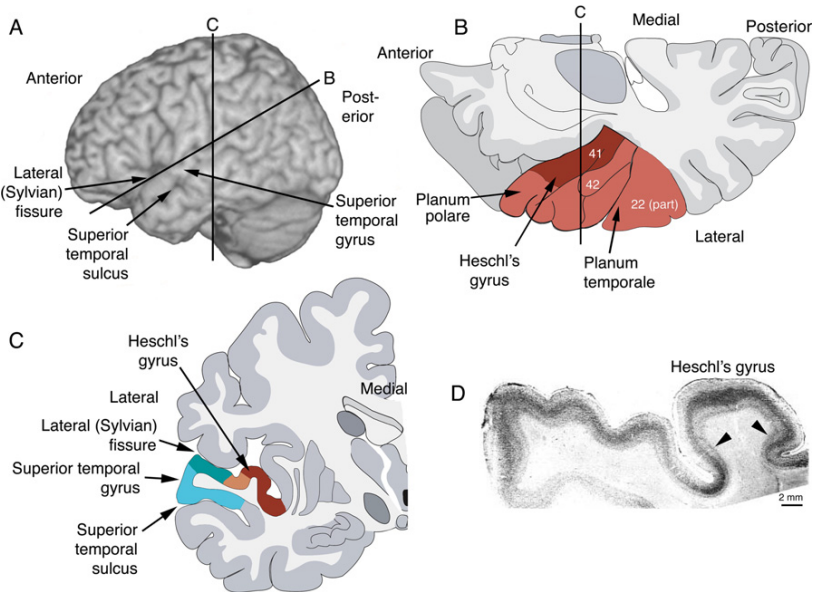


Fig. 7.4 The human auditory cortex (left hemisphere) (see also Plate 2). (A) Lateral view of left cerebral hemisphere, showing planes of section in parts B and C. (B) Sloping section in the plane shown in part A. Top view of upper surface of temporal lobe (shaded) with area of koniocortex within Heschl's gyrus marked (darker grey). The division of the surface anterior to Heschl's gyrus is known as the planum polare, and the large division posterior to Heschl's gyrus is known as the planum temporale. Numbers show areas according to Brodmann (1909). In some individuals, Heschl's gyrus divides into two. (C) Transverse section of left cerebral hemisphere in the vertical plane shown in part A, showing Heschl's gyrus (darker grey) and further auditory cortex of the superior temporal plane (shaded). Exactly how the latter areas are distributed over the superior temporal gyrus and sulcus varies between individuals. (D) Transverse histological section as in part C, showing Heschl's gyrus and laterally adjacent parts of the superior temporal plane. Arrowheads: borders of AI. Nissl stain. (E) Cytoarchitectonic areas of the human auditory cortex according to Galaburda and Sanides (1980). The dotted line (S) shows the position of the Sylvian sulcus: the cortical surface lateral to this line curves down over the external surface of the temporal lobe, over the superior temporal gyrus. The area corresponds to shaded area in part B but extending slightly more anteriorly and further laterally over the superior temporal gyrus. Numbers show areas according to Brodmann (1909). (F) Tonotopic frequency progressions in the cortex, according to Langers and van Dijk (2012), superimposed on the cytoarchitectonic areas of Galaburda and Sanides. The arrows mark the direction of the progressions from low frequencies to high. The heavy dotted line marks the line of frequency reversal along the crest of Heschl's gyrus. Because of variation in positions of gyri and sulci from individual to individual, it is not possible to definitively align the fMRI data precisely with the cytoarchitectonic data. KAlt, lateral koniocortex; KAm, medial koniocortex; PaAc/d: caudo-dorsal parakoniocortex; PaAe, external parakoniocortex; PaAi, internal parakoniocortex; PaAr, rostral parakoniocortex; ProA, prokoniocortex; S, Sylvian (lateral) sulcus or fissure; Tpt, temporoparietal area. Figure 7.4B and C from Harasty *et al.* (2003), Fig. 1; Figure 7.4D from Wallace *et al.* (2002a), Fig. 1A, with kind permission from Springer Science and Business Media; Figure 7.4E used with permission from Talavage *et al.* (2004), Fig. 7. See Plate 2.

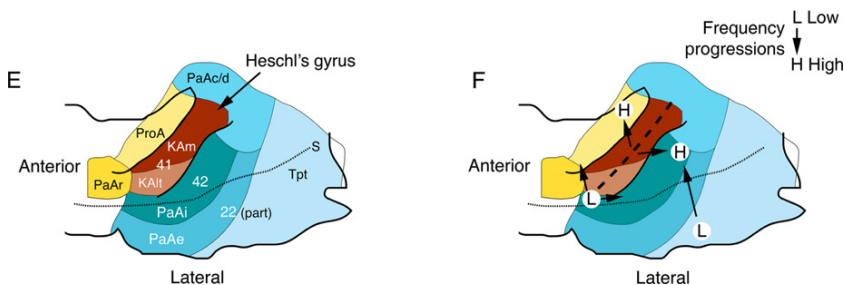


Fig. 7.4 Continued.

Galaburda and Sanides described five further cytoarchitecturally distinct fields in the surrounding cortex which were related to koniocortex, though they were distinguishable from each other in various ways (e.g. by bulkier pyramidal cells in layer III). These are therefore included with the auditory cortex, but are identified as belt and parabelt (Fig. 7.4E; see also Sweet *et al.*, 2005). In addition, in the scheme of Fullerton and Pandya (2007), the medial belt areas (called 'root') are distinguished from the lateral belt areas because of different cytoarchitectonic properties (see also Galaburda and Pandya, 1983). There is a further area situated more caudally (the temporoparietal area Tpt) which has properties more similar to association cortex than to sensory cortex. Cytochrome oxidase and acetylcholinesterase staining can also be used to define the five to seven belt areas surrounding the core (Rivier and Clarke, 1997; Wallace *et al.*, 2002a; Sweet *et al.*, 2005).

Functional magnetic resonance imaging (fMRI) confirms the presence of auditory responses on the superior surface of the temporal lobe. Distinct frequency progressions have been critical for defining core and many of the belt areas in other primates. Similarly, multiple and separate frequency progressions have been found in human beings. However because of the limited spatial resolution of the fMRI, and the closeness of the different frequency progressions, it has been difficult to use these to provide definitive evidence on the separate sub-areas. The more recent studies show three separate frequency progressions, with a frequency reversal at the centre of Heschl's gyrus. Two fields are therefore centred on Heschl's gyrus, with low frequencies represented along the centre of the ridge of the gyrus, and separate progressions towards higher frequencies on the two sides. The more caudal and lateral of these progressions lies substantially within lateral koniocortex KAlt, and is likely to correspond to AI. The more rostral and medial of these progressions lies substantially within medial koniocortex KAm, and is likely to correspond to the rostral (R) field of other primates. A further progression is found more posteriorly on the planum temporale (Fig. 7.4F; Langers and van Dijk, 2012). There are further areas with auditory responses but which do not give rise to frequency progressions. These include the greater part of PaAe and PaAc/d (see Fig. 7.4E). Therefore, these areas are probably not tonotopically organized, and it is not possible to use this criterion to say whether they are separate auditory areas, although the cytoarchitecture would suggest that they are.

7.1.2 Tonotopic organization

If the cortical surface of AI is sampled with a microelectrode, and the best or characteristic frequencies of the cells plotted as a function of distance across the cortex, a progression of characteristic frequency with position is found (Fig. 7.5A). Figure 7.5A shows data points obtained along five parallel lines of sampling across the cortex in the cat. All data points follow the same function, showing that there is a similar frequency progression along each of the five lines. If the data for AI are plotted in two dimensions, a map of frequency representation is obtained for the cortical surface (e.g. as in Fig. 7.5B). Figure 7.5B shows a frequency progression across the cortex and approximately at right angles to that progression it shows frequency-band strips or iso-frequency lines, along which the best frequency stays constant.

In human beings, similar maps can be obtained by fMRI, although at a lower resolution. Fig. 7.4F shows three separate frequency progressions, and Fig. 7.5C shows the progressions in more detail, by way of iso-frequency contours. In this experiment, the frequencies ran from 0.25 kHz (L) to 8 kHz (H) (Langers and van Dijk, 2012). Low frequencies are represented on the crest of Heschl's gyrus (white line, and white arrow), and higher frequencies are represented on either side. The finding of low frequencies being represented along the crest of Heschl's gyrus, with higher frequencies on either side, has also been found in another investigation (Da Costa *et al.*, 2011). The rostral progression (R) in Fig. 7.5C is likely to correspond to the primate R field, and the caudal progression (C) to AI. The third progression in Fig. 7.5C (starting at the L on the extreme lower right of the sub-figure) lies in the planum temporale (P), and coincides with the macaque caudal areas CL and CM.

In summary, the map of frequency undergoes a series of transformations up the auditory pathway. A sound of one frequency is represented by a single point in the cochlea, by one- or more two-dimensional sheets of cells in each of the intervening auditory nuclei, and by a one-dimensional strip of cells on the surface of each of the tonotopically organized fields in the cortex, with multiple representations in the different fields.

7.1.3 Organization along the frequency-band strips

The visual cortex in primates contains functional modules that are repeated across the surface of the cortex, representing line orientation, eye of stimulation and colour, within the overall spatiotopic representation of the visual field. Within each module, there is a columnar organization, such that all cells in one column have related properties. These findings led to a search for analogous functional modules within the auditory cortex, superimposed on the tonotopic representation of frequency. Such an organization has been found, although the situation is not as distinct as in the visual cortex, and the relations between the different functional components are not as clear.

Imig and Adrian (1977) showed that in cat AI, cells that are excited by stimuli in one ear but inhibited by stimuli in the other (EI or IE cells) were located in discrete areas of the cortex. They were separate from cells excited by stimuli in

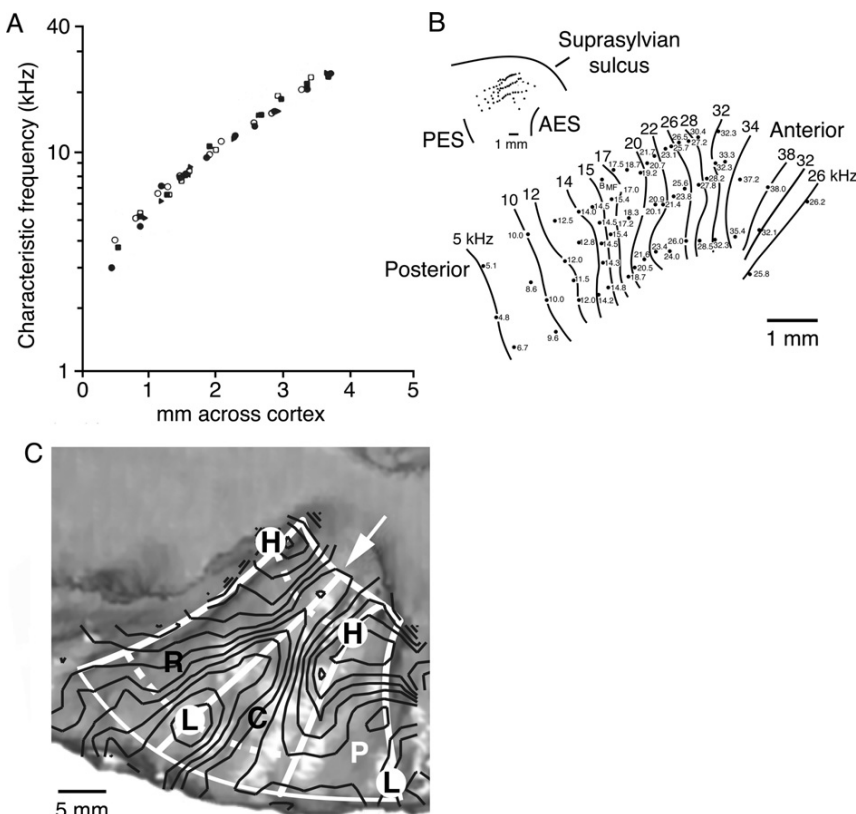


Fig. 7.5 Tonotopic organization within the cortex. (A) Best frequencies of neurones in a cat's auditory cortex are plotted as a function of distance across the cortex. The neurones were located on five parallel lines across the cortex, and different symbols are used for each line. Used with permission from Merzenich *et al.* (1975), Fig. 6. (B) Frequency-band strips in a cat's auditory cortex, interpolated from the characteristic frequencies of neurones measured in multiple recording sites (see insert for position on the cat's cortex). Numbers on curves, frequency in kHz. AES, anterior ectosylvian sulcus; PES, posterior ectosylvian sulcus. From Rajan *et al.* (1993), Fig. 1A. (C) Iso-frequency contours in the human left auditory cortex, aligned as in Fig. 7.4E and F, according to Langers and van Dijk (2012). The iso-frequency contours are spaced logarithmically from 0.25 kHz (L) to 8 kHz (H). Low frequencies are primarily represented rostrally and laterally on Heschl's gyrus, with high frequencies more medially and caudally. A ridge of low-frequency representation runs along the centre of the crest of Heschl's gyrus (arrow and white line). The frequency progression rostral to the centre of Heschl's gyrus (R) is likely to correspond to field R of the macaque (Fig. 7.2), and the field caudal to it (C) to AI. A further more caudal frequency progression on the planum temporale (P) is likely to correspond to the macaque fields CM and CL. From Langers and van Dijk (2012), Fig. 7A.

both ears (EE cells). Through the depth of the cortex, the different categories of cells were located in discrete radial columns, with cells in the same vertical alignment in the cortex tending to have the same spatial selectivity to binaural stimulation. In a surface view, the EI or EE cells are grouped into patches wandering over the surface of the cortex (Middlebrooks *et al.*, 1980; see also Razak, 2011, in a bat). This reflects a pattern of input from segregated zones within the medial geniculate body (Middlebrooks and Zook, 1983; Velenovsky *et al.*, 2003). There is also a close association between the electrophysiological responses and the callosal innervation, because those areas with EE responses have a particularly rich innervation from the contralateral auditory cortex via the corpus callosum (Imig and Brugge, 1978; see also Liu and Suga, 1997).

In AI, there are further multiple types of organization that are independent of the frequency-band strips, although the relation to the binaural groupings has not been explored (Fig. 7.6). While all cells tend to have a narrow bandwidth near threshold, in some cells the bandwidths expand enormously, to several octaves, well above threshold. Cells with broad suprathreshold bandwidths are segregated in patches from those with narrow bandwidths (e.g. Read *et al.*, 2002). In addition to variations measured well above threshold, there are also variations in the sharpness of tuning near threshold. Tuning measured in this way shows a spatial clustering in different regions of the cortex (e.g. as Fig. 7.6C for the squirrel monkey).

The spatial distribution of the patterns of tuning varies between species; in the cat, cells situated in the ventral division of AI have sharply tuned narrowband responses, while cells in the dorsal division have complex and multiband response areas. The results suggest that in the cat the central region of AI is involved in analysing narrowband sounds, while the dorsal division is responsible for analysing complex patterns across frequency (Sutter *et al.*, 1999).

The latency of response also varies across the cortex, gradually increasing along each frequency-band strip (shown in the squirrel monkey; Fig. 7.6B; Cheung *et al.*, 2001; see also Carrasco and Lomber, 2011 for the cat). Sensitivity to frequency modulation also shows organization along the frequency-band strips, cells having high sensitivity to frequency modulation tending to be segregated in groups, although with no clear spatial pattern (Heil *et al.*, 1992). It is possible to speculate how the different areas of cells within AI could be specialized for the detection of different aspects of the stimulus, although at the moment the exact details of the different groupings, their interrelation and their functional importance are not clear (see, e.g. Read *et al.*, 2002; Wallace and Palmer, 2009 and Bizley *et al.*, 2009).



7.2 THE RESPONSES OF SINGLE NEURONES

7.2.1 Responses in the core

Analysis of the auditory cortex is more difficult than that of lower auditory centres because anaesthesia, and particularly barbiturate anaesthesia, suppresses cortical

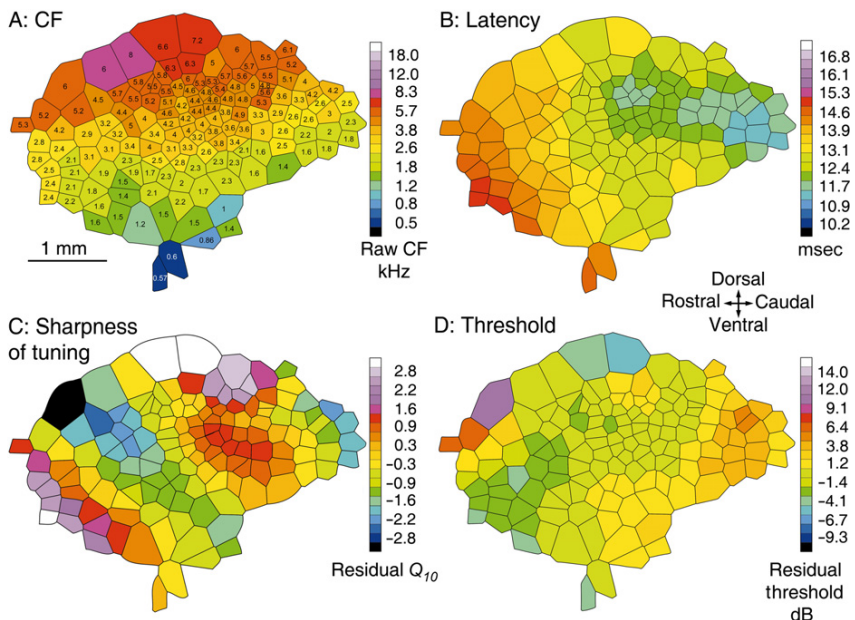


Fig. 7.6 Spatial variation in monaural response properties across the squirrel monkey primary auditory cortex (AI). Single unit and multiunit clusters were measured in many recording sites across the cortex. The characteristics of each recording site are shown within a polygon centred on the recording site. All parts of the figure show results from the same animal. (A) Tonotopic map: in this species, high frequencies are represented dorsally and low frequencies ventrally. Characteristic frequencies (CFs) are shown in kHz. (B) Latency gradient: rostral cells have shortest latencies and caudal cells longest. (C) Variation in sharpness of tuning: sharpness of tuning was determined near threshold. The ‘residual Q_{10} ’ is the variation from the mean Q_{10} for that frequency, measured over all cells at that frequency [Q_{10} : a measure of sharpness of tuning, defined as $(CF)/(bandwidth \text{ of } tuning \text{ curve measured } 10 \text{ dB above lowest threshold})$ see also Chapter 4]. (D) Gradient in thresholds: residual thresholds (threshold of area minus mean threshold of all cells at that CF), shows variation of thresholds in dB. In addition to the groupings shown here, we expect further groupings based on binaural dominance. In Fig. 7.6B–D, the values have been interpolated and smoothed to show trends in spite of the variability from area to area. Used with permission from Cheung *et al.* (2001), Figs. 1B, 5B, 11C and 8C.

responses. It reduces spontaneous activity and converts the sustained excitatory and inhibitory responses commonly seen in unanaesthetized animals to transient on or off responses with only a few action potentials per stimulus presentation. However, even in barbiturate-anaesthetized animals, the proportion of responsive neurones has been reported to be as high as 80–90% (e.g. Phillips and Irvine, 1981). In unanaesthetized animals, cells with many different patterns of response are seen in

AI, including many cells with sustained and transient responses, and also cells with only on, off or on-off responses, with the most preferred stimuli tending to give the more sustained responses (Abeles and Goldstein, 1972; Wang, 2007).

Most responsive neurones in AI have sharp tuning with a single frequency region of maximum sensitivity (e.g. Phillips and Irvine, 1981). In awake, unanaesthetized, marmosets, some neurones (27%) have very sharp tuning, much sharper than seen in the auditory nerve. The sharp tuning is particularly found in the sustained, rather than the onset, part of the response (Bartlett *et al.*, 2011). In addition, many neurones have two or more regions of maximum sensitivity, giving what are known as multipeaked responses (Fig. 7.7A and B). Multipeaked neurones consisted of 20% of the sample recorded by Kadia and Wang (2003) in the unanaesthetized marmoset; in many cases, the peaks were harmonically related to the cell's characteristic frequency (e.g. at twice characteristic frequency, or three times characteristic frequency). Multipeaked neurones are spatially segregated from single-peaked neurones, in the cat being found primarily in the dorsal rather than the central region of AI (Sutter and Schreiner, 1991; Schreiner *et al.*, 2000). Other neurones have very broad tuning curves, covering several octaves. In the cat, as in primates, broadly tuned neurones are spatially segregated from those showing sharp tuning.

As in other parts of the auditory system, neurones in AI can be inhibited by stimuli presented outside the excitatory response area, although this can be difficult to detect with single stimuli in cases where neurones have little or no spontaneous activity. In many cases, the inhibitory areas immediately surround the central

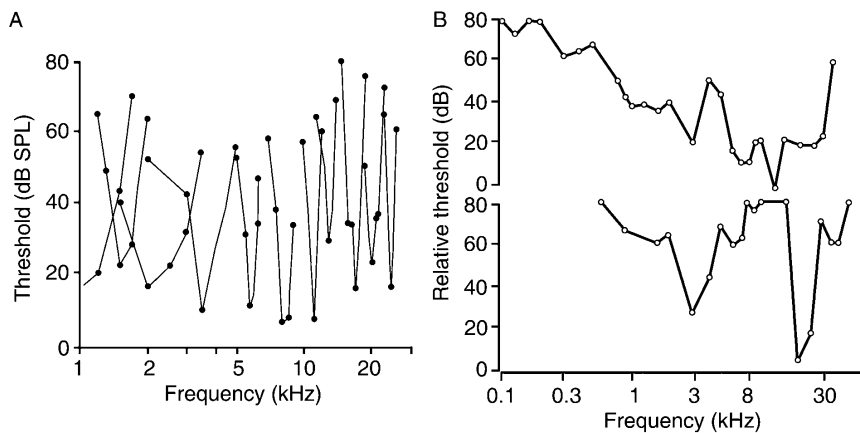


Fig. 7.7 (A) Tuning curves of single-peaked neurones in primary auditory cortex show a single frequency region of maximum sensitivity. Cat. Used with permission from Phillips and Irvine (1981), Fig. 2. (B) Broadly tuned neurones (top) and multi-peaked neurones (bottom) have a wide frequency range and can have two or more frequency regions of maximum sensitivity. Cat. From Onishi and Katsuki (1965), Fig. 1.

excitatory area. However in addition, a high proportion of cells can be inhibited by stimuli presented in one or more discrete frequency bands which are remote from the central excitatory or inhibitory area (Sutter *et al.*, 1999; Kadia and Wang, 2003). Some of the inhibition is generated within the cortex, since it can be reduced by the local application of the GABA blocker bicuculline, while anatomical studies have shown the presence of richly interconnected local inhibitory networks (Wang *et al.*, 2000; Yuan *et al.*, 2011). Some of the complex mechanisms and roles of inhibition in the auditory cortex have been reviewed by O'Connell *et al.* (2011) and Ojima (2011).

Cells in AI commonly show strongly non-monotonic responses, with the firing rate sometimes falling by 50% or more for deviations of stimulus intensity by 10 dB or so from the optimum (e.g. Sutter *et al.*, 1999). As in the subcortical auditory nuclei, non-monotonic responses are associated with inhibitory bands which overlap the excitatory area at higher stimulus intensities, and in multipeaked units, the degree of non-monotonicity can be different in the different response peaks. Cells can also be responsive to the location of the stimulus (see Section 7.3).

The cat anterior auditory field (AAF) (Fig. 7.1) is also classed as part of the core. Whereas AI receives most of its projections from the tonotopically organized ventral MGB, AAF receives a greater proportion of its input from the rostral pole of the MGB and from the non-tonotopic dorsal and medial divisions of the MGB (see Chapter 6). Nevertheless, the AAF is tonotopically organized, although compared with AI a greater proportion of the area is devoted to high frequencies (Imaiizumi *et al.*, 2004). Receptive field properties cluster into modules, but not as clearly as in AI. Compared with AI, neurones in cat AAF are more broadly tuned, have shorter latencies of response and are particularly responsive to tones with rapid frequency sweeps, in many cases being selective for the direction of the sweep (Tian and Rauschecker, 1994). No multipeaked neurones have been reported in AAF as they have been in AI. These results do not give a clear indication for a special function for AAF, although they suggest that it is involved in faster higher frequency processing than AI.

The posterior field PAF is the remaining part of the core in the cat. It receives projections from the tonotopic ventral nucleus of the medial geniculate body and in addition from some of the non-tonotopic divisions, including the dorsal cap and ventralateral divisions of the ventral nucleus, and subdivisions of the medial nucleus and the lateral part of the Po group of thalamic nuclei (Morel and Imig, 1987). The PAF is tonotopically organized, with the neural excitatory response areas having a wide variety of shapes, to include some multipeaked and some very broadly tuned neurones (Loftus and Sutter, 2001). Neurones commonly have inhibitory sidebands, usually flanking the excitatory response area on both sides, although compared with AI a greater proportion of cells have multiple inhibitory bands. The more complex inhibitory responses appear relatively slowly after a stimulus, suggesting that the neurones might be involved in the temporal and spectral integration of complex signals. Neurones in PAF are also sensitive to the location of sound sources, more so than neurones in AI, and are also particularly responsive to frequency modulation (Stecker *et al.*, 2003; Tian and Rauschecker, 1998). These results together do not give a single specific role for PAF in auditory

processing, except to suggest that it is involved in analysing the more complex aspects of the auditory stimulus including sound localization (see Section 7.3).

Relatively few comparisons of responses in the different core areas have been published in primates. Recanzone *et al.* (2000) found that neurones in the R core area of unanaesthetized and behaving macaque monkey were more sharply tuned to frequency, and more non-monotonic, than in AI. Similarly, spatial tuning is broader in AI, and other core areas, than in the caudal belt (Woods *et al.*, 2006; for reviews see Recanzone, 2011 and Recanzone *et al.*, 2011). There is a progression of processing on the macaque superior temporal plane, with responses to attended stimuli (bursts of white noise or monkey calls) evoking shortest latency responses in AI, and with longer latencies more anteriorly in the core (RT), and with still longer latencies in the areas of the parabelt situated more anteriorly in the superior temporal plane (Kikuchi *et al.*, 2010).

7.2.2 Responses in the belt

There are multiple separate areas in the belt, four of which are tonotopically organized in the macaque and one or possibly two in the cat (see Figs. 7.1 and 7.2). These areas have been incompletely investigated, and because of the large numbers of areas present and the many analyses possible, only a few examples will be given to illustrate the properties of the belt areas and the types of analyses that have been undertaken. In general, the responses suggest that, compared with the core, the belt areas have a particular role in the processing of the more complex aspects of the stimulus, such as decoding communication calls.

Responses from single cells or small clusters of cells in cat AII show that some regions of AII (dorsal and ventral strips) are tonotopically organized, although the organization is poor, with much variability of characteristic frequencies (CFs), including islands of low-frequency neurones, and with many of the neurones having wide bandwidths. Neuronal thresholds are 10–15 dB higher in AII than in AI (Schreiner and Cynader, 1984). While in AI binaural interactions show clear spatial patterns, in AII the spatial patterns of binaural interaction are more patchy and more variable from animal to animal.

This pattern may be compared with the cat dorsal zone (DZ), which borders AI dorsally on the ventral surface of the suprasylvian sulcus. DZ may in fact be part of AI, that is part of the core, rather than the belt. Here, Stecker *et al.* (2005) found that cells had complex frequency tuning with multiple excitatory and inhibitory domains, more so than in AI, with long response latencies and more non-monotonic rate-intensity functions. Many neurones had sharp spatial selectivity for azimuth (direction in the horizontal plane), probably associated with their generally high-frequency sensitivity and their complex frequency response areas. Neurones in this area are predominantly binaural, in that they respond well to binaural stimuli, but not at all to monaural ones. This may be contrasted with the position in AI, where binaurally sensitive neurones can in general also be stimulated by monaural sounds. These results suggest that DZ might have a role in the spatial representation of sounds.

Further areas that have been investigated are thought to be involved in sound localization and in the processing of complex stimuli. In the cat, this includes AES, which contains many partially overlapping visual and somatosensory as well as auditory fields (Clarey and Irvine, 1990). In the marmoset, neurones in the area known as CM have been found to be just as responsive to tones as are neurones in AI, though with lower thresholds, shorter response latencies and broader tuning curves (Kajikawa *et al.*, 2005). Neurones in the lateral belt areas (AL, ML and CL) are much less responsive to pure tones than are neurones in AI. However, they seem particularly responsive to frequency sweeps and are selective to both the rate and direction of the sweeps (Tian and Rauschecker, 2004). The maximal sensitivity of AL neurones was in the range of communication sounds, and it was suggested that AL was specialized for the decoding communication, while CL was specialized for localization.

Because most analyses of cortical function in the belt areas have been undertaken in the context of specific functions such as sound localization and the processing of complex stimuli, the further description of the belt areas will be continued in terms of those analyses.

7.3 CORTICAL PROCESSING OF SOUND LOCATION

7.3.1 Behavioural experiments

The importance of the auditory cortex for sound localization has been shown by many experiments that show deficits in localization after lesions of the auditory cortex. The initial experiments showed that after large bilateral lesions, cats were unable to localize sounds in space (e.g. Neff, 1968). Later experiments showed that unilateral lesions interfered with the localization of sounds in the contralateral hemifield of space. This suggests that, as expected, each cortex preferentially processes stimuli on the contralateral side.

Over the years, a variety of tasks have been used, and a variety of results have been found (for reviews, see Lomber *et al.*, 2007; King *et al.*, 2007; Malhotra and Lomber, 2007). The results of the experiments become clarified if three conditions are observed: (i) the sound signals are brief, possibly so that the subject cannot orient or explore within the sound field while the stimulus is sounding; (ii) there must be several speakers within the hemifield, so that the subject has to make a genuine choice of direction within the hemifield, rather than for instance making a simple left-right decision and (iii) the subject has to make a learned response to direction, rather than a simple reflexive orientation to the sound source (Thompson and Masterton, 1978; Jenkins and Masterton, 1982). These points suggest that the auditory cortex is necessary for the representation of auditory space.

Using the techniques described above, Jenkins and Merzenich (1984) showed that cats had profound deficits in sound localization after being given unilateral

lesions that were confined to AI. The deficits were confined to the hemifield contralateral to the lesion. Performance in the ipsilateral hemifield was unaffected, and if the stimuli bridged across the midline, performance also remained intact (Kavanagh and Kelly, 1987). Jenkins and Merzenich also showed that if the lesions were confined to a single frequency-band strip in AI, deficits in localization were found for tone pips of only the corresponding frequency. If the complementary experiment was performed, and a narrow frequency-band strip was left in AI while the rest of AI was removed, sound localization was possible only for the frequencies represented by the strip.

These results show that AI is essential for processing the location of sound sources and shows that it does so in a frequency-specific way. The critical involvement of further cortical areas has been shown by reversible cooling of specific cortical areas.

Malhotra and Lomber (2007) placed cooling probes over different cortical areas in the cat (see also Malhotra *et al.*, 2004). The cats were trained to approach 1 of 13 speakers situated in a semicircle around the animal, covering the full ipsilateral and contralateral hemifields. In addition to the effect of disrupting AI as described above (together with the dorsal zone DZ; Fig. 7.1), deficits in sound localization were found after unilateral cooling of a further area of the core, that is the posterior auditory field (PAF), or a field in the belt, the field of the anterior ectosylvian sulcus (AES). While the animals were still able to orient generally to the hemifield that contained the stimulus, they could not accurately locate the source of the stimulus. Cooling of any of these fields (AI/DZ, PAF or AES) on their own disrupted localization, indicating that they all need to be operating together for effective sound localization. On the other hand, cooling of the remaining area in the core, AAF, or any of the other fields in the belt, left sound localization unaffected, although cooling of AAF alone could affect sound pattern discrimination (Lomber and Malhotra, 2008). Varying the degree of cooling to affect different depths of cortex suggested that in A1/DZ and PAF only the superficial layers were critical, while in AES, the deepest layers had to be involved for a deficit to be found. In conjunction with the known anatomical connections, the results were interpreted to suggest that sound localization is first processed in AI/DZ and PAF. The information is then passed to AES, which transmits the information to the superior colliculus, where lesions have a yet more profound effect on orientation to auditory stimuli (Lomber *et al.*, 2007).

It has been difficult to obtain a clear picture in human beings because of the variability of the effects between patients. Spierer *et al.* (2009), analysing patients with a variety of lesions in the auditory cortex, found that lesions in the right hemisphere affected the localization of both contralateral and ipsilateral sound sources. The deficits were more profound and severe than those arising from left hemisphere lesions, which affected the localization only of contralateral sound sources. With right hemisphere lesions, both interaural timing and level cues tended to be affected together, suggesting that this hemisphere was dominant in spatial localization and had an integrative role in representing sound location.

7.3.2 Electrophysiological responses

7.3.2.1 Responses in AI

Electrophysiological experiments show that cells in the auditory cortex can be responsive to interaural intensity (i.e. interaural level) differences, as seen in lower stages of the auditory system (e.g. Fig. 6.16). According to [Irvine et al. \(1996\)](#), approximately 70% of cells in AI are responsive to differences in interaural intensity, and of those, approximately 70% are more strongly driven by stimuli in the contralateral ear. They therefore preferentially respond to sounds on the contralateral side of the head. In many cells, the functions relating interaural intensity difference to firing rate are steep, so the cells encode direction with great sensitivity to small changes in direction (for review, see [Clarey et al., 1992](#)). Cells with similar localizing properties are found close together in the cortex, and cells in the same column through the depth of the cortex localize sounds from the same direction in space ([Yuan and Shen, 2011](#), in the mouse).

Cortical responses show a greater degree of complexity in their responses than at lower levels of the auditory system, with a higher proportion of neurones having binaural responses, and a change from the almost exclusively contralateral responses seen in the inferior colliculus, to a greater variety of interactions. This presumably reflects processing in the medial geniculate body, as well as in the cortex itself.

[Figure 7.8A and B](#) show the responses of two typical high-frequency neurones in cat AI, to stimuli presented to the two ears, as a function of intensity difference between the ears. The horizontal axis shows the intensity difference, with zero in the centre and with more intense contralateral stimuli plotted on the right. The majority of cells in AI follow the form shown in [Fig. 7.8A](#), where greatest responses are produced when the contralateral stimulus is more intense than the ipsilateral one, and the response falls to near zero when the ipsilateral stimulus is more intense. [Fig. 7.8A](#) also shows the most common situation, in that the position and shape of the function vary with the mean overall intensity of the stimulus ([Irvine et al., 1996](#)). Such a cell would preferentially respond to sound sources on the contralateral side, although the representation of space will vary with the overall stimulus intensity. Binaural responses which are independent of overall stimulus intensity are seen in only a minority of neurones, such as shown in [Fig. 7.8B](#) (the actual proportion of neurones depends on the strictness of the criterion for invariance used, but can be taken to be approximately 15%).

Some of the factors underlying the different response types can be seen if the responses are plotted as a function of intensities in the ipsilateral and contralateral ears separately, rather than only as a function of difference between them. [Figure 7.8C](#) shows the response areas for 10 neurones in cat AI plotted in this way. All the neurones illustrated show non-monotonic intensity functions, common in auditory cortex, and hence have closed response areas when plotted in this way. In some neurones where the response area is approximately circular (e.g. the neurone labelled '1' in the figure), the response can most economically be described as depending on the coincidence of activity separately driven by the two

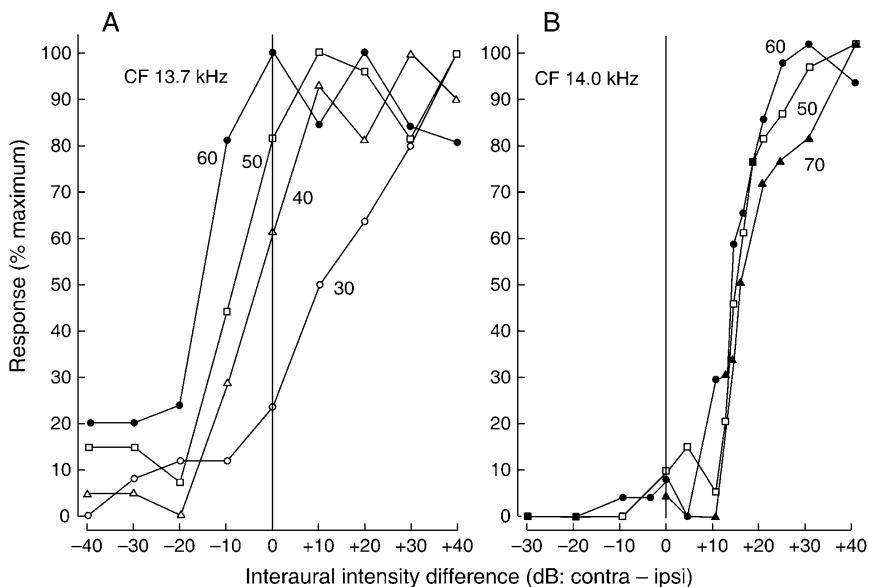


Fig. 7.8 (A, B) Firing rate of two cortical neurones in cat AI (plotted as % of maximum firing rate) in response to tone pips at the characteristic frequency presented to the two ears. The responses are shown as a function of intensity difference between the two ears. In each graph, more intense contralateral stimuli are plotted to the right. Part A shows the most common type of response, where the function varies with overall stimulus intensity; part B a less common type where the functions are relatively invariant. Used with permission from [Irvine et al. \(1996\)](#), Figs. 3D and 4D. (C) Increases in firing for 10 different cortical neurones in cat AI, plotted as a function of the intensities of the stimuli in both ipsilateral and contralateral ears. Combinations producing increases in firing that are >70% of maximum are shown in grey, >90% of maximum are shown in black. Most neurones are stimulated most strongly when the contralateral stimulus is more intense. ILD, interaural level difference. '1' and '2', neurones with different response patterns (see text). Used with permission from [Semple and Kitzes \(1993b\)](#), Fig. 10 modified.

ears, each of which has a similar non-monotonic intensity function. In other neurones (for instance, as marked '2'), where the response area is elongated in the direction of the diagonal line representing constant interaural intensity difference, the responses cannot be described in this way, and therefore reflect a more complex neural extraction of differences in interaural intensity ([Semple and Kitzes, 1993a,b](#); see also [Zhang et al., 2004](#) and [King et al., 2007](#)).

As in the lower stages of the auditory system, cells in AI can also be sensitive to interaural timing differences. Also as in the lower stages of the auditory system, cells show evidence of both inhibitory and excitatory interactions in their response to interaural timing differences, in that the response of both stimuli together when

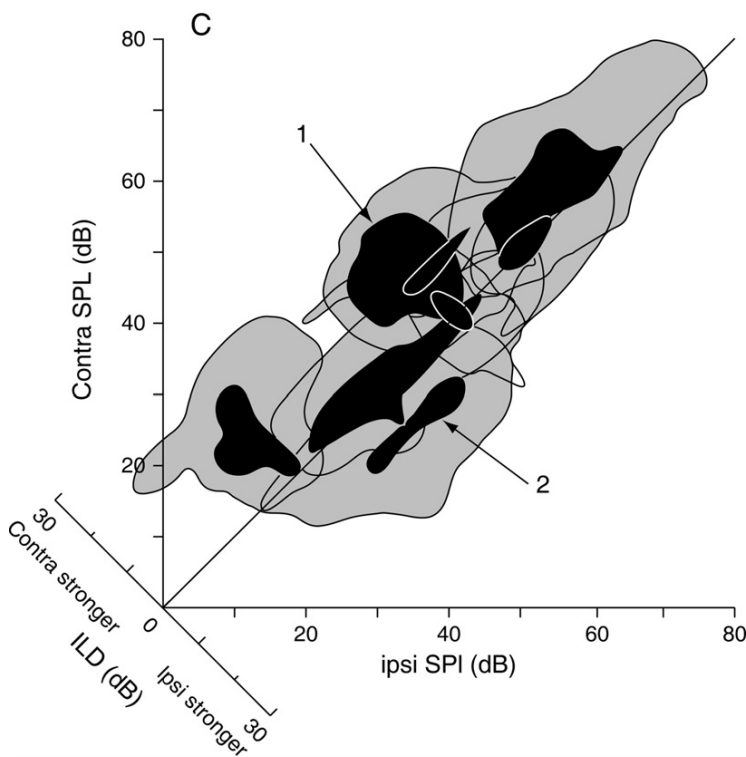


Fig. 7.8 Continued.

in the most favourable timing relation can be much larger, and when in the least favourable relation, much smaller, than to either stimulus alone. Whereas low-frequency stimuli (e.g. below 2 kHz) can reveal sound direction as a result of shifts in the phase of the waveforms arriving at the two ears, onset transients can also encode sound direction, even in high-frequency neurones. As an example from a bat, Fig. 7.9 shows that a cell's response to the onset transients in high-frequency tones varies with the interaural time difference between the transients (Lohuis and Fuzessery, 2000). Figure 7.9 also shows that, as in the lower levels of the auditory system, the time differences generating the maximum response are generally found to be as large as, or larger than, those that can be generated by stimuli outside the head in space, that is as calculated from the separation of the ears divided by the speed of sound. These neurones will not therefore reach any peak in their firing rate for any directions of the source that are less than 90° to the side. However, the neurones will represent the laterality of the sound, that is whether the sound is on the left or the right, and the overall population response will indicate the direction more precisely. Because the steepest slopes of the functions in

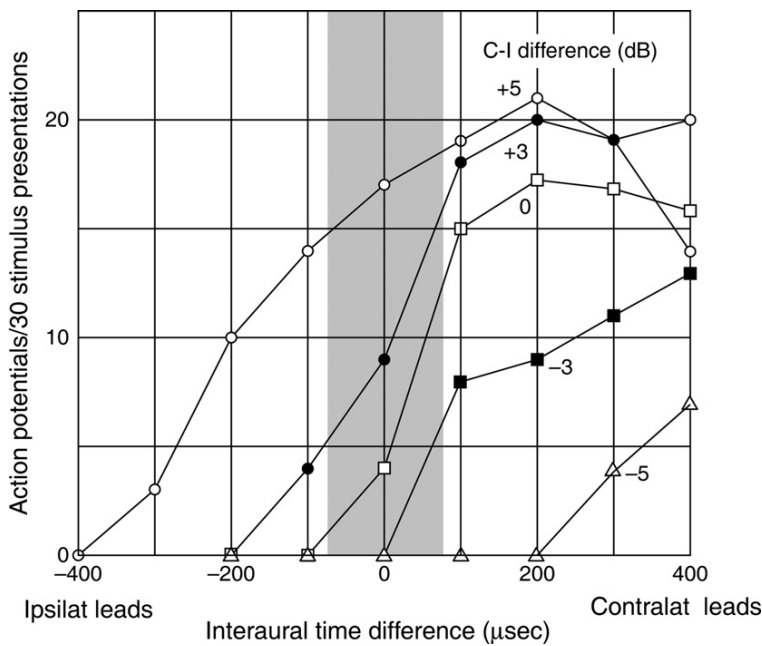


Fig. 7.9 Response of a cell in AI of the pallid bat, to tone pips presented to the two ears, as a function of time delay between the two ears. The firing rate shows a sigmoidal dependence on the time difference. The numbers on the curves show the intensity of the contralateral stimulus relative to the ipsilateral one, in dB. Increasing the relative intensity of the contralateral stimulus means that it becomes more effective at driving the neurone. The grey area shows the range of interaural time delays ($\pm 70 \mu\text{sec}$) that could be produced in this species by real acoustic stimuli in space. Stimulus intensity: 40 dB SPL at characteristic frequency. From Lohuis and Fuzessery (2000), Fig. 4A.

Fig. 7.9 are generally found at zero interaural delay, the population response will be particularly sensitive to changes of direction around the midline. Figure 7.9 also shows that increasing the intensity of one of the binaural stimuli makes it more effective in driving the neurone, so that the cell is sensitive to differences in interaural intensity as well as in timing.

In a real situation, the overall response of binaurally driven cells will be determined by many different factors. The pinna introduces its own transformations, increasing the effective intensity of stimuli that are presented along the acoustic axis of the pinna. Figure 7.10 shows spatial receptive fields as determined from the responses to clicks, where the simulated directions of the clicks in virtual acoustic space were varied by presenting synthesized click stimuli to the two ears, with the appropriate intensities, waveforms and timings chosen to simulate the different directions (Brugge *et al.*, 1994). In the neurone shown in Fig. 7.10B, the

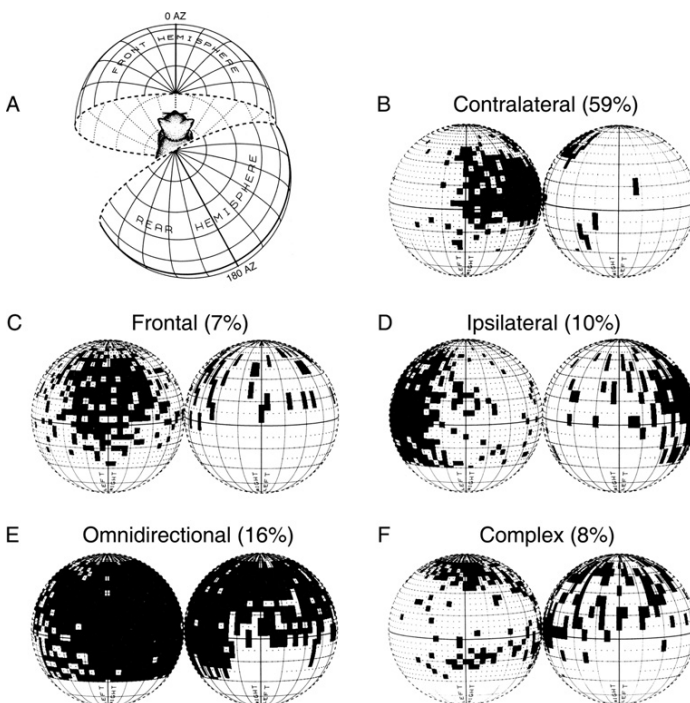


Fig. 7.10 Responses of cells in cat AI are plotted on hemispheres, according to the simulated position of the sound source in virtual space. Part A shows how the responses are plotted: the virtual hemisphere behind the animal is depicted in parts B–F as folded out beside the hemisphere that is in front of the animal. In parts B–F, the occurrence of each action potential is marked by a black square at the virtual position of the stimulus that drove it. Straight ahead corresponds to the centre of the left circle of each pair of circles. The sound stimulus was 20 dB above the lowest threshold for the neurone being tested, parts B–F, cells with different response areas. The proportion of each type of response area is indicated, as found in a sample of 164 cells. Elevations more than 36° below the horizontal were not investigated and are shown blank. From Brugge *et al.* (1994), Figs. 1 and 5.

response area is aligned to the acoustic axis of the pinna contralateral to the recording site.

Neurones with similar, localized, responses to stimuli on the contralateral side form the majority of cells found in the cortex (59% in the sample of Brugge *et al.*). Figure 7.10C–E also shows cells of the less common types, where responses are largest in the cortex ipsilateral to the ear being stimulated (10% of the sample), symmetrically to stimuli in front (7%), or show no spatial selectivity (omnidirectional, 15%), and where no simple spatial field can be defined (complex, 8%).

Some neurones show a loss of spatial selectivity with increasing intensity. In other neurones the response area is roughly confined to the contralateral side at all

intensities, termed ‘bounded’ responses by Brugge *et al.* (1996). Neurones with bounded responses receive a particularly strong inhibitory input from the non-preferred hemifield. It should also be noted that the behavioural ability to localize sounds is always far better than the localizing ability of individual neurones, so additional processing, possibly involving a population response, is likely to occur.

7.3.2.2 Responses outside AI

The behavioural experiments described above showed that in the cat fields AES and PAF, as well as AI, were essential for sound localization. AES contains multiple adjacent and partially overlapping fields with neurones that are responsive to visual, somatosensory or auditory stimuli, some of the neurones showing cross-modal interactions (Dehner *et al.*, 2004). The auditory neurones commonly have a binaural input (Clarey and Irvine, 1990). As described above, the AES is also a major source of inputs to the superior colliculus, which as well as being involved in visual orientation is involved in acoustic orientation in space. As was described in Chapter 6, the deep layers of the superior colliculus contains a map of acoustic space, in approximate register with the visual map in the more superficial layers.

Neurones in PAF have a great variety of tuning curves, many neurones having very broad and complex excitatory and inhibitory response areas (Loftus and Sutter, 2001). These response areas would be suitable for extracting information on stimulus location, based on the spectral transformations introduced by the pinna. Overall, neurones in PAF respond with much longer latencies than neurones in AI, with the timing of the responses depending particularly strongly on the location of the sound source. If the animal is able to use information on the latency of the neural response, then this may be a further way that PAF contributes to sound localization (Stecker *et al.*, 2003).

In the macaque monkey, Woods *et al.* (2006) used an array of speakers situated around the animal to investigate responses to sound location in the belt areas. They found that the spatial selectivity for sounds was lowest in AL, where it was comparable to those in AI. Selectivity was higher in ML, still higher in CM and highest in CL (see Fig. 7.2 for definition of areas). Therefore, the more caudal (i.e. posterior) areas in the monkey belt seem specialized for processing sound location. The rostral (i.e. anterior) areas, in contrast, seem more specialized for pattern recognition. This forms the beginning of a postulated division of auditory information into ‘what’ and ‘where’ streams within the cerebral cortex (Rauschecker and Tian, 2000).

In human beings, both functional magnetic resonance imaging (fMRI) and positron emission tomography (PET) have shown that the major response to changing the location of a sound source occurs posterior to Heschl’s gyrus, in the planum temporale (e.g. Warren *et al.*, 2002; Barrett and Hall, 2006; van der Zwaag *et al.*, 2011; see Fig. 7.4 for definition of areas). In contrast, auditory spectral patterns activate Heschl’s gyrus and the auditory areas anterior to Heschl’s gyrus (the planum polare), although in addition they also activate the more anterior part

of the planum temporale. Therefore, as in the macaque, there seems to be a distinction between an anterior ‘what’ stream and a more posterior ‘where’ stream, with the posterior stream also carrying some ‘what’ information.

Further imaging studies in human beings have shown the spread of the possible ‘what’ and ‘where’ streams outside these areas. Non-spatial stimuli, as well as preferentially activating areas anterior to the primary auditory cortex, activate the area around the inferior frontal gyrus, forming the proposed ‘what’ stream (Fig. 7.11). Spatial tasks preferentially activate the parietal cortex and the superior frontal area around the superior temporal gyrus, forming the proposed ‘where’ stream. Moving sounds are also more effective at activating the latter stream than are static sounds. There is also a hemispheric specialization in responding to sound movement: while the left cortex responds preferentially to sounds in the right hemifield, the right cortex responds to sound movement in both hemifields (Krumbholz *et al.*, 2005). The posterior temporal area, posterior to the auditory areas discussed above, responds equally to spatial and non-spatial stimuli. It should

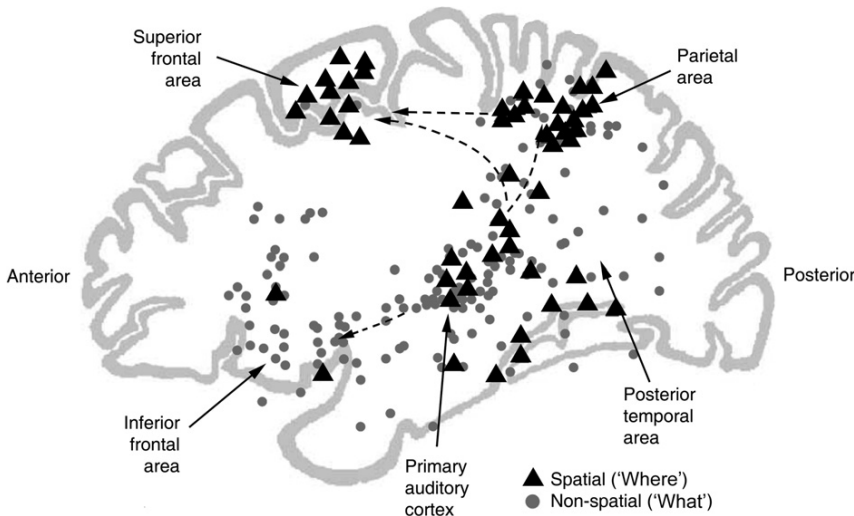


Fig. 7.11 Activation by spatial tasks (black triangles) or non-spatial auditory tasks (grey circles), according to a meta-analysis of data from 38 human positron emission tomography and functional magnetic resonance imaging studies. Spatial tasks, as well as activating the area immediately posterior to the primary auditory cortex, activate the parietal area (superior and inferior parietal cortex) and the superior frontal area (near the superior frontal sulcus) (the ‘where’ pathway). The posterior temporal area is equally activated by spatial and non-spatial tasks. Non-spatial tasks preferentially activate the anterior part of the primary auditory cortex, and the inferior frontal area (inferior frontal gyrus) (the ‘what’ pathway). Dotted lines: putative lines of information flow, based on anatomical connections (Rauschecker and Tian, 2000). Data are only shown for the areas indicated by labels. Reproduced from Arnott *et al.* (2004b), Fig. 1, with permission of the Association for Research in Otolaryngology.

also be remarked that the function of the dorsal/posterior ‘where’ pathway remains speculative and controversial. Others have argued that it is more involved in generating temporally sequenced representations of the auditory stimulus that are preparatory to making a motor response, including preparing for speech articulations (e.g. Warren *et al.*, 2005). Warren *et al.* suggested that the more dorsal pathway should instead be called the auditory ‘do’ pathway.

7.4 CORTICAL PROCESSING AND STIMULUS COMPLEXITY

7.4.1 Behavioural experiments

The auditory cortex is necessary both for the simple detection of sound and for the discrimination of frequency. While the earliest experiments showed no changes after bilateral cortical lesions, more recent experiments have shown deficits in these basic functions. Talwar *et al.* (2001) found that temporary bilateral inactivation of AI in rats by the GABA agonist muscimol raised rats’ auditory detection thresholds for several hours. After recovery of detection thresholds, frequency discrimination was found to be impaired for a further 10–15 hours. Conflicting results on simple detection thresholds have been found in macaque monkeys: Heffner and Heffner (1986) found substantial increases after large bilateral lesions which removed most of the core, belt and parabelt areas, while Harrington *et al.* (2001) found normal detection thresholds after similar lesions. However, even in the latter experiments, frequency discrimination thresholds were raised, and the ability to discriminate between frequency sweeps and steady tones was very poor indeed. And after lesions of the auditory cortex, animals seem to have particular difficulty with very short stimuli, suggesting that the area is important for registering the trace left by short stimuli (e.g. Cranford, 1979).

In one human patient, Tramo *et al.* (2005) reported that large bilateral lesions in the auditory cortex were associated with raised thresholds for the detection of frequency change, with particularly large impairments in detecting the direction of the change. In other patients with unilateral lesions, right side involvement was found to be critical, giving deficits in determining the direction of the frequency change, while frequency discrimination thresholds remained normal (Tramo *et al.*, 2005).

As might be expected from these findings, cortical lesions also affect more complex auditory tasks. Lomber and Malhotra (2008) showed in cats that after bilateral cooling of AAF, that is an anterior field in the core, the discrimination of auditory temporal patterns was significantly disrupted. Discrimination was also lost after large lesions of the auditory cortex which included AI, AII, Ep and I-T, but survived lesions of AI alone, suggesting a particular role for the core outside AI and for the belt and parabelt in this task (Diamond and Neff, 1957).

Further complex tasks affected by auditory cortical lesions include the discrimination of species-specific vocalizations in non-human primates, and

complex auditory perceptual tasks, including the perception of speech, in human beings (see [Stewart et al., 2006](#) and [Goll et al., 2010](#), for reviews of human data). Speech will be discussed further in Chapter 9. Given that the auditory cortex seems necessary for performance of complex auditory tasks, it is therefore not surprising that many cells in the auditory cortex respond selectively to complex aspects of the stimulus.

7.4.2 Physiological responses

Many neurones in AI have multipeaked tuning curves, containing response areas with two or more frequency regions of maximum sensitivity ([Section 7.2.1](#)). Responses to stimuli presented in the different peaks can be facilitatory, that is the neurone responds non-linearly such that response to both of the stimuli together can be greater than the arithmetic sum of the responses to the two stimuli separately ([Kadia and Wang, 2003](#)). Commonly, the constituent peaks are harmonically related; clearly, such neurones would be specialized for representing stimulus complexes where the stimulus components are harmonically related. Such stimuli include the vocalizations of the species concerned (the marmoset) which are rich in harmonics. Other neurones have only one excitatory peak in response to single tones, but Kadia and Wang found that multitone interactions could be detected by superimposing a second tone on the first. Where the second tone had an excitatory effect on the overall response, the frequency relations between the effective peaks tended not to be harmonically related. These neurones could be specialized for representing stimuli with multiple frequency components that were not harmonically related. However, where the second tone was inhibitory, the tones tended to be harmonically related: such neurones would therefore tend to be inhibited by stimuli with harmonically related components. Kadia and Wang speculate that this inhibition could serve to remove harmonics from a percept that contains the fundamental.

Outside AI, complex stimuli seem particularly effective at driving neurones, with frequency modulation (FM) being one critical cue. In the cat, neurones in AAF and PAF (non-AI parts of the core) are particularly responsive to frequency sweeps, with responses that are larger than to steady tones, and with many neurones being selectively responsive to the direction of the sweep ([Tian and Rauschecker, 1998](#)). Neurones in PAF are also particularly responsive to changes in the carrier frequency of species-specific vocalizations ([Gourevitch and Eggermont, 2007](#)). In cat PAF, unlike in AI and AAF, the response to frequency modulation cannot be simply predicted from the response to steady tones, suggesting that the responses reflect processing at a more complex level ([Tian and Rauschecker, 1998](#)). In the macaque lateral belt areas, neurones are also particularly strongly driven by FM stimuli. Neurones in CL have been found to be responsive to the fast sweep rates, while in AL, neurones responded to slow sweep rates, in the range found in species-specific vocalizations, and those in ML responded to the whole range of sweep rates ([Tian and Rauschecker, 2004](#)). Neurones in the lateral belt also seem particularly responsive to bandpass noise, another example of a

complex stimulus (Rauschecker and Tian, 2004). Wang (2007) has given further views on the coding of complex sounds in the primate auditory cortex.

Bats have formed a valuable model for analysis of the auditory cortex, because of their extreme specialization for echolocation. The echolocation pulse of CF-FM bats consists of a long constant frequency (CF) portion followed by a short downward sweeping FM component. In the moustached bat, each component consists of four harmonics. Therefore, the total stimulus and its Doppler frequency-shifted echo (the delay of the echo depending on the target's range, and the extent of the frequency shift depending on its velocity) contain a rich set of combinations of frequencies and frequency sweeps, which give information about the target's range and velocity. In the FM–FM cortical area (outside AI), the neurones respond poorly to the pulse or echo alone, but respond strongly to pairs of stimuli mimicking the pulse and echo where there were specific delays between the two stimuli. An essential requirement for facilitation is that the stimulus consists of the fundamental plus one or more of its harmonics. Here, as with the simpler case of multipeaked neurones, a specific combination of fundamental stimuli is required to activate the neurones (Kanwal *et al.*, 1999; Jen *et al.*, 2002).

In responding to complex stimuli, the auditory cortex seems to be responding to specific combinations of fundamental stimuli. Such responses could be determined by coincidence networks in the cortex. The combinations that are effective probably depend both on genetic programming, and on the stimuli that the animal has been previously exposed to. The influence of afferent activity was shown dramatically by Sharma *et al.* (2000), who cut the auditory afferent inputs to the medial geniculate body, and ablated the superior colliculus, one of the normal targets of neurones in the visual pathway, in early developing ferrets. The ferrets were then allowed to develop until adulthood. This resulted in rerouting of visual input to the medial geniculate body, with the result that visual inputs could drive neurones in the auditory cortex. The auditory cortex developed an organization reminiscent of the visual cortex, with a pattern of anatomical interconnectivity more similar to that of visual cortex, and with modules of cells responsive to visual stimuli of specific orientations. In other words, a novel patterned input had imposed quite a different anatomical and functional organization on the auditory cortex. We would therefore expect that with natural auditory stimuli, the selectivity of responses in the auditory cortex would similarly come to reflect the patterns of stimuli existing in the auditory input.

fMRI studies in human beings have shown that stimuli with complex spectral features preferentially activate lateral Heschl's gyrus, the anterior superior temporal gyrus, the planum polare and the area around the inferior frontal gyrus, all of which are included in the proposed 'what' stream (e.g. Arnott *et al.*, 2004a,b; Ahveninen *et al.*, 2006; Barrett and Hall, 2006; Viceic *et al.*, 2006; Fig. 7.11; see Figs. 7.4 and 9.16 for definition of areas). Moreover, vowel sounds and sounds that evoke a strong sensation of pitch produce strong responses in anterolateral Heschl's gyrus, or in the anterior planum temporale, suggesting that they might be centres for the extraction of pitch (Stewart *et al.*, 2006; Gutschalk and Uppenkamp, 2011; Barker *et al.*, 2011). Correlations between the variation in responses in the different cortical areas evoked by variation in stimulus structure have suggested that there is a hierarchical analysis of information, running from Heschl's gyrus to the planum

temporale and from the planum temporale to the superior temporal sulcus (Kumar *et al.*, 2007). On the other hand, stimuli with a spatial component activate areas that are situated only more posteriorly. This reflects the activation of the more posterior ‘where’ stream described above (Fig. 7.11).

Speech sounds are one example of a complex stimulus. Speech is processed in a special way in the auditory cortex and particularly involves activation of the areas posterior to Heschl’s gyrus, on the planum temporale of the dominant, usually left, side. Speech first appears to be treated differently from non-speech stimuli in an area lateral and inferior to Heschl’s gyrus, distributed along the superior temporal gyrus. Cortical responses to speech and to species-specific vocalizations will be discussed in detail in Chapter 9.

Finally, it should be remarked that the responsiveness and connectivity of the auditory cortex is continually and dynamically adjusted in response to the behavioural demands at the time (e.g. Fritz *et al.*, 2003; Ohl and Scheich, 2005; Chait *et al.*, 2012). Cortical responses to acoustic stimuli are particularly clearly enhanced when the stimulus is associated with another stimulus of strong significance for the animal, such as an electric shock (reviewed by Weinberger, 1998, 2004). Electrical stimulation of the auditory cortex can also modify the responses of the lower auditory centres such as the medial geniculate and the inferior colliculus, enhancing their responses to frequencies represented in the areas of the cortex being stimulated (for review, see Suga and Ma, 2003; see also Chapter 8). The cortex therefore appears able to enhance the responses of stimuli of significance, not only in the cortex, but at other stages of the auditory system. These responses will then be reflected in further enhanced responses in the cortex. The cortex is therefore likely to be able to devote larger numbers of neurones to stimuli which are of particular current significance for the organism.

7.5 OVERVIEW OF FUNCTIONS OF THE AUDITORY CORTEX

In contrast with earlier results, recent studies have shown deficits in relatively simple functions such as stimulus detection, frequency discrimination and sound localization, after lesions of the auditory cortex. Theories of function for the auditory cortex have therefore moved from previous suggestions that it is only involved in higher level cognitive functions to suggestions that it is also involved in processing stimuli in a more direct way, with stimulus features being first analysed in the core, then in the belt and then the parabelt.

Responses to complex stimuli suggest that in AI, neurones can respond specifically to sound location, and to stimuli such as multitone complexes, where the cross-frequency interaction is made possible by the neuronal processes that connect across frequency-band strips. The functional pattern of connectivity at any one time would be a combination of genetic programming, the history of exposure of the animal to such stimuli and the continual moment-by-moment modulations produced by the current demands of the behavioural state of the animal. In this

way, the neurones would come to respond to the complex stimuli that are present in the environment, with particular emphasis on those that are of current significance to the animal. Once the stimulus complexes have been analysed in the core areas, the neuronal activity is combined with analyses undertaken in the belt, and the parabelt, where higher and higher levels of analysis are carried out.

It can be hypothesized that the auditory cortex can develop these analyses not only because its number and range of interconnections allow a greater degree of complex interaction than in lower centres, but also because of its larger number of neurones and greater degree of plasticity. In addition, the inputs and interactions between the different specialized auditory and non-auditory areas allow it to adjust its responses to the current demands of the auditory environment and the animal, to a greater extent and in a more complex and versatile way.

The pathways for sound identification and sound location are partially segregated in the early stages of the auditory system, as a result of the different analyses required by the very different acoustic cues for these two aspects of the stimulus (see Chapter 6). Information on identification and location is then progressively combined in the inferior colliculus, medial geniculate body and primary auditory cortex. After this stage, the two types of information are segregated again, into more anterior and more dorsal/posterior pathways, suggested to correspond to hypothetical 'what' and 'where' pathways. This points to the cortex, which is the final stage of convergence of the identification and location streams, and also the first stage of divergence of the 'what' and 'where' streams, as having a special function. It can be hypothesized that in the primary auditory cortex, neuronal activity can be driven specifically by certain auditory objects. Such activity would combine information about the spatial source of the sound derived from the localization pathway, with information about its spectral and temporal nature being derived from the sound identification pathway. Coincidences in the activation of inputs to these neurones during previous auditory experience would facilitate the activation of neurones driven by common combinations of stimuli. This would promote neuronal circuits that could be said to represent the objects. Objects seem to be represented in a pattern of activity over many neurones. Conversely, each neurone may contribute to the representation of many different auditory objects.

The combined information about location and identity is then passed along the hypothetical dorsal/caudal 'where' or 'do' pathway, which responds to both aspects of the stimulus, and which may be involved in preparing the auditory stimulus so that it can be linked with a motor response. In contrast, the more ventral/rostral 'what' pathway seems to be concerned only with the identity of the stimulus and does not respond to information about location.



7.6 SUMMARY

1. Auditory cortex consists of a core surrounded by a belt and a parabelt. The core contains multiple (e.g. three) areas, including AI. The core receives its major

input from the specific or lemniscal division of the thalamic nucleus, namely the ventral division of the medial geniculate body that projects to the auditory cortex. The belt and parabelt areas predominantly receive their inputs from other divisions of the medial geniculate body. The belt also receives intracortical projections from the core, and the parabelt receives intracortical projections from the belt.

2. Auditory cortical areas are defined by the following criteria: (i) cell types and histological appearance; (ii) connections with the thalamus; (iii) pattern of staining for cytochrome oxidase, acetylcholinesterase and parvalbumin and (iv) the existence of separate tonotopic progressions in some areas.
3. In human beings, the primary auditory cortex is situated in the posterior and medial part of Heschl's gyrus on the superior temporal plane on the upper surface of the temporal lobe, deep in the lateral (Sylvian) sulcus. Belt and parabelt areas surround it rostrally (the planum polare), caudally (the planum temporale) and laterally (the superior temporal gyrus).
4. Primary cortical areas, and some of the belt areas, are tonotopically organized, that is the characteristic frequencies of neurones change in a progressive manner across the cortex. Lines joining neurones of similar characteristic frequency run orthogonal to the frequency progression and make what are called frequency-band strips. Cells whose responses are dominated by one ear or the other are grouped in patches on the surface of the cortex. Other groupings of cells, not related to the above patterns, can be found when cells are analysed in terms of latency, sharpness of tuning, threshold or sensitivity to frequency modulation. The significance of these groupings is not known.
5. Single neurones in the core areas show many different shapes of tuning curves in response to pure tones. Some neurones have sharp tuning curves with a single frequency region of maximum sensitivity. Others have very broad tuning curves, or 'multipeaked' tuning curves with two or more frequency regions of maximum sensitivity. Stimuli in the different regions of maximum sensitivity can be facilitatory, so that the neurones are particularly responsive to certain complex stimuli. In many of these cases, the frequencies of maximum sensitivity are harmonically related, so that the neurones would be particularly sensitive to stimuli with a rich harmonic structure, such as vocalizations. In other cases, although only a single excitatory peak is visible in the tuning curve in response to single tones, multiple bands of excitation or inhibition are revealed when further tones are superimposed.
6. Outside AI, in other parts of the core and in the belt areas, neurones seem particularly responsive to complex stimuli, including frequency- and amplitude-modulated tones, with different cortical areas being responsive to different modulation rates.
7. Sound location is represented in the auditory cortex, and unilateral lesions in the auditory cortex interfere with behavioural sound localization on the contralateral side. In the cat, local reversible cooling shows that AI, another core area (PAF) and a belt area (AES) are all essential for behavioural sound localization. In these areas, as well as in other cortical areas, a high proportion of neurones are sensitive to the location of sound sources and use interaural intensity and/or timing as cues.

8. Microelectrode studies in non-human primates, and fMRI in human and non-human primates, suggest that after the core areas, spatial information is processed more caudally and dorsally in the cortex, in what has been called the ‘where’ or ‘do’ stream. This includes the posterior temporal gyrus, the inferior parietal cortex and a more anteriorly situated area, near the superior frontal sulcus. On the other hand, complex stimuli particularly activate areas anterior to the auditory core, including in human the planum polare and area around the inferior frontal gyrus. These areas are part of the more rostral ‘what’ stream. However, there is some crossover and some ‘what’ information is also represented in the other stream.
9. It is suggested that one role of the auditory cortex in perception, among others, is that of representing auditory objects. Different objects are likely to be represented in overlapping patterns of activity spread over many neurones. The pattern of responsiveness of the cortex at any one time reflects the current behavioural state of the animal, with the neuronal responses modifiable such that a larger proportion of cortex is devoted to stimuli of particular current significance.



7.7 FURTHER READING

The anatomy of the auditory cortex has been reviewed by Winer (1992), with updates by Kaas and Hackett (2000), Winer *et al.* (2005) and Hackett (2011). The latter is one of many commentaries on auditory cortical function that appeared in a special issue of ‘Hearing Research’ (2011, Vol. 271, pp. 1–158). Cortical processing of location and complex stimuli, particularly in relation to single-neurone analysis in animals, has been reviewed by Middlebrooks *et al.* (2002) and Nelken (2002) respectively, in two chapters of ‘Integrative Functions in the Mammalian Auditory Pathway’ (Springer Handbook of Auditory Research, Vol. 15, eds D. Oertel, R.R. Fay and A. N. Popper), and also by Wang (2007), Recanzone (2011) and Recanzone *et al.* (2011). Complex stimulus processing in relation to ‘auditory objects’ has been reviewed by Goll *et al.* (2010). Cortical processing in human beings, with particular reference to fMRI, has been reviewed by Scheich *et al.* (2007), Zatorre (2007) and Woods and Alain (2009), and with particular reference to temporal processing by Nourski and Brugge (2011). The cortical processing of music has been reviewed by Stewart *et al.* (2006) and Limb (2006), and information on the relation between speech and music processing as revealed by fMRI is given by Rogalsky *et al.* (2011). ‘What’ and ‘where’ streams have been reviewed in relation to human beings by Barrett and Hall (2006), and summarized by van der Zwaag *et al.* (2011), with an alternative view being given by Warren *et al.* (2005). Cortical plasticity has been reviewed by Weinberger (2004) and for human beings by Froemke and Martins (2011) and Spierer *et al.* (2011).

THE CENTRIFUGAL PATHWAYS

The centrifugal pathways run from the higher stages of the auditory system to the lower. The auditory cortex sends a particularly rich centrifugal innervation to the medial geniculate body and further centrifugal innervations run to the inferior colliculus and other areas of the brainstem including some motor areas. The inferior colliculus sends centrifugal fibres to the superior olivary complex and the cochlear nucleus, while other centrifugal pathways run from the superior olivary complex to the cochlear nucleus and, as the olivocochlear bundle, to the hair cells and afferent nerve fibres within the cochlea. It is suggested that the more central centrifugal auditory pathways help to enhance responses to stimuli that are of particular significance for the animal. It is suggested that the olivocochlear bundle (i) helps protect the cochlea from acoustic trauma, (ii) assists in the detection of signals in noise and (iii) is involved in selective attention.



8.1 INTRODUCTION

So far we have considered the auditory pathway as one in which information is handed exclusively from the lower to the higher levels of the nervous system. Such a view is, however, far from that of the whole picture. In particular, the auditory system possesses a large number of nerve fibres running in the reverse direction, from the higher levels of the nervous system to the lower. The fibres run close to, but not generally within, the tracts carrying the ascending information. In this way, the activity of the lower levels of the nervous system can be influenced by the complex responses of the highest. We might therefore expect the central state of the animal to affect the responses of the earlier stages of the auditory pathway. Centrifugal pathways have been known since the end of the nineteenth century (e.g. [Held, 1893](#)); later interest was triggered by Rasmussen's description in 1946 of the olivocochlear bundle, running from the superior olive to the hair cells. Further interest was triggered by the possibilities that the centrifugal pathways could modify the sensory input according to the demands of the animal and help protect the cochlea from acoustic overstimulation.

8.2 THE OLIVOCOCHLEAR BUNDLE

The olivocochlear bundle is able to alter the sensitivity of the cochlea, by reducing the degree of active amplification of the travelling wave in the cochlea (see Chapters 3 and 5) and by modifying the input to the brain at a neural level.

8.2.1 Anatomy

The bundle arises bilaterally in the superior olivary complex. The fibres from the contralateral superior olivary complex cross the midline just below the floor of the fourth ventricle on the dorsal surface of the brainstem (Fig. 8.1). The fibres are then joined by ipsilateral fibres, and some branch off to enter the cochlear nucleus. The others leave the brainstem by way of the vestibular nerve, cross over into the auditory nerve and enter the cochlea.

There are two divisions of the olivocochlear bundle. Fibres of the medial olivocochlear bundle (MOC) arise medially in the superior olivary complex and terminate with large, vesiculated, synaptic terminals around the lower ends of the outer hair cells, mainly contralaterally. They surround both the base of the outer

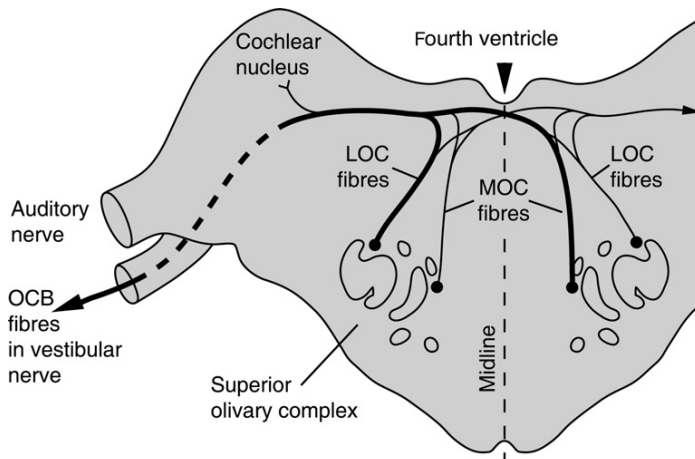


Fig. 8.1 The olivocochlear bundle (OCB) arises in the superior olivary complex of both sides. Fibres of the medial olivocochlear bundle (MOC) arise medially in the superior olive and innervate the outer hair cells, mainly on the contralateral side. Fibres of the lateral olivocochlear bundle (LOC) arise more laterally and innervate the afferent nerve dendrites near the inner hair cells, mainly on the ipsilateral side. Some of the fibres send collaterals to innervate the cochlear nucleus. Arrowhead: the point in the midline in the floor of the fourth ventricle where it is possible to stimulate or lesion the crossing fibres. Paths are shown on a schematic cross section of the cat's brainstem.

hair cells and the afferent terminals on the outer hair cells and are able to modulate the state of the outer hair cells. Fibres of the lateral olivocochlear bundle (LOC) arise more laterally in the superior olive. They end mainly ipsilaterally in the region of the inner hair cells and make axodendritic synapses en passant with the afferent fibres under the inner hair cells (Warr *et al.*, 1997). Sometimes, they make contact with the inner hair cells themselves (e.g. Liberman, 1980). For both groups, the density of efferent terminals is greater towards the middle and basal or high-frequency end of the cochlea, although the density is lower towards the extreme base (Liberman *et al.*, 1990).

The details of the sites of origin in the brainstem were worked out by means of axonal transport techniques by Warr and Guinan (1979). In the cat, there are about 1400 olivocochlear neurones in all, of which about two-thirds belong to the LOC (see Warr, 1992). The cell bodies lie in the superior olive, in many of the pre-olivary and peri-olivary nuclei surrounding the lateral olivary nucleus, as well as in the lateral olivary nucleus itself, though this is highly variable with species (Fig. 8.2; see also Fig. 6.13 for definition of nuclei). Such an association of the centrifugal system with the areas surrounding, but not generally identical with, the ascending pathway seems to be reproduced at many levels of the auditory system.

The cells of origin of the medial olivocochlear bundle (MOC) are scattered around the medial side of the superior olivary complex. The cells have relatively large bodies, give rise to large, myelinated axons and terminate on the outer hair cells, predominantly on the contralateral side (Guinan *et al.*, 1983).

The cells of origin of the lateral olivocochlear bundle (LOC) are tightly clustered mainly within but also around the lateral superior olivary nucleus (LSO). The cells have relatively small bodies and give rise to small, unmyelinated axons, which terminate on the dendrites of the afferent nerve fibres below the inner hair cells, predominantly on the ipsilateral side (Fig. 8.3). Those with cell bodies just outside the LSO are known as 'shell' neurones, and are likely to form a functionally separate subgroup (Warr *et al.*, 1997).

The separation into two systems, the LOC to the afferent nerve fibres below the inner hair cells and the MOC to the outer hair cells, is associated with a functional separation, related to the different roles of the inner and outer hair cells in transduction. The division into lateral and medial systems supersedes an earlier division into the crossed (COCB) and uncrossed (UOCB) olivocochlear bundles. The olivocochlear bundle also shows considerable anatomical variation between species, and the description above does not apply to all species. In addition, some fibres give rise to collaterals that innervate the cochlear nucleus. These arise from fibres of the MOC, and also from a subset of fibres of the LOC, namely those that arise from the LOC 'shell' neurones, which have their cell bodies in the peri-olivary nuclei around the LSO (Horvath *et al.*, 2000).

8.2.2 Neurotransmitters

There is clear evidence that acetylcholine is a transmitter of the medial and lateral olivocochlear bundles (for reviews, see Wersinger and Fuchs, 2011; Elgoyhen and

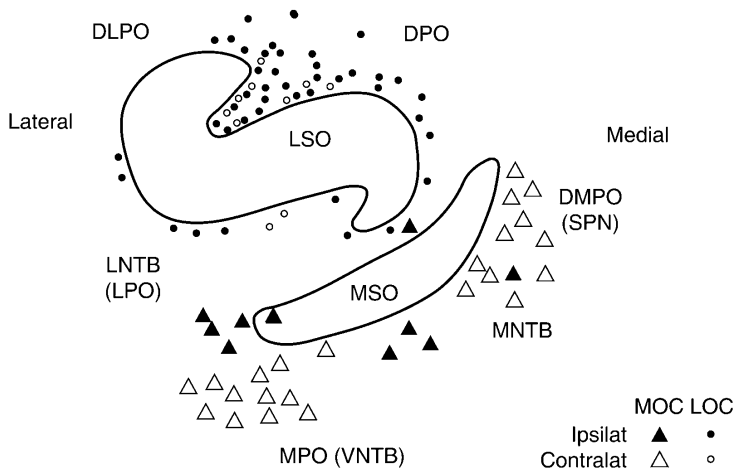


Fig. 8.2 The cells of origin of the lateral and medial olivocochlear bundles as shown in the cat by applying horseradish peroxidase to either the contralateral or ipsilateral cochleae. Large cells (\blacktriangle , \triangle) are the cells of origin of the medial olivocochlear system (MOC) and project to the outer hair cells. Small cells (\circ , \bullet) are the cells of origin of the lateral olivocochlear system (LOC) and project to the afferent dendrites below the inner hair cells. Cells projecting ipsilaterally are shown by filled symbols and those projecting contralaterally by open symbols. The cells of origin, here represented schematically, lie in the pre-olivary and peri-olivary cell groups and on the borders of the LSO. In rodents, in addition to the LOC cells with bodies situated around the LSO as shown above (shell neurones), there are also some LOC cells with bodies situated within the LSO (intrinsic neurones: not shown above; Warr *et al.*, 1997). DLPO, dorsal peri-olivary nucleus; DMPO, dorsomedial peri-olivary nucleus or superior para-olivary nucleus (SPN); DPO, dorsal peri-olivary nucleus; LNTB, lateral nucleus of the trapezoid body, or lateral pre-olivary nucleus (LPO); LOC, lateral olivocochlear system or bundle; LSO, lateral superior olive nucleus; MNTB, medial nucleus of the trapezoid body; MOC, medial olivocochlear system or bundle; MPO, medial pre-olivary nucleus, or ventral nucleus of the trapezoid body (VNTB); MSO, medial superior olive nucleus. Data from different levels of the cat brainstem have been projected onto one cross section. Data from Warr *et al.* (1986), Fig. 1.

Katz, 2012). Unusually for a cholinergic system, however, strychnine is also a powerful blocker. The acetylcholine receptors on outer hair cells are likely to be a composite of two types of receptor subunits, known as the $\alpha 9$ and $\alpha 10$ subunits, responsible for the unusual pattern of blocking at the synapse (Elgoeyen *et al.*, 2001; Lustig, 2006). In addition to acetylcholine, however, both the LOC and MOC systems contain further neurotransmitters or neuromodulators, including GABA and enkephalins, dynorphins and calcitonin gene-related peptide (CGRP), with a subset of LOC fibres, probably in rodents corresponding to some of the ‘shell’ neurones (see caption to Fig. 8.2), using dopamine instead of acetylcholine as a neurotransmitter (e.g. Maison *et al.*, 2003a; Darrow *et al.*, 2006b; Lendvai

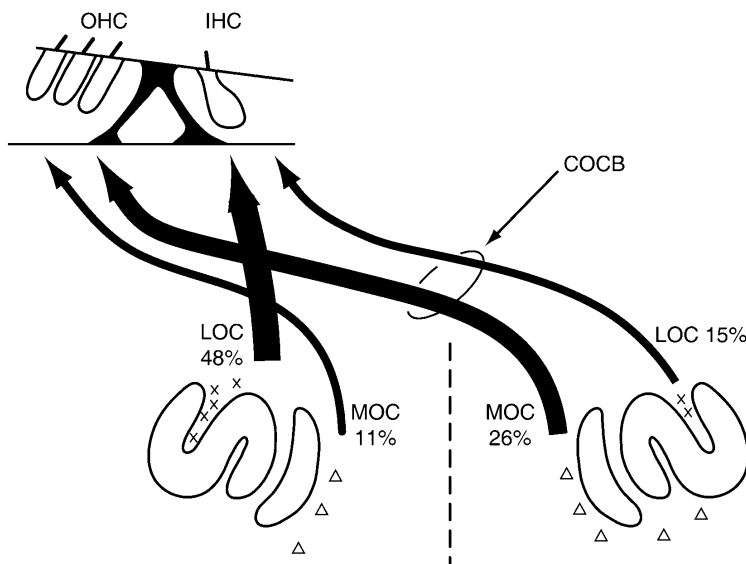


Fig. 8.3 The contribution of the MOC cells (Δ , to region of outer hair cells) and LOC cells (\times , to region of inner hair cells) to the different components of the olivocochlear bundle in the cat. The percentages show the contribution that each tract makes to the overall innervation of one cochlea. COCB, crossing fibres of the crossed olivocochlear bundle; LOC, lateral olivocochlear bundle; MOC, medial olivocochlear bundle. Data from Warr (1978) to incorporate the data of Warren and Liberman (1989a).

et al., 2011). The extent to which some of these neurotransmitters and neuromodulators play a functional role is still controversial. Mice with knockout of some subtypes of GABA receptors have raised auditory thresholds. In these animals, both the afferent and efferent nerves degenerate over time, suggesting that the GABA receptors are necessary for the normal maintenance of the innervation, in ways that are not currently understood (Maisond et al., 2006).

8.2.3 Physiology and function

8.2.3.1 Effect on the ascending system

8.2.3.1.1 MOC effects on outer hair cell membranes. MOC neurones are able to alter the motile response of outer hair cells, reducing the degree of active amplification of the travelling wave, and hence its magnitude in the cochlea. The release of acetylcholine by MOC neurones activates the acetylcholine receptors on the outer hair cells, causing the influx of Ca^{2+} into the cytoplasm of outer hair cells. Some of this Ca^{2+} may be released from within the cells, from the subsurface cisternae that line the basal membranes of the outer hair cells (see Fig. 3.5C). The

raised cytoplasmic Ca^{2+} then acts as a second messenger inside the cell, with a number of subsequent effects, including opening Ca^{2+} -activated K^+ channels in the membrane, known as the SK2 channels (Maison *et al.*, 2007). There are dual effects on outer hair cells, occurring over fast (tens of milliseconds) and slow (seconds) timescales (e.g. Cooper and Guinan, 2003).

Both the fast and slow effects are thought to reduce the outer hair cells' active amplification of the mechanical travelling wave, by affecting the hair cells' active motile process. The active amplification normally increases the magnitude of the mechanical travelling wave as it travels up the cochlear duct and is responsible for the great sensitivity and high degree of frequency resolution of the cochlea (see Chapters 3 and 5). The fast effect is likely to depend on the opening of the SK2 channels and the consequent exit of K^+ , because mice that overexpress SK2 channels show enhanced suppression of neural responses upon electrical stimulation of the MOC (Maison *et al.*, 2007). There may be two mechanisms for the downstream effects of opening the SK2 channels. (i) The opening may increase the conductance of the outer hair cell membrane, partially short-circuiting the transducer currents through the membrane. This could be expected to reduce the sound-evoked intracellular potential changes and hence reduce the degree of active amplification. (ii) A second mechanism may be that the exit of K^+ through the SK channels, by hyperpolarizing the outer hair cells, shifts the membrane potential, and possibly the resting operating points of the mechanotransducer channels and the basilar membrane, further away from their optimum values for active amplification (Santos-Sacchi *et al.*, 1998; Abel *et al.*, 2009).

The slow effect is thought to be due to the reduction in the stiffness of the outer hair cells. Acetylcholine reduces the axial (longitudinal) stiffness of the outer hair cell by about half. This is thought to occur via a number of mechanisms. The Ca^{2+} that enters through the acetylcholine-receptor channels could act as a second messenger inside the cell, to alter the mechanical properties (e.g. degree of polymerization) of the cytoskeleton within the cell which helps to give the cell its rigidity. The slow effect could also reduce the amount of active amplification more directly: the properties of the motor molecules themselves could possibly be altered, perhaps also as a result of modifications induced by second messengers (He *et al.*, 2003).

8.2.3.1.2 MOC effects on cochlear responses. Activation of MOC neurones, by electrical stimulation of the crossing fibres in the floor of the fourth ventricle (at arrowhead; Fig. 8.1), reduces the magnitude of the mechanical response on the basilar membrane. This is reflected in the tuning curves for the basilar membrane mechanical response and in the tuning curves of inner hair cells as shown in Fig. 5.17A and B. The changes are greatest at the characteristic frequency, where the degree of active amplification of the travelling wave is greatest, in agreement with the idea that the MOC works by reducing the degree of active amplification produced by the outer hair cells.

Intensity functions form another way of expressing the responses of the basilar membrane, inner hair cells and auditory nerve fibres; here, the magnitude of

response is plotted as a function of the intensity of the acoustic stimulus. Fig. 8.4A–C shows responses for tones at the characteristic frequency, where the effect is greatest. The action of the MOC is to shift the intensity functions to the right (horizontal arrows in the figure), that is to reduce the effective intensity of the stimulus. The effects are greatest for low-intensity stimuli, so the overall effect is to reduce the dynamic range of hearing (i.e. the number of dB between the threshold and the maximum response). Again, it must be emphasized that the fibres of the MOC innervate the outer hair cells, and so the effects on the inner hair cells (Fig. 8.4B) or auditory nerve fibres (Fig. 8.4C) which are driven by the inner hair cells, must be indirect, and are highly likely to be derived from the changed response of the basilar membrane (Fig. 8.4A). Figure 8.4D shows the effect of MOC stimulation on the tuning curve of an auditory nerve fibre, showing that, as expected, it is similar to the effect on the tuning of the basilar membrane and inner hair cells (Fig. 5.17A and B).

The active amplification of the mechanical travelling wave is intrinsically non-linear, because the input–output functions of the outer hair cells, which drive the amplification, are also non-linear (Fig. 3.20). Reducing the contribution from outer hair cells reduces the non-linearity from this source and can make the response of the basilar membrane more linear (e.g. Fig. 8.4A). This can reduce the amplitude of the non-linear intermodulation distortion tones produced within the cochlea, such as the cubic distortion tone at the frequency $2f_1-f_2$, where f_1 and f_2 are the frequencies of two tones presented (Liberman *et al.*, 1996; see Chapter 4, Section 4.2.4.3 and Chapter 5, Section 5.6.3).

However, and in spite of the expected reduced drive from the outer hair cells, MOC stimulation can sometimes *increase* the magnitude of the difference tone (i.e. quadratic distortion product) f_2-f_1 . The difference tone arises from a square-law non-linearity in cochlear function, and square-law non-linearity can be introduced by a d.c. bias in the operating point of a non-linear system (see Chapter 5, Section 5.6.3). Introducing a low-frequency biasing tone into the cochlea at the same time as MOC stimulation interacts in such a way as to suggest that MOC stimulation indeed affects the resting or zero operating point of the outer hair cells (Abel *et al.*, 2009). Whether it is a direct effect on the operating point of the outer hair cells' mechanotransducer channels, or occurs via a shift in the resting position of the basilar membrane, is at the moment controversial, direct measurements of the latter having shown no effect of the MOC (Murugasu and Russell, 1996).

The active mechanical process of the outer hair cells also gives rise to cochlear emissions; that is acoustic vibrations that can be detected in the external ear as a result of the active process within the cochlea (Chapter 5). The emitted tones can contain non-linear or intermodulation products, also driven by the outer hair cell non-linearity. The emitted cubic distortion tone, reflecting the above two aspects of the active process, is a particularly valuable measure of outer hair cell function, because it contains frequencies not present in the input, and so can be detected relatively easily. Suppression of cochlear emissions, and particularly of emissions of the distortion tone, can be used as a sensitive non-invasive measure of MOC function, an effect which is particularly useful in human beings (e.g. Guinan, 2006). Unfortunately, the difference tone f_2-f_1 , otherwise a sensitive indicator of

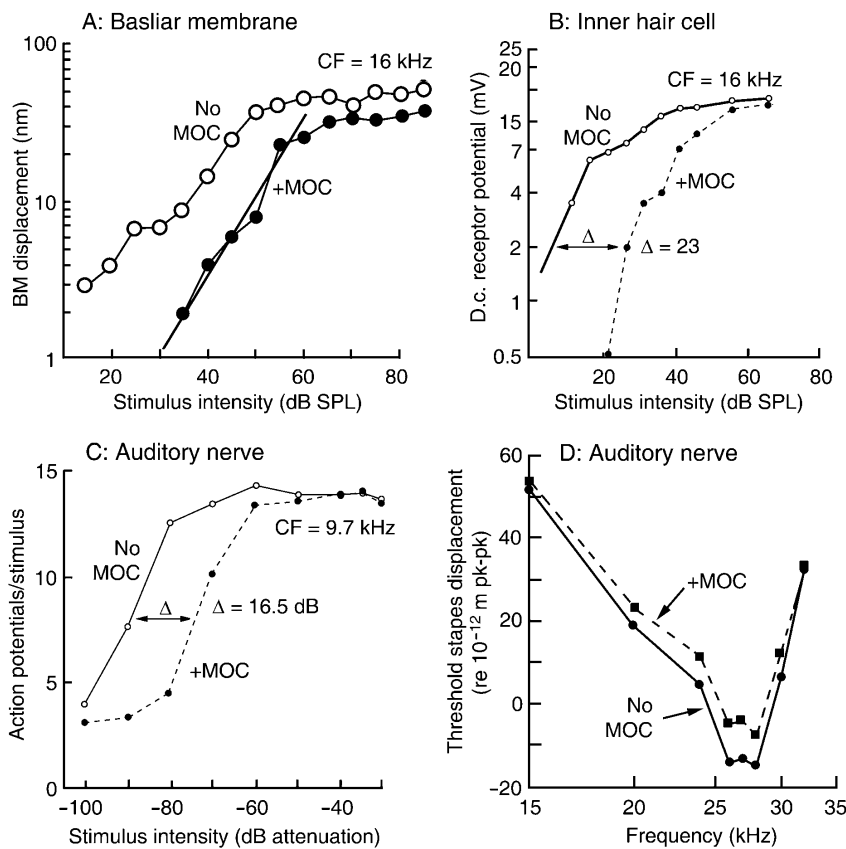


Fig. 8.4 (A–C) Effects of stimulation of the medial olivocochlear bundle (MOC) on cochlear responses, determined at the characteristic frequency (CF). Intensity functions are shown with (+ MOC) and without (no MOC) stimulation. (A) Magnitude of basilar membrane vibration, as a function of stimulus intensity in the guinea pig. MOC stimulation shifts the curve to higher intensities (i.e. reduces sensitivity) by 10–25 dB, depending on the point chosen on the curve. The diagonal line fitted to the data points marked + MOC has a slope of 1 (i.e. linear growth of response). Guinea pig. (B) Reduction of inner hair cell potentials by MOC stimulation. At low intensities, there is a 23-dB shift in sensitivity. Guinea pig. (C) Reduction of firing of auditory nerve fibres by MOC stimulation. The shift is 16.5 dB. Cat. (D) Effect of MOC stimulation on the tuning curve of an auditory nerve fibre. (A) Reprinted from Russell and Murugasu (1997), Fig. 3D, Copyright (1977), with permission from American Institute of Physics. (B) From Brown and Nuttal (1984), Fig. 3D. (C) Reprinted from Wiederhold (1970), Fig. 4C, Copyright (1970), with permission from American Institute of Physics. (D) From Wiederhold (1970), Fig. 8.

MOC effects, is not a good indicator in human beings, because in human beings it is only present at very low levels and is often difficult to detect.

The MOC also affects the gross stimulus-evoked potentials of the cochlea, namely the massed neural potential N_1 and the cochlear microphonic (see Chapter 3). The neural potential is suppressed along with the other neural responses; however, the cochlear microphonic, which under many stimulus conditions is dominated by the vibration in the tail of the tuning curve and hence is not amplified by the active mechanical process, is slightly increased, possibly because opening the Ca^{2+} -activated K^+ channels in the hair cells' membranes increases the stimulus-evoked currents through the cells. The endocochlear potential is also reduced by a few millivolts, in agreement with the idea that MOC stimulation increases current flows through the hair cells.

8.2.3.1.3 LOC effects. It has been difficult to analyse the effects of activation of the LOC, because the results are so easily contaminated by effects from the MOC. Local intracochlear application of the potential neurotransmitters of the LOC or interference with their synthesis or uptake suggest that the acetylcholine is excitatory to the afferent nerve fibres, while dopamine and GABA are inhibitory (e.g. Felix and Ehrenberger, 1992; Ruel *et al.*, 2006). Effects from the LOC may possibly be mixed and complex, and contradictory results have been obtained in the different experiments. Presumed activation of the cells of origin of the LOC in the superior olive, by the focal application of noradrenaline, increases spontaneous and evoked neural responses from the cochlea (Mulders and Robertson, 2005a). The interpretation of this experiment is that some components at least of the LOC can enhance the spontaneous and sound-evoked activity of the auditory nerve fibres. Results suggesting a similar influence were found by Maison *et al.* (2003b), who analysed auditory responses in mice with knockout of calcitonin gene-related peptide (CGRP), one of the neurotransmitters of the LOC. Although thresholds were normal, supra-threshold neuronal responses were reduced by 20%, suggesting that the CGRP component of the LOC normally enhances supra-threshold neuronal excitability. On the other hand, Darrow *et al.* (2006a, 2007) found that partial lesions of the cells of origin of the LOC enhanced supra-threshold neural responses ipsilaterally, suggesting that normally this innervation suppresses the responses. Dual effects of the LOC were found by Groff and Liberman (2003), who stimulated sites in the inferior colliculus, and found that some sites produced suppression, and others enhancement, of the neural responses of the cochlea.

8.2.3.2 What normally activates the olivocochlear bundle?

Anatomically, the olivocochlear fibres are organized into reflex arcs so that sound can influence the responsiveness of the cochlea. The shortest arc is likely to be a three-neurone loop from the cochlea to the ipsilateral posteroventral cochlear nucleus and then to the superior olive of both sides, with the involvement of

the posteroventral cochlear nucleus being shown by the effect of local kainic acid-induced lesions, which interrupt the reflex (de Venecia *et al.*, 2005). The MOC cells of origin in the superior olivary complex receive synaptic inputs from the T-stellate cells of the posteroventral cochlear nucleus (i.e. the planar multipolar cells in the alternative terminology; Darrow *et al.*, 2012). T-stellate cells have narrow excitatory bandwidths, and are therefore suited to conveying frequency-specific activation.

It is possible to selectively record from fibres of the olivocochlear bundle in the anastomosis of Oort, where they cross from the vestibular to the cochlear branches of the auditory nerve, or alternatively from within the intraganglionic spiral bundle within the cochlea. Recordings here show that the fibres have little or no spontaneous activity, although the apparent ‘spontaneous’ activity can be raised for some minutes after the end of acoustic stimulation, and so depends on the history of exposure of the animal. The fibres have regular firing patterns, in comparison with the irregular ones of auditory nerve afferent fibres. Their thresholds are similar to those of the auditory afferent fibres, and their tuning curves are as sharp, or nearly as sharp (Robertson and Gummer, 1985; Brown, 1989). When recordings are made in the cochlea, just before the fibres enter the organ of Corti, it is possible to relate fibre properties to the site of termination along the cochlear duct. In this case, it can be shown that in response to tonal stimulation, fibres are tuned to the frequency of the region they themselves innervate. Evidence for such an organized tonotopic projection, in frequency-specific loops, can also be found anatomically (Robertson *et al.*, 1987). Approximately two-thirds of efferents are preferentially driven by the ipsilateral ear, one-third by the contralateral ear and a small proportion are activated equally by both (Brown, 1989). Therefore as well as each ear being influenced by its own activity, it can be influenced by activity in the contralateral ear. Stimulating the contralateral ear is a convenient way to measure olivocochlear influences on the ear being analysed.

While contralateral tones can drive olivocochlear effects, bands of noise have been found to be much more effective at doing so (Warren and Liberman, 1989b). In human beings, when the olivocochlear suppression is tested by looking for its effects on otoacoustic emissions, the wider the band of noise, the more effective is the olivocochlear suppression. With bands of noise, ipsilateral and contralateral noise are equally effective, but the effects interact so that bilateral noise is far more effective than either ipsilateral and contralateral noise alone (Lilaonitkul and Guinan, 2009a,b).

The olivocochlear bundle can also be influenced by more central structures, so that for instance the MOC can be activated by stimulation within the inferior colliculus, to affect cochlear responses (Mulders and Robertson, 2005b). The olivocochlear bundle can also be affected by stimulation of the cortex, part of the evidence that the centrifugal control of the cochlea is likely to be organized in a system that connects from cortex to cochlea. However, in unanaesthetized cats, the activity of the olivocochlear bundle does not appear to fluctuate either with general motor activity or with vocalizations, so does not appear to control the auditory input during self-produced movements or sounds (Banks *et al.*, 1979).

8.2.3.3 Functional significance of the olivocochlear bundle

In spite of a large number of experiments, we are still unsure of the overall importance of the olivocochlear bundle in hearing. For instance, changes in auditory performance after lesions in the midline in the floor of the fourth ventricle, where approximately two-thirds of the MOC fibres cross to the other side, have in many cases produced either no, or only very slight, changes in performance.

8.2.3.3.1 Protection from acoustic trauma. Figure 8.5A shows how a tone exposure raises auditory thresholds measured after the traumatizing tone has ended. The raised threshold, which recovers over a period of hours to days, is called a temporary threshold shift and is an indication that incipient damage has been caused to the cochlea. If the tone exposure is accompanied by electrical stimulation

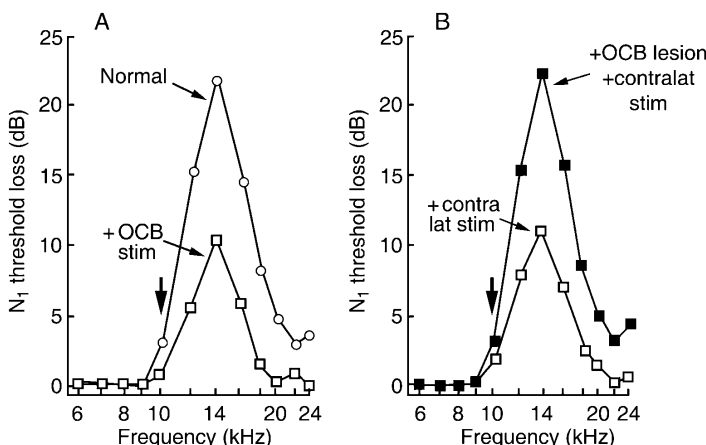


Fig. 8.5 Effects of the olivocochlear bundle (OCB) on temporary threshold shifts produced by a loud sound presented unilaterally. (A) Guinea pigs were stimulated with a 10-kHz tone in one ear at 103 dB SPL for 10 min (at frequency marked by vertical arrow). Auditory thresholds for the N₁ potential were measured 5 min after the end of the exposure. The exposure produced an increase in thresholds, with a maximum loss of 22 dB at 14 kHz (○; for explanation of why the maximum threshold loss is at a higher frequency than the traumatizing frequency; see Chapter 10, Section 10.3.2.1). If the crossing fibres of the OCB (mainly MOC fibres) are electrically stimulated during the traumatizing exposure, the maximum threshold loss is reduced from 22 to 10 dB (+ OCB stim, □). (B) Effects of contralateral stimulation on the threshold losses. If the contralateral ear is stimulated acoustically (10 kHz, 80 dB SPL for 1 min) simultaneously with the traumatizing stimulus, the threshold losses are reduced (+ contralat stim, □). If the same stimulating conditions are used but the crossing fibres of the OCB are lesioned beforehand, the protection is lost (+ OCB lesion + contralat stim, ■), i.e. giving losses as in part A. Used with permission from Rajan (1988), Fig. 2A, and from Rajan and Johnstone (1988), Fig. 5A.

of the crossing fibres of the OCB, the increase in threshold is halved. This reduction is likely to occur because the crossing fibres of the OCB, which mainly consist of MOC fibres to the outer hair cells, reduce the magnitude of the mechanical travelling wave in the cochlear duct and so reduce the magnitude of the traumatizing stimulus to the hair cells.

Figure 8.5 also shows an interesting phenomenon: the traumatizing tone exposure in Fig. 8.5A was unilateral, and if the contralateral ear was stimulated at the same time as the one being traumatized, threshold losses were reduced (open squares, Fig. 8.5B). This contralateral protection also occurs via the OCB, because it disappears, and the losses return to those seen as in Fig. 8.5A, if the crossing fibres of the OCB are lesioned (filled squares, Fig. 8.5B).

The above results relate to temporary threshold shifts after acoustic trauma. However, the OCB can also protect from the permanent threshold shifts seen after more severe trauma. While sectioning the crossing fibres of the OCB in the midline has produced only small or ambiguous effects, if both crossing and uncrossed OCB fibres are cut by unilateral sectioning within the brainstem, animals become more vulnerable to permanent threshold shifts after overstimulation, with threshold losses increasing by some 15–20 dB (e.g. Kujawa and Liberman, 1997). Overexpression of the $\alpha 9$ acetylcholine receptor subtype, one of the subtypes used by the acetylcholine receptors on the outer hair cells, renders mice more resistant to permanent threshold shifts after acoustic overstimulation, presumably because the MOC has become more effective than normal (Maison *et al.*, 2002). Similarly, a point mutation in the $\alpha 9$ receptor that enhances the effect of acetylcholine, by increasing the receptor's sensitivity to acetylcholine and by prolonging the open time of the receptor channel, also renders mice more resistant to acoustic trauma (Taranda *et al.*, 2009). Both of these results suggest that the MOC can help to protect the ear against acoustic trauma.

While some of the manipulations described above will have affected both the MOC and LOC, genetically manipulating the $\alpha 9$ acetylcholine receptors, which affects only the OHCs, shows that the MOC is certainly involved. Further experiments have shown that mice that overexpress SK2 channels had no enhanced protection from acoustic injury, although in these animals MOC fast effects were enhanced when tested with electrical stimulation of the MOC. This suggests that normally protection from acoustic overstimulation occurs independently of the SK2 channels and hence is likely to be due to the MOC slow effect, possibly because of a reduction of the active amplification of the cochlear travelling wave by the slow effect (Maison *et al.*, 2007).

It is also possible that the LOC may be able to modify the effects of acoustic trauma, this time to the nerve supply. Darrow *et al.* (2007) unilaterally destroyed cells of origin of the LOC by precise local injections of a cellular toxin in the mouse. In these animals, there were temporary increases in neural thresholds after an acoustic traumatizing stimulus that were 10–15 dB greater on the damaged side. There were no changes in the emissions of distortion products from the ear, indicating that the effects had not occurred as a result of changed active amplification of the travelling wave, that is they were not mediated via the MOC on the outer hair cells. These results suggest that normally the LOC is able to

reduce sound-induced excitotoxic damage to the afferent auditory nerve fibres, perhaps by its ability to modify neural responsiveness (see above; see also Chapter 10 and [Lendvai *et al.*, 2011](#)).

8.2.3.3.2 Improving the detection of signals in noise. Winslow and Sachs (1987) showed that electrical stimulation of the crossed olivocochlear bundle in the floor of the fourth ventricle (i.e. mainly the MOC) could reduce masking in single auditory nerve fibres. Fig. 8.6 shows the rate-intensity functions (solid lines) of an auditory nerve fibre for tone pulses in silence (Fig. 8.6A), and for tone pulses heavily masked by a constant broadband background noise (Fig. 8.6B). In this figure, the firing rates are plotted as a function of tone level. With no OCB stimulation, the background noise flattened the tone-intensity function (full line in Fig. 8.6B: compare with full line in Fig. 8.6A). The flattening occurred because, at low tone intensities, the noise itself drove the fibre, and at higher tone intensities, the noise suppressed the response to the tone.

Electrical stimulation of the OBC (dotted line, Fig. 8.6A) shifts the rate-intensity functions for the tone to the right, similar to the effect shown in Fig. 8.4C. However, in the presence of background masking noise, OCB stimulation suppresses the response to both the noise and the tone. The suppression of the response to the tone shifts its rate-intensity function to the right (dotted line,

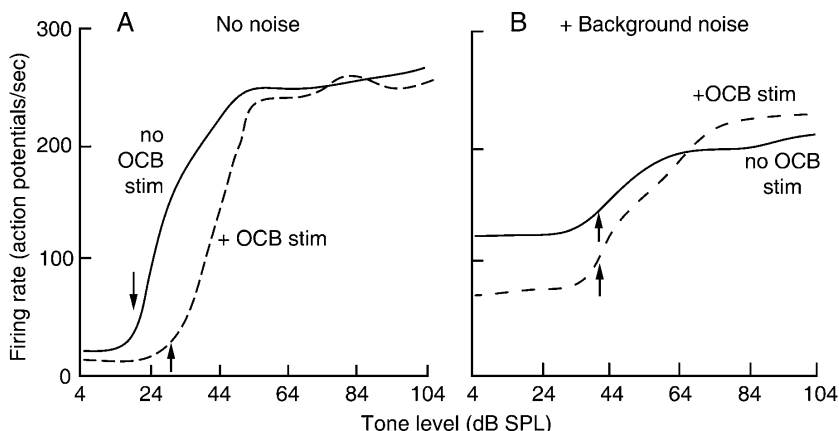


Fig. 8.6 Rate-intensity functions for an auditory nerve fibre, without (—) and with (----) electrical stimulation of the olivocochlear bundle (OCB; mainly MOC). (A) No masking noise. The fibre here is activated only by the tone pulses and shows the standard sigmoidal relation between tone intensity and firing rate. OCB stimulation shifted the function along the intensity axis by 12 dB. (B) With continuous masking noise, the function is flatter (see text). OCB stimulation reverses the effects and steepens the function. Arrows: point at which the tone increases the firing rate by 20 spikes/sec. For clarity the original published functions have been slightly smoothed. Used with permission from Winslow and Sachs (1987), Fig. 4A and D.

Fig. 8.6B). The suppression of the response to the noise by the OCB reduces the extent to which the noise adapts the response to the tone, so that for higher-level tones, the response to the tone itself is actually increased. For low-intensity tones, when the noise itself was driving the fibre, the firing of the fibre is reduced. The result is that the rate-intensity function to the tone is steepened as well as being shifted. For stimuli well above threshold, therefore, the OCB stimulation enhanced the response of the fibre to the tone, when in the presence of background noise.

However, the masked detection threshold for the tone in noise was unchanged. As shown in Fig. 8.6, the tone intensity for a small (20 spikes/sec) increment in firing is the same with and without OCB stimulation (arrows, Fig. 8.6B). Kawase *et al.* (1993) confirmed this in more detail in a later experiment and showed that it particularly applied to fibres measured in the presence of relatively low levels of background noise. On the other hand, they found that in some fibres, particularly those with high spontaneous firing rates, and for higher levels of background masking noise, OCB stimulation could lower the detection thresholds of tones in noise, commonly by about 5 dB.

The improvement is also shown in higher levels of the auditory system, in both the cochlear nucleus and inferior colliculus (Seluakumaran *et al.*, 2008; Mulders *et al.*, 2009). In the inferior colliculus, Seluakumaran *et al.* showed a strong enhancement in the response of neurones to tones in noise, when the tone was presented at an intensity which was well above its masked detection threshold. In a minority of neurones, the masked detection threshold was lowered as well.

A role in the discrimination of signals in noise was first suggested by the behavioural experiments of Dewson (1968). He trained rhesus monkeys to discriminate between two vowel sounds in the presence of masking noise. Performance was reduced by cutting the fibres of the crossed component of the olivocochlear bundle. Similar results have been obtained by Hienz *et al.* (1998) in cats. In human beings, contralateral acoustic stimulation can activate the MOC, as detected by suppression of otoacoustic emissions produced by the ear being tested (for reviews, see Guinan, 2006, 2010; Robertson, 2009). In some reports, contralateral stimulation has been found to enhance the detection of tones in noise, likely also to occur via an effect on the MOC. For instance, in the experiment of Micheyl and Collet (1996), in those subjects where contralateral noise was particularly effective at suppressing otoacoustic emissions in the tested ear (i.e. presumably those subjects where the crossed MOC reflex was particularly effective), masked thresholds for tone pips in the tested ear tended to be better than in the other subjects, by a few dB. This result was however contradicted by Garinis *et al.* (2011), who showed that individuals who tended to have stronger MOC reflexes tended to have poorer masked thresholds. Effects on the discrimination of speech in noise have also been contradictory: one report showed better perception in those subjects with presumed more effective MOC reflexes as assessed by the above criteria. Moreover, the improvement was absent in patients in whom the vestibular nerve had been cut, severing all OCB efferents (Giraud *et al.*, 1997). In another report, however, the opposite effect was found (de Boer *et al.*, 2012).

8.2.3.3.3 Adjusting the dynamic range of hearing. The effects on the intensity functions (Fig. 8.4) and on masking (Fig. 8.6) are both examples of the ways that the OCB can reduce the sensitivity of the auditory system in the presence of intense stimuli. Moderate and intense stimuli can drive auditory nerve fibres into the saturated range of their firing. If the OCB is activated by high-intensity stimuli, the OCB may be able to enhance the dynamic range of the cochlea by reducing the response of the auditory nerve to the high-intensity stimuli. However, tests of patients with a severed vestibular nerve and hence no OCB fibres to that ear have provided no support for this hypothesis (Scharf *et al.*, 1997).

8.2.3.3.4 Role in attention. Could the olivocochlear bundle be involved in attention, attenuating the peripheral response to an auditory signal when it is judged to be irrelevant? Such a hypothesis could explain some of the common experience of fluctuations in the awareness of auditory stimuli. The OCB can be activated by more central auditory stimulation, for instance in the inferior colliculus (e.g. Mulders and Robertson, 2005b), so there is the possibility that OCB effects could be modulated by the behavioural state of the subject. In one example, Delano *et al.* (2007) showed that when chinchillas attended to a visual task, cochlear neural responses were decreased, and cochlear microphonics were increased, suggestive of an effect of the olivocochlear bundle on the cochlea. However, the important control, of showing that the effects disappeared when the effect of the bundle was blocked, was not done.

In a second example, this time with human subjects, Maison *et al.* (2001) measured otoacoustic emissions to test tones in one ear, while asking the subjects to count probe tones in noise in the other ear. When the test and probe tones had the same frequency, there were small (0.3 dB) reductions in the levels of otoacoustic emissions from the ear being tested, but not when the subject was attending to probes of different frequencies. This suggests that MOC activation is used to suppress responses, albeit by only a small amount, in the ear not being attended to and that this occurs in a frequency-specific way. This is supported by findings in patients with a unilaterally severed vestibular nerve and hence no OCB fibres to that ear. On the normal, unlesioned side, it was found that tones of unexpected frequency were detected less readily than tones of expected frequency. However, on the lesioned side, all tones were detected with equal facility. This suggests that the OCB can reduce the sensitivity of the cochlea to signals of unexpected frequencies (Scharf *et al.*, 1997).



8.3 CENTRIFUGAL PATHWAYS TO THE COCHLEAR NUCLEI

8.3.1 Anatomy

The cochlear nuclei receive centrifugal fibres from several sources. By far the largest innervation appears to arise in the superior olivary complex. Centrifugal

inputs from the interior colliculus and the reticular formation have also been described. Some of the centrifugal fibres from the superior olivary complex consist of branches of the olivocochlear bundle: Horvath *et al.* (2000) showed that probably all MOC fibres send collaterals to the cochlear nucleus, as do those LOC fibres arising in the area surrounding the LSO (the 'shell' neurones; Fig. 8.2). Other fibres run ipsilaterally by rather more direct paths in the dorsal and intermediate acoustic striae and bilaterally in the trapezoid body (Fig. 8.7). As with the olivocochlear bundle, the centrifugal innervation does not arise in the main nuclei associated with the ascending system, but in some of the surrounding pre-olivary and peri-olivary nuclei, and particularly densely in the lateral and ventral nuclei of the trapezoid body (see Fig. 6.13 for definition of nuclei; Spangler *et al.*, 1987; Shore *et al.*, 1991). These nuclei, of course, receive an auditory input, so the centrifugal pathways can be activated by sound as well as by central influences.

The centrifugal innervation from the inferior colliculus arises in all areas of the colliculus. Cells that belong to the descending pathway, that is those that project to the cochlear nucleus, seem to be segregated from those belonging to the ascending pathway, being situated in separate groups within the colliculus (Coomes and Schofield, 2004). The fibres descend and run along the ventral surface of the brainstem, where they turn and ascend dorsally into the granule areas of the VCN and the middle layers of the DCN (Shore and Moore, 1998; Alibardi, 2002).

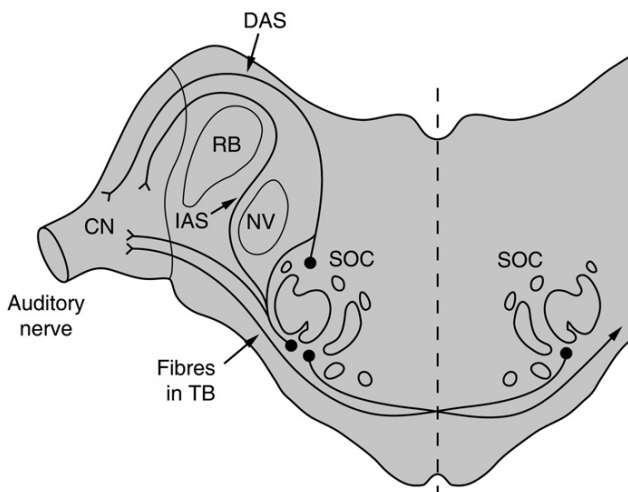


Fig. 8.7 A schematic representation of some of the centrifugal pathways from the superior olivary complex (SOC) to the cochlear nucleus (CN). Branches of the olivocochlear bundle also run from the SOC to the CN but are not shown here. The fibres run by three routes: the dorsal acoustic stria (DAS), the intermediate acoustic stria (IAS) and in the trapezoid body (TB). RB, restiform body (inferior cerebellar peduncle); NV, fifth nerve nucleus. Data from Elverland (1977).

The nucleus of the trigeminal nerve and the reticular formation also send projections to the cochlear nucleus (Shore and Zhou, 2006). All divisions of the cochlear nuclei receive centrifugal fibres in different degrees from the different sources. There is considerable detail in the projections – for instance, Cant and Morest (1978) described six groups of centrifugal axons ending in different ways in the anteroventral cochlear nucleus alone.

8.3.2 Neurotransmitters

As in the cochlea, knowledge of the neurotransmitters and pharmacology of the centrifugal system has been useful for discovering the function of the pathways. The collaterals of the OCB to the cochlear nucleus are cholinergic, with many of the terminals in the cochlear nucleus and many of the cells of origin, particularly in the superior olive, reacting positively for acetylcholinesterase and choline acetyltransferase. Combined retrograde tracer and choline acetyltransferase staining shows that there is a further ipsilateral cholinergic projection from the ventral nucleus of the trapezoid body within the superior olivary complex, that runs ventrally over the brainstem to the cochlear nucleus via the trapezoid body (Sherriff and Henderson, 1994). In the guinea pig, approximately three-quarters of the cholinergic input arises from the superior olivary complex, while the remaining cholinergic inputs arise from the pontomesencephalic tegmentum, an area associated with arousal, sensory gating, sleep–wake cycle, reward and motor functions (Mellott *et al.*, 2011).

Other pathways to the cochlear nucleus from the superior olivary complex are inhibitory and use GABA or glycine as a neurotransmitter (Ostapoff *et al.*, 1997). In addition, the cochlear nucleus receives a noradrenergic input from several brainstem areas including the locus coeruleus and possibly the nuclei of the lateral lemniscus (Thompson, 2003a,b).

8.3.3 Physiology and function

Acetylcholine, a centrifugal neurotransmitter within the cochlear nucleus, is excitatory when applied to the cells of the ventral cochlear nucleus, and mainly inhibitory when applied to the dorsal cochlear nucleus (Caspary *et al.*, 1983). Fujino and Oertel (2001) showed in mouse tissue slices that T-stellate (T-multipolar) cells of the posteroventral cochlear nucleus could be excited by acetylcholine, via both muscarinic and nicotinic receptors, while D-stellate (D-multipolar) cells were not affected. But by intracellular recording *in vivo* in guinea pigs, Mulders *et al.* (2009) showed that onset-chopper cells (D-stellate cells) gave excitatory postsynaptic potentials (EPSPs) in response to electrical stimulation of the olivocochlear bundle in the floor of the fourth ventricle, that is in response to activation of the cholinergic collaterals of the olivocochlear bundle to the cochlear nucleus. The reason for the difference in results is not clear; the application of acetylcholine will of course affect all cholinergic receptors, whether associated with the OCB or not. In addition, the results were obtained in

different species. [Mulders *et al.* \(2009\)](#) also observed excitatory and inhibitory effects in primary-like (bushy) and chopper (T-stellate) and neurones. They suggested that these effects were produced indirectly via the excitatory effects on the onset-chopper cells.

A role for the cholinergic input to the cochlear nucleus in the discrimination of signals in noise was shown in behavioural experiments by [Pickles and Comis \(1973\)](#). A cannula was chronically implanted over the nucleus in cats, and atropine was applied to the nucleus. Atropine can block the excitatory input from the superior olive, blocking the muscarinic component of the cholinergic excitation ([Comis and Whitfield, 1968](#); [Fujino and Oertel, 2001](#)). Cats were trained to detect tone pips both in silence and against masking noise. In such behavioural test, atropine applied to the cochlear nucleus raised the absolute thresholds for tone pips by a few dB, but raised masked thresholds by on average 9 dB more. This suggests that atropine might have been blocking a system whose normal action was to help the animal hear signals in masking noise. It was also shown that tones masked by narrowband noise were not affected, while tones masked by wideband maskers were affected. When the bandwidth of the noise was systematically varied, it was shown that the bandwidth of the noise around the signal that contributed to masking the tone, known as the critical band (Chapter 9), had been increased ([Pickles, 1976](#)). This agrees with suggestions that the cholinergic centrifugal innervation enhances the responses of neurones which help extract narrowband signals from a wideband noise background. It is interesting that both of the cholinergic centrifugal innervations so far analysed, namely the olivocochlear bundle and the innervation of the cochlear nucleus, affect the discrimination of signals in noise.

[Shore \(1998\)](#) cut pathways central to the cochlear nucleus in guinea pigs, interrupting both the outflow from the nucleus and the centrifugal input to the nucleus. The time course of masking was changed in the cochlear nucleus, depending on neurone type. In some types of neurones, the masking of one stimulus by a later stimulus was decreased, while in other types of neurones, the delayed masking was increased, suggesting the removal of either delayed excitation or delayed inhibition on the neurones. Stimulation of one of the nuclei of origin of the pathways, the spinal trigeminal nucleus, was able to affect the timing of neuronal spikes in the dorsal cochlear nucleus ([Koehler *et al.*, 2011](#)). It is therefore possible that the centrifugal pathways modify temporal processing and via that, sensory integration in the cochlear nucleus, according to the demands of the task.



8.4 CENTRIFUGAL PATHWAYS IN HIGHER CENTRES

Centrifugal pathways are found at all levels of the auditory system, from cortex to cochlea, with the result that the highest levels of the auditory system are able to influence all lower levels (for reviews, see [Spangler and Warr, 1991](#); [Smith and Spirou, 2002](#)).

8.4.1 Anatomy

8.4.1.1 Corticofugal system

Two descending systems have been described as originating in the auditory cortex. Firstly, the cortical areas send massive descending projections to the medial geniculate body, particularly to the division from which they receive an ascending innervation. Secondly, the cortex also sends descending projections to a wide range of other areas, including auditory brainstem nuclei (the inferior colliculus, the superior olivary complex and the cochlear nucleus) as well as non-auditory areas, including other nuclei of the thalamus, the tegmentum, the amygdala and the central grey matter, and areas connected to the motor system (for reviews, see Winer, 2006; Suga, 2012).

The tonotopic areas of the auditory cortex project primarily to the tonotopic divisions of the medial geniculate, while the non-tonotopic areas project primarily to the non-tonotopic areas of the medial geniculate and to the polymodal areas of the thalamus. Within the tonotopic projections, the descending fibres terminate in a spatially organized way on the cells that project back to the cortex. It seems, therefore, that there is a close coupling in the loop of afferent and efferent fibres, so that each part of the cortex can influence the part of the medial geniculate body that sends its connections, and suggesting that, within each functional division, the thalamus and cortex can act as a single integrated unit. In addition to this area-specific projection, there is also a more divergent projection, with each cortical area projecting to multiple areas of the thalamus (Winer *et al.*, 2001).

The cortical projection to the inferior colliculus ends mainly in the external nucleus and dorsal cortex, that is in the extralemniscal areas of the colliculus, which are part of the less specific and sometimes multisensory auditory pathway (Chapter 6). There is also a much smaller projection from the cortex to the superior olivary complex, running mainly ipsilaterally to the ventral nucleus of the trapezoid body (medial pre-olivary nucleus) and ending on the cells of origin of the MOC (Mulders and Robertson, 2000). The projection to the cochlear nucleus also ends primarily ipsilaterally, in the granule cell layers of all divisions and in all parts of the dorsal nucleus, in particular in its pyramidal (fusiform) layer, ending on cells that project centripetally to the inferior colliculus (Schofield and Coomes, 2005). In addition, the auditory cortex projects to the motor nuclei of the pons, a major source of mossy fibres to the cerebellum, and to the striatum, both of which form parts of the extrapyramidal motor system (Winer, 2006).

8.4.1.2 Centrifugal fibres from the inferior colliculus

The inferior colliculus is a further rich source of centrifugal fibres, sending projections to the lateral lemniscus, the superior olivary complex and the cochlear nucleus. The projections to the superior olivary complex end in the ventral nucleus of the trapezoid body and the peri-olivary region rostral to the nucleus; the centrifugal neurones end on neurones that themselves project to the cochlear

nucleus and to the cochlea, the latter via the MOC (Vetter *et al.*, 1993; Schofield and Cant, 1999). The connections from cortex to inferior colliculus and to superior olive, and the olivocochlear bundle to the cochlea, form a way that the cortex can modulate the responses of the cochlea.

8.4.2 Physiology and function

Ma and Suga (2001) recorded from cells in the inferior colliculus of bats (big brown bats), while stimulating in the auditory cortex within the cortical projection areas of the neurones being recorded from. When the characteristic frequencies of the areas being stimulated and recorded from matched, the neural frequency response areas of the neurones in the lower nuclei became sharpened – that is the responses to tones at the best frequency were enhanced, and the responses to adjacent frequencies were inhibited. On the other hand, if the characteristic frequencies were unmatched, the stimulation inhibited the response at the characteristic frequency, but enhanced the responses at other frequencies. This shifted the best frequencies of the cells in the lower nuclei, in most cases towards that of the stimulated neurones. The effect is that the cortical activation enhances the responses and sharpens the frequency selectivity of the cells that project to the same area. The direction of the frequency shift in unmatched neurones means that a greater portion of the auditory pathway becomes devoted to the frequencies that are being activated by the cortical stimulation (reviewed by Suga, 2012). Zhang and Suga (2005) later showed that similar frequency shifts could be obtained by stimulation within the inferior colliculus itself. The effect was mediated by a loop that went up to the auditory cortex and back, because it could be prevented by inactivating the primary auditory cortex (AI) by the topical application of a local anaesthetic. The effect is mediated by muscarinic cholinergic synapses, because it can be blocked by atropine applied to the inferior colliculus (Ji *et al.*, 2001). Analogous results have been obtained in the mouse by Yan and Ehret (2002). This suggests that centrifugal pathways might be a mechanism by which the cortex can enhance its responses and devote a larger number of neurones to stimuli which are of current and particular significance for the animal.

The auditory cortex can influence other types of processing in the inferior colliculus. For instance, inactivation of the auditory cortex can change the sensitivity of cells in the colliculus to interaural differences in sound intensity (Nakamoto *et al.*, 2008). This will be expected to alter the spatial sensitivity of neurones in the inferior colliculus. While animals can still localize sounds after selective inactivation of the descending pathways from the primary auditory cortex to the colliculus, they are unable to relearn localization if the cues are altered by plugging one ear (Bajo *et al.*, 2010). And as also shown by cortical inactivation, the auditory cortex can change temporal processing in the inferior colliculus. The interpretation is that some complex temporal fluctuations become selectively more prominent. This could enhance the detection of some harmonically complex sounds when in the presence of other similar sounds (Nakamoto *et al.*, 2010).

The descending fibres from the inferior colliculus to lower levels of the auditory system can also affect the responses of the cochlea and auditory nerve, since the fibres end on the cells of origin of the olivocochlear bundle. [Mulders and Robertson \(2005b\)](#) stimulated the inferior colliculus and produced a variety of effects in auditory nerve fibres. Most effects were inhibitory but some were excitatory, increasing the responsiveness of the fibres and enhancing spontaneous activity. The effects were blocked by gentamycin, which affects outer hair cells' function, showing that the effects occurred via the MOC system which runs to the outer hair cells. Focal stimulation within the inferior colliculus produces frequency-specific effects in the cochlea, with the frequency region targeted in the cochlea being matched to the best frequency of the area stimulated in the inferior colliculus. This shows that the inferior colliculus is capable of controlling the cochlea in a precise, frequency-specific way ([Ota et al., 2004](#)).

As expected from their close anatomical relationship, the auditory cortex has a strong influence on the responses in the medial geniculate body. As an example, [Zhang and Suga \(2000\)](#) found that focal stimulation of the auditory cortex shifted the frequency representation in the medial geniculate body, as it did in the inferior colliculus as described above. However, the changes were found to be greater in the medial geniculate, suggesting that there was an additional effect on the nucleus.

Stimulus-specific adaptation (SSA) refers to a decline in response to repeated stimuli, without any change in the responsiveness to other stimuli. It can be seen in all stages of the auditory system from the inferior colliculus upwards and is clearly a mechanism for picking out novel or important stimuli. [Bäuerle et al. \(2011\)](#) found that SSA in neurones of the ventral nucleus of the medial geniculate disappeared after pharmacological inactivation of the auditory cortex, suggesting that the auditory cortex has a role in priming the lower stages of the auditory system to respond to novel stimuli of significance.

In summary, the anatomical evidence suggests that there are multiple centrifugal pathways that can influence all stages of the auditory system. There is a chain of efferent command, starting at the auditory cortex, influencing the cochlea and all stages in between. Cortical effects on the cochlea have been supported by functional observations in unanaesthetized mustached bats by [Xiao and Suga \(2002\)](#), who showed that cortical stimulation could modify the responses of the cochlea, as detected by changes in the cochlear microphonic. In cases of human patients with unilateral lesions of the auditory cortex, there was found to be reduced MOC-induced suppression of otoacoustic emissions, the MOC activation being induced by stimulation of the contralateral ear ([Khalfa et al., 2001](#)). The deficit was greatest in the ear contralateral to the lesion. The corticofugal effects could therefore enhance the responsiveness of the earliest stages of the system to stimuli of significance, as described for centrifugal pathways from the auditory cortex earlier in this section. Cortical control of the olivocochlear system could also underlie the attentional effects of the olivocochlear bundle described above (Section 8.2.3.3.4).



8.5 SUMMARY

1. Centrifugal (efferent) pathways parallel the centripetal (afferent) auditory pathways along the length of the system, forming a system which runs from the cortex to the hair cells. In many stages of the auditory pathways, the centrifugal fibres run adjacent to, but not actually within, the tracts and nuclei principally associated with the ascending system.
2. The cochlea is innervated by the olivocochlear bundle, which arises bilaterally in the superior olivary complex. The medial olivocochlear bundle (MOC) arises medially in the superior olivary complex, and projects to the outer hair cells, predominantly on the contralateral side. The cells of origin have relatively large bodies and give rise to relatively large, myelinated axons. The lateral olivocochlear bundle (LOC) arises laterally in the superior olivary complex, and projects to the dendrites of the auditory nerve fibres near the inner hair cells, predominantly on the ipsilateral side. The cells of origin have relatively small bodies and give rise to relatively small, unmyelinated axons. Both the MOC and LOC use acetylcholine as a neurotransmitter. In addition, they use neurotransmitters or neuromodulators such as GABA, enkephalins, dynorphins and CGRP (calcitonin gene-related peptide), with a subset of LOC fibres using dopamine instead of acetylcholine as a neurotransmitter.
3. The MOC reduces the active amplification of the travelling wave in the cochlea by the outer hair cells. It does this by opening Ca^{2+} channels in the membrane, which then are likely to open Ca^{2+} -activated K^+ channels (SK2 channels) in the membrane. There are effects over two different timescales in hair cells, and both may affect mechanical amplification. Fast effects (tens of milliseconds) are thought to occur because opening the K^+ channels (i) partially short-circuits the membrane (so that transducer currents do not produce such large voltage changes, reducing active amplification) and (ii) moves the active amplifier and possibly the mechanotransducer channels away from their optimal operating points, also reducing active amplification. Slow effects (over seconds) are thought to occur because the outer hair cells become less stiff, likely to be as a result of a Ca^{2+} -dependent second messenger cascade acting on the cytoskeleton and possibly the motor proteins, also affecting active amplification. The result is that the amplitude of the travelling wave in the cochlea is reduced, especially in the region of the sensitive, sharply tuned peak. Inner hair cell responses and auditory nerve fibre responses are also changed.
4. The functions of the LOC are uncertain: it is likely to modulate the neural excitability of the afferent nerve fibres.
5. Nerve fibres of the olivocochlear bundle can be driven by sound, and respond to sounds of the best frequencies of the areas that they themselves innervate. The fibres therefore are able to make closed frequency-specific feedback loops. They can also be driven by descending fibres from the more central auditory nuclei, also in a frequency-specific way.

6. The olivocochlear bundle is likely to (i) help protect the cochlea from acoustic trauma, both by reducing the size of the travelling wave in the cochlea, and by direct effects of the LOC on the afferent nerve fibres, (ii) enhance the response to narrowband signals in wideband masking noise and (iii) may modify the auditory input in attention.
7. The cochlear nucleus receives a centrifugal innervation, including branches of the olivocochlear bundle, together with other centrifugal fibres from the superior olive, the inferior colliculus and from several other brainstem areas. The neurotransmitters include acetylcholine, GABA, glycine and noradrenaline. The cholinergic innervation of the nucleus may assist in the detection of signals in wideband masking noise. The centrifugal pathways also can modulate temporal integration in the nucleus and affect delayed masking.
8. The auditory cortex is a rich source of centrifugal fibres running to the inferior colliculus, to all parts of the nucleus though mainly to the non-specific (extralemniscal) divisions of the colliculus. In the inferior colliculus, the corticofugal fibres can affect frequency-specific processing, temporal processing and the representation of sound location. It can also enhance sounds with certain temporal structures at the expense of other sounds.
9. The auditory cortex also sends many centrifugal connections to the medial geniculate body. The centrifugal and centripetal fibres make closed feedback loops suggesting that within each functional division, the thalamus and cortex work as a closely integrated unit. The auditory cortex enhances the responses and sharpens the frequency selectivity of the cells that project to the area being stimulated. The centrifugal input is also able to enhance stimulus-specific adaptation (SSA) in the medial geniculate, and therefore also helps prime the system to respond to novel stimuli. Electrical stimulation of the auditory cortex is also able to activate the olivocochlear bundle, forming a mechanism by which the cortex could also modify the auditory input as early as the cochlea.
10. The general conclusion is that centrifugal pathways allow the higher levels of the auditory system to modify sensory processing at the lower levels. They enhance the responses of the system, and allow it to devote a larger numbers of neurones to stimuli that are of particular current significance for the animal.



8.6 FURTHER READING

The anatomy and function of the olivocochlear bundle have been reviewed by Robertson (2009), Guinan (2010) and Wersinger and Fuchs (2011). Olivocochlear effects on the vibration of the basilar membrane have been reviewed by Cooper and Guinan (2006). The anatomy and function of the olivocochlear bundle have also been reviewed in Chapters 2–5 in Vol. 38 of the Springer Handbook of Auditory Physiology ‘Auditory and Vestibular Efferents’

(2011), eds D.K. Ryugo and R.R. Fay. The anatomy and physiology of central centrifugal pathways have been reviewed in Chapters 9–11 of the same volume. The anatomy of the central auditory centrifugal pathways, particularly with reference to the corticofugal pathways, has been reviewed by [Winer \(2006\)](#), and in relation to corticofugally induced tuning shifts, by [Suga \(2012\)](#).

PHYSIOLOGICAL CORRELATES OF AUDITORY PSYCHOPHYSICS AND PERFORMANCE

Basic auditory psychophysical phenomena have correlates in the physiological responses of the different stages of the auditory system. For most of the audible range, the variation of the absolute threshold with frequency appears to be set by the efficiency of the outer and middle ears in transmitting the incident acoustic energy to the cochlea. The overall frequency resolving power of the auditory system is set by the mechanical frequency resolution of the cochlea, as revealed in the vibration of the basilar membrane and the firing of the auditory nerve fibres. Pitch discrimination depends on multiple mechanisms, including the frequency resolution of the cochlea, and temporal analyses undertaken by unknown mechanisms. Loudness can be related to the total amount of activity in the auditory nerve, although the sensation is likely to be modified by central mechanisms. Sound localization depends on both monaural and binaural cues, the latter involving differences in intensity and timing at the two ears, as extracted in the superior olive. Related mechanisms assist in the extraction of signals from noise on the basis of differences in interaural timing. Speech sounds are initially analysed in terms of their basic acoustic properties in the auditory brainstem and core areas of the auditory cortex. They are then passed for higher-level analyses in surrounding cortical areas, including the superior temporal gyrus and the inferior frontal gyrus, which form parts of the ‘language network’ of the brain. This chapter requires knowledge of the information contained in Chapters 1–4. In addition, there are some specific referrals back to Chapters 6 and 7.



9.1 INTRODUCTION

In this chapter, we shall try to analyse the extent to which some aspects of auditory performance can be explained in terms of known physiological processes. The chapter by no means attempts to be a balanced review of the psychology or psychophysics of hearing, but deals with certain phenomena whose explanation has, or seems to have, a close correlate with physiology.



9.2 THE ABSOLUTE THRESHOLD

The absolute threshold seems to be a reasonably close match to the minimum thresholds of auditory nerve fibres (Fig. 4.4). The behavioural audiogram is near, or is about 10 dB below, the lowest neuronal thresholds. A small discrepancy is not surprising. Even if subjects use only mean neural firing rates, they may be able to do better than suggested by the thresholds of individual fibres, because they are able to combine information over many fibres. The discrepancy between the neural and behavioural data is more serious at high frequencies. The reason for this is not clear; the surgical preparation for the electrophysiological experiment may well have had an influence. However, more recent reports, from experiments where the necessary controls are better understood, show a close match at all frequencies (e.g. Sayles and Winter, 2010).

What determines the form of the relation between absolute threshold and frequency? Calculations from the efficiency of power transfer through the outer and middle ears shows that in human beings the absolute threshold corresponds to a power of 10^{-18} Watts being delivered to the cochlea, for much of the audible range (Rosowski, 1991). Similar relations have also been shown for cats and chinchillas. Put in other words, for much of the audible range, the shape of the audiogram is determined by the transmission characteristics of the outer and middle ears. These observations have the intriguing implication that, for much of the audible range, the cochlea itself is approximately equally responsive to all tones, irrespective of frequency.

However, this conclusion does not hold towards the upper and lower ends of the frequency range. The high-frequency absolute cut-off of hearing is likely to arise because the cochlea itself becomes unresponsive to tones above a certain frequency, different for each species (Ruggero and Temchin, 2002). At lower frequencies (below 450 Hz), the threshold rises more rapidly than predicted from the power transmission. It has been suggested that this arises because the stimulus coupling to the stereocilia of the inner hair cells, by viscous drag of the fluid in the cochlea, becomes less effective below this frequency. At still lower frequencies, some of the sound energy is shunted through the helicotrema at the extreme apical termination of the cochlea (Cheatham and Dallos, 2001).



9.3 FREQUENCY RESOLUTION

9.3.1 A review of the psychophysics of frequency resolution

9.3.1.1 Frequency resolution and frequency discrimination

Psychophysically, we distinguish two distinct phenomena that are related to how frequencies are separated in the auditory system. One is known as frequency or pitch discrimination. Two tones are presented one after the other, and we have to

tell whether there is a difference between them. Frequency difference limens in this case can be very small, as small as 0.2 or 0.3% of the stimulus frequency. The fine resolution comes from our ability to compare two neural patterns that are separated in time. This phenomenon is related to the analysis of pitch, and the relation between frequency and pitch will be discussed later ([Section 9.4](#)). The other phenomenon is known as frequency resolution and corresponds more closely to the physiological phenomena of frequency selectivity studied by the electrophysiologist. In this case, the subject has to detect one frequency component of a complex stimulus in the presence of other frequency components, all presented simultaneously. It measures the extent to which the subject is able to filter one stimulus out from others on the basis of frequency. In an analogy, we can think of tuning an analogue (AM band) radio receiver so that the filter in the input circuit receives the desired station and rejects all others. The resolution of the filter tells us how good it is at passing one station while rejecting others that are close to it in frequency. In the auditory system, such resolution bandwidths are a measure of the basic frequency filtering properties of the auditory system. These resolution bandwidths are much larger than frequency difference limens and are perhaps 10–20% of the stimulus frequency. It is the latter case of frequency resolution that will be dealt with in this section; frequency (i.e. pitch) discrimination will be dealt with later.

9.3.1.2 Masking patterns as an indication of frequency resolution

One of the most immediate demonstrations of psychophysical frequency resolution is provided by the masking pattern produced by a narrowband stimulus, such as a narrow band of noise ([Fig. 9.1](#)). The masker is presented as a background, and the threshold of a superimposed tonal signal, called the probe, is plotted as a function of probe frequency. It is assumed that the threshold of the probe is a measure of the amount of activity produced by the masker in neurones with characteristic frequencies near to the probe's frequency. The logic is that the probe is detected only if it produces more activity than the masker alone. The masking pattern therefore becomes a correlate of the iso-intensity curves shown in [Fig. 4.7B](#). The masked threshold is greatest near the masker frequency, and at high masker levels, the pattern spreads more to high than to low frequencies. The asymmetry has an obvious correlate in the asymmetry of tuning curves, which in the cat for neurones above 1 kHz extend further below than above the characteristic frequency.¹ The reversal of the pattern of asymmetry between the psychophysical and neural cases stems simply from the method of measurement. An electrophysiologist plots the response of one neurone to stimuli of many different frequencies. In contrast, the psychophysicist measures the response in many different frequency regions to a masker of one frequency. Viewed in

¹ In the psychophysical case, another factor affects the asymmetry, which is that the auditory filter bandwidth (see below) increases with increasing centre frequency.

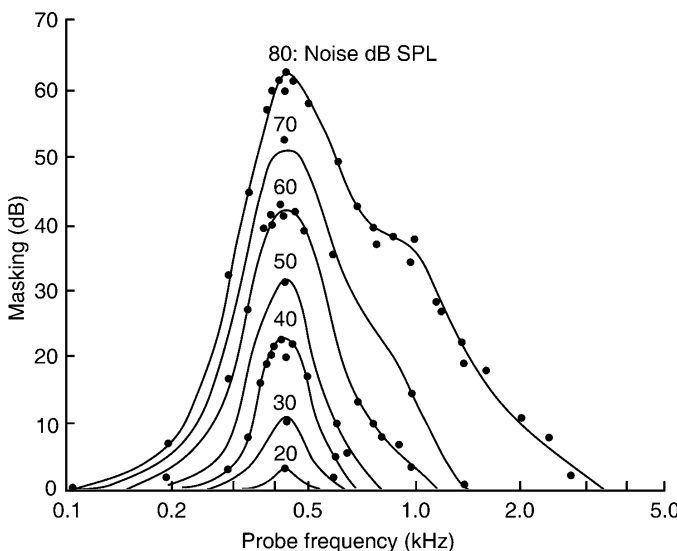


Fig. 9.1 The masking pattern produced by a narrow band of noise (intensity of noise indicated by numbers of curves). The elevation in threshold of a probe tone was plotted as a function of the probe frequency. At high masker intensities, the masking pattern spreads more to high than to low frequencies. Masker width 90 Hz, centred at 410 Hz. Reprinted from Egan and Hake (1950), Fig. 8, Copyright (1950), with permission from American Institute of Physics.

another way, a masker is able to activate the low-frequency tails of the tuning curves of neurones of much higher characteristic frequency, and so mask probes of much higher frequency. But a masker is comparatively ineffective at activating neurones of lower characteristic frequency, because the high-frequency cut-offs of their tuning curves are so sharp. Maskers are therefore not effective at masking probes of much lower frequency. This accounts for the predominantly upward spread of masking at higher masking levels.

A technique which might give a close psychophysical correlate of neural tuning curves generates what is known as a ‘psychophysical tuning curve’. In this case, the probe is fixed in frequency and is presented at a low constant intensity, such as 10 dB above threshold. Presumably, such a low-level probe will activate only a few neurones and will provide a near approximation to the electrophysiologist’s measurement of single neurones. The masker is varied in frequency and is adjusted in intensity to keep the probe at threshold. Again we presume that the probe is detected if it produces more activity in any neurones than the masker alone. We might therefore expect the probe to stay at threshold as the masker is moved in frequency and intensity around the edges of the tuning curves of the neurones at the probe frequency. The resulting psychophysical tuning curves indeed appear very similar to the tuning curves of auditory nerve fibres (Fig. 9.2).

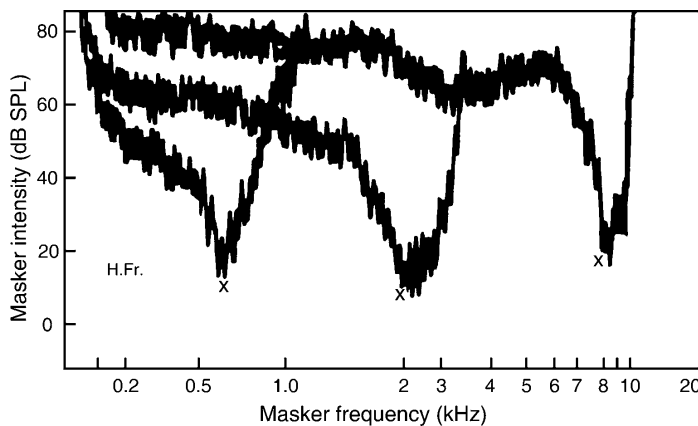


Fig. 9.2 Psychophysical tuning curves are produced by plotting the locus of frequency and intensity necessary to just mask a constant low-level probe (shown by crosses). The curves were determined with a Békésy audiometer, in which the subject continuously adjusts the masker intensity as its frequency is swept, in order to keep the probe at threshold. From Zwicker (1974), Fig. 2, with kind permission of Springer Science and Business Media).

The masking patterns of Figs. 9.1 and 9.2 appear to be similar to the frequency responses of bandpass filters. This suggests that we can think of the frequency resolving power of the auditory system as being due to a set of bandpass filters. Such filters have been measured extensively and have given us the phenomenon known as the critical band.

9.3.1.3 Critical bands and psychophysical filters

Fletcher (1940) introduced the concept of the critical band to deal with the masking of a pure-tone signal by wideband noise. He found that he could electronically filter out noise components remote in frequency from the signal without affecting the signal's threshold. However, there was a critical frequency region around the signal in which removing noise did affect masking. He called this range the critical bandwidth. We can think of critical bands, now commonly termed 'psychophysical filters', as a series of overlapping bandpass filters situated early in the auditory system. Only noise which activates the same psychophysical filter as the signal will mask it. The filters correspond to the filters underlying the masking patterns of Figs. 9.1 and 9.2. The bandwidth of the filters is commonly expressed as the 'equivalent rectangular bandwidth', that is as the bandwidth of a rectangular-shaped filter, which has the same peak transmission and the same overall power transmission, as the psychophysical filter in question. In normal subjects, the equivalent rectangular bandwidth is 10–20% of the stimulus frequency, varying systematically with stimulus frequency. Stimuli will interact

to different extents depending on whether or not they lie within the same filter. For this reason, psychophysical filters affect a wide variety of auditory tasks, including masked thresholds, frequency discrimination, sensitivity to phase relations and judgements of loudness, tonal dissonance and roughness (see Moore, 2005, 2012, for reviews).

Current techniques for measuring psychophysical filters generally depend on masking the response to one signal, often a tone, by noise of variable spectral characteristics. In one method, the tone is masked by noise which has a notch in its spectrum. The notch is centred on the signal frequency, and the signal threshold is measured as a function of the width of the noise notch. The resulting calculated auditory filter has a shape with a rounded top. This has been modelled in a number of forms, including the form known as a roex filter, and more recently, a gamma-chirp filter (see Unoki *et al.*, 2006). The filters have a form generally similar to the frequency filtering functions of auditory nerve fibres, as reflected in their tuning curves. The filters are slightly asymmetric, being wider on the low-frequency side for high-intensity maskers. The asymmetry at high masker levels contributes to the asymmetry of the masking patterns shown in Figs. 9.1 and 9.2.

9.3.1.4 Non-simultaneous masking techniques

A technique for measuring frequency resolution that produced a great deal of interest depends on non-simultaneous rather than direct or simultaneous masking (Houtgast, 1977). One technique used by Houtgast was forward masking. In forward masking, the masker is pulsed, each pulse being followed by a brief probe, lasting only 10 or 20 msec. The stimuli are ramped on and off to reduce the effects of spectral splatter. The masker will, of course, raise the threshold of the probe. If the critical band measurements are repeated with forward masking rather than with simultaneous masking a surprising difference emerges: the calculated psychophysical filters necessary to explain the results are commonly rather narrower, and surrounded, particularly on the high-frequency side, by areas of negative transmission. The negative areas can be explained by supposing that they are areas of lateral inhibition or suppression (Fig. 9.3; Houtgast, 1977).

Lateral inhibition or suppression is of course widespread in the auditory system, but had not been demonstrated convincingly by simultaneous masking techniques. Houtgast pointed out an obvious reason. We calculate the internal representation of a masker by measuring the threshold of a probe superimposed on the masker. If the elements of a complex masker interact to suppress the masker in some frequency regions, a probe in those frequency regions if presented simultaneously will be suppressed as well and to a similar extent. Because the signal-to-noise ratio is in effect unchanged, the probe threshold will be unchanged, and the suppression areas will not be reflected in the probe threshold. Forward masking acts rather differently. A complex masker will produce regions of high activity and, as a result of lateral suppression or inhibition, some regions of low activity. When the masker is turned off, its after-effects will raise the thresholds of neurones of some later stage in the auditory system, to an extent which depends on

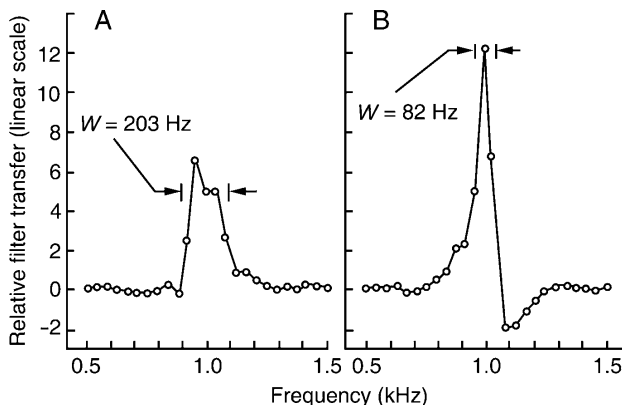


Fig. 9.3 Calculated psychophysical filter shapes derived by simultaneous masking techniques (A) are broader than those determined by non-simultaneous techniques (B). That determined by non-simultaneous masking also has an inhibitory sideband. ‘ W ’ indicates the effective bandwidth of the filter, that is the bandwidth of the equivalent rectangular filter. The filter shapes were calculated from masking the signal with wideband noise which had a rippled spectrum. The frequency spacing and positions of the ripples were varied. Test frequency 1 kHz. Reprinted from Houtgast (1977), Fig. 6, Copyright (1977), with permission from American Institute of Physics.

the amount of previous activity. If a probe is now presented, its threshold will be raised less in the areas of low activity than in the areas of high activity. In other words, the masking pattern will now reflect the influence of the inhibitory bands as well as that of the excitatory ones. The difference between simultaneous and non-simultaneous masking may reveal the effects only of cochlear non-linearity, or may include those of neuronal inhibition at later stages as well.

Non-simultaneous masking techniques have generated interest because they can reveal the effects of lateral inhibition. This has suggested that non-simultaneous masking might provide a more accurate picture of the neural representation of auditory stimuli than does simultaneous masking. On the other hand, the detection cues used by the subject in non-simultaneous masking can be more complex than in simultaneous masking, and these can have their own effect on the apparent shape of the filter (Moore and Glasberg, 1982).

9.3.2 Quantitative relations between psychophysics and physiology in frequency resolution

Although it is clear that in general terms psychophysical filters reflect the underlying frequency filtering properties of the auditory system, does the relation hold up quantitatively and in detail? In particular, how closely do psychophysical filters correspond to the frequency resolution of the cochlea, as initially suggested

by Fletcher (1940), and as reflected in the frequency filtering properties of auditory nerve fibres?

The tasks used to measure the filters psychophysically depend on interactions between two or more stimuli and are therefore more complex than those used to measure pure-tone tuning curves in single auditory nerve fibres. In order to establish the correspondence between electrophysiological and psychophysical measures of tuning, the equivalent task must be used in the two cases. One such method is to measure the equivalent of ‘psychophysical tuning curves’ on individual fibres of the auditory nerve, using a forward masking paradigm analogous to that used psychophysically. In such experiments, a pure-tone tuning curve is first determined for an auditory nerve fibre. The fibre is then excited by tone pips presented at a fixed intensity (e.g. 10 dB above threshold) at the characteristic frequency. As in the conventional psychophysical tuning curve, the response is masked by a tone that is varied in frequency, and adjusted in intensity, so that the constant tone pips produce a fixed, criterion, increment in firing above that produced by the variable masker. If forward masking is used, the resulting ‘psychophysical tuning curves’ are very similar to the corresponding excitatory pure-tone tuning curves (Fig. 9.4A; Harris and Dallos, 1979). On the other hand, if simultaneous masking is used, the single fibre ‘psychophysical tuning curves’ are wider than the pure-tone excitatory tuning curves (Fig. 9.4B). In this case, the masker is able to suppress the simultaneously presented probe, and we expect the psychophysical tuning curve, determined electrophysiologically, to be related to the fibre’s two-tone suppression areas (compare Fig. 9.4B with Fig. 4.14A; see caption of Fig. 9.4B for further details).

Figure 9.4C shows how closely these results relate to psychophysical data in human beings: tuning curves measured psychophysically by forward and simultaneous masking bear the same overall relation to one another as do the standard single-tone excitatory tuning curve and the ‘psychophysical tuning curve’ measured electrophysiologically by simultaneous masking. The difference between the two methods is particularly visible on the edge of the filter on the high-frequency side.

Therefore, where psychophysical filters are measured by simultaneous masking techniques, it is possible that the resulting filters will be wider than the underlying physiological filters as reflected in neural tuning curves, particularly on the high-frequency side. The extent to which this might occur is uncertain, because human psychophysical studies disagree on the exact extent to which filter bandwidths determined from simultaneous and non-simultaneous masking differ. The more recent data, using paradigms which would be expected to minimize the known artefacts in measuring psychophysical tuning curves, showed that the effective bandwidths determined with simultaneous masking were substantially greater (by an average of 75%) than those determined with non-simultaneous masking (Oxenham and Shera, 2003; Oxenham and Simonson, 2006). If this result is generally true, it suggests that simultaneous masking overestimates the bandwidths of the underlying physiologically defined cochlear filters.

Evidence from animals, where it is possible to measure both neural and psychophysical resolution in the same species, is contradictory. Pickles (1975, 1979)

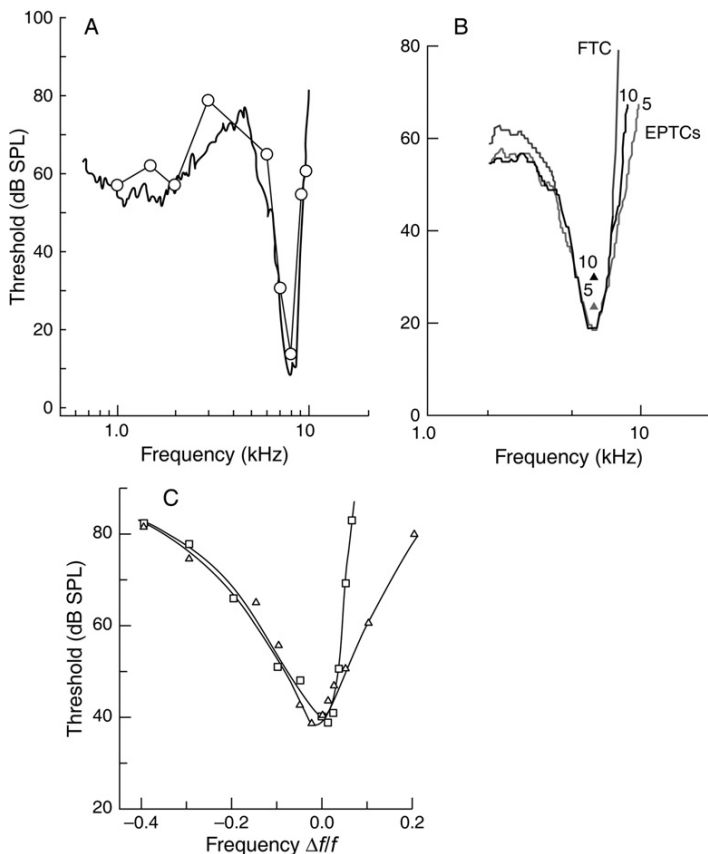


Fig. 9.4 Relation between auditory nerve tuning and ‘psychophysical tuning curves’ determined by forward and simultaneous masking. (A) The ‘psychophysical tuning curve’ determined by forward masking in a cat auditory nerve fibre (\circ) is similar to the conventional tuning curve (thick line). From Bauer (1978), Fig. 5. (B) ‘Psychophysical tuning curves’ (EPTCs) determined by simultaneous masking in an auditory nerve fibre are wider than the excitatory tuning curve (FTC). EPTCs for two probe levels, 5 and 10 dB above the fibre’s absolute threshold, are shown (numbers on curves). Measurements of firing rate showed that in determining the tuning curve, the response to the 5-dB probe was suppressed right down to the fibre’s absolute threshold; in this case, we expect the EPTC to follow a curve related to the outer edges of the fibre’s two-tone suppression areas. The response to the 10-dB probe was not suppressed to this extent; in this case, we expect the EPTC to follow a curve related to the greatest degree of suppression within the fibre’s two-tone suppression areas. The curves have been adjusted in level so that they coincide at the tip, to facilitate comparison of the shapes. Guinea pig. From Pickles (1984). (C) Psychophysical tuning curves in human beings, determined by simultaneous masking (Δ) are wider than those determined by forward masking (\square). The horizontal axis shows the masker frequency as a fractional deviation from the probe frequency. Note the similarity to the curves in panel B. Note that the frequency scale in panel C is expanded compared to that in panels A and B. Reprinted from Moore *et al.* (1984), Fig. 1, Copyright (1984), with permission from American Institute of Physics.

and Nienhuys and Clark (1979) in the cat, found that critical bands, measured behaviourally by simultaneous masking, had greater effective bandwidths than most auditory nerve fibres measured in the same species, suggesting that in this species simultaneous masking overestimates the width of the underlying cochlear filters. Similarly, in mice, Ehret (1976) found that critical bands were significantly wider than the mean excitatory bandwidths determined electrophysiologically (Egorova *et al.*, 2001, for the inferior colliculus). On the other hand, Kittel *et al.* (2002) in the gerbil found that psychophysical resolution bandwidths determined by simultaneous masking were similar to the bandwidths of auditory nerve fibres measured in the same species, suggesting that for this species at least simultaneous masking can be used as a good measure of peripheral resolution.

9.3.3 Frequency resolution in the auditory central nervous system

If the frequency resolution of the auditory system is originally set in the cochlea, it is pertinent to ask: does frequency resolution change as the signal is transmitted up the auditory pathway, and in particular, does lateral inhibition alter the frequency resolution shown by individual neurones? In this section, as in the last, we are considering frequency resolution, that is the ability to resolve a narrowband spectral component within a broadband stimulus, rather than frequency discrimination, which relates to the ability to distinguish two narrowband stimuli presented in succession.

The mean frequency resolution of later stages of the auditory pathway, as shown by the tuning curves of single neurones in anaesthetized animals, is in general similar to that of the auditory nerve, when the responses are measured with stimuli at or near threshold (Calford *et al.*, 1983). The result has been repeated by a number of different paradigms (Sayles and Winter, 2010; Mc Laughlin *et al.*, 2007; see also summary of data by Bartlett *et al.*, 2011). That is, the tips of the tuning curves, if used to define the bandwidth of an auditory filter (e.g. as $Q_{10\text{ dB}}$), have in general the same widths as those of auditory nerve fibres. This is true whether the nucleus shows a great deal of or low amounts of lateral inhibition (e.g. Goldberg and Brownell, 1973). However, there is a clear influence of lateral inhibition, in that where there are stronger inhibitory inputs onto a neurone, the response area tends not to widen at high stimulus intensities to the same extent as in the auditory nerve or in neurones without a lateral inhibitory input. Lateral inhibition therefore, while not generally increasing the fundamental frequency resolving power of the auditory system, helps to ensure that the fundamental frequency resolving power is made available to the system at all stimulus intensities.

Those results applied to mean data. There are exceptions, however. Some reports have shown that some neurones in the inferior colliculus have tuning curves that are narrower than those in the auditory nerve, sometimes dramatically so (e.g. in the cat, Aitkin *et al.*, 1975). Figure 6.27 shows an example for the moustache bat. Here, the neurones have sharper tuning curves than auditory nerve fibres. When inhibitory inputs within the nucleus are blocked by the local

application of the GABA-blocker bicuculline, the tuning curves widen a little, but are still sharper than those of auditory nerve fibres of the same characteristic frequency. In other words, some of the sharpening is produced by local inhibition within the nucleus, but even without this, the neurones have sharper tuning, which is possibly due to inhibition at other stages of the auditory system.

In unanaesthetized marmosets, Bartlett *et al.* (2011) also found some neurones with much sharper tuning, both in the medial geniculate body and in the auditory cortex. Moreover, the tuning was sharper than seen in anaesthetized animals. In the cortex, the sharp tuning was particularly shown in the sustained, rather than the onset, part of the response, suggesting that the sharp frequency selectivity might be developed over time by local cortico-thalamic or intracortical neural networks.

Bitterman *et al.* (2008) recorded single neurones from the primary auditory cortex (Heschl's gyrus; see Fig. 7.4) of human beings undergoing surgery to remove persistent epileptic foci. The patients passively listened to multitone complexes, with the notes varying randomly between presentations. By matching the neural response to the stimulus presented, and by varying the spacing of the tones, it was possible to determine the tone or tones that were driving the neurone, and its ability to distinguish one tone from another. The neurones could reliably distinguish frequency differences of less than 3%. This is finer resolution than expected from human critical bands (10–15% of the stimulus frequency) and comparable to the frequency discrimination (difference) limens sometimes seen in untrained human observers.

It should be remembered that auditory nuclei receive descending and reciprocal inputs from higher stages of the auditory system. Frequency representation in the inferior colliculus and medial geniculate can be modified as a result of electrical stimulation of the auditory cortex (see Chapter 8). The responses become modified so that greater numbers of neurones represent stimuli of significance for the subject (e.g. Edeline and Weinberger, 1991; Suga and Ma, 2003). It is reasonable to suspect that similar effects could also be produced within the auditory cortex by local intracortical circuits. These changes have the potential to enhance the frequency selectivity of the system to significant stimuli, and it is possible that some of the sharp resolution seen in the above studies may have resulted from such effects. The development of a relatively slow neural contribution to frequency selectivity may be responsible for the finding that for simultaneous masking with certain types of stimuli, the psychophysical frequency resolving power of the auditory system continues to improve for some hundreds of milliseconds after the onset of the masker (Bacon and Moore, 1986).

9.3.4 Co-modulation masking release: analysis across filters

In the model presented so far, listeners primarily make judgements using the output of a single psychophysical filter. However, there are indications that in some cases, subjects can make judgements across psychophysical filters, to pick out wideband spectrotemporal patterns. If a wideband masker undergoes temporal fluctuations, the masking of a narrowband signal is reduced, in the situation where

the fluctuations of the maskers in the different frequency bands are correlated in time, compared with the situation where they are uncorrelated (Hall *et al.*, 1984). The difference in threshold between the two conditions is known as co-modulation masking release. The frequency regions that contribute to the release from masking can lie well outside the same critical band, and therefore the auditory system must be able to make judgements by integrating information from more than one critical band.

Neurones that demonstrate co-modulation release from masking have been found in both the ventral and the dorsal cochlear nuclei. In the ventral nucleus, neurones with an onset (or transient) chopper response pattern, among others, show significant release from masking (Pressnitzer *et al.*, 2001). The cells tend to have narrow excitatory bandwidths, sometimes surrounded by wider inhibitory bands, so would be suited to picking out narrowband stimuli in the presence of wideband maskers. In the dorsal cochlear nucleus, Neuert *et al.* (2004) found release from masking in neurones that had a response area with an excitatory centre and inhibitory surrounds (i.e. Type II or III responses; see Fig. 6.9). We expect the release from masking to be generated as a result of inhibition by neurones, such as D-stellate cells (onset choppers), that integrate spectral information over a wide range of frequencies and that have rapid temporal responses so that their inhibitory outputs can follow the temporal fluctuations in the wideband masker.

A comparable release from masking has also been seen in the inferior colliculus. However, the phenomenon showed a great jump in strength in some neurones of the medial geniculate body and auditory cortex. In these areas some neurones showed an almost complete suppression of their response to a fluctuating noise envelope, when simultaneously stimulated with a much weaker tone. The suppression of the noise response took at least one cycle of the noise fluctuation to appear, far longer than the onset latency of the response to the noise, and therefore is likely to be a result of a higher-level response. It is quite possible therefore that it resulted from an enhancement, by cortico-thalamic or local cortico-cortico circuits, of responses to a signal that has been defined as a separate auditory object, and that has been extracted by a high-level process (Las *et al.*, 2005).

9.4 FREQUENCY DISCRIMINATION

9.4.1 Place and time coding

The frequency of a pure tone has a perceptual correlate known as its pitch. The frequency of a pure tone is represented in the cochlea by two mechanisms, namely the position of the travelling wave in the cochlear duct (place information) and the temporal pattern of vibration at any one point on the wave (timing information; see, e.g. Figs. 3.8 and 3.10). These two types of information are reflected in the activity of auditory nerve fibres, which are activated selectively according to their place of innervation along the cochlear duct, and by the time pattern of their

firings, at least for stimulus frequencies below the limit for phase locking, which is 5 kHz. It is reasonable to suppose that our perception of the frequency of a stimulus is dependent on one or both of these cues. In terms of place coding, a peak of activity on the basilar membrane would be sufficient to evoke a sensation of pitch. In terms of time coding, a central processor would measure the timing of the dominant intervals in neural activity and use the times to generate a sensation of pitch. Several lines of evidence have been used to assess the contribution of the two types of cue. The arguments in this section follow those given by Moore (2012), to whom the reader is referred for further information.

9.4.1.1 Frequency difference limens

If two pure tones of different frequency are presented successively, we have the opportunity to compare the patterns of excitation produced by the two tones. Figure 9.5 shows schematically how this could be done. The greatest changes in activity are produced on the low-frequency side of the nerve-fibre array (generated by the steep high-frequency slopes of the frequency response functions of the auditory nerve fibres). Since we know that human beings can detect about a 1 dB change in stimulus intensity, knowing the steepness of the frequency response functions, or in human beings, the steepness of the slopes of the psychophysical filters, allows us to predict the smallest frequency difference that can be detected (Zwicker, 1970; Heinz *et al.*, 2001). The difference limens calculated this way

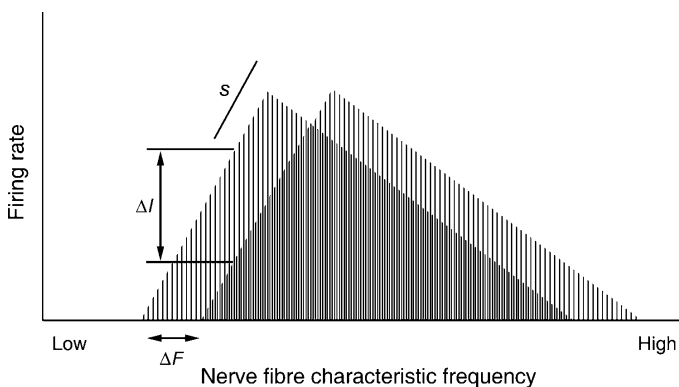


Fig. 9.5 The place mechanism of frequency discrimination, according to Zwicker (1970). The pattern of activity in the nerve fibre array is represented schematically by a series of vertical lines, each line representing the firing rate of one neurone to the stimulus. The neurones are arranged in order of ascending characteristic frequency. Shifts in the place of excitation are detected. The minimum frequency shift detectable (ΔF) can be predicted from the minimum intensity change detectable (ΔI : about 1 dB) and the slope (s) of the steepest part of the array, given by the high-frequency slopes of the auditory nerve fibre frequency response functions [$\Delta F = (\Delta I/s)$].

agree with (or are worse than) the values observed experimentally at very high frequencies, that is above 5 kHz. They also agree with the limens for detecting frequency modulation where the frequency of a steady sinusoid is modulated up and down 10 times or more per second. However, it seriously underestimates the ability of human beings to discriminate frequencies when the tones are presented successively and at a lower rate of variation, for stimuli of 2 kHz and below. This suggests that the place information is inadequate under these circumstances, with the corollary that it might be supplemented by temporal information.

9.4.1.2 Differences above and below 5 kHz

Differences in perception above and below 5 kHz suggest that timing information might be used in pitch perception below 5 kHz, in contrast to place information above. Timing information declines in the auditory nerve above 1 kHz and is lost by about 5 kHz. As an example, the sense of a melody disappears for tones above about 5 kHz. Subjects also find it difficult to adjust tones to octave intervals if the higher tone is above 5 kHz. And, as described in the last paragraph, frequency difference limens increase markedly around this limit.

9.4.1.3 The pitch of complex tones (the ‘missing fundamental’)

If tones such as 1000, 1200 and 1400 Hz are sounded together, a pitch corresponding to a tone of 200 Hz, which is not present in the stimulus, is also heard. The tones which are presented could be considered as the harmonics of the 200-Hz tone. The phenomenon is known as that of the ‘missing fundamental’ or as the ‘residue’. The low pitch is heard, even when masking noise is added to the stimulus that would be at a sufficient level to mask the low pitch, if it arose in response to an acoustic stimulus at the fundamental frequency. This suggests that it is not present in the response of the cochlea, but is generated more centrally in the central nervous system. In contrast to the position predicted by simple place theories, the pitch heard does not correspond to the position of the peak of activity on the basilar membrane, but to that of the construed low tone.

Two general types of theories have been used to account for residue pitch. In pattern theories, the central nervous system identifies the frequencies of the individual tones presented, and, recognizing that they could be the harmonics of a low tone, supplies the fundamental that could have generated them. These models require that at least some of the tones presented can be resolved by the auditory system. The harmonics which contribute most strongly to residue pitch are around the 3rd to the 5th. These harmonics for most frequencies are spatially resolved in the cochlea, and therefore could be used for pattern recognition. However, residue pitch can be perceived under some circumstances with stimuli which consist only of high, unresolved harmonics, that is in cases where pattern recognition is not possible (Houtsma and Smurzynski, 1990).

Alternative theories are temporal theories. A tone complex such as that described above will have a temporally repeating pattern at 200 Hz, which corresponds to the pitch heard. This pattern will be present in the time pattern of action potentials in auditory nerve fibres, if the patterns of excitation to the constituent tones overlap on the basilar membrane. Although the 3rd–5th harmonics are resolvable, they also overlap to some extent, and therefore could generate the temporal pattern corresponding to the low pitch. If a decision mechanism was able to measure the time intervals between corresponding points on the waveform, then it would generate intervals corresponding to the pitch heard. For this to occur, the central nervous system must be able to measure time intervals and use them to generate a sensation of pitch.

In some cases, weak pitches can be heard on the basis of purely temporal information, for example by noise being presented separately to the two ears, where there are certain relations between the stimuli at the two ears (reviewed by Moore, 2012). Where purely temporal information is presented by electrical stimulation of the cochlea through a prosthesis (the cochlear implant), a pitch sensation is perceived, though it is usually a weak one and with a harsh buzzing atonal quality. However, the place of stimulation has an influence as well: stimulation at sites more apical in the cochlea produces sensations with a lower ascribed pitch, although in this case the change is described more as one of timbre than of pitch (see Chapter 10).

The overall conclusion from psychophysical studies is that both place and time information can contribute to the perception of pitch. Moreover, for most naturally occurring sounds, it is the periodicity of the stimulus that makes the major contribution to the sensation of pitch (see, e.g. Schnupp *et al.*, 2011).

9.4.2 A psychophysical model for pitch perception and its relation to physiology

A current successful conceptual model of temporal pitch extraction was described by Moore with later modifications by others. In this model, the auditory stimulus is first filtered into channels by a set of bandpass filters, corresponding to the filtering of the stimulus on the basilar membrane. After neural transduction, and at some stage in the auditory nervous system, the intervals between action potentials are measured for each channel separately. The interval or intervals that are common across all channels are extracted, and a decision mechanism uses the most prominent interval or intervals to ascribe a pitch. This model therefore has timing information as the key element for pitch extraction. It explains all the main phenomena of pitch perception, in cases where stimuli are presented monaurally (see Moore, 2012; see also Schnupp *et al.*, 2011 for a further discussion of pitch in relation to its possible physiological basis).

Temporal models of pitch perception require that the temporal information is available to the pitch decision mechanism, over the frequency range of stimuli that give rise to the perception of residue pitch. The information has to be present in the output neurones of the previous stage, though it may not necessarily be

recordable by an experimenter at the decision stage itself. The required frequency range certainly includes 1 kHz and at its upper limit stretches to 5 kHz. The upper frequency limit of phase locking gradually declines through the auditory system, from 5 kHz in the auditory nerve and 4 kHz in the cochlear nucleus (Winter and Palmer, 1990), to 1 kHz in the medial geniculate (Rouiller *et al.*, 1979), and 250–300 Hz in the auditory cortex (Wallace *et al.*, 2002b).

In other words, at all stages after the cochlear nucleus, the upper frequency limit for phase locking is too low to account for the highest frequencies used in periodicity detection. Because the fast timing information is lost at later stages of the auditory system, it would be advantageous for the decision mechanism to be situated early in the auditory pathway, and for it to translate the information into a non-temporal code, such as a place-based code.

In the cochlear nucleus, chopper cells might at first sight appear to be strong candidates for cells that translate a timing code into a place-based code. In response to a sustained auditory input, they fire at a regular rate, which depends on the cell and is not primarily a function of the repetition rate of the stimulus itself (Fig. 6.6). It may be surmised that if the repetition rate of the stimulus coincides with the intrinsic repetition rate of the neurone, a particularly strong response will be produced. This indeed occurs; however, the resulting selectivity for time periods is very broad indeed (Kim *et al.*, 1990; Wiegrefe and Winter, 2001). With this very poor selectivity, it is difficult to see how different neurones could transform the time pattern of firings into a spatial code, sufficient to underlie a model with the high degree of selectivity as found psychophysically.

In the central nucleus of the inferior colliculus, a high proportion of cells show selective responses to the amplitude modulation of an ongoing stimulus (Langner and Schreiner, 1988). The responses are largest at certain frequencies of modulation, giving a bandpass characteristic (Fig. 9.6). These neurones would be able to extract temporal information in the stimulus, to affect the overall rate of firing. Given that different neurones are tuned to different frequencies of modulation, the neurones would be able to transform temporal intervals into a place code.

Although the results of Langner and Schreiner (1988) might suggest a mechanism for the periodicity detection that underlies the discrimination of pitch, in fact there are serious reservations. (1) Later researchers have not found best modulation frequencies over the range (up to 1 kHz) shown in Fig. 9.6. In one major study, only 2% of neurones had best modulation frequencies over 100 Hz (the highest was 140 Hz), and 50% of neurones had best modulation frequencies below 50 Hz (Krishna and Semple, 2000). Therefore the neurones do not nearly cover the range over which periodicity detection gives rise to the sensation of pitch in human beings or experimental animals where it has been tested (e.g. up to 5 kHz in cats; Heffner and Whitfield, 1976). (2) The tuning functions for best modulation frequency are very broad indeed – in most of the neurones illustrated in the study of Krishna and Semple, the bandwidth for 50% response was greater than 100% of the best modulation frequency (e.g. a neurone with a best modulation frequency of 50 Hz, might have response that falls to 50% of maximum at 20 and 150 Hz). It is difficult to see how, even with a great deal of averaging, this could produce discrimination limens of 1% or less. (3) The responses appear to be driven by the

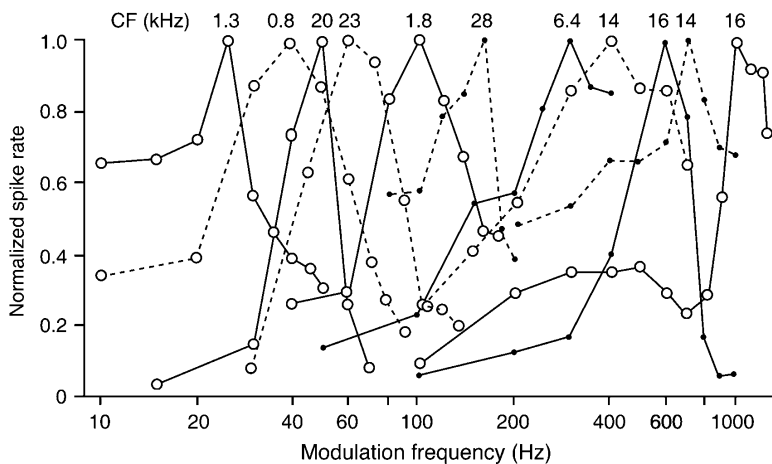


Fig. 9.6 Firing rate as a function of amplitude modulation frequency for neurones in the central nucleus of the inferior colliculus. Each neurone was stimulated by a tone (the carrier) at its characteristic frequency (in kHz, numbers on curves). The tone was modulated in amplitude at the frequency shown on the abscissa. For clarity, all curves have been scaled to the same maximum rate. Used with permission from Langner and Schreiner (1988), Fig. 3.

envelope of the stimulus, not to the individual waveforms within it. In other words they would not explain how the perceived pitch changes when the overall envelope is kept constant, but the frequencies of the tones within it are varied (Shackleton *et al.*, 2009).

In summary, while many experiments describe how timing information is transferred up the auditory pathway, they do not address the way that the pitch decision mechanism could operate in neural terms. This is likely to involve the cross-correlation or comparison of many different inputs by networks or by single cells; however cells or systems with appropriate properties have not been found. Overall, the conclusion is that no central mechanisms are known that might extract periodicity as a basis of pitch, in the way that is required by the models that are derived from psychophysics. Given the prominence of pitch in the subjective auditory experience, this mismatch is intriguing.



9.5 INTENSITY AND LOUDNESS

9.5.1 Stimulus coding as a function of intensity

The human auditory system is able to process signals over an enormous range of signal intensities, greater than 100 dB, and it is interesting to consider the neural

mechanisms that allow this, and the extent to which performance changes over the intensity range.

9.5.1.1 Frequency resolution and intensity

Above about 30 dB SPL, the vibration of the basilar membrane starts to saturate, that is starts to grow more slowly as a function of intensity (Fig. 3.13A). The tuning of the basilar membrane also broadens. That is shown in the iso-intensity functions of Figs. 3.10B and 3.11A. Both phenomena occur because the active amplification provided by the outer hair cells, which enhances the magnitude of the response around the peak of the wave, starts saturating at this level. Psychophysical filters in human beings also broaden with intensity. Rosen *et al.* (1998) reported that this change started at about 15 dB above the absolute threshold, which was the lowest level at which they could make measurements.

Figure 9.7 shows how the filter shape changes with intensity. It can be directly compared to the functions for the basilar membrane in Fig. 3.13B, which are plotted in a similar way, that is as a gain or (magnitude of response)/(stimulus intensity). In addition to the increases in bandwidth, both figures show that the peak gain decreases by about 20 dB for a 40 dB increase in stimulus intensity. It is

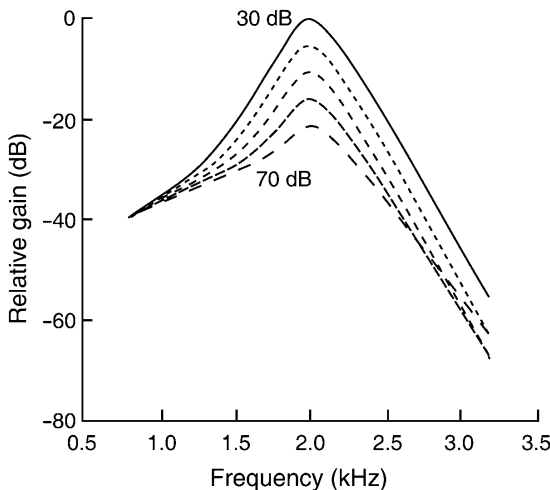


Fig. 9.7 Calculated changes in the shape and gain of the psychophysical filter in human beings, as a function of signal intensity. The curves have been adjusted along the vertical axis so that they coincide at low frequencies. Curves were derived from the mean results for three listeners. Probe frequency: 2 kHz. Filter shapes were determined by masking the probe with noise which has a spectral notch and by varying the bandwidth and frequency position of the notch. Reprinted from Rosen *et al.* (1998), Fig. 7, Copyright (1998), with permission from American Institute of Physics.

reasonable to suppose that these results directly reflect changes in cochlear frequency resolution.

To what extent are auditory nerve fibres able to signal the frequency resolution of the cochlea to the auditory central nervous system over this wide range of stimulus intensities? The firing of the auditory nerve fibre in Fig. 4.6A saturates, that is reaches a clear maximum, at around 30 dB SPL for tones at its characteristic frequency. Frequency resolution as reflected only in the mean firing rate of this fibre will start to deteriorate beyond that point, due to saturation of firing, in addition to that imposed by the non-linearity of the basilar membrane. The combined effect of basilar membrane non-linearity and saturation of firing are shown in the iso-intensity plots of auditory nerve firing in Fig. 4.7B, indicating a marked widening of the response area, and concomitant reduction in frequency selectivity as shown in the mean firing rate of this fibre, as the stimulus intensity is raised.

However, there is a 60-dB to 80-dB spread of thresholds for nerve fibres of any one characteristic frequency (Fig. 4.4). This occurs because the different synapses on each inner hair cell have different sensitivities (see Chapter 4). Nerve fibres with high thresholds, that is in the intensity range in which the basilar membrane response grows slowly as a function of stimulus intensity (e.g. above about 30 dB SPL in Fig. 3.13A), will have a correspondingly slow growth in their own responses with stimulus intensity. This will extend their dynamic range to higher stimulus intensities. These fibres are said to show ‘sloping saturation’ or sometimes ‘straight’ functions (Fig. 4.6B). The high-threshold fibres will be more closely able to reflect the details of basilar membrane vibration, and hence basilar membrane frequency resolution and small changes in stimulus intensity, even at high stimulus intensities. However, it is still a matter of debate as to whether the information in their mean firing rates is sufficient, given the small numbers of these fibres and the shallowness of their rate-intensity functions (e.g. Colburn *et al.*, 2003).

9.5.1.2 Two-tone suppression and lateral inhibition

Could two-tone suppression in the cochlea further extend the dynamic range of auditory nerve fibres? After all, lateral inhibition in vision preserves the response to a pattern relatively unchanged over a wide range of overall light intensities. However, two-tone suppression in the cochlea operates rather differently. It arises because the active amplification of the mechanical stimulus on the basilar membrane is reduced by the suppressing stimulus, so decreasing the magnitude of the response to the suppressed stimulus. In some cases, this can indeed extend the dynamic range – for instance, where there is a strong narrowband stimulus such as a tone presented in a lower level broadband background. As an example, Costalupes *et al.* (1984) recorded the response of auditory nerve fibres to tones in background noise and showed that the background noise could shift the rate-intensity functions to the tones upwards by as much as 30 dB. However, with complex stimuli having many frequency components, such as speech, two-tone suppression can reduce the

dynamic range. The response to some critical stimulus components can be suppressed by the other stimulus components. At high stimulus intensities, this can flatten out the separate peaks of activity in the auditory nerve fibre array produced by the spectral peaks in the stimulus (Sachs and Young, 1979; see Section 9.7.2.1).

Lateral inhibition in the cochlear nucleus and in the later stages of the auditory system can however act powerfully in preserving the dynamic range. This can of course only occur if the information is present in the auditory nerve in the first place (probably in the high-threshold fibres). Cells with an excitatory centre and inhibitory sidebands will be very effective at picking out differences in activity and representing them as peaks of excitation separated by regions of inhibition (Fig. 9.8). Cells with this property include the Type II or Type III cells, which are found widely in the cochlear nucleus. This information will be preserved in later stages of the auditory nervous system and strengthened in those nuclei, such as the inferior colliculus, that show enhanced degrees of lateral inhibition. Cells in the inferior colliculus appear to be able to adapt their sensitivity not only to the mean

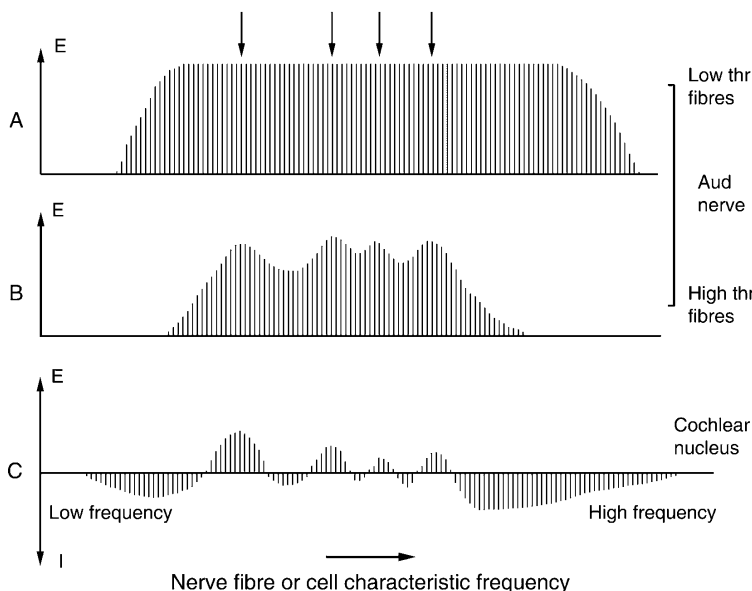


Fig. 9.8 Schematic response of different groups of auditory nerve fibres and cells of the cochlear nucleus to a high-intensity complex stimulus with four spectral peaks (marked by arrows). Nerve fibres or cells are represented in order of characteristic frequency, and the height of each line indicates the amount of activity in each fibre or cell. (A) At high stimulus intensities, the firing in low-threshold fibres is saturated, and no separate peaks of activity are visible. (B) However, peaks of activity are visible in the responses of the high-threshold fibres. (C) In the cochlear nucleus, the spectral peaks are clearly preserved, as a result of lateral inhibition.

level of the stimulus, but to other properties such as its variance, in such a way as to respond optimally to the stimuli presented (Dean *et al.*, 2005).

The preservation and enhancement of spectral features by these mechanisms are an example of the way that the auditory central nervous system recodes stimuli so as to emphasize their critical features.

9.5.1.3 Role of temporal information

Timing information is preserved in the firing of auditory nerve fibres, even though the mean rate has saturated. Figure 4.8 shows how the period histogram of the response to a low-frequency tone continues to follow the sinusoidal shape of the stimulus waveform, even at high stimulus intensities. In response to complex stimuli, with multiple frequency components, and under some circumstances, the phase locking to each of the components considered separately, is proportional to the strength with which that frequency component drives the fibre. Mathematical techniques which relate the time pattern of firings to the temporal structure of the stimulus waveform can be used to show that the drive to the fibre is still tuned according to the pattern of vibration on the basilar membrane, even though the stimulus intensity is well into the range in which the fibre's firing is saturated (Section 4.2.3).

Is temporal information in fact used in this way to reveal frequency resolution? The auditory nerve does not phase-lock above 5 kHz, so that if performance deteriorates with intensity more above, than below, this frequency limit, the implication is that timing information might be used below the limit. Moore (1975) found that masked thresholds increased with intensity more above, than below, the 5-kHz frequency limit. Also, many conceptual models of auditory processing include timing information and obtain matches to psychophysical data that are closer than those obtained using only mean rates of firing (e.g. Colburn *et al.*, 2003; Tan and Carney, 2006). However, it is very difficult to obtain definitive evidence that timing information is actually used in this way.

One type of model uses the temporal relations between the firings in different neural channels, that is spatiotemporal information, to extract information about the stimulus. A simple and physiologically realistic way of doing this, and which enhances rate-place information in the cochlear nucleus, was proposed by Shamma (1985a,b). Shamma pointed out that the relative timing of nerve action potentials in the different fibres of the auditory nerve would be affected by the place of activation along the cochlea. The cochlear travelling wave shows large phase shifts near its peak of vibration. Nerve fibres innervating adjacent regions near the peak will therefore tend to be activated in different phases of the input stimulus. Cells in the cochlear nucleus show lateral inhibition, so that they are excited by nerve fibres innervating one region of the cochlear duct and inhibited by nerve fibres from adjacent regions. If the spatial separations of the excitatory and inhibitory inputs from different parts of the cochlea are suitable, it is possible that excitation will be transmitted in one phase of the stimulus, while the inhibition from adjacent regions is transmitted in the opposite phase. The net effect is that the (opposite) excitatory

and inhibitory phases of the waveform will summate, giving large fluctuations of excitation and inhibition in the cell during a cycle of the stimulus (Fig. 9.9). Phase-locked responses in the cell will be thereby enhanced. If the mean firing rate responds non-linearly to changes in membrane potential, the fluctuations will be reflected in an increase in the mean rate.

However, where nerve fibres are activated towards the tail of the travelling wave, where phase changes are smaller as a function of distance, excitation and inhibition will tend to arrive with similar phases at cells of the cochlear nucleus, and the net response of the cell will be small.

Simulations of the model shows that it can preserve the spectral information present in a complex stimulus in the cochlea, over a wide range of intensities, even when the intensity is so high that it has been lost in the mean-rate information in the auditory nerve (Shamma, 1985b). A more recent analysis of the actual spatiotemporal patterns of firing of auditory nerve fibres by [Cedolin and Delgutte \(2010\)](#) showed the information in the combined spatiotemporal array, based on

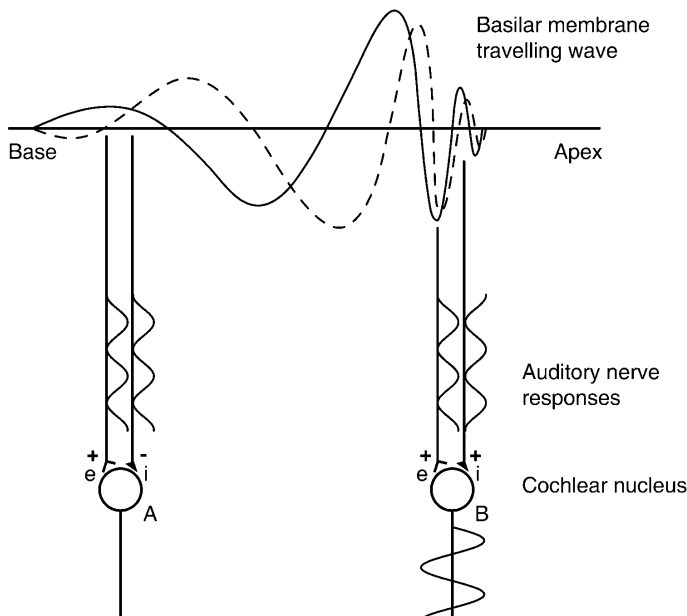


Fig. 9.9 Phase shifts in the travelling wave, combined with lateral inhibitory interactions in the cochlear nucleus, could decode timing information into place information, according to the theory presented by Shamma. Excitatory (e) and inhibitory (i) synapses on neurone A are activated with similar phases, so their effects cancel (+, -). However, excitatory (e) and inhibitory (i) synapses on neurone B are activated in opposite phases, so the responses summate (+, +). Open symbols, excitatory synapses; filled symbols, inhibitory synapses. Reprinted from [Shamma \(1985a\)](#), Fig. 4c, Copyright (1985), with permission from American Institute of Physics.

phase-locked firing and phase shifts along the fibre array, was indeed more invariant with stimulus level than with a simple rate-place representation.

Other types of model extract timing on the basis of the repetition rates or timing intervals of action potentials within the same, rather than across, neural channels. However, as pointed out in Section 9.4.2, neural substrates for temporal detection are not known.

Overall, models incorporating temporal information have two general problems: (i) that of proposing a neural basis for the extraction of the temporal information that is realistic in physiological terms and (ii) obtaining clear and independent physiological evidence that the models are actually valid.

9.5.1.4 The middle ear muscle reflex

Sound-elicited contractions of the middle ear muscles may attenuate the sound input by as much as 20 dB. Such powerful control will only be expected to occur for sound frequencies in the range where transmission is strongly affected by the middle ear muscle reflex, that is below 1 kHz (Chapter 2). It will not explain the wide dynamic range of hearing for frequencies of 1 kHz and above.

9.5.1.5 The olivocochlear bundle

The olivocochlear bundle attenuates the responses of auditory nerve fibres by reducing the degree of active amplification of the travelling wave in the cochlea. Stimulation of the olivocochlear bundle can enhance the contrast in a spectral pattern for certain types of stimuli at high intensity and give a small increase in the upper limit of the dynamic range (Fig. 8.6; Winslow and Sachs, 1987; Kawase *et al.*, 1993). However, observations in human beings with unilateral lesions of the olivocochlear bundle have shown no changes in the dynamic range on that side (Scharf *et al.*, 1997). The possible mechanism was discussed in Chapter 8.

9.5.1.6 Conclusions

At high stimulus intensities, changes in psychophysical frequency resolution reflect the changes in the frequency resolution of the cochlea. However, the way that the auditory nerve transmits spectral information in this intensity range has not been definitively explained. Plausible hypotheses suggest that information in the time pattern of neural firings is used together with the information from small variations in mean firing rates (based on a range of thresholds in auditory nerve fibres, sloping saturations of the rate-intensity functions and two-tone suppression). The middle ear muscle reflex and possibly the olivocochlear bundle may also contribute.

9.5.2 Loudness

It has been suggested that the sensation of loudness depends on the total sum of activity transmitted in the auditory nerve (e.g. [Wever, 1949](#)). While this is likely to be true in general terms, it may not hold up in detail. The hypothesis moreover does not inform us about all the actual physiological mechanisms determining the sensation of loudness, which are likely to have a contribution from central processes.

Loudness can be assessed by asking the subject to adjust the levels of two stimuli so that one seems for instance twice as loud as the other. Clearly, this is a very subjective judgement, and one amenable to many biases. The overall conclusion is that, for stimuli above about 40 dB SPL, a 10-dB increase in intensity generates approximately a doubling of loudness. Given that $\log_{10}(2)$ is approximately 0.3, this means that the amplitude of the loudness can be written as, $\text{Loudness} = k \times \text{Intensity}^{0.3}$, where k is a constant.

This suggests that the activity generating the sensation of loudness is a compressive function of stimulus intensity.

In some ways, the growth of loudness mirrors the responses of the auditory periphery. As shown in Fig. 3.13A, above about 30 dB SPL, the amplitude of vibration on the basilar membrane grows non-linearly with stimulus intensity, with a compressive relation and with a slope of about 0.3. Further stages of compression are the hair cell neural synapse, and all neural stages thereafter.

The growth of loudness mirrors other aspects of the response at the auditory periphery as well. Near threshold, and to a lesser extent at very high stimulus intensities, loudness grows more steeply with stimulus intensity (see, e.g. [Moore et al., 1997](#), Fig. 12). Similarly, basilar membrane intensity functions grow more steeply at very low stimulus intensities, that is before the outer hair cells have started to saturate, and there is evidence from some researchers that it may start to grow more steeply again at very high intensities, when the passive component of basilar membrane vibration overtakes the saturating active component (see Chapter 3 and Fig. 5.23).

The concepts described above have been applied to a quantitative model, where the possible physiological correlates of each stage have been spelled out. After an initial compressive stage, corresponding to the non-linear growth of the basilar membrane, the stimulus is detected by multiple auditory nerve fibres (or in psychophysical terms, by multiple psychophysical filters), and the outputs of all the filters summed. The parameters of the model have been chosen so as to fit the empirical data most closely: the rate of growth of the amplitude on the basilar membrane has been chosen to be 0.2 dB/dB, rather than the value 0.3 dB/dB which is observed in many animal studies (see Chapter 3). This value was chosen because it generates a growth of loudness at the final output of the model which increases as $\text{Intensity}^{0.3}$, in closest accordance with the psychophysical findings ([Moore et al., 1997](#)).

Other aspects of loudness judgements have a correlate in the responses in the auditory periphery. [Zwicker et al. \(1957\)](#) asked subjects to judge the overall loudness of a band of noise, of constant total power, but variable bandwidth. They

found that when the band of noise was narrower than the equivalent bandwidth of one psychophysical filter, the judgement of loudness was independent of the bandwidth of the noise. However, if the noise was spread beyond one psychophysical filter, the loudness increased, even though the total power of the noise remained the same (Fig. 9.10A). This can be seen as another expression of the amplitude compression mentioned above, where a greater total response is produced by putting half the total energy into each of two channels, rather than concentrating it all on one channel.

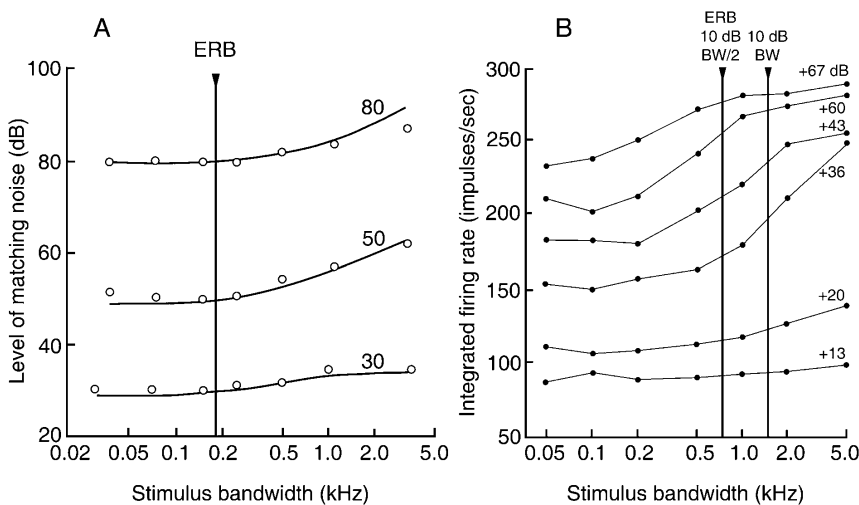


Fig. 9.10 (A) Judgement of loudness of a band of noise of constant power, but variable bandwidth. The band was matched in loudness to a 210-Hz wide band centred on the test frequency. The loudness stays approximately constant for bandwidths narrower than the width of a single psychophysical filter (ERB, arrowhead) and increases for wider bandwidths. ERB: equivalent rectangular bandwidth calculated for a psychophysical filter centred on the test frequency (1.42 kHz). Numbers on curves: total signal level in dB SPL. Solid lines: predictions from model of Moore *et al.* (1997). Data points from Zwicker *et al.* (1957). From Moore *et al.* (1997), Fig. 14. (B) Integrated firing rate of an auditory nerve fibre, as a function of stimulus bandwidth, for noise bands of constant total intensity. The integrated firing rate was calculated as described in the text. The numbers marked on the curves show the stimulus intensity, with respect to the fibre's absolute threshold. Near threshold, the integrated firing rate is relatively independent of stimulus bandwidth. At higher intensities, the integrated firing rate increases with stimulus bandwidth. The ERB of a fibre is expected to be about half the 10-dB bandwidth (arrowhead: 10-dB bandwidth, that is the bandwidth of the tuning curve measured 10 dB above the tip). Unlike in the original publication, a logarithmic scale of stimulus bandwidth is used, so that the results are more easily comparable with panel A. Fibre characteristic frequency: 3.76 kHz. Data from Pickles (1983), Fig. 2.

Pickles (1983) imitated the paradigm in measuring the responses of single fibres of the guinea pig auditory nerve. Instead of measuring the responses of many fibres to a band centred on one frequency, the converse experiment was performed, of measuring the response of one fibre to bands of noise centred on many frequencies, and summing the results. The results have the advantage that between-fibre variability is eliminated and give results for an array of fibres each of which is identical to the fibre being stimulated. In this case, as with the experiment of Zwicker *et al.*, the summed activity tended to remain constant for narrow stimulus bandwidths and increased for wider bandwidths, even though the total stimulus power remained constant. The curves followed the psychophysical results at least in the low and middle range of stimulus intensities (Fig. 9.10B).

Although the above model fits with the physiological data in general terms, it may not always agree quantitatively and in detail. Relkin and Doucet (1997) presented a method for measuring the total integrated activity of auditory nerve fibres, by measuring the gross potentials of the auditory nerve. They found that the total auditory nerve response grew with a slope that was about half that expected if loudness was proportional to the total activity in the auditory nerve.

Relkin and Doucet pointed out another problem. Although human beings are able to match the loudness of intense low-frequency tones to those of intense high-frequency tones, this is not always possible when considering the integrated activity of the auditory nerve. The reason is that intense low-frequency tones activate a large stretch of the basilar membrane, while intense high-frequency tones activate a much shorter stretch. This means that there are certain low-frequency tones which can never be matched in total activity by intense high-frequency tones, because the high-frequency tones can never generate enough total activity.

It is also highly likely that transformations of the auditory stimulus by the central nervous system play a critical part in determining the loudness of stimuli. Using functional magnetic resonance imaging (fMRI), Röhl and Uppenkamp (2012) looked at individual differences in the magnitude of the responses to noise and compared them with individual differences in the judgements of loudness. They found that when comparing different individuals, variation in the magnitude of the fMRI signal in the auditory cortex was related to variation in the subjective magnitude of the loudness. This relationship was not observed at lower levels of the auditory system, where the responses were more closely described by the physical parameters of the stimulus than by its subjective loudness.

Retro-cochlear tumours, such as vestibular schwannomas (also known as acoustic neuromas), that grow in the sheath of the vestibular nerve and affect hearing by pressing on the cochlear nerve and associated brainstem nuclei, can lead to an unusually slow growth in loudness, presumably because of decreased activity in the affected structures (e.g. Nieschalk *et al.*, 1999). This is in contrast to sensorineural hearing loss arising in the cochlea, which tends to lead to over-recruitment, that is abnormally rapid growth of loudness with stimulus intensity (see Chapter 10).

9.6 SOUND LOCALIZATION AND SPATIAL HEARING

9.6.1 Introduction

A sound source in space will stimulate both ears. Experiments with headphones have suggested that the side on which a source is heard depends on timing and intensity differences at the two ears. A sound source on one side will stimulate the nearest ear first, because the sound path to that ear is shorter (Fig. 9.11A). This cue is particularly important for low-frequency sounds, because with low-frequency sounds, the phase differences at the two ears produced by the difference in path length are unambiguous. The intensity at the nearest ear will also be greater, because the farther ear is shadowed by the head. The degree of shadowing will be greatest at high frequencies, because of the reduced diffraction, that is the reduced bending of the sound waves around the head, at high frequencies. Localization depending only on these binaural cues lead to potential ambiguities, because they do not give information on the elevation of a sound source, or whether the source is in front of or behind the head. Information on these is contributed by the pinna, which for high-frequency sounds produces further shadows and reflections (see

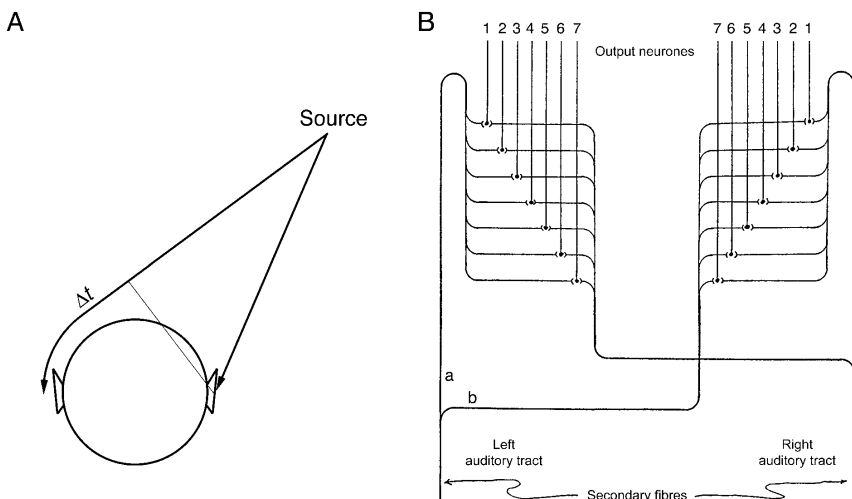


Fig. 9.11 (A) Sounds from a source to one side of the head will strike the nearer ear first (Δt : extra delay to farther ear) and will also be more intense in the nearer ear. (B) Jeffress's model of sound localization, based on neural delay lines. The output neurones marked '1' have the shortest neural paths from the ipsilateral side and the longest paths from the contralateral side. If the output neurones are driven by coincidence in their inputs, they will be activated when the difference in neural delays exactly compensates for the interaural delay Δt . Therefore different output neurones will code different directions of the sound source. Reprinted from Jeffress (1948), Fig. 1, by permission of the American Psychological Association.

Chapter 2; Fig. 2.2). The cues from the pinna also mean that some localization is possible when using only one ear.

Models for sound localization based on these and similar observations have an extensive history. They fall into four groups (see, e.g. Colburn and Kulkarni, 2005).

1. In models of the first group, the inputs from the two ears are cross-correlated, with differences in timing being picked out in such a way as to produce a maximum response in the channel coding the direction of the source.
2. In second type of model, differences in intensity are used to produce a maximum response in the channel coding the direction of the source.
3. In the third class of models, the overall levels of neural activity in the inputs from the two sides are compared and used as the basis for a decision.
4. The above models all deal with localization in the horizontal plane and comparisons of inputs from the two ears: localization in the vertical plane, and removal of in-front/behind ambiguities, require additional mechanisms.

9.6.2 Mechanisms of sound localization

9.6.2.1 Cross-correlation: timing cues

With ongoing stimuli in the frequency range for phase locking, differences in the times of arrival of the stimuli at the two ears produce a difference in the phase of stimulation at the ears. In the model of Jeffress (1948), this is detected by the input from one ear being compared with multiple time-shifted versions of the input from the other ear. The time shift that produces the maximum degree of similarity indicates the direction of the sound source in the horizontal plane. In the formulation of Jeffress, the time shifts are produced by axons of different lengths. The output neurones detect coincidence in the time-shifted inputs from the two ears (Fig. 9.11B). The circuit in Fig. 9.11B is repeated for each frequency band in the range in which timing cues are used for localization.

The model has considerable support in birds. In the external nucleus of the barn owl's homologue of the inferior colliculus, the nucleus laminaris, the neurones form a map of auditory space, with the timing cues decoded by differences in path length (Overholt *et al.*, 1992; for review, see Konishi, 2003).

Some aspects of Jeffress's model are applicable to mammals. In the mammalian medial superior olive, which predominantly represents low frequencies, neurones are indeed driven by stimuli from the two ears, with different neurones having different relative delays of activation from the two ears (Fig. 6.18). As described in Chapter 6, the cells act as temporal coincidence detectors, so that when stimuli have the optimum relation between their delays, the response to the two stimuli together can be greater than the sum of the responses to the stimuli presented separately. When in the optimum relation, binaural stimuli can drive the neurones far harder than even more intense monaural stimuli (Fig. 6.18B). Similarly, at the minimum, the response is less than the response to either separately. This shows that when the stimuli coincide, the interaction is one of facilitation rather than

simple summation. Different neurones have different characteristic delays, that is different delays between the inputs from the two ears, as expected from the model. Cells respond preferentially to sounds on the contralateral side of the head, not surprising as the stimuli arrive earlier at the contralateral ear. The earlier arrival time is compensated for by the longer neuronal pathways from the contralateral side (Fig. 6.15B).

However, in mammals, there are two major problems with the applicability of the model.

9.6.2.1.1 Generation of characteristic delays. In the original model of Jeffress (1948), the differences in times of arrival from the two ears arose from systematic variation in the lengths of axons from the two ears. Anatomical studies in mammals of inputs from the anteroventral cochlear nucleus to the medial superior olive have indeed shown a gradient in axonal lengths, particularly from the contralateral side (Beckius *et al.*, 1999). However, Beckius *et al.* also found considerable scatter in the path lengths and in the travel times that they calculated from the anatomical data, and suggested that further factors must affect the responses, to produce the characteristic delays that have been observed physiologically.

The critical delays may in fact arise from a separate inhibitory input. If the glycinergic inhibitory inputs to cells are blocked by the application of strychnine, the characteristic delays shift to zero (Brand *et al.*, 2002). The inhibition has to arrive in the correct temporal window, because if the glycine is applied tonically, the characteristic delays also shift towards zero (Pecka *et al.*, 2008). It was suggested that fast and temporally precise inhibitory inputs via the LNTB and MNTB instead drive the coincidence detection (for review, see Grothe *et al.*, 2010). A further suggested factor is that asymmetric terminations of the input axons on the cell bodies of the MSO may generate some of the asymmetric delays in response to stimuli from two sides (Zhou *et al.*, 2005).

9.6.2.1.2 Range of characteristic delays. A second issue with the physiological realization of Jeffress's model is that many of the characteristic delays found physiologically are outside the range required by the model. In the original formulation, the different characteristic delays cover the range of delays expected to arise from single sound sources external to the head, that is the delays that could arise from the potential range of different travel times to the two ears. In fact, in the guinea pig and cat, many cells have characteristic delays that are much greater. Figure 9.12 shows data on this point obtained in the inferior colliculus, where the methodological problems of recording are much less than in the medial superior olive, but where we expect the binaural responses to follow the pattern set in the superior olive.

This is particularly marked in the guinea pig, where the head is smaller than in the cat, but the distribution of characteristic delays is almost the same. Figure 9.12A shows that for cells responding preferentially to stimuli on the contralateral side, 85% of cells in the guinea pig and 49% of cells in the cat have characteristic delays that are larger than the delays that could have been produced by single sound sources

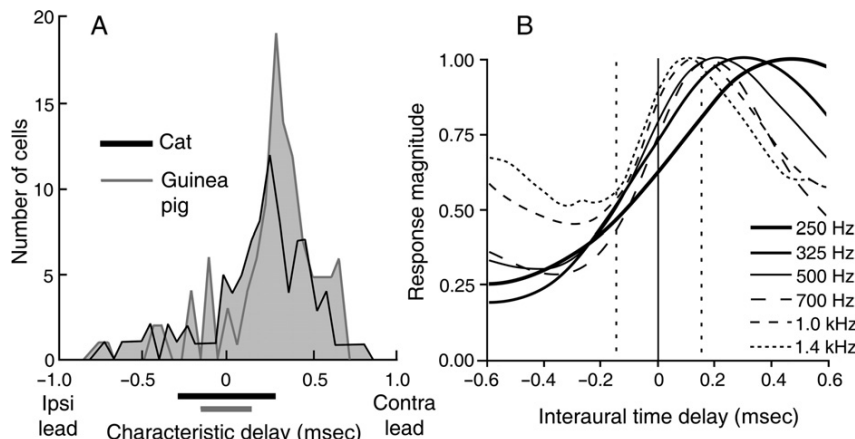


Fig. 9.12 (A) In the cat and guinea pig, many binaural cells have characteristic, or best, delays that are larger than needed to match the delays that could be produced by sound sources external to the head. The figure shows the distribution of characteristic delays, for sound stimuli to the two ears, measured in cells of the inferior colliculus. Like the medial superior olive, the inferior colliculus preferentially represents sounds on the contralateral side. The distributions peak at around 320 μ sec. The range of delays expected for sound sources external to the head are marked by the horizontal bars (closed bar: cat, $\pm 300 \mu$ sec, Hancock and Delgutte, 2004; grey bar: guinea pig, $\pm 150 \mu$ sec, McAlpine *et al.*, 2001). Data from Palmer *et al.* (1992) (guinea pig), which includes data from Yin *et al.* (1986) in the cat. (B) Firing rates as a function of interaural delay, averaged over neurones with characteristic frequencies in different bands (250 Hz–1.4 kHz). The curves have been normalized to the same maximum firing rate. The greatest slopes of the functions are found nearest 0 μ sec interaural delay. Moreover, neurones of low characteristic frequency tend to have longer characteristic delays. Inferior colliculus; guinea pig. Dotted lines: the range of delays expected for single sound sources external to the head. From McAlpine *et al.* (2001), Fig. 3b.

external to the head. Similar findings have been made in other species (see, e.g. Fig. 6.18). For the cells that lie outside this range, the cells can represent only which side of the head the source is on, and not its actual angle. However, when the functions relating firing rate to binaural delay are plotted, the functions usually have their steepest slopes near zero delay. And as shown in Fig. 9.12B, the characteristic delay is systematically dependent on the cell's characteristic frequency, so that the steepest slopes are always around zero delay at the cell's optimal frequency of stimulation. The result is that these cells are also most accurate at detecting small deviations in direction around the midline (McAlpine *et al.*, 2001).

It should be remarked that the distribution of characteristic delays has been generally found to be invariant with species, in spite of differences in head size. If the same range of delays occurs in human beings, with their larger head sizes, then sound sources which are in different directions in the horizontal plane would preferentially activate different neural channels.

The above model detects coincidences of neural firing from the two ears. The coincidence detection occurs in the medial superior olive and can be considered to be related to a multiplication of activity. However, temporal effects have also been found in the lateral superior olive, although the nucleus primarily extracts differences in interaural intensity. The contralateral input arrives via an inhibitory synapse from the medial trapezoid body. As described in Chapter 6, this input is delayed by on average 200 μ sec with respect to the excitatory ipsilateral input (Joris and Yin, 1998). Therefore, for maximum inhibition of the ipsilateral response, the contralateral stimulus has to be applied 200 μ sec before the ipsilateral one. Maximum inhibition will therefore occur when the sound source is on the contralateral side of the head, with the result that cells of the lateral superior olive have overall best excitation with sound sources on the ipsilateral side.

With low-frequency stimuli in the (relatively few) low-frequency cells of the lateral superior olive, the temporal effects can be seen on a cycle-by-cycle basis and can summate with cues arising from intensity differences. Above the frequency range for phase locking, with high-frequency stimuli and in the high-frequency cells of the lateral superior olive, the temporal effects will be detectable in the onset responses and in temporal fluctuations of the stimulus envelope (Tollin and Yin, 2005).

9.6.2.2 Binaural intensity cues

Differences in stimulus intensity at the two ears will be greatest for high-frequency stimuli, because sound waves are least able to bend, or diffract, around the head at high frequencies. As described in the previous section and in Chapter 6, differences in intensity at the two ears are extracted in the lateral superior olive (LSO). Because cells of the LSO are excited by activity from the ipsilateral ear, and inhibited by activity from the contralateral ear, the LSO preferentially represents sounds on the ipsilateral side of the head. The intensity effects will therefore summate with the timing effects described in the previous paragraph. The LSO then projects to the contralateral inferior colliculus, so that the colliculus represents the contralateral side of space. Here its responses summate with an uncrossed projection from the medial superior olive which also represents the contralateral side of space. Because the LSO is mainly a high-frequency nucleus (Fig. 6.14B), it is most effective at extracting cues in the frequency range where the intensity cues are greatest.

In mammals such as bats, cats and rodents, the LSO is much larger than the medial superior olive (MSO), commensurate with the high-frequency range of these species and with the dominance of binaural intensity cues at high frequencies. However, in human beings the position is reversed, with the LSO being small and the MSO much larger. This is in agreement with the generally lower-frequency range of human beings, and with the consequent presumed greater importance of timing cues in sound localization. While some previous reports suggested that human beings do not have an MNTB (which gives inputs to the LSO and MSO), it now appears that this is not the case, and resulted from difficulties in identification (Grothe *et al.*, 2010).

9.6.2.3 Comparison of activity on the two sides

A further class of models suggests that direction is assessed from the relative amounts of total activity in hypothetical neural populations driven by sounds on the left, or on the right, sides of the head (e.g. [van Bergeijk, 1962](#)).

As was pointed out above, in small mammals, the majority of cells have characteristic delays that are larger than would be required to match the delays generated by sound sources external to the head (e.g. for the guinea pig data shown in Fig. 9.12A). These cells would therefore be only able to signal whether a source was on the left or on the right and would not be able to signal its direction more precisely. However, the balance of activity between the left and right sides of the brain, as seen in the total neural population responses, would be able to indicate the direction more precisely. In addition, in the majority of cells, the steepest part of the functions relating firing rate to interaural delay falls near the point of zero delay ([McAlpine et al., 2001](#)). The balance of total activity between the two sides of the brain would change most rapidly as sources moved across the midline, meaning that the discrimination of directions would be most accurate for sources which are most nearly straight ahead. This is indeed the case ([Mills, 1958](#)). Functionally, this would be extremely valuable in guiding a behavioural orientation of the head towards a sound source after a cruder estimation of direction has been obtained by other means.

This model requires that at some stage or stages in the auditory system, neural networks are available for comparing the levels of activity on the two sides of the brain. The dorsal nucleus of the lateral lemniscus (DNLL) appears to be one such stage. As described in Chapter 6, it receives inputs bilaterally from the superior olivary complex and the contralateral cochlear nucleus, as well as receiving an inhibitory input from the contralateral DNLL. Most neurones of the DNLL are sensitive to interaural time and level differences such that they represent sounds on the opposite side of the head ([Kuwada et al., 2006](#)). The interactions within the DNLL and between the DNLL of the two sides serve to increase the accuracy, contrast and dynamic range of the localization information, compared with that found in the superior olive ([Pecka et al., 2010](#)). The crossed inhibitory input from the contralateral DNLL to the inferior colliculus further increases the neural contrast between the responses to sound sources localized in different positions in the horizontal plane. If the crossing paths are interfered with, by either chemical or surgical lesions, the animals' ability to localize sounds behaviourally is substantially reduced (see Chapter 6; [Kelly, 1997](#)).

9.6.2.4 Localization in the vertical direction

The pinna introduces cues which allow localization in the vertical direction and which also permit distinctions to be made between sounds in front of and behind the head. The pinna introduces spectral notches in the frequency response of the outer ear, the exact frequency at which the notches occur being dependent on the elevation of the sound source (Fig. 2.2B). These cues appear to be decoded at least in part within the dorsal cochlear nucleus (see Chapter 6). Lesions of the output

pathways of the nucleus, the dorsal and intermediate acoustic striae, mean that animals lose the ability to make reflexive responses dependent on the elevation of sound sources. However, they are still able to make learned discriminations of the elevation, suggesting that it is the reflexive component of the action that is critical for the involvement of the dorsal nucleus. This also suggests that the other divisions of the cochlear nucleus or their output nuclei have the ability to extract the spectral cues that permit localization in the vertical plane, to subserve the learned decisions (Sutherland *et al.*, 1998a,b). The ability of the principal cells of the dorsal nucleus, the fusiform cells, to respond to localization cues in the vertical direction is ascribed to their complex excitatory–inhibitory response areas. This means that the cells’ responses could be driven by the sound energy in an upper, rising edge of a high-frequency spectral notch in a wideband sound stimulus (see Type V response area in Fig. 6.9E and discussion in Section 6.2.7.4; Reiss and Young, 2005).

In some species, the pinna provides selective amplification for sound sources along a narrow axis. In these species, pinna cues not only contribute to localization in the vertical direction, but also to localization in the horizontal plane (e.g. Musicant *et al.*, 1990; see also Chapter 2).

9.6.3 Spatial release from masking and the binaural masking level difference

We have a remarkable ability to distinguish signals from competing stimuli, when the sound sources are separated in space. One example is the ‘cocktail party effect’, where voices can be easily heard in the presence of other voices, if the speakers are in different locations. In one of the most basic demonstrations of the effect, a signal and noise are both presented by a headphone to the same ear, and the signal is adjusted in level so that it is just inaudible. However, if a copy of the noise is simultaneously presented to the opposite ear, the signal becomes audible again, even though the total amount of noise presented to the auditory system has increased. One can speculate that the presentation of the masker without the signal has allowed the nervous system to calculate what the signal would have been without the masker in the waveform and has allowed it to be audible again. The greatest effects are found when the same masker is presented in phase to the two ears, but the signal in one ear is inverted with respect to the other ear. Under these circumstances, the release from masking or binaural masking level difference (BMLD) can reach 15 dB.

The phenomenon is largest for stimuli below about 1.5 kHz, which is in the frequency range for phase locking, and depends on differences in the phases of the signals and maskers at the two ears. This suggests that it is subserved by low-frequency neurones which are sensitive to interaural phase, such as neurones of the medial superior olive (MSO). However, as with the studies mentioned above, because of the difficulties of recording in the MSO, physiological investigations of the phenomenon are usually undertaken in the inferior colliculus. Jiang *et al.* (1997) measured the activity of neurones in low-frequency areas of the inferior colliculus, in response to the binaural stimuli that generate a BMLD in human beings. Tones, when presented to the two ears, gave firing rates that varied with

interaural delay, producing functions similar to those shown in Fig. 6.18A. The functions generally showed a peak of response at the characteristic delay of the cell, with dips on either side. Responses to broadband noise commonly showed similar functions as a function of interaural delay. The similar pattern of response to tones and broadband noise is not surprising, since the tuning of the cochlea means that the neurone is stimulated with a narrowband-filtered version of the noise which is centred on the neurone's characteristic frequency.

If however noise and tone were both presented simultaneously to the two ears, and the tone level was varied, the rate-intensity function to the tone could vary markedly with the phase of the tone. In some neurones, the masked response to the tone when it was presented in one phase could be an increase in activity, while in the opposite phase, the masked response could be a decrease in activity. In other neurones, tones always produced an increase in activity, but the rate-intensity function was shifted along the intensity axis. Differences in response as a function of phase, whether increases or decreases, can theoretically be used as a detection cue, and when the sizes of these cues are calculated over a population of neurones, BMLDs can be measured, although they are rather smaller than those found psychophysically in human beings (Palmer *et al.*, 2000). Analogous results have also been found with more complex stimuli (Lane and Delgutte, 2005). The mechanism behind the effect is likely to be the coincidence in activity from the two ears in driving the neurone, which then would be perturbed by the addition of a superimposed signal to one ear. Suppose a neurone as illustrated in Fig. 6.18A is stimulated with broadband noise, identical at the two ears, but with the contralateral ear leading by 200 μ sec. The neurone is driven by the coincidence of identical inputs from the two ears, which are in the optimal phase relation to give the maximal response. However, if a tone is superimposed on the input from one ear, the input waveforms from the two ears will no longer be identical. The phase difference between the waveforms from the two ears will vary from moment to moment because of summation of noise and tone in the input from one ear. Therefore, the stimuli from the two ears will no longer always be in an ideal phase relation to drive the neurone strongly. The firing rate of the neurone will therefore be lowered. In other neurones, with different relations between neurone characteristic frequency, tone frequency and characteristic delay, the effect of summation may be to increase the average firing rate.

The physiological data are in closest accordance with the model of interaural cross-correlation proposed by Colburn and Durlach (1978). In this model, the stimuli from each ear are initially narrowband filtered by a bank of filters, corresponding to the auditory nerve fibre filter functions. The inputs from the two ears are then cross-correlated within each frequency channel separately, so that the output signal from each channel is a function that plots the magnitude of the cross-correlation in that channel, as a function of all possible delays between the inputs from the two ears. Where the stimuli are identical at the two ears apart from being shifted in time, the function in any channel responding to the stimulus will have a single major peak. The value of the delay corresponding to the peak can be used to calculate the actual interaural delay, and hence the direction of the sound source at that frequency. The presence of stimuli which are different at the two ears will

decorrelate the inputs and cause other, smaller peaks to appear in the functions, which can be used as a basis for detection (see, e.g. Trahiotis *et al.*, 2005).

An alternative model to explain the BMLD is the Equalization and Cancellation model. In this model, the activity from the two ears is subtracted, and the result is used to detect the signal (Durlach, 1972). Subtraction of the activity from the two ears can occur in the lateral superior olive (LSO). However, the LSO is mainly a high-frequency nucleus. One can speculate that the subtraction could instead occur in low-frequency cells of the LSO, if the LSO indeed has an inhibitory input in human beings, or it may be due to subtraction of the excitatory and the minority inhibitory inputs to the medial superior olive (see Section 9.6.2.2). However, physiological experiments with the stimuli that generate the BMLD, as described above, have not produced responses in accordance with this proposed mechanism.

The overall conclusion from the physiological studies is that the ability to hear sounds in a spatially complex auditory environment, known as spatial release from masking, uses mechanisms that are closely allied to those subserving sound localization and is based primarily on temporal cross-correlation occurring in the medial superior olive.



9.7 SPEECH

9.7.1 What is special about speech?

Speech is a highly practiced form of auditory perception. Speech sounds have many characteristics that are critical in the communication of meaning which mark them as different from other auditory stimuli. This carries the further implication that specialized neural structures have developed for the analysis of speech.

- (i) As pointed out by Liberman *et al.* (1967), the individual perceived components of speech, that is phonemes,² are not necessarily represented by individual sounds. Single acoustic cues often carry information simultaneously and in parallel about multiple phonemes, and information about single phonemes may be spread over successive acoustic cues. The acoustic cues used in identifying a single phoneme can vary enormously with the context and can depend on the sounds that come before or after. This permits the very rapid communication of meaning in speech and suggests that speech perception is based on learning patterns of speech on a larger scale than the phonemes, rather than by identifying the individual phonemes separately and in succession.
- (ii) Speech sounds commonly show categorical perception. If one speech stimulus is manipulated so that it is gradually transformed to another speech stimulus, perception does not change gradually, but discontinuously (e.g. as when the

² Phonemes are defined as the smallest units of speech that change the meaning of a word if one is substituted for another.

sound ‘ba’ is transformed into the sound ‘pa’). Moreover, thresholds for discrimination of differences well within one reported category are high, while thresholds for discrimination near the border between categories are much lower.

In speech, categorical perception is particularly seen in discriminating between phonemes based on their onsets (e.g. ‘ba’ vs. ‘pa’ above) and in discriminating between vowel sounds. Experiments measuring perception via conditioned reflexes show that very soon after birth newborn babies can discriminate well within single categories, and discriminate between the categories used in all languages equally well. However by 12 months of age perception becomes dominated by the categories used in their native language. For instance, Japanese-learning babies lose the ability to discriminate ‘la’ and ‘ra’, which are both mapped to the same category in Japanese, while in English-learning babies the ability becomes enhanced (see Kuhl, 2010, for review). Some non-speech stimuli can also show categorical perception. It seems that categorical perception is valuable for the rapid and reliable detection and utilization of stimuli where identification of the category is critical, but discrimination within categories is not.

- (iii) There are indications that listeners can switch between hearing some stimuli as speech or as non-speech, and that when they do, their ability to discriminate details of the stimuli change (for discussion of further evidence and for summary, see Moore, 2012).
- (iv) Studies of brain function in human beings show that there are specialized regions for the analysis of speech. Observations from patients with lesions, and imaging the brain by functional magnetic resonance imaging (fMRI) or positron emission tomography (PET), suggest that some areas in the left hemisphere are more critical for the analysis of speech than of other stimuli. These findings will be discussed in more detail below.

In summary, many lines of psychophysical, anatomical, clinical and physiological data suggest that speech is at some stage analysed by specialized neural structures. It is quite possible that non-speech stimuli can also be analysed by these structures, and it is controversial as to what stage in the auditory pathway the structures become ‘speech specific’, if indeed they ever do. It is generally assumed, from the similarity of auditory anatomy in human and non-human species, that all structures up to and including the inferior colliculus and possibly the medial geniculate body deal with stimuli purely on the basis of their acoustic properties. To this extent, they are expected to deal equally with speech and non-speech stimuli. At some stage in cortical processing, structures are likely to become specialized for speech, and it is at the moment controversial whether this difference starts in the auditory core areas (e.g. AI) or develops only in higher order cortical areas (see discussion below).

It is therefore probably valid to analyse speech processing in the auditory brainstem by means of electrophysiological experiments in non-human species, using either human speech sounds or non-speech sounds that have been tailored to probe the mechanisms under consideration. However, at some level of the cortex, the mechanisms underlying the analysis of human speech can only be undertaken

using speech stimuli in human beings. This means studies depend on functional imaging and anatomy in normal human beings and on data from, for example lesions, microstimulation or neuronal multiunit and very occasionally single-unit recording, in clinical patients. Electrophysiological analyses of AI and other early cortical areas in animals have an uncertain status for the understanding of human processing of speech, with the interpretation of these experiments depending on the extent to which speech-specialized structures have developed in these areas in human beings. Some experimenters probe the responses of the cortex in non-human species with vocalizations specific to those species. This may give information on the mechanisms behind the responses to stimuli with speech-like levels of complexity that are of critical importance for the species concerned.

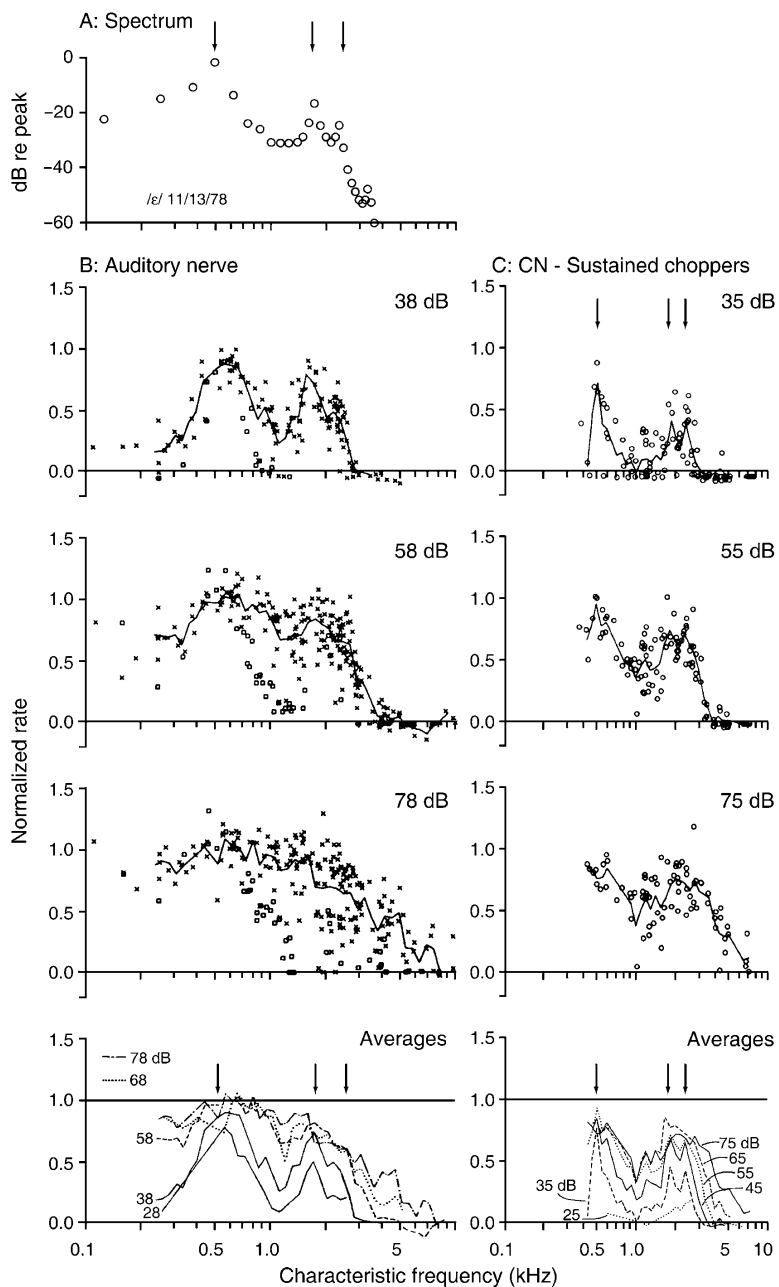
To the extent that these underlying mechanisms are common across species, the interpretation of the experiments may also be applicable to human beings.

9.7.2 Auditory nerve and brainstem responses

9.7.2.1 Vowel sounds

Given that the brainstem is likely to process speech sounds on the basis of their fundamental acoustic properties, analysis of speech sounds at this level can be undertaken with artificial speech-like stimuli in experimental animals. The coding of steady vowel sounds was studied by [Sachs and Young \(1979\)](#), who presented anaesthetized cats with steady-state synthesized vowel sounds, consisting of three formants, or spectral peaks, the lowest in frequency being called F_1 , the next F_2 and the next F_3 . They used a limited set of vowels, and each was presented at several intensities. The activity of a large number of auditory nerve fibres was sampled in each animal in response to the same stimulus set. In this way, a picture was built up of the response of the whole nerve fibre array to each of the stimuli.

When mean firing rates were plotted as a function of fibre characteristic frequency, clear peaks at the frequencies of the formants could be seen in response to stimuli presented at low intensities ([Fig. 9.13B](#)). However, as the stimulus intensity was raised to 78 dB SPL and above, still in the range in which speech is easily comprehensible to human beings, the separate peaks disappeared, leaving a broad band of activation. The changes are most clearly shown in the graphs of the average responses at the bottom of the figure. Such a loss of spectral detail at medium and high stimulus intensities corresponds to that seen with other types of stimuli, when the responses of all fibres together are considered. The loss is due to three factors: (i) the flattening of the rate-intensity functions of the low-threshold fibres at high stimulus intensities, (ii) the reduction in cochlear frequency resolution expected at high stimulus intensities and (iii) two-tone suppression. Two-tone suppression means that the response to F_1 suppresses the responses to F_2 and F_3 . However, activity in the fibres tuned to frequencies in the gap between F_1 and F_2 is not suppressed: activity in those fibres is driven by F_1 itself, and therefore is not suppressed by F_1 . Therefore, two-tone suppression reduces, rather than enhances, the spectral contrast in the responses of the nerve fibre array. However, and as with



other types of stimuli, we expect the high-threshold fibres, which include those with sloping saturations or straight intensity functions, to convey some spectral details even at the higher stimulus levels (see Section 9.5.1.1 and Chapter 4).

In the cochlear nucleus, cells with excitatory tuning curves and inhibitory surrounds (Type II or III responses; Fig. 6.9) are able to represent spectral patterns in their mean firing rates over a wider range of stimulus intensities. Figure 9.13C shows the responses of sustained chopper cells in the cochlear nucleus, obtained by methods similar to those for the auditory nerve fibres in Fig. 9.13B. The peak of response to the lowest formant F_1 is separate from the peaks to the two upper formants F_2 and F_3 at all stimulus intensities, although at the highest intensity, the peaks to F_2 and F_3 are not separable (see also averages at bottom of the figure). Sustained chopper cells are identified as T-stellate (T-multipolar) cells and have narrow tuning curves that are excitatory with inhibitory sidebands (Type III responses; see Chapter 6). These cells are clearly able to adjust their sensitivity, so that with more intense stimuli their pattern of response becomes dominated by the high-threshold, rather than by the more numerous low-threshold, auditory nerve fibres (see also May *et al.*, 1998). On the other hand, cells without strong inhibitory sidebands, such as the primary-like cells, are unable to represent the stimulus spectrum at higher stimulus intensities (Recio and Rhode, 2000).

Although the pattern of mean-rate activity becomes flattened in auditory nerve fibres at moderate and high stimulus intensities, temporal information is preserved in the auditory nerve at all stimulus intensities. Young and Sachs (1979) made Fourier transforms of the temporal firing patterns of auditory nerve fibres, so as to measure the degree of phase locking to the individual components of the stimulus. They showed that the representation of the stimulus spectrum, determined in the way, was preserved without degradation at all stimulus levels. And as shown by Delgutte and Kiang (1984a), for most vowel sounds, the fibres phase-lock to one or other of the formants in the stimulus. This was as true for fibres tuned to frequencies in the gaps between the formants, as it was for the fibres tuned to the frequencies of the formants themselves. In the fibres tuned to

Fig. 9.13 Auditory nerve and cochlear nucleus responses to a vowel sound. (A) Spectrum of the vowel sound /ɛ/ used as the stimulus. The arrows mark the frequencies of the spectral peaks or formants F_1 , F_2 and F_3 . (B) Neurograms of auditory nerve fibre activity to the vowel sound. The activity of a large number of auditory nerve fibres was sampled in responses to the one stimulus, and the activity of each fibre plotted against its characteristic frequency. Solid lines show the running averages. Responses for three of the five stimulus intensities used in the experiment are shown here (dB marked on curves). The bottom panel shows the average curves for all five stimulus intensities and how representation of the formants is lost in the average above about 55 dB SPL. Reprinted from Sachs and Young (1979), Figs. 1 and 6, Copyright (1979), with permission from American Institute of Physics. (C) Neurograms for sustained chopper neurones in the cochlear nucleus to the same stimulus. The averaged curves (bottom panel) show that the spectral peaks are preserved in the averages even at the highest stimulus intensities. Used with permission from Blackburn and Sachs (1990), Figs. 15 and 16.

frequencies in the gaps between the formants, the strong responses to the formants suppress the phase-locking responses to other frequency components.

While these results show that temporal information in the stimulus gives rise to temporal information in the responses of auditory nerve fibres, the results cannot be taken as proof that this information is actually used for analysing the spectrum of the vowel. For this to occur, there must be a mechanism to decode the temporal information. One possible way this could occur in the cochlear nucleus was proposed by Shamma (1985a), presented in Fig. 9.9, where inhibitory sidebands, activated in different phases of the stimulus waveform, could be used to emphasize spectral contrasts at the cochlear nucleus. This could account for some of the results in the sustained choppers shown in Fig. 9.13C. Recordings of auditory nerve activity by Cedolin and Delgutte (2010) showed that once the phase information was taken into account, spectral contrasts could indeed be emphasized, although they did not show a neural mechanism for the extraction of the information. However, at some stage of the auditory system, we expect the temporal activity to be translated into a code which is more resistant to temporal degradation. As discussed in Section 9.4.2, we have no idea of the mechanism.

9.7.2.2 Consonants

Transient speech sounds, such as consonants, produce temporally varying patterns of activity in different neurones, the pattern being determined by the time pattern of energy in the frequency channel to which the neurone is tuned.

In auditory nerve fibres, the patterns of firing can be predicted from the spectrotemporal pattern (spectrogram) of the speech sound and the frequency tuning of the fibres (Delgutte and Kiang, 1984b). At higher stimulus intensities, transient onset responses become relatively more prominent in the temporal pattern, probably because auditory nerve fibres have a greater dynamic range to transient than to steady-state stimuli.

In the cochlear nucleus and at higher levels, the responses of many neurones to frequency-modulated stimuli are enhanced. This emphasizes the responses to speech transients and to the temporal fluctuations in the speech waveform. Figure 9.14 compares sample responses from the auditory nerve, cochlear nucleus and inferior colliculus and shows how transients are particularly emphasized in the inferior colliculus (see also Miller *et al.*, 2002; and Suta *et al.*, 2008, for review). This forms an example of how certain critical features, in this case temporal transients and modulations, are progressively emphasized at higher and higher levels of the auditory system.

9.7.3 Cortical responses to vocalizations in non-human species

In an attempt to identify cortical mechanisms for the analysis of species-specific vocalizations, many experimenters have measured neuronal responses to specific,

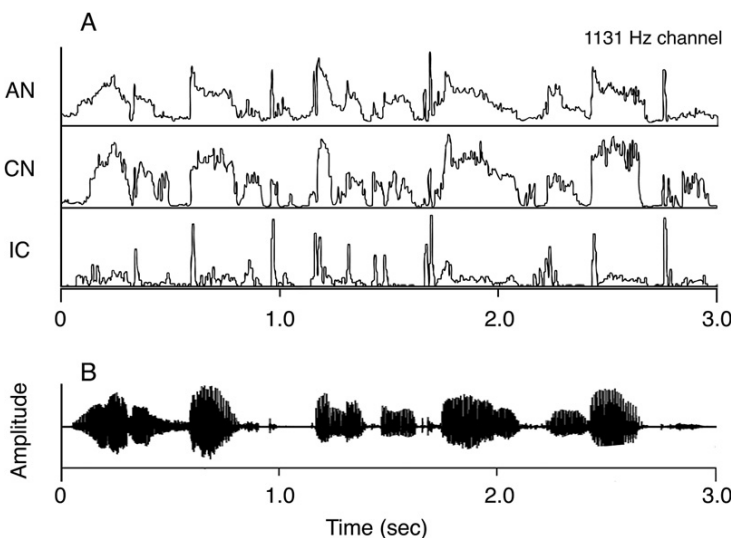


Fig. 9.14 (A) Responses of neurones in the auditory nerve (AN), cochlear nucleus (CN) and inferior colliculus (IC) to the speech sound ‘wood is best for making toys and blocks’ (waveform in B). Responses in the IC in particular show enhanced responses to the transients in the stimulus. For this figure, responses for neurones with characteristic frequencies within half an octave of 1131 Hz were averaged. The CN responses were recorded mainly from primary-like, chopper and pauser neurones. Data from Delgutte *et al.* (1998).

stereotyped animal vocalizations. For instance, Nagarajan *et al.* (2002) measured the responses of cells in the marmoset primary auditory cortex to a common call in the marmoset, the twitter call. When comparing different cells, the strength of response to the twitter calls could be related to the magnitude of the response to amplitude-modulated tones modulated at similar rates. The neurones appeared to be predominantly driven by the temporal properties of the stimulus, rather than by its spectral characteristics. Outside AI, a greater responsiveness to spectrally complex stimuli and to temporal modulation has been found, which further enhances the response to vocalizations in many of the areas (e.g. Tian *et al.*, 2001; Tian and Rauschecker, 2004; Gourevitch and Eggermont, 2007; Recanzone, 2008; Kajikawa *et al.*, 2008).

The overall conclusion from these and similar studies in animals has been that in the core areas, the responses of cortical neurones are determined by the general frequency and temporal properties of the sounds. In these areas, there has been no evidence for specialized detectors of specific vocalizations. Rather, current models of coding suggest that the stimuli are represented as a pattern over a distributed neuronal population and use neuronal circuits that are shared with other auditory stimuli of similar complexity. However in some belt areas, the parabelt areas, and some of the surrounding cortical areas, the responses become

more and more selective for the features contained in vocalizations. In some of these areas and the further surrounding areas, the responses become so specific that they can indeed be said to be specialized for species-specific vocalizations (e.g. Remedios *et al.*, 2009).

9.7.4 Responses to speech in the human cortex

9.7.4.1 The initial stage of speech processing in the human auditory cortex (pre-lexical processing)

Pre-lexical processing includes the acoustic analysis of speech sounds and the categorization of phonemes so as to allow the subsequent recognition of words. Imaging studies in human beings show that both speech and non-speech stimuli activate areas in and around the superior temporal plane, which includes the auditory core areas (including AI in Heschl's gyrus) together with activation in other areas of the lateral surface of the brain (Fig. 9.15A; see Figs. 7.4 and 9.16A for description of areas). The cortex is activated bilaterally, in the great majority of people to a greater extent on the left side when speech stimuli are used. The extent of overall cortical activation varies between studies, being dependent on the type of task required by the subject in response to the speech.

Figure 9.15B shows a detailed view of activation within the superior temporal plane, in a single slice 6 mm thick through the plane. The figure shows the response to words, when the subject had the task of distinguishing between words and 'pseudo-words', which were meaningless concatenations of syllables (Behne *et al.*, 2006). It shows how speech sounds bilaterally activate structures on the superior temporal plane. The stripes of activation visible in the image result from the gyri on the superior temporal plane moving in and out of the plane of section. In accordance with other studies, we also expect activation in many other areas, outside the section illustrated here.

Many of these areas respond to both speech and the speech-like components of sounds. For instance, magnetoencephalographic imaging (in which the magnetic fields resulting from electrical activity in the cortex are measured) shows that vowel sounds and sounds evoking a sensation of pitch both activate the same areas within lateral Heschl's gyrus. It is reasonable to suppose that at this stage these two types of sound are processed by the same mechanism (Gutschalk and Uppenkamp, 2011).

At what stage in the cortex are speech stimuli analysed by speech-specific mechanisms, that is where are speech stimuli treated differently from non-speech stimuli? This issue, which has been the object of many investigations over the years, is unfortunately an immensely difficult one to resolve. One of the problems is the difficulty of devising stimuli that are perceived as speech rather than as non-speech, while not differing in any other acoustic properties. Another difficulty is that any response to the speech may represent a high-level response to a semantic aspect of the stimulus, rather than the initial processing of the stimulus as speech.

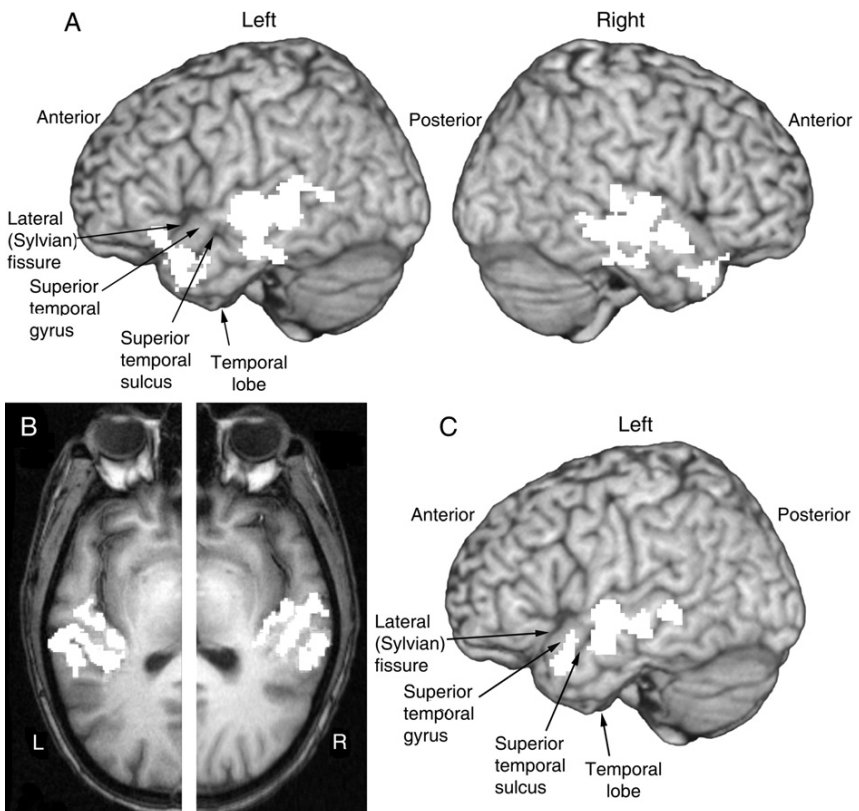


Fig. 9.15 Cortical responses to speech, shown in white in this figure and in red/yellow in Plate 3. (A) Response during passive listening to speech sounds, imaged in left and right hemispheres in a single subject by functional magnetic resonance imaging (fMRI). fMRI detects the local drop in oxygen level in the blood, consequent on activity. In this view, surface and subsurface signals from fMRI (coloured) are projected onto a standard cortical surface obtained from structural MRI. Areas (yellow/red) are shown where the signal with the speech sound is statistically greater than the signal in silence. Areas are bilaterally activated in the temporal lobe. Data for figure were provided by Professor C. Price. (B) Response to spoken words, imaged by fMRI in a 6-mm-thick slice along the surface of the superior temporal plane, in a single subject. The data from fMRI are superimposed on a high resolution structural MRI scan of the brain. There is a bilateral response, in Heschl's gyrus and extending over the superior temporal plane. The illustrated image is the average of the responses to the two ears and is the activity measured during presentation of the signal minus the activity measured in silence. Used with permission from Behne *et al.* (2006), Fig. 3, digital average of left halves of original sub-figures. (C) Responses to speech sounds, when the subjects had to make a later response based on the meaning of the sounds. The figure shows the activity in response to the speech sounds, minus the activity in response environmental sounds which were approximately matched in acoustic properties. There are discrete areas of specific activation in the region of the superior temporal gyrus and sulcus. Left hemisphere. Data from Thierry *et al.* (2003), as reanalysed by Price *et al.* (2005). From Price *et al.* (2005), Fig. 1A. See also Plate 3.

For these reasons, different investigators have produced different results over the years. Figure 9.15C shows areas activated more by speech than by environmental sounds, as reported by Thierry *et al.* (2003). Analogous results have been found by others (e.g. Crinion *et al.*, 2003; Liebenthal *et al.*, 2005). The areas shown in Fig. 9.15C lie in the left middle and superior temporal gyri (Brodmann areas 21 and 22) and more anteriorly in the left temporal lobe (Brodmann area 38, near the temporal pole: see Fig. 9.16A for definition of areas). The areas lie within and just outside the cortical lateral parabelt areas (see Fig. 7.4). However, other investigators have pointed out that the stimuli used in such studies differ markedly from speech in their acoustic properties. A study where these were more closely controlled found only a single patch of potentially speech-specific activation in the centre of the areas shown in Fig. 9.15C (Uppenkamp *et al.*, 2006).

Further analysis of more advanced pre-lexical processing, for example by looking for changes in fMRI responses when one vowel stimulus was changed to another, showed that there were specific responses from an area situated more anteriorly on the left superior temporal lobe (Leff *et al.*, 2009). These results support a general model in which there is a hierarchy of more and more complex analyses, which are undertaken serially as information is passed forward in a major stream running anteriorly in the temporal lobe (Rauschecker and Scott, 2009; DeWitt and Rauschecker, 2012). Moreover, even in Heschl's gyrus and immediately adjacent areas, the responses can depend on the task required of the subject and not just on the stimulus. This suggests that starting in AI and immediately surrounding areas, the analysis is varied according to the high-level demands on the subject, and is therefore affected by top-down or antihierarchical control (Harinen *et al.*, 2012).

In addition to the major anteriorly directed stream, there is a major posterior and dorsalward-stream, projecting to the posterior superior temporal plane, the angular gyrus and adjacent areas (Fig. 9.16A). This stream feeds into the dorsal and posterior areas involved in the further analysis of speech, and in the production of speech (see Rauschecker and Scott, 2009; Turkeltaub and Coslett, 2010; Hickok *et al.*, 2011, for reviews). It is also possible that the pathway of activation is varied by top-down commands, and adjusted to the requirements of the particular task.

9.7.4.2 Higher levels of speech processing

Analysis of speech involves not only phonology and pre-lexical analysis, that is the initial processing of speech sounds, but lexical analysis (analysis of words or groups of words), analysis of syntax (grammar) and semantics (meaning). Many of the relevant studies have used the production of speech or visual reading as tools. They are part of the large subject area of neurolinguistics and lie outside the scope of this book (see further reading at the end of this chapter).

A meta-analysis of studies in which a decision was made whether a sound was a word or a pseudo-word (i.e. a lexical decision) showed that there was widespread activation by words in the left hemisphere, outside many of the areas shown as activated in Fig. 9.15A. These included posterior areas such as the angular gyrus

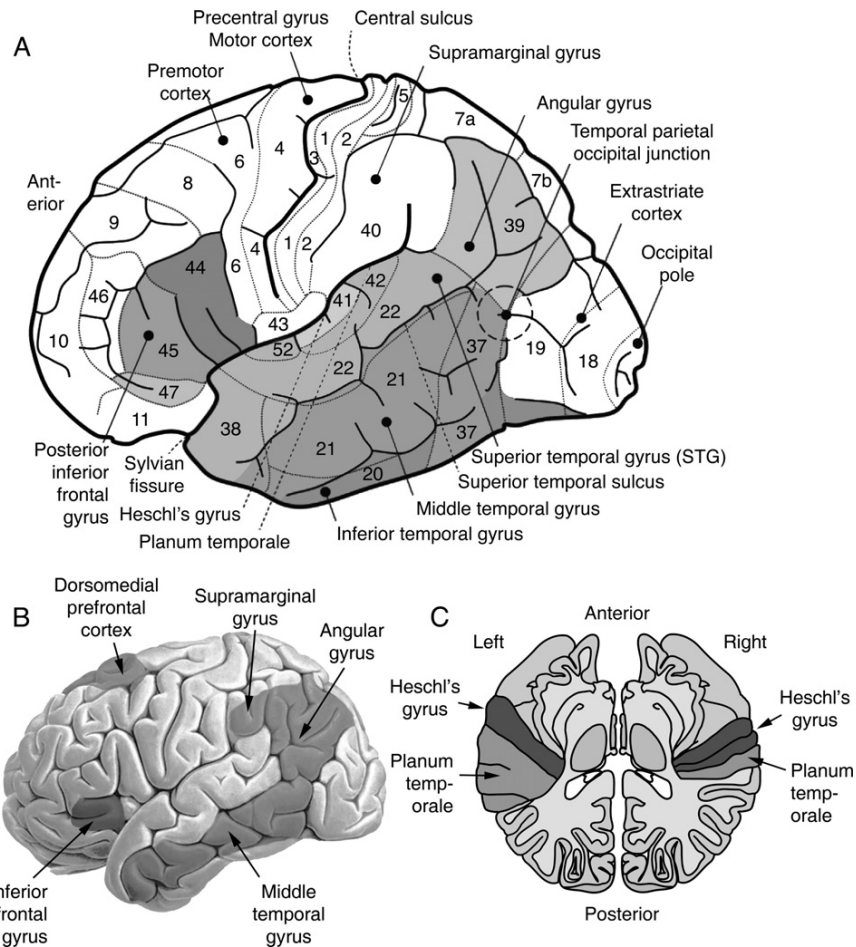


Fig. 9.16 (A) Cortical areas involved in language processing, shown in the left hemisphere, according to Démonet *et al.* (2005). Areas are numbered according to Brodmann (1909). Compare to Fig. 7.4 for more information. Solid lines indicate sulci, dotted lines the divisions between Brodmann areas. Used with permission from Démonet *et al.* (2005), Fig. 6. (B) Areas implicated in semantic processing as shown by fMRI (shaded), shown on a canonical left hemisphere, according to Binder *et al.* (2009), Fig. 7, by permission of Oxford University Press. (C) Cortical asymmetry as reported by Geschwind and Levitsky. The figure shows an approximately horizontal section through the brain to reveal the upper surface of the superior temporal plane. The planum temporale is larger on the left side; the difference in this particular subject was unusually dramatic. Based on data from Geschwind and Levitsky (1968) and Pickles (2007b).

and adjacent areas, the middle temporal gyrus and more anteriorly, the inferior frontal gyrus (Davis and Gaskell, 2009). Other studies have included areas in the left frontal cortex, around the posterior inferior frontal gyrus (parts of Brodmann's areas 44 and 45, previously known as Broca's area (Vigneau *et al.*, 2006; see Fig. 9.16A).

In semantic analysis, the meaning of sentences is determined. Semantic analysis has been detected by comparing responses to grammatically correct sentences that have plausible and implausible meanings. In a meta-analysis of 120 papers, Binder *et al.* (2009) found left-dominated activation foci in several areas, including among other areas, all along the middle temporal gyrus, more posteriorly in the angular gyrus and adjacent supramarginal gyrus, the dorsomedial prefrontal cortex (just anterior to pre-motor cortex) and in the inferior frontal gyrus (shaded areas, Fig. 9.16B). As with the areas for lexical analysis, some of these areas surround the areas for phonological analysis, and it has been suggested that information resulting from the phonological processing in the superior temporal plane is passed to the surrounding areas for lexical and semantic processing. The widespread participation of these structures may also reflect the involvement of working memory in semantic analysis.

Data from patients with lesions have, as commonly interpreted, pointed to two areas specifically involved in speech, previously known as Wernicke's and Broca's areas. Wernicke's area is now referred to as the posterior left superior temporal gyrus, that is the most posterior part of Brodmann's area 22 (see Fig. 9.16A). Broca's area is now referred to as the left posterior inferior frontal gyrus, that is parts of Brodmann's areas 44 and 45.

Lesions in the posterior left superior temporal gyrus give rise to problems in comprehension. While speech production may be grammatically normal, the resulting sentences can be meaningless, suggestive of the problems in comprehension. Imaging shows that this area has however multiple and diverse functions, being activated by a variety of events, including the perception of language-related sounds, monitoring the speakers own voice and the retrieval of words (for reviews, see Wise *et al.*, 2001; Saur and Hartwigsen, 2012). Studies have found that lesions in this area do not in fact affect the comprehension of some sentences at all, although lesions in the middle temporal gyrus and anterior superior temporal gyrus can do so (reviewed by Dronkers *et al.*, 2004; see also Tsapkini *et al.*, 2011). The latter areas on the temporal gyri are also the ones shown to be activated by speech in Fig. 9.15C. On the other hand, the left posterior inferior frontal gyrus is predominantly involved in the production of speech. Lesions here leave comprehension relatively unaffected, although there can be problems in understanding long and syntactically complex sentences, commensurate with a suggested role of this area in processing complex hierarchical or sequential structures.

9.7.4.3 Left–right cortical asymmetries in auditory processing

Observations from brain lesions in human beings originally pointed to the importance of the left hemisphere for speech processing in the great majority

(96%) of cases. Anatomical studies show that the superior temporal cortex usually has a larger surface area on the left than on the right side (Fig. 9.16C; Geschwind and Levitsky, 1968; see also Dorsaint-Pierre *et al.*, 2006). The difference is particularly apparent in the planum temporale, which extends farther posteriorly on the left and which on average is one-third larger in area than on the right. The left planum temporale contains more white matter than the right, suggesting a greater extent of myelination, together with more interconnecting nerve fibres and a greater number of afferent fibres (Seldon, 1981; Penhune *et al.*, 1996). The cells are organized in columns; a wider separation of columns in the left hemisphere is associated with a lower number of short-range connections between the columns, suggesting that there is a higher possibility of independent local processing within this hemisphere. However there are also an increased number of long-range connections within the left cortex, suggesting a greater degree of integration of the results of the local processing (for review, see Hutsler and Galuske, 2003).

Observations in aphasic patients have for many years suggested that deficits in temporal processing underlie some of the language disturbances seen with left hemisphere lesions. Imaging studies using positron emission tomography show that tonal stimuli with many rapid temporal transitions activate the region around Heschl's gyrus to a greater degree on the left than on the right side (Zatorre and Belin, 2001). Recordings from human patients with electrodes placed within the auditory areas also have shown that stimuli with more temporal contrasts activated Heschl's gyrus and the planum temporale on the left more than the right side (Liégeois-Chauvel *et al.*, 1999). The results did not apply only to speech sounds, but also to non-speech sounds with similar temporal structure. On the other hand, stimuli with slow temporal transitions preferentially activate the right hemisphere (for review, see Nourski and Brugge, 2011). In addition, stimuli to the right ear have a small but significant advantage for the perception of speech. Because of the stronger crossed projection in the auditory system, we would expect these stimuli to preferentially activate the left hemisphere. The right ear advantage is particularly marked for stimuli with strong acoustic transients, such as consonants, whereas vowels which have slower temporal variations do not show a right ear advantage. This suggests that the left hemisphere is specialized for processing faster temporal variations than the right hemisphere. The greater degree of local processing in the left auditory areas, together with the higher degree of myelination of interconnecting fibres, would enhance the processing of stimuli where timing is critical.

The asymmetry is carried through to complex syntactic function, since patients with left hemisphere lesions have more severe impairments in grammar and syntax than do patients with right hemisphere lesions. However, it appears that the right hemisphere preferentially, although not exclusively, processes the emotional content of words. For instance, patients with lesions of the parietal area of the right hemisphere are more impaired in the perception of the emotional content of speech than are those with lesions in the left hemisphere. However, patients with frontal lesions are equally impaired with lesions on either side (Shamay-Tsoory *et al.*, 2004; Schirmer and Kotz, 2006).



9.8 SUMMARY

1. The behavioural absolute threshold is related to the minimum thresholds of single auditory nerve fibres, determined from the mean firing rate.
2. The shape of the audiogram (the relation between threshold and stimulus frequency) is, for the middle part of the audible frequency range, governed by the efficiency of the middle and outer ears in delivering energy to the cochlea. The cochlea itself has approximately equal sensitivity to energy of all frequencies, except at low (<450 Hz) and very high frequencies.
3. Frequency resolution describes the ability to filter out, on the basis of frequency, one stimulus component from another in a complex stimulus. Psychophysical frequency resolving power, as shown by ‘psychophysical filters’ or critical bands, seems to approximately match the frequency resolving power of the mechanical travelling wave in the cochlea and that of auditory nerve fibres. However, the degree of correspondence varies with the psychophysical method used to measure the frequency resolution.
4. Because the cochlea behaves non-linearly, psychophysical methods using simultaneous masking, where the signal and masker have the opportunity to interact non-linearly, give different results from those determined by non-simultaneous masking, for example forward masking. In general, we expect psychophysical filters measured with simultaneous masking to be broader than those of the underlying physiological filters, especially on the high-frequency side of the filters. Non-simultaneous masking techniques are expected to give more accurate measures of underlying physiological frequency resolution.
5. Psychophysical filters, and mechanical filtering functions on the basilar membrane, broaden with increases in stimulus intensity, and both do so in the same way. It is therefore very likely that the changes in frequency resolution with stimulus intensity at least partly reflect changes in cochlear filtering. Different nerve fibres have different thresholds and dynamic ranges. At high stimulus intensities, information reflecting mean firing rates is carried by a smaller subpopulation of fibres with high thresholds and wider dynamic ranges (those with ‘sloping’ and ‘straight’ saturations). In the cochlear nucleus and beyond, neurones with strong lateral inhibition are able to signal details of the stimulus in their mean firing rates over a wide range of stimulus intensities. Temporal information is preserved in the firing of auditory nerve fibres over the whole intensity range.
6. Some auditory phenomena, such as co-modulation masking release, require information to be combined over multiple psychophysical filters. Correlates have been found in the responses of T-stellate (T-multipolar) cells in the cochlear nucleus, which receive inhibition that has been integrated over a wide range of frequencies.
7. In pitch discrimination, two tones are presented successively, and we have to tell whether there is a difference between them on the basis of frequency. At high frequencies (above the frequency limit for phase locking, 5 kHz), it is

likely that pitch discrimination takes place on the basis of differences in the place of activation along the cochlear duct. At lower frequencies, it is likely that temporal information is used. This is likely to involve extracting the timing between corresponding points on the stimulus waveform. However, the underlying neural mechanisms are not known.

8. Loudness is likely to depend on the total integrated activity in the auditory nerve, as modulated by central mechanisms.
9. Sound localization depends on both monaural and binaural mechanisms. Monaural mechanisms, where the auditory stimulus is modified by the pinna and head in a direction-dependent manner, allow judgements of elevation and whether sound sources are in front or behind. Some of the neural circuits processing this information are found in the dorsal cochlear nucleus, where cells extract the information for elevation and form part of an automatic reflex orienting pathway. However, it is likely that learned judgments of elevation use other neural circuits.
10. Binaural mechanisms of localization depend on comparing timing and intensity differences at the two ears. Low-frequency cells in the medial superior olive are able to detect differences in the timing of activity arriving from the two ears and give maximum responses for certain time differences (compensating for the so-called characteristic delay of the cells). However, for many cells, their characteristic delays are greater than the delays that could be produced by sound sources external to the head. Such cells would only indicate which side of the head the stimulus is on, although the relative activation in the population response of cells on the left and right sides could indicate direction more precisely. The functions relating firing rate and interaural delay are commonly steepest near the midline, meaning that these cells would be particularly accurate at responding to changes in direction around the midline.
11. Differences in the times of arrival at the two ears of stimulus onsets, or of temporal fluctuations in the envelope of high-frequency stimuli, can be detected in the lateral superior olive. The lateral and medial superior olive project to the dorsal nucleus of the lateral lemniscus, and then the inferior colliculus, where the results of the different types of analyses are combined.
12. Spatial information can be used to help distinguish signals from competing stimuli, when they are separated in space (the 'cocktail party effect'). This is also shown in the phenomenon known as the binaural masking level difference (BMLD) or as the spatial release from masking. Physiological recordings in the inferior colliculus suggest that the effect is likely to depend on timing information and on the coincidence or correlation of activity from the two ears. The superimposition of a monaural signal on identical noise to the two ears can decorrelate the inputs to the two ears. This modifies the responses in some binaural neurones, allowing the signal to be detected.
13. Speech sounds are likely to be processed by the same neural mechanisms as other auditory stimuli in the brainstem and possibly in the core areas of the auditory cortex. Vowel formants are represented in the firing of neurones

- tuned to their frequency in the cochlear nucleus and very likely in higher auditory nuclei. The temporal transitions in consonants are progressively emphasized in the higher auditory nuclei.
14. At some stage in the auditory system, it is likely that speech is analysed by specialized neural mechanisms, that is, speech becomes treated differently from other auditory stimuli. It is controversial as to where in the cortex this separation occurs. Some evidence suggests that areas on the upper surface of the temporal lobe (Heschl's gyrus and immediately adjacent planum temporale) analyse the phonological properties (i.e. acoustic characteristics) of speech and that other auditory stimuli can share the same neural mechanisms. However, imaging suggests that speech-specific analyses are likely to take place in the surrounding areas, that is in the superior temporal gyrus and the inferior frontal gyrus and the areas surrounding those, particularly on the left side of the brain (to include areas previously known as Wernicke's and Broca's areas). These areas are part of a 'language network' that includes many areas of the brain.
15. The planum temporale on the posterior part of the superior temporal plane is larger on the left than on the right side in most people. It is also more heavily myelinated, suitable for the rapid conduction of neural impulses. Stimuli with many rapid temporal transitions preferentially activate the left side of the brain, while stimuli with slow temporal transitions preferentially activate the right side of the brain. The emotional content of speech is also preferentially processed in some areas on the right side of the brain.

9.9 FURTHER READING

For an introduction to the psychology and psychophysics of hearing, see 'An Introduction to the Psychology of Hearing' by B.C.J. Moore (Emerald, 2012). Many of the issues discussed in this chapter are also discussed in 'Auditory Neuroscience: Making Sense of Sound' by J. Schnupp, I. Nelken and A. King (MIT Press, 2011).

For more advanced treatments see chapters in several volumes of the Springer Handbook of Auditory Research: 'Human Psychophysics', eds W.A. Yost, A.N. Popper and R.R. Fay (Vol. 3, 1993); 'Pitch: Neural Coding and Perception', eds C.J. Plack, A.J. Oxenham, A.N. Popper and R.R. Fay (Vol. 24, 2005); 'Sound Source Localization', eds A.N. Popper and R.R. Fay (Vol. 25, 2005); 'Music Perception', eds M.R. Jones, R.R. Fay and A.N. Popper (Vol. 36, 2010) and 'Loudness', eds M. Florentine, A.N. Popper and R.R. Fay (Vol. 37, 2011).

Brainstem mechanisms of sound localization have been reviewed by [Grothe et al. \(2010\)](#) for mammals, and by [Konishi \(2003\)](#) for birds.

Cortical processing of spatial and temporal stimuli in macaque has been reviewed by [Recanzone et al. \(2011\)](#). Cortical encoding of pitch and stimulus periodicity have been reviewed by [Walker et al. \(2011\)](#) for both human beings and

animals, and by Nourski and Brugge (2011) for human beings with a further emphasis on speech processing and cortical asymmetries.

The basic psychoacoustic processes underlying speech perception have been reviewed by Moore (2005), and the development of phoneme recognition in human beings by Kuhl (2010). Responses to communication calls in the non-human brainstem and cortex have been reviewed by Suta *et al.* (2008).

The cortical structures involved in the analysis of language have been reviewed by Price (2010), and results from structural MRI (i.e. static brain structure) in relation to language processing were reviewed by Richardson and Price (2009). Left-right asymmetries in the auditory system and in auditory processing were reviewed by Lazard *et al.* (2012). Asymmetries in cortical neural organization and connections were reviewed by Hutsler and Galuske (2003).

Streams in the cortical processing of speech were reviewed by Rauschecker and Scott (2009), Turkeltaub and Coslett (2010), Hickok *et al.* (2011) and Smith (2011). Localization of the semantic system in the brain was reviewed by Binder *et al.* (2009). The role of posterior left superior temporal gyrus ('Wernicke's area') in speech was reviewed by Wise *et al.* (2001).

The effects of stroke on speech processing in the left anterior pole were reviewed by Tsapkini *et al.* (2011). Recovery of language function after stroke was reviewed by Saur and Hartwigsen (2012).

For an introduction to neurolinguistics, see a text such as 'Neurolinguistics: An Introduction to Spoken Language Processing and its Disorders' (Cambridge Textbooks in Linguistics) by J.C.L. Ingram (2007). For a more specialized treatment, with an emphasis on clinical aspects, see 'Handbook of the Neuroscience of Language' eds B. Stemmer and H.A. Whitaker (Elsevier, 2008).

SENSORINEURAL HEARING LOSS

Hearing loss that arises in the cochlea, from damage to the hair cells or auditory nerve, is known as sensorineural hearing loss. Further cochlear losses can arise in the stria vascularis. In many cases, the causes of these losses are now known. In addition, sensorineural hearing loss has provided us with many models that have led to greater understanding of basic biological processes within the cochlea. The biological origin of the major forms of hearing loss will be discussed, and their correlates in terms of auditory performance will be described. The possibilities of reversing or restoring lost hearing by therapy at a cellular level, including stem cell therapy, gene therapy and antioxidant therapy, will be discussed, as will the restoration of hearing by cochlear prostheses. This chapter requires knowledge of Chapter 3 and the first part of Chapter 4.



10.1 TYPES OF HEARING LOSS

Hearing loss arising in the auditory periphery is divided into two types, known as conductive and sensorineural loss. Hearing loss due to an abnormality in the outer or middle ears is known as conductive loss. Conductive loss may arise for a number of reasons: the outer ear may be blocked or the tympanic membrane damaged, or the coupling of energy to the cochlea is reduced, because for instance the ossicles are immobilized, or because the differential transfer of pressure to the oval and round windows is otherwise impaired. Conductive loss produces a simple though frequency-dependent attenuation of the stimulus and can be well compensated for by hearing aids. In some cases, the causes are amenable to treatment by antibiotics, and in severe cases, the loss may be amenable to surgical intervention, for instance by a prosthesis replacing an ossified stapes in the oval window.

Hearing loss arising in the hair cells or auditory nerve is known as sensorineural hearing loss. Loss arising in the nerve sometimes results from a benign tumour around the sheath of the vestibular nerve (vestibular schwannoma, otherwise called an acoustic neuroma). However, the most common form of sensorineural impairment arises within the cochlea. Cochlear hearing loss can also be caused by acoustic trauma, drugs, infections or may be congenital. A further common type of cochlear hearing loss arises in middle and old age, when degenerative changes can produce an impairment known as presbyacusis (presbycusis), which can be severe and progressive, and is without cure. The sensitive transducer cells, the hair cells,

are particularly vulnerable and if destroyed in mammals cannot be replaced. The stria vascularis is a further vulnerable structure, giving a ‘metabolic’ or ‘strial’ type of loss. Because treatment is so often inadequate, because hearing aids prove to be of limited use and because the condition is widespread, the importance of sensorineural hearing loss of cochlear origin cannot be overestimated. This chapter will be mainly concerned with the mechanisms of sensorineural hearing loss in the vulnerable cell types, the consequences of the loss in terms of the changes in physiological responses and attempts that have been made to reverse some of the effects of the loss, either by electrical stimulation of the inner ear using cochlear implants, or through intervention at the molecular level.



10.2 SENSORINEURAL HEARING LOSS OF COCHLEAR ORIGIN: MECHANISMS OF PATHOLOGY

10.2.1 Ototoxicity

10.2.1.1 Aminoglycosides

Ototoxic drugs fall into a number of categories. The most powerfully ototoxic drugs in general therapeutic use are the aminoglycosides, which include drugs such as gentamicin and kanamycin (Box 10.1).

In spite of decades of research, we are not yet sure of all the mechanisms of aminoglycoside ototoxicity, although it is likely that oxidative damage forms one of the major mechanisms (see below).

Box 10.1 The aminoglycosides

The aminoglycosides are amikacin, dibekacin, gentamicin, isepamicin, kanamycin, neomycin, netilmicin, paromomycin, sisomicin, streptomycin and tobramycin and their variants.

The ending ‘-mycin’ or ‘-micin’ denotes that the substance is produced by the soil actinomycetes, ‘mycins’ by *Streptomyces*, ‘micins’ by *Micromonospora*. Not all drugs with these endings are aminoglycosides.

In bacteria, aminoglycosides bind to the small (16S) component of ribosomal RNA (involved in the production of protein), and this is the presumed mechanism of toxicity in bacteria. However, this binding does not occur in cells with nuclei (eukaryotes), which have a different configuration of their ribosomal DNA (except in the unusual case of an inherited mutation in mitochondrial DNA – see text). This is presumably why eukaryotic cells are less vulnerable to the effects of aminoglycosides.

Data from Forge and Schacht (2000).

It is likely that there are multiple routes of entry of aminoglycosides into the cells of the cochlea. After administration of fluorescently labelled gentamicin *in vivo*, there was found to be rapid uptake into the cells of the stria vascularis as well as those of the spiral ligament, the spiral limbus and the organ of Corti (Wang and Steyger, 2009; for explanation of structures, see Fig. 3.1). The entry into the stria vascularis could form a route by which aminoglycosides enter the scala media and then gain access to the apical surfaces of hair cells. It is possible that at least one of the routes of entry into hair cells is via the mechanotransduction channels on the apical surfaces of the cells. Hair cells may also take up aminoglycosides by transporters within the membrane, or by endocytosis (i.e. taken up in pinched-off vesicles derived from the external membrane of the cell). However, the binding factors or receptors driving the uptake are not known, and multiple mechanisms are likely to operate (for review, see Xie *et al.*, 2011). Within the hair cells, aminoglycosides can be detected by immuno-electron microscopy first in endocytic vesicles (i.e. the vesicles resulting from the uptake described above) and then in liposomes, the intracellular structures that contain large concentrations of degradative enzymes and which are used by the cell to destroy macromolecules (e.g. Hashino *et al.*, 1997). In addition, there is evidence of early uptake by the endoplasmic reticulum and the Golgi apparatus of the cell. The uptake into all the above structures can precede other signs of cellular damage by some days, and therefore is likely to be early in the chain of events, rather than being subsequent to the cell damage. Once in the liposomes, some of the aminoglycoside molecules, rather than being degraded, may be spilt into the cell's cytosol, where they may be able to cause their ototoxic damage. These mechanisms were initially described for the kidney and are less established for the hair cells of the inner ear. In hair cells, and with scanning electron microscopy, the early external signs of damage are often seen as fusion and loss of the stereocilia (Figs. 10.1 and 10.2). As damage progresses, the whole cell is lost.

The aspects of the aminoglycoside molecules that confer their particular reactivity and ability to interfere with biochemical reactions within the cell are still a matter of debate. Aminoglycosides can trigger the formation of free radicals (e.g. reactive oxygen species – forms or compounds of oxygen that have an unpaired electron and so are highly reactive, or reactive nitrogen species, and hydroxyl radicals), the reaction being catalysed by compounds formed between aminoglycosides, membrane lipids and iron (Lesniak *et al.*, 2005). Mice engineered to over-express the antioxidant enzyme copper/zinc superoxide dismutase (SOD1) are less vulnerable to aminoglycosides (Sha *et al.*, 2001a). Protection from oxidative damage by a wide variety of applied antioxidants can also reduce aminoglycoside ototoxicity, suggesting that this is the critical mechanism of damage (Forge and Schacht, 2000). Aspirin (acetyl salicylate) is hydrolyzed on ingestion to become salicylate in the blood serum, where it can act as an antioxidant. Concurrent administration of high levels of aspirin with the gentamicin can substantially protect against gentamicin-induced hearing loss in human beings, supporting this hypothesis (Sha *et al.*, 2006).

In the absence of protection, the free radicals damage lipids, proteins and DNA. The intracellular organelles and membranes are disrupted, and the mitochondria

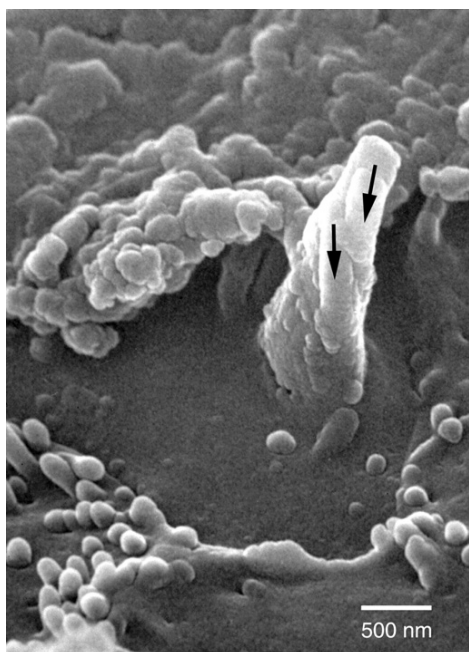


Fig. 10.1 Fused stereocilia remaining on an outer hair cell of the guinea pig cochlea after treatment with kanamycin. Arrows: remains of two individual stereocilia. From Pickles *et al.* (1987a), Fig. 1.

become swollen and fragmented, inducing cell death (see Box 10.2). There are two mechanisms of cell death in hair cells after aminoglycoside intoxication *in vivo*: in apoptosis, the cellular contents are systematically broken down and fragmented within intact cell membranes. In necrosis, the external cell membrane breaks and releases the fragmented cell contents into the surroundings. Evidence from Jiang *et al.* (2006) suggests that hair cell loss after chronic aminoglycoside intoxication *in vivo* occurs by both necrotic and apoptotic mechanisms, although they found that many of the classic markers for apoptosis were absent. According to Abrashkin *et al.* (2006), after the death of hair cells, the cell fragments are phagocytosed by the surrounding supporting cells.

Although aminoglycosides are taken up by many types of cells in the cochlea, the ototoxic effects are primarily seen in the cochlear outer hair cells and vestibular hair cells. The reason for the targeting of ototoxicity to hair cells is not known, but may be related to their higher sensitivity to oxidative damage. Different aminoglycosides also have a different spectrum of effects on the two organs. For example in human beings neomycin is primarily toxic to the cochlea, while gentamicin is more toxic to the vestibular system; again, the reasons are not known. The greater vulnerability of basal in comparison to apical outer hair cells may arise because of lower antioxidant defences in the basal outer hair cells (Sha *et al.*, 2001b).

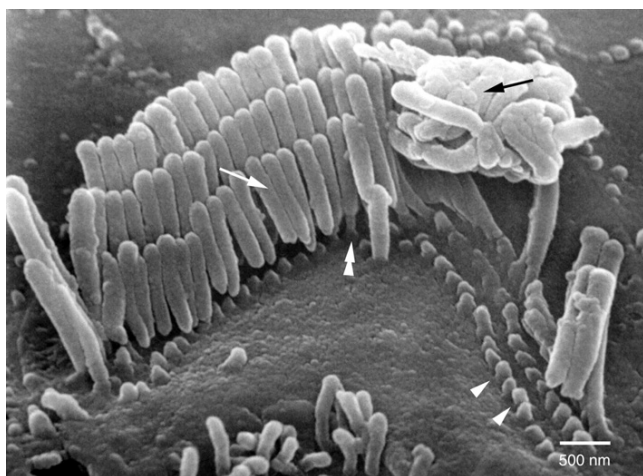


Fig. 10.2 In outer hair cells less severely affected by kanamycin, the stereocilia may be detached or fused (arrows), and the tip links lost. Single arrowheads: rootlets of stereocilia remaining in the cuticular plate. Double arrowhead: constricted rootlet of stereocilium. Guinea pig. From [Pickles et al. \(1987a\)](#), Fig. 4.

Box 10.2 Mitochondria and cell death

Mitochondria play a key role in cell death. Normally, the mitochondria generate the high-energy compound ATP by oxidizing the products of glucose metabolism. During this process, a negative potential (-140 mV , the 'mitochondrial potential') is generated within the mitochondria. When mitochondrial oxidation is compromised, the mitochondrial potential falls. As a result of this, a structure known as the permeability transition pore opens in the mitochondrial inner membrane, allowing the entry of small-molecular-weight solutes, following which the mitochondria break open from osmotic stress. This releases factors, called 'apoptosis-inducing factors', which trigger a series of changes culminating in cell death.

The apoptosis-inducing factors activate proteins called caspases, which activate other members of the caspase family in an amplifying cascade. The caspases then cleave other proteins and activate degradative enzymes, causing disassembly of the cell. Cell death is also regulated by other factors, including the mitogen-activated protein kinase/c-Jun N-terminal kinase (MAPK/JNK) pathway, and by members of the Bcl-2 family. Some members of the Bcl-2 family promote cell death, and others inhibit it. Other protein cascades such as the calpains and cathepsins also produce cell death.

For information on cell death pathways in hair cells, see [Cheng et al. \(2005\)](#) and [Sha et al. \(2009\)](#).

10.2.1.2 Other ototoxic agents

Other agents will be mentioned only briefly. Cisplatin (cisplatinum), an anticancer compound that can cause permanent hearing loss, targets outer hair cells, cells of the spiral ganglion (auditory nerve) and the lateral wall of the cochlea, including the stria vascularis. It probably also works by oxidative damage, because anti-oxidants provide some protection (for review, see Mukherjea and Rybak, 2011). Loop diuretics (e.g. ethacrynic acid, furosemide and bumetanide) reduce the absorption of fluid in the kidney by inhibiting the active absorption of Cl^- in the loop of Henle. In the cochlea, they affect the endocochlear potential, targeting the $\text{Na}^+/\text{2Cl}^-/\text{K}^+$ cotransporter in the marginal cells of the stria vascularis (for review, see Ikeda *et al.*, 1997; see also Chapter 3). Aspirin (acetyl salicylate) causes a temporary hearing loss, by reversibly competing with Cl^- for a binding site on prestin, the outer hair cell motor protein that is responsible for the active amplification of the mechanical travelling wave in the cochlea (Santos-Sacchi *et al.*, 2006). Salicylate induces tinnitus by mechanisms unknown, but may act by both peripheral and central mechanisms (for review, see Eggermont, 2012). Organic solvents such as styrene and toluene are also ototoxic, although the mechanisms of the ototoxicity are not clear (Hoet and Lison, 2008).

10.2.2 Acoustic trauma

Hair cells have been examined from cochleae either immediately after the induction of experimental acoustic trauma or after a period in which the degenerative or repair processes have had a chance to operate.

In the mildest cases of acoustic trauma, the stereocilia of outer hair cells can be slightly splayed and tip links broken, while the rootlets of the stereocilia become less dense in transmission electron micrographs (Liberman and Dodds, 1987; Clark and Pickles, 1996). It was suggested, on the basis of the losses in associated electrophysiological recordings, that these changes are fully reversible. In more severe cases, leading to permanent damage, the stereocilia kink or fracture at the rootlet and the packed actin filaments which give the stereocilia their rigidity depolymerize (Liberman and Dodds, 1987). The links between the stereocilia break and the stereocilia separate widely, with loss of tip links and consequent loss of transduction. In inner hair cells, however, the tallest stereocilia in the bundle tend to break away from the others, the shorter stereocilia keeping their linkages intact and hence presumably still being able to transduce (Fig. 10.3; Pickles *et al.*, 1987b). In other cases, the stereocilia become fused, bent, splayed apart or detached (Fig. 10.4). In more severe cases, changes are also found in the supporting cells, and in very severe acoustic trauma, such as blast noise, the whole organ of Corti can be ripped apart mechanically (Patterson and Hamernik, 1997).

Intracellularly, hair cells show changes associated with metabolic stress, including breakdown of internal structures and swelling and disruption of mitochondria, which can be expected to lead to cell death over hours or days (Lim, 1986). As with ototoxicity, oxidative damage may contribute to cell death, since enhanced levels of reactive oxygen species can be demonstrated in hair cells after

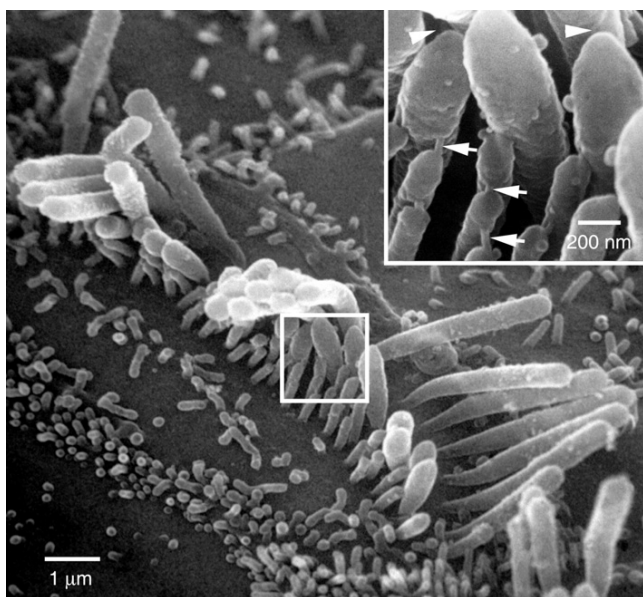


Fig. 10.3 The tallest stereocilia on an inner hair cell can show disarray after acoustic trauma, while the shorter stereocilia and their tip links remain intact. The inset shows the region outlined in the main figure and shows that tip links (arrows) remain on the shorter stereocilia. However, the tip links connecting the shorter stereocilia to the tallest stereocilia are broken (arrowheads). It is therefore possible that the shorter stereocilia may still be able to transduce, being moved by viscous drag from the surrounding fluid during acoustic stimulation. Scale bar: 1 μm in the main figure and 200 nm in the inset. From [Pickles *et al.* \(1987b\)](#), Figs. 15 and 16.

acoustic overstimulation. The reactive oxygen species are likely to have been produced by impaired oxidation in partially damaged mitochondria (for review, see [Henderson *et al.*, 2006](#)).

Further changes are produced in the afferent nerve supply. The synapses of the majority Type I afferent nerve fibres below the inner hair cells become swollen and can fragment. The changes are produced by excitotoxicity, that is by the afferent neurotransmitter, glutamate, which activates channels in the nerve fibre membranes allowing high levels of Ca^{2+} to enter the cell. The Ca^{2+} has a number of effects: it activates many enzymes which damage cell structures such as the cytoskeleton, membranes and DNA as well as opening the permeability transition pores of mitochondria which can trigger cell death (see [Box 10.2](#)). In mild cases, the synapses can recover after a few days, but in more severe cases, the afferent nerve fibres degenerate. Anoxia can also cause excitotoxic damage to the afferent nerve fibres (for review, see [Pujol and Puel, 1999](#)). Dopamine released from the lateral olivocochlear bundle (see Chapter 8) can reduce the excitotoxicity, presumably via inhibitory dopaminergic synapses on the peripheral terminals of the afferent auditory nerve

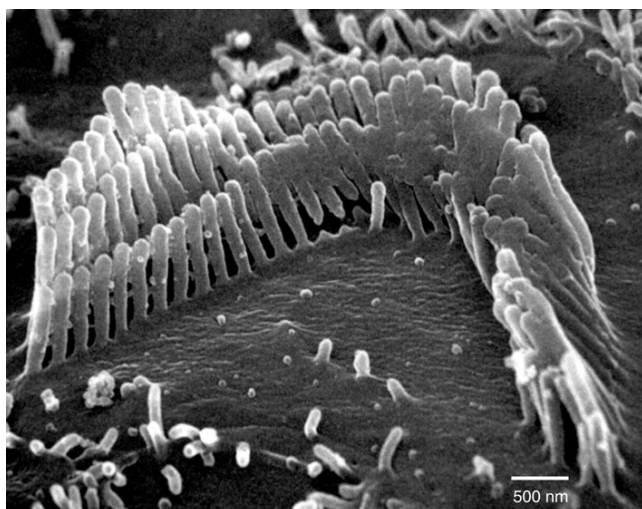


Fig. 10.4 An outer hair cell after acoustic trauma, showing fused and detached stereocilia and loss of tip links. Scale bar: 500 nm. From Pickles *et al.* (1987b), Fig. 6.

fibres (Darrow *et al.*, 2007; Lendvai *et al.*, 2011; see also Ohlemiller, 2008, for a general overview of cochlear acoustic trauma).

10.2.3 Genetic causes

There are a large number of inherited diseases that can directly affect hearing. Many of these, though rare in the population as a whole, have been invaluable to researchers as a means of tracking down critical molecular components of the inner ear.

The most common genetic form of sensorineural deafness, in some national populations accounting for 35% of all cases of inherited hearing loss, is a mutation in the gene encoding connexin-26 (the CX26 or *GJB2* gene), which gives rise to the form of deafness classed as DFNB1 (see Box 10.3). Connexin-26 is a component of gap junctions which allow ions and small molecules to pass between cells. In the inner ear, gap junctions in the supporting cells of the cochlea, in the spiral ligament and in the cochlear wall, allow K^+ to be recycled from the scala tympani, through the spiral ligament, and to the marginal cells of the stria vascularis, from where the K^+ is pumped back into the scala media (see Chapter 3). DFNB1 is severe and of early onset. In gap junctions, connexin-26 can co-assemble with other connexins (e.g. connexin-30) to make a complete junction, and the gene for connexin-30 (*GJB6*) is sometimes also mutated, also giving rise to DFNB1 (for reviews, see del Castillo and del Castillo, 2011; Pfenniger *et al.*, 2011).

Among the many non-syndromic recessively inherited genetic diseases affecting hair cells, among the first to be characterized was one arising from mutations in the

Box 10.3 Nomenclature of genetic hearing losses

Genetic hearing losses are divided into syndromic forms (where deafness is only one component of whole syndrome of changes, including, e.g. blindness), and non-syndromic or isolated forms (affecting hearing only).

Non-syndromic forms are further divided according to their mode of transmission:

- (1) X chromosome-linked (labelled DFN).
- (2) Y chromosome-linked.
- (3) Not linked to X or Y chromosomes (i.e. autosomal) and dominant (labelled DFNA).
- (4) Not linked to X or Y chromosomes (i.e. autosomal) and recessive (labelled DFNB).
- (5) Mitochondrial genes (maternally inherited).

Within the different categories, the type is labelled in order of date of identification, that is DFNB1 was the first to be identified in the DFNB category. Human gene names are written in capitals, while other species have species-specific nomenclatures. In all species, gene names are written in italics, while gene protein products are written in non-italics.

Different mutations in the same gene can lead to different patterns of deficit (i.e. can give rise to different non-syndromic or syndromic losses).

From Petit (2006).

MYO7A gene. *MYO7A* codes for myosin 7A and gives rise to the DFNB2 hearing loss. Depending on the region mutated, mutations in *MYO7A* can also give rise to a syndromic hearing loss, Usher syndrome Type IB, which includes loss of vision as well as deafness. Myosin 7A is important for the integrity of the hair cell stereocilia. As a further example, the *CDH23* gene codes for cadherin-23 (otocadherin), a major component of the tip link, loss of which leads not only to loss of transduction, but also to gross disorganization of the stereocilia and to the DFNB12 type of hearing loss. In a third example, the *USH1C* gene was found to code for a cytoskeletal protein called harmonin, which is expressed in stereocilia and which cooperates with myosin 7A and cadherin-23 in generating the hair cell bundle (Schwander *et al.*, 2010). While mutations in this gene can give rise to the non-syndromic hearing loss labelled DFNB18, the pattern of mutations more commonly lead to Usher syndrome Type 1C, which includes blindness as well as deafness. Many further genes also affect hair cells and also give rise to deafness when mutated (for reviews, see Raviv *et al.*, 2010; Richardson *et al.*, 2011).

Mitochondria have their own genetic systems, reminiscent of the bacteria from which they evolved. Mitochondria are passed down in the ovum, and only very rarely in the sperm, so the inheritance of the mitochondrial genome is

exclusively or almost exclusively from the mother. Mitochondrial genes encode some of the proteins involved in mitochondrial metabolism, which involves oxidation and energy production. Because of the importance of mitochondria for energy production in all cells of the body, mitochondrial mutations with severe effects, and where a high proportion of the inherited mitochondria carry the mutation, are fatal early in life. However, some mutations have relatively mild effects and allow the organism to survive, only showing their influence later in life or when the organism is stressed. Because some cells of the inner ear (e.g. in the stria vascularis and auditory nerve) have a high energy consumption, and because some of these cells and hair cells are postmitotic (i.e. dead cells cannot be replaced by mitosis – cell division), these are among the sites at which mitochondrial mutations first make their presence felt. Many of the several mitochondrial syndromes that affect hearing also affect brain, muscle and kidney, where, as in the inner ear, the cells are postmitotic, have heavy energy consumption and are heavily involved in ion pumping. One typical example is MELAS (standing for mitochondrial encephalomyopathy, lactic acidosis and stroke-like episodes), the name indicating the further involvement of muscle and brain. Mitochondrial diseases tend to progress over time: the mutant load in the vulnerable cells increases over time, with individual cells continuing to function apparently normally until a certain mutant load is reached, at which point energy production fails, the cell death pathways are triggered and the cell dies (see Box 10.2).

One intriguing human mitochondrial mutation is known as the A1555G mutation (because the adenine at position 1555 in the mitochondrial genome is changed to a guanine). Patients with the A1555G mutation have a very high susceptibility to aminoglycoside-induced hearing loss. This mutation is found in the DNA coding for the mitochondrial small ribosomal RNA (involved in protein synthesis). It has been suggested that the mutation makes the ribosomal RNA assume the conformation of bacterial ribosomal RNA, which is effective at binding with aminoglycoside antibiotics ([Hutchin and Cortopassi, 2000](#)). However, it should be remarked that the pattern of ototoxicity in these patients differs from the normal pattern of aminoglycoside-induced damage. In addition, even without aminoglycosides, patients with this mutation tend to show a mild and progressive hearing loss.

Mitochondrial involvement in hearing loss has been reviewed by [Fischel-Ghodsian et al. \(2004\)](#), [Kokotas et al. \(2007\)](#) and [Cacace and Pinheiro \(2011\)](#).

10.2.4 Ageing

Sensorineural hearing loss due to ageing is known as presbycusis (presbycusis). In the cochlea, age-related morphological changes have been shown in the hair cells, auditory nerve and stria vascularis, with the marginal cells of the latter being particularly vulnerable ([Schuknecht and Gacek, 1993](#)). One debate concerns whether the changes are due to accumulated small degrees of trauma, for example acoustic or ototoxic damage, over the lifespan. A second debate concerns the extent to which genetic factors also contribute. In a study of male twins, about half the variability of

age-related hearing loss had a genetic origin, although in the older age groups non-genetic (i.e. environmental) factors became relatively more important (Karlsson *et al.*, 1997). Studies of a large cohort in human beings have shown the existence of a ‘sensory’ pattern associated with hair cell changes and a ‘strial’ pattern associated with the stria vascularis. Both of these have inherited components, with the strial losses being particularly strongly inherited in females (Gates *et al.*, 1999). A third debate concerns the factors underlying the vulnerability of the different structures of the inner ear. Many of the most vulnerable structures have a high energy consumption, or are composed of predominantly postmitotic cells which therefore cannot be replaced after damage, or share both properties.

We would expect cells with a high energy consumption to be most vulnerable to the effects of mitochondrial dysfunction. Mitochondrial dysfunction and damage by free radicals are likely to lead to accumulated damage to the mitochondrial proteins and lipids, as well as to accumulated mutations in the mitochondrial DNA, all of which would render the mitochondrial oxidative chain increasingly inefficient. Increasing amounts of free radicals would therefore be formed. The free radicals would further damage the mitochondria, so that the production of free radicals further increases, leading eventually to a runaway vicious cycle, culminating in death of the cells (see Box 10.2) and hearing loss (reviewed by Pickles, 2004; Seidman *et al.*, 2004). Post-mortem analysis of mitochondrial DNA from the cochlea of patients has indeed shown an accumulation of mutations in the mitochondrial DNA associated with presbycusis, suggesting that these mutations are a contributor in some individuals (Fischel-Ghodsian *et al.*, 1997).



10.3 SENSORINEURAL HEARING LOSS OF COCHLEAR ORIGIN: FUNCTIONAL CHANGES

10.3.1 Physiological changes

10.3.1.1 Damage to outer hair cells

As was discussed in Chapters 3 and 5, outer hair cells help produce the sharp tuning and great sensitivity of the mechanical travelling wave in the cochlea. They do this by means of the active mechanical process, which feeds mechanical energy of biological origin back into the wave. After the administration of ototoxic drugs such as the aminoglycoside antibiotics, which preferentially damage the outer hair cells, neural tuning curves are raised in threshold and broadened in tuning, losing their sensitive, sharply tuned tips (Fig. 10.5). The changes are reminiscent of those seen in the tuning of the basilar membrane itself as the preparation deteriorates (Fig. 3.13B, line marked ‘p.m.’). Because the very great majority of auditory nerve fibres innervate the inner hair cells, it is concluded that the changes in Fig. 10.5 occur because loss of the outer hair cells has altered the mechanical pattern of vibration on the basilar membrane.

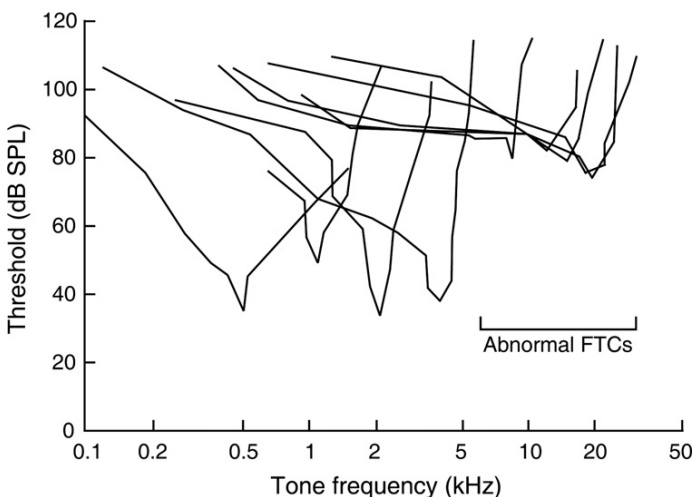


Fig. 10.5 After kanamycin, the tuning curves of auditory nerve fibres are raised in threshold and broadened in shape. In this experiment, fibres from the high-frequency end of the cochlea were most affected ('Abnormal FTCs'). Guinea pig. From Evans and Harrison (1976), Fig. 1.

In a series of careful experiments, Liberman and colleagues recorded from auditory nerve fibres in acoustically damaged ears. The nerve fibres were filled with horseradish peroxidase after recording, so that the fibres could be traced back to the inner hair cells of origin. The cochlea was then analysed morphologically. It was found that if only the outer hair cell stereocilia had been damaged in the region of the cochlea innervated, the tuning curve was raised in threshold and broadened in shape (Fig. 10.6A; Liberman and Dodds, 1984b). If however some outer hair cell stereocilia remained, a small, sharply tuned tip could remain on the upper edge of the tuning curves, presumably resulting from only a partial loss of the sharply tuned response (Fig. 10.6B). These results confirm the role of the outer hair cells in increasing the sharp tuning and sensitivity of the travelling wave.

10.3.1.2 Damage to inner hair cells

The majority of experimental manipulations affect outer hair cells rather than inner hair cells. However, by tracing horseradish peroxidase-filled afferents to the inner hair cells after electrophysiological recordings, Liberman and Dodds (1984b) were able to show that where there was disarray mainly of inner hair cell stereocilia, the tuning curves were raised in threshold, but were of nearly normal shape (Fig. 10.6C). The results are in agreement with the idea that inner hair cells are only involved in detecting the movement of the basilar membrane and are not involved in producing the sharp tuning. The disarray was mainly seen in the tallest

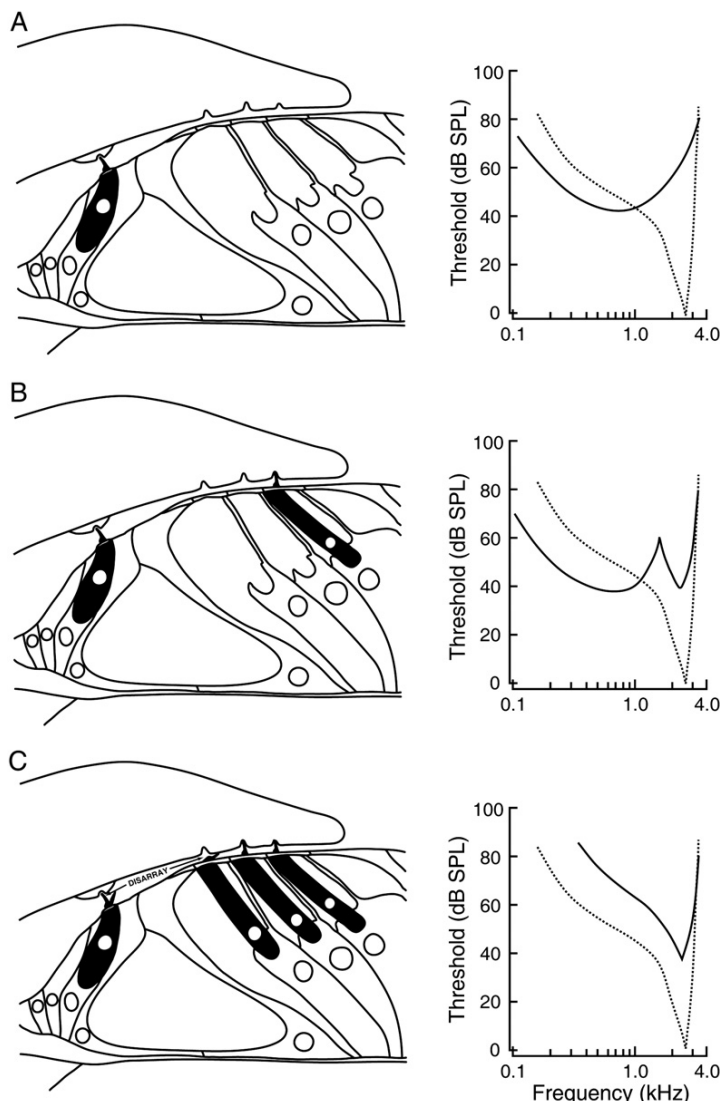


Fig. 10.6 (A) If the stereocilia of outer hair cells are lost, the auditory nerve fibres innervating the adjacent inner hair cells are raised in threshold and broadened in tuning (solid line in tuning curve vs. dotted line – normal). The low-frequency tail of the tuning curve becomes hypersensitive. (B) If some outer hair cell stereocilia remain, a short, sharply tuned tip can be seen on the tuning curve. (C) If inner hair cell stereocilia are damaged while most outer hair cell stereocilia remain apparently normal, the tuning curve can have a nearly normal shape but be raised in threshold. From Liberman and Dodds (1984b), Fig. 14.

stereocilia; the morphological changes shown in Fig. 10.3, where the tip links remain intact on the shorter stereocilia, suggest that such inner hair cells might indeed be able to continue transducing, though with reduced sensitivity. Auditory nerve fibres from these inner hair cells have much lowered rates of spontaneous activity, perhaps because of reduced standing currents through the disconnected, and therefore possibly shut, mechanotransducer channels (Liberman and Dodds, 1984a).

10.3.2 Psychophysical correlates

10.3.2.1 Threshold and loudness

The neural data lead us to expect a loss of sensitivity in sensorineural hearing loss of cochlear origin, combined with a loss in frequency resolution.

The loss of sensitivity is of course an easily recognizable sign of cochlear damage. In ototoxicity and ageing, high frequencies are generally affected first, in accordance with the generally greater vulnerability of basal outer hair cells (see Section 10.2). However, with acoustic trauma, the losses are determined by the frequency of exposure as well as by the pattern of vulnerability of the hair cells.

With intense narrowband traumatizing stimuli, it can be shown that the losses are concentrated at the point of maximum vibration of the basilar membrane, which leads to a loss of sensitivity to frequencies represented in that region. However, it should be noted that the frequency of maximum loss and the frequency of exposure are not always the same. As shown in Fig. 3.10B, with intense stimuli the peak of mechanical vibration occurs basal to the peak measured with less intense stimuli (compare lines for 100 and 20 dB SPL). This occurs because the peak of vibration for less intense stimuli is dominated by the active process. The active process starts to grow more slowly beyond around 30 dB SPL. However, the passive component of the travelling wave, though smaller at low stimulus intensities, increases linearly with intensity, and so comes to dominate at high stimulus intensities. The peak of vibration for the 15-kHz, 100-dB SPL stimulus in Fig. 3.10B, at around 3.1 mm from the base, corresponds to the 18 kHz point in the cochlea, if measured with low-intensity test stimuli. In this example, intense 15-kHz tones will therefore produce their greatest losses at around 18 kHz. The phenomenon, of intense narrowband stimuli producing maximum losses in sensitivity at higher frequencies, is known as ‘the half-octave shift’. The same phenomenon is depicted in Fig. 8.5, where a 10-kHz traumatizing tone produces the greatest threshold loss at 14 kHz.

In human beings, general broadband noise exposure, as found for instance in a noisy environment, commonly produces its first loss at 4 kHz, producing a phenomenon in the audiogram known as the ‘4 kHz notch’. A selective loss at this frequency is generally taken as a sign of previous noise exposure, though with limited reliability (see, e.g. McBride and Williams, 2001). The mechanisms behind the development of the 4-kHz notch are not known. It may correspond to a particular vulnerability of the cochlea in this region, combined with the overall spectrum of the noise to which individuals tend to be exposed. A 4-kHz notch is

also seen in the behavioural audiograms of apparently normal cats, and in the thresholds of auditory nerve fibres with characteristic frequencies in that region (Fig. 4.4). These small losses in apparently normal cats seem to be pathological, because they are reduced in cats raised from birth in a soundproofed chamber (Liberman and Kiang, 1978).

Patients with sensorineural hearing loss show a characteristic feature, namely that of loudness recruitment. Once stimuli become supra-threshold, perceived loudness grows abnormally quickly with increases in stimulus intensity. Originally, it was thought that this had a cochlear origin and could be explained by the transition from the generally shallow slope of the amplitude functions that are seen in sensitive cochleae, to the steeper more linear growth seen in insensitive cochleae (see, e.g. Fig. 3.13A, compare curves marked 9, 10 and 11 kHz with that marked 9 p.m.). However, recordings from auditory nerve fibres are inconsistent with this hypothesis: loudness functions calculated from the responses of auditory nerve fibres are no steeper after hearing loss than before (Heinz *et al.*, 2005). In contrast, in the ventral cochlear nucleus, some types of cells show steepened rate-level functions and higher maximum firing rates some weeks after acoustic trauma (Cai *et al.*, 2009). The cells showing these changes are those with chopper responses and other non-primary-like responses, generally identified with T- or D-stellate morphology and octopus cells (see also Chapter 6). The reason for the enhanced responses was not shown; it was suggested that a decrease in inhibition on the cells might be responsible, as well as perhaps a change in the strength of the excitatory synaptic inputs.

10.3.2.2 Frequency resolution

The change in neural frequency resolution has a correlate in psychophysical data. Psychophysical tuning curves, which are thought to be an approximation to neural turning curves (Figs. 9.2 and 9.4), are broadened (e.g. Moore and Glasberg, 1986). The sharply tuned tip of the psychophysical tuning curve is shortened or abolished, and the low-frequency slope in particular becomes shallower (Fig. 10.7). These changes parallel those seen in auditory nerve fibres (Fig. 10.5). In some cases, W-shaped FTCs are found. These do not have an obvious correlate in the tuning curves of auditory nerve fibres. Instead, Kluk and Moore (2005) showed that W-shaped tuning curves in impaired ears occurred when the signal frequency fell within or near a cochlear ‘dead’ region, that is one in which no responses were detectable because for instance none of the inner hair cells are functional. In these cases, the signal was detected in other frequency regions of the cochlea, as a result of beats or difference tones produced between the signal and the masker. Additional masking of these components returned the FTCs to a simple shape, with a single broad dip.

Critical bandwidths, being the bandwidths of the psychophysical filter (see Section 9.3.1.3), are also affected. Psychophysical filters, measured by a great variety of methods, all become broader with increases in threshold. For instance, Laroche *et al.* (1992) asked subjects to detect a probe tone masked by wideband

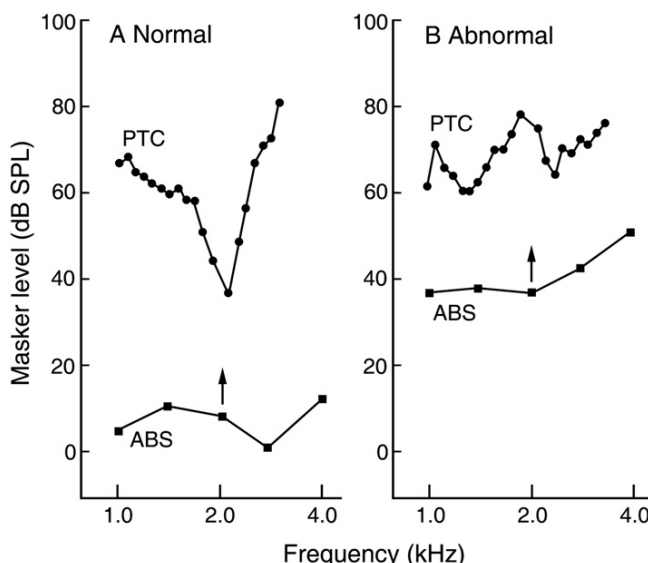


Fig. 10.7 Psychophysical tuning curves (PTCs) determined with simultaneous masking in a normal subject (A) and in a subject with sensorineural hearing loss (B). ABS, absolute threshold (audiogram). Arrows: frequency and intensity of probe. Reprinted from Carney and Nelson (1983), Figs. 1 and 3, Copyright (1983), with permission from American Institute of Physics.

noise, where the noise had a notch in its spectrum centred on the frequency of the probe. They plotted the masked threshold as a function of the width of the notch and used the results to calculate the shape of the psychophysical filter. There was little change in the effective bandwidth of the psychophysical filter with threshold losses of up to about 30 dB, and thereafter bandwidths increased approximately 1.5-fold for each 10 dB increase in threshold. The same trend was apparent in a summary of data published by Moore (2005). These patterns of change have a parallel in the single-unit data where for small losses the tips of the tuning curves are raised but do not become any broader, but after a certain point, the tuning curves broaden substantially.

There is also a very large scatter in the psychophysical data, some patients with hearing losses of up to 70 dB showing normal frequency resolution bandwidths. This may reflect variation in the factors underlying the loss (e.g. the relative degrees of damage to inner and outer hair cells).

The loss of resolution leads to a particular difficulty in understanding broadband complex sounds. While acoustic amplifying hearing aids can increase the magnitude of the acoustic signal, and so restore sensitivity, they cannot restore the cochlea's frequency resolution, so that the sounds, though now audible, may sound incomprehensible or garbled. This particularly affects the understanding of speech, especially in a noisy background.

10.3.2.3 Tinnitus

One of the sometimes distressing accompaniments of sensorineural hearing loss is tinnitus, which can deprive the sufferers of even the dubious consolation of living in a silent world. Tinnitus is defined as an auditory sensation in the absence of an auditory input. Originally, tinnitus was divided into objective tinnitus, which could be recordable as a real sound in the ear, and subjective tinnitus, which could not. Objective tinnitus was thought to arise peripheral to the cochlea, in say the muscles or vasculature of the middle ear, while subjective tinnitus arose in the cochlea or more centrally. The discovery of cochlear emissions showed that some 'objective' tinnitus could arise in the cochlea. Figure 5.19A shows a recording of spontaneous objective tinnitus of cochlear origin, recorded in the ear canal. It is likely that this arises when the gain of the outer hair cell active process becomes temporarily high, enhancing the energy fed back into the basilar membrane. If the spatial relations are right, mechanical energy may be reflected back and forth along the cochlea, further stimulating the hair cells, leading to a self-sustaining oscillation, and so to tinnitus. It is common to experience transient periods of tinnitus of this type, when a sudden tonal 'ping' is heard in the ear, which then gradually fades over several seconds or minutes. In these cases, an emission of sound of the same frequency can be recorded in the ear canal.

Although this is an intriguing explanation of one type of tinnitus, it is not likely to explain the majority of the cases of clinical importance. We expect tinnitus associated with cochlear emissions to be continuous and narrowband or tonal. In contrast, much tinnitus is continuous and atonal, like high-pitched hissing or knocking noises. Moreover, cochlear emissions disappear in experimental cochlear deafness, while tinnitus can be particularly prominent in patients with severe hearing loss.

In contrast, most of the tinnitus of clinical importance is likely to arise centrally. This is supported by findings that cutting the auditory nerve is commonly ineffective in relieving tinnitus. Since tinnitus is usually associated with some degree of hearing loss, the most reasonable explanation is that tinnitus results from compensating central hypersensitivity following a reduction in peripheral input.

Animal models have proved invaluable for analysing possible neural mechanisms for the generation of tinnitus. In a typical behavioural test, animals are trained to drink in the presence of noise, but trained to stop drinking when in silence (Jastreboff *et al.*, 1988). Before the induction of tinnitus, animals are tested in alternating periods of noise and silence. After the experimental manipulation, continued drinking in the periods of silence is taken as an indication that the animals can in fact hear a stimulus, that is can hear tinnitus. Factors that induce tinnitus when tested this way are similar to those inducing tinnitus in human beings, including systemically administered ototoxic drugs (aminoglycosides, salicylate and quinine) and acoustic overstimulation.

The tinnitus-inducing manipulations do not in general produce sustained increases in the spontaneous activity of primary auditory nerve fibres; rather, the activity decreases or stays the same (e.g. Mulheran, 1999). However, spontaneous activity may increase in certain central structures of the auditory pathway,

including the dorsal cochlear nucleus, the inferior colliculus and areas of the auditory cortex.

As an example, Kaltenbach *et al.* (1998) exposed hamsters to an intense (125–130 dB SPL) 10-kHz tone for 4 h. Thirty days after the exposure, rates of spontaneous activity were found to be raised three- to fourfold in the dorsal cochlear nucleus. Neural thresholds were also raised, consistent with the suggestion that increased thresholds can lead to increased spontaneous activity. In the inferior colliculus, Bauer *et al.* (2008) also found increases in neural spontaneous activity and in neural synchronization in subsets of neurones in all areas of the colliculus following a variety of tinnitus-inducing manipulations of the cochlea.

GABA and glycine are major inhibitory neurotransmitters within the central auditory nuclei. Middleton *et al.* (2011) showed a decrease in GABAergic inhibition within the dorsal cochlear nucleus, using brain slices taken from mice with behavioural evidence of tinnitus. Similarly, a decrease in the expression of glycine receptors has been found in the dorsal cochlear nuclei of rats with behavioural evidence of tinnitus (Wang *et al.*, 2009a). These and similar results suggest that decrease in central inhibition is one of the consequences of the reduction in peripheral input. GABAergic inhibition can be enhanced by the anti-epileptic drugs vigabatrin and gabapentin. In experimental animals, both drugs were found to reduce tinnitus, as judged by behavioural tests. Trials with human beings have also found some positive effects in a subset of patients (discussed by Bauer and Brozoski, 2007; see also Wang *et al.*, 2011a; Richardson *et al.*, 2012, for reviews).

Changes in GABAergic and glycinergic inhibition could also explain the increased tinnitus commonly found with ageing, since GABAergic and glycinergic inhibition are reduced in the auditory brainstem of ageing rats (Caspary *et al.*, 1995; Wang *et al.*, 2009b).

Another mechanism has been suggested by Pilati *et al.* (2012). They showed in rats that a few days after acoustic overstimulation which caused hearing loss, fusiform cells in the dorsal cochlear nucleus developed an irregular bursting pattern of firing. They presented evidence that this was associated with a downregulation in the channels known as Kv3 high voltage activated potassium channels. These channels could therefore potentially be a target for pharmacological therapy.

One of the critical features of tinnitus is the way that it can dominate the patient's attention. This can occur even though the tinnitus may be perceived at only a low subjective level, as judged by comparisons of loudness. It is noteworthy that the nuclei of the extralemniscal auditory pathway trigger automatic orienting reflexes, which may explain the effect (see Chapter 6). The dorsal cochlear nucleus, the first site at which increases in activity have been shown with tinnitus, is the first stage at which the extralemniscal pathway starts to diverge from the more specific lemniscal pathway. A further common finding is that tinnitus is enhanced by anxiety. Activity of the locus coeruleus induces anxiety, and the locus coeruleus sends projections to the dorsal cochlear nucleus (Kromer and Moore, 1980; Tanaka *et al.*, 2000). Cross-sensory interactions in tinnitus may also be explicable: in some patients, tinnitus can be enhanced by clenching the jaws or contracting muscles of the neck. Stimulation of the trigeminal and other somatosensory nerves can

enhance responses in auditory neurones situated in the dorsal cochlear nucleus and external nucleus of the inferior colliculus, sites in the extralemniscal auditory pathway where neuronal activity is increased in tinnitus (Shore and Zhou, 2006; for review, see Kaltenbach, 2006).

Notwithstanding the preliminary results described above, tinnitus in human beings is currently poorly controlled by drugs or by surgery. However, behavioural intervention, in the form known as tinnitus retraining therapy, can be highly successful. Tinnitus retraining therapy aims to reduce the perception of tinnitus by reducing its significance for the patient. In this way, it is hoped that the mechanisms of neural plasticity that have enhanced the tinnitus in the patient's awareness will be put into reverse. Tinnitus retraining therapy uses multiple strategies, including counselling and the use of distracting sounds, to bring this about, with a reported success rate of 80% or higher (reviewed by Jastreboff, 2007).



10.4 PHYSIOLOGICAL ASPECTS OF THE COCHLEAR PROSTHESIS

10.4.1 Introduction

When the hair cells of the cochlea are lost in human beings, they cannot currently be replaced. Therefore, natural hearing cannot be restored. Under these circumstances, the best hope for restoring some auditory function seems to be to bypass the transducer mechanism and to attempt to stimulate what remains of the auditory nerve directly, by electrical means. It is intended, by stimulating early in the auditory pathway, that the complex and specialized signal processing capabilities of the auditory system will be utilized. Cochlear implants have been highly successful, restoring useful hearing at the time of writing to over 200 000 people worldwide. The successful development of effective cochlear prostheses has depended on the simultaneous solution to problems in physiology, bioengineering, psychophysics and signal processing.

The earliest attempts to stimulate the cochlea by means of a prosthesis ranged from the use of a single extracochlear electrode on the round window to intra-cochlear stimulation with one or a few electrodes. These devices generally gave poor sound quality, and unaided speech perception was rarely attainable. Development of an effective prosthesis, with free-running conversational speech being understood by a high proportion of patients, has depended on (i) the development of longer electrode arrays, so that a greater length of the cochlea can be stimulated, (ii) the use of multiple electrodes, so that the stimulus could be delivered to localized regions of the cochlea, (iii) the development of novel patterns of electrical stimulation and advanced signal pre-processing, which present the cues to the remaining auditory nerve fibres in the most effective manner and (iv) advances in electrode design which have permitted the electrodes to be inserted accurately in the correct places in the cochlea while causing minimal damage and tissue reaction.

10.4.2 Physiological background

10.4.2.1 Condition of the nerve

A critical question is: Are there any auditory nerve fibres left to stimulate when all hearing has been lost through cochlear deafness? In a summary of seven studies in human beings, [Leake and Rebscher \(2004\)](#) reported that the mean survival of cochlear ganglion cells varied between 41% and 77% of normal (range of averages for the different studies). The extent of the loss depends on the original cause of the deafness. There were large losses if the original deafness was due to viral labyrinthitis, fewer losses if it was due to congenital deafness or to bacterial meningitis and only small losses if the original deafness was due to aminoglycosides or to sudden idiopathic deafness. In addition, the losses tended to be greater towards the base of the cochlea where most cochlear prostheses are placed, and the losses increased with longer durations of deafness ([Nadol, 1997](#); see also [Shepherd et al., 2004](#), for animal studies). However, it is difficult to assess this ahead of implantation: pre-operative testing for the presence of nerve fibres with, for example extracochlear electrical stimulation, has been shown to have limited predictive value and is therefore normally not undertaken (e.g. [Frohne et al., 1997](#)). However, imaging of the temporal bone, either by high-resolution X-ray computerized tomography or by high-resolution magnetic resonance imaging (MRI), is routinely used. This not only shows whether there are any structural abnormalities that may compromise insertion of an implant, but with appropriate techniques can show the anatomical condition of the nerve.

A second problem is that intracochlear insertion of the electrode array may produce further loss of nerve fibres. The major factor causing this arises from trauma during insertion, which may extend to the array breaking through the spiral lamina or through the covering of Rosenthal's canal, the latter containing the cells of the cochlear ganglion. A further complication is the growth of new bone around the electrode, which is probably determined both by the previous pathology and by the degree of trauma occurring during the insertion ([Nadol, 1997](#)).

10.4.2.2 Responses of auditory nerve fibres to electrical stimulation

In normal subjects, the auditory nerve transmits information by two methods of coding, namely (i) the place principle, by which the place of maximum activation in the cochlear duct depends on the frequency of the stimulus and (ii) the timing principle, by which individual action potentials tend to be locked to the temporal waveform of the stimulus. With normal acoustic stimulation, these are not independent factors, but are tied together by the mechanics of the cochlea. Furthermore at any one frequency, the firing rate increases sigmoidally with the stimulus intensity over a range of input intensities, depending on the fibre, of 20–60 dB. It is worth examining the extent to which these aspects can be reproduced by electrical stimulation.

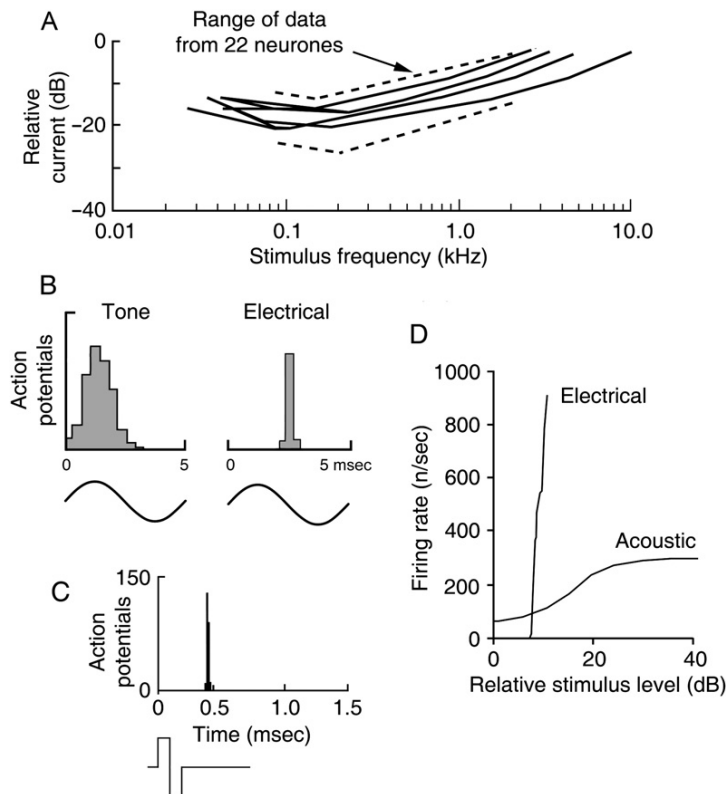


Fig. 10.8 Auditory nerve responses to electrical stimulation. (A) Auditory nerve fibres show negligible intrinsic tuning to electrical stimuli applied across the cochlea. These broad ‘tuning curves’ should be compared to the sharp tuning curves to acoustic stimuli shown in Fig. 4.3. (B) Period histogram in response to a 200 Hz sinusoidal acoustic stimulus in a normal cat (left) and of a sinusoidal electric stimulus in a deafened cat (right). With electrical stimulation, the action potentials are triggered in a highly restricted region of the waveform. (C) Response to biphasic pulsatile stimulation, as currently used by cochlear implants. The latency of the response (depending on the neural travel time to the recording site) is approximately 0.5 msec. (D) The steep rate-intensity functions seen with electrical stimuli (here, delivered at 1000/sec), compared with the shallower function with acoustic stimuli. A derived using data from Kiang and Moxon (1972), B author data and data derived from Kiang and Moxon (1972), C from Javel and Shepherd (2000), Fig. 3, D from Shepherd and Javel (1997), Fig. 18, and author data (for acoustic stimulation).

10.4.2.2.1 The place principle. If auditory nerve fibres are stimulated electrically, nerve fibres are seen not to have any intrinsic tuning at all. In the experiment illustrated in Fig. 10.8A, the cats were first deafened with an ototoxic antibiotic, so that there was no chance that the electrical stimulus would trigger a

normal travelling wave. The electrical stimulus was applied to the round window. Irrespective of the fibre's place of origin along the cochlear duct, the lowest thresholds were produced with stimulus frequencies of around 100–200 Hz, and there was a gradual rise in thresholds towards higher frequencies of stimulation.

Analogous results have since been found by many other investigators (e.g. van den Honert and Stypulkowski, 1984). Therefore, if frequency information is to be transmitted as place information in the auditory nerve, ways must be found to restrict the stimulus to local regions of the cochlea. Current spread in the cochlea makes localized stimulation difficult. With monopolar stimulation, the current is applied to one electrode in the cochlear duct and flows to a remote electrode. With this configuration, there is a wide pattern of activation in the cochlear duct. In bipolar stimulation, currents flow between members of a pair of closely spaced electrodes, both of which are within the cochlear duct. Bipolar stimulation produces much more confined pattern of activation along the duct (van den Honert and Stypulkowski, 1987). However, and surprisingly, bipolar stimulation does not generally improve perception through the implant and therefore it is not usually used. A further reason for not using bipolar stimulation is that it needs much higher currents, by an order of magnitude or so, which results in significantly greater power consumption.

10.4.2.2.2 The timing principle. Temporal information is preserved with electrical stimulation. Indeed, firing tends to be restricted more closely to one point on the waveform than with acoustic stimulation, as shown in response to sinusoidal stimulation in Fig. 10.8B. This presumably occurs because as soon as the electric potential has reached the threshold for activation, the nerve fibre fires with a high probability. Figure 10.8C shows the precise timing of action potentials to the bipolar pulsatile stimuli as used in current implants. Although with electrical stimuli the maximum firing rates of auditory nerve fibres are in the range 800–1000/sec (e.g. Shepherd and Javel, 1997), some degree of phase-locking can be detected with much higher frequencies of stimulation (e.g. to 2.5 kHz; Parkins, 1989).

10.4.2.2.3 Rate-intensity functions. Fig. 10.8D shows that rate-intensity functions to electrical stimulation are very steep indeed; that is as with the time-varying stimuli discussed in Section 10.4.2.2.2, once threshold is reached, the fibre fires with a high degree of probability. The dynamic range is often less than 10 dB. This can be compared with 20–30 dB for low-threshold fibres, and 60 dB for high-threshold fibres, to acoustic stimulation. Moreover, the spread of thresholds in different fibres is very small, being less than 20 dB (van den Honert and Stypulkowski, 1987). This means that the spread of activity to extra fibres can provide only a very small extension of the dynamic range. The results mean that very accurate amplitude compression of the stimulus is necessary.

10.4.2.3 Insertion and pattern of stimulation

Multichannel cochlear implants contain a pre-formed set of electrodes (between 12 and 22 electrodes in current devices) fixed in the surface of a long, tapered,

silicone carrier. The cochlear wall is opened near the round window, and the electrode array is inserted into the scala tympani, generally to a maximum depth of between 20 and 25 mm, although insertions of up to 31 mm are used with some devices (the human cochlea has a length of 35 mm). The implant can be pre-formed with a curve, so that after insertion, it hugs the inner, modiolar wall of the scala tympani as much as possible, with the result that the electrodes come to lie as close as possible to the cell bodies of the spiral ganglion, giving lower thresholds and a wider dynamic range (Shepherd *et al.*, 1993). Because implants with pre-formed curves lie closer to the modiolus, they insert relatively more deeply, in terms of distance along the cochlear spiral, than straight arrays of similar length. Greater depths of insertion can allow the lower frequencies of stimulation to be applied closer to their natural tonotopic place in the cochlea. Cells of the spiral ganglion are situated in the basal half of the cochlea, with fibres to the apical turn arising from cell bodies situated more basally in modiolus, which means that insertions over the basal half of the cochlea can cover the length of the ganglion (Stakhovskaya *et al.*, 2007). However, in practice even modiolus-hugging arrays generally only extend along the lower 60–80% of the length of the spiral ganglion. In addition, greater physical depths of insertion have the potential for causing greater damage to the cochlea, and the potential payoff in terms of improved performance is uncertain (see, e.g. Boyd, 2011, for discussion).

It has been found best to use brief (e.g. 25 μ sec) current pulses for stimulation. The pulses are delivered in a charge-balanced configuration, so that in one electrode a pulse of one polarity is followed by a second pulse of opposite polarity (Fig. 10.9). This means that during stimulation, there is ideally no net current flow

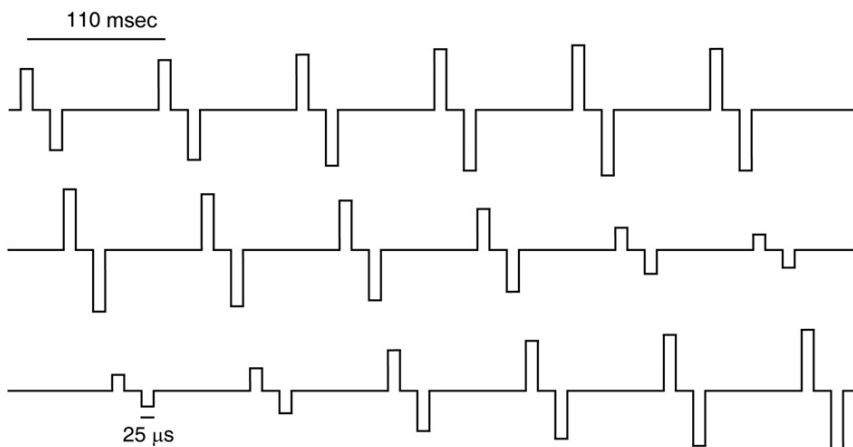


Fig. 10.9 The pattern of electrical stimulation commonly used in a cochlear implant, illustrated for three electrodes. Brief charge-balanced pulses (10–50 μ sec each) are presented at a rate of between 200 Hz and 2 kHz per channel (900 Hz illustrated here). The amplitude of stimulation is varied independently at each electrode. The different channels are activated at different times to reduce current flow between channels.

through an electrode, so that any ionic changes produced during the first pulse should be exactly reversed during the second pulse. Pulses are delivered asynchronously to the different channels in the implant, to reduce electrical interaction between the different channels. Each channel is stimulated at a rate of between 200 and 2000 pulses/sec. For most patients, the electrodes are driven in a monopolar configuration, that is with current applied between the active scala tympani electrode and a remote ground, which is typically an electrode on the implanted receiver-stimulator or located in the temporalis muscle. However, many devices are reprogrammable, so that bipolar stimulation or ‘common ground’ stimulation (where all the inactive electrodes can be used as a ground for the electrode in use) can also be used. Modern cochlear implants also include an option for telemetry, with signals being transmittable in reverse from the device to an external receiver, so that the patient’s neural responses to stimulation can be measured by the clinician. This facility can also measure the impedance of each electrode.

10.4.3 Results

10.4.3.1 Intensity coding

As expected from the physiological experiments, the dynamic range, being the range between threshold and discomfort, is small. Dynamic ranges are commonly around 10 dB, though much smaller and much larger values can be found (e.g. Nelson *et al.*, 1996; McKay, 2004). The dynamic range can be markedly different between electrodes in a single patient. It might be thought that if the stimulus were more localized in the cochlea by using for instance bipolar stimulation, increased current spread with intensity might increase the dynamic range. However, this does not appear to occur (e.g. Cohen *et al.*, 2001). The narrow dynamic range, presumably associated with a steep dependence of loudness on stimulus intensity, does not seem to have correlate in particularly small difference limens for intensity. Difference limens are about 1 dB, similar to those found with acoustic stimuli. Over the whole dynamic range, therefore, there may be only about 10–20 just noticeable difference for intensity, although with enormous variations between subjects and electrodes, compared with well over 100 for normal hearing.

10.4.3.2 Frequency, pitch and stimulus quality

If we believe the extreme position that at low frequencies information is carried purely by the temporal pattern of nerve impulses, then periodic electrical stimulation should produce faithful representation of auditory sensations and good discrimination of frequencies. The results of electrical stimulation have been disappointing for such a prediction. In only a few cases do electrical stimuli produce clear tonal sensations. A typical report is that tones sound harsh or like a buzz.

Nevertheless, a subjective pitch can often be ascribed to the stimulus based on the rate of activation of an electrode. Commonly, the assigned pitch increases with

the rate of stimulation up to about 300 Hz, with no further increases for higher rates of stimulation.

The subjective pitch through an electrode also depends on the position of the electrode in the cochlea, with more basal electrodes giving higher pitches and more apical electrodes giving lower pitches. More apical insertion of electrodes also produces lower perceived pitches (e.g. Hamzavi and Arnoldner, 2006). However, the change with place of stimulation is more commonly described as a change in timbre rather than of pitch itself.

Most patients can accurately rank electrodes in the cochlea according to place of stimulation. Commonly, the change in sensation occurs progressively and relatively smoothly with electrode position along the array, although discontinuities and even reversals are sometimes found. Patients can generally distinguish between the sensations produced by changes in the rate of stimulation and those produced by changes in the place of stimulation, the sensations of which are perceived independently and in a non-interacting way (Tong *et al.*, 1983).

Although available devices contain up to 22 electrodes (i.e. channels), in practice between 8 and 16 electrodes are generally used. The large number of channels potentially available, however, means that the configuration can be optimally selected for each patient, with any high-threshold electrodes, or electrodes that evoke unpleasant effects (e.g. very high pitch; or stimulation of the facial nerve), not being used. The usefulness of an electrode may be affected by, for instance, exactly how the electrode lies within the cochlear duct (e.g. either too near nor too far from the modiolus), survival of the nerve in the region being stimulated and local tissue reaction or bone growth around the electrode. Mapping the effects produced by the different electrodes, including matching the stimulus to the threshold and dynamic range of each electrode, is an essential preliminary step in programming the prosthesis for each patient, and one which has to be repeated regularly during the life of the implant.

10.4.3.3 Perception of speech

Current devices use variants of a common method of conveying speech. The acoustic stimulus is filtered through multiple bandpass filters (up to 20), with the overall frequency range adjustable for each patient but typically covering the range from 200 Hz to 8 kHz. After filtering, the envelope of the acoustic waveform is calculated for each channel. Those channels with the highest amplitudes are selected, with six channels commonly being chosen. The electrodes are stimulated with brief biphasic current pulses as illustrated in Fig. 10.9, with the amplitude of the pulses presented to any one electrode depending on the amplitude of the acoustic stimulus in the corresponding channel. In some implementations the stimulation is adaptive, with the number of channels selected varying with the number of clear spectral peaks in the stimulus, and with the mapping of the filter bank to the electrode array being dynamically altered to optimize the discriminability of the peaks. Because the amplitude in each channel is calculated at a high rate, and the biphasic pulses are presented at a high rate, the overall

stimulation in each channel can follow the rapid temporal fluctuations in the stimulus waveform, while the spatial pattern represents the short-term spectrum of the stimulus.

While the initial sensations through an implant can be perceived as highly unnatural and poor at conveying speech sounds, with practice many patients achieve good speech recognition in quiet with free-running speech. However, in noise, perception drops more rapidly than with normal-hearing subjects, particularly for stimuli containing rapidly changing spectral patterns (Munson and Nelson, 2005). In addition, music perception is generally poor, as is speech recognition with tonal languages such as Mandarin Chinese (Gfeller *et al.*, 2010; Wang *et al.*, 2011b).

In cases of partial loss of hearing, acoustic hearing aids are particularly poor at compensating for the losses at high frequencies. Therefore, where patients have residual low-frequency hearing, it may be worth implanting with hybrid or electroacoustic device. A cochlear implant is used to deliver some of the high-frequency information, while an acoustic hearing aid is used to deliver the low-frequency stimuli. In these cases, a short electrode may be used, to avoid damaging the more apical regions of the cochlea (Turner *et al.*, 2010).

One critical issue is to what extent stimulation enhances the functional abilities of the auditory nervous system. As far as survival of the auditory nerve fibres themselves is concerned, animal studies are in conflict as to whether stimulation encourages survival, some authors having reported only small effects and others none; the effect therefore seems minor at best (reviewed by Miller, 2001).

However, it has become clear that early implantation has major and overwhelming advantages for the development of the auditory central nervous system. For this reason, where deafness can be reliably diagnosed, implantation may be undertaken as early as 6–12 months of age. The cochlea is fully grown at birth, so implantation at this age does not pose problems for insertion, while later revision surgery if necessary is usually successful (Fayad *et al.*, 2006). Children receiving implants before the age of 12 months typically develop both receptive and expressive speech at the same rate as normal-hearing children, and at significantly greater rates than those implanted later (Dettman *et al.*, 2007). On the other hand, without early auditory input or implantation, the development of the central nervous system, and in particular the thalamo-cortical system, is delayed or prevented (see, e.g. Gordon *et al.*, 2011, for review).



10.5 CELLULAR REPLACEMENT, PROTECTION AND GENE THERAPY IN THE INNER EAR

10.5.1 Introduction

As pointed out above, if hair cells are destroyed in human beings and other mammals they are not replaced. Therefore, it was a surprise to find that in birds,

hair cells regenerate after being destroyed by noise or by ototoxic drugs, leading to functional restoration of hearing (Cotanche, 1987; Cruz *et al.*, 1987). This opened the possibility of inducing hair cell regeneration in human beings, prompting the question ‘If it works in birds, why not in man?’ (Girod and Rubel, 1991).

Box 10.4 Cell fates in the inner ear

In most cases, many of the genes that control the developmental decisions are known: the reader is referred to the original sources for details (e.g. Driver and Kelley, 2009).

A pointed arrow (Fig. 10.10) indicates that one cell type can develop into another cell type. A flat-ended arrow (Fig. 10.10) indicates that one cell type can inhibit the formation of the other cell type.

Modified and simplified from Kelley (2006), Fig. 5.

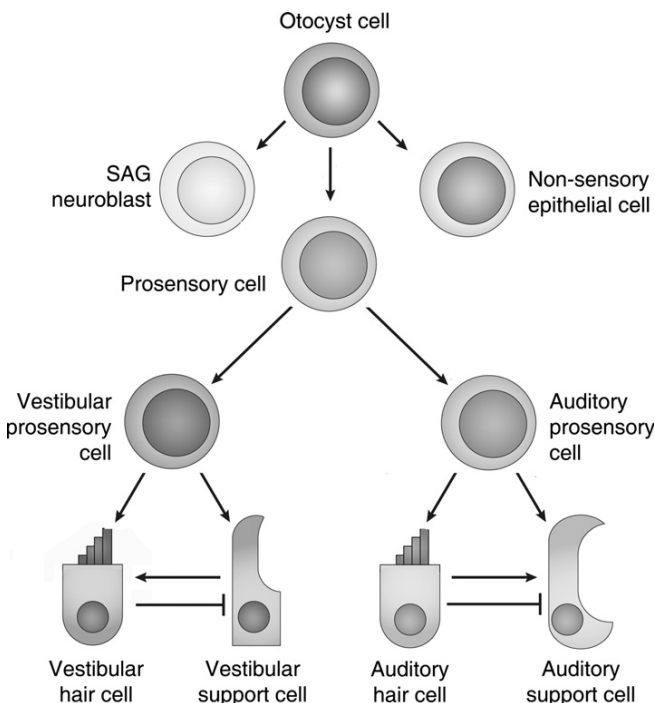


Fig. 10.10 Cells of the otocyst (primordial ear) develop either into cells of the statoacoustic ganglion, prosensory cells or non-sensory cells. Adapted from Kelley (2006), Fig. 5.

The aim of restoring functional hearing in human beings has been one of the drivers of a large research effort aimed at discovering the basic developmental programmes that lead to the generation of hair cells and at discovering the genes that control them (Box 10.4; see review by [Driver and Kelley, 2009](#)). This section is not intended to be a summary of that work (see Further Reading at the end of this chapter), but a description of the more direct applications to reversing hearing loss.

The bird cochlea is composed of relatively unspecialized hair cells situated in a simple columnar epithelium. The hair cells do not show the extreme specializations of, for instance, the outer hair cells, nor do the supporting cells show the extreme specialization of the pillar cells or Deiters' cells. It is possible that this unspecialized organization has allowed new hair cells to be produced from supporting cells after damage. Mammalian vestibular organs also have relatively unspecialized sensory epithelia, and mature vestibular epithelia may be able to produce new hair cells after damage, albeit sometimes at a low rate ([Forge et al., 1993](#); [Kawamoto et al., 2009](#)). However, restoration of cochlear function by hair cell regeneration is likely to represent a different order of difficulty. In order to re-establish near-normal sensitivity and tuning, outer hair cell function has to be re-established. This may mean, as well as replacing the outer hair cells, recreating at least some of the complex three-dimensional arrangement of the outer hair cell region of the organ of Corti, as shown in Figs. 3.1D and 3.4B. However, in severely deafened cochleae, the supporting cells change, in some species forming a simple undifferentiated flat or cuboidal epithelium, though in other species some remnants of supporting cell morphology and specific protein markers remain ([Kim and Raphael, 2007](#); [Oesterle and Campbell, 2009](#)). This implies that if effective repair is to occur, it may only be feasible while much of the structure of the organ of Corti is still intact.

10.5.2 Production of new hair cells by transdifferentiation of supporting cells

The possibility that mammalian supporting cells could transdifferentiate (i.e. transform without cell division or mitosis) directly into hair cells was shown in the vestibular sensory epithelium by [Li and Forge \(1997\)](#). One key gene, *Math-1*, has since been shown to be necessary for the development of hair cells from their precursors ([Birmingham et al., 1999](#)). *Math-1* (alternatively called *Atoh1*) codes for a gene transcription factor. [Izumikawa et al. \(2005\)](#) first unilaterally deafened guinea pigs with a local injection of an ototoxic antibiotic, which destroyed the hair cells in that ear. They then inoculated the ear with a virus engineered to contain *Math-1*. Some of the supporting cells in the organ of Corti trans-differentiated into cells with the appearance of hair cells, generating substantial numbers of both inner and outer hair cell-like cells. Moreover, the thresholds for the auditory brainstem response, a measure of auditory sensitivity, were lowered in the inoculated cochleae, in some animals to near normal, but remained high in the contralateral non-inoculated cochlea.

The transdifferentiated cells had many of the cellular and morphological characteristics of hair cells, including intact stereociliary bundles of the appropriate shape. However, as a result of the transdifferentiation, the normal structure of the organ of Corti, with its array of phalanges of Deiters' cells bracing the upper surface of the organ, was missing. These results were obtained in mature cochleae, in young adult guinea pigs, and form the first findings of the replacement of functional hair cells, with the consequent improvement of auditory thresholds, in adult cochleae.

In the above experiment, the cochleae were inoculated with the virus 4 days after the ototoxic lesion. However, if cochleae were not inoculated within this period, by 6 days not only had the hair cells degenerated but the supporting cells had been replaced by an undifferentiated flat epithelium. If the inoculation took place 7 days after the lesion, the epithelium remained flat and undifferentiated, and no hair cells were formed (Izumikawa *et al.*, 2008). This emphasizes that a transdifferentiation requires a set of progenitor cells that are able to undergo the change, and means that the technique would not be viable with a well-degenerated organ of Corti.

The prosensory cells of the developing cochlea (i.e. the cells that have the potential to be either hair cells or supporting cells; see Box 10.4) express a surface receptor called notch. Activation of notch by ligands on an adjacent cell represses the transcription of *Math-1*, with the result that the target cell does not develop into a hair cell. In cultured organs, the notch signalling cascade can be inhibited by the application of external agents, leading to the upregulation of *Math-1*. This induces supporting cells to become hair cells, both in neonatal cochleae and in adult vestibular organs (Yamamoto *et al.*, 2006; Lin *et al.*, 2011; Zhao *et al.*, 2011). However, in adult cochleae, only very occasional extra hair cells have been produced by this method (Hori *et al.*, 2007). Manipulation of the pathway may nevertheless one day form another potential method for the replacement of hair cells, assuming that competent progenitor cells are available.

10.5.3 Production of new hair cells by mitosis in the mammalian cochlea

In bird cochleae, some of the regenerated hair cells develop as a result of supporting cells dividing after cochlear damage (Girod *et al.*, 1989; reviewed by Stone and Cotanche, 2007). The hair cells become innervated and are functional (e.g. Wang and Raphael, 1996; Woolley *et al.*, 2001). Can mammalian cochlear supporting cells also be induced to divide and produce new and functional hair cells?

The possibility was shown in cultured supporting cells, isolated from the neonatal mouse cochlea. The cells were co-cultured with other cells to promote cellular proliferation and were shown to produce further cells by mitosis (cell division), some of which later developed elementary hair cell-like characteristics (White *et al.*, 2006). However, these results were obtained *in vitro* using cells from immature cochleae where developmental processes are still continuing, and it is not known whether they will lead to an effective therapy in mature organs. Supporting cells in the mature guinea pig cochlea have an ability, though a limited one, to

proliferate after damage and therefore could possibly provide a source for the new hair cells (Yamasoba and Kondo, 2006). The proliferation of supporting cells is controlled in mammalian cochleae by a cell cycle inhibitor known as p27Kip1, and knockout of the *p27Kip1* gene in mice allows the proliferation of excess supporting cells, with the consequential production of excess hair cells even in the adult (Chen and Segil, 1999; Löwenheim *et al.*, 1999). However, these animals have severely deformed organs of Corti and severe hearing loss (e.g. Kanzaki *et al.*, 2006a). Nevertheless, the results do suggest that at some time in the future it might be possible to trigger the development of further supporting cells in the organ of Corti and that they could be used as a source for new hair cells, either by mitosis or by transdifferentiation.

Analogous experiments with the retinoblastoma gene *Rb* showed that inactivation of the gene in the inner ear, when the hair cells were still in the proliferative phase, led to the development of supernumerary inner and outer hair cells, in multiple rows and in a disorganized pattern (Sage *et al.*, 2006). In the early postnatal period, the hair cells transduced mechanical stimuli as judged by the uptake of the fluorescent dye FMI-43, which is known to enter hair cells through the mechano-transducer channels. However, the hair cells then progressively degenerate, and a profound hearing loss develops. Inactivation of *Rb* in postnatal cells also leads to the cells re-entering the cell cycle, though they die soon after (Weber *et al.*, 2008; also reviewed by Liu and Zuo, 2008). Nevertheless, if this latter aspect of *Rb*'s role could be controlled, this may lead to a way of generating new functional hair cells (see, e.g. Huang *et al.*, 2011).

10.5.4 Gene therapy

In the cases of inherited hearing losses, there is a theoretical possibility of using gene therapy to prevent the loss in the first place, or of restoring function after the loss has occurred. Gene therapy could consist either of replacing a functional gene, or interfering with the abnormal function of a damaged gene (reviewed by Maeda *et al.*, 2009; Lustig and Akil, 2012). As an example, human DFNB3 is a defect in the gene coding for myosin 15a, with a mouse correlate in the mouse mutant known as shaker 2. In a pioneering study, the hearing defect in a shaker 2 mouse was corrected by making a transgenic mouse that incorporated a normal copy of the myosin 15a gene into its genome. Shaker 2 mice normally have high auditory thresholds and show circling behaviour, while their hair cells degenerate. In contrast, the transgenic rescued mice had normal thresholds, normal behaviour and normal cochlear morphology (Probst *et al.*, 1998; Kanzaki *et al.*, 2006b).

10.5.5 Stem cell therapy

10.5.5.1 Cochlear hair cells

Stem cells are cells that have the capacity to self-renew and differentiate into a variety of types of cells. Pluripotent embryonic stem cells can be isolated from the

cells of the inner cell mass of the blastocyst (precursor of the embryo) to generate a wide range of cell types. Pluripotency can also be induced in already differentiated cells such as fibroblasts from adults, opening the possibility of generating stem cells from a patient's own cells. Stem cells can moreover be induced to enter a particular lineage (e.g. to become neuroectoderm) by treatment with a programme of growth factors. Supporting cells from the inner ear can also act as stem cells with more restricted abilities in that they can renew and produce cells that express some of the biochemical markers of hair cells and other types of cells from the inner ear (e.g. *Oshima et al.*, 2007).

Mouse embryonic stem cells can be induced to become hair cell progenitors by treating with a succession of specific growth factors in culture. When implanted into embryonic chicken inner ears, the cells can integrate into the sensory epithelium and develop some of the markers of hair cells (*Li et al.*, 2003). However, similar incorporation has not been observed in mammals; undifferentiated and partially differentiated embryonic stem cells introduced into the scala media of adult guinea pigs cochlea have been found attached to the membranes of the scalae, but did not incorporate into the tissues, nor was there any sign of further differentiation (*Hildebrand et al.*, 2005).

Greater degrees of differentiation can also be attempted before implantation. Early human foetal (9- to 11-week-old) cochleae contain stem cells that can be induced to differentiate into hair cell-like cells and neurones. The hair cell-like cells expressed some of the molecular markers of hair cells, and showed some of the electrophysiological characteristics of hair cells, but did not develop any stereociliary bundles (*Chen et al.*, 2009). Implantation has not been shown, but such cells may be possible candidates as replacement hair cells in damaged cochleae, if they can be implanted and incorporated successfully.

10.5.2 Auditory nerve

Neural replacement seems to offer greater promise. Many of the differentiated stem cells seem to enter the neural lineage relatively easily, and incorporation into the spiral ganglion has been reported. Neural therapy could accompany the cochlear implant, in patients where nerve survival has been compromised. Many studies have shown delivery and incorporation of stem cells or neural progenitors into neural structures of the inner ear (reviewed by *Gunewardene et al.*, 2012). In one example, *Reyes et al.* (2008) induced stem cells towards the glutamatergic neuronal cell type by treatment with growth factors, and then transplanted the cells into the scala tympani of deafened young adult guinea pigs. Many cells settled in the scala; and some entered the modiolus, while a few entered Rosenthal's canal to settle among the cell bodies of the spiral ganglion. Most of the cells expressed neural markers, with many showing the markers for glutamatergic neurones. In other studies, when the treated stem cells are co-cultured with cochlear explants, they extended neurites towards the hair cells within the explants (*Nishimura et al.*, 2009).

Stem cells could also be engineered to provide growth factors to support the cells of the spiral ganglion, not only reducing the loss with for instance ageing, but

to provide a trophic support for the nerve after implantation of the cochlear prosthesis (Gillespie and Shepherd, 2005; Richardson *et al.*, 2009).

10.5.6 Cell protection

Although replacing hair cells after they have been lost is a major focus of current effort, protecting hair cells from damage in the first place is a more conservative goal and for that reason may be more achievable. A number of different approaches are under investigation, including chemically protecting the cells from free radicals, identifying and enhancing the cells' own defensive mechanisms and inhibiting cell death once the cell is damaged.

Free radicals (e.g. reactive oxygen species) are highly damaging to cells. It may therefore be possible to reduce the loss of hair cells by protecting the cells from their effects. Such an effect has been shown conclusively for drug-induced hearing loss in animals, and for aminoglycoside antibiotics in human beings, where aspirin (which is metabolized to an antioxidant) was co-administered with aminoglycoside antibiotics, with a resulting complete protection from ototoxic damage (Sha *et al.*, 2006). Many agents are able to act as antioxidants, and we have the possibility of reducing cell damage in the inner ear, either by applying them directly to the inner ear or applying them systemically (e.g. via the blood stream), so reducing the effects of aminoglycosides, acoustic trauma and possibly ageing (e.g. Bielefeld *et al.*, 2011; see Poirier *et al.*, 2010, for review).

One enigmatic observation has been that following repeated bouts of acoustic stimulation, the cochlea becomes more resistant to acoustic damage, a process known as sound conditioning or toughening (Canlon *et al.*, 1988). The effect can be substantial, with permanent hearing losses being reduced by 20 dB or more. Enhanced protection can be seen after a number of other stressors, including heat stress, restraint stress, hypoxia, sham surgery and kanamycin. Glucocorticoid-dependent processes form part of the mechanism, since the protection can be removed by inhibiting the synthesis of corticosteroids (Tahera *et al.*, 2006). A corticosteroid-responsive gene transcription protein PLZF (promyelocytic leukemia zinc finger protein) mediates at least some of the effect, since mice with mutation of the gene coding for PLZF do not show the protection (Peppi *et al.*, 2011). Immunohistology showed that the PLZF protein was normally strongly expressed in the auditory nerve, organ of Corti, and stria vascularis, all structures which are vulnerable to damage after acoustic trauma or to oxidative damage. The protection therefore seems to depend on downstream protective pathways that are induced by PLZF.

Cochlear protection, from acoustic and other stressors, can also be induced by applied corticosteroids, such as dexamethasone (see Dinh and Van De Water, 2009). Heat shock proteins, which can be released by activation of the glucocorticoid receptor and become elevated as part of a stress response, may be involved in the effect. Transgenic mice that over-express the heat shock protein HSP70 show protection against aminoglycoside ototoxicity (Taleb *et al.*, 2009). A drug known as celastrol which induces heat shock proteins is also able to protect

hair cells and reduce hearing loss after the application of aminoglycosides in mice, and has the potential to form a practical treatment (Francis *et al.*, 2011).

Damage to the hair cells may initiate a sequence of events leading either to necrosis or to programmed cell death (apoptosis). This is presumably appropriate if the cells can be replaced by mitosis, and therefore may be a general mechanism favoured by evolution for that reason. However, if the cell cannot be replaced, this may not be advantageous. Under these circumstances, it may be more favourable to inhibit apoptosis. In cultures of mammalian or bird vestibular epithelia, inhibition of cell death pathways can lead to survival of hair cells after an aminoglycoside insult that otherwise would have been lethal to the cells (Cheng *et al.*, 2005). Similarly, cells of the spiral ganglion can survive in culture conditions under which they would otherwise die, if pro-survival members of the pathways controlling apoptosis are over-expressed in the cells (Hansen *et al.*, 2007). Corresponding effects have been shown in intact animals, with the intracochlear injection of inhibitors of cell death pathways protecting against the effects of both aminoglycoside ototoxicity and acoustic trauma (Wang *et al.*, 2003; Coleman *et al.*, 2007). The inhibition of cell death pathways is at least one of the mechanisms by which the heat shock proteins referred to above confer their protection (Francis *et al.*, 2011). Overall, the results suggest that the extent of apoptosis after insults to the inner ear may not always be at a level that is optimal for the organism, and that the survival of functional hair cells and cells of the spiral ganglion can be enhanced by reducing the extent of apoptosis in the cochlea (for review, see Dinh and Van De Water, 2009).

10.6 SUMMARY

1. Hearing loss can arise in the conductive apparatus before the oval window, when it is known as conductive loss. Alternatively, it may arise in the cochlea or more centrally, when it is known as sensorineural hearing loss. If it arises in the cochlea, it is known as sensorineural hearing loss of cochlear origin.
2. Sensorineural hearing loss of cochlear origin can be caused by ototoxic drugs. Aminoglycoside antibiotics are ototoxic and have been extensively investigated; they damage hair cells, and particularly outer hair cells, in the high-frequency parts of the cochlea. They are likely to cause their damage at least in part by oxidative mechanisms, and antioxidants can provide some protection.
3. Other ototoxic agents include Cisplatin (an anticancer drug), some loop diuretics (bumetanide, furosemide and ethacrynic acid), aspirin (reversibly) and some organic solvents (e.g. styrene and toluene).
4. With acoustic overstimulation, for milder degrees of damage, there is minor disruption of the stereocilia. These degrees of damage are probably reversible. Greater degrees of damage cause loss of the hair cells.
5. Some forms of hearing losses have genetic causes. The commonest inherited hearing loss, accounting for some 35% of all congenital hearing losses (depending on the population), is the type known as DFNB1. DFNB1 is

caused by a mutation in the gene coding for the gap junction protein connexin-26. Patients with this mutation have problems cycling K⁺ from the cochlear scalae through the cochlear walls back to the stria vascularis. This and many other inherited hearing losses have been invaluable for revealing basic mechanisms of the inner ear.

6. Mutations in the mitochondrial genome may also give rise to hearing loss. These syndromes are maternally inherited, commonly affect multiple organ systems and tend to increase with severity over time.
7. Ageing causes sensorineural hearing loss (presbyacusis), which can have both cochlear and central components. In the cochlea, vulnerable sites are the hair cells, the nerve and the stria vascularis.
8. Damage to the outer hair cells causes a loss of the active amplification of the mechanical travelling wave in the cochlear duct. This leads to a reduction in the magnitude of the travelling wave and to a broadening of the peak of the wave. The changes lead to a loss in the sensitivity of auditory nerve fibres, and a broadening of their tuning curves, that is to a loss of frequency resolution. Damage to the inner hair cells leads to a loss of sensitivity of the auditory nerve fibres, without changes in frequency resolution.
9. The psychophysical results fit in with the physiological results. In sensorineural loss of cochlear origin, a loss of frequency resolution is often seen in addition to the loss in sensitivity. The loss in frequency resolution can be seen in widened psychophysical tuning curves and in widened psychophysical filters (critical bands). These factors lead to a particular difficulty in understanding broadband complex sounds, such as speech, and particularly against noisy backgrounds.
10. Some forms of tinnitus, that is those arising in the cochlea from the active mechanical amplification of the travelling wave, may give rise to objectively measurable sound emissions in the ear canal. However, this is unlikely to explain the clinically most important forms of tinnitus. Tinnitus is commonly associated with some degree of hearing loss. This suggests that it arises from a hypersensitivity of the central auditory nervous system when it is deprived of its normal input. It appears that neural activity increases in the auditory pathway, starting at the dorsal cochlear nucleus, and at later stages. The tinnitus may arise from a reduction in inhibition by the neurotransmitters GABA and glycine, and the anti-epileptic drugs vigabatrin and gabapentin that increase GABA inhibition have been reported to reverse tinnitus in experimental animals and in some patients. Tinnitus may also arise from down-regulation of K⁺ channels in the nucleus. Where there is no effective drug treatment, the behavioural method known as 'tinnitus retraining therapy' has proved effective in many patients.
11. With profound sensorineural hearing loss of cochlear origin, hearing can often be restored by a cochlear prosthesis. Current prostheses consist of multiple electrodes inserted deep into the cochlear duct, where they can stimulate what cells remain of the auditory nerve. Stimuli are pre-processed to pick out the major spectral components of the stimuli, and electrodes at the appropriate positions in the cochlea (depending on the tonotopicity of the cochlea) are stimulated electrically. The amplitude of stimulation depends on the

- amplitude of the relevant spectral component at each moment, so that the final pattern of stimulation is able to mirror both the place-frequency and temporal aspects of cochlear function. After practice, good communication is achieved with running speech, and 80–90% of open-set sentences are understood correctly.
12. Attempts are being made to replace damaged cells in the inner ear, including the hair cells, cells of the spiral ganglion (auditory nerve) and the stria vascularis. These include (i) stimulating the division of the supporting cells, to produce new hair cells, (ii) inoculating the cochlea with a virus engineered to contain a gene *Math-1*, which encourages the supporting cells to trans-differentiate (i.e. transform without undergoing cell division) into hair cells and (iii) the injection of stem cells. The transdifferentiation of supporting cells induced by *Math-1* has been able to partially restore some hearing in adult animals even after complete loss of all hair cells. However, these methods require some remaining differentiated supporting cells in the organ of Corti, which is not usually the case with advanced sensorineural hearing loss. Stem cells may however form a possible treatment for repair of the auditory nerve.
13. Gene therapy may be possible, where the function of a damaged gene is replaced by an introduced normal copy of the gene. Protection of hair cells may also be possible by (i) inhibiting apoptotic pathways, (ii) use of antioxidant therapy and (iii) manipulations which increase the ear's own biochemical protective mechanisms, for example those arising in the phenomenon known as 'sound conditioning' or 'toughening', which work via corticosteroid defences.



10.7 FURTHER READING

Ototoxicity in general has been reviewed by Tabuchi *et al.* (2011), aminoglycoside ototoxicity by Warchol (2010) and aminoglycoside ototoxicity together with protective therapy by Xie *et al.* (2011). Cisplatin ototoxicity has been reviewed by Mukherjea and Rybak (2011).

Acoustic trauma has been reviewed by Henderson *et al.* (2006) and Ohlemiller (2008). Acoustic trauma in relation to potential drug treatments has been reviewed by Oishi and Schacht (2011), and in relation to genetic studies by Konings *et al.* (2009).

Genetic bases of hearing loss have been reviewed by Raviv *et al.* (2010), and in particular relation to hair cells and the tectorial membrane by Richardson *et al.* (2011). Connexin-26 and DFNB1 have been reviewed by del Castillo and del Castillo (2011) and by Pfenniger *et al.* (2011). Mitochondrial involvement in hearing loss has been reviewed by Fischel-Ghodsian *et al.* (2004), Pickles (2004), Kokotas *et al.* (2007) and Cacace and Pinheiro (2011).

A general overview of presbyacusis has been given by Huang and Tang (2010). Strial presbyacusis was reviewed by Ohlemiller (2009). Ageing was reviewed in relation to loss of spiral ganglion cells by Bao and Ohlemiller (2010), and in relation to changes in both the cochlea and the central auditory system by

Frisina (2009). Ageing and its effects on temporal processing in brainstem were reviewed by Walton (2010).

Animal models of tinnitus have been reviewed by Eggemont (2012), and central changes in tinnitus by Kaltenbach (2006). An overview of treatments for tinnitus was given by Savage and Waddell (2012), while tinnitus retraining therapy has been reviewed by Jastreboff (2007). Human trials of vigabatrin and gabapentin for the treatment of tinnitus have been reviewed by Wang *et al.* (2011a) and Richardson *et al.* (2012), and gabapentin by Bauer and Brozoski (2007).

For a surgical and clinical perspective on cochlear prostheses; Chapters 158–161 in ‘Cummings Otolaryngology Head and Neck Surgery’ (eds P.W. Flint, B.H. Haughey, V.J. Lund, *et al.*, 5th ed., 2010; Mosby/Elsevier) are recommended. Schnupp *et al.* (2011), Chapter 8, has a valuable discussion of the physiology and psychophysics of the cochlear implant. Brain maturation in relation to the cochlear prosthesis has been reviewed by Gordon *et al.* (2011).

Hair cell development has been reviewed by Kelley (2006), Kros (2007), Driver and Kelley (2009), and in many chapters of ‘Development of the Ear’ (eds M.W. Kelley, D.K. Wu, A.N. Popper and R.R. Fay; Springer Handbook of Auditory Research, Vol. 26, 2005). Hair cell regeneration in birds has been reviewed by Stone and Cotanche (2007).

An overview of hair cell regeneration has been given by Parker (2011) and particularly in relation to regulation of cell fate by Cotanche and Kaiser (2010). Cell cycle genes in hair cell development and regeneration have been reviewed by Liu and Zuo (2008). Gene therapy has been reviewed by Maeda *et al.* (2009) and Lustig and Akil (2012).

Stem cells, hair cell regeneration and transdifferentiation have also been reviewed in ‘Regeneration and Repair’ (eds R.J. Salvi, A.N. Popper and R.R. Fay; Springer Handbook of Auditory Research, Vol. 33, 2008). In addition, hair cell regeneration has been reviewed by Groves (2010), Brigande and Heller (2009) and Warchol (2011). Stem cell therapy has also been reviewed by Jongkamonwiwat *et al.* (2010), while stem cells in neural repair, particularly in relation to cochlear prosthesis, have been reviewed by Gunewardene *et al.* (2012).

Inner ear protection and repair have been reviewed by Shibata and Raphael (2010). Oxidative stress and antioxidant therapy have been reviewed by Poirrier *et al.* (2010). Glucocorticoid protection has been reviewed by Meltser and Canlon (2011). Cell death pathways in relation to the protection of hair cells have been reviewed by Dinh and van de Water (2009).

REFERENCES

- Abel, C., Wittekindt, A., Kössl, M. 2009. Contralateral acoustic stimulation modulates low-frequency biasing of DPOAE: efferent influence on cochlear amplifier operating state? *J Neurophysiol* 101, 2362–2371.
- Abeles, M., Goldstein, M.H., Jr. 1972. Responses of single units in the primary auditory cortex of the cat to tones and to tone pairs. *Brain Res* 42, 337–352.
- Abrashkin, K.A., Izumikawa, M., Miyazawa, T., et al. 2006. The fate of outer hair cells after acoustic or ototoxic insults. *Hear Res* 218, 20–29.
- Adams, J.C. 1979. Ascending projections to the inferior colliculus. *J Comp Neurol* 183, 519–538.
- Adams, J.C., Mugnaini, E. 1984. Dorsal nucleus of the lateral lemniscus: a nucleus of GABAergic projection neurons. *Brain Res Bull* 13, 585–590.
- Aerts, J.R., Dirckx, J.J. 2010. Nonlinearity in eardrum vibration as a function of frequency and sound pressure. *Hear Res* 263, 26–32.
- Ahveninen, J., Jaaskelainen, I.P., Raji, T., et al. 2006. Task-modulated “what” and “where” pathways in human auditory cortex. *Proc Natl Acad Sci USA* 103, 14608–14613.
- Aibara, R., Welsh, J.T., Puria, S., Goode, R.L. 2001. Human middle-ear sound transfer function and cochlear input impedance. *Hear Res* 152, 100–109.
- Aitkin, L.M. 1973. Medial geniculate body of the cat: responses to tonal stimuli of neurons in medial division. *J Neurophysiol* 36, 275–283.
- Aitkin, L.M., Prain, S.M. 1974. Medial geniculate body: unit responses in the awake cat. *J Neurophysiol* 37, 512–521.
- Aitkin, L.M., Webster, W.R. 1972. Medial geniculate body of the cat: organization and responses to tonal stimuli of neurons in ventral division. *J Neurophysiol* 35, 365–380.
- Aitkin, L.M., Webster, W.R., Veale, J.L., Crosby, D.C. 1975. Inferior colliculus. I. Comparison of response properties of neurons in central, pericentral, and external nuclei of adult cat. *J Neurophysiol* 38, 1196–1207.
- Aitkin, L.M., Dickhaus, H., Schult, W., Zimmermann, M. 1978. External nucleus of inferior colliculus: auditory and spinal somatosensory afferents and their interactions. *J Neurophysiol* 41, 837–847.
- Alibardi, L. 2002. Putative inhibitory collicular boutons contact large neurons and their dendrites in the dorsal cochlear nucleus of the rat. *J Submicrosc Cytol Pathol* 34, 433–446.
- Alkhatib, A., Biebel, U.W., Smolders, J.W. 2006. Inhibitory and excitatory response areas of neurons in the central nucleus of the inferior colliculus in unanesthetized chinchillas. *Exp Brain Res* 174, 124–143.
- Ammer, J.J., Grothe, B., Felmy, F. 2012. Late postnatal development of intrinsic and synaptic properties promotes fast and precise signaling in the dorsal nucleus of the lateral lemniscus. *J Neurophysiol* 107, 1172–1185.

- Anderson, L.A., Linden, J.F. 2011. Physiological differences between histologically defined subdivisions in the mouse auditory thalamus. *Hear Res* 274, 48–60.
- Anderson, L.A., Christianson, G.B., Linden, J.F. 2009. Stimulus-specific adaptation occurs in the auditory thalamus. *J Neurosci* 29, 7359–7363.
- Anniko, M., Wroblewski, R. 1986. Ionic environment of cochlear hair cells. *Hear Res* 22, 279–293.
- Antunes, F.M., Nelken, I., Covey, E., Malmierca, M.S. 2010. Stimulus-specific adaptation in the auditory thalamus of the anesthetized rat. *PLoS One* 5, e14071.
- Arnott, R.H., Wallace, M.N., Shackleton, T.M., Palmer, A.R. 2004a. Onset neurones in the anteroventral cochlear nucleus project to the dorsal cochlear nucleus. *J Assoc Res Otolaryngol* 5, 153–170.
- Arnott, S.R., Binns, M.A., Grady, C.L., Alain, C. 2004b. Assessing the auditory dual pathway model in humans. *Neuroimage* 22, 401–408.
- Arthur, R.M., Pfeiffer, R.R., Suga, N. 1971. Properties of ‘two-tone inhibition’ in primary auditory neurones. *J Physiol* 212, 593–609.
- Ashmore, J. 2008. Cochlear outer hair cell motility. *Physiol Rev* 88, 173–210.
- Ashmore, J., Avan, P., Brownell, W.E., et al. 2010. The remarkable cochlear amplifier. *Hear Res* 266, 1–17.
- Assad, J.A., Shepherd, G.M., Corey, D.P. 1991. Tip-link integrity and mechanical transduction in vertebrate hair cells. *Neuron* 7, 985–994.
- Bacon, S.P., Moore, B.C. 1986. Temporal effects in masking and their influence on psychophysical tuning curves. *J Acoust Soc Am* 80, 1638–1645.
- Bajo, V.M., Nodal, F.R., Moore, D.R., King, A.J. 2010. The descending corticocollicular pathway mediates learning-induced auditory plasticity. *Nat Neurosci* 13, 253–260.
- Banks, W.F., Saunders, J.C., Lowry, L.D. 1979. Olivocochlear bundle activity recorded in awake cats. *Otolaryngol Head Neck Surg* 87, 463–471.
- Bao, J., Ohlemiller, K.K. 2010. Age-related loss of spiral ganglion neurons. *Hear Res* 264, 93–97.
- Barker, D., Plack, C.J., Hall, D.A. 2011. Human auditory cortical responses to pitch and to pitch strength. *Neuroreport* 22, 111–115.
- Barrett, D.J., Hall, D.A. 2006. Response preferences for “what” and “where” in human non-primary auditory cortex. *Neuroimage* 32, 968–977.
- Bartlett, E.L., Wang, X. 2011. Correlation of neural response properties with auditory thalamus subdivisions in the awake marmoset. *J Neurophysiol* 105, 2647–2667.
- Bartlett, E.L., Sadagopan, S., Wang, X. 2011. Fine frequency tuning in monkey auditory cortex and thalamus. *J Neurophysiol* 106, 849–859.
- Bauer, J.W. 1978. Tuning curves and masking functions of auditory-nerve fibers in cat. *Sens Processes* 2, 156–172.
- Bauer, C.A., Brozoski, T.J. 2007. Gabapentin. *Prog Brain Res* 166, 287–301.
- Bauer, C.A., Turner, J.G., Caspary, D.M., Myers, K.S., Brozoski, T.J. 2008. Tinnitus and inferior colliculus activity in chinchillas related to three distinct patterns of cochlear trauma. *J Neurosci Res* 86, 2564–2578.
- Bäuerle, P., von der Behrens, W., Kössl, M., Gaese, B.H. 2011. Stimulus-specific adaptation in the gerbil primary auditory thalamus is the result of a fast frequency-specific habituation and is regulated by the corticofugal system. *J Neurosci* 31, 9708–9722.
- Beckius, G.E., Batra, R., Oliver, D.L. 1999. Axons from anteroventral cochlear nucleus that terminate in medial superior olive of cat: observations related to delay lines. *J Neurosci* 19, 3146–3161.

- Behne, N., Wendt, B., Scheich, H., Brechmann, A. 2006. Contralateral white noise selectively changes left human auditory cortex activity in a lexical decision task. *J Neurophysiol* 95, 2630–2637.
- Békésy, G. von 1947. The variation in phase along the basilar membrane with sinusoidal vibrations. *J Acoust Soc Am* 19, 452–460.
- Békésy, G. von 1949. On the resonance curve and the decay period at various points on the cochlear partition. *J Acoust Soc Am* 21, 245–254.
- Békésy, G. von 1953. Description of some mechanical properties of the organ of Corti. *J Acoust Soc Am* 25, 770–785.
- Békésy, G. von. 1960. Experiments in Hearing, Wever, E.G. (Ed.). McGraw-Hill, New York. Reissued 1989, Acoustical Society of America.
- Bermingham, N.A., Hassan, B.A., Price, S.D., et al. 1999. Math1: an essential gene for the generation of inner ear hair cells. *Science* 284, 1837–1841.
- Beurg, M., Evans, M.G., Hackney, C.M., Fettiplace, R. 2006. A large-conductance calcium-selective mechanotransducer channel in mammalian cochlear hair cells. *J Neurosci* 26, 10992–11000.
- Beurg, M., Fettiplace, R., Nam, J.H., Ricci, A.J. 2009. Localization of inner hair cell mechanotransducer channels using high-speed calcium imaging. *Nat Neurosci* 12, 553–558.
- Biebel, U.W., Langner, G. 2002. Evidence for interactions across frequency channels in the inferior colliculus of awake chinchilla. *Hear Res* 169, 151–168.
- Bielefeld, E.C., Wantuck, R., Henderson, D. 2011. Postexposure treatment with a Src-PTK inhibitor in combination with N-l-acetyl cysteine to reduce noise-induced hearing loss. *Noise Health* 13, 292–298.
- Billig, I., Yeager, M.S., Blikas, A., Raz, Y. 2007. Neurons in the cochlear nuclei controlling the tensor tympani muscle in the rat: A study using pseudorabies virus. *Brain Res* 1154, 124–136.
- Binder, J.R., Desai, R.H., Graves, W.W., Conant, L.L. 2009. Where is the semantic system? A critical review and meta-analysis of 120 functional neuroimaging studies. *Cereb Cortex* 19, 2767–2796.
- Binns, K.E., Grant, S., Withington, D.J., Keating, M.J. 1992. A topographic representation of auditory space in the external nucleus of the inferior colliculus of the guinea-pig. *Brain Res* 589, 231–242.
- Bitterman, Y., Mukamel, R., Malach, R., Fried, I., Nelken, I. 2008. Ultra-fine frequency tuning revealed in single neurons of human auditory cortex. *Nature* 451, 197–201.
- Bizley, J.K., Walker, K.M., Silverman, B.W., King, A.J., Schnupp, J.W. 2009. Interdependent encoding of pitch, timbre, and spatial location in auditory cortex. *J Neurosci* 29, 2064–2075.
- Blackburn, C.C., Sachs, M.B. 1990. The representations of the steady-state vowel sound /ɛ/ in the discharge patterns of cat anteroventral cochlear nucleus neurons. *J Neurophysiol* 63, 1191–1212.
- Blauert, J. 1997. Spatial hearing: the psychophysics of human sound localization. MIT Press, Cambridge.
- Boudreau, J.C., Tsuchitani, C. 1968. Binaural interaction in the cat superior olive S segment. *J Neurophysiol* 31, 442–454.
- Boyd, P.J. 2011. Potential benefits from deeply inserted cochlear implant electrodes. *Ear Hear* 32, 411–427.
- Brand, A., Behrend, O., Marquardt, T., McAlpine, D., Grothe, B. 2002. Precise inhibition is essential for microsecond interaural time difference coding. *Nature* 417, 543–547.

- Brigande, J.V., Heller, S. 2009. Quo vadis, hair cell regeneration? *Nat Neurosci* 12, 679–685.
- Brodmann, K. 1909. *Vergleichende Localisationslehre der Grosshirnrinde*, Barth, Leipzig (Eng. Tr. by Garey, L.J. as *Localisation in the Cerebral Cortex*, 1994, Smith-Gordon, London).
- Brown, A.M., Pye, J.D. 1975. Auditory sensitivity at high frequencies in mammals. *Adv Comp Physiol Biochem* 6, 1–73.
- Brown, M., Webster, W.R., Martin, R.L. 1997. The three-dimensional frequency organization of the inferior colliculus of the cat: a 2-deoxyglucose study. *Hear Res* 104, 57–72.
- Brown, M.C. 1987. Morphology of labeled afferent fibers in the guinea pig cochlea. *J Comp Neurol* 260, 591–604.
- Brown, M.C. 1989. Morphology and response properties of single olivocochlear fibers in the guinea pig. *Hear Res* 40, 93–109.
- Brown, M.C., Nuttall, A.L. 1984. Efferent control of cochlear inner hair cell responses in the guinea-pig. *J Physiol* 354, 625–646.
- Brownell, W.E., Bader, C.R., Bertrand, D., de Ribaupierre, Y. 1985. Evoked mechanical responses of isolated cochlear outer hair cells. *Science* 227, 194–196.
- Brugge, J.F., Reale, R.A., Hind, J.E., Chan, J.C., Musicant, A.D., Poon, P.W. 1994. Simulation of free-field sound sources and its application to studies of cortical mechanisms of sound localization in the cat. *Hear Res* 73, 67–84.
- Brugge, J.F., Reale, R.A., Hind, J.E. 1996. The structure of spatial receptive fields of neurons in primary auditory cortex of the cat. *J Neurosci* 16, 4420–4437.
- Burnett, L.R., Stein, B.E., Chaponis, D., Wallace, M.T. 2004. Superior colliculus lesions preferentially disrupt multisensory orientation. *Neuroscience* 124, 535–547.
- Cacace, A.T., Pinheiro, J.M. 2011. The mitochondrial connection in auditory neuropathy. *Audiol Neurotol* 16, 398–413.
- Cai, S., Ma, W.L., Young, E.D. 2009. Encoding intensity in ventral cochlear nucleus following acoustic trauma: implications for loudness recruitment. *J Assoc Res Otolaryngol* 10, 5–22.
- Caird, D., Klinke, R. 1983. Processing of binaural stimuli by cat superior olfactory complex neurons. *Exp Brain Res* 52, 385–399.
- Cajal, S.R. 1909. *Histologie du Système Nerveux de l'Homme et des Vertébrés*. Maloine, Paris, Reissued (Eng. Tr. by Swanson, N. and Swanson, L., 1995, Oxford University Press, New York).
- Calford, M.B. 1983. The parcellation of the medial geniculate body of the cat defined by the auditory response properties of single units. *J Neurosci* 3, 2350–2364.
- Calford, M.B., Aitkin, L.M. 1983. Ascending projections to the medial geniculate body of the cat: evidence for multiple, parallel auditory pathways through thalamus. *J Neurosci* 3, 2365–2380.
- Calford, M.B., Webster, W.R., Semple, M.M. 1983. Measurement of frequency selectivity of single neurons in the central auditory pathway. *Hear Res* 11, 395–401.
- Campbell, R.A., Doubell, T.P., Nodal, F.R., Schnupp, J.W., King, A.J. 2006. Interaural timing cues do not contribute to the map of space in the ferret superior colliculus: A virtual acoustic space study. *J Neurophysiol* 95, 242–254.
- Canlon, B., Borg, E., Flock, A. 1988. Protection against noise trauma by pre-exposure to a low level acoustic stimulus. *Hear Res* 34, 197–200.
- Cant, N.B., Benson, C.G. 2003. Parallel auditory pathways: projection patterns of the different neuronal populations in the dorsal and ventral cochlear nuclei. *Brain Res Bull* 60, 457–474.

- Cant, N.B., Morest, D.K. 1978. Axons from non-cochlear sources in the anteroventral cochlear nucleus of the cat. A study with the rapid Golgi method. *Neuroscience* 3, 1003–1029.
- Cao, X.J., Oertel, D. 2010. Auditory nerve fibers excite targets through synapses that vary in convergence, strength, and short-term plasticity. *J Neurophysiol* 104, 2308–2320.
- Carmel, P.W., Starr, A. 1963. Acoustic and nonacoustic factors modifying middle-ear muscle activity in waking cats. *J Neurophysiol* 26, 598–616.
- Carney, A.E., Nelson, D.A. 1983. An analysis of psychophysical tuning curves in normal and pathological ears. *J Acoust Soc Am* 73, 268–278.
- Carrasco, A., Lomber, S.G. 2011. Neuronal activation times to simple, complex, and natural sounds in cat primary and nonprimary auditory cortex. *J Neurophysiol* 106, 1166–1178.
- Caspari, D.M., Havey, D.C., Faingold, C.L. 1983. Effects of acetylcholine on cochlear nucleus neurons. *Exp Neurol* 82, 491–498.
- Caspari, D.M., Backoff, P.M., Finlayson, P.G., Palombi, P.S. 1994. Inhibitory inputs modulate discharge rate within frequency receptive fields of anteroventral cochlear nucleus neurons. *J Neurophysiol* 72, 2124–2133.
- Caspari, D.M., Milbrandt, J.C., Helfert, R.H. 1995. Central auditory aging: GABA changes in the inferior colliculus. *Exp Gerontol* 30, 349–360.
- Caspari, D.M., Palombi, P.S., Hughes, L.F. 2002. GABAergic inputs shape responses to amplitude modulated stimuli in the inferior colliculus. *Hear Res* 168, 163–173.
- Casseday, J.H., Fremouw, T., Covey, E. 2002. The inferior colliculus: a hub for the central nervous system. In: Oertel, D., Fay, R.R., Popper, A.N. (Eds), *Integrative Functions in the Mammalian Auditory Pathway*, Springer Handbook of Auditory Research Vol. 15. Springer, New York. pp. 238–318.
- Cedolin, L., Delgutte, B. 2010. Spatiotemporal representation of the pitch of harmonic complex tones in the auditory nerve. *J Neurosci* 30, 12712–12724.
- Cetas, J.S., Price, R.O., Velenovsky, D.S., Sinex, D.G., McMullen, N.T. 2001. Frequency organization and cellular lamination in the medial geniculate body of the rabbit. *Hear Res* 155, 113–123.
- Cetas, J.S., Price, R.O., Velenovsky, D.S., Crowe, J.J., Sinex, D.G., McMullen, N.T. 2002. Cell types and response properties of neurons in the ventral division of the medial geniculate body of the rabbit. *J Comp Neurol* 445, 78–96.
- Cetas, J.S., Price, R.O., Crowe, J., Velenovsky, D.S., McMullen, N.T. 2003. Dendritic orientation and laminar architecture in the rabbit auditory thalamus. *J Comp Neurol* 458, 307–317.
- Chait, M., Ruff, C.C., Griffiths, T.D., McAlpine, D. 2012. Cortical responses to changes in acoustic regularity are differentially modulated by attentional load. *Neuroimage* 59, 1932–1941.
- Cheatham, M.A., Dallos, P. 1997. Intermodulation components in inner hair cell and organ of Corti responses. *J Acoust Soc Am* 102, 1038–1048.
- Cheatham, M.A., Dallos, P. 1999. Response phase: a view from the inner hair cell. *J Acoust Soc Am* 105, 799–810.
- Cheatham, M.A., Dallos, P. 2000. The dynamic range of inner hair cell and organ of Corti responses. *J Acoust Soc Am* 107, 1508–1520.
- Cheatham, M.A., Dallos, P. 2001. Inner hair cell response patterns: implications for low-frequency hearing. *J Acoust Soc Am* 110, 2034–2044.
- Chen, F., Zha, D., Fridberger, A., et al. 2011. A differentially amplified motion in the ear for near-threshold sound detection. *Nat Neurosci* 14, 770–774.

- Chen, P., Segil, N. 1999. p27(Kip1) links cell proliferation to morphogenesis in the developing organ of Corti. *Development* 126, 1581–1590.
- Chen, W., Johnson, S.L., Marcotti, W., Andrews, P.W., Moore, H.D., Rivolta, M.N. 2009. Human fetal auditory stem cells can be expanded in vitro and differentiate into functional auditory neurons and hair cell-like cells. *Stem Cells* 27, 1196–1204.
- Cheng, A.G., Cunningham, L.L., Rubel, E.W. 2005. Mechanisms of hair cell death and protection. *Curr Opin Otolaryngol Head Neck Surg* 13, 343–348.
- Cheung, E.L., Corey, D.P. 2006. Ca^{2+} changes the force sensitivity of the hair-cell transduction channel. *Biophys J* 90, 124–139.
- Cheung, S.W., Bedenbaugh, P.H., Nagarajan, S.S., Schreiner, C.E. 2001. Functional organization of squirrel monkey primary auditory cortex: responses to pure tones. *J Neurophysiol* 85, 1732–1749.
- Choudhury, N., Song, G., Chen, F., et al. 2006. Low coherence interferometry of the cochlear partition. *Hear Res* 220, 1–9.
- Clarey, J.C., Irvine, D.R. 1990. The anterior ectosylvian sulcal auditory field in the cat: I. An electrophysiological study of its relationship to surrounding auditory cortical fields. *J Comp Neurol* 301, 289–303.
- Clarey, J.C., Barone, P., Imig, T.J. 1992. Physiology of thalamus and cortex. In: Popper, A.N., Fay, R.R. (Eds), *The Mammalian Auditory Pathway: Neurophysiology*, Springer Handbook of Auditory Research Vol. 2. Springer, New York. pp. 232–334.
- Clark, J.A., Pickles, J.O. 1996. The effects of moderate and low levels of acoustic overstimulation on stereocilia and their tip links in the guinea pig. *Hear Res* 99, 119–128.
- Code, R.A., Winer, J.A. 1986. Columnar organization and reciprocity of commissural connections in cat primary auditory cortex (AI). *Hear Res* 23, 205–222.
- Cody, A.R., Russell, I.J. 1987. The response of hair cells in the basal turn of the guinea-pig cochlea to tones. *J Physiol* 383, 551–569.
- Cohen, L.T., Saunders, E., Clark, G.M. 2001. Psychophysics of a prototype peri-modiolar cochlear implant electrode array. *Hear Res* 155, 63–81.
- Colburn, H.S., Durlach, N.I. 1978. Models of binaural interaction. In: Carterette, E., Friedman, M. (Eds), *Handbook of Perception: Hearing* Vol. 4. Academic Press, New York. pp. 467–518.
- Colburn, H.S., Kulkarni, A. 2005. Models of sound localization. In: Popper, A.N., Fay, R.R. (Eds), *Sound Source Localization*, Springer Handbook of Auditory Research Vol. 25. Springer, New York. pp. 272–316.
- Colburn, H.S., Carney, L.H., Heinz, M.G. 2003. Quantifying the information in auditorynerve responses for level discrimination. *J Assoc Res Otolaryngol* 4, 294–311.
- Coleman, J.K., Littlesunday, C., Jackson, R., Meyer, T. 2007. AM-111 protects against permanent hearing loss from impulse noise trauma. *Hear Res* 226, 70–78.
- Comis, S.D., Whitfield, I.C. 1968. Influence of centrifugal pathways on unit activity in the cochlear nucleus. *J Neurophysiol* 31, 62–68.
- Comis, S.D., Pickles, J.O., Osborne, M.P. 1985. Osmium tetroxide postfixation in relation to the crosslinkage and spatial organization of stereocilia in the guinea-pig cochlea. *J Neurocytol* 14, 113–130.
- Coomes, D.L., Schofield, B.R. 2004. Separate projections from the inferior colliculus to the cochlear nucleus and thalamus in guinea pigs. *Hear Res* 191, 67–78.
- Cooper, N.P. 1998. Harmonic distortion on the basilar membrane in the basal turn of the guinea-pig cochlea. *J Physiol* 509, 277–288.
- Cooper, N.P., Guinan, J.J., Jr. 2003. Separate mechanical processes underlie fast and slow effects of medial olivocochlear efferent activity. *J Physiol* 548, 307–312.

- Cooper, N.P., Guinan, J.J., Jr. 2006. Efferent-mediated control of basilar membrane motion. *J Physiol* 576, 49–54.
- Cooper, N.P., Rhode, W.S. 1997. Mechanical responses to two-tone distortion products in the apical and basal turns of the mammalian cochlea. *J Neurophysiol* 78, 261–270.
- Corey, D.P. 2006. What is the hair cell transduction channel? *J Physiol* 576, 23–28.
- Corey, D.P., Hudspeth, A.J. 1979a. Ionic basis of the receptor potential in a vertebrate hair cell. *Nature* 281, 675–677.
- Corey, D.P., Hudspeth, A.J. 1979b. Response latency of vertebrate hair cells. *Biophys J* 26, 499–506.
- Corey, D.P., Hudspeth, A.J. 1983. Kinetics of the receptor current in bullfrog saccular hair cells. *J Neurosci* 3, 962–976.
- Corey, D.P., Garcia-Anoveros, J., Holt, J.R., et al. 2004. TRPA1 is a candidate for the mechanosensitive transduction channel of vertebrate hair cells. *Nature* 432, 723–730.
- Costalupes, J.A., Young, E.D., Gibson, D.J. 1984. Effects of continuous noise backgrounds on rate response of auditory nerve fibers in cat. *J Neurophysiol* 51, 1326–1344.
- Cotanche, D.A. 1987. Regeneration of hair cell stereociliary bundles in the chick cochlea following severe acoustic trauma. *Hear Res* 30, 181–195.
- Cotanche, D.A., Kaiser, C.L. 2010. Hair cell fate decisions in cochlear development and regeneration. *Hear Res* 266, 18–25.
- Counter, S.A., Borg, E. 1993. Acoustic middle ear muscle reflex protection against magnetic coil impulse noise. *Acta Otolaryngol* 113, 483–488.
- Cranford, J.L. 1979. Detection versus discrimination of brief tones by cats with auditory cortex lesions. *J Acoust Soc Am* 65, 1573–1575.
- Crawford, A.C., Evans, M.G., Fettiplace, R. 1991. The actions of calcium on the mechanoelectrical transducer current of turtle hair cells. *J Physiol* 434, 369–398.
- Crinion, J.T., Lambon-Ralph, M.A., Warburton, E.A., Howard, D., Wise, R.J. 2003. Temporal lobe regions engaged during normal speech comprehension. *Brain* 126, 1193–1201.
- Cruz, R.M., Lambert, P.R., Rubel, E.W. 1987. Light microscopic evidence of hair cell regeneration after gentamicin toxicity in chick cochlea. *Arch Otolaryngol Head Neck Surg* 113, 1058–1062.
- D'Angelo, W.R., Sterbing, S.J., Ostapoff, E.M., Kuwada, S. 2005. Role of GABAergic inhibition in the coding of interaural time differences of low-frequency sounds in the inferior colliculus. *J Neurophysiol* 93, 3390–3400.
- Da Costa, S., van der Zwaag, W., Marques, J.P., Frackowiak, R.S., Clarke, S., Saenz, M. 2011. Human primary auditory cortex follows the shape of Heschl's gyrus. *J Neurosci* 31, 14067–14075.
- Dallos, P. 1985. Response characteristics of mammalian cochlear hair cells. *J Neurosci* 5, 1591–1608.
- Dallos, P. 1986. Neurobiology of cochlear inner and outer hair cells: intracellular recordings. *Hear Res* 22, 185–198.
- Dallos, P. 2008. Cochlear amplification, outer hair cells and prestin. *Curr Opin Neurobiol* 18, 370–376.
- Dallos, P., Evans, B.N. 1995a. High-frequency motility of outer hair cells and the cochlear amplifier. *Science* 267, 2006–2009.
- Dallos, P., Evans, B.N. 1995b. High-frequency outer hair cell motility: corrections and addendum. *Science* 268, 1420–1421.
- Dallos, P., Billone, M.C., Durrant, J.D., Wang, C., Raynor, S. 1972. Cochlear inner and outer hair cells: functional differences. *Science* 177, 356–358.

- Dallos, P., Santos-Sacchi, J., Flock, A. 1982. Intracellular recordings from cochlear outer hair cells. *Science* 218, 582–584.
- Dallos, P., Zheng, J., Cheatham, M.A. 2006. Prestin and the cochlear amplifier. *J Physiol* 576, 37–42.
- Dallos, P., Wu, X., Cheatham, M.A., et al. 2008. Prestin-based outer hair cell motility is necessary for mammalian cochlear amplification. *Neuron* 58, 333–339.
- Darrow, K.N., Maison, S.F., Liberman, M.C. 2006a. Cochlear efferent feedback balances interaural sensitivity. *Nat Neurosci* 9, 1474–1476.
- Darrow, K.N., Simons, E.J., Dodds, L., Liberman, M.C. 2006b. Dopaminergic innervation of the mouse inner ear: evidence for a separate cytochemical group of cochlear efferent fibers. *J Comp Neurol* 498, 403–414.
- Darrow, K.N., Maison, S.F., Liberman, M.C. 2007. Selective removal of lateral olivocochlear efferents increases vulnerability to acute acoustic injury. *J Neurophysiol* 97, 1775–1785.
- Darrow, K.N., Benson, T.E., Brown, M.C. 2012. Planar multipolar cells in the cochlear nucleus project to medial olivocochlear neurons in mouse. *J Comp Neurol* 520, 1365–1375.
- Daudet, N., Lebart, M.C. 2002. Transient expression of the t-isoform of plastins/fimbrin in the stereocilia of developing auditory hair cells. *Cell Motil Cytoskeleton* 53, 326–336.
- Davis, H. 1958. Transmission and transduction in the cochlea. *Laryngoscope* 68, 359–382.
- Davis, K.A. 2005. Spectral processing in the inferior colliculus. *Int Rev Neurobiol* 70, 169–205.
- Davis, K.A., Ramachandran, R., May, B.J. 1999. Single-unit responses in the inferior colliculus of decerebrate cats. II. Sensitivity to interaural level differences. *J Neurophysiol* 82, 164–175.
- Davis, M., Antoniadis, E.A., Amaral, D.G., Winslow, J.T. 2008. Acoustic startle reflex in rhesus monkeys: a review. *Rev Neurosci* 19, 171–185.
- Davis, M.H., Gaskell, M.G. 2009. A complementary systems account of word learning: neural and behavioural evidence. *Philos Trans R Soc Lond B Biol Sci* 364, 3773–3800.
- de Boer, E. 1996. Mechanics of the cochlea: modeling efforts. In: Dallos, P., Popper, A.N., Fay, R.R. (Eds), *The Cochlea*, Springer Handbook of Auditory Research Vol. 8. Springer, New York. pp. 258–317.
- de Boer, E., de Jongh, H.R. 1978. On cochlear encoding: potentialities and limitations of the reverse-correlation technique. *J Acoust Soc Am* 63, 115–135.
- de Boer, E., Nuttall, A.L. 1999. The “inverse problem” solved for a three-dimensional model of the cochlea. III. Brushing-up the solution method. *J Acoust Soc Am* 105, 3410–3420.
- de Boer, E., Nuttall, A.L. 2002. Properties of amplifying elements in the cochlea. In: Gummer, A.W., Dalhoff, E., Nowotny, M., Scherer, M.P. (Eds), *Biophysics of the Cochlea: From Molecules to Models* (pp. 331–342). World Scientific, Singapore.
- de Boer, J., Thornton, A.R., Krumbholz, K. 2012. What is the role of the medial olivocochlear system in speech-in-noise processing? *J Neurophysiol* 107, 1301–1312.
- de La Rochefoucauld, O., Olson, E.S. 2007. The role of organ of Corti mass in passive cochlear tuning. *Biophys J* 93, 3434–3450.
- de Venecia, R.K., Liberman, M.C., Guinan, J.J., Jr., Brown, M.C. 2005. Medial olivocochlear reflex interneurons are located in the posteroventral cochlear nucleus: A kainic acid lesion study in guinea pigs. *J Comp Neurol* 487, 345–360.

- Dean, I., Harper, N.S., McAlpine, D. 2005. Neural population coding of sound level adapts to stimulus statistics. *Nat Neurosci* 8, 1684–1689.
- DeBello, W.M., Knudsen, E.I. 2004. Multiple sites of adaptive plasticity in the owl's auditory localization pathway. *J Neurosci* 24, 6853–6861.
- Defourney, J., Lallemend, F., Malgrange, B. 2011. Structure and development of cochlear afferent innervation in mammals. *Am J Physiol Cell Physiol* 301, C750–C761.
- Dehmel, S., Kopp-Scheinplug, C., Weick, M., Dorrscheidt, G.J., Rubsam, R. 2010. Transmission of phase-coupling accuracy from the auditory nerve to spherical bushy cells in the Mongolian gerbil. *Hear Res* 268, 234–249.
- Dehner, L.R., Keniston, L.P., Clemo, H.R., Meredith, M.A. 2004. Cross-modal circuitry between auditory and somatosensory areas of the cat anterior ectosylvian sulcal cortex: a 'new' inhibitory form of multisensory convergence. *Cereb Cortex* 14, 387–403.
- del Castillo, F.J., del Castillo, I. 2011. The DFNB1 subtype of autosomal recessive non-syndromic hearing impairment. *Front Biosci* 17, 3252–3274.
- Delano, P.H., Elgueda, D., Hamame, C.M., Robles, L. 2007. Selective attention to visual stimuli reduces cochlear sensitivity in chinchillas. *J Neurosci* 27, 4146–4153.
- Delgutte, B., Kiang, N.Y. 1984a. Speech coding in the auditory nerve: I. Vowel-like sounds. *J Acoust Soc Am* 75, 866–878.
- Delgutte, B., Kiang, N.Y. 1984b. Speech coding in the auditory nerve: III. Voiceless fricative consonants. *J Acoust Soc Am* 75, 887–896.
- Delgutte, B., Hammond, B.M., Cariani, P.A. 1998. Neural coding of the temporal envelope of speech: relation to modulation transfer functions. In: Palmer, A.R., Rees, A., Summerfield, A.Q., Meddis, R. (Eds), *Psychophysical and Physiological Advances in Hearing* (pp. 595–602). Whurr, London.
- Démonet, J.F., Thierry, G., Cardebat, D. 2005. Renewal of the neurophysiology of language: functional neuroimaging. *Physiol Rev* 85, 49–95.
- Denk, W., Holt, J.R., Shepherd, G.M., Corey, D.P. 1995. Calcium imaging of single stereocilia in hair cells: localization of transduction channels at both ends of tip links. *Neuron* 15, 1311–1321.
- Dettman, S.J., Pinder, D., Briggs, R.J., Dowell, R.C., Leigh, J.R. 2007. Communication development in children who receive the cochlear implant younger than 12 months: risks versus benefits. *Ear Hear* 28, 11S–18S.
- DeWitt, I., Rauschecker, J.P. 2012. Phoneme and word recognition in the auditory ventral stream. *Proc Natl Acad Sci USA* 109, E505–E514.
- Dewson, J.H. 1968. Efferent olivocochlear bundle: some relationships to stimulus discrimination in noise. *J Neurophysiol* 31, 122–130.
- Diamond, I.T., Neff, W.D. 1957. Ablation of temporal cortex and discrimination of auditory patterns. *J Neurophysiol* 20, 300–315.
- Dinh, C.T., Van De Water, T.R. 2009. Blocking pro-cell-death signal pathways to conserve hearing. *Audiol Neurotol* 14, 383–392.
- Dolan, D.F., Guo, M.H., Nuttal, A.L. 1997. Frequency-dependent enhancement of basilar membrane velocity during olivocochlear bundle stimulation. *J Acoust Soc Am* 102, 3587–3596.
- Donaudy, F., Zheng, L., Ficarella, R., et al. 2006. Espin gene (ESPN) mutations associated with autosomal dominant hearing loss cause defects in microvillar elongation or organisation. *J Med Genet* 43, 157–161.
- Dorsaint-Pierre, R., Penhune, V.B., Watkins, K.E., et al. 2006. Asymmetries of the planum temporale and Heschl's gyrus: relationship to language lateralization. *Brain* 129, 1164–1176.

- Doucet, J.R., Ryugo, D.K. 1997. Projections from the ventral cochlear nucleus to the dorsal cochlear nucleus in rats. *J Comp Neurol* 385, 245–264.
- Drenckhahn, D., Schafer, T., Prinz, M. 1985. Actin, myosin and associated proteins in the auditory and vestibular organs: immunocytochemical and biochemical studies. In: Drescher, D.G. (Ed), *Auditory Biochemistry* (pp. 436–472). Thomas, Springfield.
- Driver, E.C., Kelley, M.W. 2009. Specification of cell fate in the mammalian cochlea. *Birth Defects Res C Embryo Today* 87, 212–221.
- Dronkers, N.F., Wilkins, D.P., Van Valin, R.D., Jr., Redfern, B.B., Jaeger, J.J. 2004. Lesion analysis of the brain areas involved in language comprehension. *Cognition* 92, 145–177.
- Dumont, R.A., Zhao, Y.D., Holt, J.R., Bahler, M., Gillespie, P.G. 2002. Myosin-I isozymes in neonatal rodent auditory and vestibular epithelia. *J Assoc Res Otolaryngol* 3, 375–389.
- Durlach, N.I. 1972. Binaural signal detection: equalization and cancellation theory. In: Tobias, J.V. (Ed), *Foundations of Modern Auditory Theory* (Vol. 2). Academic Press, New York.
- Duvel, A.D., Smith, D.M., Talk, A., Gabriel, M. 2001. Medial geniculate, amygdalar and cingulate cortical training-induced neuronal activity during discriminative avoidance learning in rabbits with auditory cortical lesions. *J Neurosci* 21, 3271–3281.
- Edeline, J.M., Weinberger, N.M. 1991. Subcortical adaptive filtering in the auditory system: associative receptive field plasticity in the dorsal medial geniculate body. *Behav Neurosci* 105, 154–175.
- Egan, J.P., Hake, H.W. 1950. On the masking pattern of a simple auditory stimulus. *J Acoust Soc Am* 22, 622–630.
- Eggermont, J.J. 2012. Hearing loss, hyperacusis, or tinnitus: what is modeled in animal research? *Hear Res*. In Press.
- Egorova, M., Ehret, G., Vartanian, I., Esser, K.H. 2001. Frequency response areas of neurons in the mouse inferior colliculus. I. Threshold and tuning characteristics. *Exp Brain Res* 140, 145–161.
- Ehret, G. 1976. Critical bands and filter characteristics in the ear of the housemouse (*Mus musculus*). *Biol Cybern* 24, 35–42.
- Eldredge, D.H. 1974. Inner ear-cochlear mechanics and cochlear potentials. In: Keidel, W.D., Neff, W.D. (Eds), *Handbook of Sensory Physiology* Vol. 5/1. Springer, Berlin. pp. 549–584.
- Elgoyen, A.B., Katz, E. 2012. The efferent medial olivocochlear-hair cell synapse. *J Physiol Paris* 106, 47–56.
- Elgoyen, A.B., Vetter, D.E., Katz, E., Rothlin, C.V., Heinemann, S.F., Boulter, J. 2001. Alpha10: a determinant of nicotinic cholinergic receptor function in mammalian vestibular and cochlear mechanosensory hair cells. *Proc Natl Acad Sci USA* 98, 3501–3506.
- Elliott, D.N., Stein, L., Harrison, M.J. 1960. Discrimination of absolute-intensity thresholds and frequency-difference thresholds in cats. *J Acoust Soc Am* 32, 380–384.
- Elverland, H.H. 1977. Descending connections between superior olivary and cochlear nuclear complexes in the cat studied by autoradiographic and horseradish peroxidase methods. *Exp Brain Res* 27, 397–412.
- Elverland, H.H. 1978. Ascending and intrinsic projections of the superior olivary complex in the cat. *Exp Brain Res* 32, 117–134.
- Emadi, G., Richter, C.P., Dallos, P. 2004. Stiffness of the gerbil basilar membrane: radial and longitudinal variations. *J Neurophysiol* 91, 474–488.

- Escabi, M.A., Schreiner, C.E. 2002. Nonlinear spectrotemporal sound analysis by neurons in the auditory midbrain. *J Neurosci* 22, 4114–4131.
- Evans, E.F. 1972. The frequency response and other properties of single fibres in the guinea-pig cochlear nerve. *J Physiol* 226, 263–287.
- Evans, E.F. 1975. Cochlear nerve and cochlear nucleus. In: Keidel, W.D., Neff, W.D. (Eds), *Handbook of Sensory Physiology Vol. 5/2*. Springer, Berlin. pp. 1–108.
- Evans, E.F. 1977. Frequency selectivity at high signal levels of single units in cochlear nerve and nucleus. In: Evans, E.F., Wilson, J.P. (Eds), *Psychophysics and Physiology of Hearing* (pp. 185–192). Academic Press, London.
- Evans, E.F., Harrison, R.V. 1976. Proceedings: correlation between cochlear outer hair cell damage and deterioration of cochlear nerve tuning properties in the guinea-pig. *J Physiol* 256, 43P–44P.
- Evans, E.F., Nelson, P.G. 1973. The responses of single neurones in the cochlear nucleus of the cat as a function of their location and the anaesthetic state. *Exp Brain Res* 17, 402–427.
- Faingold, C.L. 1999. Neuronal networks in the genetically epilepsy-prone rat. *Adv Neurol* 79, 311–321.
- Faingold, C.L. 2002. Role of GABA abnormalities in the inferior colliculus pathophysiology-audiogenic seizures. *Hear Res* 168, 223–237.
- Farris, H.E., LeBlanc, C.L., Goswami, J., Ricci, A.J. 2004. Probing the pore of the auditory hair cell mechanotransducer channel in turtle. *J Physiol* 558, 769–792.
- Fauser, C., Schimanski, S., Wangemann, P. 2004. Localization of beta1-adrenergic receptors in the cochlea and the vestibular labyrinth. *J Membr Biol* 201, 25–32.
- Fawcett, D.W. 1986. *A Textbook of Histology*. W.B. Saunders, Philadelphia.
- Fayad, J.N., Eisenberg, L.S., Gillinger, M., Winter, M., Martinez, A.S., Luxford, W.M. 2006. Clinical performance of children following revision surgery for a cochlear implant. *Otolaryngol Head Neck Surg* 134, 379–384.
- Felix, D., Ehrenberger, K. 1992. The efferent modulation of mammalian inner hair cell afferents. *Hear Res* 64, 1–5.
- Felix, H. 2002. Anatomical differences in the peripheral auditory system of mammals and man. A mini review. *Adv Otorhinolaryngol* 59, 1–10.
- Fendt, M., Li, L., Yeomans, J.S. 2001. Brain stem circuits mediating prepulse inhibition of the startle reflex. *Psychopharmacology (Berl)* 156, 216–224.
- Fettiplace, R. 2006. Active hair bundle movements in auditory hair cells. *J Physiol* 576, 29–36.
- Fettiplace, R. 2009. Defining features of the hair cell mechanoelectrical transducer channel. *Pflugers Arch* 458, 1115–1123.
- Fettiplace, R., Ricci, A.J. 2003. Adaptation in auditory hair cells. *Curr Opin Neurobiol* 13, 446–451.
- Fischel-Ghodsian, N., Bykhovskaya, Y., Taylor, K., et al. 1997. Temporal bone analysis of patients with presbycusis reveals high frequency of mitochondrial mutations. *Hear Res* 110, 147–154.
- Fischel-Ghodsian, N., Kopke, R.D., Ge, X. 2004. Mitochondrial dysfunction in hearing loss. *Mitochondrion* 4, 675–694.
- Fletcher, H. 1940. Auditory patterns. *Rev Mod Phys* 12, 47–65.
- Flock, A., Flock, B., Murray, E. 1977. Studies on the sensory hairs of receptor cells in the inner ear. *Acta Otolaryngol* 83, 85–91.
- Flock, A., Bretscher, A., Weber, K. 1982. Immunohistochemical localization of several cytoskeletal proteins in inner ear sensory and supporting cells. *Hear Res* 7, 75–89.

- Forge, A., Schacht, J. 2000. Aminoglycoside antibiotics. *Audiol Neurotol* 5, 3–22.
- Forge, A., Li, L., Corwin, J.T., Nevill, G. 1993. Ultrastructural evidence for hair cell regeneration in the mammalian inner ear. *Science* 259, 1616–1619.
- Francis, S.P., Kramarenko, II, Brandon, C.S., Lee, F.S., Baker, T.G., Cunningham, L.L. 2011. Celastrol inhibits aminoglycoside-induced ototoxicity via heat shock protein 32. *Cell Death Dis* 2, e195.
- Fridberger, A., de Monvel, J.B., Zheng, J., et al. 2004. Organ of Corti potentials and the motion of the basilar membrane. *J Neurosci* 24, 10057–10063.
- Frisina, R.D. 2009. Age-related hearing loss: ear and brain mechanisms. *Ann NY Acad Sci* 1170, 708–717.
- Fritz, J., Shamma, S., Elhilali, M., Klein, D. 2003. Rapid task-related plasticity of spectrotemporal receptive fields in primary auditory cortex. *Nat Neurosci* 6, 1216–1223.
- Froemke, R.C., Martins, A.R. 2011. Spectrotemporal dynamics of auditory cortical synaptic receptive field plasticity. *Hear Res* 279, 149–161.
- Frohne, C., Lesinski, A., Battmer, R.D., Lenarz, T. 1997. Intraoperative test of auditory nerve function. *Am J Otol* 18, S93–S94.
- Fujino, K., Oertel, D. 2001. Cholinergic modulation of stellate cells in the mammalian ventral cochlear nucleus. *J Neurosci* 21, 7372–7383.
- Fullerton, B.C., Pandya, D.N. 2007. Architectonic analysis of the auditory-related areas of the superior temporal region in human brain. *J Comp Neurol* 504, 470–498.
- Galaburda, A.M., Pandya, D.N. 1983. The intrinsic architectonic and connectional organization of the superior temporal region of the rhesus monkey. *J Comp Neurol* 221, 169–184.
- Galaburda, A., Sanides, F. 1980. Cytoarchitectonic organization of the human auditory cortex. *J Comp Neurol* 190, 597–610.
- Garinis, A., Werner, L., Abdala, C. 2011. The relationship between MOC reflex and masked threshold. *Hear Res* 282, 128–137.
- Gates, G.A., Couropmitree, N.N., Myers, R.H. 1999. Genetic associations in age-related hearing thresholds. *Arch Otolaryngol Head Neck Surg* 125, 654–659.
- Geisler, C.D., Nuttall, A.L. 1997. Two-tone suppression of basilar membrane vibrations in the base of the guinea pig cochlea using “low-side” suppressors. *J Acoust Soc Am* 102, 430–440.
- Geleoc, G.S., Lennan, G.W., Richardson, G.P., Kros, C.J. 1997. A quantitative comparison of mechanoelectrical transduction in vestibular and auditory hair cells of neonatal mice. *Proc Roy Soc Biol Sci* 264, 611–621.
- Geschwind, N., Levitsky, W. 1968. Human brain: left-right asymmetries in temporal speech region. *Science* 161, 186–187.
- Gfeller, K., Jiang, D., Oleson, J.J., Driscoll, V., Knutson, J.F. 2010. Temporal stability of music perception and appraisal scores of adult cochlear implant recipients. *J Am Acad Audiol* 21, 28–34.
- Gilbert, A.G., Pickles, J.O. 1980. Responses of auditory nerve fibres in the guinea pig to noise bands of different widths. *Hear Res* 2, 327–333.
- Gillespie, L.N., Shepherd, R.K. 2005. Clinical application of neurotrophic factors: the potential for primary auditory neuron protection. *Eur J Neurosci* 22, 2123–2133.
- Gillespie, P.G. 2004. Myosin I and adaptation of mechanical transduction by the inner ear. *Philos Trans R Soc Lond B Biol Sci* 359, 1945–1951.
- Gillespie, P.G., Dumont, R.A., Kachar, B. 2005. Have we found the tip link, transduction channel, and gating spring of the hair cell? *Curr Opin Neurobiol* 15, 389–396.

- Giraud, A.L., Garnier, S., Micheyl, C., Lina, G., Chays, A., Chery-Croze, S. 1997. Auditory efferents involved in speech-in-noise intelligibility. *Neuroreport* 8, 1779–1783.
- Girod, D.A., Rubel, E.W. 1991. Hair cell regeneration in the avian cochlea: if it works in birds, why not in man? *Ear Nose Throat J* 70, 343–350, 353–354.
- Girod, D.A., Duckert, L.G., Rubel, E.W. 1989. Possible precursors of regenerated hair cells in the avian cochlea following acoustic trauma. *Hear Res* 42, 175–194.
- Glendenning, K.K., Baker, B.N., Hutson, K.A., Masterton, R.B. 1992. Acoustic chiasm V: inhibition and excitation in the ipsilateral and contralateral projections of LSO. *J Comp Neurol* 319, 100–122.
- Glueckert, R., Pfaller, K., Kinnefors, A., Schrott-Fischer, A., Rask-Andersen, H. 2005. High resolution scanning electron microscopy of the human organ of Corti. A study using freshly fixed surgical specimens. *Hear Res* 199, 40–56.
- Goblick, T.J., Jr., Pfeiffer, R.R. 1969. Time-domain measurements of cochlear nonlinearities using combination click stimuli. *J Acoust Soc Am* 46, 924–938.
- Goldberg, J.M., Brown, P.B. 1969. Response of binaural neurons of dog superior olfactory complex to dichotic tonal stimuli: Some physiological mechanisms of sound localization. *J Neurophysiol* 32, 613–636.
- Goldberg, J.M., Brownell, W.E. 1973. Discharge characteristics of neurons in anteroventral and dorsal cochlear nuclei of cat. *Brain Res* 64, 35–54.
- Goldstein, J.L. 1967. Auditory nonlinearity. *J Acoust Soc Am* 41, 676–689.
- Goldstein, J.L., Kiang, N.Y.S. 1968. Neural correlates of the aural combination tone $2f_1-f_2$. *Proc IEEE* 56, 981–992.
- Goll, J.C., Crutch, S.J., Warren, J.D. 2010. Central auditory disorders: toward a neuropsychology of auditory objects. *Curr Opin Neurol* 23, 617–627.
- Gordon, K.A., Wong, D.D., Valero, J., Jewell, S.F., Yoo, P., Papsin, B.C. 2011. Use it or lose it? Lessons learned from the developing brains of children who are deaf and use cochlear implants to hear. *Brain Topogr* 24, 204–219.
- Gourevitch, B., Eggermont, J.J. 2007. Spatial representation of neural responses to natural and altered conspecific vocalizations in cat auditory cortex. *J Neurophysiol* 97, 144–158.
- Gow, A., Davies, C., Southwood, C.M., et al. 2004. Deafness in Claudin 11-null mice reveals the critical contribution of basal cell tight junctions to stria vascularis function. *J Neurosci* 24, 7051–7062.
- Grant, L., Yi, E., Glowatzki, E. 2010. Two modes of release shape the postsynaptic response at the inner hair cell ribbon synapse. *J Neurosci* 30, 4210–4220.
- Grati, M., Kachar, B. 2011. Myosin VIIa and sans localization at stereocilia upper tip-link density implicates these Usher syndrome proteins in mechanotransduction. *Proc Natl Acad Sci USA* 108, 11476–11481.
- Greene, N.T., Lomakin, O., Davis, K.A. 2010. Monaural spectral processing differs between the lateral superior olive and the inferior colliculus: physiological evidence for an acoustic chiasm. *Hear Res* 269, 134–145.
- Greenwood, D.D., Goldberg, J.M. 1970. Response of neurons in the cochlear nuclei to variations in noise bandwidth and to tone-noise combinations. *J Acoust Soc Am* 47, 1022–1040.
- Groff, J.A., Liberman, M.C. 2003. Modulation of cochlear afferent response by the lateral olivocochlear system: activation via electrical stimulation of the inferior colliculus. *J Neurophysiol* 90, 3178–3200.
- Grosh, K., Zheng, J., Zou, Y., de Boer, E., Nuttall, A.L. 2004. High-frequency electromotile responses in the cochlea. *J Acoust Soc Am* 115, 2178–2184.

- Grothe, B., Koch, U. 2011. Dynamics of binaural processing in the mammalian sound localization pathway – the role of GABA(B) receptors. *Hear Res* 279, 43–50.
- Grothe, B., Pecka, M., McAlpine, D. 2010. Mechanisms of sound localization in mammals. *Physiol Rev* 90, 983–1012.
- Groves, A.K. 2010. The challenge of hair cell regeneration. *Exp Biol Med (Maywood)* 235, 434–446.
- Guinan, J.J., Jr. 2006. Olivocochlear efferents: anatomy, physiology, function, and the measurement of efferent effects in humans. *Ear Hear* 27, 589–607.
- Guinan, J.J., Jr. 2010. Cochlear efferent innervation and function. *Curr Opin Otolaryngol Head Neck Surg* 18, 447–453.
- Guinan, J.J., Jr., Peake, W.T. 1967. Middle-ear characteristics of anesthetized cats. *J Acoust Soc Am* 41, 1237–1261.
- Guinan, J.J., Jr., Warr, W.B., Norris, B.E. 1983. Differential olivocochlear projections from lateral versus medial zones of the superior olfactory complex. *J Comp Neurol* 221, 358–370.
- Gummer, A.W., Hemmert, W., Zenner, H.P. 1996. Resonant tectorial membrane motion in the inner ear: its crucial role in frequency tuning. *Proc Natl Acad Sci USA* 93, 8727–8732.
- Gunewardene, N., Dottori, M., Nayagam, B.A. 2012. The convergence of cochlear implantation with induced pluripotent stem cell therapy. *Stem Cell Rev and Reports*. In Press.
- Gutfreund, Y., Knudsen, E.I. 2006. Adaptation in the auditory space map of the barn owl. *J Neurophysiol* 96, 813–825.
- Gutschalk, A., Uppenkamp, S. 2011. Sustained responses for pitch and vowels map to similar sites in human auditory cortex. *Neuroimage* 56, 1578–1587.
- Gyo, K., Aritomo, H., Goode, R.L. 1987. Measurement of the ossicular vibration ratio in human temporal bones by use of a video measuring system. *Acta Otolaryngol* 103, 87–95.
- Hackett, T.A. 2011. Information flow in the auditory cortical network. *Hear Res* 271, 133–146.
- Hackett, T.A., Stepniewska, I., Kaas, J.H. 1998. Subdivisions of auditory cortex and ipsilateral cortical connections of the parabelt auditory cortex in macaque monkeys. *J Comp Neurol* 394, 475–495.
- Hackett, T.A., Stepniewska, I., Kaas, J.H. 1999. Callosal connections of the parabelt auditory cortex in macaque monkeys. *Eur J Neurosci* 11, 856–866.
- Hall, J.W., Haggard, M.P., Fernandes, M.A. 1984. Detection in noise by spectro-temporal pattern analysis. *J Acoust Soc Am* 76, 50–56.
- Halverson, H.E., Poremba, A., Freeman, J.H. 2008. Medial auditory thalamus inactivation prevents acquisition and retention of eyeblink conditioning. *Learn Mem* 15, 532–538.
- Hamill, O.P., Martinac, B. 2001. Molecular basis of mechanotransduction in living cells. *Physiol Rev* 81, 685–740.
- Hamzavi, J., Arnoldner, C. 2006. Effect of deep insertion of the cochlear implant electrode array on pitch estimation and speech perception. *Acta Otolaryngol* 126, 1182–1187.
- Hancock, K.E., Delgutte, B. 2004. A physiologically based model of interaural time difference discrimination. *J Neurosci* 24, 7110–7117.
- Hansen, M.R., Roehm, P.C., Xu, N., Green, S.H. 2007. Overexpression of Bcl-2 or Bcl-xL prevents spiral ganglion neuron death and inhibits neurite growth. *Dev Neurobiol* 67, 316–325.
- Harasty, J., Seldon, H.L., Chan, P., Halliday, G., Harding, A. 2003. The left human speech-processing cortex is thinner but longer than the right. *Laterality* 8, 247–260.

- Harinen, K., Aaltonen, O., Salo, E., Salonen, O., Rinne, T. 2012. Task-dependent activations of human auditory cortex to prototypical and nonprototypical vowels. *Hum Brain Mapp.* In Press.
- Harrington, I.A., Heffner, R.S., Heffner, H.E. 2001. An investigation of sensory deficits underlying the aphasia-like behavior of macaques with auditory cortex lesions. *Neuroreport* 12, 1217–1221.
- Harris, D.M., Dallos, P. 1979. Forward masking of auditory nerve fiber responses. *J Neurophysiol* 42, 1083–1107.
- Harrison, J.M., Howe, M.E. 1974a. Anatomy of the afferent auditory nervous system of mammals. In: Keidel, W.D., Neff, W.D. (Eds), *Handbook of Sensory Physiology* Vol. 5/1. Springer, Berlin. pp. 283–336.
- Harrison, J.M., Howe, M.E. 1974b. Anatomy of the descending auditory system (mammalian). In: Keidel, W.D., Neff, W.D. (Eds), *Handbook of Sensory Physiology* Vol. 5/1. Springer, Berlin. pp. 363–388.
- Hashino, E., Shero, M., Salvi, R.J. 1997. Lysosomal targeting and accumulation of aminoglycoside antibiotics in sensory hair cells. *Brain Res* 777, 75–85.
- He, D.Z., Jia, S., Dallos, P. 2003. Prestin and the dynamic stiffness of cochlear outer hair cells. *J Neurosci* 23, 9089–9096.
- He, W., Nuttall, A.L., Ren, T. 2007. Two-tone distortion at different longitudinal locations on the basilar membrane. *Hear Res* 228, 112–122.
- Heffner, H.E., Heffner, R.S. 1986. Hearing loss in Japanese macaques following bilateral auditory cortex lesions. *J Neurophysiol* 55, 256–271.
- Heffner, H., Whitfield, I.C. 1976. Perception of the missing fundamental by cats. *J Acoust Soc Am* 59, 915–919.
- Heil, P., Rajan, R., Irvine, D.R. 1992. Sensitivity of neurons in cat primary auditory cortex to tones and frequency-modulated stimuli. II: organization of response properties along the ‘isofrequency’ dimension. *Hear Res* 63, 135–156.
- Heinz, M.G., Colburn, H.S., Carney, L.H. 2001. Evaluating auditory performance limits: i. one-parameter discrimination using a computational model for the auditory nerve. *Neural Comput* 13, 2273–2316.
- Heinz, M.G., Issa, J.B., Young, E.D. 2005. Auditory-nerve rate responses are inconsistent with common hypotheses for the neural correlates of loudness recruitment. *J Assoc Res Otolaryngol* 6, 91–105.
- Held, G. 1893. Die Centrale Gehörleitung. *Arch Anat Physiol Anat Abt* 1893, 201–248.
- Helfert, R.H., Bonneau, J.M., Wenthold, R.J., Altschuler, R.A. 1989. GABA and glycine immunoreactivity in the guinea pig superior olivary complex. *Brain Res* 501, 269–286.
- Helmholtz, H.L.F. 1863. Die Lehre von den Tonempfindungen als Physiologische Grundlage für die Theorie der Musik, Friedrich Vieweg und Sohn, Braunschweig (Eng. Tr. by A.J. Ellis as On the Sensations of Tone, 1875, Longmans, Green, London).
- Henderson, D., Bielefeld, E.C., Harris, K.C., Hu, B.H. 2006. The role of oxidative stress in noise-induced hearing loss. *Ear Hear* 27, 1–19.
- Henkel, C.K., Gabriele, M.L., McHaffie, J.G. 2005. Quantitative assessment of developing afferent patterns in the cat inferior colliculus revealed with calbindin immunohistochemistry and tract tracing methods. *Neuroscience* 136, 945–955.
- Hibino, H., Nin, F., Tsuzuki, C., Kurachi, Y. 2010. How is the highly positive endocochlear potential formed? The specific architecture of the stria vascularis and the roles of the ion-transport apparatus. *Pflugers Arch* 459, 521–533.

- Hickok, G., Houde, J., Rong, F. 2011. Sensorimotor integration in speech processing: computational basis and neural organization. *Neuron* 69, 407–422.
- Hienz, R.D., Stiles, P., May, B.J. 1998. Effects of bilateral olivocochlear lesions on vowel formant discrimination in cats. *Hear Res* 116, 10–20.
- Hildebrand, M.S., Dahl, H.H., Hardman, J., Coleman, B., Shepherd, R.K., de Silva, M.G. 2005. Survival of partially differentiated mouse embryonic stem cells in the scala media of the guinea pig cochlea. *J Assoc Res Otolaryngol* 6, 341–354.
- Hoet, P., Lison, D. 2008. Ototoxicity of toluene and styrene: state of current knowledge. *Crit Rev Toxicol* 38, 127–170.
- Holley, M.C., Kalinec, F., Kachar, B. 1992. Structure of the cortical cytoskeleton in mammalian outer hair cells. *J Cell Sci* 102(Pt 3), 569–580.
- Holt, J.R., Corey, D.P. 2000. Two mechanisms for transducer adaptation in vertebrate hair cells. *Proc Natl Acad Sci USA* 97, 11730–11735.
- Holton, T., Hudspeth, A.J. 1986. The transduction channel of hair cells from the bull-frog characterized by noise analysis. *J Physiol* 375, 195–227.
- Homma, K., Du, Y., Shimizu, Y., Puria, S. 2009. Ossicular resonance modes of the human middle ear for bone and air conduction. *J Acoust Soc Am* 125, 968–979.
- Hori, R., Nakagawa, T., Sakamoto, T., Matsuoka, Y., Takebayashi, S., Ito, J. 2007. Pharmacological inhibition of Notch signaling in the mature guinea pig cochlea. *Neuroreport* 18, 1911–1914.
- Horst, J.W., Javel, E., Farley, G.R. 1990. Coding of spectral fine structure in the auditory nerve. II: level-dependent nonlinear responses. *J Acoust Soc Am* 88, 2656–2681.
- Horvath, M., Kraus, K.S., Illing, R.B. 2000. Olivocochlear neurons sending axon collaterals into the ventral cochlear nucleus of the rat. *J Comp Neurol* 422, 95–105.
- Hotz, M.A., Harris, F.P., Probst, R. 1994. Otoacoustic emissions: an approach for monitoring aminoglycoside-induced ototoxicity. *Laryngoscope* 104, 1130–1134.
- Houtgast, T. 1977. Auditory-filter characteristics derived from direct-masking data and pulsation-threshold data with a rippled-noise masker. *J Acoust Soc Am* 62, 409–415.
- Houtsma, A.J.M., Smurzynski, J. 1990. Pitch identification and discrimination for complex tones with many harmonics. *J Acoust Soc Am* 87, 304–310.
- Howard, J., Hudspeth, A.J. 1988. Compliance of the hair bundle associated with gating of mechanoelectrical transduction channels in the bullfrog's saccular hair cell. *Neuron* 1, 189–199.
- Howard, J., Roberts, W.M., Hudspeth, A.J. 1988. Mechanoelectrical transduction by hair cells. *Annu Rev Biophys Biophys Chem* 17, 99–124.
- Huang, C.L., Larue, D.T., Winer, J.A. 1999. GABAergic organization of the cat medial geniculate body. *J Comp Neurol* 415, 368–392.
- Huang, M., Sage, C., Tang, Y., et al. 2011. Overlapping and distinct pRb pathways in the mammalian auditory and vestibular organs. *Cell Cycle* 10, 337–351.
- Huang, Q., Tang, J. 2010. Age-related hearing loss or presbycusis. *Eur Arch Otorhinolaryngol* 267, 1179–1191.
- Hubbard, A.E., Mountain, D.C. 1996. Analysis and synthesis of cochlear mechanical models. In: Hawkins, H.L., McMullen, T.A., Popper, A.N., Fay, R.R. (Eds). *Auditory Computation*, Springer Handbook of Auditory Research Vol. 6. Springer, New York. pp. 62–120.
- Hubel, D.H., Wiesel, T.N. 1962. Receptive fields, binocular interaction and functional architecture in the cat's visual cortex. *J Physiol* 160, 106–154.
- Hudspeth, A.J. 1982. Extracellular current flow and the site of transduction by vertebrate hair cells. *J Neurosci* 2, 1–10.

- Hudspeth, A.J. 2008. Making an effort to listen: mechanical amplification in the ear. *Neuron* 59, 530–545.
- Hudspeth, A.J., Corey, D.P. 1977. Sensitivity, polarity, and conductance change in the response of vertebrate hair cells to controlled mechanical stimuli. *Proc Natl Acad Sci USA* 74, 2407–2411.
- Hudspeth, A.J., Jacobs, R. 1979. Stereocilia mediate transduction in vertebrate hair cells. *Proc Natl Acad Sci USA* 76, 1506–1509.
- Hutchin, T.P., Cortopassi, G.A. 2000. Mitochondrial defects and hearing loss. *Cell Mol Life Sci* 57, 1927–1937.
- Hutsler, J., Galuske, R.A. 2003. Hemispheric asymmetries in cerebral cortical networks. *Trends Neurosci* 26, 429–435.
- Ikeda, K., Oshima, T., Hidaka, H., Takasaka, T. 1997. Molecular and clinical implications of loop diuretic ototoxicity. *Hear Res* 107, 1–8.
- Imaizumi, K., Priebe, N.J., Crum, P.A., Bedenbaugh, P.H., Cheung, S.W., Schreiner, C.E. 2004. Modular functional organization of cat anterior auditory field. *J Neurophysiol* 92, 444–457.
- Imig, T.J., Adrian, H.O. 1977. Binaural columns in the primary field (A1) of cat auditory cortex. *Brain Res* 138, 241–257.
- Imig, T.J., Brugge, J.F. 1978. Sources and terminations of callosal axons related to binaural and frequency maps in primary auditory cortex of the cat. *J Comp Neurol* 182, 637–660.
- Ingham, N.J., McAlpine, D. 2005. GABAergic inhibition controls neural gain in inferior colliculus neurons sensitive to interaural time differences. *J Neurosci* 25, 6187–6198.
- Irvine, D.R.F. 1986. The auditory brainstem. *Prog Sens Physiol* 7, 1–279.
- Irvine, D.R., Rajan, R., Aitkin, L.M. 1996. Sensitivity to interaural intensity differences of neurons in primary auditory cortex of the cat. I. Types of sensitivity and effects of variations in sound pressure level. *J Neurophysiol* 75, 75–96.
- Ito, M., van Adel, B., Kelly, J.B. 1996. Sound localization after transection of the commissure of Probst in the albino rat. *J Neurophysiol* 76, 3493–3502.
- Ito, T., Oliver, D.L. 2010. Origins of glutamatergic terminals in the inferior colliculus identified by retrograde transport and expression of VGLUT1 and VGLUT2 genes. *Front Neuroanat* 4, article 135.
- Izumikawa, M., Minoda, R., Kawamoto, K., et al. 2005. Auditory hair cell replacement and hearing improvement by Atoh1 gene therapy in deaf mammals. *Nat Med* 11, 271–276.
- Izumikawa, M., Batts, S.A., Miyazawa, T., Swiderski, D.L., Raphael, Y. 2008. Response of the flat cochlear epithelium to forced expression of Atoh1. *Hear Res* 240, 52–56.
- Kawamoto, K., Izumikawa, M., Beyer, L.A., Atkin, G.M., Raphael, Y. 2009. Spontaneous hair cell regeneration in the mouse utricle following gentamicin ototoxicity. *Hear Res* 247, 17–26.
- Jain, R., Shore, S. 2006. External inferior colliculus integrates trigeminal and acoustic information: unit responses to trigeminal nucleus and acoustic stimulation in the guinea pig. *Neurosci Lett* 395, 71–75.
- Jastreboff, P.J. 2007. Tinnitus retraining therapy. *Prog Brain Res* 166, 415–423.
- Jastreboff, P.J., Brennan, J.F., Coleman, J.K., Sasaki, C.T. 1988. Phantom auditory sensation in rats: an animal model for tinnitus. *Behav Neurosci* 102, 811–822.
- Javel, E., Shepherd, R.K. 2000. Electrical stimulation of the auditory nerve. III. Response initiation sites and temporal fine structure. *Hear Res* 140, 45–76.

- Javel, E., McGee, J., Walsh, E.J., Farley, G.R., Gorga, M.P. 1983. Suppression of auditory nerve responses. II. Suppression threshold and growth, iso-suppression contours. *J Acoust Soc Am* 74, 801–813.
- Jeffress, L.A. 1948. A place theory of sound localization. *J Comp Physiol Psychol* 41, 35–39.
- Jen, P.H., Chen, Q.C., Wu, F.J. 2002. Interaction between excitation and inhibition affects frequency tuning curve, response size and latency of neurons in the auditory cortex of the big brown bat, *Eptesicus fuscus*. *Hear Res* 174, 281–289.
- Jenkins, W.M., Masterton, R.B. 1982. Sound localization: effects of unilateral lesions in central auditory system. *J Neurophysiol* 47, 987–1016.
- Jenkins, W.M., Merzenich, M.M. 1984. Role of cat primary auditory cortex for soundlocalization behavior. *J Neurophysiol* 52, 819–847.
- Ji, W., Gao, E., Suga, N. 2001. Effects of acetylcholine and atropine on plasticity of central auditory neurons caused by conditioning in bats. *J Neurophysiol* 86, 211–225.
- Jia, S., He, D.Z. 2005. Motility-associated hair-bundle motion in mammalian outer hair cells. *Nat Neurosci* 8, 1028–1034.
- Jia, S., Dallos, P., He, D.Z. 2007. Mechanoelectric transduction of adult inner hair cells. *J Neurosci* 27, 1006–1014.
- Jiang, D., McAlpine, D., Palmer, A.R. 1997. Detectability index measures of binaural masking level difference across populations of inferior colliculus neurons. *J Neurosci* 17, 9331–9339.
- Jiang, H., Sha, S.H., Forge, A., Schacht, J. 2006. Caspase-independent pathways of hair cell death induced by kanamycin *in vivo*. *Cell Death Differ* 13, 20–30.
- Johnson, S.L., Beurg, M., Marcotti, W., Fettiplace, R. 2011. Prestin-driven cochlear amplification is not limited by the outer hair cell membrane time constant. *Neuron* 70, 1143–1154.
- Johnstone, B.M., Sellick, P.M. 1972. The peripheral auditory apparatus. *Q Rev Biophys* 5, 1–57.
- Johnstone, B.M., Patuzzi, R., Yates, G.K. 1986. Basilar membrane measurements and the travelling wave. *Hear Res* 22, 147–153.
- Johnstone, B.M., Patuzzi, R., Syka, J., Sykova, E. 1989. Stimulus-related potassium changes in the organ of Corti of guinea-pig. *J Physiol* 408, 77–92.
- Jones, E.G. 2003. Chemically defined parallel pathways in the monkey auditory system. *Ann NY Acad Sci* 999, 218–233.
- Jongkamonwiwat, N., Zine, A., Rivolta, M.N. 2010. Stem cell based therapy in the inner ear: appropriate donor cell types and routes for transplantation. *Curr Drug Targets* 11, 888–897.
- Joris, P.X. 1998. Response classes in the dorsal cochlear nucleus and its output tract in the chloralose-anesthetized cat. *J Neurosci* 18, 3955–3966.
- Joris, P.X., Yin, T.C. 1998. Envelope coding in the lateral superior olive. III. Comparison with afferent pathways. *J Neurophysiol* 79, 253–269.
- Joris, P.X., Smith, P.H., Yin, T.C.T. 1998. Coincidence detection in the auditory system: 50 years after Jeffress. *Neuron* 21, 1235–1238.
- Joris, P.X., Schreiner, C.E., Rees, A. 2004. Neural processing of amplitude-modulated sounds. *Physiol Rev* 84, 541–577.
- Kaas, J.H., Hackett, T.A. 2000. Subdivisions of auditory cortex and processing streams in primates. *Proc Natl Acad Sci USA* 97, 11793–11799.
- Kachar, B., Parakkal, M., Kurc, M., Zhao, Y., Gillespie, P.G. 2000. High-resolution structure of hair-cell tip links. *Proc Natl Acad Sci USA* 97, 13336–13341.

- Kadia, S.C., Wang, X. 2003. Spectral integration in A1 of awake primates: neurons with single- and multipeaked tuning characteristics. *J Neurophysiol* 89, 1603–1622.
- Kajikawa, Y., de La Mothe, L., Blumell, S., Hackett, T.A. 2005. A comparison of neuron response properties in areas A1 and CM of the marmoset monkey auditory cortex: tones and broadband noise. *J Neurophysiol* 93, 22–34.
- Kajikawa, Y., de la Mothe, L.A., Blumell, S., et al. 2008. Coding of FM sweep trains and twitter calls in area CM of marmoset auditory cortex. *Hear Res* 239, 107–125.
- Kaltenbach, J.A. 2006. The dorsal cochlear nucleus as a participant in the auditory, attentional and emotional components of tinnitus. *Hear Res* 216/217, 224–234.
- Kaltenbach, J.A. 2011. Tinnitus: models and mechanisms. *Hear Res* 276, 52–60.
- Kaltenbach, J.A., Godfrey, D.A., Neumann, J.B., McCaslin, D.L., Afman, C.E., Zhang, J. 1998. Changes in spontaneous neural activity in the dorsal cochlear nucleus following exposure to intense sound: relation to threshold shift. *Hear Res* 124, 78–84.
- Kanold, P.O., Davis, K.A., Young, E.D. 2011. Somatosensory context alters auditory responses in the cochlear nucleus. *J Neurophysiol* 105, 1063–1070.
- Kanwal, J.S., Fitzpatrick, D.C., Suga, N. 1999. Facilitatory and inhibitory frequency tuning of combination-sensitive neurons in the primary auditory cortex of mustached bats. *J Neurophysiol* 82, 2327–2345.
- Kanzaki, S., Beyer, L.A., Swiderski, D.L., et al. 2006a. p27(Kip1) deficiency causes organ of Corti pathology and hearing loss. *Hear Res* 214, 28–36.
- Kanzaki, S., Beyer, L., Karolyi, I.J., et al. 2006b. Transgene correction maintains normal cochlear structure and function in 6-month-old Myo15a mutant mice. *Hear Res* 214, 37–44.
- Karlsson, K.K., Harris, J.R., Svartengren, M. 1997. Description and primary results from an audiometric study of male twins. *Ear Hear* 18, 114–120.
- Kavanagh, G.L., Kelly, J.B. 1987. Contribution of auditory cortex to sound localization by the ferret (*Mustela putorius*). *J Neurophysiol* 57, 1746–1766.
- Kawamoto, K., Izumikawa, M., Beyer, L.A., Atkin, G.M., Raphael, Y. 2009. Spontaneous hair cell regeneration in the mouse utricle following gentamicin ototoxicity. *Hear Res* 247, 17–26.
- Kawase, T., Delgutte, B., Liberman, M.C. 1993. Antimasking effects of the olivocochlear reflex. II. Enhancement of auditory-nerve response to masked tones. *J Neurophysiol* 70, 2533–2549.
- Kazmierczak, P., Sakaguchi, H., Tokita, J., et al. 2007. Cadherin 23 and protocadherin 15 interact to form tip-link filaments in sensory hair cells. *Nature* 449, 87–91.
- Kelley, M.W. 2006. Regulation of cell fate in the sensory epithelia of the inner ear. *Nat Rev Neurosci* 7, 837–849.
- Kelly, J.B. 1997. Contributions of the dorsal nucleus of the lateral lemniscus to binaural processing in the auditory brainstem. In: Syka, J. (Ed), *Acoustical Signal Processing in the Central Auditory System* (pp. 329–352). Plenum, New York.
- Kelly, J.B., Li, L., van Adel, B. 1996. Sound localization after kainic acid lesions of the dorsal nucleus of the lateral lemniscus in the albino rat. *Behav Neurosci* 110, 1445–1455.
- Kelly, J.B., van Adel, B.A., Ito, M. 2009. Anatomical projections of the nuclei of the lateral lemniscus in the albino rat (*Rattus norvegicus*). *J Comp Neurol* 512, 573–593.
- Kemp, D.T. 1978. Stimulated acoustic emissions from within the human auditory system. *J Acoust Soc Am* 64, 1386–1391.
- Kemp, D.T. 2002. Otoacoustic emissions, their origin in cochlear function, and use. *Br Med Bull* 63, 223–241.

- Kennedy, H.J., Evans, M.G., Crawford, A.C., Fettiplace, R. 2003. Fast adaptation of mechanoelectrical transducer channels in mammalian cochlear hair cells. *Nat Neurosci* 6, 832–836.
- Kennedy, H.J., Crawford, A.C., Fettiplace, R. 2005. Force generation by mammalian hair bundles supports a role in cochlear amplification. *Nature* 433, 880–883.
- Kennedy, H.J., Evans, M.G., Crawford, A.C., Fettiplace, R. 2006. Depolarization of cochlear outer hair cells evokes active hair bundle motion by two mechanisms. *J Neurosci* 26, 2757–2766.
- Kessel, R.G., Kardon, R.H. 1979. *Tissues and Organs*. W.H. Freeman and Company, San Francisco.
- Khalfa, S., Bougeard, R., Morand, N., et al. 2001. Evidence of peripheral auditory activity modulation by the auditory cortex in humans. *Neuroscience* 104, 347–358.
- Khan, K.M., Drescher, M.J., Hatfield, J.S., Ramakrishnan, N.A., Drescher, D.G. 2007. Immunohistochemical localization of adrenergic receptors in the rat organ of corti and spiral ganglion. *J Neurosci Res* 85, 3000–3012.
- Khanna, S.M., Tonndorf, J. 1972. Tympanic membrane vibrations in cats studied by timeaveraged holography. *J Acoust Soc Am* 51, 1904–1920.
- Kiang, N.Y. 1980. Processing of speech by the auditory nervous system. *J Acoust Soc Am* 68, 830–835.
- Kiang, N.Y. 1990. Curious oddments of auditory-nerve studies. *Hear Res* 49, 1–16.
- Kiang, N.Y., Moxon, E.C. 1972. Physiological considerations in artificial stimulation of the inner ear. *Ann Otol Rhinol Laryngol* 81, 714–730.
- Kiang, N.Y.S., Watanabe, T., Thomas, E.C., Clark, L.F. 1965. *Discharge Patterns of Single Fibers in the Cat's Auditory Nerve*. MIT Press, Cambridge.
- Kiang, N.Y., Sachs, M.B., Peake, W.T. 1967. Shapes of tuning curves for single auditorynerve fibers. *J Acoust Soc Am* 42, 1341–1342.
- Kidd, S.A., Kelly, J.B. 1996. Contribution of the dorsal nucleus of the lateral lemniscus to binaural responses in the inferior colliculus of the rat: interaural time delays. *J Neurosci* 16, 7390–7397.
- Kikuchi, Y., Horwitz, B., Mishkin, M. 2010. Hierarchical auditory processing directed rostrally along the monkey's supratemporal plane. *J Neurosci* 30, 13021–13030.
- Kim, D.O., Molnar, C.E., Matthews, J.W. 1980. Cochlear mechanics: nonlinear behavior in two-tone responses as reflected in cochlear-nerve-fiber responses and in ear-canal sound pressure. *J Acoust Soc Am* 67, 1704–1721.
- Kim, D.O., Sirianni, J.G., Chang, S.O. 1990. Responses of DCN-PVCN neurons and auditory nerve fibers in unanesthetized decerebrate cats to AM and pure tones: analysis with autocorrelation/power-spectrum. *Hear Res* 45, 95–113.
- Kim, Y.H., Raphael, Y. 2007. Cell division and maintenance of epithelial integrity in the deafened auditory epithelium. *Cell Cycle* 6, 612–619.
- King, A.J., Bajo, V.M., Bizley, J.K., et al. 2007. Physiological and behavioral studies of spatial coding in the auditory cortex. *Hear Res* 229, 106–115.
- Kittel, M., Wagner, E., Klump, G.M. 2002. An estimate of the auditory-filter bandwidth in the Mongolian gerbil. *Hear Res* 164, 69–76.
- Kluk, K., Moore, B.C. 2005. Factors affecting psychophysical tuning curves for hearing-impaired subjects with high-frequency dead regions. *Hear Res* 200, 115–131.
- Knudsen, E.I., Konishi, M. 1978. A neural map of auditory space in the owl. *Science* 200, 795–797.
- Koch, M. 1999. The neurobiology of startle. *Prog Neurobiol* 59, 107–128.

- Koch, U., Grothe, B. 2003. Hyperpolarization-activated current (I_h) in the inferior colliculus: distribution and contribution to temporal processing. *J Neurophysiol* 90, 3679–3687.
- Koehler, S.D., Pradhan, S., Manis, P.B., Shore, S.E. 2011. Somatosensory inputs modify auditory spike timing in dorsal cochlear nucleus principal cells. *Eur J Neurosci* 33, 409–420.
- Koike, T., Wada, H., Kobayashi, T. 2002. Modeling of the human middle ear using the finite-element method. *J Acoust Soc Am* 111, 1306–1317.
- Kokotas, H., Petersen, M.B., Willems, P.J. 2007. Mitochondrial deafness. *Clin Genet* 71, 379–391.
- Konings, A., Van Laer, L., Van Camp, G. 2009. Genetic studies on noise-induced hearing loss: a review. *Ear Hear* 30, 151–159.
- Konishi, M. 2003. Coding of auditory space. *Annu Rev Neurosci* 26, 31–55.
- Kopp-Scheinpflug, C., Dehmel, S., Dorrscheidt, G.J., Rübsamen, R. 2002. Interaction of excitation and inhibition in anteroventral cochlear nucleus neurons that receive large endbulb synaptic endings. *J Neurosci* 22, 11004–11018.
- Kopp-Scheinpflug, C., Lippe, W.R., Dorrscheidt, G.J., Rübsamen, R. 2003. The medial nucleus of the trapezoid body in the gerbil is more than a relay: comparison of pre- and postsynaptic activity. *J Assoc Res Otolaryngol* 4, 1–23.
- Kringlebotn, M. 1988. Network model for the human middle ear. *Scand Audiol* 17, 75–85.
- Krishna, B.S., Semple, M.N. 2000. Auditory temporal processing: responses to sinusoidally amplitude-modulated tones in the inferior colliculus. *J Neurophysiol* 84, 255–273.
- Kromer, L.F., Moore, R.Y. 1980. Norepinephrine innervation of the cochlear nuclei by locus coeruleus neurons in the rat. *Anat Embryol (Berl)* 158, 227–244.
- Kros, C.J. 1996. Physiology of mammalian cochlear hair cells. In: Dallos, P., Popper, A.N., Fay, R.R. (Eds), *The Cochlea*, Springer Handbook of Auditory Research Vol. 8. Springer, New York. pp. 318–385.
- Kros, C.J. 2007. How to build an inner hair cell: challenges for regeneration. *Hear Res* 227, 3–10.
- Kros, C.J., Rüsch, A., Richardson, G.P. 1992. Mechano-electrical transducer currents in hair cells of the cultured neonatal mouse cochlea. *Proc Roy Soc Biol Sci* 249, 185–193.
- Krumbholz, K., Schonwiesner, M., von Cramon, D.Y., et al. 2005. Representation of interaural temporal information from left and right auditory space in the human planum temporale and inferior parietal lobe. *Cereb Cortex* 15, 317–324.
- Kuenzel, T., Borst, J.G., van der Heijden, M. 2011. Factors controlling the input-output relationship of spherical bushy cells in the gerbil cochlear nucleus. *J Neurosci* 31, 4260–4273.
- Kuhl, P.K. 2010. Brain mechanisms in early language acquisition. *Neuron* 67, 713–727.
- Kuijpers, W., Bonting, S.L. 1969. Studies on $(\text{Na}^+ - \text{K}^+)$ -activated ATPase. XXIV. Localization and properties of ATPase in the inner ear of the guinea pig. *Biochim Biophys Acta* 173, 477–485.
- Kuijpers, W., Bonting, S.L. 1970. The cochlear potentials. I. The effect of ouabain on the cochlear potentials of the guinea pig. *Pflugers Arch* 320, 348–358.
- Kujawa, S.G., Liberman, M.C. 1997. Conditioning-related protection from acoustic injury: effects of chronic deafferentation and sham surgery. *J Neurophysiol* 78, 3095–3106.
- Kulesza, R.J., Jr. 2007. Cytoarchitecture of the human superior olivary complex: medial and lateral superior olive. *Hear Res* 225, 80–90.

- Kumar, S., Stephan, K.E., Warren, J.D., Friston, K.J., Griffiths, T.D. 2007. Hierarchical processing of auditory objects in humans. *PLoS Comput Biol* 3, e100. Epub 2007 Apr 24.
- Kummer, P., Janssen, T., Arnold, W. 1995. Suppression tuning characteristics of the $2f_1-f_2$ distortion-product otoacoustic emission in humans. *J Acoust Soc Am* 98, 197–210.
- Kuwada, S., Fitzpatrick, D.C., Batra, R., Ostapoff, E.M. 2006. Sensitivity to interaural time differences in the dorsal nucleus of the lateral lemniscus of the unanesthetized rabbit: comparison with other structures. *J Neurophysiol* 95, 1309–1322.
- Kuwada, S., Bishop, B., Alex, C., Condit, D.W., Kim, D.O. 2011. Spatial tuning to sound-source azimuth in the inferior colliculus of unanesthetized rabbit. *J Neurophysiol* 106, 2698–2708.
- Kwan, K.Y., Allchorne, A.J., Vollrath, M.A., et al. 2006. TRPA1 contributes to cold, mechanical, and chemical nociception but is not essential for hair-cell transduction. *Neuron* 50, 277–289.
- Kwon, J., Pierson, M. 1997. Fos-immunoreactive responses in inferior colliculi of rats with experimental audiogenic seizure susceptibility. *Epilepsy Res* 27, 89–99.
- Lane, C.C., Delgutte, B. 2005. Neural correlates and mechanisms of spatial release from masking: single-unit and population responses in the inferior colliculus. *J Neurophysiol* 94, 1180–1198.
- Langers, D.R., van Dijk, P. 2012. Mapping the tonotopic organization in human auditory cortex with minimally salient acoustic stimulation. *Cereb Cortex*. In Press.
- Langner, G. 2004. Topographic representation of periodicity information: the 2nd neural axis of the auditory system. In: Syka, J., Merzenich, M.M. (Eds), *Plasticity of the Central Auditory System and Processing of Complex Acoustic Signals* (pp. 19–33). Plenum, New York.
- Langner, G. 2005. Neuronal mechanisms underlying the perception of pitch and harmony. *Ann NY Acad Sci* 1060, 50–52.
- Langner, G., Schreiner, C.E. 1988. Periodicity coding in the inferior colliculus of the cat. I. Neuronal mechanisms. *J Neurophysiol* 60, 1799–1822.
- Langner, G., Albert, M., Briede, T. 2002. Temporal and spatial coding of periodicity information in the inferior colliculus of awake chinchilla (*Chinchilla laniger*). *Hear Res* 168, 110–130.
- Laroche, C., Hetu, R., Quoc, H.T., Josserand, B., Glasberg, B. 1992. Frequency selectivity in workers with noise-induced hearing loss. *Hear Res* 64, 61–72.
- Las, L., Stern, E.A., Nelken, I. 2005. Representation of tone in fluctuating maskers in the ascending auditory system. *J Neurosci* 25, 1503–1513.
- Lazard, D.S., Collette, J.L., Perrot, X. 2012. Speech processing: from peripheral to hemispheric asymmetry of the auditory system. *Laryngoscope* 122, 167–173.
- Leake, P.A., Rebscher, S.J. 2004. Anatomical considerations and long-term effects of electrical stimulation. In: Zeng, F.G., Popper, A.N., Fay, R.R. (Eds), *Cochlear Implants: Auditory Prostheses and Electric Hearing*, Springer Handbook of Auditory Research Vol. 20. Springer, New York. pp. 101–148.
- LeBeau, F.E., Malmierca, M.S., Rees, A. 2001. Iontophoresis *in vivo* demonstrates a key role for GABA(A) and glycinergic inhibition in shaping frequency response areas in the inferior colliculus of guinea pig. *J Neurosci* 21, 7303–7312.
- Lee, C.C., Sherman, S.M. 2011. On the classification of pathways in the auditory midbrain, thalamus, and cortex. *Hear Res* 276, 79–87.
- Leff, A.P., Iverson, P., Schofield, T.M., et al. 2009. Vowel-specific mismatch responses in the anterior superior temporal gyrus: an fMRI study. *Cortex* 45, 517–526.

- Lendvai, B., Halmos, G.B., Polony, G., *et al.* 2011. Chemical neuroprotection in the cochlea: the modulation of dopamine release from lateral olivocochlear efferents. *Neurochem Int* 59, 150–158.
- Lesniak, W., Pecoraro, V.L., Schacht, J. 2005. Ternary complexes of gentamicin with iron and lipid catalyze formation of reactive oxygen species. *Chem Res Toxicol* 18, 357–364.
- Li, H., Roblin, G., Liu, H., Heller, S. 2003. Generation of hair cells by stepwise differentiation of embryonic stem cells. *Proc Natl Acad Sci USA* 100, 13495–13500.
- Li, L., Forge, A. 1997. Morphological evidence for supporting cell to hair cell conversion in the mammalian utricular macula. *Int J Dev Neurosci* 15, 433–446.
- Li, L., Kelly, J.B. 1992. Inhibitory influence of the dorsal nucleus of the lateral lemniscus on binaural responses in the rat's inferior colliculus. *J Neurosci* 12, 4530–4539.
- Liberman, A.M., Cooper, F.S., Shankweiler, D.P., Studdert-Kennedy, M. 1967. Perception of the speech code. *Psychol Rev* 74, 431–461.
- Liberman, L.D., Wang, H., Liberman, M.C. 2011. Opposing gradients of ribbon size and AMPA receptor expression underlie sensitivity differences among cochlear-nerve/hair-cell synapses. *J Neurosci* 31, 801–808.
- Liberman, M.C. 1978. Auditory-nerve response from cats raised in a low-noise chamber. *J Acoust Soc Am* 63, 442–455.
- Liberman, M.C. 1980. Efferent synapses in the inner hair cell area of the cat cochlea: an electron microscopic study of serial sections. *Hear Res* 3, 189–204.
- Liberman, M.C. 1982. Single-neuron labeling in the cat auditory nerve. *Science* 216, 1239–1241.
- Liberman, M.C., Dodds, L.W. 1984a. Single-neuron labeling and chronic cochlear pathology. II. Stereocilia damage and alterations of spontaneous discharge rates. *Hear Res* 16, 43–53.
- Liberman, M.C., Dodds, L.W. 1984b. Single-neuron labeling and chronic cochlear pathology. III. Stereocilia damage and alterations of threshold tuning curves. *Hear Res* 16, 55–74.
- Liberman, M.C., Dodds, L.W. 1987. Acute ultrastructural changes in acoustic trauma: serial-section reconstruction of stereocilia and cuticular plates. *Hear Res* 26, 45–64.
- Liberman, M.C., Kiang, N.Y. 1978. Acoustic trauma in cats. Cochlear pathology and auditory-nerve activity. *Acta Otolaryngol Suppl* 358, 1–63.
- Liberman, M.C., Dodds, L.W., Pierce, S. 1990. Afferent and efferent innervation of the cat cochlea: quantitative analysis with light and electron microscopy. *J Comp Neurol* 301, 443–460.
- Liberman, M.C., Puria, S., Guinan, J.J., Jr. 1996. The ipsilaterally evoked olivocochlear reflex causes rapid adaptation of the $2f_1-f_2$ distortion product otoacoustic emission. *J Acoust Soc Am* 99, 3572–3584.
- Liberman, M.C., Gao, J., He, D.Z., Wu, X., Jia, S., Zuo, J. 2002. Prestin is required for electromotility of the outer hair cell and for the cochlear amplifier. *Nature* 419, 300–304.
- Liebenthal, E., Binder, J.R., Spitzer, S.M., Possing, E.T., Medler, D.A. 2005. Neural substrates of phonemic perception. *Cereb Cortex* 15, 1621–1631.
- Liégeois-Chauvel, C., de Graaf, J.B., Laguitton, V., Chauvel, P. 1999. Specialization of left auditory cortex for speech perception in man depends on temporal coding. *Cereb Cortex* 9, 484–496.
- Lilaonitkul, W., Guinan, J.J., Jr. 2009a. Human medial olivocochlear reflex: effects as functions of contralateral, ipsilateral, and bilateral elicitor bandwidths. *J Assoc Res Otolaryngol* 10, 459–470.

- Lilaonitkul, W., Guinan, J.J., Jr. 2009b. Reflex control of the human inner ear: a half-octave offset in medial efferent feedback that is consistent with an efferent role in the control of masking. *J Neurophysiol* 101, 1394–1406.
- Lim, D.J. 1986. Effects of noise and ototoxic drugs at the cellular level in the cochlea: a review. *Am J Otolaryngol* 7, 73–99.
- Lim, K.M., Steele, C.R. 2002. A three-dimensional nonlinear active cochlear model analyzed by the WKB-numeric method. *Hear Res* 170, 190–205.
- Limb, C.J. 2006. Structural and functional neural correlates of music perception. *Anat Rec A Discov Mol Cell Evol Biol* 288, 435–446.
- Lin, V., Golub, J.S., Nguyen, T.B., Hume, C.R., Oesterle, E.C., Stone, J.S. 2011. Inhibition of Notch1 activity promotes nonmitotic regeneration of hair cells in the adult mouse utricles. *J Neurosci* 31, 15329–15339.
- Liu, W., Suga, N. 1997. Binaural and commissural organization of the primary auditory cortex of the mustached bat. *J Comp Physiol [A]* 181, 599–605.
- Liu, Z., Zuo, J. 2008. Cell cycle regulation in hair cell development and regeneration in the mouse cochlea. *Cell Cycle* 7, 2129–2133.
- Loftus, W.C., Sutter, M.L. 2001. Spectrotemporal organization of excitatory and inhibitory receptive fields of cat posterior auditory field neurons. *J Neurophysiol* 86, 475–491.
- Loftus, W.C., Bishop, D.C., Saint Marie, R.L., Oliver, D.L. 2004. Organization of binaural excitatory and inhibitory inputs to the inferior colliculus from the superior olive. *J Comp Neurol* 472, 330–344.
- Loftus, W.C., Bishop, D.C., Oliver, D.L. 2010. Differential patterns of inputs create functional zones in central nucleus of inferior colliculus. *J Neurosci* 30, 13396–13408.
- Lohuis, T.D., Fuzessery, Z.M. 2000. Neuronal sensitivity to interaural time differences in the sound envelope in the auditory cortex of the pallid bat. *Hear Res* 143, 43–57.
- Lomber, S.G., Malhotra, S. 2008. Double dissociation of ‘what’ and ‘where’ processing in auditory cortex. *Nat Neurosci* 11, 609–616.
- Lomber, S.G., Malhotra, S., Hall, A.J. 2007. Functional specialization in non-primary auditory cortex of the cat: areal and laminar contributions to sound localization. *Hear Res* 229, 31–45.
- Löwenheim, H., Furness, D.N., Kil, J., et al. 1999. Gene disruption of p27(Kip1) allows cell proliferation in the postnatal and adult organ of Corti. *Proc Natl Acad Sci USA* 96, 4084–4088.
- Löwenstein, O., Wersäll, J. 1959. A functional interpretation of the electron-microscopic structure of sensory hairs in the cristae of the elasmobranch *Raja clavata* in terms of directional sensitivity. *Nature* 184, 1807–1808.
- Lukashkin, A.N., Richardson, G.P., Russell, I.J. 2010. Multiple roles for the tectorial membrane in the active cochlea. *Hear Res* 266, 26–35.
- Lumani, A., Zhang, H. 2010. Responses of neurons in the rat’s dorsal cortex of the inferior colliculus to monaural tone bursts. *Brain Res* 1351, 115–129.
- Lumpkin, E.A., Hudspeth, A.J. 1995. Detection of Ca^{2+} entry through mechanosensitive channels localizes the site of mechanoelectrical transduction in hair cells. *Proc Natl Acad Sci USA* 92, 10297–10301.
- Lustig, L.R. 2006. Nicotinic acetylcholine receptor structure and function in the efferent auditory system. *Anat Rec A Discov Mol Cell Evol Biol* 288, 424–434.
- Lustig, L.R., Akil, O. 2012. Cochlear gene therapy. *Curr Opin Neurol* 25, 57–60.
- Lynch, T.J., Nedzelnitsky, V., Peake, W.T. 1982. Input impedance of the cochlea in cat. *J Acoust Soc Am* 72, 108–130.

- Ma, W.L., Brenowitz, S.D. 2012. Single-neuron recordings from unanesthetized mouse dorsal cochlear nucleus. *J Neurophysiol* 107, 824–835.
- Ma, X., Suga, N. 2001. Plasticity of bat's central auditory system evoked by focal electric stimulation of auditory and/or somatosensory cortices. *J Neurophysiol* 85, 1078–1087.
- Maeda, Y., Sheffield, A.M., Smith, R.J. 2009. Therapeutic regulation of gene expression in the inner ear using RNA interference. *Adv Otorhinolaryngol* 66, 13–36.
- Maier, J.X., Groh, J.M. 2009. Multisensory guidance of orienting behavior. *Hear Res* 258, 106–112.
- Maison, S., Micheyl, C., Collet, L. 2001. Influence of focused auditory attention on cochlear activity in humans. *Psychophysiology* 38, 35–40.
- Maison, S.F., Luebke, A.E., Liberman, M.C., Zuo, J. 2002. Efferent protection from acoustic injury is mediated via alpha9 nicotinic acetylcholine receptors on outer hair cells. *J Neurosci* 22, 10838–10846.
- Maison, S.F., Adams, J.C., Liberman, M.C. 2003a. Olivocochlear innervation in the mouse: immunocytochemical maps, crossed versus uncrossed contributions, and transmitter colocalization. *J Comp Neurol* 455, 406–416.
- Maison, S.F., Emeson, R.B., Adams, J.C., Luebke, A.E., Liberman, M.C. 2003b. Loss of alpha CGRP reduces sound-evoked activity in the cochlear nerve. *J Neurophysiol* 90, 2941–2949.
- Maison, S.F., Rosahl, T.W., Homanics, G.E., Liberman, M.C. 2006. Functional role of GABAergic innervation of the cochlea: phenotypic analysis of mice lacking GABA(A) receptor subunits alpha 1, alpha 2, alpha 5, alpha 6, beta 2, beta 3, or delta. *J Neurosci* 26, 10315–10326.
- Maison, S.F., Parker, L.L., Young, L., Adelman, J.P., Zuo, J., Liberman, M.C. 2007. Overexpression of SK2 channels enhances efferent suppression of cochlear responses without enhancing noise resistance. *J Neurophysiol* 97, 2930–2936.
- Maison, S.F., Le, M., Larsen, E., et al. 2010. Mice lacking adrenergic signaling have normal cochlear responses and normal resistance to acoustic injury but enhanced susceptibility to middle-ear infection. *J Assoc Res Otolaryngol* 11, 449–461.
- Malhotra, S., Lomber, S.G. 2007. Sound localization during homotopic and heterotopic bilateral cooling deactivation of primary and nonprimary auditory cortical areas in the cat. *J Neurophysiol* 97, 26–43.
- Malhotra, S., Hall, A.J., Lomber, S.G. 2004. Cortical control of sound localization in the cat: unilateral cooling deactivation of 19 cerebral areas. *J Neurophysiol* 92, 1625–1643.
- Malmierca, M.S., Leergaard, T.B., Bajo, V.M., Bjaalie, J.G., Merchan, M.A. 1998. Anatomic evidence of a three-dimensional mosaic pattern of tonotopic organization in the ventral complex of the lateral lemniscus in cat. *J Neurosci* 18, 10603–10618.
- Malmierca, M.S., Merchan, M.A., Henkel, C.K., Oliver, D.L. 2002. Direct projections from cochlear nuclear complex to auditory thalamus in the rat. *J Neurosci* 22, 10891–10897.
- Malmierca, M.S., Izquierdo, M.A., Cristaudo, S., et al. 2008. A discontinuous tonotopic organization in the inferior colliculus of the rat. *J Neurosci* 28, 4767–4776.
- Mancilla, J.G., Manis, P.B. 2009. Two distinct types of inhibition mediated by cartwheel cells in the dorsal cochlear nucleus. *J Neurophysiol* 102, 1287–1295.
- Marcus, D.C., Wu, T., Wangemann, P., Kofuji, P. 2002. KCNJ10 (Kir4.1) potassium channel knockout abolishes endocochlear potential. *Am J Physiol Cell Physiol* 282, C403–C407.
- Markin, V.S., Hudspeth, A.J. 1995. Gating-spring models of mechanoelectrical transduction by hair cells of the internal ear. *Annu Rev Biophys Biomol Struct* 24, 59–83.

- Martin, P., Bozovic, D., Choe, Y., Hudspeth, A.J. 2003. Spontaneous oscillation by hair bundles of the bullfrog's sacculus. *J Neurosci* 23, 4533–4548.
- Masterton, B., Diamond, I.T. 1967. Medial superior olive and sound localization. *Science* 155, 1696–1697.
- Matsubara, J.A., Phillips, D.P. 1988. Intracortical connections and their physiological correlates in the primary auditory cortex (AI) of the cat. *J Comp Neurol* 268, 38–48.
- Matsumoto, N., Kalinec, F. 2005. Prestin-dependent and prestin-independent motility of guinea pig outer hair cells. *Hear Res* 208, 1–13.
- May, B.J. 2000. Role of the dorsal cochlear nucleus in the sound localization behavior of cats. *Hear Res* 148, 74–87.
- May, B.J., Prell, G.S., Sachs, M.B. 1998. Vowel representations in the ventral cochlear nucleus of the cat: effects of level, background noise, and behavioral state. *J Neurophysiol* 79, 1755–1767.
- McAlpine, D., Palmer, A.R. 2002. Blocking GABAergic inhibition increases sensitivity to sound motion cues in the inferior colliculus. *J Neurosci* 22, 1443–1453.
- McAlpine, D., Jiang, D., Palmer, A.R. 2001. A neural code for low-frequency sound localization in mammals. *Nat Neurosci* 4, 396–401.
- McBride, D.I., Williams, S. 2001. Audiometric notch as a sign of noise induced hearing loss. *Occup Environ Med* 58, 46–51.
- McEchron, M.D., Green, E.J., Winters, R.W., Nolen, T.G., Schneiderman, N., McCabe, P.M. 1996. Changes of synaptic efficacy in the medial geniculate nucleus as a result of auditory classical conditioning. *J Neurosci* 16, 1273–1283.
- McGinley, M.J., Oertel, D. 2006. Rate thresholds determine the precision of temporal integration in principal cells of the ventral cochlear nucleus. *Hear Res* 216/217, 52–63.
- McKay, C. 2004. Psychophysics and electrical stimulation. In: Zeng, F.G., Popper, A.N., Fay, R.R. (Eds), *Cochlear Implants: Auditory Prostheses and Electric Hearing*, Springer Handbook of Auditory Research Vol. 20. Springer, New York. pp. 286–333.
- McLaughlin, M., Van de Sande, B., van der Heijden, M., Joris, P.X. 2007. Comparison of bandwidths in the inferior colliculus and the auditory nerve. I. Measurement using a spectrally manipulated stimulus. *J Neurophysiol* 98, 2566–2579.
- McMullen, N.T., Velenovsky, D.S., Holmes, M.G. 2005. Auditory thalamic organization: cellular slabs, dendritic arbors and tectothalamic axons underlying the frequency map. *Neuroscience* 136, 927–943.
- Melichar, I., Syka, J. 1987. Electrophysiological measurements of the stria vascularis potentials *in vivo*. *Hear Res* 25, 35–43.
- Mellott, J.G., Motts, S.D., Schofield, B.R. 2011. Multiple origins of cholinergic innervation of the cochlear nucleus. *Neuroscience* 180, 138–147.
- Meltser, I., Canlon, B. 2011. Protecting the auditory system with glucocorticoids. *Hear Res* 281, 47–55.
- Merchan, M.A., Berbel, P. 1996. Anatomy of the ventral nucleus of the lateral lemniscus in rats: a nucleus with a concentric laminar organization. *J Comp Neurol* 372, 245–263.
- Merchan, M., Aguilar, L.A., Lopez-Poveda, E.A., Malmierca, M.S. 2005. The inferior colliculus of the rat: quantitative immunocytochemical study of GABA and glycine. *Neuroscience* 136, 907–925.
- Merzenich, M.M., Knight, P.L., Roth, G.L. 1975. Representation of cochlea within primary auditory cortex in the cat. *J Neurophysiol* 38, 231–249.
- Meyer, A.C., Moser, T. 2010. Structure and function of cochlear afferent innervation. *Curr Opin Otolaryngol Head Neck Surg* 18, 441–446.

- Micheyl, C., Collet, L. 1996. Involvement of the olivocochlear bundle in the detection of tones in noise. *J Acoust Soc Am* 99, 1604–1610.
- Middlebrooks, J.C., Green, D.M. 1991. Sound localization by human listeners. *Annu Rev Psychol* 42, 135–159.
- Middlebrooks, J.C., Zook, J.M. 1983. Intrinsic organization of the cat's medial geniculate body identified by projections to binaural response-specific bands in the primary auditory cortex. *J Neurosci* 3, 203–224.
- Middlebrooks, J.C., Dykes, R.W., Merzenich, M.M. 1980. Binaural response-specific bands in primary auditory cortex (AI) of the cat: topographical organization orthogonal to isofrequency contours. *Brain Res* 181, 31–48.
- Middlebrooks, J.C., Makous, J.C., Green, D.M. 1989. Directional sensitivity of soundpressure levels in the human ear canal. *J Acoust Soc Am* 86, 89–108.
- Middlebrooks, J.C., Xu, L., Furukawa, S., Mickey, B.J. 2002. Location signaling by cortical neurons. In: Oertel, D., Fay, R.R., Popper, A.N. (Eds), *Integrative Functions in the Mammalian Auditory Pathway*, Springer Handbook of Auditory Research Vol. 15. Springer, New York. pp. 319–357.
- Middleton, J.W., Kiritani, T., Pedersen, C., Turner, J.G., Shepherd, G.M., Tzounopoulos, T. 2011. Mice with behavioral evidence of tinnitus exhibit dorsal cochlear nucleus hyperactivity because of decreased GABAergic inhibition. *Proc Natl Acad Sci USA* 108, 7601–7606.
- Miller, A.L. 2001. Effects of chronic stimulation on auditory nerve survival in ototoxically deafened animals. *Hear Res* 151, 1–14.
- Miller, L.M., Escabi, M.A., Read, H.L., Schreiner, C.E. 2002. Spectrotemporal receptive fields in the lemniscal auditory thalamus and cortex. *J Neurophysiol* 87, 516–527.
- Mills, A.W. 1958. On the minimum audible angle. *J Acoust Soc Am* 30, 237–246.
- Möller, A.R. 1965. An experimental study of the acoustic impedance of the middle ear and its transmission properties. *Acta Otolaryngol* 60, 129–149.
- Moore, B.C. 1975. Mechanisms of masking. *J Acoust Soc Am* 57, 391–399.
- Moore, B.C. 2002. Interference effects and phase sensitivity in hearing. *Philos Transact Roy Soc A Math Phys Eng Sci* 360, 833–858.
- Moore, B.C. 2005. Basic psychophysics of human spectral processing. *Int Rev Neurobiol* 70, 49–86.
- Moore, B.C.J. 2012. *An Introduction to the Psychology of Hearing* (6th ed). Emerald Publishing, Bingley, UK.
- Moore, B.C., Glasberg, B.R. 1982. Contralateral and ipsilateral cueing in forward masking. *J Acoust Soc Am* 71, 942–945.
- Moore, B.C., Glasberg, B.R. 1986. Comparisons of frequency selectivity in simultaneous and forward masking for subjects with unilateral cochlear impairments. *J Acoust Soc Am* 80, 93–107.
- Moore, B.C., Glasberg, B.R., Roberts, B. 1984. Refining the measurement of psychophysical tuning curves. *J Acoust Soc Am* 76, 1057–1066.
- Moore, B.C.J., Glasberg, B.R., Baer, T. 1997. A model for the prediction of threshold, loudness, and partial loudness. *J Audio Eng Soc* 45, 224–240.
- Moore, J.K. 1980. The primate cochlear nuclei: loss of lamination as a phylogenetic process. *J Comp Neurol* 193, 609–629.
- Moore, J.K. 1987. The human auditory brain stem: a comparative view. *Hear Res* 29, 1–32.
- Moore, J.K., Guan, Y.L. 2001. Cytoarchitectural and axonal maturation in human auditory cortex. *J Assoc Res Otolaryngol* 2, 297–311.
- Morel, A., Imig, T.J. 1987. Thalamic projections to fields A, AI, P, and VP in the cat auditory cortex. *J Comp Neurol* 265, 119–144.

- Morest, D.K., Oliver, D.L. 1984. The neuronal architecture of the inferior colliculus in the cat: defining the functional anatomy of the auditory midbrain. *J Comp Neurol* 222, 209–236.
- Morest, D.K., Kiang, N.Y.S., Kane, E.C., Guinan, J.J., Godfrey, D.A. 1973. Stimulus coding at caudal levels in the cat's auditory nervous system. In: Möller, A. (Ed), *Basic Mechanisms in Hearing* (pp. 479–504). Academic Press, New York.
- Mountain, D.C. 1980. Changes in endolymphatic potential and crossed olivocochlear bundle stimulation alter cochlear mechanics. *Science* 210, 71–72.
- Mukerji, S., Windsor, A.M., Lee, D.J. 2010. Auditory brainstem circuits that mediate the middle ear muscle reflex. *Trends Amplif* 14, 170–191.
- Mukherjea, D., Rybak, L.P. 2011. Pharmacogenomics of cisplatin-induced ototoxicity. *Pharmacogenomics* 12, 1039–1050.
- Mulders, W.H., Robertson, D. 2000. Evidence for direct cortical innervation of medial olivocochlear neurones in rats. *Hear Res* 144, 65–72.
- Mulders, W.H., Robertson, D. 2005a. Noradrenergic modulation of brainstem nuclei alters cochlear neural output. *Hear Res* 204, 147–155.
- Mulders, W.H., Robertson, D. 2005b. Diverse responses of single auditory afferent fibres to electrical stimulation of the inferior colliculus in guinea-pig. *Exp Brain Res* 160, 235–244.
- Mulders, W.H., Paolini, A.G., Needham, K., Robertson, D. 2009. Synaptic responses in cochlear nucleus neurons evoked by activation of the olivocochlear system. *Hear Res* 256, 85–92.
- Mulheran, M. 1999. The effects of quinine on cochlear nerve fibre activity in the guinea pig. *Hear Res* 134, 145–152.
- Munson, B., Nelson, P.B. 2005. Phonetic identification in quiet and in noise by listeners with cochlear implants. *J Acoust Soc Am* 118, 2607–2617.
- Murugasu, E., Russell, I.J. 1995. Salicylate ototoxicity: the effects on basilar membrane displacement, cochlear microphonics, and neural responses in the basal turn of the guinea pig cochlea. *Aud Neurosci* 1, 139–150.
- Murugasu, E., Russell, I.J. 1996. The effect of efferent stimulation on basilar membrane displacement in the basal turn of the guinea pig cochlea. *J Neurosci* 16, 325–332.
- Musicant, A.D., Chan, J.C., Hind, J.E. 1990. Direction-dependent spectral properties of cat external ear: new data and cross-species comparisons. *J Acoust Soc Am* 87, 757–781.
- Nadol, J.B., Jr. 1997. Patterns of neural degeneration in the human cochlea and auditory nerve: implications for cochlear implantation. *Otolaryngol Head Neck Surg* 117, 220–228.
- Nagarajan, S.S., Cheung, S.W., Bedenbaugh, P., Beitel, R.E., Schreiner, C.E., Merzenich, M.M. 2002. Representation of spectral and temporal envelope of twitter vocalizations in common marmoset primary auditory cortex. *J Neurophysiol* 87, 1723–1737.
- Nakajima, H.H., Dong, W., Olson, E.S., Merchant, S.N., Ravicz, M.E., Rosowski, J.J. 2009. Differential intracochlear sound pressure measurements in normal human temporal bones. *J Assoc Res Otolaryngol* 10, 23–36.
- Nakamoto, K.T., Jones, S.J., Palmer, A.R. 2008. Descending projections from auditory cortex modulate sensitivity in the midbrain to cues for spatial position. *J Neurophysiol* 99, 2347–2356.
- Nakamoto, K.T., Shackleton, T.M., Palmer, A.R. 2010. Responses in the inferior colliculus of the guinea pig to concurrent harmonic series and the effect of inactivation of descending controls. *J Neurophysiol* 103, 2050–2061.

- Nakamura, P.A., Cramer, K.S. 2011. Formation and maturation of the calyx of Held. *Hear Res* 276, 70–78.
- Nam, J.H., Fettiplace, R. 2010. Force transmission in the organ of Corti micromachine. *Biophys J* 98, 2813–2821.
- Nayagam, B.A., Muniak, M.A., Ryugo, D.K. 2011. The spiral ganglion: connecting the peripheral and central auditory systems. *Hear Res* 278, 2–20.
- Nayagam, D.A., Clarey, J.C., Paolini, A.G. 2005. Powerful, onset inhibition in the ventral nucleus of the lateral lemniscus. *J Neurophysiol* 94, 1651–1654.
- Nedzelnitsky, V. 1980. Sound pressures in the basal turn of the cat cochlea. *J Acoust Soc Am* 68, 1676–1689.
- Neely, S.T., Kim, D.O. 1986. A model for active elements in cochlear biomechanics. *J Acoust Soc Am* 79, 1472–1480.
- Neff, W.D. 1968. Localization and lateralization of sound in space. In: de Reuck, A.V.S., Knight, J. (Eds), *Hearing Mechanisms in Vertebrates* (pp. 207–231). Churchill, London.
- Nelken, I. 2002. Feature detection by the auditory cortex. In: Oertel, D., Fay, R.R., Popper, A.N. (Eds), *Integrative Functions in the Mammalian Auditory Pathway*, Springer Handbook of Auditory Research Vol. 15. Springer, New York. pp. 358–416.
- Nelken, I., Young, E.D. 1994. Two separate inhibitory mechanisms shape the responses of dorsal cochlear nucleus type IV units to narrowband and wideband stimuli. *J Neurophysiol* 71, 2446–2462.
- Nelken, I., Young, E.D. 1997. Linear and nonlinear spectral integration in type IV neurons of the dorsal cochlear nucleus. I. Regions of linear interaction. *J Neurophysiol* 78, 790–799.
- Nelson, D.A., Schmitz, J.L., Donaldson, G.S., Viemeister, N.F., Javel, E. 1996. Intensity discrimination as a function of stimulus level with electric stimulation. *J Acoust Soc Am* 100, 2393–2414.
- Neuert, V., Verhey, J.L., Winter, I.M. 2004. Responses of dorsal cochlear nucleus neurons to signals in the presence of modulated maskers. *J Neurosci* 24, 5789–5797.
- Nicol, M.J., Walmsley, B. 2002. Ultrastructural basis of synaptic transmission between endbulbs of Held and bushy cells in the rat cochlear nucleus. *J Physiol* 539, 713–723.
- Nienhuys, T.G., Clark, G.M. 1979. Critical bands following the selective destruction of cochlear inner and outer hair cells. *Acta Otolaryngol* 88, 350–358.
- Nieschalk, M., Schmal, F., Delank, K.W., Stoll, W. 1999. Category loudness scaling to evaluate sound perception in cochlear and retro-cochlear lesions. *HNO* 47, 787–795.
- Nilsen, K.E., Russell, I.J. 2000. The spatial and temporal representation of a tone on the guinea pig basilar membrane. *Proc Natl Acad Sci USA* 97, 11751–11758.
- Nishimura, K., Nakagawa, T., Ono, K., et al. 2009. Transplantation of mouse induced pluripotent stem cells into the cochlea. *Neuroreport* 20, 1250–1254.
- Nourski, K.V., Brugge, J.F. 2011. Representation of temporal sound features in the human auditory cortex. *Rev Neurosci* 22, 187–203.
- Nuttall, A.L., Dolan, D.F., Avinash, G. 1991. Laser Doppler velocimetry of basilar membrane vibration. *Hear Res* 51, 203–213.
- Nuttall, A.L., Grosh, K., Zheng, J., de Boer, E., Zou, Y., Ren, T. 2004. Spontaneous basilar membrane oscillation and otoacoustic emission at 15 kHz in a guinea pig. *J Assoc Res Otolaryngol* 5, 337–348.
- O'Connor, K.N., Puria, S. 2006. Middle ear cavity and ear canal pressure-driven stapes velocity responses in human cadaveric temporal bones. *J Acoust Soc Am* 120, 1517–1528.

- O'Connell, M.N., Falchier, A., McGinnis, T., Schroeder, C.E., Lakatos, P. 2011. Dual mechanism of neuronal ensemble inhibition in primary auditory cortex. *Neuron* 69, 805–817.
- Oertel, D. 1983. Synaptic responses and electrical properties of cells in brain slices of the mouse anteroventral cochlear nucleus. *J Neurosci* 3, 2043–2053.
- Oertel, D. 1991. The role of intrinsic neuronal properties in the encoding of auditory information in the cochlear nuclei. *Curr Opin Neurobiol* 1, 221–228.
- Oertel, D., Young, E.D. 2004. What's a cerebellar circuit doing in the auditory system? *Trends Neurosci* 27, 104–110.
- Oertel, D., Wu, S.H., Garb, M.W., Dizack, C. 1990. Morphology and physiology of cells in slice preparations of the posteroventral cochlear nucleus of mice. *J Comp Neurol* 295, 136–154.
- Oertel, D., Wright, S., Cao, X.J., Ferragamo, M., Bal, R. 2011. The multiple functions of T stellate/multipolar/chopper cells in the ventral cochlear nucleus. *Hear Res* 276, 61–69.
- Oesterle, E.C., Campbell, S. 2009. Supporting cell characteristics in long-deafened aged mouse ears. *J Assoc Res Otolaryngol* 10, 525–544.
- Offner, F.F., Dallos, P., Cheatham, M.A. 1987. Positive endocochlear potential: mechanism of production by marginal cells of stria vascularis. *Hear Res* 29, 117–124.
- Ohl, F.W., Scheich, H. 2005. Learning-induced plasticity in animal and human auditory cortex. *Curr Opin Neurobiol* 15, 470–477.
- Ohlemiller, K.K. 2008. Recent findings and emerging questions in cochlear noise injury. *Hear Res* 245, 5–17.
- Ohlemiller, K.K. 2009. Mechanisms and genes in human stria presbycusis from animal models. *Brain Res* 1277, 70–83.
- Oishi, N., Schacht, J. 2011. Emerging treatments for noise-induced hearing loss. *Expert Opin Emerg Drugs* 16, 235–245.
- Ojima, H. 2011. Interplay of excitation and inhibition elicited by tonal stimulation in pyramidal neurons of primary auditory cortex. *Neurosci Biobehav Rev* 35, 2084–2093.
- Oliver, D.L., Morest, D.K. 1984. The central nucleus of the inferior colliculus in the cat. *J Comp Neurol* 222, 237–264.
- Oliver, D.L., Winer, J.A., Beckius, G.E., Saint Marie, R.L. 1994. Morphology of GABAergic neurons in the inferior colliculus of the cat. *J Comp Neurol* 340, 27–42.
- Oliver, D.L., Beckius, G.E., Bishop, D.C., Kuwada, S. 1997. Simultaneous anterograde labeling of axonal layers from lateral superior olive and dorsal cochlear nucleus in the inferior colliculus of cat. *J Comp Neurol* 382, 215–229.
- Oonishi, S., Katsuki, Y. 1965. Functional organization and integrative mechanism on the auditory cortex of the cat. *Jap J Physiol* 15, 342–365.
- Osborne, M.P., Comis, S.D., Pickles, J.O. 1988. Further observations on the fine structure of tip links between stereocilia of the guinea pig cochlea. *Hear Res* 35, 99–108.
- Osen, K.K. 1969. Cytoarchitecture of the cochlear nuclei in the cat. *J Comp Neurol* 136, 453–484.
- Osen, K.K., Roth, K. 1969. Histochemical localization of cholinesterases in the cochlear nuclei of the cat, with notes on the origin of acetylcholinesterase-positive afferents and the superior olive. *Brain Res* 16, 165–185.
- Oshima, K., Grimm, C.M., Corrales, C.E., et al. 2007. Differential distribution of stem cells in the auditory and vestibular organs of the inner ear. *J Assoc Res Otolaryngol* 8, 18–31.

- Ostapoff, E.M., Feng, J.J., Morest, D.K. 1994. A physiological and structural study of neuron types in the cochlear nucleus. II. Neuron types and their structural correlation with response properties. *J Comp Neurol* 346, 19–42.
- Ostapoff, E.M., Benson, C.G., Saint Marie, R.L. 1997. GABA- and glycineimmunoreactive projections from the superior olfactory complex to the cochlear nucleus in guinea pig. *J Comp Neurol* 381, 500–512.
- Ota, Y., Oliver, D.L., Dolan, D.F. 2004. Frequency-specific effects on cochlear responses during activation of the inferior colliculus in the Guinea pig. *J Neurophysiol* 91, 2185–2193.
- Overholt, E.M., Rubel, E.W., Hyson, R.L. 1992. A circuit for coding interaural time differences in the chick brainstem. *J Neurosci* 12, 1698–1708.
- Oxenham, A.J., Shera, C.A. 2003. Estimates of human cochlear tuning at low levels using forward and simultaneous masking. *J Assoc Res Otolaryngol* 4, 541–554.
- Oxenham, A.J., Simonson, A.M. 2006. Level dependence of auditory filters in nonsimultaneous masking as a function of frequency. *J Acoust Soc Am* 119, 444–453.
- Özdamar, O., Dallos, P. 1978. Synchronous responses of the primary auditory fibers to the onset of tone burst and their relation to compound action potentials. *Brain Res* 155, 169–175.
- Palmer, A.R., King, A.J. 1982. The representation of auditory space in the mammalian superior colliculus. *Nature* 299, 248–249.
- Palmer, A.R., Russell, I.J. 1986. Phase-locking in the cochlear nerve of the guinea-pig and its relation to the receptor potential of inner hair-cells. *Hear Res* 24, 1–15.
- Palmer, A.R., Rees, A., Caird, D. 1992. Binaural masking and sensitivity to interaural delay in the inferior colliculus. *Philos Trans R Soc Lond B Biol Sci* 336, 415–422.
- Palmer, A.R., Jiang, D., McAlpine, D. 2000. Neural responses in the inferior colliculus to binaural masking level differences created by inverting the noise in one ear. *J Neurophysiol* 84, 844–852.
- Pang, X.D., Guinan, J.J., Jr. 1997a. Effects of stapedius-muscle contractions on the masking of auditory-nerve responses. *J Acoust Soc Am* 102, 3576–3586.
- Pang, X.D., Guinan, J.J., Jr. 1997b. Growth rate of simultaneous masking in cat auditory-nerve fibers: relationship to the growth of basilar-membrane motion and the origin of two-tone suppression. *J Acoust Soc Am* 102, 3564–3575.
- Paolini, A.G., Clark, G.M. 1999. Intracellular responses of onset chopper neurons in the ventral cochlear nucleus to tones: evidence for dual-component processing. *J Neurophysiol* 81, 2347–2359.
- Park, T.J., Klug, A., Holinstat, M., Grothe, B. 2004. Interaural level difference processing in the lateral superior olive and the inferior colliculus. *J Neurophysiol* 92, 289–301.
- Parker, M.A. 2011. Biotechnology in the treatment of sensorineural hearing loss: foundations and future of hair cell regeneration. *J Speech Lang Hear Res* 54, 1709–1731.
- Parkins, C.W. 1989. Temporal response patterns of auditory nerve fibers to electrical stimulation in deafened squirrel monkeys. *Hear Res* 41, 137–168.
- Patterson, J.H., Jr., Hamernik, R.P. 1997. Blast overpressure induced structural and functional changes in the auditory system. *Toxicology* 121, 29–40.
- Patuzzi, R.B. 1996. Cochlear micromechanics and macromechanics. In: Dallos, P., Popper, A.N., Fay, R.R. (Eds), *The Cochlea*, Springer Handbook of Auditory Research Vol. 8. Springer, New York. pp. 186–257.
- Patuzzi, R., Sellick, P.M. 1984. The modulation of the sensitivity of the mammalian cochlea by low frequency tones. II. Inner hair cell receptor potentials. *Hear Res* 13, 9–18.

- Pecka, M., Zahn, T.P., Saunier-Rebori, B., *et al.* 2007. Inhibiting the inhibition: a neuronal network for sound localization in reverberant environments. *J Neurosci* 27, 1782–1790.
- Pecka, M., Brand, A., Behrend, O., Grothe, B. 2008. Interaural time difference processing in the mammalian medial superior olive: the role of glycinergic inhibition. *J Neurosci* 28, 6914–6925.
- Pecka, M., Siveke, I., Grothe, B., Lesica, N.A. 2010. Enhancement of ITD coding within the initial stages of the auditory pathway. *J Neurophysiol* 103, 38–46.
- Peng, A.W., Salles, F.T., Pan, B., Ricci, A.J. 2011. Integrating the biophysical and molecular mechanisms of auditory hair cell mechanotransduction. *Nat Commun* 2, 523.
- Penhune, V.B., Zatorre, R.J., MacDonald, J.D., Evans, A.C. 1996. Interhemispheric anatomical differences in human primary auditory cortex: probabilistic mapping and volume measurement from magnetic resonance scans. *Cereb Cortex* 6, 661–672.
- Peppi, M., Kujawa, S.G., Sewell, W.F. 2011. A corticosteroid-responsive transcription factor, promyelocytic leukemia zinc finger protein, mediates protection of the cochlea from acoustic trauma. *J Neurosci* 31, 735–741.
- Petit, C. 2006. From deafness genes to hearing mechanisms: harmony and counterpoint. *Trends Mol Med* 12, 57–64.
- Petkov, C.I., Kayser, C., Augath, M., Logothetis, N.K. 2006. Functional imaging reveals numerous fields in the monkey auditory cortex. *PLoS Biol* 4, e215.
- Pfeiffer, R.R. 1966. Anteroventral cochlear nucleus: wave forms of extracellularly recorded spike potentials. *Science* 154, 667–668.
- Pfenniger, A., Wohlwend, A., Kwak, B.R. 2011. Mutations in connexin genes and disease. *Eur J Clin Invest* 41, 103–116.
- Phillips, D.P., Irvine, D.R. 1981. Responses of single neurons in physiologically defined primary auditory cortex (AI) of the cat: frequency tuning and responses to intensity. *J Neurophysiol* 45, 48–58.
- Pickles, J.O. 1975. Normal critical bands in the cat. *Acta Otolaryngol* 80, 245–254.
- Pickles, J.O. 1976. Role of centrifugal pathways to cochlear nucleus in determination of critical bandwidth. *J Neurophysiol* 39, 394–400.
- Pickles, J.O. 1979. Psychophysical frequency resolution in the cat as determined by simultaneous masking and its relation to auditory-nerve resolution. *J Acoust Soc Am* 66, 1725–1732.
- Pickles, J.O. 1983. Auditory-nerve correlates of loudness summation with stimulus bandwidth, in normal and pathological cochleae. *Hear Res* 12, 239–250.
- Pickles, J.O. 1984. Frequency threshold curves and simultaneous masking functions in single fibres of the guinea pig auditory nerve. *Hear Res* 14, 245–256.
- Pickles, J.O. 1992. Tip links and hair cells. *Curr Biol* 2, 48–50.
- Pickles, J.O. 1993. A model for the mechanics of the stereociliary bundle on acousticolateral hair cells. *Hear Res* 68, 159–172.
- Pickles, J.O. 2004. Mutation in mitochondrial DNA as a cause of presbyacusis. *Audiol Neurotol* 9, 23–33.
- Pickles, J.O. 2007a. The physiology of the ear. In: Wright, D. (Ed), *Scott-Brown's Otolaryngology* (Vol. 1), 7th ed. Butterworth Medical, London.
- Pickles, J.O. 2007b. Illustrations of the Inner Ear. Graceville Press, Graceville.
- Pickles, J.O., Comis, S.D. 1973. Role of centrifugal pathways to cochlear nucleus in detection of signals in noise. *J Neurophysiol* 36, 1131–1137.
- Pickles, J.O., Comis, S.D., Osborne, M.P. 1984. Cross-links between stereocilia in the guinea pig organ of Corti, and their possible relation to sensory transduction. *Hear Res* 15, 103–112.

- Pickles, J.O., Comis, S.D., Osborne, M.P. 1987a. The effect of chronic application of kanamycin on stereocilia and their tip links in hair cells of the guinea pig cochlea. *Hear Res* 29, 237–244.
- Pickles, J.O., Osborne, M.P., Comis, S.D. 1987b. Vulnerability of tip links between stereocilia to acoustic trauma in the guinea pig. *Hear Res* 25, 173–183.
- Pickles, J.O., Brix, J., Comis, S.D., et al. 1989. The organization of tip links and stereocilia on hair cells of bird and lizard basilar papillae. *Hear Res* 41, 31–41.
- Pickles, J.O., Rouse, G.W., von Perger, M. 1991. Morphological correlates of mechanotransduction in acousticolateral hair cells. *Scanning Microsc* 5, 1115–1124, Discussion 1124–1128.
- Pickles, J.O., Billieux-Hawkins, D.A., Rouse, G.W. 1996. The incorporation and turnover of radiolabelled amino acids in developing stereocilia of the chick cochlea. *Hear Res* 101, 45–54.
- Pilati, N., Large, C., Forsythe, I.D., Hamann, M. 2012. Acoustic over-exposure triggers burst firing in dorsal cochlear nucleus fusiform cells. *Hear Res* 283, 98–106.
- Poirrier, A.L., Pincemail, J., Van Den Ackerveken, P., Lefebvre, P.P., Malgrange, B. 2010. Oxidative stress in the cochlea: an update. *Curr Med Chem* 17, 3591–3604.
- Pollak, G.D., Burger, R.M., Klug, A. 2003. Dissecting the circuitry of the auditory system. *Trends Neurosci* 26, 33–39.
- Poon, P.W., Chen, X., Cheung, Y.M. 1992. Differences in FM response correlate with morphology of neurons in the rat inferior colliculus. *Exp Brain Res* 91, 94–104.
- Portfors, C.V., Roberts, P.D. 2007. Temporal and frequency characteristics of cartwheel cells in the dorsal cochlear nucleus of the awake mouse. *J Neurophysiol* 98, 744–756.
- Pralong, D., Carlile, S. 1994. Measuring the human head-related transfer functions: a novel method for the construction and calibration of a miniature “in-ear” recording system. *J Acoust Soc Am* 95, 3435–3444.
- Prescott, E.D., Zenisek, D. 2005. Recent progress towards understanding the synaptic ribbon. *Curr Opin Neurobiol* 15, 431–446.
- Pressnitzer, D., Meddis, R., Delahaye, R., Winter, I.M. 2001. Physiological correlates of comodulation masking release in the mammalian ventral cochlear nucleus. *J Neurosci* 21, 6377–6386.
- Price, C.J. 2010. The anatomy of language: a review of 100 fMRI studies published in 2009. *Ann NY Acad Sci* 1191, 62–88.
- Price, C., Thierry, G., Griffiths, T. 2005. Speech-specific auditory processing: where is it? *Trends Cogn Sci* 9, 271–276.
- Prieto, J.J., Peterson, B.A., Winer, J.A. 1994. Morphology and spatial distribution of GABAergic neurons in cat primary auditory cortex (AI). *J Comp Neurol* 344, 349–382.
- Probst, F.J., Fridell, R.A., Raphael, Y., et al. 1998. Correction of deafness in shaker-2 mice by an unconventional myosin in a BAC transgene. *Science* 280, 1444–1447.
- Pujol, R., Puel, J.L. 1999. Excitotoxicity, synaptic repair, and functional recovery in the mammalian cochlea: a review of recent findings. *Ann NY Acad Sci* 884, 249–254.
- Puria, S., Allen, J.B. 1991. A parametric study of cochlear input impedance. *J Acoust Soc Am* 89, 287–309.
- Rabinowitz, W.M. 1981. Measurement of the acoustic input immittance of the human ear. *J Acoust Soc Am* 70, 1025–1035.
- Rajan, R. 1988. Effect of electrical stimulation of the crossed olivocochlear bundle on temporary threshold shifts in auditory sensitivity. I. Dependence on electrical stimulation parameters. *J Neurophysiol* 60, 549–568.

- Rajan, R., Johnstone, B.M. 1988. Binaural acoustic stimulation exercises protective effects at the cochlea that mimic the effects of electrical stimulation of an auditory efferent pathway. *Brain Res* 459, 241–255.
- Rajan, R., Irvine, D.R., Wise, L.Z., Heil, P. 1993. Effect of unilateral partial cochlear lesions in adult cats on the representation of lesioned and unlesioned cochleas in primary auditory cortex. *J Comp Neurol* 338, 17–49.
- Ramachandran, R., May, B.J. 2002. Functional segregation of ITD sensitivity in the inferior colliculus of decerebrate cats. *J Neurophysiol* 88, 2251–2261.
- Ramachandran, R., Davis, K.A., May, B.J. 1999. Single-unit responses in the inferior colliculus of decerebrate cats. I. Classification based on frequency response maps. *J Neurophysiol* 82, 152–163.
- Rasmussen, G.L. 1946. The olfactory peduncle and other fiber projections to the superior olfactory complex. *J Comp Neurol* 84, 141–220.
- Rauschecker, J.P., Scott, S.K. 2009. Maps and streams in the auditory cortex: nonhuman primates illuminate human speech processing. *Nat Neurosci* 12, 718–724.
- Rauschecker, J.P., Tian, B. 2000. Mechanisms and streams for processing of “what” and “where” in auditory cortex. *Proc Natl Acad Sci USA* 97, 11800–11806.
- Rauschecker, J.P., Tian, B. 2004. Processing of band-passed noise in the lateral auditory belt cortex of the rhesus monkey. *J Neurophysiol* 91, 2578–2589.
- Raviv, D., Dror, A.A., Avraham, K.B. 2010. Hearing loss: a common disorder caused by many rare alleles. *Ann NY Acad Sci* 1214, 168–179.
- Razak, K.A. 2011. Systematic representation of sound locations in the primary auditory cortex. *J Neurosci* 31, 13848–13859.
- Read, H.L., Winer, J.A., Schreiner, C.E. 2002. Functional architecture of auditory cortex. *Curr Opin Neurobiol* 12, 433–440.
- Read, H.L., Nauen, D.W., Escabi, M.A., Miller, L.M., Schreiner, C.E., Winer, J.A. 2011. Distinct core thalamocortical pathways to central and dorsal primary auditory cortex. *Hear Res* 274, 95–104.
- Reale, R.A., Imig, T.J. 1980. Tonotopic organization in auditory cortex of the cat. *J Comp Neurol* 192, 265–291.
- Recanzone, G.H. 2008. Representation of con-specific vocalizations in the core and belt areas of the auditory cortex in the alert macaque monkey. *J Neurosci* 28, 13184–13193.
- Recanzone, G.H. 2011. Perception of auditory signals. *Ann NY Acad Sci* 1224, 96–108.
- Recanzone, G.H., Guard, D.C., Phan, M.L. 2000. Frequency and intensity response properties of single neurons in the auditory cortex of the behaving macaque monkey. *J Neurophysiol* 83, 2315–2331.
- Recanzone, G.H., Engle, J.R., Juarez-Salinas, D.L. 2011. Spatial and temporal processing of single auditory cortical neurons and populations of neurons in the macaque monkey. *Hear Res* 271, 115–122.
- Recio, A., Rhode, W.S. 2000. Representation of vowel stimuli in the ventral cochlear nucleus of the chinchilla. *Hear Res* 146, 167–184.
- Recio, A., Rich, N.C., Narayan, S.S., Ruggero, M.A. 1998. Basilar-membrane responses to clicks at the base of the chinchilla cochlea. *J Acoust Soc Am* 103, 1972–1989.
- Recio-Spinoso, A., Temchin, A.N., van Dijk, P., Fan, Y.H., Ruggero, M.A. 2005. Wiener kernel analysis of responses to noise of chinchilla auditory-nerve fibers. *J Neurophysiol* 93, 3615–3634.
- Reiss, L.A., Young, E.D. 2005. Spectral edge sensitivity in neural circuits of the dorsal cochlear nucleus. *J Neurosci* 25, 3680–3691.

- Relkin, E.M., Doucet, J.R. 1997. Is loudness simply proportional to the auditory nerve spike count? *J Acoust Soc Am* 101, 2735–2740.
- Remedios, R., Logothetis, N.K., Kayser, C. 2009. An auditory region in the primate insular cortex responding preferentially to vocal communication sounds. *J Neurosci* 29, 1034–1045.
- Ren, T. 2002. Longitudinal pattern of basilar membrane vibration in the sensitive cochlea. *Proc Natl Acad Sci USA* 99, 17101–17106.
- Ren, T., He, W., Porsov, E. 2011. Localization of the cochlear amplifier in living sensitive ears. *PLoS One* 6, e20149.
- Reyes, J.H., O'Shea, K.S., Wys, N.L., et al. 2008. Glutamatergic neuronal differentiation of mouse embryonic stem cells after transient expression of neurogenin 1 and treatment with BDNF and GDNF: in vitro and in vivo studies. *J Neurosci* 28, 12622–12631.
- Rhode, W.S. 1971. Observations of the vibration of the basilar membrane in squirrel monkeys using the Mössbauer technique. *J Acoust Soc Am* 49, 1218–1231.
- Rhode, W.S. 1999. Vertical cell responses to sound in cat dorsal cochlear nucleus. *J Neurophysiol* 82, 1019–1032.
- Rhode, W.S. 2007. Mutual suppression in the 6 kHz region of sensitive chinchilla cochleae. *J Acoust Soc Am* 121, 2805–2818.
- Rhode, W.S., Greenberg, S. 1994. Encoding of amplitude modulation in the cochlear nucleus of the cat. *J Neurophysiol* 71, 1797–1825.
- Rhode, W.S., Recio, A. 2000. Study of mechanical motions in the basal region of the chinchilla cochlea. *J Acoust Soc Am* 107, 3317–3332.
- Rhode, W.S., Geisler, C.D., Kennedy, D.T. 1978. Auditory nerve fiber response to wideband noise and tone combinations. *J Neurophysiol* 41, 692–704.
- Rhode, W.S., Oertel, D., Smith, P.H. 1983a. Physiological response properties of cells labeled intracellularly with horseradish peroxidase in cat ventral cochlear nucleus. *J Comp Neurol* 213, 448–463.
- Rhode, W.S., Smith, P.H., Oertel, D. 1983b. Physiological response properties of cells labeled intracellularly with horseradish peroxidase in cat dorsal cochlear nucleus. *J Comp Neurol* 213, 426–447.
- Ricci, A.J., Wu, Y.C., Fettiplace, R. 1998. The endogenous calcium buffer and the time course of transducer adaptation in auditory hair cells. *J Neurosci* 18, 8261–8277.
- Ricci, A.J., Crawford, A.C., Fettiplace, R. 2000. Active hair bundle motion linked to fast transducer adaptation in auditory hair cells. *J Neurosci* 20, 7131–7142.
- Ricci, A.J., Crawford, A.C., Fettiplace, R. 2003. Tonotopic variation in the conductance of the hair cell mechanotransducer channel. *Neuron* 40, 983–990.
- Ricci, A.J., Kennedy, H.J., Crawford, A.C., Fettiplace, R. 2005. The transduction channel filter in auditory hair cells. *J Neurosci* 25, 7831–7839.
- Rice, J.J., May, B.J., Spirou, G.A., Young, E.D. 1992. Pinna-based spectral cues for sound localization in cat. *Hear Res* 58, 132–152.
- Richardson, B.D., Brozoski, T.J., Ling, L.L., Caspary, D.M. 2012. Targeting inhibitory neurotransmission in tinnitus. *Brain Res. In Press*.
- Richardson, F.M., Price, C.J. 2009. Structural MRI studies of language function in the undamaged brain. *Brain Struct Funct* 213, 511–523.
- Richardson, G.P., de Monvel, J.B., Petit, C. 2011. How the genetics of deafness illuminates auditory physiology. *Annu Rev Physiol* 73, 311–334.
- Richardson, R.T., Wise, A.K., Thompson, B.C., et al. 2009. Polypyrrole-coated electrodes for the delivery of charge and neurotrophins to cochlear neurons. *Biomaterials* 30, 2614–2624.

- Riquelme, R., Saldana, E., Osen, K.K., Ottersen, O.P., Merchan, M.A. 2001. Colocalization of GABA and glycine in the ventral nucleus of the lateral lemniscus in rat: an *in situ* hybridization and semiquantitative immunocytochemical study. *J Comp Neurol* 432, 409–424.
- Rivier, F., Clarke, S. 1997. Cytochrome oxidase, acetylcholinesterase, and NADPHdiaphorase staining in human supratemporal and insular cortex: evidence for multiple auditory areas. *Neuroimage* 6, 288–304.
- Robertson, D. 1984. Horseradish peroxidase injection of physiologically characterized afferent and efferent neurones in the guinea pig spiral ganglion. *Hear Res* 15, 113–121.
- Robertson, D. 2009. Centrifugal control in mammalian hearing. *Clin Exp Pharmacol Physiol* 36, 603–611.
- Robertson, D., Gummer, M. 1985. Physiological and morphological characterization of efferent neurones in the guinea pig cochlea. *Hear Res* 20, 63–77.
- Robertson, D., Johnstone, B.M. 1979. Aberrant tonotopic organization in the inner ear damaged by kanamycin. *J Acoust Soc Am* 66, 466–469.
- Robertson, D., Anderson, C.J., Cole, K.S. 1987. Segregation of efferent projections to different turns of the guinea pig cochlea. *Hear Res* 25, 69–76.
- Robertson, D., Sellick, P.M., Patuzzi, R. 1999. The continuing search for outer hair cell afferents in the guinea pig spiral ganglion. *Hear Res* 136, 151–158.
- Robles, L., Ruggero, M.A. 2001. Mechanics of the mammalian cochlea. *Physiol Rev* 81, 1305–1352.
- Robles, L., Ruggero, M.A., Rich, N.C. 1997. Two-tone distortion on the basilar membrane of the chinchilla cochlea. *J Neurophysiol* 77, 2385–2399.
- Rogalsky, C., Rong, F., Saberi, K., Hickok, G. 2011. Functional anatomy of language and music perception: temporal and structural factors investigated using functional magnetic resonance imaging. *J Neurosci* 31, 3843–3852.
- Röhl, M., Uppenkamp, S. 2012. Neural coding of sound intensity and loudness in the human auditory system. *J Assoc Res Otolaryngol* 13, 369–379.
- Rose, J.E. 1949. The cellular structure of the auditory region of the cat. *J Comp Neurol* 91, 409–439.
- Rose, J.E., Hind, J.E., Anderson, D.J., Brugge, J.F. 1971. Some effects of stimulus intensity on response of auditory nerve fibers in the squirrel monkey. *J Neurophysiol* 34, 685–699.
- Rosen, S., Baker, R.J., Darling, A. 1998. Auditory filter nonlinearity at 2 kHz in normal hearing listeners. *J Acoust Soc Am* 103, 2539–2550.
- Rosowski, J.J. 1991. The effects of external- and middle-ear filtering on auditory threshold and noise-induced hearing loss. *J Acoust Soc Am* 90, 124–135.
- Rosowski, J.J. 1994. Outer and middle ears. In: Fay, R.R., Popper, A.N. (Eds), *Comparative Hearing: Mammals*, Springer Handbook of Auditory Research Vol. 4. Springer, New York. pp. 172–247.
- Ross, K.C., Coleman, J.R. 2000. Developmental and genetic audiogenic seizure models: behavior and biological substrates. *Neurosci Biobehav Rev* 24, 639–653.
- Rouiller, E., de Ribaupierre, V., de Ribaupierre, F. 1979. Phase-locked responses to low frequency tones in the medial geniculate body. *Hear Res* 1, 213–226.
- Ruel, J., Chen, C., Pujol, R., Bobbin, R.P., Puel, J.L. 1999. AMPA-preferring glutamate receptors in cochlear physiology of adult guinea-pig. *J Physiol* 518, 667–680.
- Ruel, J., Wang, J., Dememes, D., Gobaille, S., Puel, J.L., Rebillard, G. 2006. Dopamine transporter is essential for the maintenance of spontaneous activity of auditory nerve neurones and their responsiveness to sound stimulation. *J Neurochem* 97, 190–200.

- Ruggero, M.A. 1992. Physiology and coding of sound in the auditory nerve. In: Popper, A.N., Fay, R.R. (Eds), *The Mammalian Auditory Pathway: Neurophysiology*, Springer Handbook of Auditory Research Vol. 2. Springer, New York. pp. 34–93.
- Ruggero, M.A., Rich, N.C. 1987. Timing of spike initiation in cochlear afferents: dependence on site of innervation. *J Neurophysiol* 58, 379–403.
- Ruggero, M.A., Rich, N.C. 1991a. Application of a commercially-manufactured Dopplershift laser velocimeter to the measurement of basilar-membrane vibration. *Hear Res* 51, 215–230.
- Ruggero, M.A., Rich, N.C. 1991b. Furosemide alters organ of Corti mechanics: evidence for feedback of outer hair cells upon the basilar membrane. *J Neurosci* 11, 1057–1067.
- Ruggero, M.A., Temchin, A.N. 2002. The roles of the external, middle, and inner ears in determining the bandwidth of hearing. *Proc Natl Acad Sci USA* 99, 13206–13210.
- Ruggero, M.A., Santi, P.A., Rich, N.C. 1982. Type II cochlear ganglion cells in the chinchilla. *Hear Res* 8, 339–356.
- Ruggero, M.A., Rich, N.C., Robles, L., Shivapuja, B.G. 1990. Middle-ear response in the chinchilla and its relationship to mechanics at the base of the cochlea. *J Acoust Soc Am* 87, 1612–1629.
- Ruggero, M.A., Rich, N.C., Recio, A., Narayan, S.S., Robles, L. 1997. Basilar-membrane responses to tones at the base of the chinchilla cochlea. *J Acoust Soc Am* 101, 2151–2163.
- Ruggero, M.A., Narayan, S.S., Temchin, A.N., Recio, A. 2000. Mechanical bases of frequency tuning and neural excitation at the base of the cochlea: comparison of basilar-membrane vibrations and auditory-nerve-fiber responses in chinchilla. *Proc Natl Acad Sci USA* 97, 11744–11750.
- Russell, I.J. 1983. Origin of the receptor potential in inner hair cells of the mammalian cochlea – evidence for Davis' theory. *Nature* 301, 334–336.
- Russell, I.J., Kössl, M. 1991. The voltage responses of hair cells in the basal turn of the guinea-pig cochlea. *J Physiol* 435, 493–511.
- Russell, I.J., Murugasu, E. 1997. Medial efferent inhibition suppresses basilar membrane responses to near characteristic frequency tones of moderate to high intensities. *J Acoust Soc Am* 102, 1734–1738.
- Russell, I.J., Nilsen, K.E. 1997. The location of the cochlear amplifier: spatial representation of a single tone on the guinea pig basilar membrane. *Proc Natl Acad Sci USA* 94, 2660–2664.
- Russell, I.J., Sellick, P.M. 1978. Intracellular studies of hair cells in the mammalian cochlea. *J Physiol* 284, 261–290.
- Russell, I.J., Sellick, P.M. 1983. Low-frequency characteristics of intracellularly recorded receptor potentials in guinea-pig cochlear hair cells. *J Physiol* 338, 179–206.
- Russell, I.J., Richardson, G.P., Cody, A.R. 1986a. Mechanosensitivity of mammalian auditory hair cells in vitro. *Nature* 321, 517–519.
- Russell, I.J., Cody, A.R., Richardson, G.P. 1986b. The responses of inner and outer hair cells in the basal turn of the guinea-pig cochlea and in the mouse cochlea grown in vitro. *Hear Res* 22, 199–216.
- Rzadzinska, A.K., Schneider, M.E., Davies, C., Riordan, G.P., Kachar, B. 2004. An actin molecular treadmill and myosins maintain stereocilia functional architecture and self-renewal. *J Cell Biol* 164, 887–897.
- Rzadzinska, A., Schneider, M., Noben-Trauth, K., Bartles, J.R., Kachar, B. 2005. Balanced levels of espin are critical for stereociliary growth and length maintenance. *Cell Motil Cytoskeleton* 62, 157–165.

- Sachs, M.B., Kiang, N.Y. 1968. Two-tone inhibition in auditory-nerve fibers. *J Acoust Soc Am* 43, 1120–1128.
- Sachs, M.B., Young, E.D. 1979. Encoding of steady-state vowels in the auditory nerve: representation in terms of discharge rate. *J Acoust Soc Am* 66, 470–479.
- Sage, C., Huang, M., Vollrath, M.A., *et al.* 2006. Essential role of retinoblastoma protein in mammalian hair cell development and hearing. *Proc Natl Acad Sci USA* 103, 7345–7350.
- Sakaguchi, H., Tokita, J., Naoz, M., Bowen-Pope, D., Gov, N.S., Kachar, B. 2008. Dynamic compartmentalization of protein tyrosine phosphatase receptor Q at the proximal end of stereocilia: implication of myosin VI-based transport. *Cell Motil Cytoskeleton* 65, 528–538.
- Salt, A.N., Plontke, S.K. 2010. Endolymphatic hydrops: pathophysiology and experimental models. *Otolaryngol Clin North Am* 43, 971–983.
- Salt, A.N., Melichar, I., Thalmann, R. 1987. Mechanisms of endocochlear potential generation by stria vascularis. *Laryngoscope* 97, 984–991.
- Samson, F.K., Barone, P., Irons, W.A., Clarey, J.C., Poirier, P., Imig, T.J. 2000. Directionality derived from differential sensitivity to monaural and binaural cues in the cat's medial geniculate body. *J Neurophysiol* 84, 1330–1345.
- Santi, P.A., Anderson, C.B. 1987. A newly identified surface coat on cochlear hair cells. *Hear Res* 27, 47–65.
- Santi, P.A., Mancini, P. 2005. Cochlear anatomy and central auditory pathways. In: Cummings, C.W., Haughey, B.H., Thomas, J.R., *et al.* (Eds), *Cummings: Otolaryngology, Head and Neck Surgery*, Vol. 4, Part 14. Elsevier, Philadelphia. pp. 3373–3401.
- Santos-Sacchi, J. 1993. Harmonics of outer hair cell motility. *Biophys J* 65, 2217–2227.
- Santos-Sacchi, J., Kakehata, S., Takahashi, S. 1998. Effects of membrane potential on the voltage dependence of motility-related charge in outer hair cells of the guinea-pig. *J Physiol* 510(Pt 1), 225–235.
- Santos-Sacchi, J., Song, L., Zheng, J., Nuttall, A.L. 2006. Control of mammalian cochlear amplification by chloride anions. *J Neurosci* 26, 3992–3998.
- Saunders, J.C., Bock, G.R., James, R., Chen, C.S. 1972. Effects of priming for audiogenic seizure on auditory evoked responses in the cochlear nucleus and inferior colliculus of BALB-c mice. *Exp Neurol* 37, 388–394.
- Saur, D., Hartwigsen, G. 2012. Neurobiology of language recovery after stroke: lessons from neuroimaging studies. *Arch Phys Med Rehabil* 93, S15–S25.
- Savage, J., Waddell, A. 2012. Feb 3, 2012. pii: 0506. *Tinnitus. Clin Evid (Online)* 2012. <http://www.clinicalevidence.bmjjournals.org/x/systematic-review/0506/archive/02/2012.html>
- Sayles, M., Winter, I.M. 2010. Equivalent-rectangular bandwidth of single units in the anaesthetized guinea-pig ventral cochlear nucleus. *Hear Res* 262, 26–33.
- Scharf, B., Magnan, J., Chays, A. 1997. On the role of the olivocochlear bundle in hearing: 16 case studies. *Hear Res* 103, 101–122.
- Scheibel, M.E., Scheibel, A.B. 1974. Neuropil organization in the superior olive of the cat. *Exp Neurol* 43, 339–348.
- Scheich, H., Brechmann, A., Brosch, M., Budinger, E., Ohl, F.W. 2007. The cognitive auditory cortex: task-specificity of stimulus representations. *Hear Res* 229, 213–224.
- Schirmer, A., Kotz, S.A. 2006. Beyond the right hemisphere: brain mechanisms mediating vocal emotional processing. *Trends Cogn Sci* 10, 24–30.

- Schneider, M.E., Dose, A.C., Salles, F.T., *et al.* 2006. A new compartment at stereocilia tips defined by spatial and temporal patterns of myosin IIIa expression. *J Neurosci* 26, 10243–10252.
- Schnupp, J., Nelken, I., King, A. 2011. Auditory neuroscience: making sense of sound. MIT Press, Cambridge, MA.
- Schofield, B.R., Cant, N.B. 1999. Descending auditory pathways: projections from the inferior colliculus contact superior olivary cells that project bilaterally to the cochlear nuclei. *J Comp Neurol* 409, 210–223.
- Schofield, B.R., Coomes, D.L. 2005. Projections from auditory cortex contact cells in the cochlear nucleus that project to the inferior colliculus. *Hear Res* 206, 3–11.
- Schreiner, C.E., Cynader, M.S. 1984. Basic functional organization of second auditory cortical field (AII) of the cat. *J Neurophysiol* 51, 1284–1305.
- Schreiner, C.E., Langner, G. 1988. Periodicity coding in the inferior colliculus of the cat. II. Topographical organization. *J Neurophysiol* 60, 1823–1840.
- Schreiner, C.E., Langner, G. 1997. Laminar fine structure of frequency organization in auditory midbrain. *Nature* 388, 383–386.
- Schreiner, C.E., Read, H.L., Sutter, M.L. 2000. Modular organization of frequency integration in primary auditory cortex. *Annu Rev Neurosci* 23, 501–529.
- Schuknecht, H.F. 1960. Neuroanatomical correlates of auditory sensitivity and pitch discrimination in the cat. In: Rasmussen, G.L., Windle, W.F. (Eds), *Neural Mechanisms of the Auditory and Vestibular Systems* (pp. 76–90). Thomas, Springfield.
- Schuknecht, H.F., Gacek, M.R. 1993. Cochlear pathology in presbycusis. *Ann Otol Rhinol Laryngol* 102, 1–16.
- Schwander, M., Kachar, B., Muller, U. 2010. Review series: the cell biology of hearing. *J Cell Biol* 190, 9–20.
- Schwartz, I.R. 1992. The superior olive and lateral lemniscal nuclei. In: Webster, D.B., Popper, A.R., Fay, R.R. (Eds), *The Mammalian Auditory Pathway: Neuroanatomy*, Springer Handbook of Auditory Research Vol. 1. Springer, New York. pp. 117–167.
- Sedlacek, M., Tipton, P.W., Brenowitz, S.D. 2011. Sustained firing of cartwheel cells in the dorsal cochlear nucleus evokes endocannabinoid release and retrograde suppression of parallel fiber synapses. *J Neurosci* 31, 15807–15817.
- Seidman, M.D., Ahmad, N., Joshi, D., Seidman, J., Thawani, S., Quirk, W.S. 2004. Age-related hearing loss and its association with reactive oxygen species and mitochondrial DNA damage. *Acta Otolaryngol Suppl* 552, 16–24.
- Seldon, H.L. 1981. Structure of human auditory cortex. I. Cytoarchitectonics and dendritic distributions. *Brain Res* 229, 277–294.
- Sellick, P.M., Russell, I.J. 1979. Two-tone suppression in cochlear hair cells. *Hearing Res* 1, 227–236.
- Sellick, P.M., Russell, I.J. 1980. The responses of inner hair cells to basilar membrane velocity during low frequency auditory stimulation in the guinea pig cochlea. *Hear Res* 2, 439–445.
- Sellick, P.M., Patuzzi, R., Johnstone, B.M. 1982. Measurement of basilar membrane motion in the guinea pig using the Mössbauer technique. *J Acoust Soc Am* 72, 131–141.
- Seluakumaran, K., Mulders, W.H., Robertson, D. 2008. Unmasking effects of olivocochlear efferent activation on responses of inferior colliculus neurons. *Hear Res* 243, 35–46.
- Semple, M.N., Aitkin, L.M. 1979. Representation of sound frequency and laterality by units in central nucleus of cat inferior colliculus. *J Neurophysiol* 42, 1626–1639.

- Semple, M.N., Kitzes, L.M. 1993a. Binaural processing of sound pressure level in cat primary auditory cortex: evidence for a representation based on absolute levels rather than interaural level differences. *J Neurophysiol* 69, 449–461.
- Semple, M.N., Kitzes, L.M. 1993b. Focal selectivity for binaural sound pressure level in cat primary auditory cortex: two-way intensity network tuning. *J Neurophysiol* 69, 462–473.
- Sha, S.H., Zajic, G., Epstein, C.J., Schacht, J. 2001a. Overexpression of copper/zinc-superoxide dismutase protects from kanamycin-induced hearing loss. *Audiol Neurotol* 6, 117–123.
- Sha, S.H., Taylor, R., Forge, A., Schacht, J. 2001b. Differential vulnerability of basal and apical hair cells is based on intrinsic susceptibility to free radicals. *Hear Res* 155, 1–8.
- Sha, S.H., Qiu, J.H., Schacht, J. 2006. Aspirin to prevent gentamicin-induced hearing loss. *N Engl J Med* 354, 1856–1857.
- Sha, S.H., Chen, F.Q., Schacht, J. 2009. Activation of cell death pathways in the inner ear of the aging CBA/J mouse. *Hear Res* 254, 92–99.
- Shackleton, T.M., Liu, L.F., Palmer, A.R. 2009. Responses to diotic, dichotic, and alternating phase harmonic stimuli in the inferior colliculus of guinea pigs. *J Assoc Res Otolaryngol* 10, 76–90.
- Shamay-Tsoory, S.G., Tomer, R., Goldsher, D., Berger, B.D., Aharon-Peretz, J. 2004. Impairment in cognitive and affective empathy in patients with brain lesions: anatomical and cognitive correlates. *J Clin Exp Neuropsychol* 26, 1113–1127.
- Shamma, S.A. 1985a. Speech processing in the auditory system. I: The representation of speech sounds in the responses of the auditory nerve. *J Acoust Soc Am* 78, 1612–1621.
- Shamma, S.A. 1985b. Speech processing in the auditory system. II: lateral inhibition and the central processing of speech evoked activity in the auditory nerve. *J Acoust Soc Am* 78, 1622–1632.
- Sharma, J., Angelucci, A., Sur, M. 2000. Induction of visual orientation modules in auditory cortex. *Nature* 404, 841–847.
- Shaw, E.A.G. 1974. The external ear. In: Keidel, W.D., Neff, W.D. (Eds), *Handbook of Sensory Physiology Vol. 5/1*. Springer, Berlin. pp. 455–490.
- Shepherd, R.K., Javel, E. 1997. Electrical stimulation of the auditory nerve. I. Correlation of physiological responses with cochlear status. *Hear Res* 108, 112–144.
- Shepherd, R.K., Hatsushika, S., Clark, G.M. 1993. Electrical stimulation of the auditory nerve: the effect of electrode position on neural excitation. *Hear Res* 66, 108–120.
- Shepherd, R.K., Roberts, L.A., Paolini, A.G. 2004. Long-term sensorineural hearing loss induces functional changes in the rat auditory nerve. *Eur J Neurosci* 20, 3131–3140.
- Shera, C.A., Guinan, J.J., Jr., Oxenham, A.J. 2002. Revised estimates of human cochlear tuning from otoacoustic and behavioral measurements. *Proc Natl Acad Sci USA* 99, 3318–3323.
- Sherriff, F.E., Henderson, Z. 1994. Cholinergic neurons in the ventral trapezoid nucleus project to the cochlear nuclei in the rat. *Neuroscience* 58, 627–633.
- Shibata, S.B., Raphael, Y. 2010. Future approaches for inner ear protection and repair. *J Commun Disord* 43, 295–310.
- Shneiderman, A., Henkel, C.K. 1987. Banding of lateral superior olive nucleus afferents in the inferior colliculus: a possible substrate for sensory integration. *J Comp Neurol* 266, 519–534.
- Shofner, W.P., Young, E.D. 1985. Excitatory/inhibitory response types in the cochlear nucleus: relationships to discharge patterns and responses to electrical stimulation of the auditory nerve. *J Neurophysiol* 54, 917–939.

- Shore, S.E. 1998. Influence of centrifugal pathways on forward masking of ventral cochlear nucleus neurons. *J Acoust Soc Am* 104, 378–389.
- Shore, S.E., Moore, J.K. 1998. Sources of input to the cochlear granule cell region in the guinea pig. *Hear Res* 116, 33–42.
- Shore, S.E., Zhou, J. 2006. Somatosensory influence on the cochlear nucleus and beyond. *Hear Res* 216/217, 90–99.
- Shore, S.E., Helfert, R.H., Bledsoe, S.C., Jr., Altschuler, R.A., Godfrey, D.A. 1991. Descending projections to the dorsal and ventral divisions of the cochlear nucleus in guinea pig. *Hear Res* 52, 255–268.
- Sidi, S., Friedrich, R.W., Nicolson, T. 2003. NompC TRP channel required for vertebrate sensory hair cell mechanotransduction. *Science* 301, 96–99.
- Siegel, J.H., Kim, D.O. 1982. Efferent neural control of cochlear mechanics? Olivocochlear bundle stimulation affects cochlear biomechanical nonlinearity. *Hear Res* 6, 171–182.
- Siemens, J., Lillo, C., Dumont, R.A., et al. 2004. Cadherin 23 is a component of the tip link in hair-cell stereocilia. *Nature* 428, 950–955.
- Simmons, D.D., Liberman, M.C. 1988. Afferent innervation of outer hair cells in adult cats: I. Light microscopic analysis of fibers labeled with horseradish peroxidase. *J Comp Neurol* 270, 132–144.
- Simmons, F.B. 1964. Perceptual theories of middle ear muscle function. *Ann Otol Rhinol Laryngol* 73, 724–739.
- Siveke, I., Pecka, M., Seidl, A.H., Baudoux, S., Grothe, B. 2006. Binaural response properties of low-frequency neurons in the gerbil dorsal nucleus of the lateral lemniscus. *J Neurophysiol* 96, 1425–1440.
- Slama, M.C., Ravicz, M.E., Rosowski, J.J. 2010. Middle ear function and cochlear input impedance in chinchilla. *J Acoust Soc Am* 127, 1397–1410.
- Slepicky, N.B. 1996. Structure of the mammalian cochlea. In: Dallos, P., Popper, A.N., Fay, R.R. (Eds), *The Cochlea*, Springer Handbook of Auditory Research Vol. 8. Springer, New York. pp. 44–129.
- Smith, E.H. 2011. Temporal processing in the auditory core: transformation or segregation? *J Neurophysiol* 106, 2791–2793.
- Smith, P.H., Populin, L.C. 2001. Fundamental differences between the thalamocortical recipient layers of the cat auditory and visual cortices. *J Comp Neurol* 436, 508–519.
- Smith, P.H., Rhode, W.S. 1987. Characterization of HRP-labeled globular bushy cells in the cat anteroventral cochlear nucleus. *J Comp Neurol* 266, 360–375.
- Smith, P.H., Rhode, W.S. 1989. Structural and functional properties distinguish two types of multipolar cells in the ventral cochlear nucleus. *J Comp Neurol* 282, 595–616.
- Smith, P.H., Spirou, G.A. 2002. From the cochlea to cortex and back. In: Oertel, D., Fay, R.R., Popper, A.N. (Eds), *Integrative Functions in the Mammalian Auditory Pathway*, Springer Handbook of Auditory Research Vol. 15. Springer, New York. pp. 6–71.
- Smith, P.H., Joris, P.X., Carney, L.H., Yin, T.C. 1991. Projections of physiologically characterized globular bushy cell axons from the cochlear nucleus of the cat. *J Comp Neurol* 304, 387–407.
- Smith, P.H., Joris, P.X., Yin, T.C. 1993. Projections of physiologically characterized spherical bushy cell axons from the cochlear nucleus of the cat: evidence for delay lines to the medial superior olive. *J Comp Neurol* 331, 245–260.
- Smith, P.H., Massie, A., Joris, P.X. 2005. Acoustic stria: anatomy of physiologically characterized cells and their axonal projection patterns. *J Comp Neurol* 482, 349–371.

- Smith, P.H., Uhlrich, D.J., Manning, K.A., Banks, M.I. 2012. Thalamocortical projections to rat auditory cortex from the ventral and dorsal divisions of the medial geniculate nucleus. *J Comp Neurol* 520, 34–51.
- Smith, R.L. 1979. Adaptation, saturation, and physiological masking in single auditory nerve fibers. *J Acoust Soc Am* 65, 166–178.
- Söllner, C., Rauch, G.J., Siemens, J., et al. 2004. Mutations in cadherin 23 affect tip links in zebrafish sensory hair cells. *Nature* 428, 955–959.
- Sotomayor, M., Corey, D.P., Schulter, K. 2005. In search of the hair-cell gating spring elastic properties of ankyrin and cadherin repeats. *Structure* 13, 669–682.
- Sotomayor, M., Weihofen, W.A., Gaudet, R., Corey, D.P. 2010. Structural determinants of cadherin-23 function in hearing and deafness. *Neuron* 66, 85–100.
- Spangler, K.M., Warr, W.B. 1991. The descending auditory system. In: Altschuler, R.A., Bobbin, R.P., Clopton, B.M., Hoffman, D.W. (Eds), *Neurobiology of Hearing: The Central Auditory System* (pp. 27–45). Raven Press, New York.
- Spangler, K.M., Cant, N.B., Henkel, C.K., Farley, G.R., Warr, W.B. 1987. Descending projections from the superior olfactory complex to the cochlear nucleus of the cat. *J Comp Neurol* 259, 452–465.
- Spicer, S.S., Schulte, B.A. 2005. Novel structures in marginal and intermediate cells presumably relate to functions of apical versus basal strial strata. *Hear Res* 200, 87–101.
- Spierer, L., Bellmann-Thiran, A., Maeder, P., Murray, M.M., Clarke, S. 2009. Hemispheric competence for auditory spatial representation. *Brain* 132, 1953–1966.
- Spierer, L., De Lucia, M., Bernasconi, F., et al. 2011. Learning-induced plasticity in human audition: objects, time, and space. *Hear Res* 271, 88–102.
- Spirou, G.A., Davis, K.A., Nelken, I., Young, E.D. 1999. Spectral integration by type II interneurons in dorsal cochlear nucleus. *J Neurophysiol* 82, 648–663.
- Spoendlin, H. 1972. Innervation densities of the cochlea. *Acta Otolaryngol* 73, 235–248.
- Spoendlin, H. 1978. The afferent innervation of the cochlea. In: Naunton, R.F., Fernandez, C. (Eds), *Evoked Electrical Activity in the Auditory Nervous System* (pp. 21–39). Academic Press, London.
- Srinivasan, G., Friauf, E., Lohrke, S. 2004. Functional glutamatergic and glycinergic inputs to several superior olivary nuclei of the rat revealed by optical imaging. *Neuroscience* 128, 617–634.
- Stach, B.A., Jerger, J.F., Jenkins, H.A. 1984. The human acoustic tensor tympani reflex. A case report. *Scand Audiol* 13, 93–99.
- Stakhovskaya, O., Sridhar, D., Bonham, B.H., Leake, P.A. 2007. Frequency map for the human cochlear spiral ganglion: implications for cochlear implants. *J Assoc Res Otolaryngol* 8, 220–233.
- Stecker, G.C., Mickey, B.J., Macpherson, E.A., Middlebrooks, J.C. 2003. Spatial sensitivity in field PAF of cat auditory cortex. *J Neurophysiol* 89, 2889–2903.
- Stecker, G.C., Harrington, I.A., Macpherson, E.A., Middlebrooks, J.C. 2005. Spatial sensitivity in the dorsal zone (area DZ) of cat auditory cortex. *J Neurophysiol* 94, 1267–1280.
- Sterkers, O., Ferrary, E., Amiel, C. 1984. Inter- and intracompartimental osmotic gradients within the rat cochlea. *Am J Physiol* 247, F602–F606.
- Stewart, L., von Kriegstein, K., Warren, J.D., Griffiths, T.D. 2006. Music and the brain: disorders of musical listening. *Brain* 129, 2533–2553.
- Stone, J.S., Cotanche, D.A. 2007. Hair cell regeneration in the avian auditory epithelium. *Int J Dev Biol* 51, 633–647.

- Suga, N. 2012. Tuning shifts of the auditory system by corticocortical and corticofugal projections and conditioning. *Neurosci Biobehav Rev* 36, 969–988.
- Suga, N., Ma, X. 2003. Multiparametric corticofugal modulation and plasticity in the auditory system. *Nat Rev Neurosci* 4, 783–794.
- Suga, N., Zhang, Y., Yan, J. 1997. Sharpening of frequency tuning by inhibition in the thalamic auditory nucleus of the mustached bat. *J Neurophysiol* 77, 2098–2114.
- Sukharev, S., Corey, D.P. 2004. Mechanosensitive channels: multiplicity of families and gating paradigms. *Sci STKE* 2004, 219, re4.
- Suta, D., Popelar, J., Syka, J. 2008. Coding of communication calls in the subcortical and cortical structures of the auditory system. *Physiol Res* 57(Suppl. 3), S149–S159.
- Sutherland, D.P., Masterton, R.B., Glendenning, K.K. 1998a. Role of acoustic striae in hearing: reflexive responses to elevated sound-sources. *Behav Brain Res* 97, 1–12.
- Sutherland, D.P., Glendenning, K.K., Masterton, R.B. 1998b. Role of acoustic striae in hearing: discrimination of sound-source elevation. *Hear Res* 120, 86–108.
- Sutter, M.L., Schreiner, C.E. 1991. Physiology and topography of neurons with multipeaked tuning curves in cat primary auditory cortex. *J Neurophysiol* 65, 1207–1226.
- Sutter, M.L., Schreiner, C.E., McLean, M., O'Connor, K.N., Loftus, W.C. 1999. Organization of inhibitory frequency receptive fields in cat primary auditory cortex. *J Neurophysiol* 82, 2358–2371.
- Sweet, R.A., Dorph-Petersen, K.A., Lewis, D.A. 2005. Mapping auditory core, lateral belt, and parabelt cortices in the human superior temporal gyrus. *J Comp Neurol* 491, 270–289.
- Tabuchi, K., Nishimura, B., Nakamagoe, M., Hayashi, K., Nakayama, M., Hara, A. 2011. Ototoxicity: mechanisms of cochlear impairment and its prevention. *Curr Med Chem* 18, 4866–4871.
- Tahera, Y., Meltsner, I., Johansson, P., Hansson, A.C., Canlon, B. 2006. Glucocorticoid receptor and nuclear factor-kappa B interactions in restraint stress-mediated protection against acoustic trauma. *Endocrinology* 147, 4430–4437.
- Talavage, T.M., Sereno, M.I., Melcher, J.R., Ledden, P.J., Rosen, B.R., Dale, A.M. 2004. Tonotopic organization in human auditory cortex revealed by progressions of frequency sensitivity. *J Neurophysiol* 91, 1282–1296.
- Taleb, M., Brandon, C.S., Lee, F.S., Harris, K.C., Dillmann, W.H., Cunningham, L.L. 2009. Hsp70 inhibits aminoglycoside-induced hearing loss and cochlear hair cell death. *Cell Stress Chaperones* 14, 427–437.
- Talwar, S.K., Musial, P.G., Gerstein, G.L. 2001. Role of mammalian auditory cortex in the perception of elementary sound properties. *J Neurophysiol* 85, 2350–2358.
- Tan, Q., Carney, L.H. 2006. Predictions of formant-frequency discrimination in noise based on model auditory-nerve responses. *J Acoust Soc Am* 120, 1435–1445.
- Tanaka, M., Yoshida, M., Emoto, H., Ishii, H. 2000. Noradrenaline systems in the hypothalamus, amygdala and locus coeruleus are involved in the provocation of anxiety: basic studies. *Eur J Pharmacol* 405, 397–406.
- Taranda, J., Maisond, S.F., Ballesteros, J.A., et al. 2009. A point mutation in the hair cell nicotinic cholinergic receptor prolongs cochlear inhibition and enhances noise protection. *PLoS Biol* 7, e18.
- Tasaki, I. 1954. Nerve impulses in individual auditory nerve fibers of guinea pig. *J Neurophysiol* 17, 97–122.
- Tasaki, I., Spyropoulos, C.S. 1959. Stria vascularis as source of endocochlear potential. *J Neurophysiol* 22, 149–155.

- Tasaki, I., Davis, H., Legouix, J.P. 1952. The space-time pattern of the cochlear microphonics (guinea pig), as recorded by differential electrodes. *J Acoust Soc Am* 24, 502–519.
- Tasaki, I., Davis, H., Eldredge, D.H. 1954. Exploration of cochlear potentials in guinea pig with a microelectrode. *J Acoust Soc Am* 26, 765–773.
- Temchin, A.N., Ruggero, M.A. 2010. Phase-locked responses to tones of chinchilla auditory nerve fibers: implications for apical cochlear mechanics. *J Assoc Res Otolaryngol* 11, 297–318.
- Temchin, A.N., Rich, N.C., Ruggero, M.A. 1997. Low-frequency suppression of auditory nerve responses to characteristic frequency tones. *Hear Res* 113, 29–56.
- Temchin, A.N., Rich, N.C., Ruggero, M.A. 2008a. Threshold tuning curves of chinchilla auditory-nerve fibers. I. Dependence on characteristic frequency and relation to the magnitudes of cochlear vibrations. *J Neurophysiol* 100, 2889–2898.
- Temchin, A.N., Rich, N.C., Ruggero, M.A. 2008b. Threshold tuning curves of chinchilla auditory nerve fibers. II. Dependence on spontaneous activity and relation to cochlear nonlinearity. *J Neurophysiol* 100, 2899–2906.
- Thierry, G., Giraud, A.L., Price, C. 2003. Hemispheric dissociation in access to the human semantic system. *Neuron* 38, 499–506.
- Thompson, A.M. 2003a. A medullary source of norepinephrine in cat cochlear nuclear complex. *Exp Brain Res* 153, 486–490.
- Thompson, A.M. 2003b. Pontine sources of norepinephrine in the cat cochlear nucleus. *J Comp Neurol* 457, 374–383.
- Thompson, G.C., Masterton, R.B. 1978. Brain stem auditory pathways involved in reflexive head orientation to sound. *J Neurophysiol* 41, 1183–1202.
- Thornton, S.K., Withington, D.J. 1996. The role of the external nucleus of the inferior colliculus in the construction of the superior collicular auditory space map in the guinea pig. *Neurosci Res* 25, 239–246.
- Tian, B., Rauschecker, J.P. 1994. Processing of frequency-modulated sounds in the cat's anterior auditory field. *J Neurophysiol* 71, 1959–1975.
- Tian, B., Rauschecker, J.P. 1998. Processing of frequency-modulated sounds in the cat's posterior auditory field. *J Neurophysiol* 79, 2629–2642.
- Tian, B., Rauschecker, J.P. 2004. Processing of frequency-modulated sounds in the lateral auditory belt cortex of the rhesus monkey. *J Neurophysiol* 92, 2993–3013.
- Tian, B., Reser, D., Durham, A., Kustov, A., Rauschecker, J.P. 2001. Functional specialization in rhesus monkey auditory cortex. *Science* 292, 290–293.
- Tilney, L.G., Derosier, D.J., Mulroy, M.J. 1980. The organization of actin filaments in the stereocilia of cochlear hair cells. *J Cell Biol* 86, 244–259.
- Tilney, L.G., Saunders, J.C., Egelman, E., DeRosier, D.J. 1982. Changes in the organization of actin filaments in the stereocilia of noise-damaged lizard cochleae. *Hear Res* 7, 181–197.
- Tollin, D.J., Yin, T.C. 2002. The coding of spatial location by single units in the lateral superior olive of the cat. II. The determinants of spatial receptive fields in azimuth. *J Neurosci* 22, 1468–1479.
- Tollin, D.J., Yin, T.C. 2005. Interaural phase and level difference sensitivity in low-frequency neurons in the lateral superior olive. *J Neurosci* 25, 10648–10657.
- Tollin, D.J., Koka, K., Tsai, J.J. 2008. Interaural level difference discrimination thresholds for single neurons in the lateral superior olive. *J Neurosci* 28, 4848–4860.
- Tolnai, S., Hernandez, O., Englitz, B., Rubsam, R., Malmierca, M.S. 2008. The medial nucleus of the trapezoid body in rat: spectral and temporal properties vary with anatomical location of the units. *Eur J Neurosci* 27, 2587–2598.

- Tong, Y.C., Blamey, P.J., Dowell, R.C., Clark, G.M. 1983. Psychophysical studies evaluating the feasibility of a speech processing strategy for a multiple-channel cochlear implant. *J Acoust Soc Am* 74, 73–80.
- Trahiotis, C., Bernstein, L.R., Stern, R.M., Buell, T.N. 2005. Interaural correlation as the basis of a working model of binaural processing: an introduction. In: Popper, A.N., Fay, R.R. (Eds), *Sound Source Localization*, Springer Handbook of Auditory Research Vol. 25. Springer, New York. pp. 238–271.
- Tramo, M.J., Cariani, P.A., Koh, C.K., Makris, N., Braida, L.D. 2005. Neurophysiology and neuroanatomy of pitch perception: auditory cortex. *Ann NY Acad Sci* 1060, 148–174.
- Tsapkini, K., Frangakis, C.E., Hillis, A.E. 2011. The function of the left anterior temporal pole: evidence from acute stroke and infarct volume. *Brain* 134, 3094–3105.
- Tsuchitani, C. 1997. Input from the medial nucleus of trapezoid body to an interaural level detector. *Hear Res* 105, 211–224.
- Tsuchitani, C., Boudreau, J.C. 1966. Single unit analysis of cat superior olive S segment with tonal stimuli. *J Neurophysiol* 29, 684–697.
- Tsuji, J., Liberman, M.C. 1997. Intracellular labeling of auditory nerve fibers in guinea pig: central and peripheral projections. *J Comp Neurol* 381, 188–202.
- Tsuprun, V., Goodyear, R.J., Richardson, G.P. 2004. The structure of tip links and kinocilial links in avian sensory hair bundles. *Biophys J* 87, 4106–4112.
- Turkeltaub, P.E., Coslett, H.B. 2010. Localization of sublexical speech perception components. *Brain Lang* 114, 1–15.
- Turner, C.W., Gantz, B.J., Karsten, S., Fowler, J., Reiss, L.A. 2010. Impact of hair cell preservation in cochlear implantation: combined electric and acoustic hearing. *Otol Neurotol* 31, 1227–1232.
- Ulehlova, L., Voldrich, L., Janisch, R. 1987. Correlative study of sensory cell density and cochlear length in humans. *Hear Res* 28, 149–151.
- Unoki, M., Irino, T., Glasberg, B., Moore, B.C., Patterson, R.D. 2006. Comparison of the roex and gammachirp filters as representations of the auditory filter. *J Acoust Soc Am* 120, 1474–1492.
- Uppenkamp, S., Johnsrude, I.S., Norris, D., Marslen-Wilson, W., Patterson, R.D. 2006. Locating the initial stages of speech-sound processing in human temporal cortex. *Neuroimage* 31, 1284–1296.
- Vachon-Presseau, E., Martin, A., Lepore, F., Guillemot, J.P. 2009. Development of the representation of auditory space in the superior colliculus of the rat. *Eur J Neurosci* 29, 652–660.
- van Bergeijk, W.A. 1962. Variation on a theme of von Békésy: a model of binaural interaction. *J Acoust Soc Am* 34, 1431–1437.
- van den Honert, C., Stypulkowski, P.H. 1984. Physiological properties of the electrically stimulated auditory nerve. II. Single fiber recordings. *Hear Res* 14, 225–243.
- van den Honert, C., Stypulkowski, P.H. 1987. Single fiber mapping of spatial excitation patterns in the electrically stimulated auditory nerve. *Hear Res* 29, 195–206.
- van der Heijden, M., Joris, P.X. 2005. The speed of auditory low-side suppression. *J Neurophysiol* 93, 201–209.
- van der Heijden, M., Louage, D.H., Joris, P.X. 2011. Responses of auditory nerve and anteroventral cochlear nucleus fibers to broadband and narrowband noise: implications for the sensitivity to interaural delays. *J Assoc Res Otolaryngol* 12, 485–502.
- van der Zwaag, W., Gentile, G., Gruetter, R., Spierer, L., Clarke, S. 2011. Where sound position influences sound object representations: a 7T fMRI study. *Neuroimage* 54, 1803–1811.

- van Dijk, P., Wit, H.P., Segenhout, J.M., Tubis, A. 1994. Wiener kernel analysis of inner ear function in the American bullfrog. *J Acoust Soc Am* 95, 904–919.
- Velenovsky, D.S., Cetas, J.S., Price, R.O., Sinex, D.G., McMullen, N.T. 2003. Functional subregions in primary auditory cortex defined by thalamocortical terminal arbor: an electrophysiological and anterograde labeling study. *J Neurosci* 23, 308–316.
- Vetter, D.E., Saldana, E., Mugnaini, E. 1993. Input from the inferior colliculus to medial olivocochlear neurons in the rat: a double label study with PHA-L and cholera toxin. *Hear Res* 70, 173–186.
- Viceic, D., Fornari, E., Thiran, J.P., et al. 2006. Human auditory belt areas specialized in sound recognition: a functional magnetic resonance imaging study. *Neuroreport* 17, 1659–1662.
- Vicente-Torres, M.A., Gil-Loyzaga, P. 2002. Age- and gender-related changes in the cochlear sympathetic system of the rat. *Neurosci Lett* 319, 177–179.
- Viergever, M.A., Diependaal, R.J. 1986. Quantitative validation of cochlear models using the Liouville-Green approximation. *Hear Res* 21, 1–15.
- Vigneau, M., Beaucousin, V., Herve, P.Y., et al. 2006. Meta-analyzing left hemisphere language areas: phonology, semantics, and sentence processing. *Neuroimage* 30, 1414–1432.
- Voigt, H.F., Young, E.D. 1980. Evidence of inhibitory interactions between neurons in dorsal cochlear nucleus. *J Neurophysiol* 44, 76–96.
- Vollrath, M.A., Kwan, K.Y., Corey, D.P. 2007. The micromachinery of mechanotransduction in hair cells. *Annu Rev Neurosci* 30, 339–365.
- von Economo, C., Koskinas, G.N. 1925. Die Cytoarchitektonik der Hirnrinde des erwachsenen Menschen. Julius Springer, Berlin.
- Voss, S.E., Shera, C.A. 2004. Simultaneous measurement of middle-ear input impedance and forward/reverse transmission in cat. *J Acoust Soc Am* 116, 2187–2198.
- Walker, K.M., Bizley, J.K., King, A.J., Schnupp, J.W. 2011. Cortical encoding of pitch: recent results and open questions. *Hear Res* 271, 74–87.
- Wallace, M.N., Palmer, A.R. 2009. Functional subdivisions in low-frequency primary auditory cortex (AI). *Exp Brain Res* 194, 395–408.
- Wallace, M.N., Johnston, P.W., Palmer, A.R. 2002a. Histochemical identification of cortical areas in the auditory region of the human brain. *Exp Brain Res* 143, 499–508.
- Wallace, M.N., Shackleton, T.M., Palmer, A.R. 2002b. Phase-locked responses to pure tones in the primary auditory cortex. *Hear Res* 172, 160–171.
- Walton, J.P. 2010. Timing is everything: temporal processing deficits in the aged auditory brainstem. *Hear Res* 264, 63–69.
- Wang, H., Brozoski, T.J., Turner, J.G., et al. 2009a. Plasticity at glycinergic synapses in dorsal cochlear nucleus of rats with behavioral evidence of tinnitus. *Neuroscience* 164, 747–759.
- Wang, H., Turner, J.G., Ling, L., Parrish, J.L., Hughes, L.F., Caspary, D.M. 2009b. Age-related changes in glycine receptor subunit composition and binding in dorsal cochlear nucleus. *Neuroscience* 160, 227–239.
- Wang, H., Brozoski, T.J., Caspary, D.M. 2011a. Inhibitory neurotransmission in animal models of tinnitus: maladaptive plasticity. *Hear Res* 279, 111–117.
- Wang, J., Caspary, D., Salvi, R.J. 2000. GABA-A antagonist causes dramatic expansion of tuning in primary auditory cortex. *Neuroreport* 11, 1137–1140.
- Wang, J., Van De Water, T.R., Bonny, C., de Ribaupierre, F., Puel, J.L., Zine, A. 2003. A peptide inhibitor of c-Jun N-terminal kinase protects against both aminoglycoside and acoustic trauma-induced auditory hair cell death and hearing loss. *J Neurosci* 23, 8596–8607.

- Wang, Q., Steyger, P.S. 2009. Trafficking of systemic fluorescent gentamicin into the cochlea and hair cells. *J Assoc Res Otolaryngol* 10, 205–219.
- Wang, W., Zhou, N., Xu, L. 2011b. Musical pitch and lexical tone perception with cochlear implants. *Int J Audiol* 50, 270–278.
- Wang, X. 2007. Neural coding strategies in auditory cortex. *Hear Res* 229, 81–93.
- Wang, Y., Raphael, Y. 1996. Re-innervation patterns of chick auditory sensory epithelium after acoustic overstimulation. *Hear Res* 97, 11–18.
- Wangemann, P. 2006. Supporting sensory transduction: cochlear fluid homeostasis and the endocochlear potential. *J Physiol* 576, 11–21.
- Wangemann, P., Schacht, J. 1996. Homeostatic mechanisms in the cochlea. In: Dallos, P., Popper, A.N., Fay, R.R. (Eds), *The Cochlea*, Springer Handbook of Auditory Research Vol. 8. Springer, New York. pp. 130–185.
- Wangemann, P., Liu, J., Marcus, D.C. 1995. Ion transport mechanisms responsible for K⁺ secretion and the transepithelial voltage across marginal cells of stria vascularis in vitro. *Hear Res* 84, 19–29.
- Wangemann, P., Itza, E.M., Albrecht, B., et al. 2004. Loss of KCNJ10 protein expression abolishes endocochlear potential and causes deafness in Pendred syndrome mouse model. *BMC Med* 2, 30 (15pp.).
- Warchol, M.E. 2010. Cellular mechanisms of aminoglycoside ototoxicity. *Curr Opin Otolaryngol Head Neck Surg* 18, 454–458.
- Warchol, M.E. 2011. Sensory regeneration in the vertebrate inner ear: differences at the levels of cells and species. *Hear Res* 273, 72–79.
- Warr, W.B. 1978. The olivocochlear bundle: its origins and terminations in the cat. In: Naunton, R.F., Fernandez, C. (Eds), *Evoked Electrical Activity in the Auditory Nervous System* (pp. 43–63). Academic Press, New York.
- Warr, W.B. 1992. Organization of cochlear efferent systems in mammals. In: Webster, D.B., Popper, A.N., Fay, R.R. (Eds), *The Mammalian Auditory Pathway: Neuroanatomy*, Springer Handbook of Auditory Research Vol. 1. Springer, New York. pp. 410–448.
- Warr, W.B., Guinan, J.J., Jr. 1979. Efferent innervation of the organ of corti: two separate systems. *Brain Res* 173, 152–155.
- Warr, W.B., Guinan, J.J., White, J.S. 1986. Organization of efferent fibers: the lateral and medial olivocochlear systems. In: Altschuler, R.A., Bobbin, R.P., Hoffman, D.W. (Eds), *Neurobiology of Hearing: The Cochlea* (pp. 333–348). Raven Press, New York.
- Warr, W.B., Boche, J.B., Neely, S.T. 1997. Efferent innervation of the inner hair cell region: origins and terminations of two lateral olivocochlear systems. *Hear Res* 108, 89–111.
- Warren, E.H., Liberman, M.C. 1989a. Effects of contralateral sound on auditory-nerve responses. I. Contributions of cochlear efferents. *Hear Res* 37, 89–104.
- Warren, E.H., Liberman, M.C. 1989b. Effects of contralateral sound on auditory-nerve responses. II. Dependence on stimulus variables. *Hear Res* 37, 105–121.
- Warren, J.D., Zielinski, B.A., Green, G.G., Rauschecker, J.P., Griffiths, T.D. 2002. Perception of sound-source motion by the human brain. *Neuron* 34, 139–148.
- Warren, J.E., Wise, R.J., Warren, J.D. 2005. Sounds do-able: auditory-motor transformations and the posterior temporal plane. *Trends Neurosci* 28, 636–643.
- Weber, T., Corbett, M.K., Chow, L.M., Valentine, M.B., Baker, S.J., Zuo, J. 2008. Rapid cell-cycle reentry and cell death after acute inactivation of the retinoblastoma gene product in postnatal cochlear hair cells. *Proc Natl Acad Sci USA* 105, 781–785.
- Weddell, T.D., Mellado-Lagarde, M., Lukashkina, V.A., Lukashkin, A.N., Zuo, J., Russell, I.J. 2011. Prestin links extrinsic tuning to neural excitation in the mammalian cochlea. *Curr Biol* 21, R682–R683.

- Weinberger, N.M. 1998. Physiological memory in primary auditory cortex: characteristics and mechanisms. *Neurobiol Learn Mem* 70, 226–251.
- Weinberger, N.M. 2004. Specific long-term memory traces in primary auditory cortex. *Nat Rev Neurosci* 5, 279–290.
- Weinberger, N.M. 2011. The medial geniculate, not the amygdala, as the root of auditory fear conditioning. *Hear Res* 274, 61–74.
- Wersinger, E., Fuchs, P.A. 2011. Modulation of hair cell efferents. *Hear Res* 279, 1–12.
- Wever, E.G. 1949. Theory of Hearing. Wiley, New York.
- Wever, E.G., Bray, C.W. 1930. Action currents in the auditory nerve in response to acoustical stimulation. *Proc Natl Acad Sci USA* 16, 344–350.
- Wever, E.G., Lawrence, M. 1954. Physiological Acoustics. Princeton University Press, Princeton.
- Wever, E.G., Vernon, J.A. 1955. The effects of the tympanic muscle reflexes upon sound transmission. *Acta Otolaryngol* 45, 433–439.
- White, P.M., Doetzlhofer, A., Lee, Y.S., Groves, A.K., Segil, N. 2006. Mammalian cochlear supporting cells can divide and trans-differentiate into hair cells. *Nature* 441, 984–987.
- Wiederhold, M.L. 1970. Variations in the effects of electric stimulation of the crossed olivocochlear bundle on cat single auditory-nerve-fiber responses to tone bursts. *J Acoust Soc Am* 48, 966–977.
- Wiegrebé, L., Winter, I.M. 2001. Temporal representation of iterated rippled noise as a function of delay and sound level in the ventral cochlear nucleus. *J Neurophysiol* 85, 1206–1219.
- Wiener, F.M., Ross, D.A. 1946. The pressure distribution in the auditory canal in a progressive sound field. *J Acoust Soc Am* 18, 401–408.
- Wilson, J.P. 1980. Evidence for a cochlear origin for acoustic re-emissions, threshold fine-structure and tonal tinnitus. *Hear Res* 2, 233–252.
- Winer, J.A. 1985. The medial geniculate body of the cat. *Adv Anat Embryol Cell Biol* 86, 1–97.
- Winer, J.A. 1992. The functional architecture of the medial geniculate body and the primary auditory cortex. In: Webster, D.B., Popper, A.N., Fay, R.R. (Eds), *The Mammalian Auditory Pathway: Neuroanatomy*, Springer Handbook of Auditory Research Vol. 1. Springer, New York. pp. 222–409.
- Winer, J.A. 2006. Decoding the auditory corticofugal systems. *Hear Res* 212, 1–8.
- Winer, J.A., Saint Marie, R.L., Larue, D.T., Oliver, D.L. 1996. GABAergic feedforward projections from the inferior colliculus to the medial geniculate body. *Proc Natl Acad Sci USA* 93, 8005–8010.
- Winer, J.A., Diehl, J.J., Larue, D.T. 2001. Projections of auditory cortex to the medial geniculate body of the cat. *J Comp Neurol* 430, 27–55.
- Winer, J.A., Miller, L.M., Lee, C.C., Schreiner, C.E. 2005. Auditory thalamocortical transformation: structure and function. *Trends Neurosci* 28, 255–263.
- Winslow, R.L., Sachs, M.B. 1987. Effect of electrical stimulation of the crossed olivocochlear bundle on auditory nerve response to tones in noise. *J Neurophysiol* 57, 1002–1021.
- Winter, I.M., Palmer, A.R. 1990. Responses of single units in the anteroventral cochlear nucleus of the guinea pig. *Hear Res* 44, 161–178.
- Wise, R.J., Scott, S.K., Blank, S.C., Mummery, C.J., Murphy, K., Warburton, E.A. 2001. Separate neural subsystems within ‘Wernicke’s area’. *Brain* 124, 83–95.
- Woods, D.L., Alain, C. 2009. Functional imaging of human auditory cortex. *Curr Opin Otolaryngol Head Neck Surg* 17, 407–411.

- Woods, T.M., Lopez, S.E., Long, J.H., Rahman, J.E., Recanzone, G.H. 2006. Effects of stimulus azimuth and intensity on the single-neuron activity in the auditory cortex of the alert macaque monkey. *J Neurophysiol* 96, 3323–3337.
- Woolley, S.M., Wissman, A.M., Rubel, E.W. 2001. Hair cell regeneration and recovery of auditory thresholds following aminoglycoside ototoxicity in Bengalese finches. *Hear Res* 153, 181–195.
- Wu, S.H., Kelly, J.B. 1992. Synaptic pharmacology of the superior olivary complex studied in mouse brain slice. *J Neurosci* 12, 3084–3097.
- Wu, S.H., Ma, C.L., Kelly, J.B. 2004. Contribution of AMPA, NMDA, and GABA(A) receptors to temporal pattern of postsynaptic responses in the inferior colliculus of the rat. *J Neurosci* 24, 4625–4634.
- Wu, Y.C., Ricci, A.J., Fettiplace, R. 1999. Two components of transducer adaptation in auditory hair cells. *J Neurophysiol* 82, 2171–2181.
- Xiao, Z., Suga, N. 2002. Modulation of cochlear hair cells by the auditory cortex in the mustached bat. *Nat Neurosci* 5, 57–63.
- Xie, J., Talaska, A.E., Schacht, J. 2011. New developments in aminoglycoside therapy and ototoxicity. *Hear Res* 281, 28–37.
- Yamamoto, N., Tanigaki, K., Tsuji, M., Yabe, D., Ito, J., Honjo, T. 2006. Inhibition of Notch/RBP-J signaling induces hair cell formation in neonate mouse cochleas. *J Mol Med (Berl)* 84, 37–45.
- Yamasoba, T., Kondo, K. 2006. Supporting cell proliferation after hair cell injury in mature guinea pig cochlea in vivo. *Cell Tissue Res* 325, 23–31.
- Yan, J., Ehret, G. 2002. Corticofugal modulation of midbrain sound processing in the house mouse. *Eur J Neurosci* 16, 119–128.
- Yates, G.K., Winter, I.M., Robertson, D. 1990. Basilar membrane nonlinearity determines auditory nerve rate-intensity functions and cochlear dynamic range. *Hear Res* 45, 203–219.
- Yeomans, J.S., Frankland, P.W. 1996. The acoustic startle reflex: neurons and connections. *Brain Res Brain Res Rev* 21, 301–314.
- Yin, T.C.T., Chan, J.C. 1990. Interaural time sensitivity in medial superior olive of cat. *J Neurophysiol* 64, 465–488.
- Yin, T.C.T., Chan, J.C., Irvine, D.R. 1986. Effects of interaural time delays of noise stimuli on low-frequency cells in the cat's inferior colliculus. I. Responses to wideband noise. *J Neurophysiol* 55, 280–300.
- Young, E.D., Brownell, W.E. 1976. Responses to tones and noise of single cells in dorsal cochlear nucleus of unanesthetized cats. *J Neurophysiol* 39, 282–300.
- Young, E.D., Davis, K.A. 2002. Circuitry and function of the dorsal cochlear nucleus. In: Oertel, D., Fay, R.R., Popper, A.N. (Eds), *Integrative Functions in the Mammalian Auditory Pathway*, Springer Handbook of Auditory Research Vol. 15. Springer, New York. pp. 160–206.
- Young, E.D., Oertel, D. 2004. Cochlear nucleus. In: Shepherd, G.M. (Ed), *The Synaptic Organization of the Brain* (5th ed, pp. 4–163). Oxford University Press, New York.
- Young, E.D., Sachs, M.B. 1979. Representation of steady-state vowels in the temporal aspects of the discharge patterns of populations of auditory-nerve fibers. *J Acoust Soc Am* 66, 1381–1403.
- Yuan, K., Shen, J.X. 2011. Columnar and layer-specific representation of spatial sensitivity in mouse primary auditory cortex. *Neuroreport* 22, 530–534.
- Yuan, K., Shih, J.Y., Winer, J.A., Schreiner, C.E. 2011. Functional networks of parvalbumin-immunoreactive neurons in cat auditory cortex. *J Neurosci* 31, 13333–13342.

- Zatorre, R.J. 2007. There's more to auditory cortex than meets the ear. *Hear Res* 229, 24–30.
- Zatorre, R.J., Belin, P. 2001. Spectral and temporal processing in human auditory cortex. *Cereb Cortex* 11, 946–953.
- Zenner, H.P., Zimmermann, U., Schmitt, U. 1985. Reversible contraction of isolated mammalian cochlear hair cells. *Hear Res* 18, 127–133.
- Zhang, D.S., Piazza, V., Perrin, B.J., et al. 2012. Multi-isotope imaging mass spectrometry reveals slow protein turnover in hair-cell stereocilia. *Nature* 481, 520–524.
- Zhang, H., Kelly, J.B. 2006. Responses of neurons in the rat's ventral nucleus of the lateral lemniscus to monaural and binaural tone bursts. *J Neurophysiol* 95, 2501–2512.
- Zhang, H., Kelly, J.B. 2010. Time dependence of binaural responses in the rat's central nucleus of the inferior colliculus. *Hear Res* 268, 271–280.
- Zhang, J., Nakamoto, K.T., Kitzes, L.M. 2004. Binaural interaction revisited in the cat primary auditory cortex. *J Neurophysiol* 91, 101–117.
- Zhang, Y., Suga, N. 1997. Corticofugal amplification of subcortical responses to single tone stimuli in the mustached bat. *J Neurophysiol* 78, 3489–3492.
- Zhang, Y., Suga, N. 2000. Modulation of responses and frequency tuning of thalamic and collicular neurons by cortical activation in mustached bats. *J Neurophysiol* 84, 325–333.
- Zhang, Y., Suga, N. 2005. Corticofugal feedback for collicular plasticity evoked by electric stimulation of the inferior colliculus. *J Neurophysiol* 94, 2676–2682.
- Zhao, L.D., Guo, W.W., Lin, C., et al. 2011. Effects of DAPT and Atoh1 overexpression on hair cell production and hair bundle orientation in cultured Organ of Corti from neonatal rats. *PLoS One* 6, e23729.
- Zheng, J., Shen, W., He, D.Z., Long, K.B., Madison, L.D., Dallos, P. 2000. Prestin is the motor protein of cochlear outer hair cells. *Nature* 405, 149–155.
- Zhou, Y., Carney, L.H., Colburn, H.S. 2005. A model for interaural time difference sensitivity in the medial superior olive: interaction of excitatory and inhibitory synaptic inputs, channel dynamics, and cellular morphology. *J Neurosci* 25, 3046–3058.
- Zwicker, E. 1970. Masking and physiological excitation as consequences of the ear's frequency selectivity. In: Plomp, R., Smoorenburg, G. (Eds), Frequency Analysis and Periodicity Detection in Hearing (pp. 376–394). Sijthoff, Leiden.
- Zwicker, E. 1974. On a psychoacoustical equivalent of tuning curves. In: Zwicker, E., Terhardt, E. (Eds), Facts and Models in Hearing (pp. 132–141). Springer, Berlin.
- Zwicker, E., Flottorp, G., Stevens, S.S. 1957. Critical band-width in loudness summation. *J Acoust Soc Am* 29, 548–557.
- Zwislocki, J.J. 1965. Analysis of some auditory characteristics. In: Luce, R., Bush, R., Galanter, E. (Eds), Handbook of Mathematical Psychology Vol. 3. Wiley, New York. pp. 1–97.
- Zwislocki, J.J. 1980. Theory of cochlear mechanics. *Hear Res* 2, 171–182.

INDEX

Page numbers shown in **bold** indicate the most important coverage of the subject.

- α -actinin, 104
- Absolute threshold, and
- auditory nerve threshold, 78, 268
 - cochlear efficiency, 268
 - cortex, role of, 235, 238
 - outer/middle ear effect on, 268
 - sensorineural loss, 329–33, 336, 346–7
- Acetylcholine as transmitter of
- centrifugal fibres to cochlear nucleus, 259
 - olivocochlear bundle, 245–8, 251, 254
- Acetylcholinesterase (in cortex), 212, 216, 218
- Acoustic ohms, 5, 17, 18
- Acoustic (middle-ear muscle) reflex, 23, 203–4
- and discrimination at high intensity, 23, 289
- Acoustic striae
- dorsal, 157, 159, 169, 173, 299
 - intermediate, 157, 159, 163, 173, 299
 - ventral (ventral stream, trapezoid body), 159–61, 173–84
 - and sound localization, 173–84, 293–8
- Acoustic trauma, *see also* sensorineural hearing loss
- 4 kHz notch, 332
 - auditory nerve
 - excitotoxicity, 255, 325
 - synapses, 325
 - thresholds, 329–32
 - tuning, 329–31
- hair cell effects, 324–6
- stereocilia, 102, 324–5
- half-octave shift, 332
- loudness recruitment, 333
- middle ear muscles, 23
- olivocochlear protection, 253–5
- ‘toughening’ (‘conditioning’, protection), 350–1
- Actin
- in cuticular plate, 31, 104
 - in stereocilia, 30, 102–4, 108–9, 121, 123
- Action potential of cochlea, *see* N₁, N₂ potentials
- Active mechanical amplifier (cochlea),
- see also* travelling wave, 44–45, **50–2, 123–7**
- mechanisms of amplification, 51–2, 131–5
- models, 125–7
- needed theoretically?, 124–5
- noise advantage, 126–7
- nonlinearity, 51, 142–50
- olivocochlear effects, 128–31, 150, 248–51
- outer hair cells, role of, 50, 51–2, **128–37**
- and cochlear microphonic, 134–5
- Adaptation of hair cells, 122–3
- and active amplification, 135
 - Ca²⁺ effects, 122–3, 135
- fast, 122–3
- and hair cell motility, 135
- slow, 123, 145
- Adrenergic innervation of cochlea, 35

- Ageing, 319–20, 328–9, *see also*
 sensorineural hearing loss
- Aminoglycoside antibiotics, **320–3**, *see also*
 sensorineural hearing loss
- Antioxidant protection, 321
- Effects on hair cells, 321–2
- Effect on travelling wave, 128–9
- Mechanisms of ototoxicity, 320–2
- Nomenclature, 320
- Amplitude modulation
- cochlear nucleus, 171–2
 - inferior colliculus, 194, 195
 - cortex, 307
- Amplitude response (intensity functions):
- definition, 43
 - of auditory nerve fibres, 79–81
 - of cochlear partition, 43–4, 143–5
 - of hair cells, 62
- Amygdala, and auditory learning, 198, 203
- Anaesthesia, effect on responses, 164, 221–2
- Antioxidants, 321, 322, 324, 350
- Anoxia, 54, 325
- Anteroventral cochlear nucleus, *see* cochlear nucleus
- Aphasia, 312, 313
- Apoptosis, 322, 323, 324, 325, 328, 329, 350, 351
- Arch of Corti, 27–9,
- Aspirin
- antioxidant therapy, 321, 350
 - and tinnitus, 324
- ATP, 55–6
- Atoh1, 346
- ATPase, 55–6, 123
- Atropine and
- cochlear nucleus, 260
 - inferior colliculus, 262
- Attention and
- olivocochlear bundle, 257
 - tinnitus, 336
- Audiogenic seizure, 205
- Auditory cortex, *see* cortex, auditory
- Auditory filter (psychophysical frequency filter) **268–77**
- auditory nerve correlates, 273–5
 - centrifugal effects on, 260
- defined, 269
- sensorineural hearing loss, 333–4
- simultaneous vs. nonsimultaneous masking, 272–6
- Auditory nerve, **73–100**
- 10-dB bandwidths, 79
 - activation mechanisms, 139–42
 - acoustic trauma, 253–4, 330–2
 - adaptation, 75–6, 94–5
 - anatomy, 27, 33–5, 73–4, 142
 - and cochlear nucleus, 158
 - critical band correlates, 273–6
 - dynamic range, 80, 87–9, 283–9, 303–6
 - frequency-threshold curves, 42, **75–6**
 - frequency resolution
 - to broadband stimuli, 86–7
 - to tones, 75–9
 - as a function of stimulus intensity, 81, 87–9
 - in sensorineural hearing loss, 329–31 - intensity effects
 - click response, 86–7
 - firing rate, 79–81, 139–41
 - on frequency resolution, 81, 87–9
 - and loudness, 290–2
 - olivocochlear influence on, 249–50, 257 - masking, 93–5
 - N₁, N₂ potentials (CAP), 68–9
 - neurotransmitters
 - output, 158
 - input, 141–2 - numbers, 73
 - olivocochlear effects on, 128–9, 249–51, 255–7
 - phase of activation
 - to clicks, 84–5
 - to tones, 81–3, **139–41** - phase-locking, **81–3**, 85, 86–9, 97, **139–41**, 280, 282, 303–4
 - frequency limit, 83
- Q₁₀, Q₁₀ dB, 79, 276
- Rate-intensity functions, 79–80
- notches in, 139–41

- recording method, 74
response to
 f_2-f_1 , 98, 150, 249
 $2f_1-f_2$, 96–8, 148–9, 249
 clicks, 83–5
 complex stimuli, 86–7, 89–98
 combination tones, 96–8
 cubic distortion tone, 97–8,
 148–9
 electrical stimulation, 338–40
 noise bands, 86–7, 95
 speech sounds, 303–6
 tones, 75–83, 139–41
reverse correlation technique, 86–97
and sensorineural hearing loss
 intensity functions, 333
 nerve survival, 338
 threshold, 129–30
 tuning, 128–9, 329–31
sloping saturation, 80, 285
speech coding
 consonants, 306
 intensity effects, 303–5
 temporal cues, 305–6
 vowels, 303–5
spiral ganglion, 26–7, 33–5, 73–4, 338,
 341, 349
spontaneous activity, 74, 75–6, 78, 80,
 141–2
 and best threshold, 76–8, 141–2
 and inner hair cell damage, 332
 and tinnitus, 335
'straight' saturation functions, 80, 285
suppression (two-tone), **89–93**, 93–5,
 145–7
 frequency relations, 91–3
 high stimulus intensity, effects on
 response at, 285–7, 303
 latency, 90
 mechanism, 92, 145–7
 olivocochlear bundle, no effect on,
 90
 psychophysical correlates, 272–3,
 274–6
 spontaneous activity, no effect, 89
 temporal relations, 81–5
thresholds (best), 76–8
 and psychophysical absolute
 threshold, 268
 and spontaneous activity, 76–8, 142
two-tone suppression *see* suppression
 (two-tone)
tuning curves, 75–7
type I fibres, 33–4, 73–4
type II fibres, 33–4, 73–4
 responses, 74, 145
velocity responses, 138, 139, 147
waveforms, 75
Wiener kernel analysis, 87, 88, 89
Auditory object, 156, 187, 239, 278
Auditory reflexes *see* reflexes
Audiogenic seizures, 205
Azimuth (horizontal direction) of sound
 sources, 13–5, **293–8**
- Bandwidths (10 dB), *see* frequency-
 threshold curve, frequency resolution
 for main entries, *see also* Q₁₀ dB, critical
 bands, names of specific structures
auditory nerve, 79, 81, 88
comparison in different stages in system,
 201–2, **276–7**
definition, 79
BAPTA, effect on mechanotransduction, 115
Basal body (in hair cells), 31
Basal cells (of stria vascularis), 54–6
Basilar membrane
 general anatomy, 25–9
 length, 25
 mechanics, *see* travelling wave for main entry
 admittance, impedance, 47–9,
 124–5, 130
 resting position, 65, 145
 stiffness, 47–9, 124–5
Basilar (basal) tunnel fibres, 34
Battery theory (hair cell), 52, 57–8, 111,
 134–5
Bats, 194, 201–202, 221, 230, 231, 237
Belt (extra-lemniscal system),
 auditory system (in general), 157, 164,
 187, 196, 199, 202, 261
 cortex, *see* cortex belt system

- Binaural masking level difference (BMLD), 299–301
- Binaural responses, *see also* sound localization, and names of individual nuclei
in auditory cortex, 221, 222, 225, 228–33
dorsal nucleus of the lateral lemniscus, 186, 298
inferior colliculus, 191–3, 294–9
lateral superior olive, 173–80, 297, 301
medial geniculate body, 200, 202
medial superior olive, 174, 178, 182–4, 295, 297, 299
- Bionic ear, *see* cochlear prosthesis
- Bird hair cells, 344, 346, 347, 349, 351
- Blood flow (cortical), 215, 309
- Blood vessels of cochlea, 28, 35, 54
innervation, 35
- Boettcher cells, 27
- Boltzmann's law (and mechanotransduction), 118, 120, 144
- Bone vibration, and middle ear bones, 15
- Brainstem, *see also* names of individual nuclei, 155–97
main ascending pathways, 175
reflexes, 203–5
- Broca's area, 312
- Brodmann's areas, 216–7, 310, 311, 312
- Build-up responses, 164, 165
- Bulla, 21, 23
- Bushy cells (spherical, globular), 159–61, 162, 169, 170–171, 176, 180, 181, 185
projections to superior olive, 160, 161, 166, 175–6, 178, 180, 181
timing in, 160–1, 170
- Ca^{2+}
and adaptation of mechanotransduction, 122–3
and motility of hair cells, 52, 135
needed for transduction, 115
- and neurotransmitter release at inner hair cells, 142
- permeance through mechanotransducer channel, 113–4, 117
- Cadherin 108–9, 116, 121, 327
- Calbindin, 104
- Calcitonin gene-related peptide (CGRP), 246, 251
- Calmodulin, 104
- Calpains, 323
- CAP (cochlear action potential) *see* N_1 , N_2 potentials
- Caspases, 323
- Categorical perception (of speech), 301–2
- Cathepsins, 323
- Celastrol, 350–1
- Cellular therapy, replacement, protection in sensorineural hearing loss, 344–51
and cell cycle, 348
gene therapy, 348
shaker-2, 348
- hair cell development, 345–6
- math-1, 346, 347
- mitosis, 328, 346, 347–8, 351
- p27^{kip1}, 348
- protection and 'toughening', 350–1
- stem cell therapy, 348–9
- supporting cells, 346–8, 349
- transdifferentiation, 346–8
- vestibular epithelium, 346, 347, 351
- viral transfer, 346, 347
- Cell death, 322, 323, 324, 325, 328, 329, 350, 351
- Centrifugal pathways
to
cochlea, *see* olivocochlear bundle
cochlear nuclei
anatomy, 244, 257–9
behavioural experiments, 260
masking, 260
neurotransmitters, 259
physiology, 259–60
- inferior colliculus
anatomy, 195, 261
function, 262

- medial geniculate body (corticofugal), 202, 213, 238, 261, 262–3
superior olive, 261–2
- Centriole (in hair cells), 31
- CGRP (calcitonin gene-related peptide), 246, 251
- Characteristic delay, 182–3, 295–6, 298, 300
- Characteristic frequency: definition, 42
auditory nerve fibres, 75–81, 83–4
cochlear travelling wave, 42–4, 126
hair cells, 62
tectorial membrane (suggested), 136, 137
- Chick hair cells *see* bird hair cells
- Choline acetyltransferase, 259
- Chopper responses
cochlear nucleus
onset, 164, 169, 171, 278, 282
sustained, 163, 169, 282, 305–6
- Cisplatin, 324
- Cisternae (of outer hair cells), 32, 248
- Claudius cells, 26
- Click responses (auditory nerve fibres), 83–5
- Cochlea, *see also* hair cells, travelling wave, names of individual structures and potentials,
active mechanical processes, 44–5, 50–2, **123–37**
anatomy (general), 25–35
cochlear action potential (CAP) *see* N₁, N₂ potentials
echo, 128–31, *see also* cochlear emissions
electrical stimulation, 337, 338–42
see cochlear prosthesis for main entry
electrophysiology (in general), 52–69
emissions, 128–31, *see* cochlear emissions
for main entry
frequency selectivity, *see* travelling wave
for main entry, 41–2, 44, 61–2, 126–7
olivocochlear effects, 128, 129, 249, 250
gross evoked potentials, *see also* cochlear microphonics, N₁ N₂ potentials, summatting potential, 66–69
innervation, 33–5, 73–4
- input impedance, 17, 18, 21
- lever action (organ of Corti), **29–30**, 126, 139
- mechanics *see* travelling wave
- micromechanics, *see* travelling wave, micromechanics
- microphonic, *see* cochlear microphonic
for main entry, 66–8
- nerve excitation, 139–42
- nonlinearity *see* nonlinearity for main entry, 42–5, 51, 59, 62–4, 95–8, **142–50**
- nucleus, *see* cochlear nucleus
- olivocochlear effects on,
see olivocochlear bundle
- organ of Corti *see also* names of structures within
anatomy, 26–33
ionic composition of fluid in, 57
potential, 57, 67, 141
- partition, *see* basilar membrane, travelling wave
- potentials, *see* names of individual potentials
- structures, *see* names of individual structures
- summatting potential, 66, 68
- travelling wave, *see* travelling wave for main entry
- Cochlear emissions, **128–37**
diagnostic tool, 130, 150
echo demonstration, 130
energy produced, 131
olivocochlear effect on, 150, 256
ototoxic effects on, 130
sensorineural hearing loss, 130, 335
spontaneous, 131, 335
- Cochlear implant, *see* cochlear prosthesis
- Cochlear microphonic, 66–68
and active mechanical process, 134–5
intensity function, 67–8
localization, 67
olivocochlear effects, 251
origin, 67
outer hair cell contribution to, 67, 138
and outer hair cell motility, 133–5

- Cochlear nerve, *see* auditory nerve
 Cochlear nucleus, **157–73**
 anaesthesia, effect of, 164, 168
 anatomy (general), 157–9
 anteroventral nucleus, **157–64**
 cell types, 158–61, 164
 inhibition in, 161, 169–70
 innervation, 158–9
 outputs, 157, 160–1, 166, 174, 176,
 180, 181
 responses, 159–61
 tonotopicity, 158
 auditory nerve inputs, 158–9
 build-up responses, 164, 165
 bushey cells (spherical, globular), 159–61,
 162, 169, 170–1, 176, 180, 181,
 185
 timing in, 160, 161, 170
 centrifugal pathways to
 anatomy, 244, 257–60
 behavioural experiments, 260
 masking, 260
 neurotransmitters, 259
 physiology, 259–60
 chopper responses,
 onset, 163, 164, 169, 171, 278
 sustained, 163, 169, 305–6
 comodulation masking release and, 278
 complex stimuli, 157, 163, 172–3
 dorsal nucleus, 158, **164–6**
 cell types, 164–6
 comodulation masking release and,
 278
 complex stimuli, 172–3
 inhibitory input, 166, 169
 excitatory areas, 167–9
 inhibitory responses, 166–70
 innervation, 158
 outputs, 164–166, 174, 204, 298–9
 responses, 164–6, 167–70, 172–3
 sound localization, 172–3, 189, 202,
 204, 298–9
 tinnitus, 336–7
 tonotopicity, 158
 dynamic range, 170, 171, 285–6,
 304–5
 fusiform cells, 164–5, 166, 169, 172–3
 globular cells, *see* bushy cells
 human, 165
 inhibition in, 164, 165, 166, **167–71**,
 172, 287–8, 305
 innervation (inputs), 158–9
 intensity effects, 168, 170, 285–97,
 304–5
 interneurones, 161, 164, 166, 169, 172
 localization, *see* sound localization
 multipolar cells, *see* cochlear nucleus
 stellate cells
 neurotransmitters, 158, 164, 166, 169,
 336
 octopus cells, 162–3, 169, 174, 185
 olivocochlear fibres to, 244, 245, 258
 onset response type, 160–1, 162
 onset chopper, 163–4, 169, 171, 278
 outputs, 157, 160, 161, 163, 164, 165,
 166, 169, 174, 185, 189–90
 pauser response type, 164–5
 posteroventral nucleus, 158–9, **162–4**
 cell types, 162–4
 innervation, 158–9
 outputs, 163–4, **166**, 174, 185
 responses, 162–3
 tonotopicity, 158
 primary-like responses, 160–1, 171
 pyramidal cells, *see also* fusiform cells,
 164–5, 166
 sound localization, 157, 158, 159–64,
 164, 170–1, **172–3**
 spectral contrast in, 171
 speech sounds, 304–5
 spherical cells, *see* globular cells
 stellate cells (T-, D-stellate), 162–4, 166,
 169, 278, 304–5
 sustained chopper, 163, 169, 304–5,
 306
 timing information, 160–1, 170–1
 Type I – V responses, 167–9, 172
 Cochlear partition, *see* basilar membrane,
 travelling wave
 Cochlear pathology, *see* sensorineural
 hearing loss, acoustic trauma
 ototoxicity

- Cochlear prosthesis, **337–44**
aims and conclusions, 337
age at implantation, 344
auditory nerve survival, 338
auditory nerve responses to stimulation, 338–42
cochlear damage, 338, 341
development of nervous system, 344
electrical stimulation parameters, 341–2
electroacoustic (hybrid) devices, 344
multiple channels, 340–2, 343, 344
intensity functions, 340, 342
perceptual findings
 frequency and pitch, 342–3
 intensity, 342
 speech, 343–5
place information, 343
residual hearing loss, 344
supplement to acoustic hearing aids, 344
telemetry, 342
 timing information, 340, 341
Colliculus, *see* inferior colliculus, superior colliculus
Columnar organization of cortex, 212–3, 219, 221, 228, 313
Combination tones, *see also* nonlinearity, **95–8, 147–50**
 auditory nerve fibre response to, 95–98
 cubic distortion tone ($2f_1-f_2$), 95–8, 147–50, 249
 difference tone (f_2-f_1), 98, 150, 249
 middle ear (absent), 22
 olivocochlear effects on, 249–51
 origin, 95–8, 147–50
 psychophysical demonstration, 96
 travelling wave response to, 148–51
Commissures of brainstem, 175
 of Probst, 186
Comodulation masking release, 277–8
Complex stimuli
 and
 auditory nerve, 89–8
 cochlear nucleus, 170, 172–2
 cortex, 223–4, 226, 227, 234, 235–9, 302–3, 307–13
 inferior colliculus, 192–4
 medial geniculate body, 200–3
 Fourier analysis of, 5–9
 General considerations, 155–7
Compound histogram, 84–5
Concha, 11–12, 14
Conditioning *see* learning
 ‘toughening’ in relation to acoustic trauma, 350–1
Conductive hearing loss, 15–16, 319
Connexins, 53, 326
Consonants, *see* speech
‘Core’
 of auditory system in general, *see* lemniscal system
 of cortex, *see* cortex, core system
Cortex, auditory,
 anatomy, *see also* cortex, ‘belt’ system; cortex, ‘core’ system
 acetylcholinesterase in, 212, 216, 218
 areas: cat, 211–14
 areas: defining, 212–4
 areas: human being, 214–19
 areas: non-human primate, 211–15
 ‘belt’ system, *see* cortex ‘belt’ system
 Broca’s area, 312
 Brodmann’s areas, 216–17, 310, 311, 312
 callosal connections, 213, 214, 221
 cells: types and organization, 212–3
 columns, 212–13, 219, 221, 228, 313
 core system, *see* cortex, auditory, ‘core’ system
 corticofugal fibres, 213, 261, 262–3
 cytochrome oxidase in, 212, 216, 218
 fMRI, 215, 217, 218, 219, 233, 237, 292, 302, 309–11
 frequency-band strips, 213, 219–21, 227, 238
 Heschl’s gyrus, 216–20, 233, 237–8, 277, 308–10, 313
 inhibitory neurotransmitters, 213
 inputs, 211–14
 iso-frequency lines, 219–20

- Cortex, auditory, anatomy (*Continued*)
 koniocortex, 212, 216–18
 layers, 212–13, 218, 227
 maps, 219–22
 organization along frequency-band strips, 219–21
 ‘parabelt’ system, **213–16**, 218, 225, 235, 238–9, 307, 310
 parakoniocortex, 217
 parvalbumin in, 212
 planum polare, 217, 233, 237
 planum temporale, 217–20, 311, 313
 projections from thalamus, 212–13
 prokoniocortex, 217
 ‘rain-shower’ formation of cells, 213
 superior temporal plane, 213–18, 308–13
 Wernicke’s area, 312
 behavioural studies
 absolute detection threshold, 235
 complex stimuli, 235–6
 frequency discrimination, 235
 sound localization, 226–7
 ‘belt’ system,
 areas (cat), 213–14
 areas (human), 218–19
 areas (non-human primate), 213–16
 definition, 213, 218
 responses, 225–6
 Broca’s area, 312
 columnar organization, 212–13, 219, 221, 228, 313
 complex sounds, 235–8, 307–12
 ‘core’ system,
 areas (cat), 213–14
 areas (human), 214–19
 areas (non-human primate), 213–16
 definition, 212, 216
 responses, 221–5, 228–33, 236
 corticofugal effects (on MGB), 202, 213, 238, 261, 262–3
 fMRI and
 complex stimuli, 237–8
 definition of areas, 218, 219–20
 sound localization, 233–4
 speech, 238, 308–12
 tonotopic responses, 215, 217–19, 220
 functions in general, 238–9
 hemispheric differences, 312–13
 Heschl’s gyrus, 216–20, 233, 237–8, 277, 308–10, 313
 planum polare, 217, 233, 237
 planum temporale, 217–20, 233–4, 237–8, 311, 313
 asymmetries, 312–13
 speech, 237–8, 311, 313
 responses of cells
 binaural, 221, 222, 225, 228, 231, 233,
 to complex stimuli, 225, 226, 236–8
 to frequency modulation, 221, 224, 236
 frequency-threshold curves, 223, 225
 in belt, 225–6
 in core, 221–5
 inhibition, 213, 219, 222–5, 229, 233, 236
 latencies, 221, 222, 224, 225, 226, 233
 multipeaked, 223–4, 225, 236–7
 response types, 221–6
 to speech sounds, 302–3, 307–8
 to sound location, 224, **228–34**, 238
 temporal patterns of, 222–3
 tonotopic, 219–20, 222, 224, 225
 tuning, 223, 225, 236–7
 sound localization
 neuronal responses, 225, 228–33
 behavioural studies, 226–7
 speech analysis, for main entry *see*
 speech, 238, **308–13**
 tonotopy, 211, 212, 214, 215, 217, 218, **219**, 220, 222, 224, 225
 Wernicke’s area, 312
 ‘what’ stream, 211, 233–234, 237, 239
 ‘where’ stream, 211, 233–5, 238, 239
 Corti, *see* organ of Corti, cochlea, hair cells, names of individual structures
 Corticosteroids, 351
 Critical bands (psychophysical filter)

- auditory nerve correlates, 273–6
defined, 271–2
and loudness, 290–2
sensorineural hearing loss, 333–4
simultaneous vs nonsimultaneous masking, 272–3
- Cubic distortion tone, *see* combination tones, nonlinearity
- Cuticular plate, 31, **102–4**, 133
- Cytochrome oxidase (in cortex), 212, 216, 218
- Deafness, for main entry *see* sensorineural hearing loss, *see also* conductive hearing loss, stria vascularis
types defined, 319
- Death, effect on travelling wave, 44
- Decibels (dB)
definition, 3–4
dB SPL scale, 4
- Deep-water waves in cochlea, 47
- Deiters' cells (outer phalangeal cells), 26, 28, 30, 31, 136, 346
transdifferentiation of, 346–7
- Deoxyglucose, 188
- Dexamethasone, 351
- Difference tone ($f_2 - f_1$), 98, 150, 249
see also combination tones, nonlinearity
- Diffusion potentials
defined, 110–11
and hair cell currents, 111
role in endocochlear potential, 54–6
- Displacement
of air in sound wave, 1–4
response of hair cells, 137–9, 141
- Dopamine, as transmitter of olivocochlear bundle, 246, 251
- Dorsal acoustic stria, 157, 159, 163, 169, 173, 174
- Dorsal cochlear nucleus, *see* cochlear nucleus
- Dorsal stream (sound identifying and localising) of brainstem, 164–6, 173–5
- Ductus reuniens, 56
- Dynamic range
auditory nerve, 80, 89, 285–6, 303
cochlear nucleus, 170, 171, 286, 305
definition, 80
hair cells, 51, 59
middle ear reflex and, 23, 289
olivocochlear effects, 257, 289
superior olive, 178
- Dynorphins, as transmitter of olivocochlear bundle, 246
- Ear advantage (in speech perception), 313
- Ear canal, **11–15**, 18, 19
- Eardrum, *see* tympanic membrane
- Echo (cochlear) *see* cochlear emissions
- Echo (in environment), 186
- Echolocation, 194, 201–2, 237
- EE neurones, 176, 182–4, 192, 221–2, 297, 299–301
definition, 176
- El neurones, 176, 182, 192–193, 221–2, 297, 299–301
definition, 176
- Efferent fibres, *see* olivocochlear bundle, centrifugal pathways
- Efficiency of
middle ear, 18–22
outer ear, 13–14
- Electrical stimulation of cochlea, *see* cochlear prosthesis for main entry 131–2, **338–40**
- Elevation of sound source
and outer ear, 13–14, 15
and dorsal cochlear nucleus, 173, 197, 204
- Emissions (cochlear) *see* cochlear emissions
- Endocochlear potential, **52–6**
role in transduction, 57
- Endolymph, 25, 54–7
composition, 53
endolymphatic space, 52–3
flow, 56
hydrops, 56
origin, 54–7
potential, 53, 54–7
- Endolymphatic duct, sac, 56
- Energy transfer in
middle ear, 18–22

- Energy transfer in (*Continued*)
 outer ear, 13–14
 cochlea, 124–5, 268
- Enkephalins, as transmitter of olivocochlear bundle, 246
- Equalisation and Cancellation (EC) model, 301
- Equilibrium potentials, defined, 110–11
 and hair cell transduction, 110–11
- Espin, 103
- Ethacrynic acid, 55, 324
- Evoked cochlear mechanical response,
see cochlear emissions
- Excitotoxicity and acoustic trauma, 325
- External auditory meatus, 11–12, 14, 15, 18, 19
- Extralemniscal system, 157, 164, 187, 196, 199, 202
- $2f_1 - f_2$ tone, *see* combination tones, nonlinearity
- Feature detection
 auditory cortex, 211, 238
 cochlear nucleus, 170
 in general, 155–7
- Fimbrin, 103, 104
- fMRI and
 complex stimuli, 237
 definition of cortical areas, 215, 217–8, 219
 loudness, 292
 sound localization, 233
 speech, 302, 309–11
 tonotopic responses, 217–18, 219
- Formants, *see* speech
- Forward masking, *see* non-simultaneous masking
- Fourier analysis, 5–8, 9
- Free radicals, 321, 329, 350
- Frequency (definition), 1
- Frequency-band strips (in cortex), 213, 219–21, 238
 and sound localization, 227
- Frequency discrimination *see* pitch perception
- Frequency modulation
 auditory cortex, 221, 224, 236
 inferior colliculus, 194
- Frequency progressions, and definition of cortical areas, 212, 213, 217, 218, 219, 220
- Frequency resolution, *see also* tuning curve, travelling wave, critical band, Q_{10} dB, names of specific structures
 auditory nerve,
 to broadband stimuli, 86–7
 as a function of intensity, 87–9
 to tones, 75–9
- basilar membrane (travelling wave), 35–42
 and active cochlear mechanics, 50–2, 123–37
 in relation to auditory nerve, 41–2
- centrifugal effects on,
 in cochlea, 128–9, 248–9
 at central nuclei, 276–7
- in cochlear pathology (sensorineural hearing loss) 128–9, 329–32, 333–4
 with cochlear prosthesis, 339–40
- comodulation masking release, 277–8
- comparison in stages of auditory system, 201–2, 276–7
- cortical (AI) variations in, 221–2
- definition (psychophysical), 268–9
- frequency discrimination, difference from, 268–9
- influence of
 cochlear nonlinearity, 42–5
 intensity, 41–5, 79–81, 87–9
 lateral inhibition, 276–7
- in masking patterns
 nonsimultaneous masking, 272–3
 simultaneous masking, 271–2, 273–6
 in relation to auditory nerve, 274–6
- inner hair cells, 61–2
- missing fundamental, 280–1
- outer hair cells, 61, 64
- psychophysical, 268–73

- and sensorineural hearing loss, 329–32, 333–4
theories of in cochlea, 46–52, 123–8
- Frequency-threshold curve, *see also*
frequency resolution, travelling wave, critical band, Q₁₀ dB, psychophysical tuning curve
of
auditory nerve fibres, 75–8
cochlear pathology, 329–32
cochlear nucleus, 167, 169
cortex, 222–3, 226, 233, 236
hair cells, 61
inferior colliculus, 190–1, 192, 196
lateral superior olive, 178
medial geniculate body, 199–201
medial nucleus of trapezoid body, 180
nuclei of lateral lemniscus, 185
olivocochlear fibres, 252
travelling wave, 41–2, 127, 129
- comparison in different stages of auditory system, 201–2, 276–7
construction of, 42–3
definition, 42
olivocochlear effects on, 128–9
- Functional magnetic resonance imaging, *see* fMRI
- Furosemide (Frusemide), 128, 324
- Fusiform cells,
cochlear nucleus, 164–6, 169, 172–3
lateral superior olive, 176
medial superior olive, 181
- GABA, 169, 180, 185, 186, 189, 190, 193, 194, 195, 199, 201, 205, 213, 224, 235, 246, 247, 251, 259, 336
- Gating spring theory *see*
mechanotransduction for main entry, 117–22
- Gene therapy, *see* cellular therapy for main entry, 348
- Geniculate body, *see* medial geniculate body, lateral geniculate body
- Gentamicin, *see* aminoglycosides
- Globular (bushy) cells, *see* bushy cells
- Glutamate (as neurotransmitter), 33, 57, 142, 158, 176, 181, 189, 204
- Glycine (as neurotransmitter), 164, 166, 169, 176, 180, 181, 183, 185, 189, 190, 195, 259, 336
- Glycoconjugates, 105
- Habenula perforata, 26, 33
- Hair cells, *see also* stereocilia,
mechanotransduction
acoustic trauma, 102, 324–6
and active process in sharp tuning, 44–5, 50–2, 125–37
adaptation, 109, 122–3
and active amplification, 135
and basilar membrane position, 145
Ca²⁺ effects, 122–3, 135
fast, 122–3
and motility, 135
slow, 123
anatomy, 30–3, 102–110
basal body, 31
battery theory, 52, 57–8, 111–14, 133–5
birds, 344, 346, 347, 349, 351
centriole, 31
cuticular plate proteins, 30–1, 104
α-actinin, 104
actin, 104
calbindin, 104
calmodulin, 104
myosin, 104
spectrin, 104
tropomyosin, 104
cytoskeleton (and transduction), 102–10
development, 345–6
dynamic range, 51, 58–9, 62–5
inner hair cells, 27–33, 60–4
anatomy, 27, 30–3
damage and cochlear tuning, 330–2
electrophysiology, 60–4
frequency selectivity, 61–2
innervation, 33–4, 73, 141–2
input–output functions, 62–4
intensity functions, 62

- Hair cells, inner hair cells (*Continued*)
 mitochondria, 33
 neurotransmitter release, 61, 141–2
 and nerve fibre activation, 139–42
 olivocochlear effects on, 128–9,
 248–51
 olivocochlear innervation, 245
 and phase-locking in nerve, 61, 83,
 139–41
 response to tones, 60–4
 resting potential, 60
 suppression, 91, 145–7
 synapse, 33, 141–2
 velocity responses, 137–9, 147,
 268
- motility, 50–52, 131–7
 nerve activation by, 139–42
 numbers, 28
 ototoxicity, 128, 320–4
 outer hair cells, 27–33
 and active process in cochlear
 mechanics, 51–2, 102, **123–37**
 afferent (Type II) fibre response, 74,
 145
 anatomy, 27, 30–3
 contribution to cochlear
 microphonic, 67, 138–9
 damage and cochlear tuning, 128,
 329–30
 displacement response, 65, 138–9,
 147
 electrophysiology, 57–9, 64–5
 frequency limitation in motility,
 133–5
 frequency selectivity, 61, 64
 innervation, 33–5
 input-output functions, 64–5
 intensity functions, 62, 64
 mitochondria, 33
 motility, 51–2, 125–8, 131–5
 cell body motility, 133–5
 stereociliar motility, 135
 nonlinear responses and travelling
 wave, 51, 144–7
 nonlinear responses and two-tone
 suppression, 92, 144–7
- olivocochlear effects on, 128, 247–8,
 254
 olivocochlear innervation, 244–5
 response to tones, 64–5
 resting potential, 64
 submembrane cisternae, 32
 synapses, 33
 thresholds and tuning of cochlea,
 role in, 50–2, 125–8, **131–7**
- regeneration, *see* cellular therapy for
 main entry, **344–9**
- responses in general, 57–5
 stimulus coupling in cochlea, 137–9
 summating potential, role in, 68
 transduction mechanisms *see*
 mechanotransduction for main
 entry
- turtle, 116, 122–3, 135
- Half-octave shift, 332
- Harmonics
 and distortion tones, 147–0
 and “missing fundamental”, 280–1
- Head size
 relation to high frequency hearing, 184
 and sound localization, 179, 184, 296
- Hearing loss, for main entry *see*
 sensorineural hearing loss, *see also*
 conductive hearing loss, stria vascularis
 types defined, 319
- Heat shock proteins, 351–2
- Helicotrema, 25, 268
- Held, end-bulbs of, 159–60, 181
- Hemispheric differences (in cortex),
 308–10, 311, 312–14
- Hensen’s cells, 27–8
- Hensen’s stripe, 26, 29, 65, 137
- Hertz (Hz), definition, 1
- Heschl’s gyrus, 216–20, 233, 237–8, 277,
 308–10, 312–3
- Hierarchical processing (in general), 156
- Hologram analogy, 156
- HSP70 (heat shock protein 70), 350–1
- Human being
 anatomy of cochlear nucleus, 165
 anatomy of auditory cortex, 212,
 214–8

- anatomy of inferior colliculus, 187
anatomy of superior olive, 184
olivocochlear effects, 249, 251, 252, 256, 257, 263
ventral nucleus of lateral lemniscus in, 185
speech analysis, 301–3, 308–13
superior olive in sound localization, 184, 297, 301
- Hydrops, 56
- Hypersensitivity and tinnitus, 335
- IE neurones, 176–8, 182, 221–2, 297, 299–301
definition, 176
- Impedance
acoustic ohms, 5, 17, 18
cochlear input impedance, 16–17, 18
cochlear partition, 47–50, 124–5
definition, 1–2, 4–5
discontinuity and energy transmission, 4–5
transformer in middle ear, 16–19
tympanic membrane, 18
- Implant, *see* cochlear prosthesis
- Incus, *see also* middle ear bones, 15, 16–18, 21, 22
- Inner hair cell, *see* hair cells, inner
- Inferior colliculus, **186–97**
anatomy, 186–90
binaural responses, 191–3, 195, 294–9
central nucleus
amplitude modulation, response to, 194
anatomy and organization, 187–90, 192–3, 194–5
frequency modulation, response to, 194
frequency organization, 188–9
inputs, 166, 175, 188–90
lateral division, 187, 188
maps, 194–5
neurotransmitters, 189–90, 193, 194
responses, 190–5
and sound localization, 191–3, 195, 295–6
- temporal responses, 194
centrifugal innervation
anatomy, 258, 261–3
function, 261–3
- dorsal cortex
anatomy, 187, 189, 195
reflexes, 204–5
responses, 195–7
- external nucleus
anatomy, 187, 189, 195
maps, 196–7
reflexes, 204–5
responses, 195–7
tinnitus and, 336–7
- obligatory relay?, 187
- olivocochlear bundle, effects on, 252, 257
- sound localization and, 186–7, 191–3, 195, 294–9
- speech sounds, 302, 306–7
- Inhibition
not in auditory nerve, 75, 86, 89–90
in cochlear nucleus, *see also* cochlear nucleus, 164, 165, 166, **167–71**, 172, 287–8, 305
in cortex, 213, 219, 222–5, 229, 233, 236
in dorsal nucleus of lateral lemniscus, role of, 186, 298
and frequency resolution
in cochlear nucleus, 170, 286, 304–5
psychophysical, 272–3, 275
in inferior colliculus, role of, 190–1, 191–3
in lateral superior olive, 176–80, 297, 301
in medial geniculate body, 199, 200–2, 205
psychophysical demonstration of lateral inhibition, 272–3
and timing information, 170
- Inner hair cells, *see* hair cells, inner
- Innervation *see* name of structure innervated
- Intensity, and
auditory nerve
click response, 85

- Intensity, and auditory nerve (*Continued*)
 electrical stimulation (cochlear prosthesis), 338–40
 frequency resolution, 81, 87–9, 284–9, 303–5
 intensity functions, 79–80, 285–7
 sloping saturation, 80, 285
 straight saturation, 80, 285
 vowel responses, 285–7
 cochlear mechanics, 39–40, 41–5
 cochlear prosthesis, 338–40, 342
 cochlear nucleus, 167–8, 169, 171, 286–9
 cortex: rate-intensity functions, 224, 225
 definition, 2–3
 frequency resolution (psychophysical), 283–6
 lateral inhibition, 170, 286–9
 loudness,
 auditory nerve correlates, 290–2
 and cochlear prosthesis, 342
 and critical bandwidth, 272
 recruitment, 292, 333
 and hearing loss, 333
 middle ear muscle reflex, 289
 olivocochlear bundle, 248–50, 257, 289
 perception in general, **290–1**
 recruitment, 292, 333
 sound localization cues, 176–179, 184, 297–8
 speech coding, 303–5
 suppression (two-tone), 285–7
 temporal information, 82–3, 87–9, 170, 171–2, 287–9, 305–6
 travelling wave, 42–5
- Interaural disparities in timing and intensity,
see binaural responses, sound localization
- Intermediate acoustic stria, *see* dorsal stream
 for main entry, 157, 159, 163, 173, 174
- Intermediate cells (of stria vascularis), 54–6
- Intrastrial space (of stria vascularis), 31, 55–6
- Isofrequency line (in cortex), *see* frequency-band strips, 213, 219–21, 238
 and sound localization, 227
- IT field of cortex, *see* cortex
- Jeffress model for sound localization, 183, 293–5
- Jerker mouse, 103
- K⁺
 concentration in
 endolymph, 53
 intrastrial space, 55
 organ of Corti space after
 stimulation, 65, 68
 perilymph, 57
 recycling, 53, 326
 role in endocochlear potential, 53–6
 and mechanotransducer channel, 58, 65, 117
- Kanamycin, *see* aminoglycoside antibiotics
- Kinocilium, 31–2
 and hair cell polarisation, 112–13
 role in transduction, 113, 114
- Koniocortex, 212, 216–18
- Lateral inhibition, *see* inhibition
- Lateral lemniscus, nuclei of,
 dorsal, 186
 anatomy and projections, 186, 189–0
 responses, 186
 sound localization, role in, 186, 298
- intermediate, 185
- ventral, 185
 anatomy and projections, 185, 189–90
 pitch perception, possible role in, 185
- Lateral lemniscus, pathway, 157, 175, 185
- Lateral superior olive, *see* superior olivary complex
- Lateralization of sound sources, *see also* sound localization, 186, 193, 226, 298
- Learning, and categorical perception, 302
- Lemniscal system, *see also* cortex auditory ‘core’ system, 157, 187, 196, 197
- Lever action (of organ of Corti), 29–30, 126, 139

- Lexical analysis, 310–12
Limbus, spiral (of cochlea), 26, 29
Line-busy effect in masking, 93–5
Linearity, *see* nonlinearity for main entry, *see also* combination tones, two-tone suppression definition, 9 of middle ear, 21–2
Links between stereocilia side links, 30, 32, **104** tip links, 30, 32, 58, 101, 102, **104–10**, 103, 115–18, 121, 123, 135 acoustic trauma effects, 324–5 anatomy, 104–9 BAPTA effects, 105 Ca^{2+} effects, 115 composition, 108–9 and mechanotransduction, *see also* mechanotransduction, 109–10, **115**, 118–20 ototoxic effects, 322–3 spatial organization, 105–8
Lizard, 103, 107
LOC (lateral olivocochlear system or bundle) *see* olivocochlear bundle
Localization, *see* sound localization
Long waves in cochlea, 47
Loop diuretics, 324
Loudness auditory nerve correlates, 290–2 and cochlear prosthesis, 342 and critical bandwidth, 272, 290–2 recruitment, 292, 333 and sensorineural hearing loss, 292, 333
Low pitch, *see also* pitch perception, 280–1
Malleus, *see also* middle ear bones, 15, 16–19, 22
Maps in cortex, 219, 222 in inferior colliculus, 194–5, 196–7 of sound location, 233, 194–5, 196–7, 204–5
Marginal cells (of stria vascularis), 54–6 in ageing, 328
ototoxic effects on, 324 potential, 55
Masking auditory nerve fibres, 93–95 centrifugal pathways to cochlear nucleus, 260 comodulation masking release, 277–8 critical bands, 271–2 frequency resolution, 269–71 middle ear muscles, 23–4 non-simultaneous, 272–3 and auditory-nerve frequency resolution, 274–5 lateral inhibition, 272–3, 275–6 psychophysical tuning curves, 274–5
olivocochlear effects, 255–6 psychophysical tuning curves, 270–1 simultaneous auditory-nerve frequency resolution, 273–6 psychophysical tuning curves, 270–1 spatial release from, 299–301
Math-1, 346, 347
Mechanics of cochlea, *see* travelling wave
Mechanotransduction, 30, 32, 58–9, 63, **111–23** adaptation, 109, 122–3 and active mechanical process of cochlea, 135 Ca^{2+} effects, 122–3, 135 fast, 122–3 slow, 109, 123 BAPTA effects, 115 Ca^{2+} -imaging of channels, 113–14 electrophysiological analysis, **111–23** gating spring theory, **117–21** ions involved, 111, 117 manipulation of stereocilia, 58–60, 111–13 mechanotransducer channels, 30, 32, 110, 117 conductance, 116 delay, 117 direct mechanical action on, 118, 121 ionic selectivity, 117

- Mechanotransduction, mechanotransducer channels (*Continued*)
 molecular nature of channel, 109–10
 number of states of channel, 120
 numbers of channels, 116
 position, 109–10, 113–15
 single channel recording, 115–16
- Molecular identity (not known), 101, 109–10, 116
- nonlinearity, 59, 120, 144–50
- stereocilia (role of), 112–13
- tip links, role of, 30–2, 109, 115, 117–21
- theory of, 117–22
- Medial geniculate body, 197–203
 anatomy, 197–9
 centrifugal innervation, 202, 213, 238, 261, 262–3
 dorsal and medial divisions, 197–9, 202–3
 anatomy, 197–9
 inputs, 198–9
 learning in, 202–3
 projections, 198–9, 203
 responses, 202
 stimulus-specific adaptation (SSA)
 in, 202
- ventral division, 198–202
 inputs, 197–8
 lamination, 198, 199–200
 projections, 198
 responses, 200–2
 ‘slabs’ in, 199–200
 sound localization, 200, 202
 tonotopy, 198, 199–200
- MELAS, 328
- Ménière’s disease, 56
- Medial superior olive, *see* superior olivary complex, medial superior olive for main entry, 181–4
- Metabolic hearing loss, *see* stria vascularis
- Microvilli, 30
- Microtubules, 31
- Middle ear
 anatomy, 12, 15–16
 bones
 and bone vibration from skull, 15
 effect on transfer function, 18
- impedance transformer action, 17–19
 mode of vibration, 19
- efficiency of, 21–22
- hearing loss, 15–16, 319
- impedance transformer
 action, 16–19
 ratio, 17–21
- linearity, 21–22
- muscles
 acoustic trauma and, 23
 action, 23
 reflex, 22–3, 203–4
 reflex and discrimination at high intensity, 23–4, 289
 reflex and speech, 23–4
- transfer function, 19–21
- transmission (energy) losses, 19, 21
- Missing fundamental, 280–1
- Mitochondria,
 in ageing, 329
 aminoglycoside interactions, 320, 321–2, 328
 and cell death, 323
 in hair cells (anatomy), 33
 mitochondrial inheritance and hearing loss, 327–8
 pathological changes, 321–2, 324–5
- MOC (medial olivocochlear system or bundle) *see* olivocochlear bundle
- Modiolus, 25–6, 28
- Mössbauer technique, 39
- Motility in hair cells, *see* active mechanical amplifier (cochlea), *see also* adaptation of hair cells
- Multipolar cells (cochlear nucleus), *see* stellate cells
- Myosins (in hair cells), 103–4, 108–9
 slow adaptation, 123
 hair cell motility, 135
- N₁, N₂ potentials, 68–9
 olivocochlear effects, 251, 253
- Na⁺
 concentration in endolymph, 53
 concentration in perilymph, 57

- and endocochlear potential, 54, 55–6
and mechanotransducer channel, 117
 Na^+/K^+ -ATPase, role in endocochlear potential, 55–6
 $\text{Na}^+/\text{Cl}^-/\text{K}^+$ -co-transporter, role in endocochlear potential, 56
Necrosis, 322, 351
Nerve, *see* name of individual nerve (e.g. auditory nerve)
Neurotransmitters *see under* name of structure
NMDA receptors, 158
Noise, *see also* acoustic trauma, masking, centrifugal pathways to cochlear nucleus and, 260
cochlear active amplification and filtering, 126–7
olivocochlear bundle, 253–6
responses in
 auditory nerve, 86–9, 94–5
 cochlear nucleus, 168, 170, 171, 172
 cortex, 236
 inferior colliculus, 197
Non-lemniscal system, 157, 164, 187, 196, 199, 202
Nonlinearity, *see also* combination tones, suppression
cochlear mechanics, 38, 42–5, 126, **142–50**
 active contribution to, 51, 143–4
combination tones, 95–8, 147–50
 auditory nerve fibre response to, 97–8
 cubic distortion tone ($2f_1-f_2$), 96–8, 147–50
 difference tone (f_2-f_1), 98, 147–50
 origin, 95–8, 147–50
 psychophysical demonstration, 95–6
 travelling wave response to, 148–9
definition, 9
of hair cell transduction, 59, 61, 112, 120–1
of hair cell intensity responses, 59, 62–4, 142–4
of middle ear (linear), 21–2
and two-tone suppression (*see* suppression for main entry), 89–93
olivocochlear bundle effects on, 131, 249
Non-simultaneous masking, 272–3
 and auditory-nerve frequency resolution, 274–5
 and lateral inhibition or suppression, 273–5
 and psychophysical tuning curves, 274–5
Noradrenaline, 35, 251, 259
Nucleus, *see* specific name
 nucleus of lateral lemniscus, *see* lateral lemniscus, nuclei of
 nucleus of trapezoid body, *see* superior olive, trapezoid body, nuclei of
Nuel, space of, 27
Object, auditory, 156, 187, 239, 278
Octopus cells, **162–3**, 169, 174, 185
Ohms, acoustic, 5, 17, 18
Olivocochlear bundle, 32, 34–5, **243–57**
 activation, 251–3
 central effects on, 263
 cochlear nucleus, to, 258, 259, 260
 crossed bundle (COCB) *see* MOC, 244
 firing pattern, 252
 inferior colliculus, influence from, 263
 intensity control, 257
LOC (lateral olivocochlear system)
 anatomy, 244–5, 246, 247
 cells of origin, 244–6
 lateral (small) cells, 245, 246
 neurotransmitters, 246–7, 251
 numbers of fibres, 245, 247
 shell neurones, 245–6, 258
 terminations in cochlea, 245–6
LOC effects
 on acoustic trauma, 254–5
 on cochlear responses, 251
 dynamic range of hearing, 257
MOC (medial olivocochlear system)
 anatomy, 244–5, 246, 247
 cells of origin, 245–6
 medial (large) cells, 245–6

- MOC (medial olivocochlear system)
 anatomy (*Continued*)
 neurotransmitters, 246–7
 numbers of fibres, 245, 247
 terminations in cochlea, 32, 244–5
- MOC effects
 acoustic trauma, 253–5
 active process in cochlea, 128–9,
 131, 150, 248–9
 attention, 257
 auditory nerve afferents, 249–50
 on basilar membrane position?, 145
 cochlear emissions, 131, 150,
 249–50
 cochlear microphonic, 251
 cochlear responses, 248–51
 cochlear tuning, 128–9, 248
 cortical influence on, 262, 263
 dynamic range of hearing, 257, 289
 fast (at outer hair cells) 248, 254
 hair cells, 128, 247–8
 inferior colliculus effect on, 263
 intensity functions, 248–50
 masking, 255–7
 N₁ potential of cochlea, 251
 nonlinearity (of cochlea), 131,
 249–50
 signals in noise, 252, 255–7
 slow (at outer hair cells), 248, 254
 stimulus coding at high intensity,
 248–50, 257, 289
 tonotopicity of, 252
 uncrossed bundle (UOCB) *see* LOC
- Onset
 onset chopper type, 163–4, 169, 171,
 278
 onset response type, 160, 162, 179, 180,
 194, 196, 200, 202
 response to onsets in speech, 307
- Organ of Corti, *see* cochlea, individual
 names of structures, travelling wave,
 for main entries
 anatomy, 26–35
 ionic composition of fluid in, 52, 53,
 56–7
 potentials, 53, 56, 65, 134–5, 141
- Ossicles, *see* middle ear bones
- Ototoxicity, *see* sensorineural hearing loss
- Ouabain, 55
- Outer ear
 anatomy, 11–12
 and sound localization, 14–15, 197,
 231–2
 pressure gain of, 11–15
- Outer hair cells, *see* hair cells
- Oval window, 15, 16–18, 19, 22, 28,
 35–6
- Owl, localisation, 196, 197, 205, 294
- P27^{kip1}, 348
- Parakoniocortex, 217,
- Parvalbumin (in cortex), 212
- Pauser response type
 cochlear nucleus, 164–5, 307
 inferior colliculus, 194
- Perilymph, 25, 52, 54–5
 origin, composition and potential, 56–7
- Periodicity pitch, *see also* pitch perception,
 280–1
- Phalangeal cells (for Outer phalangeal cells
 see also Deiters' cells), 27, 28
 transdifferentiation, 347
- Phase, *see also* phase-locking
 of auditory nerve activation, 82–3, 84,
 139–41
 of hair-cell activation, 82–6, 137–9
 interaural and release from masking
 (BMLD), 299–301
 interaural and sound localization, 178,
 181–4, 193, 230–1, **293–7**
 of travelling wave, 36–7, **45–6**, 48–9
 of two-tone inhibition, and extraction of
 frequency information, 287–8, 306
- Phase-locking, *see also* phase
 in auditory nerve
 and combination tones, 96–7
 to electrical stimulation of cochlea,
 340
 frequency limits, 83, 282
 to noise, 86–7
 to speech, 305–6
 to tones, 82–3, 86, 139–41

- frequency limits in CNS, 281–2
intensity effects, 82–3, 88–9, 139–41
and spectral resolution, 86–7
- Phonology, 301–3, 308–10
- Pillar cells, 26, 27, 28, 29
- Pinna, 11–12, 14–15
and sound localization, 14–15, 172–3, 197, 231–2
and pressure at tympanic membrane, 14–15
- Pitch perception and frequency
discrimination, 268–9, **278–83**
cochlear nucleus, 282
complex tones, 280–1
cortex, 235, 237
definition, 268–9
difference limens, 279–80
inferior colliculus, 282–3
model for, 281–3
residue pitch, 280–1
ventral nucleus of the lateral lemniscus, 185
- Pitch and cochlear prosthesis, 342–3
- Place theory of frequency discrimination, 278–80
and cochlear prosthesis, 343
- Planum polare (of cortex) *see also* cortex, auditory
anatomy, 217
and complex stimuli, 233, 237
- Planum temporale, (of cortex) *see also* cortex, auditory
anatomy, 217–20
asymmetries, 312–13
and sound location, 233–4
speech, 237–8, 311, 313
- Plasticity, *see also* learning, 239
- Plastins, 103
- Plateau region (of travelling wave), 46
- PLZF (promyelocytic leukemia zinc finger protein), 350
- Posteroventral cochlear nucleus, *see* cochlear nucleus posteroventral
- Poststimulus-time (peri-stimulus-time) histograms
of auditory nerve activity, 75, 76, 84, 85, 90
in cochlear nucleus, 161, 162, 163, 165
- Power transfer,
and absolute threshold, 268
in cochlea, 124–5
of middle ear, 21–2
of outer ear, 13–14
- Presbyacusis (Presbycusis), *see also* sensorineural hearing loss, 319–20, **328–9**
- Pressure
gain of outer ear, 11–13
RMS definition, 3
in sound wave, 1–3
transfer function of middle ear, 19–22
- Prestin, 52, 102, 128–9, 133
- Primary-like responses
cochlear nucleus, 160–1, 171
medial nucleus of trapezoid body, 180
- Probst, commissure of, 186
- Profilin, 104
- Prokoniocortex, 217
- Prosthesis, *see* cochlear prosthesis
- Protection
acoustic trauma
cellular protection, 350–1
middle ear muscles, 23, 203–4, olivocochlear bundle, 253–5
'toughening', 350–1
hair cells, 350–1
- Protein tyrosine phosphatase receptor Q, 104
- Protocadherin-15, 108–9, 121
- Psychophysical (frequency) filter (critical band), psychophysical tuning curve
auditory nerve correlates, 274–6
defined, 271–2
sensorineural hearing loss, 333–4
simultaneous vs nonsimultaneous masking, 272–4
- Pyramidal cells
in cochlear nucleus, 164–6
in cortex, 212–3, 218
- Quality factor ($Q_{10 \text{ dB}}$), *see also* tuning curves, frequency resolution, names of specific structures
auditory nerve, 79

- Quality factor ($Q_{10 \text{ dB}}$) (*Continued*)
 comparison in stages of auditory system, 201–2, 276–7
 cortex, variations in, 221–2
 definition, 79
- Quinine, 335
- RMS pressure, definition, 3
- Rarefaction clicks, 84–5
- Rate-intensity functions
 auditory nerve, 79–80, 88, 139–41
 cochlear nucleus, and inhibition, 168
 cortex, 224, 225, 229, 231
 lateral superior olive, 176, 179
 medial superior olive, 182–3
- Reactive oxygen species, 321, 324–5, 350
- Recruitment, and hearing loss, 292, 333
- Reflexes, brainstem, 204–5
 acoustic (middle-ear muscle), 22–4, 203–4
 audiogenic seizures, 205
 orientation (to sound source), 173, 204–5
 startle response, 204
- Regeneration (hair cell), *see* cellular therapy
 for main entry, **344–9**
- Reissner's membrane, 25–6, 36, 52, 54
- Residue pitch, *see also* pitch perception, 280–1
- Resistance-modulation theory of hair cell function, 57–8, 113, 133–4
- Resonance, *see* travelling wave for main entry
 middle ear, 19, 21, 23
 middle ear muscle effects, 23
 outer ear, 11–12
 passive cochlear mechanics, 46–50
- Reticular lamina, 26, 28, 29, 52, 67, 133, 136
- Reticular formation, 199, 204–5
- Reversal potential for transducer current, 117
- Reverse correlation, 86–7, 88–9
- Rootlet (of stereocilia), 30, 103–4, 323–4
- Rosenthal's canal, 33, 338, 349
- Round window, 15, 16, 26, 35, 36, 68
- Salicylate (acetyl salicylate; aspirin)
 antioxidant therapy, 321
 and tinnitus, 324, 335
- Scala media
see also endolymph
 potential, 53, 58, 67, 68
 anatomy and spatial relations, 25–6, 28, 52
- Scala tympani
see also perilymph
 potential, 56
 anatomy and spatial relations, 25–6, 28, 52
- Scala vestibuli
see also perilymph
 potential, 56
 anatomy and spatial relations, 25–6, 28, 52
- Semantics, analysis of, 310–12
- Sensorineural hearing loss, *see also* acoustic trauma, cellular therapy, cochlear prosthesis, **319–51**
 ageing, 319–20, 328–9, 336
 aminoglycoside antibiotics, **320–3**
 antioxidant protection, 321
 effects on hair cells, 128, 321–3
 effect on travelling wave, 128
 mechanisms of ototoxicity, 320–2
 nomenclature, 320
- antioxidants, 321–2, 324, 350
- auditory nerve
 ototoxic effects, 128
 presbyacusis, 328
 responses, 329–32
 spontaneous activity, 332, 335
 survival, 338
- causes (general), 319–20
- cellular therapy, replacement or protection, **344–51**
- cochlear emissions, 130, 131
- cochlear implant (prosthesis), *see* cochlear prosthesis for main entry, **337–44**
 cochlear tuning changed, 128–9, 329–30
 definitions, 319–20
 free radicals, 321, 324–5, 329, 350
 genetic causes, 326–8

- A1555G mutation, 328
cadherin, 327
connexins, 53, 326
harmonin, 327
MELAS, 328
mitochondrial mutations, 328
myosins, 327
nomenclature, 327
ototoxicity interaction, 328
Usher syndrome, 327
hair cell changes, 321–2, 324, 329–32
hair-cell regeneration, *see cellular therapy for main entry*, 344–9
hearing aids, 319–20, 334, 344
mitochondria, involvement, 320, 321–2, 323, 324–5, 327–9
ototoxic agents, *see also aminoglycoside antibiotics*, 320–4
A1555G mutation, 328
aspirin (acetyl salicylate), 321, 324, 350
Cisplatin, 324
ethacrynic acid, 55, 324
furosemide, 324
loop diuretics, 324
styrene, 324
toluene, 324
otoxicity (in general), 320–4
oxidative damage, 320–2, 324, 329, 350
presbyacusis, 319, 328–9
psychophysical correlates
 absolute threshold, 332–3
 complex stimuli, 334
 critical bandwidth, 333–4
 frequency resolution, 333–4
 half-octave shift, 332
 loudness, 333
 psychophysical filter, 333–4
 psychophysical tuning curves, 333–4
 recruitment, 292, 333
 speech, 334
reactive oxygen species, 321, 324–5, 329, 350
speech, 334
prosthesis and, 337, 343–4
stem cells, *see cellular therapy for main entry*, 348–50
stria vascularis, 320, 321, 324, 326, 328–9, 350
tinnitus, 324, 335–7
 animal models, 335
 anxiety, 336
 and auditory nerve, 335
 brainstem structures, possible involvement, 335–6
 cochlear emissions, 131, 335
 drug treatment?, 336
 GABA, glycine, possible involvement, 336
 mechanism, possible, 336
 retraining therapy, 337
 somatosensory effects, 336
 travelling wave of cochlea changed, 128–9
Septum of middle ear, 21
Shaker-2, 348
Shallow-water waves in cochlea, 47
Short waves in cochlea, 47
SK2 channels (in outer hair cells), 248, 254
Sloping saturation (of auditory nerve fibre), 80, 285, 289, 305
Somatosensory-auditory interactions, 173, 195–6, 198–9, 336
Sound
 physics, 1–5
 wave motion, 1–2
Sound localization, 293–301
 and
 auditory cortex, 225, 226, 227–35
 cochlear nucleus, 157, 159–60, 162, 170–1, 172–3, 298–9
 dorsal nucleus of the lateral lemniscus, 186, 298
 inferior colliculus, 186–7, 191–3, 195, 294, 295–8
 lateral superior olive, 173, 175–80, 184, 267, 297–8
 medial geniculate body, 202, 204

- Sound localization, and (*Continued*)
 medial nucleus of the trapezoid
 body, 178, 180–1, 297
 medial superior olive, 178, **181–4**,
 295–7
 outer ear, 14–15, 197, 231–2, 299
 ventral stream of brainstem, 159–64,
 170–1, **173–84**
- behavioural studies, 173, 186, 226–7
 binaural masking level difference and,
299–301
 characteristic delay, 183, 295–7, 298,
 300
 comparison of activity on two sides of
 head, 298
 and head size, 184, 296
 and hierarchical analysis (general), 156–7
 intensity cues, 175–80, 297–8
 Jeffress model, 183–4, 293, 294–7
 laterality, establishment of, 186, 193, 298
 mechanisms, **294–9**
 in owl, 196–7, 205
 spatial release from masking and,
299–301
 timing cues, 181–4, 294–7
 in vertical direction, 14–15, 172–3,
 298–9
- Spatial maps (of sound location), 194–5,
 196–7, 204–5, 219–21, 233
- Spatial release from masking, **299–301**
- Specific impedance, 3–5, 14, 15, 16–18
 definition, 2
- Spectrum, definition, 5–7
- Speech, **301–14**
 aphasia, 312, 313
 categorical perception, 301–2
 learning effects, 302
 and cochlear prosthesis, 343–4
 consonants, 306–7, 313
 cortical asymmetries, 312–3
 ear advantage, 313
 temporal transitions and, 313
 emotional perception and, 313
 fMRI analysis, 302, 309–12
 formants, responses to, 303–6
 lesions, effects of, 312–3
- lexical analysis, 310–12
 and middle ear muscle reflex, 25
 neurolinguistics, 310
 and non-human vocalizations, 235–6,
 302–3, 306–8
 PET analysis, 302
 phonemes, 301–2, 308
 responses in
 angular gyrus, 310, 312
 auditory cortex, 238, **308–13**
 auditory nerve, 303–6
 Broca's area, 312
 cochlear nucleus, 163, 304–5
 Heschl's gyrus, 308–10, 313
 inferior colliculus, 306
 inferior frontal gyrus, 312
 planum temporale, 237–8, 311,
 313
 temporal lobe, 308–314
 Wernicke's area, 312
 semantics, 310, 312
 and sensorineural hearing loss, 334
 'speech mode' of perception, 301–2
 speech-specific responses?, 235, 237–8,
 302–3, 308–10
 syntax, analysis of, 310, 312, 313
 vowels, 302, 303–6, 308, 310, 313
 working memory, 312
- Spherical (bushy) cells, *see* bushy cells
- Spiral bundle, 27, 34
- Spiral ganglion, *see also* auditory nerve,
 26–7, 33–5, 73–4, 324
 adrenergic innervation, 35
 cell repair/replacement, 349, 351
 cochlear prosthesis and, 338, 341
- Spiral lamina, 25–7, 28, 33, 35
- Spiral limbus, 26, 29
- SPL, definition, 4
- Spontaneous activity
 of auditory nerve fibres, 74–8, 141–2
 and best threshold, 76, 141–2
 and hair cell damage, 332
 and inhibition in cochlear nucleus,
 167–9
 and tinnitus, 131, 335–6
- SSA, *see* Stimulus-specific adaptation

- Stapes, *see* middle ear bones for main entry, 15–18, 21–2
- Stellate cells (T-, D-stellate), 162–4, 166, 169, 181, 185, 187–9, 194
- and comodulation masking release, 278
- and stimuli at high intensity, 305
- Stem cell therapy, 348–50
- Stereocilia
- anatomy, 29–32, 33, 102–9
 - acoustic trauma effects on, 102, 324
 - composition, 102–4, 109
 - damage
 - by acoustic trauma, 102, 324
 - aminoglycosides, 322–3
 - and inner hair cell responses, 325, 330–2
 - and jerker mouse, 103
 - linkages
 - side links, 30, 32, **104–5**, 106,
 - tip links, 30, 32, 58, **101–10**
 - composition, 108–9
 - and mechanotransduction *see* mechanotransduction
 - spatial organization, 106–8
 - in lizard, 103
 - mechanical properties, 102
 - mechanotransduction *see* mechanotransduction
 - motility, 135, 137
 - ototoxic effects on, 322–3
 - protein components
 - actin (f-actin) organisation, 102–3
 - profilin, 104
 - espin, 103
 - myosins, 103–4, 123
 - plastins (fimbrin), 103
 - rootlet, 30, 103–4
 - S1 fragment (of myosin), 102
 - stimulus coupling to, 137–9, 147, 268, 324
- Stiffness
- of cochlear partition, 47–49
 - of gating spring, 118–21
 - and middle ear structures, 20–2, 23
 - of stereocilia, 30, 102, 125
- Stimulus-specific adaptation (SSA), 196, 202, 203
- Straight saturation (of auditory nerve fibres), 80, 285, 289, 305
- Stria vascularis, 35, 52–6
 - adrenergic innervation, 35
 - and hearing loss, 320, 321, 324, 326, 328–9, 350
 - and origin of endolymph and endocochlear potential, **54–6**
 - ototoxic effects on, 55, 321–4
- Strychnine, 183, 246
- Styrene, 324
- Subtectorial space, 65, 137
- Summating potential, 66, 68
- Superior colliculus, 188, 197, 198, 204–5
- Superior olivary complex, **173–84**
 - anatomy, 173–6
 - centrifugal fibres to cochlea, *see* olivocochlear bundle
 - centrifugal fibres to cochlear nucleus, 257–60
 - centrifugal innervation of, 261
 - human, 184, 297
 - innervation, 166, 173–5
 - nuclei of the trapezoid body
 - lateral (LNTB), 178, 183, 295
 - medial (MNTB), 178, **180–1**, 184
 - output, 180–1, 183
 - sound localization, 183, 184, 295–7
 - lateral superior olive (LSO), **175–80**
 - anatomy, 175–7
 - binaural responses, 176–80, 184, 297
 - inputs, 176
 - neurotransmitters, 176
 - outputs, 180, 186, 189–90, 192–3, 195
 - and sound localization, 173–4, 175–80, **184**, 297
 - medial superior olive (MSO), **181–4**
 - anatomy, 176, 181–2
 - binaural responses, 182–3
 - inputs, 178, 180, 181

- Superior olivary complex, medial superior olive (MSO) (*Continued*)
 outputs, 180–1, 186, 189–90
 and sound localization, 174, 181–4,
 295–7
- olivocochlear bundle, *see* olivocochlear bundle
- para-olivary nucleus, superior (SPN), 246
- pre-olivary nuclei
 medial (or ventral nucleus of the trapezoid body, VNTB), 176,
 180, 246, 261
- peri-olivary nuclei, in general, 174, 180,
 245, 246, 258, 261
- dorsal (DPO), 176, 246
- dorsolateral (DLPO), 176, 246
- dorsomedial (DMPO) (or superior para-olivary nucleus SPN of rodents), 176, 180, 246
- ventromedial (VMPO), 176
- superior para-olivary nucleus (SPN), 176, 180, 246
- Superior temporal plane, *see also* cortex, areas: human, *see also* speech, 213, 215–7, 225, 237–8, 308–13
- Supporting cells (of organ of Corti), *see also* names of individual cell types, 27–30, 32
 transdifferentiation in cell therapy, 346–7
- Suppression (two-tone suppression)
 auditory nerve, 89–93, 94–5, 145–7,
 274–5, 285–9, 303–6
 spontaneous activity, no effect on, 89
 frequency relations, 91–2
 hair cells, 90–2, 145–7
 high stimulus intensity, effects on
 response at, 285–7, 303–5
 latency, 90
 masking, 95–5, 272–3
 mechanism, 92, 145–7
 and noise, 94–5
 olivocochlear bundle, no effect on, 90
 and psychophysical masking patterns, 272–5
- psychophysical demonstration, 272–3
 and speech (vowel) sounds, 303–5
 travelling wave, 90–1, 145–7
- Sympathetic innervation of cochlea, 35
- Synapses
 on hair cells, 32, 33–5, 73–4, 141–2
 Synaptic bodies in hair cells, 33, 141–2
- Syntax, analysis of, 310, 313
- Tectorial membrane, 26, 28–9, 47, 65, 133, 137, 144
 and cochlear micromechanics, 125–6, 135–7, 139, 141
- Tectorin, 28
- Temporal bone, 12, 17, 19, 25, 36
- Temporal information, *see also* phase locking, binaural responses in auditory nerve
 to broadband stimuli, 86–9
 to clicks, 83–5
 to electrical stimulation, 340
 as function of intensity, 83, 287–9
 to speech sounds, 305–6
 to tones, 81–3
- in cochlear nucleus, 160–1, 162–3, 170, 171–2, 287–9, 305–6
- and cochlear prosthesis, 340, 341–3
- and frequency/pitch discrimination, 278–9, 280–3
 in cochlear nucleus?, 282
 in inferior colliculus, 282–3
- models for use of, 281–3, 287–9, and speech coding, 305–6
- Temporary threshold shift, 324, 253–4
- Tetramethylammonium (TMA), 117
- Thalamus, for main entries, *see* names of individual nuclei
- Thresholds, *see also* absolute threshold, frequency discrimination, masking absolute threshold, and energy to cochlea, 268
 auditory nerve, 76–78
 relation to psychophysical absolute threshold, 268
- cortex, 221–2, 235
 ototoxic effects, 128, 329–32

- and transduction kinetics, 121
travelling wave, 42
- Time, *see* temporal information, *see also*
binaural responses, sound localization,
phase, phase-locking
- Tinnitus, 335–7
animal models, 335
anxiety, 336
attention, 336
brainstem structures, possible
involvement, 335–6
cochlear emissions, 131, 335
drug treatments?, 336
GABA, glycine, possible involvement,
336
mechanism, possible, 335–6
quinine, 335
retraining therapy, 337
salicylate (aspirin), 335
- Tip links, *see* links
- Toluene, 324
- Tonotopicity
definition, 158
in
 cochlear nucleus, 158
 cortex, 212, 214–18, **219–20**, 222,
 224, 225
 inferior colliculus, 186, 188–9, 195
 lateral superior olive, 177
 medial geniculate body, 198–200
 nuclei of lateral lemniscus, 185
 olivocochlear bundle, 252
- ‘Toughening’ (cochlear protection), 350–1
- Trabeculae, 29
- Transdifferentiation, 346–7
- Transduction in hair cells *see*
 mechanotransduction
- Transfer function of middle ear, 19–21
- Transformer ratio of middle ear, 17–19
- Transient receptor potential channels, 110,
 116
- Trapezoid body (as ventral sound localizing
 stream of brainstem), 166, **173–84**
 for nuclei *see* superior olivary complex
- Travelling wave of cochlea, **35–52**
 active mechanical amplifier, 44–5, **123–37**
- mechanisms of amplification, 131–7
micromechanics, 135–7
models, 125–7
needed theoretically? 124–5
noise advantage, 126–7
role of outer hair cells, 128, 131–5
and cochlear microphonic, 134–5
aminoglycoside effects on, 128
amplitude plots, 41–2, 43–4
combination tones, *see* nonlinearity for
 main entry, *see also* combination
 tones, 147–50
displacement at threshold, 42
emissions *see* cochlear emissions for main
 entry, **128–37**
echo demonstration, 130
energy produced, 131
olivocochlear effect on, 150, 256
spontaneous, 131, 335
- frequency selectivity, 41–2
in active models, 126–7
relation to auditory nerve, 42,
 126–7
- relation to hair cell responses,
 61–2, 64
- relation to critical bandwidth, 273–6
after death, 36, 44
- hair cell responses to displacement and
 velocity, 137–9
- history, 35–8
- impedance of cochlear partition, 47–50,
 124–5
- intensity effects, 39–40, 41–2, 43–5
 olivocochlear influence on, 249–50
- micromechanics, 126–7, 135–7
- nonlinearity, *see* nonlinearity for main
 entry, 38, 42–5, 126, **142–50**
 and olivocochlear bundle, 131, 249
- and outer hair cells, 51–2, 102, **123–37**
- and outer hair cell nonlinearity, 51,
 144–7
- olivocochlear effects, 128–9, 248–9
- ototoxic effects, 128
- pattern (general), 35–40
 in relation to frequency, 36–8, **41–2**
 over space, 36–7, **39–40**

- Travelling wave of cochlea (*Continued*)
phase, 36–7, 45–46
power flux in cochlea, 124–5
static (d.c.) displacements, 65, 144–5
temporal effects in theory of frequency resolution, 287–9
theories
 broadly-tuned (passive) component, 46–50
 and admittance of cochlear partition, 47–9, 124–5
 micromechanics, 125–7, 135–7
 and pressure across cochlear partition, 47–9
 and resonance of cochlear partition, 47–9, 124–5
 and stiffness of cochlear partition, 47–9, 124–5
 sharply-tuned (active) component, 50–2, 125–37, 143–4
resonance in cochlea, 46–50, 125–6, 135–7
resting position (of basilar membrane), 65, 144–5
two-tone suppression, 145–7
 see suppression for main entry
- Triethyl ammonium, 117
- Tropomyosin, 104
- TRP channels, 110, 116
- Tubulin, 31
- Tuning curve *see* frequency-threshold curve
- Tunnel fibres, 27, 34, 35
- Turtle, 116, 122–3, 135
- Twitter call, 307
- Two-cell model (of stria vascularis), 55–6
- Two-tone suppression *see* suppression
- Tympanic membrane
 input impedance, 16–8
 mode of vibration, 19
- Type I auditory nerve fibres, 33–4, 73–4
 see auditory nerve for main entry
- Type II auditory nerve fibres, 73–4, 145
- Usher syndrome, 108, 327
- Velocity
 of particles in sound wave, 1–5
 responses of
 auditory nerve fibres, 139–41
 inner hair cells, 138–9
- Ventral acoustic stria, 157, 159–66, 173–84
- Ventral stream (sound localizing) of brainstem, 157, 159–66, **173–84**
- Vestibular hair cells, 110, 113–4, 123, 135
vestibulotoxicity, 322
- Vocalizations, 173, 203, 235–6, 238, 303, 306–8
- Vowels, *see* speech
- Water wave analogy for travelling wave, 46–7
- Wernicke's area, 312
- 'What' stream in cortex, 211, 233–4, 237, 239
- 'Where' stream in cortex, 211, 233–4, 235, 238, 239
- Wiener kernel analysis, 87, 89
- Zebrafish, 110
- Zonula adherens of hair cell, 104

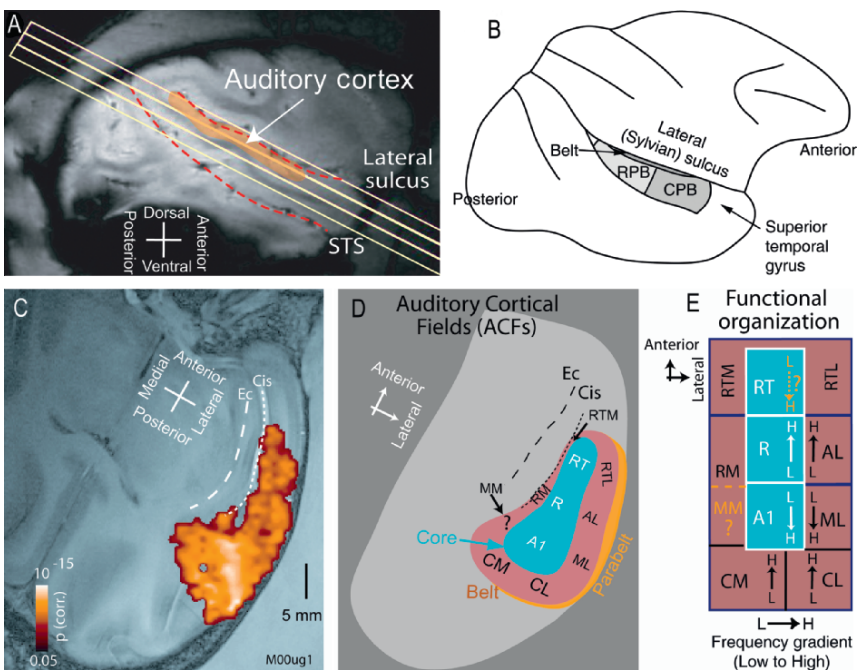


Plate 1 Areas of the monkey (macaque) right auditory cortex as shown by functional magnetic resonance imaging (fMRI). fMRI uses the response to changes in intense magnetic fields to detect activity-related changes in the oxygen depletion of blood. (A) Side view of cortex, showing the planes, through the lower edge of the lateral sulcus, over which images were taken. (B) Diagrammatic representation of the macaque cortex from the same point of view as in part A. The rostral and caudal parabelt areas (RPB, CPB) are shown on the surface of the superior temporal gyrus. (C) Response to broadband noise in one animal. (D) The three core auditory areas (blue) are surrounded by eight belt areas. (E) Tonotopicity of the three core areas and four of the belt areas, shown by representation of high (H) and low (L) frequencies. A1, primary auditory area; AL, anterolateral area; Cis, circular sulcus; CL, caudolateral area; CM, caudomedian area; CPB, caudal parabelt; Ec, external capsule; ML, middle lateral area; MM, middle medial area; R, rostral area; RM, rostromedial area; RPB, rostral parabelt; RT, rostrotemporal area; RTL, lateral rostrotemporal area; RTM, medial rostrotemporal area; STS, superior temporal sulcus. Figure 7.2A, C–E from Petkov *et al.* (2006), Fig. 7.2. (See Fig. 7.2, p. 215).

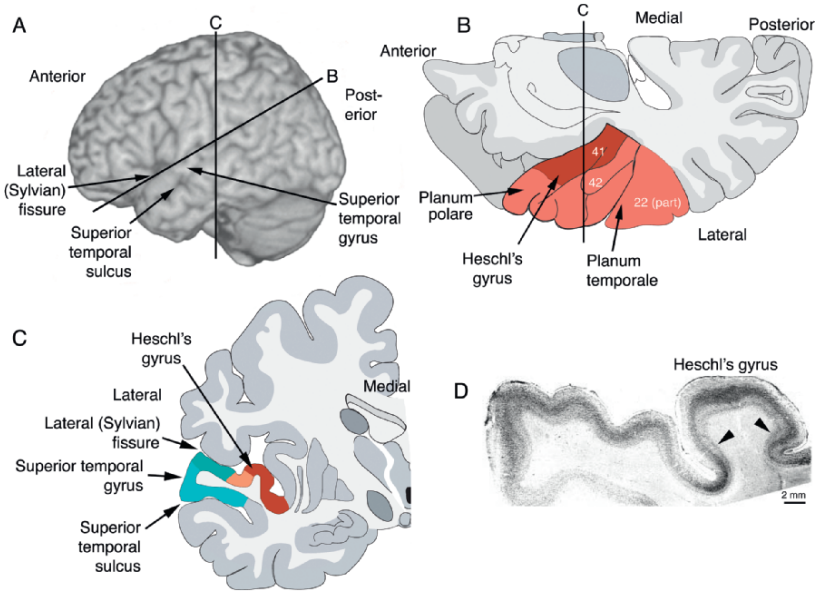


Plate 2 The human auditory cortex (left hemisphere). (A) Lateral view of left cerebral hemisphere, showing planes of section in parts B and C. (B) Sloping section in the plane shown in part A. Top view of upper surface of temporal lobe (red) with area of koniocortex within Heschl's gyrus marked (darker red). The division of the surface anterior to Heschl's gyrus is known as the planum polare, and the large division posterior to Heschl's gyrus is known as the planum temporale. Numbers show areas according to Brodmann (1909). In some individuals, Heschl's gyrus divides into two. (C) Transverse section of left cerebral hemisphere in the vertical plane shown in part A, showing Heschl's gyrus (darker red) and further auditory cortex of the superior temporal plane (lighter red, lighter and darker blue). Exactly how the latter areas are distributed over the superior temporal gyrus and sulcus varies between individuals. (D) Transverse histological section as in part C, showing Heschl's gyrus and laterally adjacent parts of the superior temporal plane. Arrowheads: borders of AI. Nissl stain.

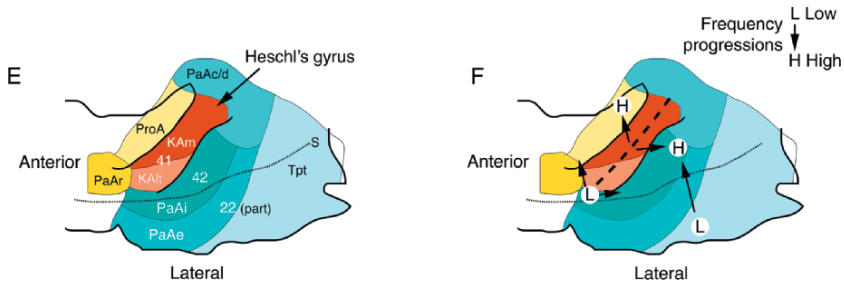


Plate 2 (Continued) (E) Cytoarchitectonic areas of the human auditory cortex according to Galaburda and Sanides (1980). The dotted line (S) shows the position of the Sylvian sulcus: the cortical surface lateral to this line curves down over the external surface of the temporal lobe, over the superior temporal gyrus. The area corresponds to coloured area in part B but extending slightly more anteriorly and further laterally over the superior temporal gyrus. Numbers show areas according to Brodmann (1909). (F) Tonotopic frequency progressions in the cortex, according to Langers and van Dijk (2012), superimposed on the cytoarchitectonic areas of Galaburda and Sanides. The arrows mark the direction of the progressions from low frequencies to high. The heavy dotted line marks the line of frequency reversal along the crest of Heschl's gyrus. Because of variation in positions of gyri and sulci from individual to individual, it is not possible to definitively align the fMRI data precisely with the cytoarchitectonic data. KAAlt, lateral koniocortex; KAm, medial koniocortex, PaAc/d: caudo-dorsal parakoniocortex; PaAe, external parakoniocortex; PaAi, internal parakoniocortex; PaAr, rostral parakoniocortex; ProA, prokoniocortex; S, Sylvian (lateral) sulcus or fissure; Tpt, temporoparietal area. Figure 7.4B and C from Harasty *et al.* (2003), Fig. 1; Figure 7.4D from Wallace *et al.* (2002a), Fig. 1A, with kind permission from Springer Science and Business Media; Figure 7.4E used with permission from Talavage *et al.* (2004), Fig. 7. (See Fig. 7.4, p. 217, 218).

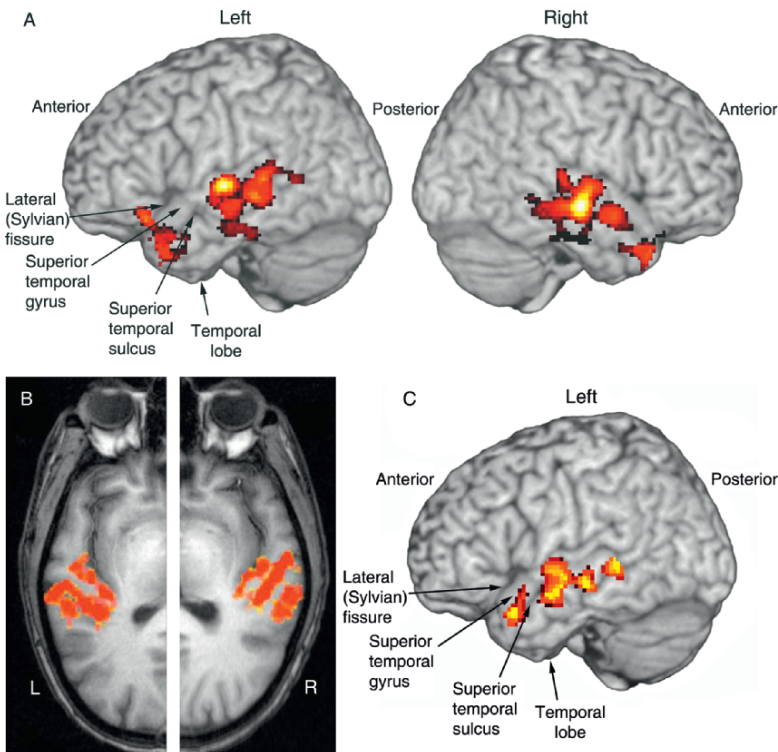


Plate 3 Cortical responses to speech, shown in red/yellow. (A) Response during passive listening to speech sounds, imaged in left and right hemispheres in a single subject by functional magnetic resonance imaging (fMRI). fMRI detects the local drop in oxygen level in the blood, consequent on activity. In this view, surface and subsurface signals from fMRI (coloured) are projected onto a standard cortical surface obtained from structural MRI. Areas (yellow/red) are shown where the signal with the speech sound is statistically greater than the signal in silence. Areas are bilaterally activated in the temporal lobe. Data for figure were provided by Professor C. Price. (B) Response to spoken words, imaged by fMRI in a 6-mm-thick slice along the surface of the superior temporal plane, in a single subject. The data from fMRI are superimposed on a high resolution structural MRI scan of the brain. There is a bilateral response, in Heschl's gyrus and extending over the superior temporal plane. The illustrated image is the average of the responses to the two ears and is the activity measured during presentation of the signal minus the activity measured in silence. Used with permission from Behne *et al.* (2006), Fig. 3, digital average of left halves of original sub-figures. (C) Responses to speech sounds, when the subjects had to make a later response based on the meaning of the sounds. The figure shows the activity in response to the speech sounds, minus the activity in response environmental sounds which were approximately matched in acoustic properties. There are discrete areas of specific activation in the region of the superior temporal gyrus and sulcus. Left hemisphere. Data from Thierry *et al.* (2003), as reanalysed by Price *et al.* (2005). From Price *et al.* (2005), Fig. 1A. (See Fig. 9.15, p. 309).